

# Deutsche Entomologische

---

## Zeitschrift

---

# 71 (1) 2024

# Deutsche Entomologische Zeitschrift

## An International Journal of Systematic Entomology

### Editor-in-Chief

**Matthias Seidel**

Natural History Museum Vienna  
matthias.seidel@nhm-wien.ac.at

### Managing Editor

**Lyubomir Penev**

Pensoft Publishers, Sofia, Bulgaria  
phone: +359-2-8704281  
fax: +359-2-8704282  
e-mail: penev@pensoft.net

### Editorial Secretary

**Boryana Ovcharova**

Pensoft Publishers, Sofia, Bulgaria  
e-mail: journals@pensoft.net

### Editorial Board

**Emmanuel Arriaga Varela**, Warszawa, Poland

**Ulrike Aspöck**, Vienna, Austria

**Silas Bossert**, Pullman, United States of America

**Alexssandro Camargo**, Vienna, Austria

**Jose Fernandez-Triana**, Ottawa, Canada

**Viktor Hartung**, Münster, Germany

**Claudia Hemp**, Bayreuth, Germany

**Zoltán László**, Cluj-Napoca, Romania

**Harald Letsch**, Vienna, Austria

**James Liebherr**, Ithaca, United States of America

**Wolfram Mey**, Berlin, Germany

**Alessandro Minelli**, Padova, Italy

**Susanne Randolph**, Vienna, Austria

**Dávid Rédei**, Tianjin, China

**Matthias Seidel**, Vienna, Austria

**Nikolaus Szucsich**, Vienna, Austria

**Sonja Wedmann**, Messel, Germany

**Frank Wieland**, Bad Dürkheim, Germany

**Michael Wilson**, Cardiff, United Kingdom

**Reza Zahiri**, Karlsruhe, Germany

**Dominique Zimmermann**, Vienna, Austria

### Deutsche Entomologische Zeitschrift

#### 2024. Volume 71. Issue 1

ISSN: 1435-1951 (print), 1860-1324 (online)  
Abbreviated journal title: Dtsch. Entomol. Z.

#### In Focus

The cover picture shows habitus of female *Gyrelon jenpani* Hu, Fikáček & Matsumoto, sp. nov.

See paper of **Hu F-S, Arriaga-Varela E, Biffi G, Bocák L, Bulirsch P, Damaška AF, Frisch J, Hájek J, Hlaváč P, Ho B-H, Ho Y-H, Hsiao Y, Jelínek J, Klimaszewski J, Kundrata R, Löbl I, Makranczy G, Matsumoto K, Phang G-J, Ruzzier E, Schülke M, Švec Z, Telnov D, Tseng W-Z, Yeh L-W, Le M-H, Fikáček M** Forest leaf litter beetles of Taiwan: first DNA barcodes and first insight into the fauna

#### Cover design

Pensoft



# Deutsche Entomologische Zeitschrift

## An International Journal of Systematic Entomology

### Content of volume **71** (1) 2024

<b>Minghetti E, Montemayor SI, Dellapé PM</b> Two new genera and four new species of Neotropical Eccritotarsini (Heteroptera, Miridae, Bryocorinae)	1
<b>Hu F-S, Arriaga-Varela E, Biffi G, Bocák L, Bulirsch P, Damaška AF, Frisch J, Hájek J, Hlaváč P, Ho B-H, Ho Y-H, Hsiao Y, Jelínek J, Klimaszewski J, Kundrata R, Löbl I, Makranczy G, Matsumoto K, Phang G-J, Ruzzier E, Schülke M, Švec Z, Telnov D, Tseng W-Z, Yeh L-W, Le M-H, Fikáček M</b> Forest leaf litter beetles of Taiwan: first DNA barcodes and first insight into the fauna	17
<b>Souma J</b> Two new species of the genus <i>Agramma</i> (Hemiptera, Heteroptera, Tingidae) from small islands of Japan, with an illustrated key to the Japanese species of the genus	49
<b>Jordal BH</b> Integrated taxonomy, biology and biogeography of the Afrotropical genus <i>Xyloctonus</i> (Coleoptera, Curculionidae, Scolytinae)	67
<b>Gustafsson DR, Tian C, Ren M, Li Z, Sun X, Zou F</b> New genus and species of lice in the <i>Oxylipeurus</i> -complex (Phthiraptera, Ischnocera, Philopteridae), with an overview of the distribution of ischnoceran chewing lice on galliform hosts	85
<b>Boudinot BE, Bock BL, Weingardt M, Tröger D, Batelka J, Li D, Richter A, Pohl H, Moosdorf OTD, Jandausch K, Hammel JU, Beutel RG</b> <i>Et latet et lucet</i> : Discoveries from the Phyletisches Museum amber and copal collection in Jena, Germany	111
<b>Rehberger S, Vogel J, Müller B, Vasilita C, Krogmann L, Schmidt S, Peters RS</b> The obligate fig-pollinator family Agaonidae in Germany (Hymenoptera, Chalcidoidea)	177
<b>Sun X-Y, Dong X-M, Jiang L</b> Larval morphology of a Palearctic Rutelini, <i>Parastasia ferrieri</i> (Coleoptera, Scarabaeidae), with discussions on their feeding habits	185
<b>Paappanen J</b> <i>Lochetica ramii</i> sp. nov. – a new species of <i>Lochetica</i> Kriechbaumer, 1892 (Hymenoptera, Ichneumonidae, Phygadeuontinae) from Finland, with a key to world species	193
<b>Clavijo-Bustos J, Castro-Vargas MI, Neita Moreno JC</b> A second species of the genus <i>Manodactylus</i> Moser, 1919 (Coleoptera, Scarabaeidae, Melolonthinae, Macroductylini) from the highlands of Colombia	209
<b>Bolshakova DS, Konstantinov FV</b> Revision of the genus <i>Kunungua</i> (Hemiptera, Heteroptera, Miridae) with descriptions of three new species and new generic synonymy	219

---

## Abstract & Indexing Information

Biological Abstracts® (Thompson ISI)  
BIOSIS Previews® (Thompson ISI)  
Cambridge Scientific Abstracts (CSA/CIG)  
Web of Science® (Thompson ISI)  
Zoological Record™ (Thompson ISI)



# Two new genera and four new species of Neotropical Eccritotarsini (Heteroptera, Miridae, Bryocorinae)

Eugenia Minghetti<sup>1</sup>, Sara Itzel Montemayor<sup>1</sup>, Pablo Matías Dellapé<sup>1</sup>

<sup>1</sup> División Entomología, Museo de La Plata, Universidad Nacional de la Plata, CONICET. Paseo del Bosque s/n B1900FWA, La Plata, Buenos Aires, Argentina

<https://zoobank.org/A0C8103C-B56C-40E9-9C38-1D2617F8A3C4>

Corresponding author: Eugenia Minghetti (eugeniaminghetti@fcnym.unlp.edu.ar)

Academic editor: Dávid Rédei ♦ Received 27 March 2023 ♦ Accepted 20 November 2023 ♦ Published 8 January 2024

## Abstract

In this study two new genera and four new species of Eccritotarsini (Hemiptera: Heteroptera: Miridae: Bryocorinae) are described. *Thomasomiris* **gen. nov.** is established to accommodate *Thomasomiris setosus* **sp. nov.** (from Panama) and *Egerocoris* **gen. nov.**, is described for *E. ecuatorianus* **sp. nov.** (the type species), *E. dimorphus* **sp. nov.** (both from Ecuador) and *E. chaparensis* **sp. nov.** (from Bolivia). Adult habitus and male genitalia photographs are provided for each species. A key to species is also provided and the affinities of the new genera are discussed.

## Key Words

Insecta, Hemiptera, Bolivia, Ecuador, Panama

## Introduction

Eccritotarsini is the most diverse among the five tribes currently recognized in Bryocorinae (Hemiptera: Heteroptera: Miridae) (Namyatova et al. 2016), with about 115 genera (Konstantinov and Knyshov 2015; Schuh and Weirauch 2020) and more than 628 species worldwide (Ferreira et al. 2015; Konstantinov et al. 2018; Henry and Menard 2020). The New World has the greatest diversity with over 70 genera and more than 450 species (Ferreira et al. 2015; Henry and Menard 2020). Carvalho and Ferreira (1995) keyed 66 Neotropical genera and Ferreira and Henry (2011) provided a key to 18 genera occurring in Minas Gerais, Brazil.

Neotropical eccritotarsines can be recognized by the reduced scent gland evaporative area; the large disc-shaped pulvilli covering nearly the entire inner surface of the claws, with a comb-like row of long setae on its outer surfaces (Konstantinov and Knyshov 2015; Namyatova et al. 2016; Konstantinov et al. 2018; Schuh and

Weirauch 2020); the bothrium of femoral trichobothria being deeply recessed and tuberculate (Konstantinov and Knyshov 2015; Namyatova et al. 2016; Schuh and Weirauch 2020); the asymmetrical setiform parempodia (Konstantinov and Knyshov 2015; Konstantinov et al. 2018; Schuh and Weirauch 2020); and the female genitalia possessing an asymmetric, complexly sclerotized vestibulum (Namyatova et al. 2016).

The Eccritotarsini have a great morphological heterogeneity, including their general appearance, size, coloration, and genitalia (Konstantinov and Knyshov 2015; Namyatova et al. 2016; Konstantinov et al. 2018). Males exhibit several projections around the aperture of the genital capsule (Mu and Liu 2012; Henry and Howard 2016; Konstantinov and Zinovjeva 2016; Konstantinov et al. 2018; Menard and Schwartz 2018; Henry and Menard 2020), and internally (Menard and Schwartz 2018). The parameres are diverse, with the right paramere usually being larger and more complex than the left one (Konstantinov 2003; Namyatova et al. 2016;

Konstantinov et al. 2018; Menard and Schwartz 2018; Henry and Menard 2020; Henry 2022). The aedeagus can be simple, membranous, or complex with sclerotizations in different areas (Kerzhner and Konstantinov 1999; Konstantinov 2003; Henry and Howard 2016; Konstantinov et al. 2018). The ductus seminis is entirely membranous or with its apical part typically sclerotized and may be needle-shaped, extends to mouth of the phalotheca in repose, and can be attached to the endosoma (Kerzhner and Konstantinov 1999; Konstantinov 2003; Konstantinov et al. 2018; Menard and Schwartz 2018; Henry and Menard 2020; Henry 2022). According to Namyatova et al. (2016) *Eccritotarsini* is the sister group of *Bryocorini*, but the phylogenetic relationships among its genera are poorly resolved.

In the present contribution two new genera, the first one with one new species from Panama and the other one with three new species from Ecuador and Bolivia, are described and illustrated, and their affinities are discussed. Colour images of the adult male and female and of the male genitalia, except for one of the species that is known only from females, are provided, together with a key to facilitate identification of the species.

## Materials and methods

Specimens are deposited in the Museo de La Plata, La Plata, Argentina (MLP) and the National Museum of Natural History, Smithsonian Institution, Washington, DC, USA (USNM).

Label data are cited verbatim. Lines on labels are separated with '/', contents of different labels are separated with '//', remarks are given between square brackets '['].

All measurements are given in millimetres; measurements of the holotype between brackets; identical measurements of the same structure of different specimens are provided only once. Anterior width of pronotum is defined as the width across behind margin of collar, and posterior width of pronotum as the width across humeral angles. Genital structures were dissected under stereomicroscope, cleared in 85% lactic acid solution for 45 min, washed in distilled water and preserved in vials with glycerinol. Terminology for male genitalia follows Kerzhner and Konstantinov (1999), Konstantinov (2003) and Menard and Schwartz (2018), except for the endosoma which follows Cassis (2008).

Images were captured using a cellphone Galaxy A52s 5G attached to an Olympus stereomicroscope SZX7 for dorsal habitus, and with a Canon EOS Rebel T7i with a Professional Grade Raynox DCR 150 DSLR Objective Tube Lens and an Objective PLAN Achromatic LWD infinity 5X for external morphology and 10X for dissected genitalia, mounted on a WeMacro's automatic focus stacking rail. Multiple focal planes were taken with Helicon Remote software and merged using Helicon Focus software. Maps were built using QGIS 3.2, localities were georeferenced with Google Earth Pro.

## Results

### Taxonomy

#### *Thomasomiris* gen. nov.

<https://zoobank.org/9FF34EA5-DAB6-426D-87B7-D9BD97CA0EC5>

#### **Type species.** *Thomasomiris setosus* sp. nov.

**Diagnosis.** Head, collar, posterior pronotal lobe, scutellum, and hemelytra with short, erect setae; eyes small, stylate, directed anteriorly (Fig. 1A), less than half head height (Figs 2A, 3A); vertex with a medial longitudinal depression; antennal segment I about half the length of vertex width and almost 4 times as short as antennal segment II; anterior pronotal lobe depressed in lateral view; cuneal fracture extending to middle of corium; cuneus wider than long (Fig. 1A); veins angled at the middle of membrane, slightly surpassing apex of cuneus; and tibiae wide, with abundant semierect setae.

**Description.** *Macropterosus female.* Body length to apex of membrane 5.6–5.7; body length to apex of cuneus 4.6–4.7.

**Surface** shiny, pilose; posterior pronotal lobe evenly punctate. Head with short and erect setae (Fig. 3A); antennal segment I with recumbent setae on distal half (Fig. 3A), antennal segments II–IV with short, recumbent and longer, semierect setae. Collar, posterior pronotal lobe, scutellum and hemelytra with short, erect setae.

**Structure.** Head width more than twice its length. Clypeus flat in lateral view (Fig. 3A), not visible from above. Frons flat in lateral view. Eyes small, less than half head height (Figs 2A, 3A), stylate, directed upwards and anteriorly, interior and posterior margins straight, interior margin at same level with lateral collar margins (Fig. 1A). Maxillary plates rectangular, large, long. Labium extending to base of abdomen. Antennal segment I shortest, about half the length of vertex width, narrower basally; segment II almost 4 times as long as antennal segment I; segment III thinner than II (Fig. 1A); segment IV shorter and thinner than III. Thorax: pronotum trapeziform, slightly directed downwards. Anterior pronotal lobe clearly distinguished from posterior pronotal lobe, depressed in lateral view (Fig. 3A); collar wider than antennal segment I; calli evident, medium-sized, depressed and separated from each other by a median depression. Posterior pronotal lobe flat, with shallow lateral depressions before humeral angles, posterior margin convex (Fig. 1A). Hemelytron flat in lateral view; lateral margin convex (Fig. 1A); embolium flat, thin and slightly expanded in posterior margin; medial fracture visible, adjacent to R+M vein; cuneus wider than long (Fig. 1A); veins angled at middle of membrane and directed posteriorly behind posterior margin of cuneus. Legs: femora flat; metafemora slightly curved; tibiae robust; protibiae flat on distal interior face.

**Male.** Unknown.

**Geographic distribution.** Panama (Fig. 11).

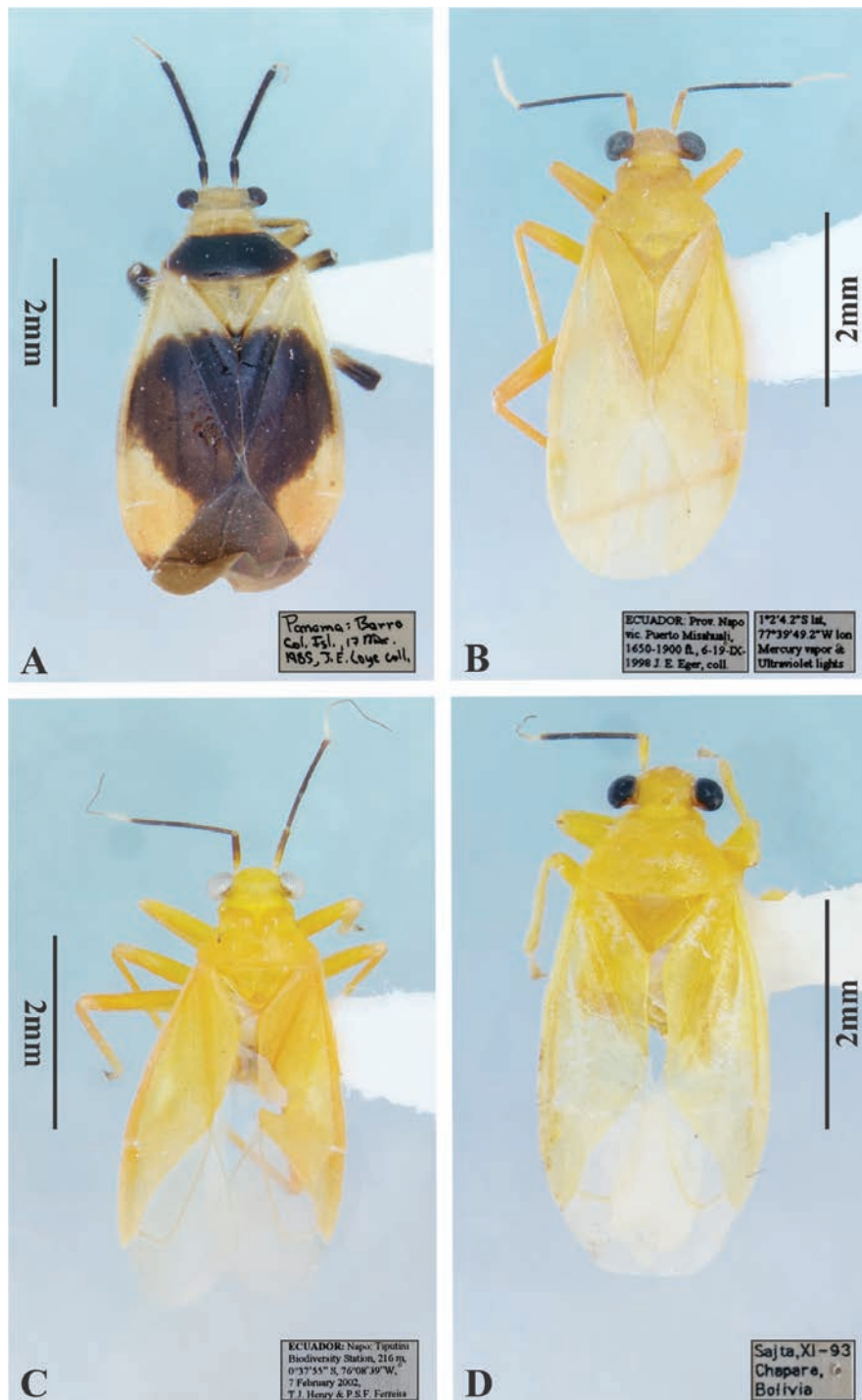


**Figure 1.** *Thomasomiris* gen. nov. and *Egerocoris* gen. nov. new species, dorsal habitus and labels. **A.** *T. setosus* sp. nov., female holotype; **B.** *E. dimorphus* sp. nov., male holotype; **C.** *E. ecuatorianus* sp. nov., male holotype; **D.** *E. chaparensis* sp. nov., male holotype.

**Etymology.** The name of the new genus is formed from the given name of our friend and colleague Dr Thomas J. Henry, who has published numerous important papers on Heteroptera, including many on Miridae, combined with *miris* in reference to its assignment to the family Miridae. Gender masculine.

**Discussion.** The first couplet of the key to the Neotropical ecritotarsine genera (Carvalho and Ferreira 1995) refers to the development of male hemelytra; we assumed

that males of *Thomasomiris* have normal hemelytra, with clavus and corium distinguished and membrane present, so we followed to couplet 3. The two monotypic genera identified in the couplet 2, *Aztecariella* Carvalho, 1951 and *Coleopteromiris* Carvalho, 1946 show different characters from *Thomasomiris*, as a pronotum coarsely punctate and females without division of clavus, corium and cuneus, and without membrane in *Aztecariella*, and sessile eyes and females with coleopteroid hemelytra in *Coleop-*

*teromiris*. Following the key, *Thomasomiris* runs to the couplet 8 where the genera *Hesperolabops* Kirkaldy, 1902 and *Aztecarina* Carvalho, 1974 are identified and are discriminated by male genitalia characters, but unlike *Thomasomiris*, *Hesperolabops* shows strongly pedunculated eyes, a lobate collar, a longer antennal segment I, and a cuneus longer than width, and *Aztecarina* shows a strongly punctate pronotum with its posterior margin sinuated and antennal segments I and II of similar length. Four Neotropical genera were omitted in the Carvalho and Ferreira' key, *Perissobasis* Reuter, 1892, *Eurycipitia* Reuter, 1905, *Bugabacoris* Carvalho & China, 1959 and *Pycnoderiella* Henry, 1993, and five genera were described after 1995, *Cubanomiris* Hernández & Stonedahl, 1996 and *Agaveocoris*, *Laterospinocoris*, *Nigrotomocoris* and *Schaffnerocoris*, described by Henry and Menard 2020 including some species with neotropical distribution. The medium size, the stylate eyes, the labium extending at least to the metacoxae, and the convex lateral margins of hemelytra are similar to those found in species of *Neoneella* Costa Lima, 1942. However, the short, erect setae, the upward and anteriorly directed eyes located far from the collar, the antennal segment II almost 4 times as long as antennal segment I, the flattened anterior pronotal lobe clearly separated from the evenly punctate posterior pronotal lobe with the posterior margin convex, the short, wide cuneus, and the concave posterior margin of cell on membrane forming an acute angle at the middle, distinguish this new genus from *Neoneella* and from all other ecritotarsines.

***Thomasomiris setosus* sp. nov.**

<https://zoobank.org/8F6E7B92-1FB9-4259-8AC5-B99C4B492E56>

Figs 1A, 2A, 3A

**Diagnosis.** Pale yellow with extensive dark areas (Fig. 1A); clypeus longer than half of head height; vertex more than two and a half times as wide as eye width; antenna shorter than length from apex of clypeus to apex of abdomen; scutellum with basal depression extended longitudinally; embolium bent upwards from its anterior end to more than half its length; cuneal fracture long; and cell in membrane with the interior margin anteriorly concave.

**Description. Macropterous female.** Coloration. Head pale yellow (Fig. 1A). Clypeus apex black (Figs 2A, 3A). Labium pale yellow, segments III–IV darker. Eyes black. Antennal segment I dark brown, base pale yellow; segment II dark brown, with faint basal ring yellow; segments III–IV brown. Thorax: collar and calli pale yellow. Posterior pronotal lobe dark brown, lateral margins pale yellow. Scutellum pale yellow, apex dark brown. Pleural area pale yellow, excepting metaepisternum dark brown dorsally. Hemelytron: embolium pale yellow; clavus basal half pale yellow and posterior half dark brown; corium anterior and posterior areas pale yellow, and medially dark brown; external apex of corium and cuneus orange, cuneus apex dark brown; membrane dark brown with dark brown veins. Legs: coxae, trochanters, femora

except apex and basal three quarters of inner face of protibiae pale yellow; apex of femora, rest of protibiae, meso- and metatibiae dark brown; tarsi dark brown with segments I–II paler. Abdomen dark brown.

**Surface.** Head with short, erect setae, more abundant on posterior margin and area adjacent to eyes in dorsal view (Fig. 1A). Labium with semierect setae. Antennal segments II–IV with abundant recumbent setae and some longer semierect setae. Collar, posterior pronotal lobe, scutellum, and hemelytra with abundant, short, erect, yellowish setae, except those on dark brown areas of hemelytra darker. Calli glabrous (Fig. 3A). Veins with very short erect setae. Pleura and abdomen with longer and more dispersed erect setae than dorsum. Coxae, trochanters, femora and tarsi with semierect setae. Tibiae with abundant dark recumbent and semierect setae, thicker than the ones in the femora.

**Structure.** Head: vertex almost twice length of antennal segment I; upper margin at eye level (Fig. 2A), with median longitudinal depression. Labrum not extending half way on labial segment I (Fig. 3A). Gular area not visible. Antennal segment II thinner and between 3–4 times as long as antennal segment I. Antennal segment III almost twice the length of antennal segment I. Thorax: anterior collar margin concave and posterior margin convex, posterior sulcus shallow medially (Fig. 1A). Posterior pronotal margin width more than twice its length; anterior pronotal width less than half posterior pronotal margin width. Calli not attaining lateral pronotal margins. Scutellum with triangular basal depression extended longitudinally. Hemelytron: embolium bent upwards from its anterior end to more than a half its length. Medial fracture shorter than one quarter of corium length. Claval commissure longer than scutellum and half of pronotum length together. Cuneal fracture evident, straight, attaining half of corium width. Interior margin of cuneus concave. Membrane with interior margin concave anteriorly, and posterior margin straight with middle weakly concave (Fig. 1A).

**Measurements** (n: 2): Body length to apex of membrane (5.60), 5.70; body length to apex of cuneus 4.60, (4.70). Head: width 1.28; interocular distance 0.73, (0.74), and (1.38), 1.42 times head height. Labium: segment I length 0.80, (0.86); II, 0.91, (0.96); III, (0.32), 0.34; IV, 0.27, (0.29). Antenna: segment I length (0.40), 0.41; II, 1.55; III, (0.75), 0.80; IV, (0.62), 0.66. Pronotum: length (0.92), 0.95; anterior width 0.95; posterior width 1.92, (1.97). Scutellum: length 0.72, (0.74); width 0.85. Cuneus: length 1.00; anterior width 1.04. Membrane cell (2.06), 2.16 times longer than wide.

**Geographic distribution.** Panama (Fig. 11).

**Type material. Holotype** ♀: Panama: Barro / Col[orado] Isl., 17 Mar. / 1985, J. E. Loye coll. [9°9'N, 79°51'W] (USNM). **Paratype** ♀: Panama: Barro / Col[orado] Isl., 17 Mar. / 1985, J. E. Loye coll. // *Neoneella* / sp. / det. T. J. Henry 1987 (MLP).

**Etymology.** The specific epithet is the Latin adjective *setosus*, -a, -um, meaning 'bristly', in allusion to the abundant short, erect setae of the dorsal surface.

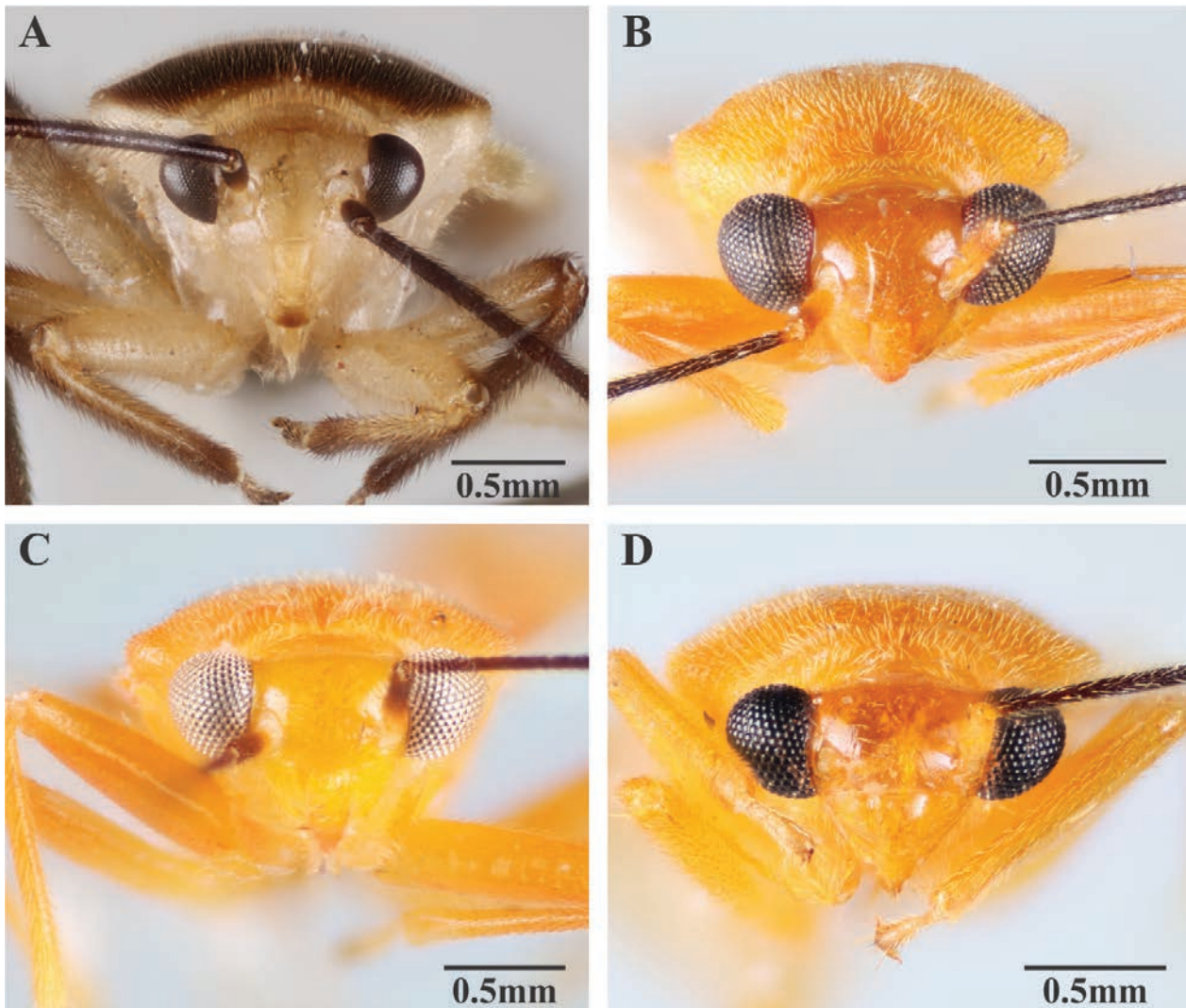


**Figure 2.** *Thomasomiris* gen. nov. and *Egerocoris* gen. nov. new species, head frontal view. **A.** *T. setosus* sp. nov., female holotype; **B.** *E. dimorphus* sp. nov., male holotype; **C.** *E. ecuatorianus* sp. nov., male holotype; **D.** *E. chaparensis* sp. nov., male holotype.

***Egerocoris* gen. nov.**

<https://zoobank.org/10DAE851-82DB-4BD4-9E51-2DEEFD77F055>

**Type species.** *Egerocoris ecuatorianus* sp. nov.

**Included species.** *Egerocoris chaparensis* sp. nov., *E. dimorphus* sp. nov., *E. ecuatorianus* sp. nov.

**Diagnosis.** Eyes large, stylate (Fig. 1B–D), partly covering collar in lateral view (Fig. 3B–D); labrum short, less than half labial segment I length; antennal segment I slightly narrowing on distal half and wider than antennal segment II; collar wider than antennal segment I; embolium flat, bent upwards from its anterior end to less than a half its length; dorsal wall of genital capsule sclerotized, left wall shorter than right wall (Fig. 6); left paramere body triangular, with apical process initially curved and V-shaped in frontal view (Fig. 8); and, ductus seminis basally expanded (Fig. 10A, B).

**Description. Macropterous male.** Body length to apex of membrane 4.42–4.66; body length to apex of cuneus 3.95–4.66; body width 1.94–2.43.

**Surface** shiny; posterior pronotal lobe evenly punctate. Head, collar, pronotum and hemelytra with abundant short, recumbent setae.

**Structure.** Head width more than twice length. Clypeus rounded in lateral view, not visible from above. Frons rounded in lateral view (Fig. 3B–D). Vertex flat (Fig. 2B–D), wider than head length. Eyes large, more than half head height, stylate, interior margin straight and at lateral collar margins level (Fig. 1B–D). Gular area not visible. Labium extending at least to metacoxae; segment I concave ventrally. Antennal segment I slightly narrowing on distal half. Antennal segment II straight, slender. Antennal segment III narrowing towards the apex, more slender than segment II. Antennal segment IV straight. Thorax: collar wider than antennal segment I; anterior margin concave and posterior margin straight. Pronotum slightly directed downwards. Calli evident, small to large, separated by a median depression, sometimes attaining to pronotal lateral margins. Posterior pronotal lobe with shallow lateral depressions before humeral angles; posterior margin straight (Fig. 1B–D). Mesoscutum exposed (Fig. 1B). Scutellum with anterior

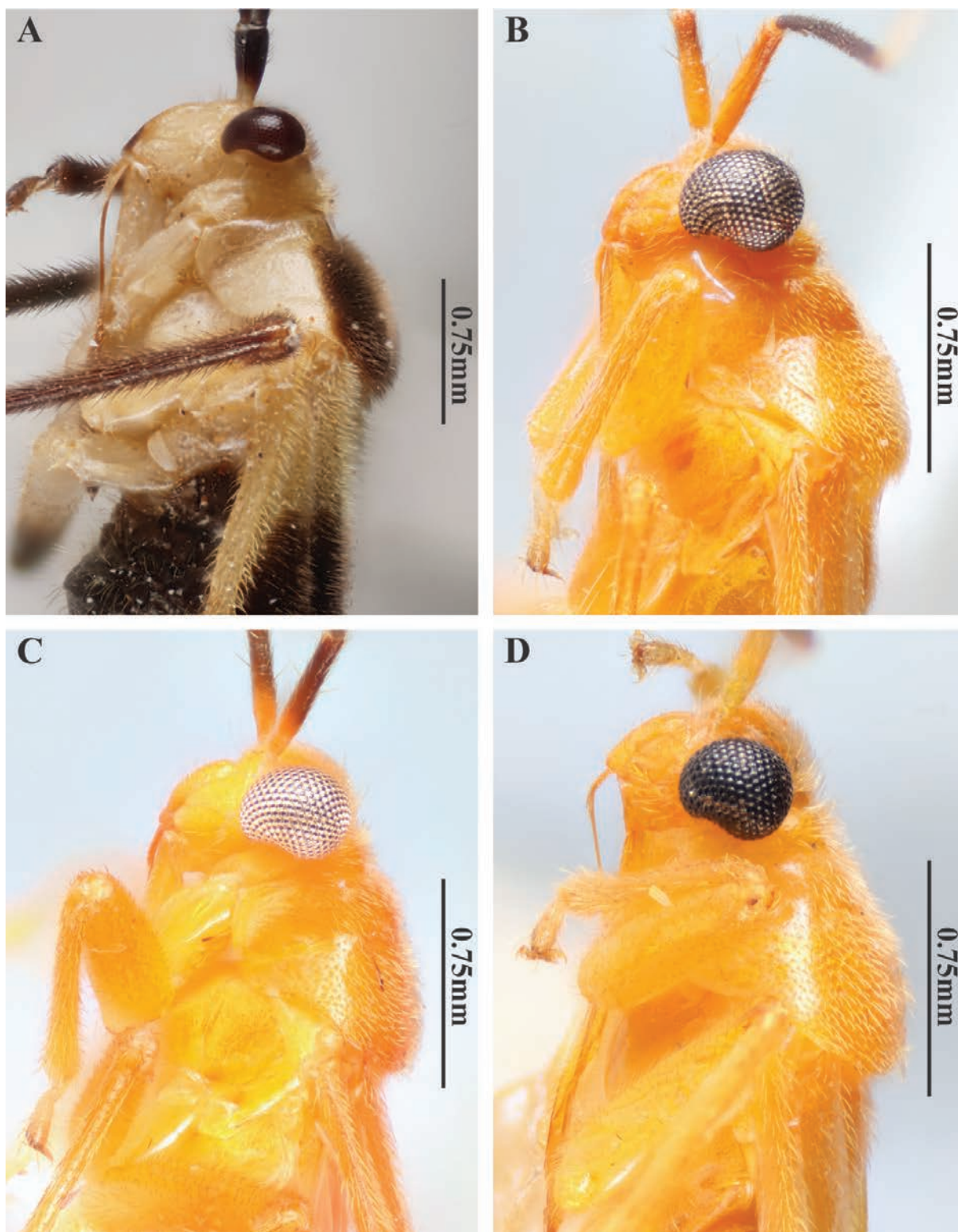


**Figure 3.** *Thomasomiris* gen. nov. and *Egerocoris* gen. nov. new species, head and pronotum lateral view. **A.** *T. setosus* sp. nov., female holotype; **B.** *E. dimorphus* sp. nov., male holotype; **C.** *E. ecuatorianus* sp. nov., male holotype; **D.** *E. chaparensis* sp. nov., male holotype.

depression. Hemelytron flat in lateral view; lateral margin convex (Fig. 1B–D). Embolium flat, straight to slightly expanded on posterior margin, bent upwards. Medial fracture visible, shorter than half the corium length. Cuneus longer than wide (in one species the length sexually dimorphic as in Fig. 4). Veins angled in middle of membrane before

posterior margin of cuneus; cell with interior and posterior margins straight (Fig. 4). Legs: profemora broader at base. Metafemora slightly curved. Protibiae wider than meso- and metatibiae. Male genitalia: genital capsule length variable relative to abdomen length, longer than wide. Right wall more developed than left wall. Dorsal wall in lateral view

straight, well developed laterally, with sclerotized processes (Fig. 5B, D, F); posterior margin concave. Ventral wall in lateral view oblique, more developed than the dorsal wall (Fig. 6); posterior margin sinuate. Subgenital plate with two processes, one on the left side and one on the right side (Fig. 7); each one embedded with corresponding paramere. Genital opening broad, dorsally directed. Left paramere (Fig. 8) smaller or larger than right paramere; body broad, triangular; apical process well developed, basally curved; expanded or not at apex. Right paramere (Fig. 9) simpler than left paramere; uniformly wide; slightly to strongly curved. Aedeagus (Fig. 10) small and simple; phallosome membranous on basal half, sclerotized on distal half. Ductus seminis basally expanded, membranous and not folded; sclerotized behind last curvature; apex extending to middle of phallosome; endosoma membranous to sclerotized.

**Macropterous female.** Body length to apex of membrane 4.28–4.94; body length to apex of cuneus 3.7–4.51; body width 1.97–2.09. Lateral margins of hemelytra either convex or (in species with sexual dimorphism) parallel with less well developed cuneus.

**Geographic distribution.** Bolivia, Ecuador (Fig. 11).

**Etymology.** The name of the genus is formed from the family name of Joe Eger, who has extensively collected Heteroptera, including one of the specimens studied herein, and published several papers on the group, combined with the latinized Greek noun *coris*, meaning “true bug”. Gender masculine.

**Discussion.** *Egerocoris* resembles *Neella* in general appearance, but in *Neella* the eyes are stylated but not covering the lateral margins of collar, the postocular region of head present a patch of setae, the antennal segment I is straight and as wide as II, the subgenital plate lacks processes and the parameres are simpler.

*Egerocoris* runs to the couplet 8 in the key to the Neotropical ecritotarsine genera (Carvalho and Ferreira 1995) where the genera *Hesperolabops* Kirkaldy, 1902 and *Aztecacarina* Carvalho, 1974 are identified. These gen-

era are quite different from *Egerocoris*, since *Hesperolabops* shows strongly pedunculated eyes, a lobate collar, and a curved spiniform projection in the genital capsule, and *Aztecacarina* shows a strongly punctate pronotum with its posterior margin sinuated and antennal segments I and II of similar length. The character states of the large, stylate eyes that partly cover the collar in lateral view, the short labrum, the long labium extending at least to metacoxae, the slightly narrowing antennal segment I on the distal half and wider than antennal segment II, the collar being wider than antennal segment I, the posterior pronotal lobe evenly punctate with its posterior margin straight, and the embolium being flat, bent upwards from its anterior end to less than a half its length, combined with characters of the male genitalia, including the presence of sclerotizations in the dorsal wall of the genital capsule, the processes on the subgenital plate embedding the parameres, and the triangular left paramere with a well-developed apical process, allow the recognition of this genus from the four genera omitted in Carvalho and Ferreira’s key and the five genera described afterwards detailed in the *Thomasomiris* discussion above.

*Egerocoris dimorphus* sp. nov. shows sexual dimorphism in the shape and length of cuneus similar to *Proneella* Carvalho, 1960, but the hemelytra are slightly more convex, and the cuneus is wider relative to its length. This species runs to the couplet 13 in the Carvalho and Ferreira’s key (1995) where *Proneella* and *Neoneella* Costa Lima, 1942 are identified. According to Carvalho (1960), the sexual dimorphism relates *Proneella* with *Neoneella*, and in both genera the included species also share several characters from internal and external morphology. Among the three species of *Egerocoris* two of them lack sexual dimorphism, but share several characters from the male genitalia and from the external morphology allowing us to infer a close relationship and justifying the inclusion of these species in the same genus, besides the absence of sexual dimorphism in *E. ecuatorianus* sp. nov. and *E. chaparensis* sp. nov.

## Key to species of *Egerocoris*

- 1 Antennal segment I unicolorous (Fig. 3D). Clypeus length less than or equal to half head height. Labial segment I deeply concave ventrally. Internal margins of cell separated with hemelytra in repose (Fig. 1D). Right paramere larger than left, C-shaped in dorsal view (Fig. 9F). Right process of subgenital plate ending in numerous asymmetric teeth (Fig. 7E, F) ..... *E. chaparensis* sp. nov.
- Antennal segment I bicolored, darker distally (Fig. 3B, C). Clypeus length greater than half head height. Labial segment I slightly concave ventrally. Internal margins of cell overlapping in anterior half with hemelytra in repose (Fig. 1B). Right paramere smaller than left, “V”-shaped in dorsal view (Fig. 9B, D). Right process of subgenital plate ending in simple pointed apex (Fig. 7A–D) ..... 2
- 2 Antennal segment III yellow (Fig. 1B). Labial segment I shorter than vertex width. Embolium longer than abdomen. Claval commissure shorter than twice scutellum length. Internal margin and length of cuneus sexually dimorphic (males with concave internal margin and cuneus extending to posterior margin of membrane, without contacting each other with hemelytra in repose; females with cuneus short, not extending to posterior margin of membrane) (Fig. 4). Female subgenital plate equal to or shorter than anterior margin width ..... *E. dimorphus* sp. nov.
- Antennal segment III basally yellow and distally darker (Fig. 1C). Labial segment I longer than vertex width. Embolium shorter than abdomen. Claval commissure longer than twice scutellum length. Internal margin and length of cuneus not sexually dimorphic, not extending to posterior margin of membrane on both sexes. Female subgenital plate longer than anterior margin width ..... *E. ecuatorianus* sp. nov.

***Egerocoris dimorphus* sp. nov.**

<https://zoobank.org/B4381DE7-5D26-4F18-A037-F2B845E097F5>

Figs 1B, 2B, 3B, 4, 5A, B, 6A, B, 7A, B, 8A, B, 9A, B, 10A

**Diagnosis.** Antennal segment I bicolored, darker distally (Figs 1B, 3B), segment III whitish; femora yellow and irregularly tinged with orange; level of vertex not attaining dorsal margin of eyes; labium extending to metacoxae and segment I slightly concave ventrally; calli large, not attaining pronotal lateral margins; embolium longer than abdomen; internal margin of cell straight; sexual dimorphism on internal margin and length of cuneus (Fig. 4A, B), which is concave in males and reaches posterior margin of membrane without contacting each other with hemelytra in repose; cell 3 times as long as wide; genital capsule with a dorsal sclerotized tooth in right side (Figs 5B, 6A); left process of subgenital plate smaller than the right, sclerotized and asymmetrically forked (Fig. 7A, B); left paramere larger than right paramere.

**Description. Macropterous male.** Coloration. Head yellow; labium yellow; eyes black. Antennal segment I yellow, darker distally; II dark brown; III pale yellow; IV pale yellow. Thorax: collar, pronotum, scutellum and pleural area yellow. Hemelytron yellow, irregularly tinged with orange; membrane yellowish; veins yellow. Legs yellow, femora and tibiae tinged with orange, tarsi darker distally, claws brown. Abdomen yellow.

**Surface.** Antennal segment I with recumbent setae and a few erect setae (Fig. 3B); segment II with semierect setae. Pleura and abdomen with longer, more dispersed setae than dorsum. Coxae, trochanters, femora and tarsi with semierect setae; tibiae with abundant, short, recumbent setae.

**Structure.** Head: level of vertex not attaining dorsal margin of eyes (Fig. 2B). Maxillary plates large. Labium extending to metacoxae and slightly concave ventrally. Antennal segment II more than 2.5 times as long as antennal segment I. Thorax: posterior pronotal margin 2 times

as wide as pronotum length. Calli large not attaining lateral pronotal margins. Pronotal width across calli half as wide as posterior margin width. Hemelytron: embolium straight, bent upwards from its anterior end to less than a half its length. Claval commissure longer than scutellum length and half of pronotal length together. Cuneus extending to posterior membrane margin, apex not contacting each other with hemelytra in repose (Fig. 4), internal margin concave. Male genitalia: Genital capsule more than one third abdomen length. Dorsal wall on right apex with one sclerotized tooth, tapering towards apex; left apex blunt and sclerotized. Left process of subgenital plate directed dorsally as a sclerotized wall, dorsally expanded, and divided into two short branches, the internal blunt and the external pointed and extended outside the genital capsule (Figs 5A, B, 6A, 7A, B). Right process of subgenital plate longer than left process, tapering towards apex, curved (Fig. 7A, B), with a basal, internal expansion. Left paramere (Fig. 8A, B) larger than the right paramere, with a sclerotized and pointed dorsal projection; apical process with tiny teeth on dorsal margin, dorsally expanded at apex. Right paramere (Fig. 9A, B) with body wider than basal and apical processes, curved; apical process blunt, with a sclerotized, pointed tooth. Aedeagus (Fig. 10A) phallosome tapering towards apex; endosoma membranous.

**Measurements** (n: 2): Body length to apex of membrane 4.42, (4.66); body length to apex of cuneus 4.42, (4.66); body width 2.23, (2.43). Head: width 1.19, (1.31); interocular distance 0.53, (0.56), 1.20 (1.27) times as wide as head length. Labium: segment I length 0.43, (0.52); II, 0.52, (0.60); III, 0.20; IV, 0.20. Antenna: segment I length 0.48, (0.56); II, 1.36, (1.49); III, 0.78, (0.85); IV, 0.84, (absent). Pronotum: length 0.74, (0.82); anterior width (0.86), 0.88; posterior width 1.49, (1.58). Scutellum: length 0.53, (0.60); width 0.77. Cuneus: length 1.58, (1.70); anterior width 0.90, (0.95). Cell 3.00 times as long as wide.

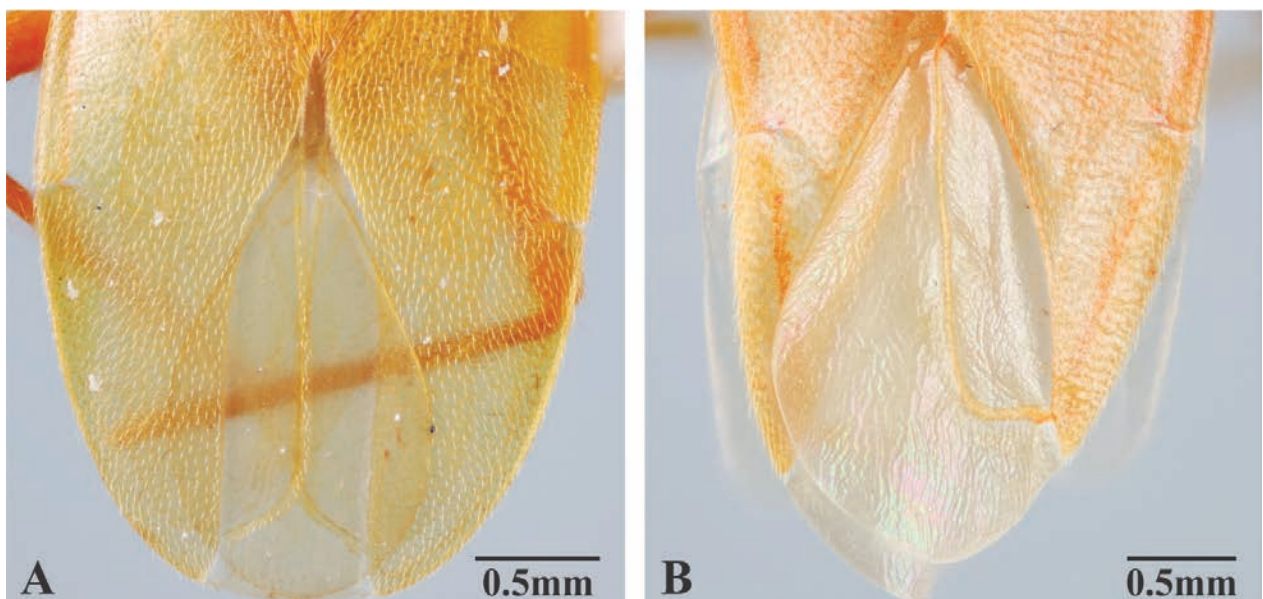


**Figure 4.** *Egerocoris dimorphus* sp. nov., dorsal view of cuneus. **A.** Male holotype; **B.** Female paratype.

**Macropterous female.** Similar to male in size, coloration, surface, and structure. Lateral margins of hemelytra parallel; cuneus less developed, without extending to posterior membrane margin, 1.5 times as long as anterior margin width, and internal margin concave with apex truncate; posterior veins margin straight. Body length to apex of membrane 4.94; body length to apex of cuneus 4.51; body width 2.02. Head: width 1.23; interocular distance 0.58. Labium: segment I length 0.46; II, 0.62; III, 0.19; IV, 0.2. Antenna: segment I length 0.52; II, 1.36; III, 0.74; IV, 0.79. Pronotum: length 0.82; anterior width 0.89; posterior width 1.66. Scutellum: length not measured; width 0.76. Cuneus: length 1.28; anterior width 0.84.

**Geographic distribution.** Ecuador (Fig. 11).

**Etymology.** The specific epithet is from the Greek *di* (two), and *morphe* (form), referring to the sexual dimorphism in cuneal development.

**Type material.** *Holotype* ♂: Ecuador: Prov. Napo [Orellana] / vic. Puerto Misahuali, / 1650–1900 ft, 6–19–IX– / 1998, J. E. Eger, coll. // 1°2'4.2"S, 77°39'49.2"W / Mercury vapor & / Ultraviolet lights (USNM). *Paratypes*: ♂, Ecuador: NAPO [Orellana] Res. Ethnica / Waorani, 1 km S. Onkone Gare / Camp, Trans. Ent. 21 June 1994 / 220m 00°39'10"S, 076°26'00"W / T. L. Erwin, et al. // Insecticidal fogging of mostly bare / green leaves, some with covering / of lichenous or bryophytic plants in / terre firme forest At 8 x-trans, / 94 m mark Project MAXUS Lot 708 (MLP); ♀, Ecuador: Napo [Orellana], Tiputini / Biodiversity Station, 216 m, / 00°37'55"S, 76°08'39"W, /

9 February 1999 / T.L Erwin et al., collectors // Insecticidal fogging of mostly / bare green leaves, some with / covering of lichenous or / bryophytic plants; / Lot #2002, Transect #T–1 (USNM).

**Remarks.** This species is sexually dimorphic in the shape and length of cuneus (Fig. 4), and in this respect it is similar to species of *Proneella*, which have the lateral margins of the hemelytra slightly convex and the cuneus narrower relative to its length. Also, in species of *Proneella* the eyes are sessile, the level of vertex attains the dorsal margin of the eyes, the antennal segment I is straight, the antennal segment II is widest in the central or distal area, the calli are small, and the posterior margin of the cell is straight.

***Egerocoris ecuatorianus* sp. nov.**

<https://zoobank.org/EB3EE0D7-40C1-4FF0-BAB9-ECE165ED5521>

Figs 1C, 2C, 3C, 5C, D, 6C, D, 7C, D, 8C, D, 9C, D, 10B

**Diagnosis.** Antennal segment I bicolored, lighter basally (Figs 2C, 3C), and segment III with basal half pale yellow, distal half darker; femora yellow and irregularly tinged with orange; level of vertex not attaining the dorsal margin of eyes (Fig. 2C); labium extending to abdominal segment III and segment I slightly concave ventrally; calli large, attaining lateral pronotal margins; embolium shorter than abdomen; internal margin of cell straight; internal margin and length of cuneus not sexually dimorphic

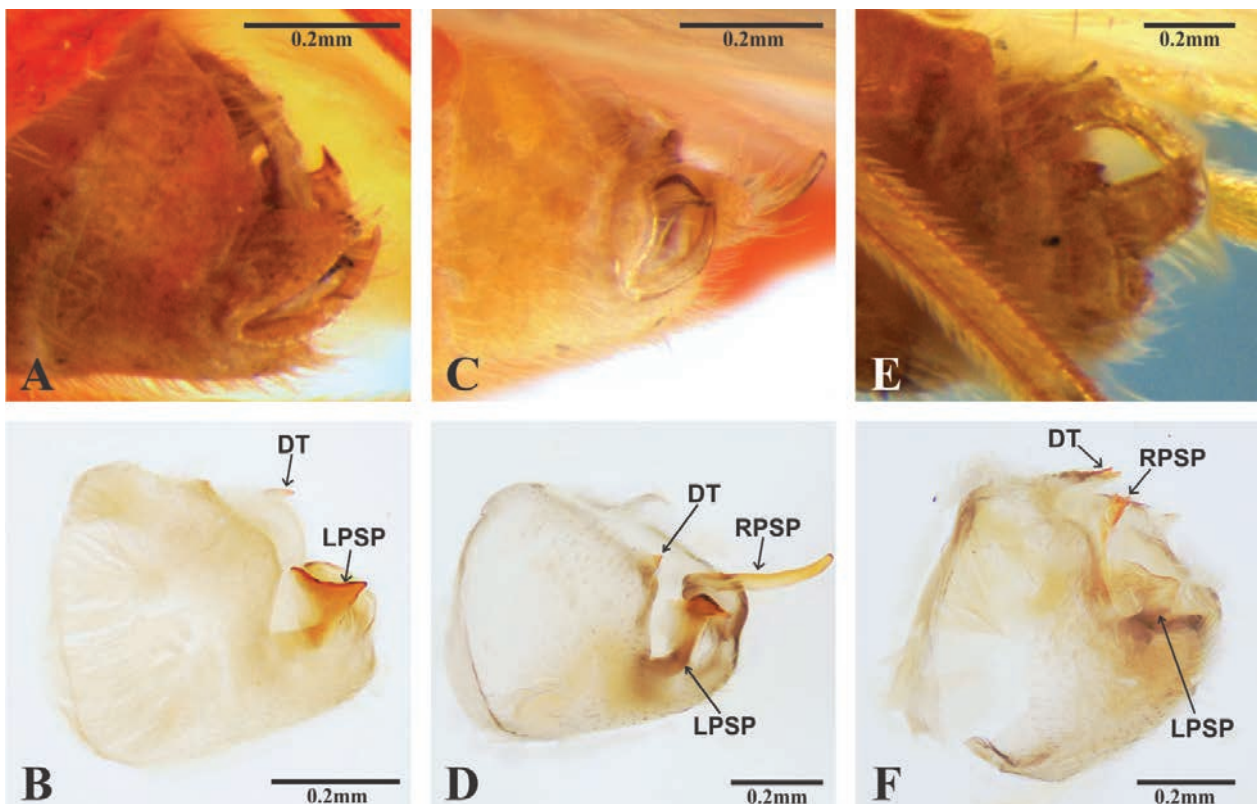


**Figure 5.** *Egerocoris* gen. nov. new species, left lateral view of genital capsule. **A, B, E.** *E. dimorphus* sp. nov.; **C, D, E.** *E. ecuatorianus* sp. nov.; **E, F.** *E. chaparensis* sp. nov.; **A, C, E.** Genital capsule not dissected; **B, D, F.** Genital capsule dissected; **DT**–dorsal tooth; **LPSP**–left process of subgenital plate; **RPSP**–right process of subgenital plate.

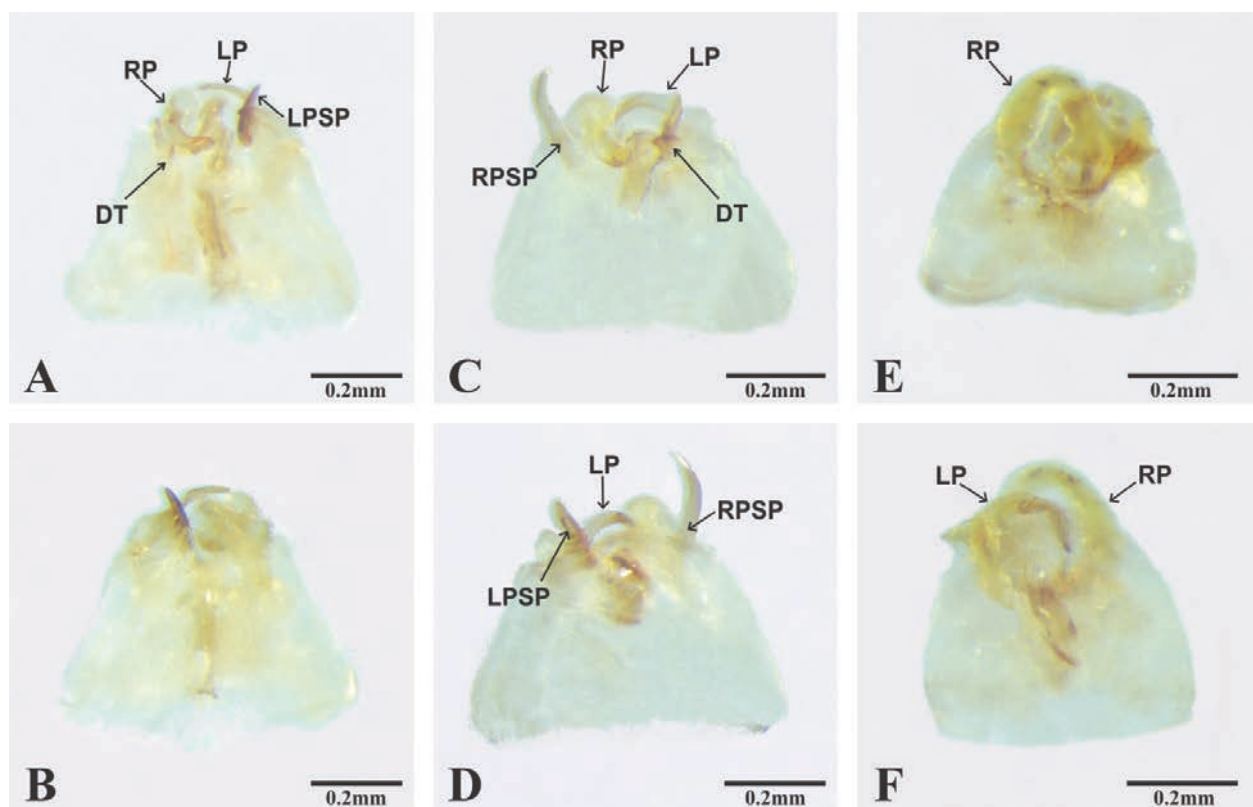


**Figure 6.** *Egerocoris* gen. nov. new species, dorsal and ventral views of genital capsule. **A, B.** *E. dimorphus* sp. nov.; **C, D.** *E. ecuatorianus* sp. nov.; **E, F.** *E. chaparensis* sp. nov.; **A, C, E.** Genital capsule dorsal view; **B, D, F.** Genital capsule ventral view; **DT**—dorsal tooth; **RP**—right paramere; **LP**—left paramere; **LPSP**—left process of subgenital plate; **RPSP**—right process of subgenital plate.

(Fig. 1C); genital capsule with a sclerotized broad tooth on left apex of posterior margin (Figs 5D, 6C); left process of the subgenital plate sclerotized, pointed, curved (Fig. 7C); left paramere same size as right paramere; and female subgenital plate longer than anterior margin width.

**Description. Macropterous male.** Coloration. Head yellow. Clypeus apex reddish. Labrum reddish. Labium yellow, segments II–IV pale yellow. Eyes silver. Antennal segment I brown, base yellow; II, brown; III, basal half pale yellow, distal half darker; IV, brown. Thorax: collar yellow. Pronotum orange. Mesoscutum yellow. Scutellum yellow, apex orange. Pleural area yellow. Hemelytron orange. Membrane and veins yellow. Legs: coxae and trochanters pale yellow. Femora and tibiae yellow and irregularly tinged with oranges. Tarsi pale yellow. Claws brown. Abdomen yellow.

**Surface.** Antennal segment I with recumbent setae and a few erect setae (Fig. 3C). Antennal segments II–III with semierect setae and some erect setae. Antennal segment IV with semierect setae. Pleural area and abdomen with longer and more dispersed setae than dorsum. Coxae, trochanters, femora, and tarsi with semierect setae. Tibiae with abundant recumbent setae.

**Structure.** Head: level of vertex not attaining dorsal margin of eyes (Fig. 2C). Maxillary plates medium-sized, wide. Labium extending to abdominal segment III, segment I extending to procoxae and slightly concave ventrally. Antennal segment II more than 2 times as long as

antennal segment I. Thorax: posterior pronotal margin 2 times as wide as pronotum length. Calli attaining lateral pronotal margins. Pronotal width across calli more than half of posterior margin width. Hemelytron: embolium slightly wider at posterior margin, bent upwards from its anterior end to less than a half its length. Internal margin of cuneus concave (Fig. 1C). Male genitalia: genital capsule less than one quarter abdomen length, almost 2 times as wide as long. Right wall straight. Left wall convex on anterior half and concave on posterior half. Dorsal wall at left apex with evident concavity, adjacent margin sclerotized and bent upwards as a broad tooth (Figs 5C, D, 6C). Left process of subgenital plate smaller than right process, flat and broad internally, curved at pointed apex (Fig. 7D). Right process of subgenital plate longer than left process, broad basally and tapered towards apex, curved, with a left basal expansion (Fig. 7C, D). Left paramere (Fig. 8C, D) almost the same size as right paramere, with a sclerotized and pointed dorsal projection; ventral margin concave; apical process tapering towards the sclerotized apex. Right paramere (Fig. 9C, D) with body wider than basal and apical processes, curved; apical process narrower apically, curved, apex rounded, flat and bent, appearing as an internal, flat, broad tooth. Aedeagus (Fig. 10B) phallosome sclerotized on distal half dorsally and at middle as a stripe. Ductus seminis sclerotized at the same level as phallosome dorsally; endosoma membranous, base sclerotized.

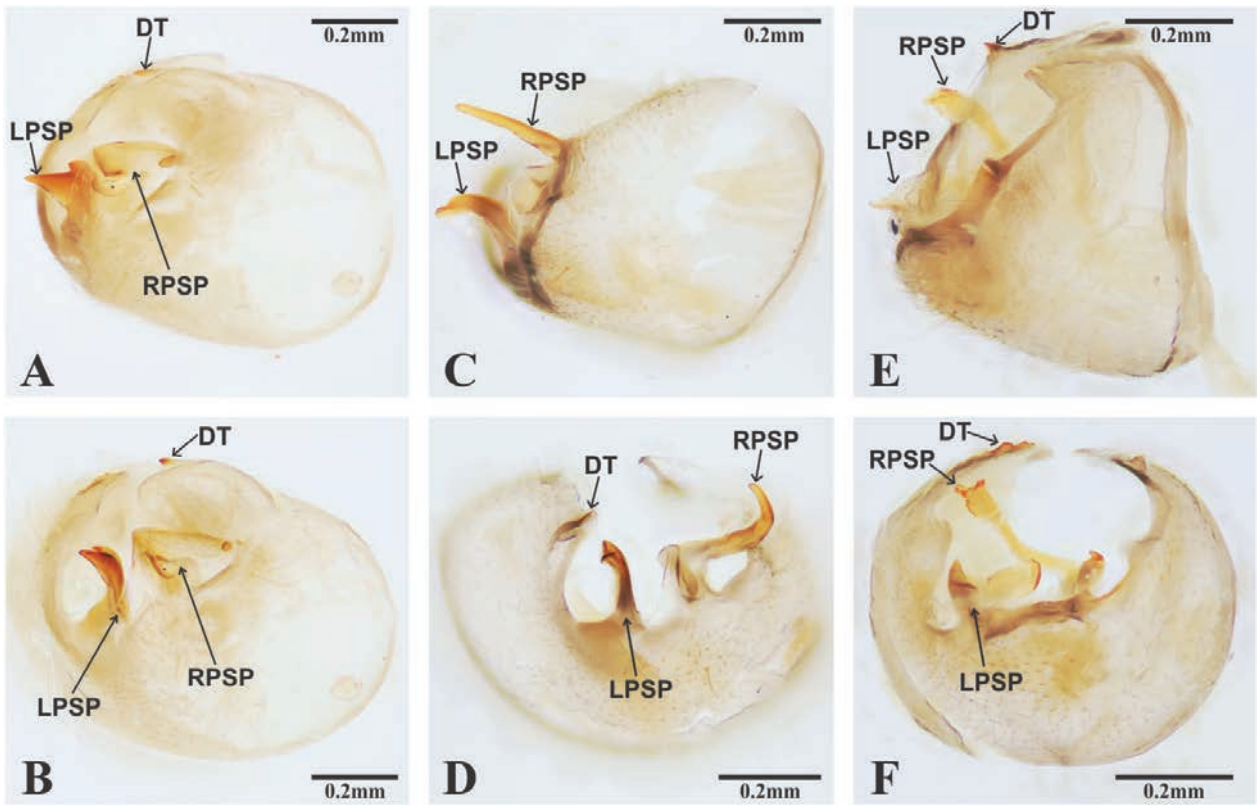


**Figure 7.** *Egerocoris* gen. nov. new species, subgenital plate. **A, B.** *E. dimorphus* sp. nov.; **C, D.** *E. ecuatorianus* sp. nov.; **E, F.** *E. chaparensis* sp. nov.; **A.** Subgenital plate right posterolateral view; **C, E.** Subgenital plate right lateral view; **B, D, F.** Subgenital plate posterior view; **DT**–dorsal tooth; **LPSP**–left process of subgenital plate; **RPSP**–right process of subgenital plate.

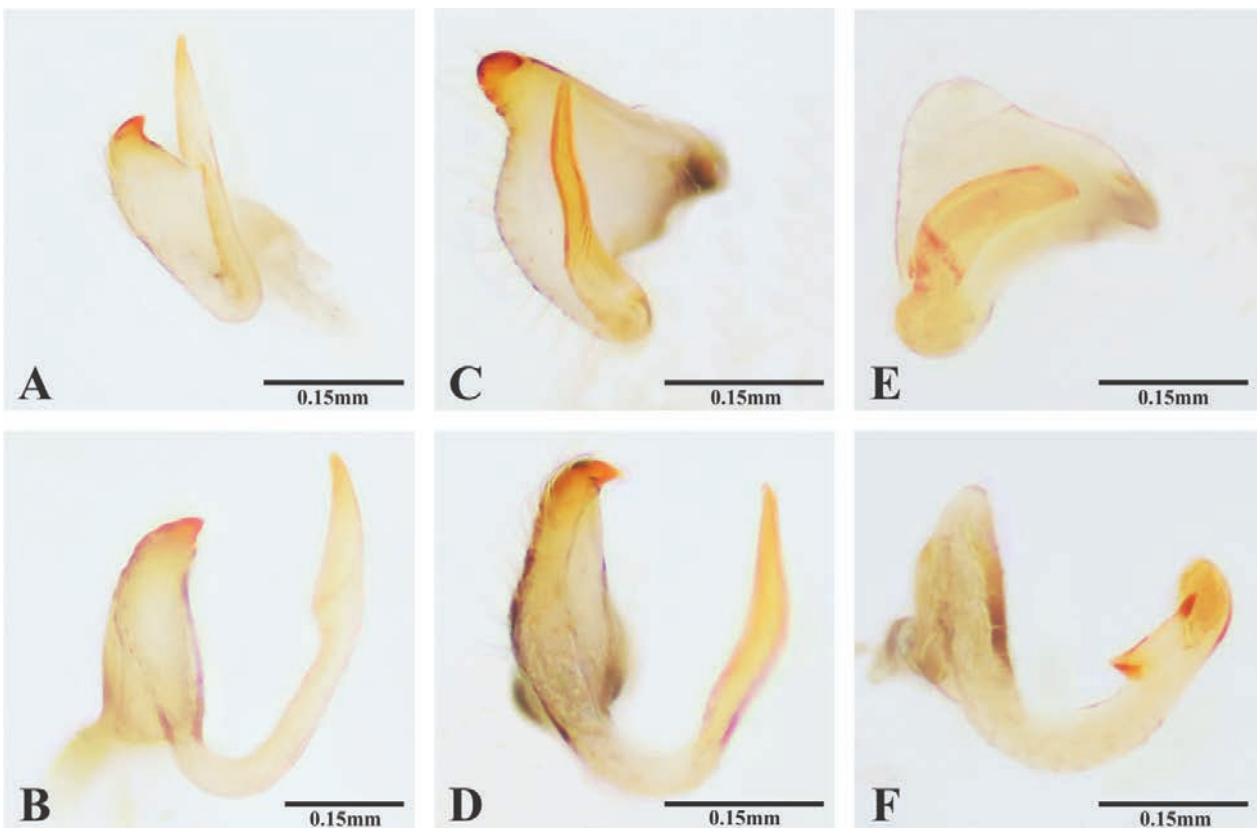


**Figure 8.** *Egerocoris* gen. nov. new species, left paramere. **A, B.** *E. dimorphus* sp. nov.; **C, D.** *E. ecuatorianus* sp. nov.; **E, F.** *E. chaparensis* sp. nov.; **A, C, E.** Interior view; **B, D, F.** Posterior view.

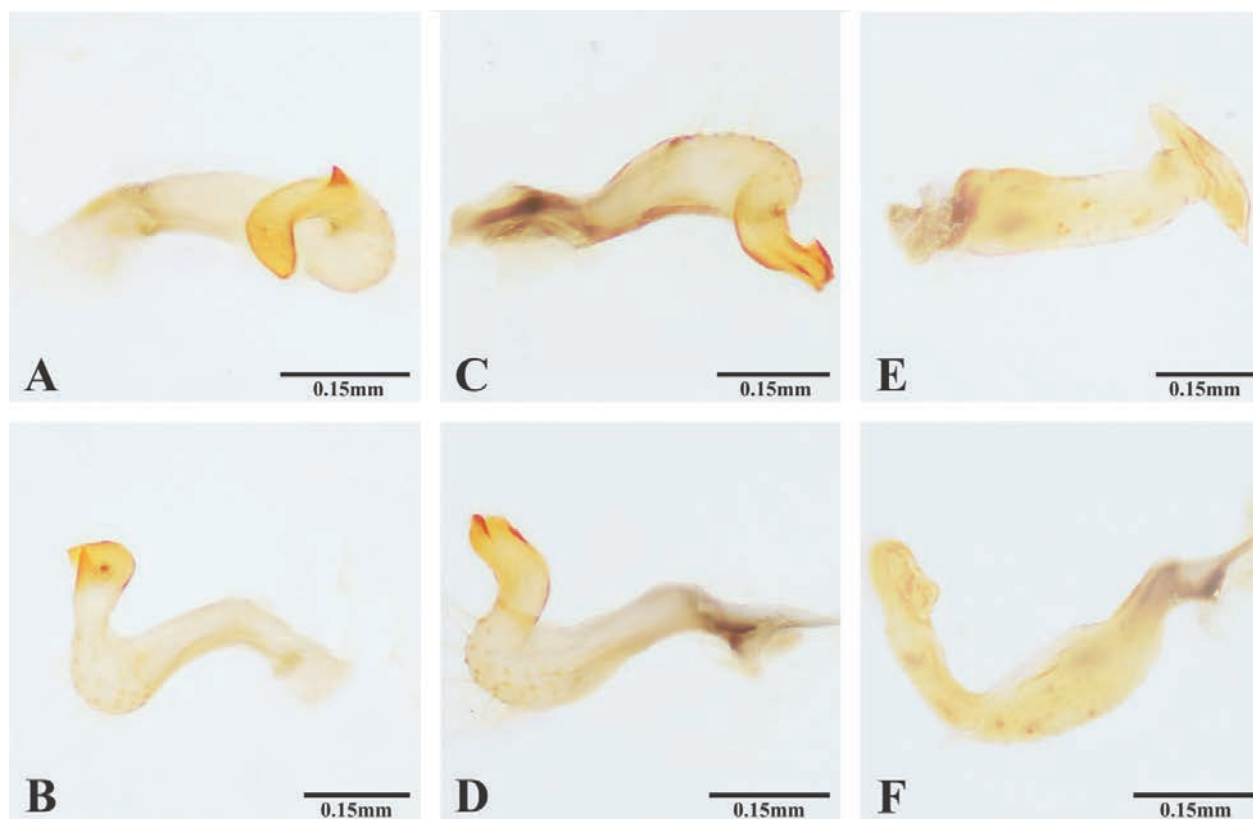


**Figure 9.** *Egerocoris* gen. nov. new species, right paramere. **A, B.** *E. dimorphus* sp. nov.; **C, D.** *E. ecuatorianus* sp. nov.; **E, F.** *E. chaparensis* sp. nov.; **A, C, E.** Interior view; **B, D, F.** Dorsal view.

**Measurements:** Body length to apex of membrane 4.61; body length to apex of cuneus 4.3; body width 2.18. Head: width 1.13; interocular distance 0.54, 1.17 times as wide as head length and 1.08 times as wide as antennal segment length. Labium: segment I length 0.56; II, 0.66; III, 0.23; IV, 0.22. Antenna: segment I length 0.5; II, 1.26; III, 0.77; IV, 0.67. Pronotum: length 0.71; anterior width 0.80; posterior width 1.42. Scutellum: length 0.48; width 0.72. Claval commissure more than 2 times as long as scutellum. Cuneus: length 1.18; anterior width 0.67. Cell 2.55 times as long as wide.

**Macropterous female.** Similar to males in size, coloration, surface, and structure, with medial fracture longer than half of corium. Body length to apex of membrane 4.84; body length to apex of cuneus 4.37; body width 2.02. Head: width 1.16; interocular distance 0.54; vertex 1.22 times as wide as head length and 1.14 times as wide as antennal segment I length. Labium: segment I length 0.58; II, 0.68; III, 0.22; IV, 0.22. Antenna: segment I length 0.50; II, 1.18; III, 0.80; IV, 0.78. Pronotum: length 0.74; anterior width 0.84; posterior width 1.50. Scutellum: length 0.47; width 0.73. Cuneus: length 1.03; anterior width 0.68. Cell 2.63 times as long as wide.

**Geographic distribution.** Ecuador (Fig. 11).

**Etymology.** The specific epithet is a latinized adjective created from the Spanish adjective *ecuatoriano*, -a, meaning “related to the Ecuador”, in reference to the country Ecuador, where the specimens were collected.

**Type material.** *Holotype* ♂: Ecuador: Napo [Orellana]: Tiputini / Biodiversity Station, 216 m, / 0°37'55"S, 76°08'39"W, / 7 February 2002, / T. J. Henry & P. S. F. Ferreira (USNM). *Paratype* ♀: Ecuador: Napo [Orellana]: Tiputini / Biodiversity Sta., Tower 1, / 0°37'55"S, 76°08'39"W, / 216 m, 3 February 2002, / T. J. Henry & P. S. F. Ferreira / Ex. Mercury vapor light (USNM).

***Egerocoris chaparensis* sp. nov.**

<https://zoobank.org/7664DCA6-2FCC-4A6C-9C82-8BD4BD8C999B>  
Figs 1D, 2D, 3D, 5E, F, 6E, F, 7E, F, 8E, F, 9E, F, 10C

**Diagnosis.** Antennal segment I yellow (Fig. 3D), segment III with basal half pale yellow, distal half darker; femora yellow; level of vertex attaining dorsal margin of eyes (Fig. 2D); labium extending at least to metacoxae and segment I deeply concave ventrally and narrowing distally; calli small, not attaining lateral pronotal margins; embolium longer than abdomen; internal margin of cell convex; without sexual dimorphism on internal margin and length of cuneus (Fig. 1D); dorsal wall of genital capsule well developed, with two tiny medial and sclerotized teeth (Figs 5F, 7E, F); left process of subgenital plate C-shaped in dorsal view, divided into two broad branches; right process ending in many asymmetrical teeth (Fig. 7E, F); left paramere smaller than the right paramere; right paramere curved, with apex expanded dorsoventrally (Fig. 9E); and aedeagus less than or as long as the genital capsule.

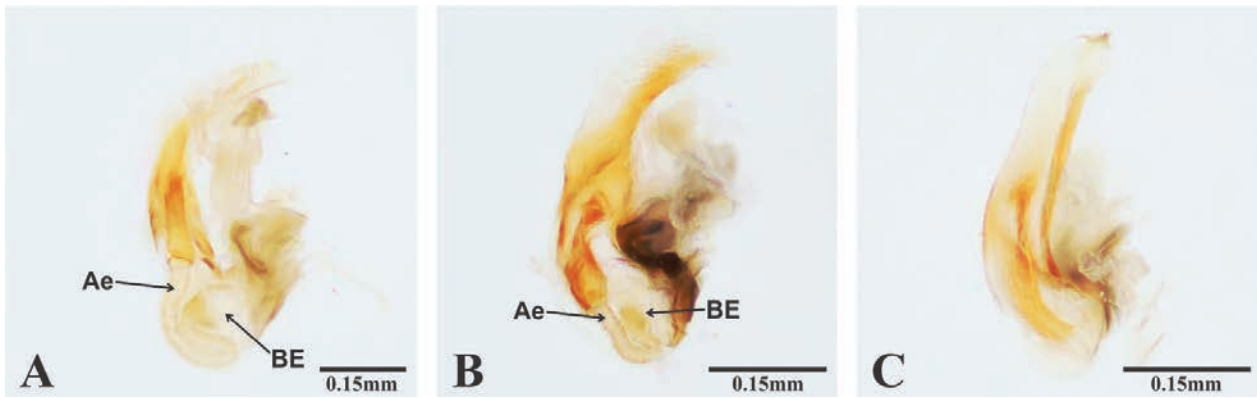


**Figure 10.** *Egerocoris* gen. nov. new species, aedeagus right lateral view. **A.** *E. dimorphus* sp. nov.; **B.** *E. ecuatorianus* sp. nov.; **C.** *E. chaparensis* sp. nov.; Ae–aedeagus; BE–basal expansion.



**Figure 11.** Distributional map of the species included in the genera *Thomasomiris* gen. nov. and *Egerocoris* gen. nov. Blue dot represents occurrence of *Thomasomiris setosus* sp. nov.; yellow dots represent occurrences of *Egerocoris dimorphus* sp. nov.; orange dot represents occurrence of *E. ecuatorianus* sp. nov.; in grey the province Chapare (Bolivia) where *E. chaparensis* sp. nov. occurs.

**Description. Macropterous male.** Coloration. Head yellow. Labium yellow. Eyes black with silver spots. Antennal segment I yellow; II, dark brown; III, basal half whitish, more than distal half brown. Thorax: collar, pronotum, scutellum and pleural area yellow. Hemelytron, legs and abdomen yellow, tarsi whitish.

**Surface.** Antennal segment I–II with recumbent setae, and a few semierect setae, more abundant on segment II. Antennal segments III with semierect setae and a few erect setae. Pleural area and abdomen with longer

and more disperse setae than dorsum. Coxae, trochanters, femora, and tarsi with semierect setae. Tibiae with abundant recumbent setae.

**Structure.** Head: level of vertex attaining dorsal margin of eyes (Fig. 2D). Maxillary plates long and thin. Labium just beyond metacoxae; segment I, deeply concave ventrally and narrowing distally; II, thin and long; III–IV, wider and short. Antennal segment II more than 2 times as long as antennal segment I. Thorax: posterior pronotal margin 2 times as wide as pronotum length.

Calli small, not attaining lateral pronotal margins. Pronotal width across calli more than half of posterior margin width. Hemelytron: embolium straight, bent upwards from its anterior end to more than anterior third; longer than abdomen. Claval commissure longer than scutellum and half pronotum length combined. Internal margin of cuneus concave (Fig. 1D). Male genitalia: genital capsule more than one third abdomen length. Dorsal wall with two tiny, medial, sclerotized teeth directed upwards; the left tooth larger than the right (Figs 5E, F, 7E, F). Subgenital plate with two large processes at the level of paramere insertions. Left process, shorter than right process, flat, broad basally and forked. Right process longer, thinner, extremely broad basally with small external tooth, C-shaped, apex with several asymmetrical teeth (Fig. 7E, F). Left paramere (Fig. 8E, F) smaller and broader than right paramere, with a blunt dorsal projection, apical process with an internal, triangular, tooth, apex flat, thin and sclerotized. Right paramere (Fig. 9E, F) curved; body wide basally, narrowed distally; apical process expanded dorsoventrally, dorsal expansion blunt, with ventral expansion pointed. Aedeagus (Fig. 10C) phallosome sclerotized on left side, with a dorsal stripe and a ventral oblique stripe sclerotized; endosoma sclerotized.

**Measurements:** Body length to apex of membrane 4.46; body length to apex of cuneus 3.95; body width 1.94. Head: width 1.08; interocular distance 0.56, 1.22 times as wide as head length and 1.47 times as wide as antennal segment I length. Labium: segment I length 0.52; II, 0.62; III, 0.17; IV, 0.18. Antenna: segment I length 0.38; II, 0.91; III, not measured; IV, absent. Pronotum: length 0.71; anterior width 0.80; posterior width 1.46. Scutellum: length 0.50; width 0.74. Cuneus: length 0.98; anterior width 0.76. Cell 2.78 times as long as wide.

**Macropterous female.** Similar to males in size, coloration, surface, and structure. Antennal segment II basally yellow, distally dark brown; IV, brown.

**Structure.** Antennal segment II more than 2.5 times as long as antennal segment I. Thorax: posterior pronotal margin more than twice as wide as pronotum length. Pronotal width across calli less than half of posterior margin width. Hemelytron: embolium bent upwards from its anterior end to a half or more than a half its length. Medial fracture attaining half corium length. Claval commissure equal to or longer than scutellum and half pronotal length combined. Cuneus not bent downwards.

**Measurements** (n: 4): Body length to apex of membrane 4.28–4.79; body length to apex of cuneus 3.7–4.23; body width 1.97–2.09. Head: width 1.07–1.10; interocular distance 0.54–0.59, 1.20–1.34 times as wide as head length and 1.50–1.64 times as wide as antennal segment I length. Labium: segment I length 0.48–0.54; II, 0.49–0.65; III, 0.18–0.19; IV, 0.18. Antenna: segment I length 0.36–0.37; II, 0.92–1.0; III, 0.44–0.46; IV, 0.58–0.62. Pronotum: length 0.74–0.80; anterior width 0.77–0.82; posterior width 1.54–1.58. Scutellum: length 0.49–0.55; width 0.72–0.77. Cuneus: length 0.98–1.09; anterior width 0.74–0.78. Cell 2.34–2.8 times as long as wide.

**Geographic distribution.** Bolivia (Fig. 11).

**Etymology.** The specific epithet refers to Chapare Province, Bolivia, where the specimens were collected. Adjective.

**Type material.** *Holotype* ♂: Sajta, XI-93 / Chapare, Bolivia (USNM). *Paratypes*: 4♀, same data as the holotype (2 USNM, 2 MLP).

## Acknowledgements

We thank Thomas Henry (Systematic Entomology Laboratory, ARS, USDA, (U.S. National Museum of Natural History (USNM), Washington, DC) for kindly reviewing the manuscript and his hospitality and support during our visit to the USNM collection, which was also made possible thanks to a Smithsonian Short-Term Visitor Grant. This work was funded by the Consejo Nacional de Investigaciones Científicas y Técnicas (CONICET).

## References

- Carvalho JCM (1946) *Mirideos neotropicales*, XXII: Tres gêneros novos do Brasil (Hemiptera). Boletim do Museu Nacional (n. s.) (Zool.), Rio de Janeiro 59: 1–6.
- Carvalho JCM (1951) Neotropical Miridae, XLV: A new genus and new species of Bryocorinae (Hemiptera). Entomologist 84: 232–234.
- Carvalho JCM (1960) *Mirideos Neotropicales*, LXXXVIII: Dois novos generos do complexo *Neella* Reuter-*Neoneella* Costa Lima (Hemiptera, Heteroptera). Arquivos do Museu Nacional, Rio de Janeiro 50: 47–60.
- Carvalho JCM (1974) Neotropical Miridae, CLXXIX: Two new genera of Bryocorinae from Costa Rica and Mexico (Hemiptera). Revista Brasileira de Biologia 34: 45–48.
- Carvalho JCM, China WE (1959) Neotropical Miridae, LXXXIV: Four new genera in the collection of the British Museum of Natural History (Hemiptera). Revista Brasileira de Biologia 19: 69–73.
- Carvalho JCM, Ferreira PSF (1995) *Mirideos Neotropicales*, CCCXC: Chave para os generos Neotropicales de Bryocorinae Baerensprung, 1860 (Heteroptera). Revista Ceres 42(243): 469–496.
- Cassis G (2008) The *Lattinova* complex of austromirine plant bugs (Hemiptera: Heteroptera: Miridae: Orthotylinae). Proceedings of the Entomological Society of Washington 110(4): 845–939. <https://doi.org/10.4289/0013-8797-110.4.845>
- da Costa Lima AM (1942) Percevejos das orquideas. (Hem. Miridae, Bryocorinae). Orquidea, Rio de Janeiro 4: 100–109.
- Ferreira PSF, Henry TJ (2011) Synopsis and keys to the tribes, genera, and species of Miridae (Hemiptera: Heteroptera) of Mina Gerais, Brazil Part I: Bryocorinae. Zootaxa 2920(1): 1–41. <https://doi.org/10.11646/zootaxa.2920.1.1>
- Ferreira PSF, Henry TJ, Coelho LA (2015) Plant Bugs (Miridae). In: Panizzi AR, Grazia J (Eds) True Bugs (Heteroptera) of the Neotropics, Springer, Dordrecht, 237–286. [https://doi.org/10.1007/978-94-017-9861-7\\_10](https://doi.org/10.1007/978-94-017-9861-7_10)
- Henry TJ (1993) A striking new genus and species of bryocorine plant bug (Heteroptera: Miridae) from eastern North America. Jeffersoniana 2: 1–9.
- Henry TJ (2022) Revision of the New World plant bug genus *Cyrtocapsus* (Heteroptera: Miridae: Bryocorinae: Ecritotarsini),

- with new and revised synonymies, lectotype designations, and descriptions of 12 new species. *Zootaxa* 5154 (1): 001–048. <https://doi.org/10.11646/zootaxa.5154.1.1>
- Henry TJ, Howard SZ (2016) Revision of the Neotropical plant bug genus *Sinervus* Stål (Heteroptera: Miridae: Bryocorinae: Eccritotarsini), with the description of four new species and a closely related new genus. *Proceedings of the Entomological Society of Washington* 118(4): 533–554. <https://doi.org/10.4289/0013-8797.118.4.533>
- Henry TJ, Menard KL (2020) Revision and phylogeny of the eccritotarsine plant bug genus *Caulotops* Bergroth, with descriptions of four new genera and 14 new species (Hemiptera: Heteroptera: Miridae: Bryocorinae) associated with *Agave* (Agavoideae: Asparagaceae) and Related Plant Genera. *Zootaxa* 4772(2): 201–252. <https://doi.org/10.11646/zootaxa.4772.2.1>
- Hernández LM, Stonedahl GM (1996) *Cubanomiris pilosus*, a new genus and species of Eccritotarsini (Heteroptera: Miridae: Bryocorinae) from Cuba. *Caribbean Journal of Science* 32: 151–157.
- Kerzhner IM, Konstantinov FV (1999) Structure of the aedeagus in Miridae (Heteroptera) and its bearing to suprageneric classification. *Acta Societatis Zoologicae Bohemicae* 63: 117–137.
- Kirkaldy GW (1902) Memoir upon the Rhyncotal family Capsidae Auctt. *Transactions of the Royal Entomological Society of London* 1902(2): 243–272. [V & VI pls] <https://doi.org/10.1111/j.1365-2311.1902.tb01384.x>
- Konstantinov FV (2003) Male genitalia in Miridae (Heteroptera) and their significance for suprageneric classification of the family. Part I: General review, Isometopinae and Psallopinae. *Belgian Journal of Entomology* 5: 3–36.
- Konstantinov FV, Knyshov AA (2015) The tribe Bryocorini (Insecta: Heteroptera: Miridae: Bryocorinae): phylogeny, description of a new genus, and adaptive radiation on ferns. *Zoological Journal of the Linnean Society* 175(3): 441–472. <https://doi.org/10.1111/zoj.12283>
- Konstantinov FV, Zinovjeva AN (2016) A new species of *Ambunticoris* from Sulawesi (Hemiptera: Heteroptera: Miridae). *Acta Entomologica Musei Nationalis Pragae* 56(1): 51–59.
- Konstantinov FV, Namyatova AA, Cassis G (2018) A synopsis of the bryocorine tribes (Heteroptera: Miridae: Bryocorinae): key, diagnoses, hosts and distributional patterns. *Invertebrate Systematics* 32(4): 866–891. <https://doi.org/10.1071/IS17087>
- Menard KL, Schwartz MD (2018) A description of a new genus and new species of sotol-feeding Eccritotarsini (Hemiptera: Heteroptera: Miridae: Bryocorinae) from Durango, Mexico. *Zootaxa* 4514(2): 283–292. <https://doi.org/10.11646/zootaxa.4514.2.11>
- Mu YR, Liu GQ (2012) New records of the genus *Jessopocoris* Carvalho, 1981 (Hemiptera: Miridae: Bryocorinae), with descriptions of two new species found in China. *Zootaxa* 3573(1): 47–54. <https://doi.org/10.11646/zootaxa.3573.1.5>
- Namyatova AA, Konstantinov FV, Cassis G (2016) Phylogeny and systematics of the subfamily Bryocorinae based on morphology with emphasis on the tribe Dicyphini sensu Schuh, 1976. *Systematic Entomology* 41(1): 3–40. <https://doi.org/10.1111/syen.12140>
- Reuter OM (1892) Voyage de M. F. Simon au Venezuela (décembre 1887-avril 1888) 20" MDSU" e mémoire. Hémiptères Hétéroptères. 1" MDSU" re partie. Capsides. *Annales de la Société Entomologique de France* 61: 391–402.
- Reuter OM (1905) Capsidae in Venezuela a D:o D:re Fr. Meinert collectae enumeratae novaeque species descriptae. *Öfversigt af Finska Vetenskaps societetens Förhandlingar* 47(19): 1–39. [1 pl.]
- Schuh RT, Weirauch C (2020) *True Bugs of the World* (Hemiptera: Heteroptera): Classification and Natural History, 2<sup>nd</sup> edn. Monograph series, London: Siri Scientific Press, 800 pp.



# Forest leaf litter beetles of Taiwan: first DNA barcodes and first insight into the fauna

Fang-Shuo Hu<sup>1</sup>, Emmanuel Arriaga-Varela<sup>2</sup>, Gabriel Biffi<sup>3</sup>, Ladislav Bocák<sup>4</sup>, Petr Bulirsch<sup>5</sup>, Albert František Damaška<sup>6</sup>, Johannes Frisch<sup>7</sup>, Jiří Hájek<sup>8</sup>, Peter Hlaváč<sup>8</sup>, Bin-Hong Ho<sup>1</sup>, Yu-Hsiang Ho<sup>9</sup>, Yun Hsiao<sup>10</sup>, Josef Jelínek<sup>8</sup>, Jan Klimaszewski<sup>11</sup>, Robin Kundrata<sup>12</sup>, Ivan Löbl<sup>13</sup>, György Makranczy<sup>14</sup>, Keita Matsumoto<sup>15</sup>, Guan-Jie Phang<sup>16</sup>, Enrico Ruzzier<sup>17,18</sup>, Michael Schülke<sup>19</sup>, Zdeněk Švec<sup>20</sup>, Dmitry Telnov<sup>15,21,22</sup>, Wei-Zhe Tseng<sup>23</sup>, Lan-Wei Yeh<sup>24</sup>, My-Hanh Le<sup>25</sup>, Martin Fikáček<sup>1,8</sup>

1 Department of Biological Sciences, National Sun Yat-sen University, Kaohsiung, Taiwan

2 Museum and Institute of Zoology, Polish Academy of Sciences, Warsaw, Poland

3 Museu de Zoologia da Universidade de São Paulo, São Paulo, Brazil

4 Czech Advanced Technology and Research Institute (CATRIN), Palacký University, Olomouc, Czech Republic

5 Milánská 461, Prague, Czech Republic

6 Department of Zoology, Faculty of Science, Charles University, Prague, Czech Republic

7 Center for Integrated Biodiversity Discovery, Museum für Naturkunde Berlin, Berlin, Germany

8 Department of Entomology, National Museum, Prague, Czech Republic

9 Department of Entomology, National Chung Hsing University, Taichung, Taiwan

10 Institute of Ecology and Evolutionary Biology, National Taiwan University, Taipei, Taiwan

11 Research Affiliate of the University of Alaska Museum Insect Collection, University of Alaska, Fairbanks, USA

12 Department of Zoology, Faculty of Science, Palacký University, Olomouc, Czech Republic

13 Muséum d'Histoire Naturelle, Genève, Switzerland

14 Department of Zoology, Hungarian Natural History Museum, Budapest, Hungary

15 Department of Life Sciences, Natural History Museum, London, UK

16 Department of Biomedical Science and Environmental Biology, College of Life Science, Kaohsiung Medical University, Kaohsiung, Taiwan

17 Department of Science, Roma Tre University, Rome, Italy

18 National Biodiversity Future Center, Palermo, Italy

19 Museum für Naturkunde, Berlin, Germany

20 Kamenická 4, Prague, Czech Republic

21 Institute of Life Sciences and Technology, Daugavpils University, Daugavpils, Latvia

22 Institute of Biology, University of Latvia, Rīga, Latvia

23 Department of Life Sciences, National Taiwan Normal University, Taipei, Taiwan

24 Department of Life Sciences, Tunghai University, Taichung, Taiwan

25 Biodiversity Research Center, Academia Sinica, Taipei, Taiwan

<https://zoobank.org/FC195427-80EA-4667-9010-AC9429FC2AB8>

Corresponding author: Martin Fikáček (mfikacek@gmail.com)

Academic editor: M. Seidel ♦ Received 6 September 2023 ♦ Accepted 29 November 2023 ♦ Published 8 January 2024

## Abstract

We report the publication of 953 DNA barcodes of forest leaf litter beetles from central Taiwan, in total representing 334 species of 36 beetle families. This is the first bulk of data from the Taiwanese Leaf Litter beetles project focused on uncovering the under-explored diversity of leaf litter beetles across Taiwan. Based on these data, we provide the first records of the following taxa for Taiwan: family Sphindidae (genus *Aspidiphorus* Ziegler, 1821); tribes Trichonychini, Ctenistini, and Bythinoplectini (all Staphylinidae: Pselaphinae); genera *Gyrelon* Hinton, 1942, *Thyroderus* Sharp, 1885, *Cautomus* Sharp, 1885 (all Cerylonidae), *Dermatohomoeus* Hlisenkovský, 1963 (Leiodidae), *Paraploderus* Herman, 1970 (Staphylinidae: Oxytelinae), *Thinocharis* Kraatz, 1859 (Staphylinidae: Paederinae), *Cephennodes* Reitter, 1884, *Napoconnus* Franz, 1957 (both Staphylinidae: Scydmaeninae),

*Bicava* Belon, 1884 (Latriidiidae), *Otibazo* Morimoto, 1961, *Seleuca* Pascoe, 1871 and *Acallinus* Morimoto, 1962 (all Curculionidae); species *Oodes* (*Lachnocrepis*) *japonicus* (Bates, 1873) (Carabidae: Liciniinae), *Drusilla obliqua* (Bernhauer, 1916) (Staphylinidae: Aleocharinae) and *Coccotrypes advena* Blandford, 1894 (Curculionidae: Scolytinae). The records of *Anapleus* Horn, 1873 (Histeridae) and *Batraxis* Reitter, 1882 (Staphylinidae: Pselaphinae) have been confirmed. The male of *Sivacrypticus taiwanicus* Kaszab, 1964 (Archeocrypticidae) is described for the first time. *Gyrelon jenpani* Hu, Fikáček & Matsumoto, **sp. nov.** (Cerylonidae) is described, illustrated, and compared with related species. DNA barcodes associated larvae of 42 species with adults, we are concisely illustrating some of these: *Oodes japonicus*, *Perigona* cf. *nigriceps* Dejean, 1831 (both Carabidae), *Ptilodactyla* sp. (Ptilodactylidae), *Maltypus ryukyuanus* Wittmer, 1970 (Cantharidae), *Drusilla obliqua*, *Myrmecocephalus brevisulcus* (Pace, 2008), *Diachus* sp., *Mimopinophilus* sp. (all Staphylinidae), *Stelidota multiguttata* Reitter, 1877, *Lasiodites inaequalis* (Grouvelle, 1914) (both Nitidulidae), *Lagriia scutellaris* Pic, 1910, and *Anaedus spinicornis* Kaszab, 1973 (both Tenebrionidae). We also report the first cases of *Rickettsia* infections in Scydmaeninae and Pselaphinae. All data (sequences, metadata, and voucher photos) are made public in BOLD database and in a Zenodo Archive.

---

## Key Words

Coleoptera, DNA barcoding, new record, new species, Oxford Nanopore

---

## Introduction

Forest leaf litter, especially in tropical regions, is recognized as a habitat comparable to coral reefs by its ability to support extremely diverse faunas (Giller 1996). Among the diverse leaf litter arthropods, beetles (Coleoptera) are the most common, remarkable and speciose group (Nadkarni and Longino 1990; Olson 1994; Sakchoowong et al. 2008), despite the fact they may be outnumbered by ants, termites and mites in the number of specimens. The immense species diversity of leaf litter beetles corresponds to the fact that leaf litter played a crucial role in the evolution and diversification of several beetle lineages, most notably those of the Staphyliniformia (e.g., McKenna et al. 2015). Consequently, the rove beetles (Staphylinidae) became one of the most species-rich families worldwide (Lü et al. 2020). Yet, our understanding of leaf litter beetle faunas remains very limited. The high number of species and specimens, small body sizes and a high local endemism due to limited dispersal abilities form a ‘toxic mix’ making the study of leaf litter beetles difficult and extremely time-consuming. Several authors of this paper have spent their whole lives processing leaf litter samples all over the world, yet only a tiny portion of the collected material has been taxonomically treated, and an even smaller part was revised in a way that makes the taxonomic knowledge accessible to non-specialists: ecologists, conservation biologists or the general public. Our knowledge of the immature stages of these beetles is even scarcer: we do not even know what the larvae of most genera look like. This limits our understanding of the biology and ecological role of these beetles, and also obscures our understanding of their evolution, since larval characters are often phylogenetically highly informative.

DNA-based tools, including DNA barcoding, have been advocated to overcome the above problems referred

to as ‘the taxonomic impediment’ (e.g., Tautz et al. 2003; Miller et al. 2016). The identification based on short mitochondrial fragments, DNA barcodes, can indeed speed up the analyses of whole faunas, especially in combination with novel methods of third-generation sequencing (e.g., Srivathsan et al. 2021) and processing of bulk samples without sorting to morphospecies (so-called metabarcoding, e.g. Liu et al. 2020), and were used to analyze species and genetic diversity of whole beetle communities (e.g., Andújar et al. 2015; Arribas et al. 2021). Yet, in most cases, these quick methods require a reference set of DNA barcodes based on specimens identified by experts, so-called DNA barcode libraries. DNA barcode libraries can also help with species identification and discovery, including the identification of pests (e.g., Madden et al. 2019) or species used in forensic entomology (Chimeno et al. 2019), or interception of newly introduced invasive species (e.g., Armstrong and Ball 2005). Importantly, the identification by comparison with expert-identified DNA barcodes may also help to train specialists in countries lacking large comparative collections and those who have limited chances to travel to visit large collections or to study historical types. Moreover, DNA barcodes may also help experts: they bring evidence independent from morphology and may attract attention to overlooked cases of cryptic or polymorphic species requiring detailed studies (e.g., Janzen and Hallwachs 2016). For all these reasons, DNA barcoding libraries have already been completed for some insect groups (e.g., British Culicidae by Hernández-Triana et al. 2019; aquatic biota including insects by Weigand et al. 2019), and a country-wide DNA-barcoding initiative have been launched by countries like Canada (Hebert et al. 2016), Germany (Hendrich et al. 2015), Finland (Pentinsaari et al. 2014) and Costa Rica (Janzen et al. 2017). The goal of our project is to build up such a reference DNA barcoding library for the forest leaf litter beetles in Taiwan.

Taiwan, a small island located in the western Pacific, lies at the intersection of the Oriental and Palaearctic biogeographical regions, which results in a rich diversity of fauna from both areas. Among the diverse insect orders found on the island, beetles (Coleoptera) stand out with an impressive number of recorded species. Taiwan is home to more than 119 families and 7711 species of beetles (Chung and Shao 2022). However, despite this extensive diversity, the taxonomic research on beetles in Taiwan has been somewhat fragmented. While there have been notable contributions such as monographs focusing on canopy phytophagous beetles (Lee and Cheng 2007; Lee et al. 2010, 2016; Ong and Hattori 2019; Ong et al. 2023), the broader study of leaf litter beetles has been largely reliant on the collections made by Aleš Smetana in the 1990s and Stanislav Vít in the 2010s. Studies based on Smetana's and Vít's material revealed a high species diversity of certain beetle groups in the leaf litter, including numerous endemic species (e.g., Smetana 1995; Angelini and De Marzo 1998; Assing 2010, 2014, 2015; Puthz 2010; Cuccodoro 2011; Löbl 2012; Borovec 2014; Cosandey 2023).

In this study, we are announcing the start of the Taiwanese Leaf Litter Beetles Barcoding project that aims at building an expert-identified DNA barcoding library of beetles inhabiting leaf litter in Taiwan. Our goals are (1) to initiate an extensive study of Taiwanese leaf litter beetles across all taxonomic groups, (2) to document the diversity of Taiwanese leaf litter beetles, including endemic and alien species, and (3) to provide a reliable tool for a quick identification facilitating the studies of biology of these beetles. Here, we are publishing the first set of DNA barcodes and the photographs of the sequenced vouchers and present the first taxonomic results: a description of a new species of Cerylonidae, the description of a male of the Taiwan-endemic species of Archeocrypticidae, and several newly recorded taxa. Since DNA barcodes associated many larvae from our samples with adults, we also provide detailed photos of some of them.

## Materials and methods

### Sampled sites

In this paper, we present the complete data (DNA barcodes, species identification, voucher photographs) of the beetle samples from the Huisun Forest Reserve (Nantou County, central Taiwan) collected from 2019 to 2021 (20 samples in total at 5 different sites at altitudes of 700–1100 m). Further samples are collected continuously from all over Taiwan: from 2021 to July 2023, we accumulated 85 additional samples, of which 27 are in the progress of barcoding (DNA barcodes are already available, but identifications and voucher photos need to be completed) and remaining samples as well as those collected in the future will be gradually processed as well (Fig. 1A). We will keep uploading the data online once the processing of these samples is completed.

### Sample collecting and morphospecies sorting

Samples were collected with the help of a sifter with a 5 mm grid. Leaf litter was collected from suitable places where it accumulates and keeps moisture. The final volume of each sample varied between 3 and 6 liters of sifted material. We originally sampled 6 liters of sifted material, but this amount was found to be too large and hence the sampling protocol was subsequently updated to (at least) 3 liters of sifted material per sample; this updated protocol is followed for all samples collected from 2022 on. Beetles were extracted using portable Winkler extractors for 3 days, leaf litter was mixed twice a day to facilitate beetle extractions (Owens and Carlton 2015). Specimens were collected in 95% alcohol. Adults and larvae of each sample were sorted into morphospecies, counted, and 1–2 specimens of each morphospecies were selected for DNA extraction and barcoding. This method allowed us to (1) compare DNA-based and morphology-based species identification and consult inconsistencies with specialists, (2) to separate larvae and adults of the species in case they co-occur, (3) to associate larvae with adults by means of DNA. Additional specimens not used for barcoding were kept in alcohol in the freezer.

### DNA extraction and PCR

Most specimens were extracted using the HotSHOT protocol (Truett et al. 2000; Srivathsan et al. 2021), using either the whole specimen in small species or few legs in specimens over 5 mm. A smaller part of the specimens was extracted using standard DNA extraction kits (Qiagen DNeasy Blood and Tissue kit or NautiaZ Tissue DNA Extraction Mini Kit) following the manufacturers' protocols, but with the cell lysis step extended to ca. 8 hours (overnight); these extracts are stored in the Laboratory of Insect Diversity, Department of Biological Sciences, National Sun Yat-sen University, Kaohsiung, Taiwan. Extracts done using HotSHOT protocol were discarded after getting the sequences because their DNA degrades over time (Srivathsan et al. 2021). We amplified the 5' part of mitochondrial cytochrome oxidase I (*cox1*) (Hebert et al. 2003) using the modified LCO1490-HCO2198 primers for 658 bp (Folmer et al. 1994) and MLEPF1-HCO2198 for 407 bp fragment (Hajibabaei et al. 2006). Each primer was tagged with a unique 13 bp tag; the combination of tagged forward and reverse primers unambiguously identifies each sample and allows demultiplexing of reads. We used 96 uniquely tagged reverse (HCO2198) primers to identify the position of the sample in the 96-well plate, and four unique forward primers to identify individual plates. For the list of tagged primers, see Fikáček et al. (2023). For PCR reaction, we mixed 6.25 µl of GoTaqR Green Master Mix (Promega Corporation, USA), 1.75 µl of dH<sub>2</sub>O, 2.00 µl of bovine serum albumin (BSA, 1 mg/ml), 1.00 µl of forward primer, 1.00 µl of reverse primer, and 2.00 µl of DNA extract. PCR conditions were: 95 °C:

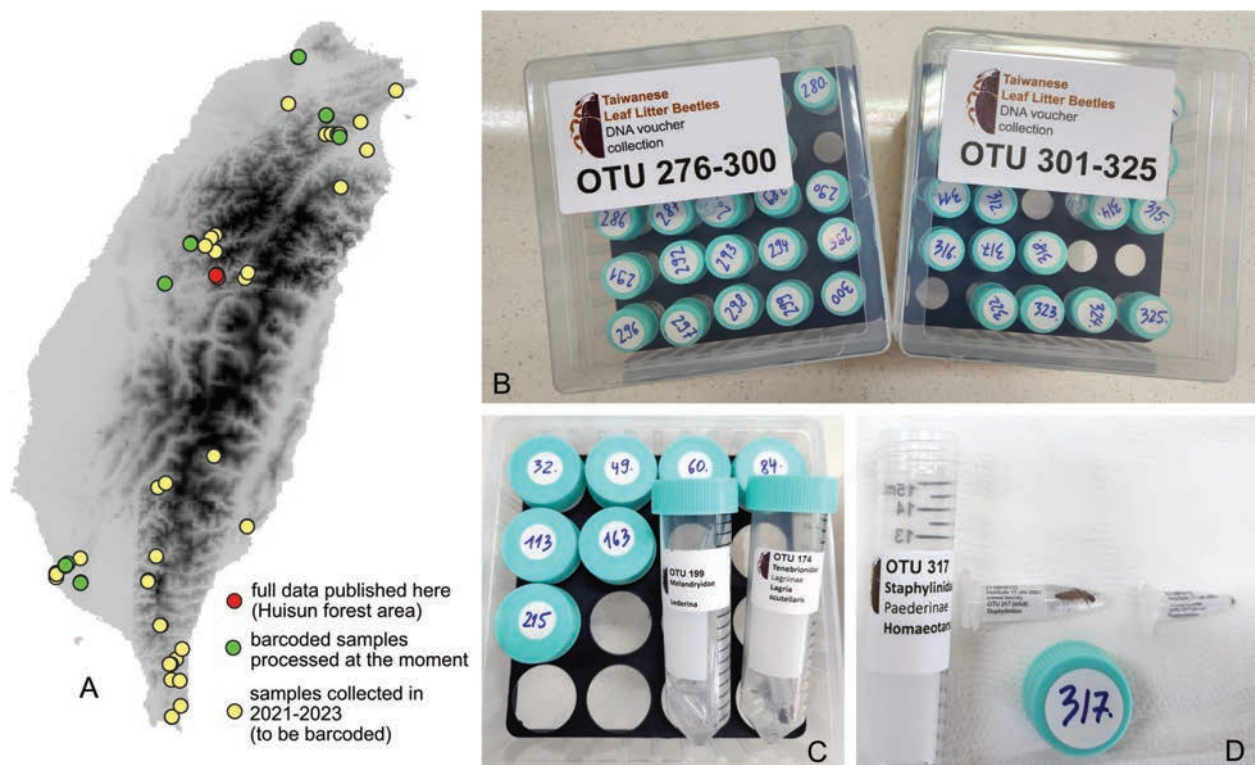


**Figure 1.** Taiwanese Leaf Litter Beetle Project: summary of the current status. **A.** Map of the samples collected in 2019–2023 (the complete data are published here for the Huisun Forest Reserve); **B–D.** Voucher collection kept in the Insect Diversity Lab, the National Sun Yatsen University, Kaohsiung, Taiwan: all vouchers and duplicates are available for study by specialists.

5 mins – 35 cycles of 94 °C: 30 seconds, 45 °C: 2 mins, 72 °C: 1 min – 72 °C: 5 mins, 12 °C: until removing samples from the machine. After the PCR, 16 samples were randomly selected from the plate and checked using gel electrophoresis to be sure that the complete plate did not fail at amplification. Individual samples were not checked, as we found that we often got sequences from samples without clear electrophoresis bands.

### ONT library preparation and sequencing

For sequencing of most samples, we used the Oxford Nanopore R9 Flongle flow cells; the only exception is the samples collected in 2019 that were sequenced using the usual Sanger protocol in Macrogen Europe. For ONT sequencing, we pooled samples from 3–4 plates into each library; 3 µl of each PCR product was used. The pooled mix was cleaned up using AMPure XP magnetic beads (Beckman Coulter, USA), typically using 500 µl of pooled PCR products and 500 µl of beads (1X ratio), using the standard protocol, but with three instead of two washes with 1 ml of 70% ethanol. The amount of DNA in the purified pooled sample was measured by Qubit (Thermo Fisher Scientific, USA). For the final library, we used 200 ng of DNA in total and the ONT Ligation Sequencing Kit SQK-LSK109. NEBNext Ultra II End repair/dA-tailing Module (New England BioLabs, Inc.) was used to repair DNA end and ligate A-tails, AMX adaptors provided in ONT Sequencing Kit were ligated using NEBNext Quick Ligation Module (New England BioLabs, Inc.). Fragment

size selection was done using the short fragment buffer (SFB) from the ONT Ligation Kit, combined with AM-Pure XP magnetic beads. The final 30 µl library consisted of 5 µl of DNA, 15 µl of SQB buffer, and 10 µl of LB buffer (both from the ONT Sequencing Kit). Sequencing was performed using MinKNOW software, for 24 to 48 hours based on the sequencing statistics. The base calling was performed subsequently in Guppy v4.0.11 software (Oxford Nanopore Technologies). For detailed protocols used, see Fikáček et al. (2023).

### Demultiplexing and consensus calling

We used ONTbarcode software (Srivathsan et al. 2021) to sort the reads from each Flongle flow cell run to the individual samples, based on the primer tags. Minimum length and length of the barcode were both set to 658 bp or 407 bp, according to the used primers, the windows for the product and primers were set to 100 bp. Consensus calling was performed using default settings (main consensus calling frequency: 0.3; range of frequencies to assess: 0.2 to 0.5; step size: 0.05) with invertebrate mitochondrial genetic code, using consensus by length (coverage used: 25, 50, 100, 200, 500; maximum deviation of read length: 50), consensus by similarity (coverage used: 100), and consensus by barcode comparison. All final consensus sequences reported in *runsummary* file are included in the final dataset, but those with the higher number of ambiguities were checked carefully in the final tree, and removed when problematic.

## Quality control

We implied three steps of the quality control of the resulting consensus sequences. Parts of the contaminations, especially by bacteria (*Wolbachia*, *Rickettsia*, etc.) or phylogenetically distant animal phyla (e.g., nematodes) were easy to recognize as exceptionally long branches not grouping with the rest of the beetles in the maximum likelihood tree constructed in MEGA v10.2.5 (Kumar et al. 2016). All such sequences were removed after their identity was checked using BLAST. This way cannot remove contaminants by other arthropods; hence, in the next step, all remaining sequences were blasted using a BLAST+ app (Camacho et al. 2009). Samples with matches of >90% identity were checked and removed in case none of the five best matches was a beetle. We also checked the match between Sanger-generated and ONT-generated sequences in our samples, as additional quality control of the ONT-generated sequences.

## Species delimitation and identification

We grouped sequences into species candidates (OTU, operational taxonomic units) by constructing the maximum likelihood tree in MEGA (Kumar et al. 2016) and searching clusters of similar sequences separated by longer internal branches. All vouchers were checked subsequently, and cases of mismatch (vouchers with different morphology in the same cluster, or identically-looking vouchers divided into separate clusters) were consulted with a specialist for the beetle family. The OTUs delimited in this way were numbered. Larval specimens nested in adult OTUs were considered conspecific with the adults. We consulted the genus and species identifications of the specimens with specialists for each family (in case these are available). All specialists providing help with identifications were offered with co-authorship.

## DNA barcodes database

All DNA barcodes which are completely processed at the moment, and the photographs of the vouchers, have been submitted to the Barcode of Life Database (BOLD; Ratnasingham and Hebert 2007; project acronym: TWHUI, 947 sequences). Voucher photos (428 photographs) are provided for at least one adult and one larva of each species. The complete data and all voucher photographs are also available in Zenodo research archive under <https://doi.org/10.5281/zenodo.10069183>. The BOLD dataset will be continuously updated once new barcodes will get available.

## DNA voucher collection

Vouchers of all sequenced specimens are deposited in the Laboratory of Insect Diversity, Department of Biological Sciences, National Sun Yat-sen University, Kaohsiung,

Taiwan (Fig. 1B–D). Individual specimens are kept in alcohol in plastic microtubes (0.2 or 0.5 ml, according to the size of the voucher), each specimen is labelled by its extraction number. Microvials with specimens belonging to the same species/OTU are grouped in 15 ml or 50 ml plastic tubes; each tube is labeled by the OTU number on the lid and by OTU number plus its identity at the side of the tube. Tubes are ordered based on the OTU numbers. Although the organization of the collection relies on OTU numbers, it remains flexible at the same moment, based on the progress on the taxonomic work on individual groups. Additional non-sequenced specimens are kept in the same lab in 95% alcohol at -20 °C. All specimens are available for study to taxonomists upon request addressed to M. Fikáček at [mfikacek@gmail.com](mailto:mfikacek@gmail.com).

## Depositories

Specimens examined in detail for taxonomy or morphology are deposited in the following collections:

<b>BHHC</b>	coll. Bin-Hong Ho, Taipei, Taiwan;
<b>BMNH</b>	Natural History Museum, London, UK (M. Barclay, K. Matsumoto);
<b>FSHC</b>	coll. Fang-Shuo Hu, Luodong, Yilan County, Taiwan;
<b>HNHM</b>	Hungarian Natural History Museum, Budapest, Hungary (Gy. Makranczy);
<b>IDL</b>	Insect Diversity Lab, Department of Biological Sciences, National Sun Yat-sen University, Kaohsiung, Taiwan (M. Fikáček);
<b>NMNS</b>	National Museum of Natural Sciences, Taichung, Taiwan (B.-C. Lai, J.-F. Tsai);
<b>NMPC</b>	National Museum, Prague, Czech Republic (J. Hájek, L. Sekerka);
<b>ZSPC</b>	coll. Zdeněk Švec, Praha, Czech Republic.

## Results

### The DNA barcode dataset

The currently released dataset is based on a total of 4629 beetle specimens collected at five sites in the Huisun Recreation Forest Area in 2019–2021 (20 samples in total). 903 specimens were larvae (19.5%); the proportion of larvae varied strongly among samples (7–36% of all specimens). In total, we extracted DNA from 1131 specimens, and obtained good-quality non-contaminated DNA barcodes for 947 of them (84%). Based on the current identification, this material represents 328 species candidates (OTUs). In most cases, the DNA-based species delimitation corresponds to that based on morphology. In a few cases, the DNA-based and morphology-based identifications are in conflict (e.g., *Stenasthetus nomurai*, *Lederina* sp., *Coccotrypes papuanus*), with DNA indicating several cryptic species within the morphology-based species.

We do not intend here to solve these cases as they will require a more diverse geographic and gene sampling. Sequenced specimens represent 36 beetle families, of which Staphylinidae are the most diverse (152 species), followed by Curculionidae (30 species), and Tenebrionidae (23 species). Staphylinidae were represented by 14 subfamilies, with Scydmaeninae (36 species), Pselaphinae (29 species) and Aleocharinae (27 species) being the most species-diverse. Larvae were associated with adults for 42 species (12.6%) belonging to 12 families. Sixty-one species (18.2%) belonging to 13 families were collected only in larval stage; they mostly belong to lineages with free-living adults (Cantharidae, Chrysomelidae, Elateridae, Lampyridae, Lycidae, Meloidae, Mordellidae, Phalacridae, Prionoceridae, Ptilodactylidae, Tenebrionidae). Eleven species were collected as accidental catches of groups not living in leaf litter (Cerambycidae, Cleridae, Melandryidae, and Zopheridae). The summary of the material from the Huisun Forest Recreation area sequenced and published here is provided in Table 1. The maximum likelihood tree of all sequences is provided in Suppl. material 1.

## Contaminations

In a few cases, we obtained sequences of other organisms than beetles, including bacteria such as *Rickettsia* and *Wolbachia*. Previous studies have reported a few cases of *Rickettsia* infection in beetles (Perlman et al. 2006; Bili et al. 2016). We identified *Rickettsia* sequences from the following taxa: Staphylinidae: Scydmaeninae, *Pseudophanias excavatus* (Staphylinidae: Pselaphinae) and Curculionidae: Scolytinae; these are the first records of *Rickettsia* infection in the Scydmaeninae and Pselaphinae. The presence of *Wolbachia* in beetles has been extensively reviewed in several studies (Kajtoch and Kotásková 2018; Kajtoch 2022). We revealed the presence of *Wolbachia* in the following taxa: Histeridae, Staphylinidae: Tachyporinae and Staphylinidae: Scydmaeninae. Additionally, we revealed several contaminations by nematodes, oomycetes and Amoebozoa in the nitidulid beetles that are possibly related to the preference of these beetles for decaying fruits. In some predatory beetles, we likely got sequences of their prey. Most interestingly, we repeated for sequences of *Burmoniscus* isopods from *Tolmerinus* sp. (both adults and larvae, 3 specimens of 16 sequenced),

**Table 1.** Summary of the dataset published here, based on 20 samples collected in the Huisun Recreation Forest area in 2019–2021.

Family	Sequences	Species: total	Species: larvae only	Species: larvae+adults	Non-arthropod contaminations
Anthicidae	2	2	–	–	–
Archeocrypticidae	2	1	–	–	–
Bothrideridae	1	1	–	–	–
Cantharidae	13	5	4	1	–
Carabidae	49	12	–	3	–
Cerambycidae	1	1	–	–	–
Cerylonidae	7	4	–	–	–
Chrysomelidae	34	17	11	1	–
Cleridae	1	1	–	–	–
Coccinellidae	2	2	–	–	–
Corylophidae	6	2	–	–	<i>Rickettsia</i>
Curculionidae	66	30	1	–	<i>Rickettsia</i>
Discolomatidae	12	2	–	1	–
Elateridae	15	9	6	–	–
Endomychidae	7	5	–	1	–
Erotylidae	11	3	–	–	–
Histeridae	4	4	1	–	<i>Wolbachia</i>
Hydrophilidae	20	4	–	–	–
Lampyridae	11	6	6	–	–
Latridiidae	8	2	–	–	–
Leiodidae	41	6	–	2	–
Lycidae	35	10	10	1	–
Melandryidae	19	1	–	–	–
Meloidae	1	1	1	–	–
Nitidulidae	16	3	–	2	Amoebozoa, oomycetes, Nematoda
Phalacridae	1	1	1	–	–
Prionoceridae	3	1	1	–	–
Ptiliidae	18	8	–	–	–
Ptilodactylidae	2	1	–	1	–
Ptinidae	2	1	–	–	–
Scarabaeidae	8	3	–	1	–
Scraptiidae	4	1	–	1	–
Sphindidae	2	2	–	–	–
Staphylinidae	449	152	6	24	<i>Rickettsia</i> , <i>Wolbachia</i>
Tenebrionidae	72	23	13	4	–
Zopheridae	2	1	–	–	–

suggesting that isopods may be the preferred food for *Tolmerinus* rove beetles. We also got one case of isopod sequence in *Erichsonius* (Staphylinidae) and one case of collembolan sequence from an unidentified Pselaphinae.

## Taxonomic part

### *Species descriptions or redescriptions*

The identification of the species barcoded so far revealed a significant number of species which may be new to science or are improperly characterized in the original descriptions. The taxonomic work on most of these species is in progress by individual specialists, several species have been already described elsewhere (*Scaphobaocera insinuata*: Löbl 2020; *Scaphisoma hui*: Löbl 2023; *Horn-iella nantouensis*: Zhang et al. 2021; *Oxyomus alligator*: Ho et al. 2022). Here we provide the complete taxonomic treatment for another two species.

### Cerylonidae

#### *Gyrelon jenpani* Hu, Fikáček & Matsumoto, sp. nov.

<https://zoobank.org/82B176D0-B4A9-4CCA-A4B3-7250E9F498B4>

Fig. 2

**Type material.** *Holotype*: male (NMNS): ‘Taiwan: Nantou County, Huisun Forest Reserve, track to Xiaochushan Mt., 24.0826139°N, 121.03115869°E, 1050 m, 4.v.2019, Damaška, Fikáček, Hu & Liu lgt., 2019-TW15’ (DNA voucher: HS2004). *Paratypes*: 1 male (NMNS): Taiwan: Nantou County, Huisun Forest Reserve, track to Xiaochushan Mt., 24.0744602°N, 121.0366337°E, 1150 m, 11.x.2020, FS Hu & YJ Chen lgt., old overgrown secondary forest on the slope, sparse understory vegetation: sifting of leaf litter accumulations (DNA voucher: 20-10HS506); 1 male (BMNH): same locality, date and collectors; 1 male (NMNS): same locality data, but 1.iii.2021, Hu, Chen, Fikáček & Peng lgt. (DNA voucher: 21-03HS508); 1 female (NMPC): same locality data, but 24.ii.2020, FS Hu lgt. (DNA voucher: 20-02HS509).

**Differential diagnosis.** The new species can be easily recognized from *G. rugosus* (Ślipiński, 1982) from southern China by the presence of both coarse and smaller punctures on the pronotum (only small and strongly elongated punctures are present in *G. rugosus*). The new species can be recognized from *G. mila* Hinton, 1942 (Sarawak) and *G. sumatrensis* Dajoz, 1974 (Sumatra) by the following characters: (1) metaventrite with punctures on the anterolateral portion much larger than posterolaterally (in contrast to small widely separated punctures in both latter species), (2) abdominal ventrite 1 with coarse punctures anteriorly and minute ones in the transverse row (with all punctures moderately large and widely spaced in both latter species), (3) transverse rows on abdominal ventrites 2–5 consisting of minute punctures (moderately large punctures in both latter species). The new species

differs from *G. compactus* Dajoz, 1979 from Singapore by (1) the presence of 8 elytral series (7 in *G. compactus*), (2) the serially arranged minute seriferous punctures on elytral intervals 1–2 (with irregularly arranged setiferous punctures in *G. compactus*), and (3) the parallel-sided posterolateral margins of the pronotum (posteriorly converging in *G. compactus*). The comparison is based on the examination of the holotype of *G. mila* and two non-type specimens of *G. sumatrensis* in coll. BMNH (from Perak and Fort de Kock). The types of *G. sumatrensis* and *G. compactus* could not be examined as they are lost (A. Mantilleri, pers. comm., March 2023). The types of *G. rugosus* were not examined as the difference is clear from the original description. We also examined unidentified specimens of *Gyrelon* from Sumatra, Borneo, Sulawesi and Thailand in coll. BMNH. All of them are similar to *G. mila* and *G. sumatrensis* in the characters listed above.

**Description.** *Body* widely oval, body length 2.8–3.2 mm (holotype: 3.2 mm), body width 1.7–1.8 mm (holotype: 1.8 mm) (n=5 including holotype). Dorsal and ventral coloration dark reddish brown to black, legs and antennae brown to reddish brown, all body parts bearing yellowish erect setae.

*Head* relatively small, eyes moderately large, globular; frons with several moderately large punctures, each bearing erect seta, interstices smooth; clypeus weakly concave on anterior margin, dorsal surface bearing many erect setae. Antenna robust, with 11 antennomeres including the 2-segmented club; antennomeres gradually widening from base to apex; antennomere with microsculptures surface, bearing moderately dense erect setae; antennal club covered by dense short setation and moderately dense set of long erect setae; apex of antennal club bluntly pointed. Mentum small, subtriangular, strongly narrowing anteriorly. Apical maxillary and labial palpomeres much narrower than the subapical ones.

*Thorax.* Pronotum subquadratic, nearly parallel-sided in posterior half, strongly narrowing in anterior half; median part of pronotum with elevated longitudinal ridge. Posterior corners nearly rectangular. Pronotal surface with large irregularly circular or oval punctures, each puncture bearing an erect seta; punctures getting smaller in posterolateral direction. Median part of pronotum lacking punctures, surface between punctures micropunctate. Prosternum widely rectangular, smooth, with coarse deep punctures; prosternal process wide, variable in shape, concave to weakly or strongly trifold posteriorly. Procoxal cavities widely separated, antennal grooves moderately wide, hypomeron with coarse punctures similar to those on prosternum. Mesoventrite anteriorly with a series of longitudinal ridges; surface microsculptured. Mesocoxal cavities widely separated by metaventral process. Each elytron with eight slightly irregular longitudinal series of punctures; serial punctures rounded, lacking setae; additional short series of coarse shallow punctures present anteriorly along elytral side; intervals flat dorsally, slightly convex laterally, smooth, each with a series of widely spaced minute punctures,

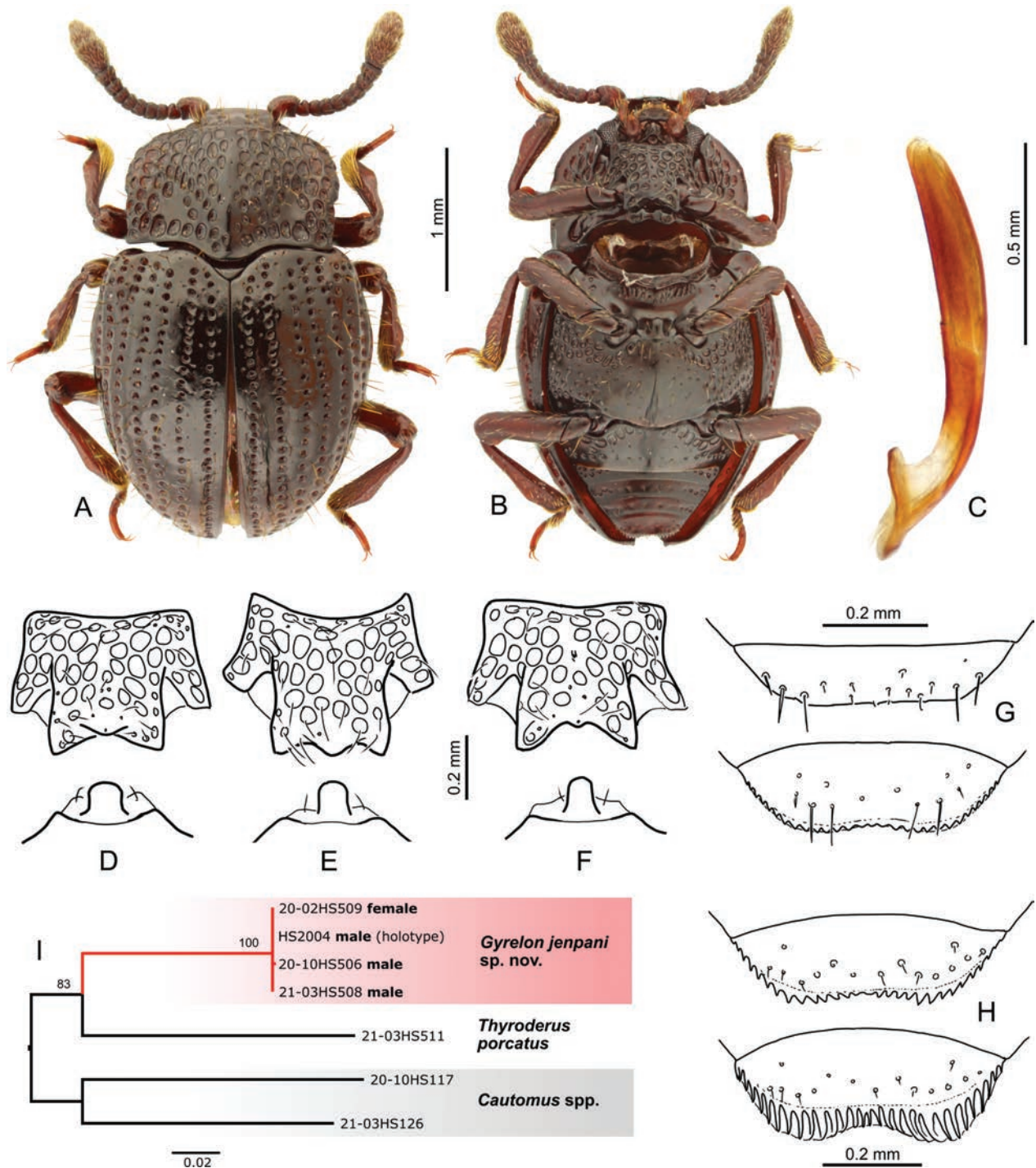


**Figure 2.** *Gyrelon jenpani* sp. nov. (Cerylonidae). **A, B.** Habitus (**A.** Dorsal view, female; **B.** Ventral view, male); **C.** Tegmen of the aedeagus; **D–F.** Variability of the shape of the prosternal process and metaventral process (**D, E.** Males; **F.** Female). Last abdominal ventrite in ventral and postero-ventral views (**G.** Male; **H.** Female); **I.** Maximum likelihood tree based on *cox1* barcodes of the sequenced Cerylonidae specimens.

each bearing erect seta; epipleuron present throughout elytral length, wide anteriorly, gradually narrowing posteriorly. Scutellar shield widely triangular. Metaventral process with a narrow median projection of variable shape. Metaventrite flat mesally, lateral portions with large closely adjacent punctures along posterior margin of mesocoxal cavities, otherwise with relatively small and widely separated punctures, each bearing a decum-

bent seta; interstices with mesh-like microsculpture. Metathoracic wings absent.

**Abdomen** with 5 visible ventrites, ventrite 1 with a row of large closely adjacent punctures along anterolateral margin, posterior part with a transverse series of minute punctures, each with a decumbent seta. Ventrites 2–5 each with a transverse series of minute punctures, each bearing a decumbent seta. Interstices of all ventrites with

fine mesh-like microsculpture. Ventrite 5 sexually dimorphic, with posterior margin nearly smooth in ventral view in male (finely crenulate in posteroventral view), and strongly crenulate in female (with a longitudinally ridged bar situated below apical part of elytral epipleuron).

**Legs** long and robust. Coxae and trochanters of all three pairs relatively small, coxa subglobular, trochanter subconical. Femora conical, with sparse erect setation, surface with mesh-like microsculpture. Tibiae flat, widening from base to apex, slightly more expanded in apical third, apical part with moderately dense erect setation; apical part of protibiae with an area of dense yellowish hair-like setae mesally. Tarsi with 4 tarsomeres, tarsomere 1 long and thick with dense long setae, tarsomeres 2–3 short, tarsomere 4 the longest.

**Male genitalia.** Aedeagus 1 mm long, simple, rod-like, without parameres, slightly widened at mid-length, rounded at apex.

**Etymology.** The species is dedicated to Dr. Jen-Pan Huang (Biodiversity Center, Academia Sinica, Taipei) as thanks for all his support of this project, including the possibility to work in his lab and for numerous inspiring discussions about evolution, diversity, and beetles.

**Distribution.** The species is so far only known from the type locality in central Taiwan.

**Notes on diagnostic characters.** Most previous studies use the form of the dorsal punctation and the shape of the prosternal process as the main diagnostic characters. Despite examining a few specimens only, we found both characters, especially the shape of the prosternal process, individually variable and/or dependent on the precise position of observation. The prosternal processes illustrated in Fig. 2D–F belong to the examined specimens whose conspecific identity was confirmed by the *cox1* barcode (Fig. 2I). A slight variation was also observed in the shape of the median projection of the metaventral process. In contrast, the character of the punctation of the metaventrite and abdominal ventrites seems to be much more distinct among species, and does not vary among the examined specimens of the new species.

## Archeocrypticidae

### *Sivacrypticus taiwanicus* Kaszab, 1964

Fig. 3

**Type material examined.** *Holotype*: female (HNMB): ‘Formosa, Sauter’, ‘Pilam, 908.II’. We have compared our specimens with the photos of the holotype provided to us by Gy. Makranczy in May 2023 (photos are available in the Zenodo Archive under <https://doi.org/10.5281/zenodo.10069183>).

**New material examined.** 1 male (NMNS): Taiwan: Nantou County, Huisun Forest Reserve, beginning of Wading trail, 24.0892139°N, 121.0297836°E, 700 m, 17.viii.2021, M. Fikáček & WR. Liang, stony disturbed forest on the slope, small leaf accumulations (DNA voucher: 21-08HS169); 1 unsexed specimen (NMPC): same

locality data, but 5.v.2019, Damaška, Fikáček, Hu & Liu lgt.; 1 female (NMNS): same locality data, but 28.ii.2021, Hu & Chen lgt. (DNA voucher: 21-03HS119); 1 male, 2 females, 3 unsexed specimens (NMNS, NMPC, BHC): Taiwan: Taichung, Wufeng, Beikeng Creek trail, 24.0451°N, 120.7827°E, 410 m, 24.v. 2023, lgt. F.S. Hu & Y.J. Chen, lowland tropical forest with large accumulation of leaf litter and sparse understory (TW2023-018, DNA voucher WF1-023 and additional non-sequenced specimens).

**Description of male genitalia.** Male genitalia 1 mm long. Median lobe thin, strongly bent in the lateral view, with a plate-like expansion on the apex. Tegmen small, freely movable along the median lobe; parameres in lateral view narrowly elongated, pointed at apex and moderately pubescent, in dorsal view plate-like, with a small indentation on lateral margin. Sperm pump present, large, bottle-like, with slightly coiled distal ductus.

**Comparison with the holotype.** Our specimens correspond to the holotype by all diagnostic characters, including body proportions, the coarse and complete series of punctures on elytra, the double-sized punctation on the pronotum, and the shape of the lateral pronotal margin. On the first view, the specimen in Fig. 3A has much weaker elytral series than the holotype. The additional specimens examined, in which most of the dorsal setation was abraded in the same way as in the holotype, prove that the character of the elytra is in fact identical. In the original description (Kaszab 1964), as well as in subsequent revisions of the genus (Kaszab 1979, 1981), the lateral pronotal ridge of *S. taiwanicus* was mentioned as narrow and not widening anteriorly. This stands in contrast to the character state in the holotype as well as in our specimens: the lateral pronotal ridge is, in fact, gradually widening from the base to anterior margin of the pronotum and bends inwards and merges with the anterior margin of the pronotum anteriorly. This fact also corresponds to the illustration of *S. taiwanicus* by Kaszab (1964) in which the anteriorly widening lateral ridge of the pronotum is clearly seen.

**Comparison with other species.** The previously unknown male of *S. taiwanicus* allows us to compare the male genitalia of the species (type species of *Sivacrypticus*) with those illustrated for other species of the genus. The male genitalia of *S. taiwanicus* are very distinct from the genitalia of most described species by (1) small tegmen, (2) strongly elongated median lobe, and (3) strongly expanded parameres in dorsal view. Its genitalia are, however, very similar to those of *S. philippinus* Merkl, 1988 from Luzon (Manila), but clearly differ from them by the apical expansion of the median lobe in lateral view, and in a less lobate shape of the parameres in dorsal view.

**Distribution.** The species was described from ‘Pilam’ (= Beinan township, Taitung County, southern Taiwan). The sequenced specimens examined by us are from lowland to lower montane forest in central Taiwan (Taichung and Nantou Counties), indicating that the species is likely widespread in lowland and lower montane forests at least in central and southern Taiwan.

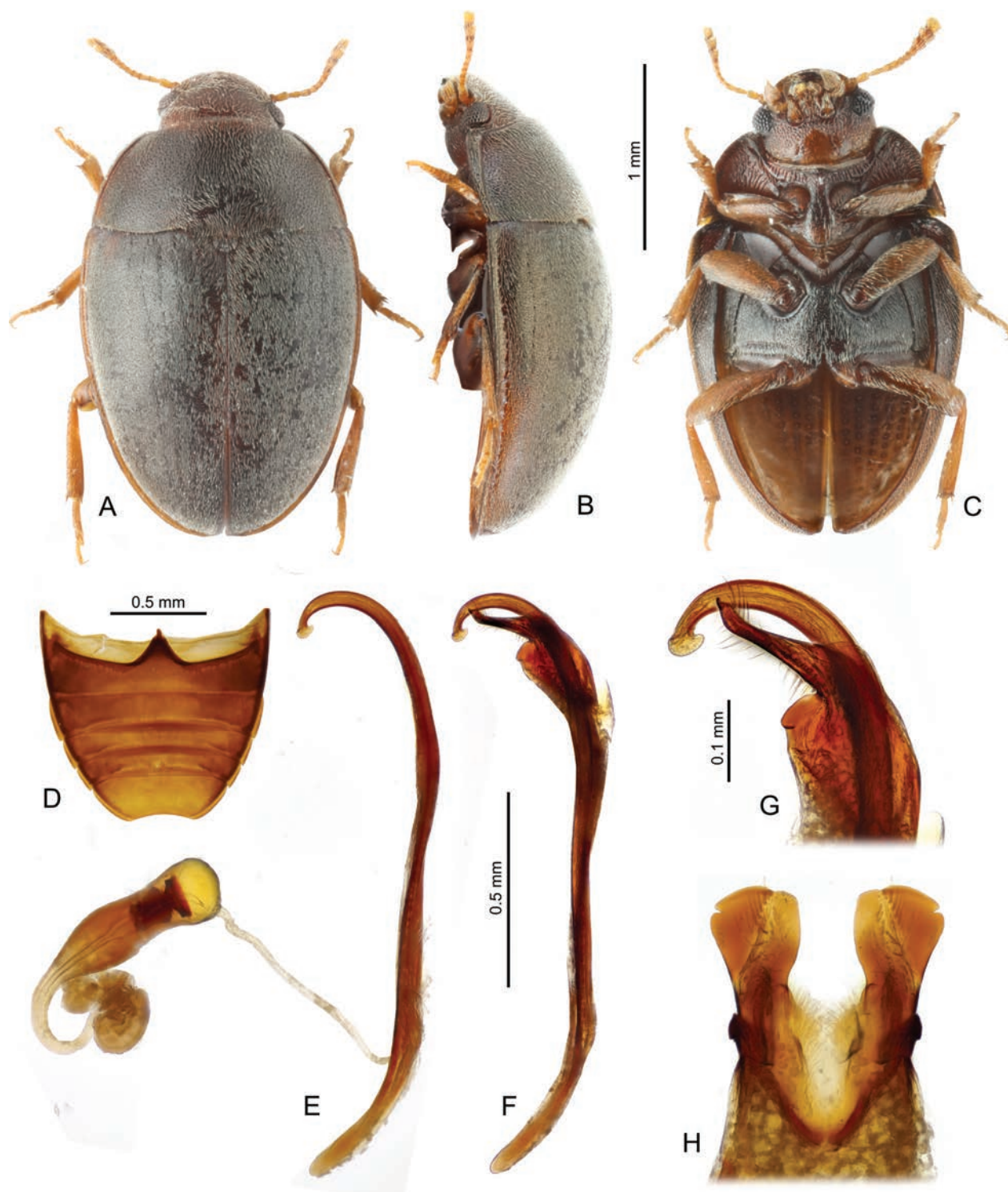


**Figure 3.** *Sivacrypticus taiwanicus* Kaszab, 1964 (Archeocrypticidae). A–C. Habitus (A. Dorsal; B. Lateral; C. Ventral); D. Abdominal ventrites, male; E–H. Male genitalia (E. Median lobe and the sperm pump, lateral view; F. Median lobe and parameres, lateral view; G. Detail of median lobe and parameres, lateral view; H. Detail of parameres, dorsal view).

#### *New records for Taiwan*

Since the leaf litter fauna of Taiwan has never been studied in detail, even our small starting dataset from the single area in central Taiwan results in many new records for Taiwan at species, genus or even family levels. Below we concisely report these new records, despite the

species-level taxonomic treatment of most of them requiring additional study. The material examined is only listed for taxa identified down to species, for genus-level records, it can be found in the Excel sheet with the complete data (Suppl. material 2). List of all species recorded in this project and identified down to genus or species is available in the Appendix 1.

**Carabidae*****Oodes (Lachnocrepis) japonicus* (Bates, 1873) (Liciniinae: Oodini)**

**Material examined.** 1 female (IDL): Taiwan: Nantou County, Huisun Forest reserve, track to Xiaochushan Mt., 24.0847025°N, 121.0274161°E, 1000 m, 20.vi.2020, F.S. Hu lgt., mixed *Cryptomeria* + sparse broadleaf forest on the slope (voucher 20-06HS304); 1 spec. (IDL): Taiwan: Nantou County, Huisun Forest res., Wading trail, 24.0892139°N, 121.0297836°E, 700 m, 17.viii.2021, M. Fikáček & W.R. Liang lgt., stony forest on the slope, small leaf accumulations (voucher 21-08HS115). 9 spec. (IDL): Taiwan: Kaohsiung City, Zuoying district (左營區), Ban-pingshan (半屏山), SW slope, 22.694262 120.305072, 100 m, 22.vii.2021, M. Fikáček lgt. (TW2021-06d), sifting of large to shallow leaf accumulations with some wood and fungi in the forest with *Ficus* in karst area (incl. voucher BP1-001); 17 spec. (IDL): same area and date but 90 m, 22.693469, 120.304979 (TW2021-06f) (incl. DNA voucher BP3-001); 8 spec. (IDL): same area, 90 m, 22.693469, 120.304979, 11.viii.2022, M. Fikáček lgt. (TW2022-006A) (incl. DNA voucher BP4-010); 2 spec. (IDL): same area and date, 100 m, 22.693469, 120.304979 (TW2022-006B) (incl. DNA voucher BP7-010); 1 spec. (IDL): same area, 22.693469, 120.304979, 90 m, 30.v.2023, M. Fikáček lgt. (TW2023-015, DNA voucher BP10-002); 1 spec. (IDL): same area, 22.694262, 120.305072, 90 m, 30.v.2023, M. Fikáček lgt. (TW2023-016, DNA voucher BP9-003).

**Comments.** Multiple species and genera of the Oodini are reported from Japan or southern China (Guéorguiev 2014; Löbl and Löbl 2017; Guéorguiev and Liang 2020), with only *Oodes desertus* Motschulsky, 1858 reported from Taiwan so far (Guéorguiev and Liang 2020). The species barcoded here belongs to *Oodes (Lachnotrepis)* based on the width of elytral interval 7 and 8 and setation of tarsomeres, and corresponds to *O. japonicus* based on all characters in the identification key by Guéorguiev and Liang (2020). The species is widespread from the Russian Far East through China and Japan to Laos and Vietnam (Guéorguiev and Liang 2020). It is recorded from Taiwan for the first time; based on our data it may be widespread in lowland to lower montane forests of central and southern Taiwan. For larval morphology, see below.

**Histeridae*****Anaples Horn, 1873* (Dendrophilinae: Anapleini)**

**Comments.** The genus was first recorded from Taiwan by Bickhardt (1913) based on *A. stigmaticus* (Schmidt, 1892). Mazur (2007) mentioned that this record might be based on a misidentification and removed the genus and species from his updated list of the Histeridae of Taiwan. The specimen sequenced here is morphologically different from *A. stigmaticus*; its identification will be done in the future.

**Leiodidae*****Dermatohomoeus* sp.**

**Material examined.** 4 females (ZSPC): Taiwan: Nantou County Huisun Forest reserve, track to Xiaochushan Mt., 24.0744602°N, 121.0366337°E, 1150 m, 24.ii.2020, F.S. Hu lgt., primary forest on the slope with sparse understory: sifting of small leaf accumulations (incl. DNA voucher 20-02HS511); 17 females (ZSPC): same locality, 20.vi.2020, F.S. Hu lgt. (incl. DNA voucher 20-06HS519); 31 females (ZSPC): same locality, 11.x.2020, F.S. Hu & Y.J. Chen lgt. (incl. DNA voucher 20-10HS521); 19 females (ZSPC): same locality, 16.viii.2021, M. Fikáček & W.R. Liang lgt. (incl. voucher 21-08HS526); 1 female (ZSPC): same locality, 1.iii.2021, M. Fikáček, F.S. Hu & G.J. Peng lgt. (voucher 21-03HS507); 10 females (ZSPC): same locality, 4.v.2019, M. Fikáček, F.S. Hu, A. Damaska & H.C. Liu lgt. (incl. DNA voucher HS1020); 4 females (ZSPC): Taiwan: Nantou County, Huisun Forest reserve, track to Xiaochushan Mt., 24.0847025°N, 121.0274161°E, 1000 m, 16.viii.2021, mixed *Cryptomeria* + sparse broadleaf forest on the slope, 16.viii.2021, M. Fikáček & W.R. Liang lgt. (incl. DNA voucher 21-08HS339); 1 female (ZSPC): same locality, 20.vi.2020, F.S. Hu lgt. (voucher 20-06HS317); 1 female (ZSPC): same locality, 11.x.2020, F.S. Hu & Y.J. Chen lgt. (voucher 20-10HS310); 8 females (ZSPC): Taiwan: Nantou County, Huisun Forest Reserve, Xiaochushan Mt. track, 0.5 km above hotels 24.0887444°N, 121.0355063°E, 850 m, 4.v.2019; Damaška, Fikáček, Hu & Liu lgt.; large accumulations of leaf litter in a small gorge with lower montane/lowland broad-leaf forest (incl. voucher HS4031); 2 females (ZSPC): Taiwan: Nantou County, Huisun Forest res., Wading trail, 24.0892139°N, 121.0297836°E, 700 m, 28.ii.2020, F.S. Hu & Y.J. Chen lgt., stony forest on the slope, small leaf accumulations (incl. DNA voucher 21-03HS120); 1 female (ZSPC): same locality, 5.v.2019, M. Fikáček, F.S. Hu, A. Damaska & H.C. Liu lgt. (DNA voucher HS5013).

**Comments.** The genus is newly recorded from Taiwan in the present paper. The previous records of the genus from Taiwan are based on the transfer of *Colenisia miyatakei* (Hisamatsu, 1985) to the *Dermatohomoeus* by Hoshina (1999) that is however not supported by diagnostic characters of *Dermatohomoeus* (Švec 2022). Consequently, *Dermatohomoeus* has not been reported from Taiwan before. All DNA-barcoded specimens from the Huisun Reserve are conspecific, and the examination of additional non-sequenced specimens confirms that all collected specimens are conspecific. Yet, they cannot be identified to species, as all of them are females (in total 99 specimens from 12 collecting events at four different collecting sites). The species of the genus are morphologically uniform, with species-specific characters being the shape of the aedeagus, including

the endophallus. Female genitalia and the spermatheca of *Dermatohomoeus* species are of the unique shape within the tribe Pseudoliadini but lack species-specific morphological features. External morphological characters detectable in *Dermatohomoeus* females are hardly sufficient for species identifications. The population of *Dermatohomoeus* consisting exclusively of females found in this study is not the first case of the absence of males. No males have been found so far for *Dermatohomoeus terrenus* (Hisamatsu, 1985), despite altogether several dozen specimens attributed to this species having been examined (Hisamatsu 1985; Hoshina 1999; Park and Ahn 2007; Švec 2022). The species is known from the Japanese islands of Honshu, Shikoku, Kyushu, Izu, Goto, from four Ryukyus islands (Hoshina 1999) and the Awaji Island (Švec 2022). Besides them, the species was recorded also from southern Korea (Park and Ahn 2007). Hoshina (1999) published a hypothesis that *D. terrenus* may be a parthenogenetic species. Perhaps, this type of reproduction is more widespread in *Dermatohomoeus* species or their populations, including those occurring in Taiwan.

### Staphylinidae

#### *Drusilla obliqua* (Bernhauer, 1916) (Aleocharinae: Lomechusini)

**Material examined.** 12 spec. (FSHC, IDL): same locality, 20.vi.2020, lgt. F.S. Hu (voucher 20-06HS129, and non-extracted specimens); 1 spec. (IDL): same locality, 17.viii.2021, lgt. M. Fikáček & W.R. Liang (voucher 21-08HS133).

**Comments.** *Drusilla obliqua* is a widespread species; it has been recorded from India, Nepal, Myanmar, China (Yunnan), Vietnam and Malaysia (Assing 2017, 2019). The species is newly recorded from Taiwan in the present paper.

#### *Paraploderus* cf. *thailandicus* Makranczy, 2016 (Oxytelinae: Thinobiini)

Fig. 4

**Material examined.** 16 spec. (HNHM, IDL): TAIWAN: Nantou County Huisun Forest reserve, track to Xiaochushan Mt., 24.0744602°N, 121.0366337°E; 1150 m 11.x.2020; Hu & Chen lgt., primary forest on the slope with sparse understory: sifting of small accumulations of leaves (DNA voucher 20-10HS531 and non-extracted specimens). 13 spec. (MHNG): TAIWAN: Taoyuan Co. Twnsh.Fushing S-BaLing km 54, road 7, 22.ii.2010 1140m, decaying wood + forest litter, leg. S. Vit #2; 3 spec. (MHNG): TAIW: Chiayi County Alishan Natural Scenic Area, 11.iv.2009 2350m, leg. S. Vit #18//Road 18, km 02 Old Lulin Tree Track, decaying Wood litter #18.

**Comments.** The genus is newly recorded from Taiwan in the present paper. György Makranczy examined the specimens of this *Paraploderus* species from

Taiwan already earlier, based on the material collected by S. Vít deposited in MHNG (see under Material examined). The male genitalia of these specimens (Fig. 4) show rather slight differences from those of *Paraploderus thailandicus* Makranczy, 2016. Therefore, it requires confirmation whether the Taiwanese populations represent a distinct species or not. This is best done by a comparison of DNA sequences from Taiwan and the mainland, including Thailand from where the species was described.

#### *Thinocharis* Kraatz, 1859 (Paederinae: Lathrobiini)

**Comments.** The genus is newly recorded from Taiwan in the present paper. The species identification will need to be done in the future.

#### Tribe Trichonychini (Pselaphinae)

**Comments.** The tribe is newly recorded from Taiwan in the present paper, as well as the supertribe Euplectitae. There are at least two species in our samples. A generic revision of the Trichonychini needs to be done before the confirmation of the generic identifications.

#### Tribe Ctenistini (Pselaphinae)

**Comments.** The tribe is here newly recorded from Taiwan. The generic revision of the Ctenistini needs to be done before the confirmation of the generic identifications.

#### Tribe Bythinoptectini (Pselaphinae)

**Comments.** The tribe, as well as the supertribe Euplectitae, are newly recorded from Taiwan here. There are at least two species in our samples.

#### *Batraxis* Reitter, 1882 (Pselaphinae: Brachyglutini)

**Comments.** The genus was listed for Taiwan in the Catalogue of Life, based on the occurrence of *B. obesa* Raftery, 1894 (Chung and Shao 2022). However, the source of the record was online only and the link is not available anymore. We formally record the genus from Taiwan for the first time.

#### *Cephennodes* Reitter, 1884 (Scydmaeninae: Cephenniini)

**Comments.** The genus is newly recorded from Taiwan in the present paper. The species identification will be done in the future.

#### *Napocconnus* Franz, 1957 (Scydmaeninae: Stenichnini)

**Comments.** The genus has been newly recorded from Taiwan in the present paper. The species identification will need to be done in the future.

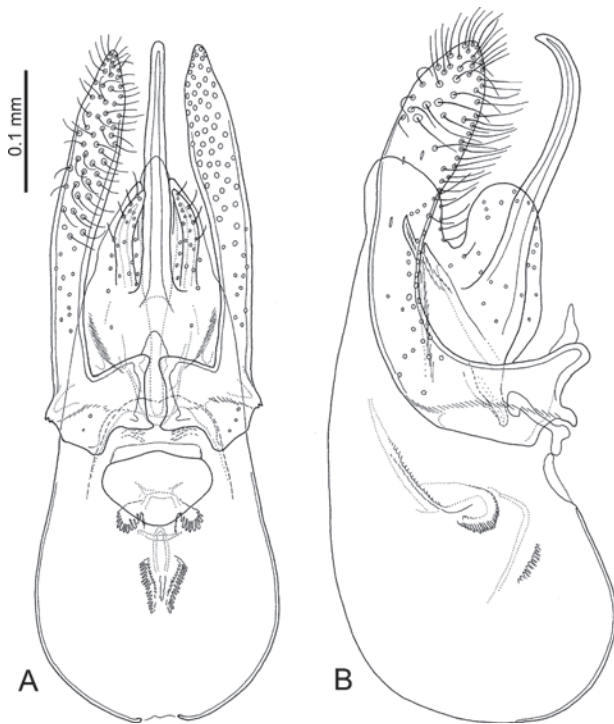


**Figure 4.** Male genitalia of *Paraploderus* cf. *thailandicus* Makranczy, 2016 from Taiwan. **A.** Frontal view (parameral setation shown on the left); **B.** Lateral view.

## Cerylonidae

### *Thyroderus porcatus* Sharp, 1885 (Ceryloninae)

**Material examined.** 2 spec. (FSHC, IDL): Taiwan: Nantou County, Huisun Forest reserve, track to Xiaochushan Mt., 24.0744602°N, 121.0366337°E; 1150 m, 1.iii.2021, M. Fikáček, F.S. Hu & G.J. Peng lgt. (voucher 21-03HS511 and an additional non-sequenced specimen).

**Comments.** The species was only known from Japan previously (Löbl and Smetana 2007), representing the only species of the genus that occurred in the Palearctic region. The genus and the species are newly recorded from Taiwan.

### *Cautomus* Sharp, 1885 (Ceryloninae)

**Comments.** The genus is newly recorded from Taiwan in this study based on two species from the Huisun Forest Reserve. Both species differ both by the DNA barcode sequences and morphologically. The species identification will be done in the future.

## Sphindidae

### *Aspidiphorus* Ziegler, 1821

**Comments.** The family and genus are newly recorded from Taiwan. There are two species in our Huisun samples identified by the DNA barcode sequences; their species identification needs to be done in the future.

## Latridiidae

### *Bicava* Belon, 1884

**Comments.** The genus is newly recorded from Taiwan in the present paper. The species identification will be done in the future.

### *Cartodere* sp.

**Comments.** The genus was first recorded from Taiwan by Yao et al. (2011) based on *C. (s. str.) constricta* (Gyllenhal, 1827). The specimens sequenced in this study differ from *C. (s. str.) constricta* by having three antennomeres clubbed (in contrast to two clubbed antennomeres in *C. constricta*). The species identification will be done in the future.

## Curculionidae

### *Otibazo* Morimoto, 1961

**Comments.** The genus is newly recorded from Taiwan in the present paper. An extensive taxonomic study on this genus in Taiwan is in preparation and will be published in the near future (Wei-Zhe Tseng, in prep.).

### *Seleuca* Pascoe, 1871

**Comments.** The genus is newly recorded from Taiwan in the present paper. The species identification needs to be completed in the future.

### *Acallinus* Morimoto, 1962

**Comments.** The genus is newly recorded from Taiwan in the present paper. Based on the DNA barcodes, the samples reported here (Taiwan: Nantou County, Huisun Forest Reserve) contain two or three species. The species identification needs to be done in the future.

### *Coccotrypes advena* Blandford, 1894

**Material examined.** 1 female (IDL): Taiwan: Nantou County, Huisun Forest reserve, track to Xiaochushan Mt., 24.0826139°N, 121.0315869°E; 1050 m, 4.v.2019, Damaška, Fikáček, Hu & Liu lgt., sparse secondary forest with dense understory incl. tree ferns on the margin of a tree plantation (voucher HS2015); 1 female (IDL): Taiwan: Nantou County, Huisun Forest res., Xiaochushan Mt. track, 0.5 km above hotels 24.0887444°N, 121.0355063°E, 850 m, 4.v.2019; Damaška, Fikáček, Hu & Liu lgt., large accumulations of leaf litter in a small gorge with lower montane/lowland broad-leaf forest (voucher HS4007); 4 females (IDL): Taiwan: Nantou County, Huisun Forest reserve, Wading trail, 24.0892139°N, 121.0297836°E, 700 m, 11.x.2020, F.S.Hu & Y.J.Chen lgt. (incl. voucher 20-10HS114); 2 females (IDL): same locality, 17.viii.2021, M. Fikáček & W.R. Liang lgt. (incl.

voucher 21-08HS170); 1 female (IDL): Taiwan: Nantou County, Huisun Forest reserve, track to Xiaochushan Mt., 24.0847025°N, 121.0274161°E, 1000 m, 11.x.2020, F.S.Hu & Y.J.Chen lgt. (voucher 20-10HS308); 1 female (IDL): Taiwan: Nantou County, Huisun Forest reserve, track to Xiaochushan Mt., 24.0744602°N, 121.0366337°E, 1150 m, 16.viii.2021, M. Fikáček & W.R.Liang lgt. (voucher 21-08HS559).

**Comments.** This is a generalist seed-boring scolytine species widespread in SE Asia, Australia and Oceania, America from Florida through the Caribbean to Suriname (Wood and Bright 1992; Bright 2021) and also recorded from Africa (Uganda: Jordal et al. 2002). In Asia, it has been recorded from India, Sri Lanka, Thailand, Vietnam, Indonesia, Malaysia, the Philippines, and Japan; here we are recording it from Taiwan for the first time. Jordal et al. (2002) report a high intraspecific variation of *cox1* sequences, possibly indicating that it represents a complex of species. The *cox1* sequences of our specimens cluster with those of the Japanese specimen sequenced by Jordal et al. (2002) (uncorrected *p*-distance to the Japanese specimen: 0.7–1.6%).

#### Examples of larvae associated with adults

#### Carabidae

#### *Oodes (Lachnocrepis) japonicus* (Bates, 1873) (Licininae: Oodini)

Fig. 5

**Material examined.** Larvae: 1 larva (IDL): Taiwan: Nantou County, Huisun Forest res., Wading trail, 24.0892139°N, 121.0297836°E, 700 m, 20.vi.2020, F.S. Hu lgt., stony forest on the slope, small leaf accumulations (voucher 20-06HS179); 1 larva (IDL): Taiwan: Nantou County, Huisun Forest reserve, track to Xiaochushan Mt., 24.0847025°N, 121.0274161°E, 1000 m, 16.viii.2021, M. Fikáček & W.R. Liang lgt., mixed *Cryptomeria* + sparse broadleaf forest on the slope (voucher 21-08HS350). Adults: see above under New records for Taiwan.

**Comments.** The knowledge on larval morphology of the Oodini is quite limited so far, with larvae of several species of *Oodes* Bonelli, 1810 described and illustrated (van Emden 1942; Lindroth 1942; Chu 1945; Thomson 1979); the larva of an unidentified North American *Oodes* illustrated by Chu (1945) differs from others in very narrow mandibles, transverse head, multidentate nasale and frontale reaching posterior margin of the head, and may actually represent a different taxon than *Oodes* or Oodini. The larva of *Oodes (Lachnocrepis) japonicus* corresponds to *Oodes* s.str. larvae illustrated by van Emden (1942) and Lindroth (1942) by general morphology, but differs from them in the shape of the nasale (*O. japonicus* with 4 sharp teeth, compared to 3 or 5 low rounded teeth in *O. helopioides* and *O. gracilis*, respectively), more slender mandibles, shorter and more robust antennomeres, and wider and more robust labial palpomere 2.

#### *Perigona cf. nigriceps* Dejean, 1831 (Lebiinae: Perigonini)

Fig. 6

**Material examined.** Larvae: 2 larvae (IDL): Taiwan: Nantou County, Huisun Forest reserve, track to Xiaochushan Mt., 24.0847025°N, 121.0274161°E, 1000 m, 20.vi.2020, F.S. Hu lgt., mixed *Cryptomeria* + sparse broadleaf forest on the slope (voucher 20-06HS344 and one additional specimen). Adults: 1 spec. (IDL): same locality, date and collector (voucher 20-06HS305); 1 spec. (IDL): same locality but 16.viii.2021, M. Fikáček & W.R. Liang lgt. (voucher 21-08HS313).

**Comments.** *Perigona* Laporte, 1835 is a species-rich world-wide genus (e.g., Baehr 2014) with larva only illustrated for *P. (Xenogona) termitis* Jeannel, 1941 (Jeannel 1941, 1942). Sequenced and examined adult specimens from Huisun belong to the subgenus *Trechicus* LeConte, 1853 based on the triangular arrangement of the subapical elytral punctures. Genetically it stands close (uncorrected *p*-distance 6.4–6.6%) but does not cluster with available sequences of the world-wide invasive *P. nigriceps* Dejean, 1831 for which DNA barcodes are available from Europe, Africa, South America, the Caribbean and New Zealand in the BOLD database (these moreover form two separate clusters). The larva examined and illustrated here corresponds to that of *P. termitis* in all characters including the multidentate slightly projecting nasale; it slightly differs from the larva of *P. termitis* by more robust labial palpomere 1.

#### Ptilodactylidae: Ptilodactylinae

#### *Ptilodactyla* sp.

Fig. 7

**Material examined.** Larvae: 3 larvae (IDL): Taiwan: Nantou County, Huisun Forest reserve, Wading trail, 24.0892139°N, 121.0297836°E, 700m, 24.ii.2020, F.S. Hu lgt., stony disturbed forest on the slope, small leaf accumulations (incl. sequenced voucher 20-02HS155). Adults: 3 adults (NMPC): same locality, 5.v.2019, Damaška, Fikáček, Hu & Liu lgt. (2019-TW18) (incl. sequenced voucher HS5011).

**Comments.** Larvae of *Ptilodactyla* Illiger, 1807 have been mentioned and illustrated by numerous authors (e.g., Costa et al. 1988), including that of *P. exotica* Chapin, 1927 which is introduced with tropical plants in the USA and Europe (e.g., Aberlenc and Allemand 1997; Mann 2006; Viñolas et al. 2020). Here we are concisely illustrating the sequenced larva of *Ptilodactyla* from subtropical lowland forest in central Taiwan. The examined specimen has clearly visible proventriculus armored with numerous spines (Fig. 7A), a structure not yet documented for larval Ptilodactylidae; we suppose this may be an adaptation for processing the food, indicating that *Ptilodactyla* larvae likely feed also on decaying wood and detritus, not only on plant roots as stated by some authors (e.g., Lawrence 2005).

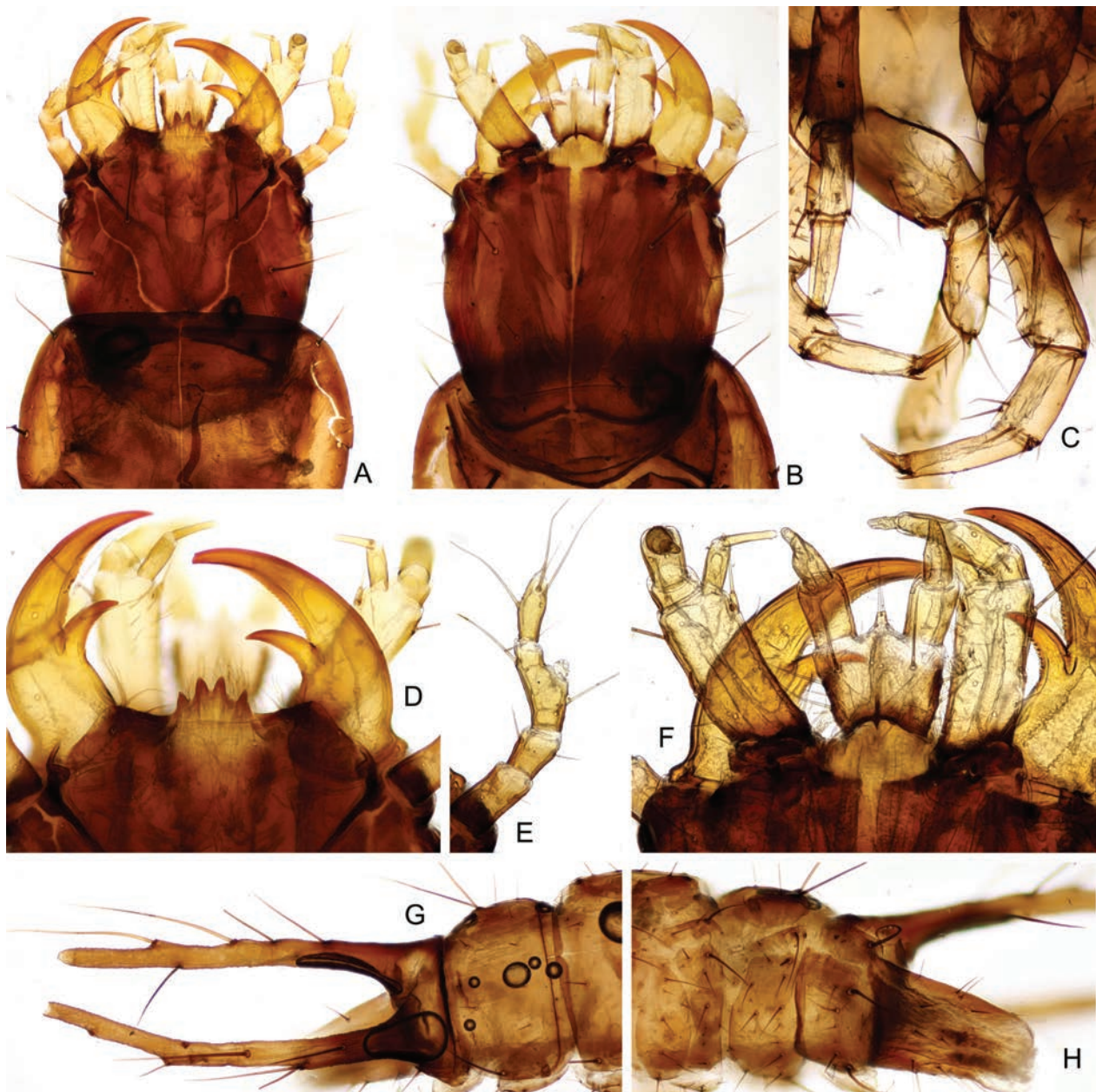


**Figure 5.** Carabidae: Oodini: larva of *Oodes* (*Lachnocrepis*) *japonicus* (Bates, 1873) (OTU159, voucher 20-08HS350) associated with adults by DNA. **A, B.** Head (**A.** Dorsal view; **B.** Ventral view); **C.** Middle and hind legs; **D.** Nasale and mandibles, dorsal view; **E.** Antenna, dorsal view; **F.** Mouthparts, ventral view; **G, H.** Abdominal apex (**G.** Dorsal view; **H.** Ventral view).

### Cantharidae: Malthininae

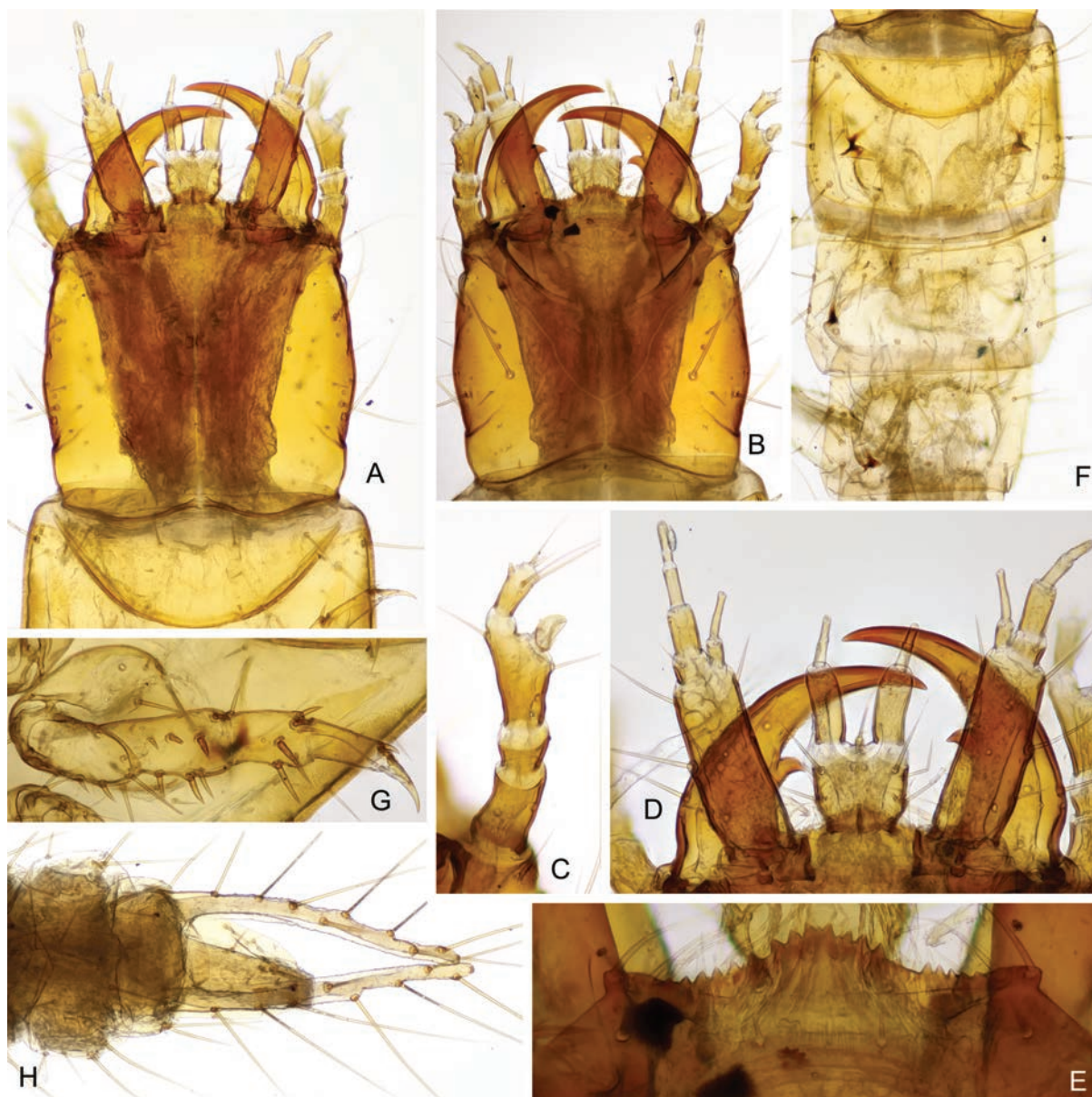
#### *Maltypus ryukyuanus* Wittmer, 1970 (Malthodini)

Fig. 8

**Material examined.** Larva: 1 larva (IDL): Taiwan: Nantou County, Huisun Forest reserve, track to Xiaochushan Mt., 24.0826139°N, 121.0315869°E; 1050 m, 4.v.2019; Damaška, Fikáček, Hu & Liu lgt., sparse secondary forest with dense understory incl. tree ferns on the margin of a tree plantation: sifting (2019-TW15) (sequenced voucher HS4055L). Adult: 1 specimen (IDL): Taiwan: Nantou County, Huisun Forest reserve, track to Xiaochushan Mt., 24.0847025°N, 121.0274161°E, 1000 m, 20.vi.2020, F.S. Hu lgt., mixed conifer/broadleaf for-

est + sparse broadleaf forest on the slope (sequenced voucher 20-06HS319).

**Comments.** In Malthininae, larvae are only known for two genera, *Malthinus* Latreille, 1806 (Malthinini) and *Malthodes* Kiesenwetter, 1852 (Malthodini), with the data about their morphology are scattered. Klausnitzer (1997) assembled all the data and proposed a key to species. Fitton (1976) presented the similarities and differences between both genera. The examined larva of *Maltypus* Motschulsky, 1860 is similar to that of *Malthodes* sp. illustrated by Fitton (1976) in the shape of the median tooth of nasale and the absence of setae on the median tooth, but resembles the larva of *Malthinus* in the inner tooth of the mandible situated more basally. The larva of *Maltypus* is illustrated for the first time here.



**Figure 6.** Carabidae: Perigonini: larva of *Perigona* cf. *nigriceps* Dejean, 1831 (OTU158, voucher 20-06HS344) associated with adults by DNA. **A, B.** Head (**A.** Ventral view; **B.** Dorsal view); **C.** Antenna; **D.** Mouthparts, ventral view; **E.** Nasale; **F.** Thorax, dorsal view; **G.** Middle leg; **H.** Abdominal apex.

### Staphylinidae Aleocharinae

#### *Drusilla obliqua* (Bernhauer, 1916) (Lomechusini)

Fig. 9

**Material examined.** Larvae: 2 larvae (IDL): Taiwan: Nantou County, Huisun Forest res., Wading trail, 24.0892139°N, 121.0297836°E, 700 m, 30.vi.2020, F.S. Hu lgt., stony forest on the slope, small leaf accumulations (vouchers 20-06HS176 and 20-06HS187); 2 larvae (IDL): same locality but 17.viii.2021, M. Fikáček & W.R. Liang lgt. (vouchers 21-08HS152 and 21-08HS153). Adults: 1 spec. (IDL): same locality, 20.vi.2020, lgt. F.S. Hu (voucher 20-06HS129); 1 spec. (IDL): same locality, 17.viii.2021, lgt. M. Fikáček & W.R. Liang (voucher 21-08HS133).

**Comments.** Larvae of two species of *Drusilla* Leach, 1819 have been described: *Drusilla canaliculata* (Fabricius, 1787) (Paulian 1941; Topp 1978; Schminke 1982) and *D. italica* (Bernhauer, 1903) (De Marzo 2007). Larvae of all species of *Drusilla* are very similar and further comparisons are needed to distinguish them.

#### *Myrmecocephalus brevisulcus* (Pace, 2008) (Falagriini)

Fig. 10

**Material examined.** Larvae: 1 larva (IDL): Taiwan: Nantou County, Huisun Forest res., Wading trail, 24.0892139°N, 121.0297836°E, 700 m, 20.ii.2020, F.S. Hu lgt., stony forest on the slope, small leaf accumulations (voucher 20-02HS154); 2 larvae (IDL): same locality but 11.x.2020, F.S. Hu & Y.J. Chen lgt. (vouchers 20-10HS163–164); 1 larva

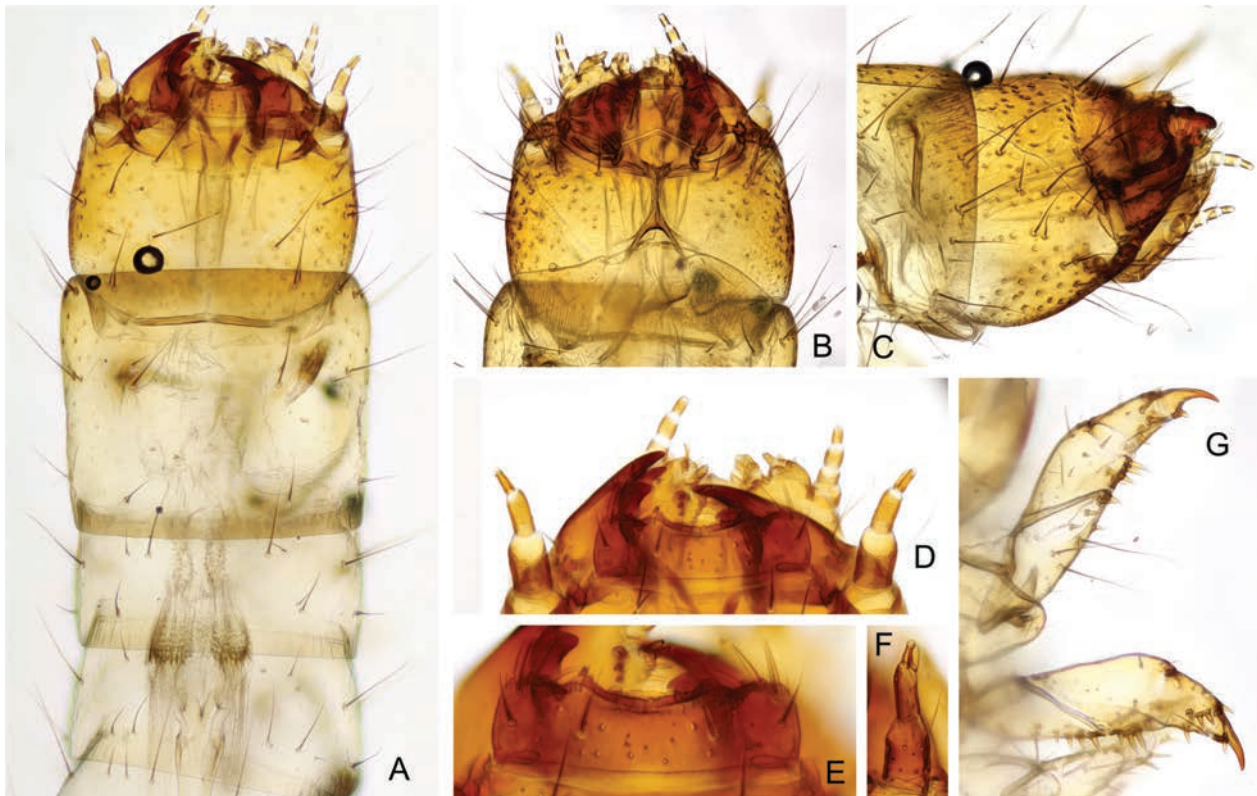


**Figure 7.** Ptilodactylidae: larva of *Ptilodactyla* sp. (OTU83, voucher 20-02HS155) associated with adults by DNA. **A.** Head and thorax in dorsal view; **B.** Head, ventral view; **C.** Head, lateral view; **D.** Anterior part of the head, dorsal view; **E.** Detail of labrum; **F.** Antenna in lateral view; **G.** Front and middle leg.

(IDL): same locality but 28.ii.2021, F.S. Hu & Y.J. Chen lgt. (voucher 21-03HS157); 1 larva (IDL): same locality but 5.v.2019, Fikáček, Hu, Damaška & Liu lgt. (voucher HS5071L); 1 larva (IDL): Taiwan: Nantou County, Huisun Forest reserve, track to Xiaochushan Mt., 24.0847025°N, 121.0274161°E, 1000 m, 4.v.2019; Damaška, Fikáček, Hu & Liu lgt., mixed conifer/broadleaf forest + sparse broadleaf forest on the slope (2019-TW16) (voucher HS3067L); 1 larva (IDL): same locality but 20.vi.2020, F.S. Hu lgt. (voucher 20-06HS348); 1 larva (IDL): Taiwan: Nantou County, Huisun Forest reserve, track to Xiaochushan Mt., 24.0744602°N, 121.0366337°E, 1150 m, 20.vi.2020, F.S. Hu lgt., oldgrown secondary forest on the slope with sparse understory (voucher 20-06HS573); 1 larva (IDL): same locality but 11.x.2020, F.S. Hu & Y.J. Chen lgt. (voucher 20-10HS563). Adults: 1 adult (FSHC): Taiwan: Nantou County, Huisun Forest res., Wading trail, 24.0892139°N, 121.0297836°E, 700 m, 20.ii.2020, F.S. Hu lgt., stony forest on the slope, small leaf accumulations (voucher 20-02HS132); 1 adult (FSHC): same locality but 20.vi.2020 (voucher 20-06HS130); 1 adult (FSHC): same locality but 11.x.2020, F.S. Hu & Y.J. Chen lgt. (voucher 20-10HS135); 1 adult (IDL): same locality but 28.ii.2021, F.S. Hu & Y.J. Chen lgt. (voucher 21-03HS139); 1 adult (IDL): Taiwan: Nantou County, Huisun Forest reserve, track to Xiaochushan Mt., 24.0744602°N, 121.0366337°E, 1150 m, 20.vi.2020, F.S. Hu lgt., oldgrown secondary forest on the slope with sparse understory (voucher 20-06HS533);

1 adult (IDL): same locality but 11.x.2020, F.S. Hu & Y.J. Chen lgt. (voucher 20-10HS529); 1 adult (IDL): same locality but 16.viii.2021, M. Fikáček & W.R. Liang lgt.

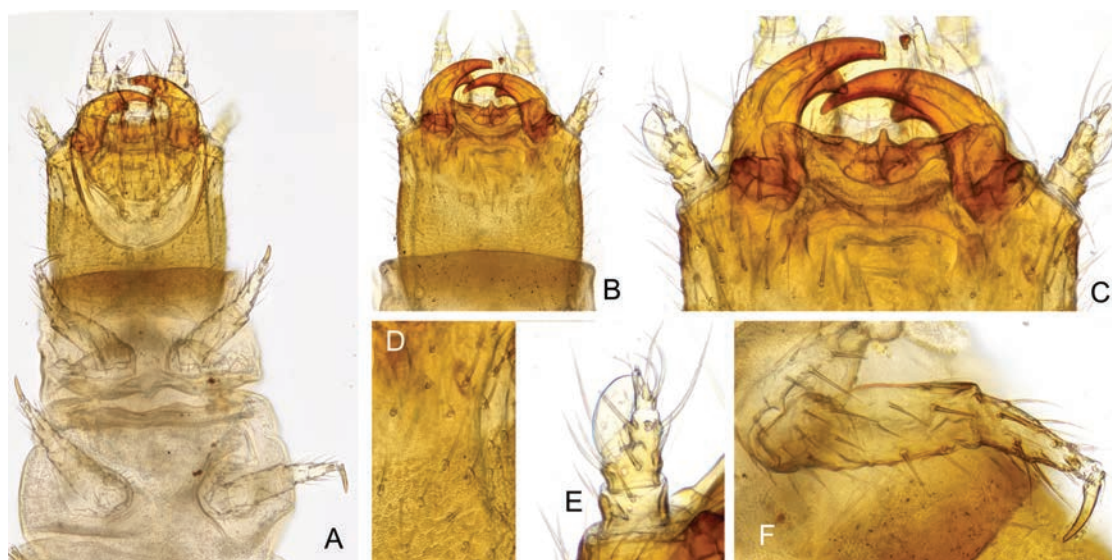
**Comments.** Larvae of several genera of Falagriini have been described or illustrated, including *Cordalia* Jacobs, 1925, *Falagria* Leach, 1819 and *Myrmecopora* Saulcy, 1864 (Topp 1978; De Marzo 2000, 2002, 2008, 2009). The larva of *Myrmecocephalus brevisulcus* is similar to that of *Myrmecopora* by the posterior part of the head becoming remarkably narrower. *Myrmecocephalus* can be distinguished from the *Myrmecopora* by the longer and stouter first antennal segment. The larva of *Myrmecocephalus* is illustrated for the first time here.

### Staphylininae

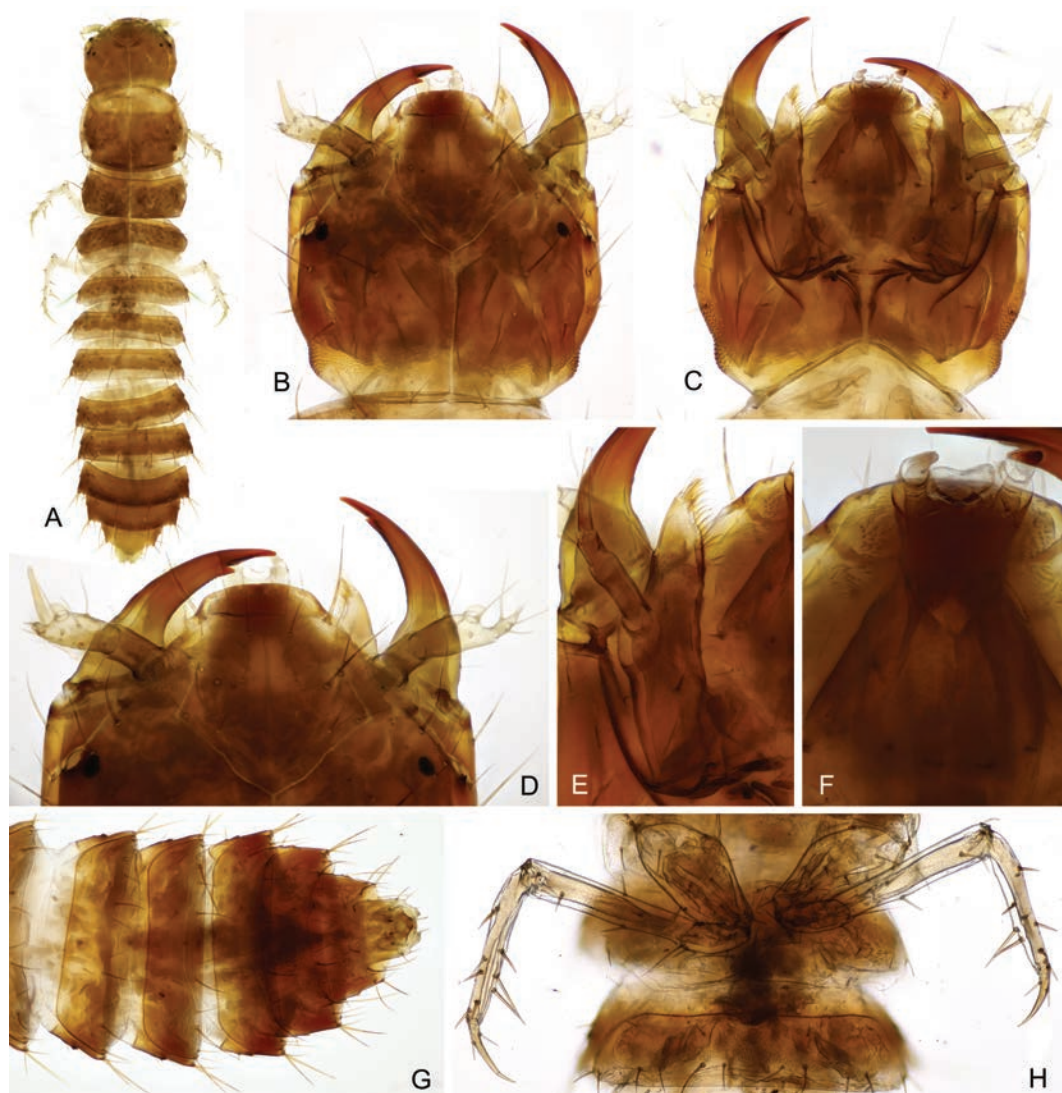
#### *Diochus* sp. (Diochini)

Fig. 11

**Material examined.** Larva: 1 larva (IDL): Taiwan: Nantou County, Huisun Forest res., Wading trail, 24.0892139°N, 121.0297836°E, 700 m, 20.vi.2020, F.S. Hu lgt., stony forest on the slope, small leaf accumulations (voucher 20-06HS182). Adults: 1 adult (coll. J. Janák, Prague): same locality but 11.x.2020, F.S. Hu & Y.J. Chen lgt. (voucher 20-10HS136); 1 adult (coll. J. Janák, Prague): same locality but 17.viii.2021, M. Fikáček & W.R. Liang lgt. (voucher 21-08HS124); 1 adult (IDL): Taiwan:



**Figure 8.** Cantharidae: larva of *Maltypus ryukyuanus* (OTU66, voucher HS4055L) associated with adults by DNA. **A.** Head and pro- and mesothorax, ventral view; **B.** Head, dorsal view; **C.** Detail of anterior part of the head, dorsal view; **D.** Detail of the head surface, with smooth anterior and sculptured posterior part; **E.** Antenna; **F.** Front leg.



**Figure 9.** Staphylinidae: Aleocharinae: Lomechusini: larva of *Drusilla obliqua*. (OTU216, voucher 21-08HS152) associated with adults by DNA. **A.** Dorsal habitus; **B–F.** Head: **B.** Dorsal view; **C.** Ventral view; **D.** Details of anterior part in dorsal view; **E.** Maxilla; **F.** Labium; **G.** Abdominal apex in ventral view; **H.** Hind legs.

Kaohsiung City, Zuoying district (左營區), Banping-shan (半屏山), SW slope, 22.694296°N, 120.305797°E, 100 m, 22.vii.2021, M. Fikáček lgt., sifting of shallow leaf accumulations with some wood and fungi and fallen figs in the forest with *Ficus* in karst area (TW2021-06e) (voucher BP2-012).

**Comments.** The tribe Diochini contains two genera: *Antarctothius* Coiffait & Sáiz, 1969 and *Diochus* Erichson, 1839; the larva of *Antarctothius* is unknown. The larva of the American *Diochus schaumii* Kraatz, 1860 is currently the only known larva in the tribe; it has been mentioned in the phylogenetic study by Solodovnikov and Newton (2005) and listed in the material examined by Irmeler (2017), but neither of these works provides a detailed description of the larva. Newton (1990) illustrated an unidentified larva of *Diochus* from Mexico, which is very similar to the *Diochus* sp. from Taiwan. Here we document the larva of *Diochus* sp. which seems to be widespread in lowland forests of Taiwan because this species was found in central (Huisun) and southern Taiwan (Banpingshan) in this study. The adult of this species is similar to one of *D. japonicus* Cameron, 1930 based on the shorter second antennal segment, but the morphology of aedeagus is completely different. The species identification needs to be done by further comparisons.

## Paederinae

### *Mimopinophilus* sp. (Pinophilini)

Fig. 12

**Material examined.** Larvae: 1 larva (IDL): Taiwan: Nantou County, Huisun Forest reserve, track to Xiaochushan Mt., 24.0744602°N, 121.0366337°E, 1150 m, 16.viii.2021, M. Fikáček & W.R. Liang lgt., old-grown secondary forest on the slope with sparse understory (voucher 21-08HS568); 1 larva (IDL): Taiwan: Nantou County, Huisun Forest reserve, track to Xiaochushan Mt., 24.0847025°N, 121.0274161°E, 1000 m, 16.viii.2021, M. Fikáček & W.R. Liang lgt., mixed conifer/broadleaf forest + sparse broadleaf forest on the slope (voucher 21-08HS346). Adults: 1 spec. (IDL): same locality, but 24.ii.2020, F.S. Hu lgt. (voucher 20-02HS316); 1 spec. (IDL): same locality, 20.vi.2020, lgt. F.S. Hu (voucher 20-06HS321); 1 spec. (IDL): same locality, 11.x.2020, lgt. F.S. Hu & Y.J. Chen (voucher 20-10HS313).

**Comments.** The larvae of Pinophilini are poorly understood (Staniec et al. 2022). Paulian (1941) described and illustrated a larva of Pinophilini from Brazil; however, the genus to which the larva belongs was not determined. Grebennikov and Newton (2009) coded the larval character states of Paederinae from Australia for the phylogenetic work, which is putative as a larva of *Pinophilus* Gravenhorst 1802. Assing (2022) subdivided the former *Pinophilus* into several separate genera; the species examined here (as well as all other Taiwanese species) correspond to the recently established *Mimopinophilus* Assing, 2022.

## Nitidulidae

### *Stelidota multiguttata* Reitter, 1877

Fig. 13A–H

**Material examined.** Larvae: 1 larva (IDL): Taiwan: Nantou County, Huisun Forest res., Wading trail, 24.0892139°N, 121.0297836°E, 700 m, 20.vi.2020, F.S. Hu lgt., stony forest on the slope, small leaf accumulations (voucher 20-06HS169); 1 larva (IDL): same locality, 17.viii.2021, M. Fikáček & W.R. Liang lgt. (voucher 21-08HS158). Adults: 1 spec. (IDL): same locality, 24.ii.2020, lgt. F.S. Hu (voucher 20-02HS116); 1 spec. (IDL): same locality, 11.x.2020, lgt. F.S. Hu & Y.J. Chen (voucher 20-10HS111); 1 spec. (IDL): Taiwan: Nantou County, Huisun Forest reserve, track to Xiaochushan Mt., 24.0847025°N, 121.0274161°E, 1000 m, 24.ii.2020, F.S. Hu lgt., mixed *Cryptomeria* + sparse broadleaf forest on the slope (voucher 20-02HS302); 1 spec. (IDL): same locality, 11.x.2020, F.S. Hu & Y.J. Chen lgt. (voucher 20-10HS302); 1 spec. (IDL): same locality, 1.iii.2021, lgt. M. Fikáček, F.S. Hu & G.J. Peng; 1 spec. (IDL): Taiwan: Nantou County, Huisun Forest reserve, track to Xiaochushan Mt., 24.0744602°N, 121.0366337°E; 1150 m, 11.x.2020, lgt. F.S. Hu & Y.J. Chen (voucher 20-10HS501).

**Comments.** The larvae of Nearctic species, *Stelidota geminata* (Say, 1825), *S. ferruginea* Reitter, 1873 and *S. octomaculata* (Say, 1825), have been described (Peng et al. 1990). The larva of *S. multiguttata* is very similar to *S. geminata*; both species possess longer second antennomere. Further comparison between *Stelidota multiguttata* and other species is needed to distinguish these similar species.

### *Lasiodites inaequalis* (Grouvelle, 1914)

Fig. 13I–N

**Material examined.** Larva: 1 spec. (IDL): Taiwan: Nantou County, Huisun Forest res., Wading trail, 24.0892139°N, 121.0297836°E, 700 m, 20.vi.2020, F.S. Hu lgt., stony forest on the slope, small leaf accumulations (voucher 20-06HS172). Adults: 1 spec. (IDL): same locality, 17.viii.2021, lgt. M. Fikáček & W.R. Liang (voucher 21-08HS107); 1 spec. (IDL): same locality, 11.x.2020, lgt. F.S. Hu & Y.J. Chen (voucher 20-10HS110); 1 spec. (NMPC): Taiwan: Nantou County, Huisun Forest reserve, track to Xiaochushan Mt., 24.0847025°N, 121.0274161°E, 1000 m, 4.v.2019; Damaška, Fikáček, Hu & Liu lgt., mixed conifer/broadleaf forest + sparse broadleaf forest on the slope: sifting (2019-TW16).

**Comments.** Although the larvae of the invasive *Lasiodites picta* are sometimes reported in literature (e.g., Serri et al. 2023), the larva of the genus has never been illustrated. Here, we are illustrating an early instar larva of *L. inaequalis*. It differs from the examined larvae of *Stelidota* Erichson, 1843 by the form of the urogomphi and

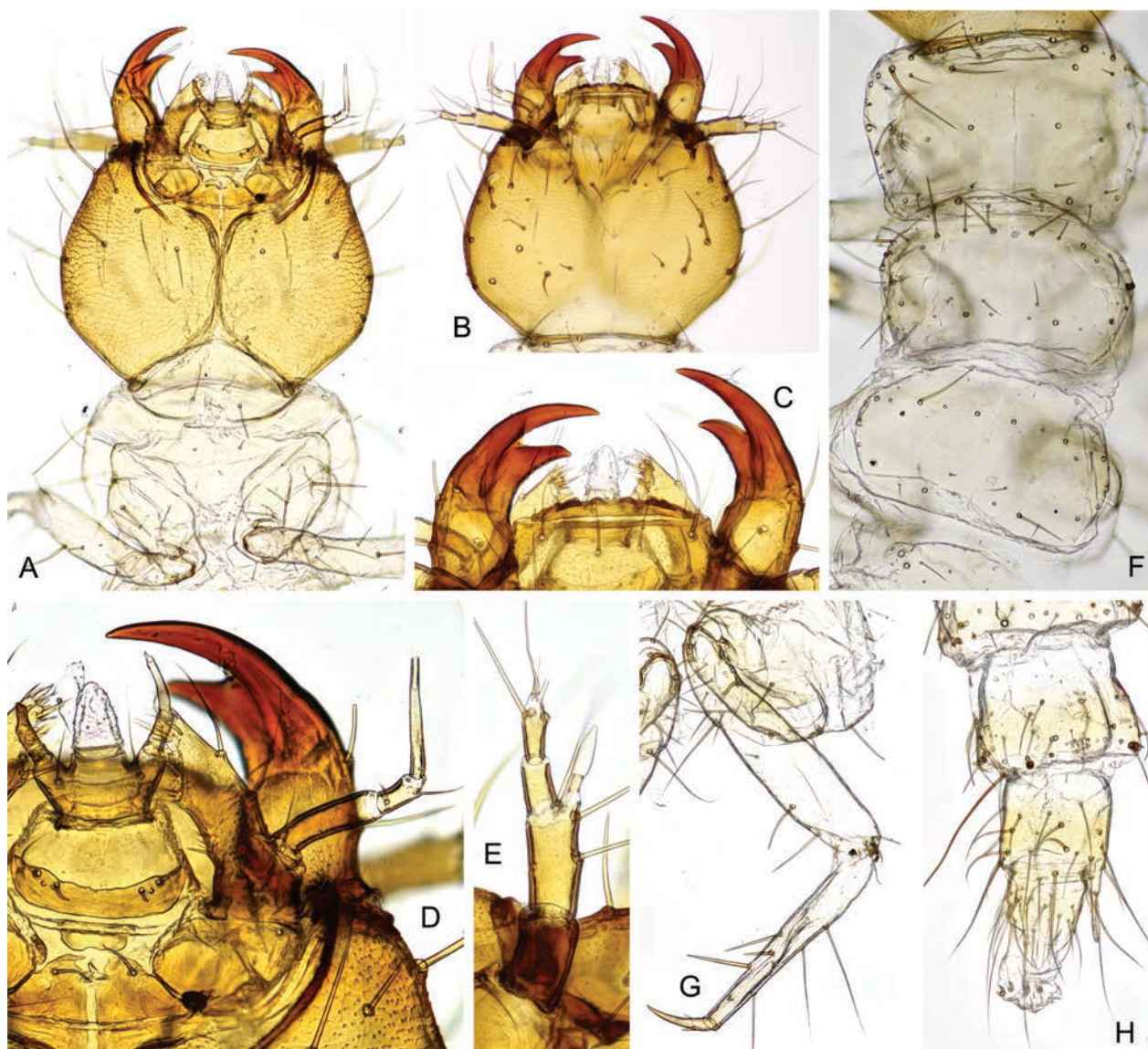


**Figure 10.** Staphylinidae: Aleocharinae: Falagriini: larva of *Myrmecocephalus brevisulcus* (OTU84, voucher 20-06HS573) associated with adults by DNA. **A.** Head and prothorax in ventral view; **B.** Head in dorsal view; **C.** Clypeus, labrum and mandibles in dorsal view; **D.** Mouthparts in ventral view; **E.** Antenna; **F.** Thorax in dorsal view; **G.** Hind leg; **H.** Abdominal apex.

by the multidentate mandibles. The species is sometimes placed in *Phenolia* Erichson, 1943 which comprises similar-looking yet unrelated American species (see Jelínek 1999; Lawrence 2019).

#### Tenebrionidae: Lagriinae

##### *Lagria scutellaris* Pic, 1910 (Lagriini)

Fig. 14

**Material examined.** Larvae: 1 larva (IDL): Taiwan: Nantou County, Huisun Forest reserve, track to Xiaochushan Mt., 24.0744602°N, 121.0366337°E; 1150 m, 24.ii.2020, lgt. F.S. Hu, old-grown forest on the slope with sparse understory (voucher 20-02HS537); 1 larva (IDL): same locality, 11.x.2020, lgt. F.S. Hu & Y.J. Chen (voucher 20-10HS556); 1 larva (IDL): Taiwan: Nantou County,

Huisun Forest reserve, Wading trail, 24.0892139°N, 121.0297836°E, 700m, 5.v.2019, Damaška, Fikáček,

Hu & Liu lgt., stony forest on the slope, small leaf accumulations (2019-TW18) (voucher HS5060L); 1 larva (IDL): same locality, 24.ii.2020, lgt. F.S. Hu (voucher 20-02HS159); 1 larva (IDL): same locality, 20.vi.2020, lgt. F.S. Hu (voucher 20-06HS167); 1 larva (IDL): same locality, 11.x.2020, lgt. F.S. Hu & Y.J. Chen (voucher 20-10HS159); 1 larva (IDL): same locality, 28.ii.2021, lgt. F.S. Hu & Y.J. Chen (voucher 21-03HS102); 1 larva (IDL): same locality, 17.viii.2021, M. Fikáček & W.R. Liang lgt. (voucher 21-08HS163). Adults: 1 spec. (IDL): same locality, 28.ii.2021, leg. F.S. Hu & Y.J. Chen (voucher 21-03HS102).

**Comments.** Although some species of *Lagria* Fabricius, 1775 are recognized as pests and are also used as model organisms and their life cycle is hence well known and studied (e.g., Zhou 1996, 2001; Janke et al. 2022), the larval morphology is rarely illustrated in detail, and are mostly available for European species *L. hirta* (Linnaeus, 1758) and the invasive African *L. villosa* Fabricius,

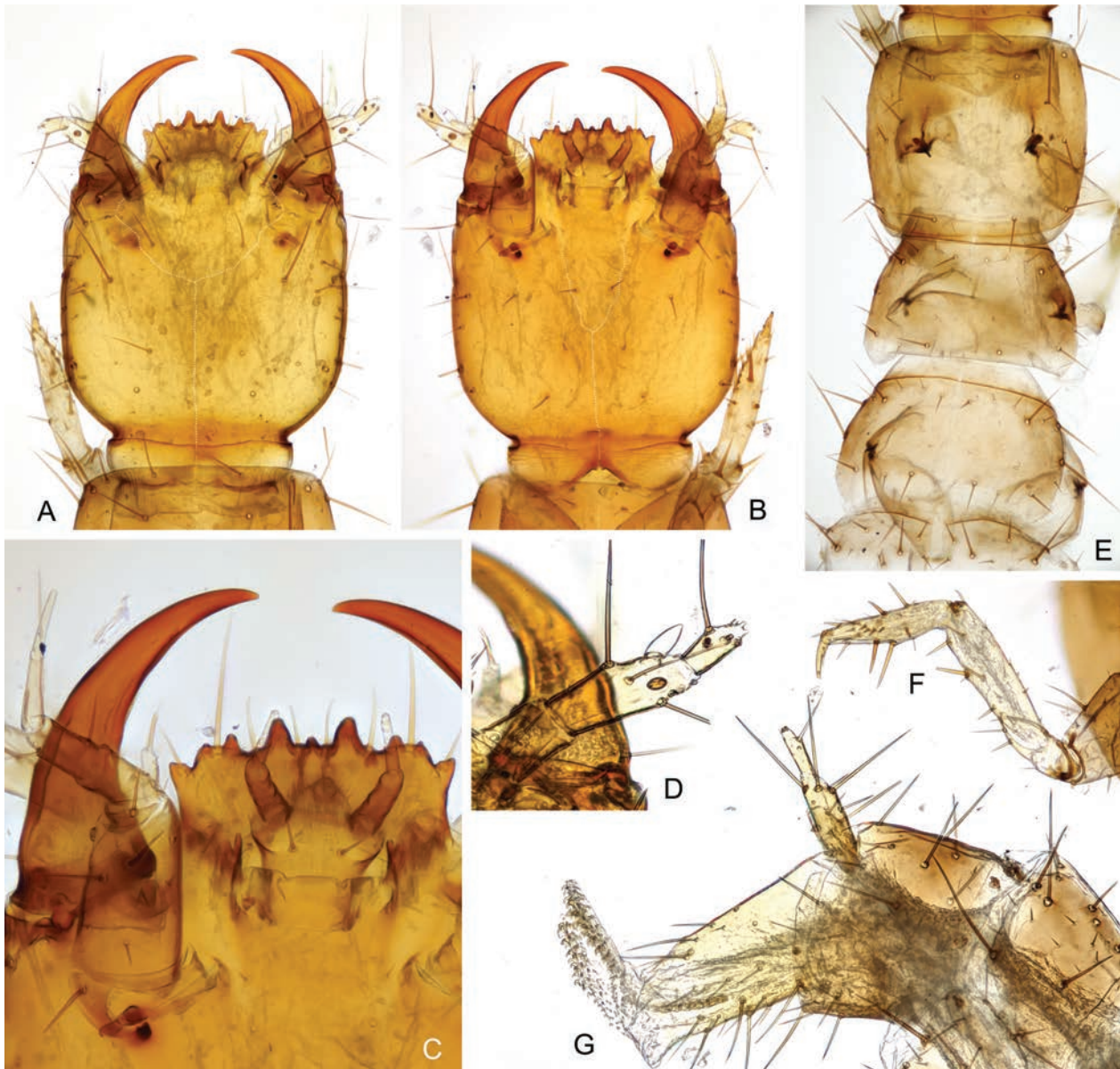


**Figure 11.** Staphylinidae: Staphylininae: Diochini: larva of *Diochus* sp. (OTU206, voucher 20-08HS182) associated with adults by DNA. **A–D.** Head: **A.** Dorsal view; **B.** Ventral view; **C.** Details of anterior part in ventral view; **D.** Antenna; **E.** Thorax in dorsal view; **F.** Fore leg; **G.** Apex of abdomen in lateral view.

1781 (see Spilman 1978 and online resources). We illustrate the larva of the Taiwan-endemic *L. scuttellaris* as it is often a dominant larval morphotype in forest leaf litter samples in Taiwan. It resembles the larva of *L. hirta* by dorsal color patterns (in contrast to uniformly black larva of *L. villosa*), but differs from it by larger and more widely separated urogomphi (very small and closely situated in *L. hirta*).

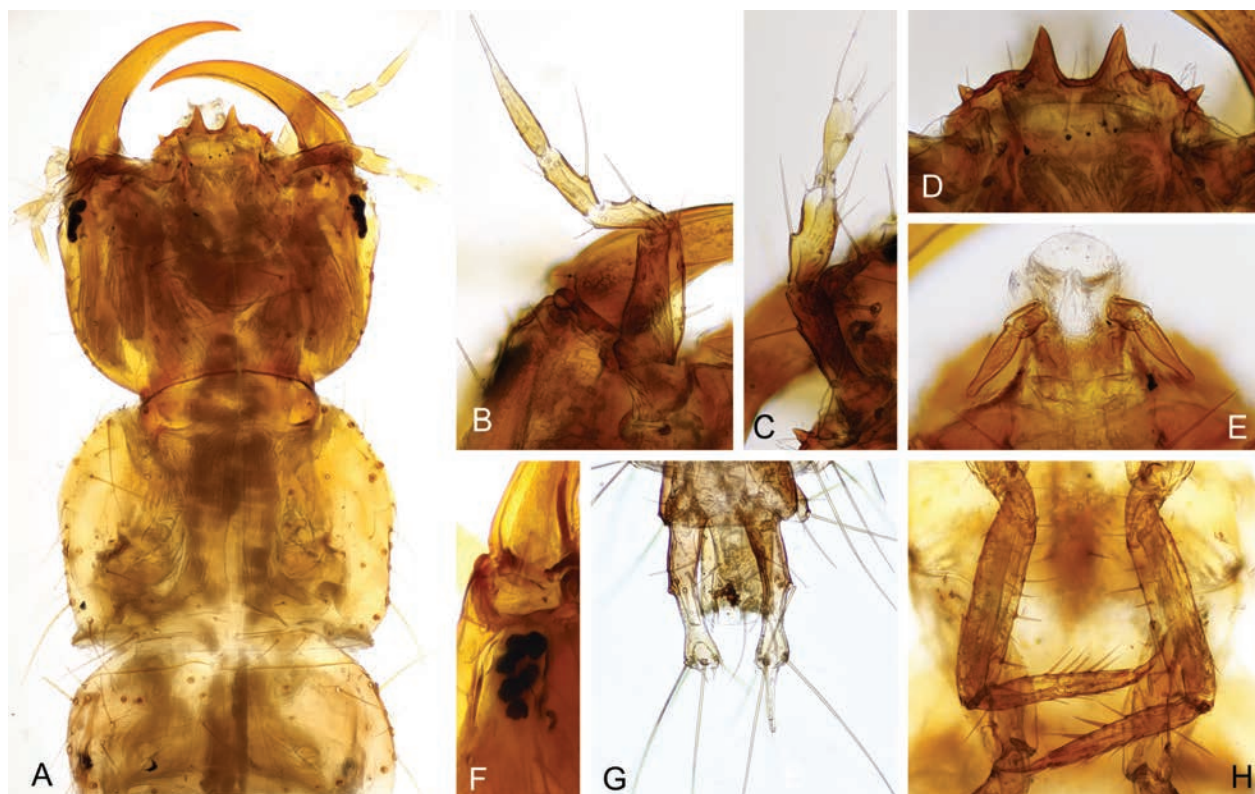
***Anaedes spinicornis* Kaszab, 1973 (Goniaderini)**

Fig. 15

**Material examined.** Larvae: 1 larva (IDL): Taiwan: Nantou County, Huisun Forest reserve, track to Xiaochushan Mt., 24.0847025°N, 121.0274161°E, 1000 m, 20.vi.2020, F.S. Hu lgt., mixed conifer/broadleaf forest + sparse broadleaf forest on the slope (voucher 20-06HS334); 1

larva (IDL): same locality, 4.v.2019, Damaška, Fikáček, Hu & Liu lgt. (2019-TW16) (voucher HS3055L); 1 larva (IDL): Taiwan: Nantou County, Huisun Forest reserve, track to Xiaochushan Mt., 24.0744602°N, 121.0366337°E; 1150 m, 20.vi.2020, lgt. F.S. Hu, old-grown forest on the slope with sparse understory (voucher 20-06HS557); 1 larva (IDL): same locality, 4.v.2019, Fikáček, Hu, Damaška, Liu lgt. (voucher HS1062L). Adults: 1 spec. (IDL): same locality, 24.ii.2020, F.S. Hu lgt. (voucher 20-02HS502); 1 spec. (IDL): same locality, 20.vi.2020, lgt. F.S. Hu (voucher 20-06HS501).

**Comments.** The larva of American *Anaedes brunneus* (Ziegler, 1844) has been illustrated without a detailed description (Böving and Craighead 1930). Arndt (1993) described the African species *Anaedes camerunus* Gebien, 1920. The larvae of *A. spinicornis* can be distinguished from the two known species by a rel-



**Figure 12.** Staphylinidae: Paederinae: Pinophilini: larva of *Mimopinophilus* sp. (OTU271, vouchers 21-08HS346 and 21-08HS568) associated with adults by DNA. **A.** Head and anterior part of thorax, dorsal view; **B.** Maxilla; **C.** Antenna; **D.** Nasale; **E.** Eye in lateral view; **F.** Labium; **G.** End of the abdomen with urogomphi, dorsal view; **H.** Front legs.

actively shorter and broader head. It can also be distinguished from *A. camerunus* by the coloration without a pair of spots on the anterior portion of the pronotum and with longer stripes on the lateral portion of the meso- and metanota.

## Discussion

The dataset published here is based on 20 samples collected in 2019–2021 in a single forest reserve in central Taiwan, and is hence limited geographically. Still, it illustrates challenges of studies on subtropical and tropical leaf litter beetle faunas: we sorted 4629 specimens that represent 334 species of 36 beetle families. It also demonstrates that the integrative approach combining DNA barcodes and morphology makes the study of largely unknown but species-diverse fauna more efficient. DNA barcodes allowed us to sort the material to species candidates for all groups, including taxonomically difficult ones or those for which taxonomic experts are not available at the moment. We were also able to sort larval specimens into species and associate part of them with co-occurring adults. This task would be impossible using morphology (see Fikáček et al. (2023)). In several widespread species, we were also able to compare DNA barcodes from Taiwan with those published from other areas: some were found nearly identical (e.g., in *Hypomedon de-*

*bilicornis* (Wollaston, 1857)), others indicate that the East Asian specimens form an isolated lineage (e.g., in *Perigona* cf. *nigriceps* and *Coccotrypes advena*) and urge for a more detailed taxonomic study.

The contribution of experts on taxonomy of particular groups is crucial for our project, providing the bridge between the DNA-based ‘species candidates’ (called OTU or MOTU in general, and BIN in the BOLD database) and taxonomic species with associated knowledge about morphology, lifestyle and evolutionary history. Although ecological studies may be based purely on numbers of unnamed species estimated by hand-sorting (e.g., Hopp et al. 2010) or DNA barcoding (e.g., Arribas et al. 2021), even these studies may benefit from accurate species identifications, especially when using functional and phylogenetic diversity measures (e.g., Basset et al. 2023). Expert-identified DNA barcodes, including those published here, make the taxonomic knowledge easily available for such studies, as well as for those focused on conservation, biogeography, physiology, etc. Moreover, DNA can help non-experts identify common species accurately. Experts can then focus on rare or newly discovered species, those with detailed lifestyle data, or species requiring further study due to differences between DNA and morphological traits.

We explicitly declare that our aim is not to support the DNA-only systematics proposed recently in some insect studies (e.g., Meierotto et al. 2019; Sharkey et al. 2021, 2023) despite the critique of such an approach (e.g.,

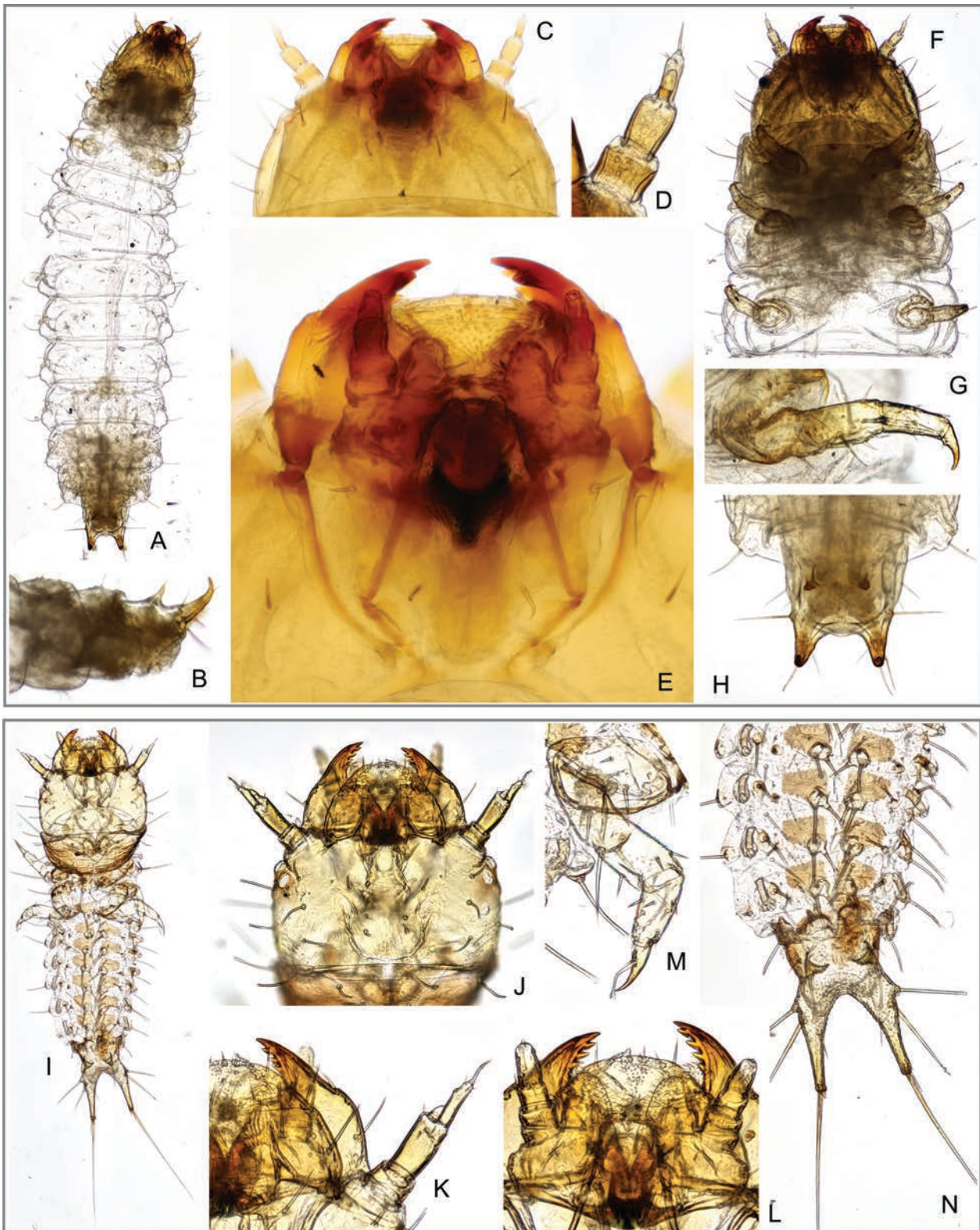


**Figure 13.** Nitidulidae. **A–G.** Late instar larva of *Stelidota multiguttata* (OTU119, voucher 21-08H158); **H–M.** Early instar larva of *Lasiodites inaequalis* (OTU180, voucher 20-08HS172). **A, I.** Habitus in dorsal view; **B.** Abdominal apex in lateral view; **C.** Head in dorsal view; **D, K.** Antenna; **E, L.** Mouthparts in ventral view; **F.** Head and thorax in ventral view; **G, M.** Detail of leg; **H, N.** End of abdomen in dorsal view; **K.** Detail of antenna and mandible in dorsal view.

Zamani et al. 2022; Meier et al. 2022). Taiwanese beetle fauna, despite island-based and highly endemic, overlaps with that of southern Japan, southern China, and north-

ern Philippines, where many beetle groups have been previously studied using traditional taxonomic methods. Taiwanese beetles have also been studied for more than

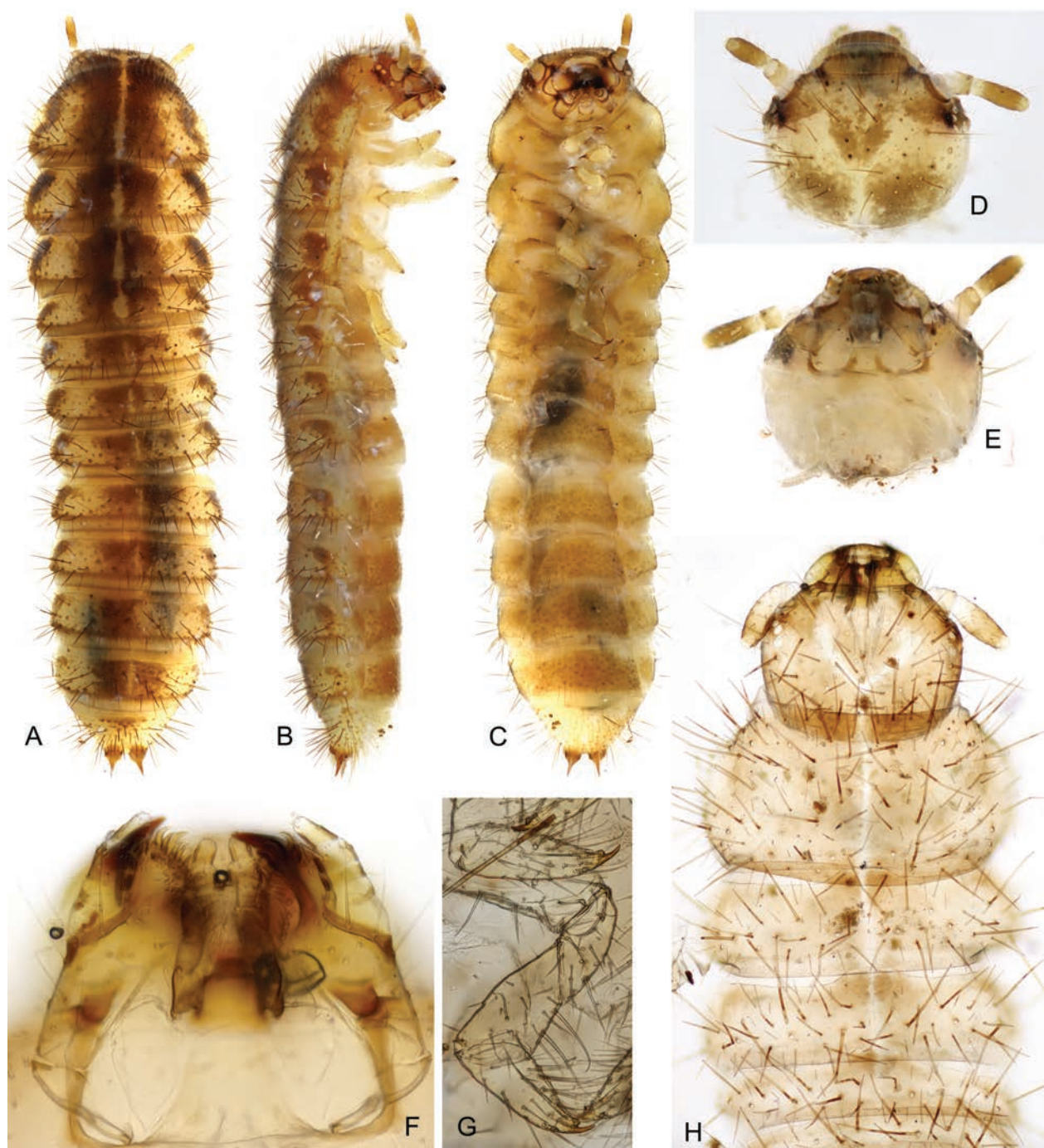


**Figure 14.** Tenebrionidae: Lagriinae: Lagriini: larvae of *Lagria scutellaris* (OTU174) associated with adults by DNA. **A–C.** Habitus of late instar larva (voucher 20-10HS556; **A.** Dorsal; **B.** Lateral; **C.** Ventral); **D, E.** Head of the late instar larva (voucher 21-08HS163; **D.** Dorsal; **E.** Ventral); **F–H.** Early instar larva (voucher HS5060L): **F.** Mouthparts, ventral view; **G.** Hind leg; **H.** Head and thorax in dorsal view.

a century as well. Taiwanese leaf litter beetles must be hence studied in geographic and taxonomic context, with DNA barcodes providing a tool for a more efficient work, not a replacement of the previous effort.

The DNA barcodes, new faunistic records and the first taxonomic conclusions reported here are the first results of the Taiwanese Leaf Litter Beetles project. Voucher specimens for all DNA sequences published here, as

well as the non-sequenced conspecific specimens from the same samples, are available for further studies by experts, e.g. those focused on particular genera and their larvae (e.g., Löbl 2020, 2023; Zhang et al. 2021; Ho et al. 2022). We will update the identifications of the DNA barcodes submitted to the BOLD database based on the subsequent research, to keep the DNA barcode dataset published here as an up-to-date resource facilitating

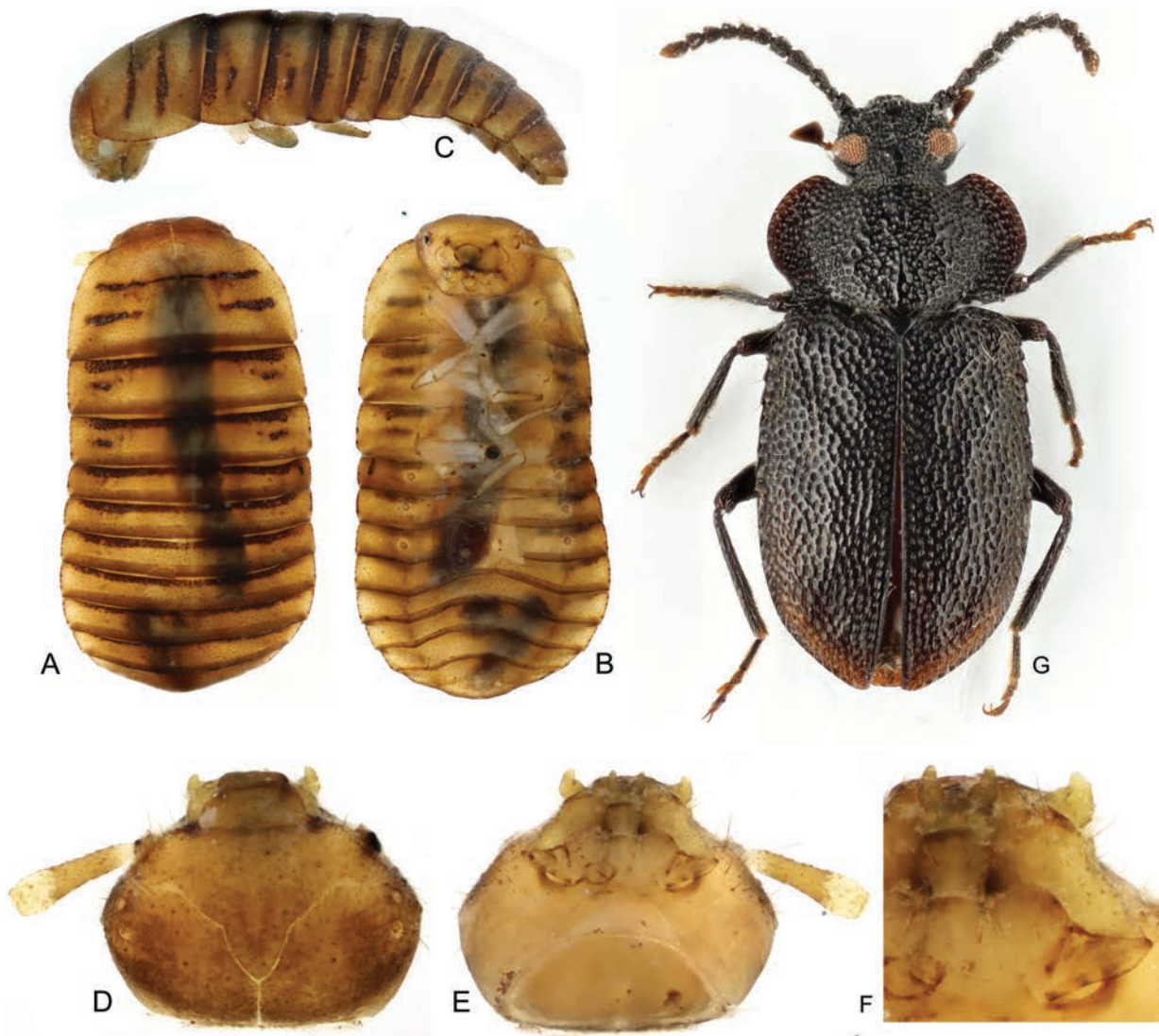


**Figure 15.** Tenebrionidae: Lagriinae: Goniaderini: larva of *Anaedus spinicornis* (OTU49, voucher HS1062L) associated with adults by DNA. A–C. Habitus (A. Dorsal; B. Ventral; C. Lateral); D–F. Head (D. Dorsal; E. Ventral; F. Ventral, close-up).

future studies. As the next step, we continue sampling across Taiwan, to cover the Taiwanese leaf litter beetle fauna more completely in all regions, altitudinal zones, and various types of forest. Based on results from the Huisun Forest Reserve, we decided to sample a smaller volume of leaf litter per sample (3 litres) which allows quicker collecting, sorting, and processing per sample, and consequently, taking multiple samples. Our data indicate that the multi-sample sampling design can detect a larger proportion of the local species diversity during a single visit: samples collected at five nearby sites on the same day in May 2019 covered ca. 40% of the estimated species richness living in the area, whereas a single 6-litre sample only covered ca. 10% of the local fauna (see also Fikáček et al. (2023)). We also continue sorting and DNA barcoding all larval morphotypes. New findings will be published continuously, either as summaries similar to this one, or as studies led by taxonomic experts and focused on particular taxa.

## Acknowledgements

We are grateful to Wei-Ren Liang (The Kyushu University Museum, Japan), Hsing-Che Liu (Taichung, Taiwan), and Yu-Jing Chen (Taichung, Taiwan) for their company and assistance with sample collecting. We are deeply indebted to Jen-Pan Huang (Biodiversity Research Centre, Academia Sinica, Taiwan) for providing his lab and massive support and encouragement for this project, and to Yi-Hsiu Kuan, Ming-Hsu Chou and Zong-Yu Shen from the same lab for lab support and discussions. Volker Assing (deceased), Ching-Shan Lin (Taichung, Taiwan), Paweł Jałoszyński (University of Wrocław, Poland), Hiroshi Sugaya (Nantou, Taiwan), Mateusz Sapieja (University of Wrocław, Poland), Shih-Pi Kao (Taichung, Taiwan), Wei-Ren Liang (Kyushu University, Japan), Adam Ślipiński (Australian National Insect Collection, Canberra), Chi-Feng Lee (Taiwan Agriculture Research Institute, Taichung), Jan Růžička (Czech University of Life Sciences Prague, Czech Republic), and

Manfred Uhlig (Museum für Naturkunde, Berlin, Germany), and Hume Douglas (Agriculture and Agri-Food Canada, Ottawa, Canada) helped with the identifications of part of the DNA-barcoded specimens. The data presented in this study were generated under the support by the Taiwanese National Science and Technology Council projects MOST 110-2621-B-110-001 and MOST 111-2621-B-110-003. The initial step of the project and the visit of Fang-Shuo Hu to Prague in 2019 was possible thanks to European Commission's SYNTHESYS project CZ-TAF-2524. The work in the National Museum, Prague was supported by the Ministry of Culture of the Czech Republic (DKRVO 2019–2023/5.I.e, National Museum, 00023272). The work of Gabriel Biffi was supported by Vale Institute of Technology and Fundação Guamá (Pará, Brazil). The project was partly funded by the SVV 260686/2023 grant to AFD.

## References

- Aberlenc HP, Allemand R (1997) Acclimatation en France de *Ptilodactyla exotica*, à mœurs anthropophiles (Coleoptera, Ptilodactylidae). Bulletin de la Société Entomologique de France 102(2): 93–102. <https://doi.org/10.3406/bsef.1997.17314>
- Andújar C, Arribas P, Ruzicka F, Crampton-Platt A, Timmermans MJTN, Vogler AP (2015) Phylogenetic community ecology of soil biodiversity using mitochondrial metagenomics. Molecular Ecology 24(14): 3603–3617. <https://doi.org/10.1111/mec.13195>
- Angelini F, De Marzo L (1998) Supplement to the knowledge of the Agathidiini of Taiwan (Coleoptera, Leiodidae). Revue Suisse de Zoologie 105(1): 125–138. <https://doi.org/10.5962/bhl.part.80034>
- Armstrong KF, Ball SL (2005) DNA barcodes for biosecurity: Invasive species identification. Philosophical Transactions of the Royal Society of London, Series B, Biological Sciences 360(1462): 1813–1823. <https://doi.org/10.1098/rstb.2005.1713>
- Arndt E (1993) Description of the larva of *Anaedes camerunus* Gebien (Coleoptera: Tenebrionidae, Lupropini). Koleopterologische Rundschau 63: 273–277.
- Arribas P, Andújar C, Salces-Castellano A, Emerson BC, Vogler AP (2021) The limited spatial scale of dispersal in soil arthropods revealed with whole-community haplotype-level metabarcoding. Molecular Ecology 31(1): 48–61. <https://doi.org/10.1111/mec.15591>
- Assing V (2010) On the Lathrobiina of Taiwan (Coleoptera: Staphylinidae: Paederinae). Beiträge zur Entomologie 60(2): 301–361. <https://doi.org/10.21248/contrib.entomol.60.2.301-361>
- Assing V (2014) Three new species and a new species group of *Medon* from China and Taiwan (Coleoptera: Staphylinidae: Paederinae). Linzer Biologische Beiträge 46: 515–523.
- Assing V (2015) A revision of the *Megalopaederus* species of Taiwan (Coleoptera: Staphylinidae: Paederinae). Stuttgarter Beiträge zur Naturkunde A, Neue Serie 8: 53–94.
- Assing V (2017) On the Lomechusini fauna of the East Palaearctic and Oriental regions, with a focus on the genera *Orphnebius* and *Amaurodera* (Coleoptera: Staphylinidae: Aleocharinae). Beiträge zur Entomologie 67(1): 63–106. <https://doi.org/10.21248/contrib.entomol.67.1.63-106>
- Assing V (2019) On the Lomechusini fauna of the Palaearctic and Oriental regions. XXVI. New species, a new synonymy, and additional records (Coleoptera: Staphylinidae: Aleocharinae). Beiträge zur Entomologie 69(1): 33–70. <https://doi.org/10.21248/contrib.entomol.69.1.033-070>
- Assing V (2022) Monograph of Palaearctic, Oriental, and New Guinean Pinophilina (Coleoptera: Staphylinidae: Paederinae). Acta Musei Moraviae. Scientiae Biologicae 107(Supplement): 1–419.
- Baehr M (2014) The species of the genus *Perigona* Castelnau from New Guinea, Sulawesi, Halmahera and Australia, and of the *parvicollis-pygmaea*-lineage (Coleoptera, Carabidae, Perigonini). Entomologische Blätter und Coleoptera 109: 1–132.
- Basset Y, Blažek P, Souto-Vilarós D, Vargas G, Ramírez Silva JA, Barrios H, Perez F, Bobadilla R, Lopez Y, Ctvrticka R, Šípek P, Solís A, Segar ST, Lamarre GPA (2023) Towards a functional classification of poorly known tropical insects: The case of rhinoceros beetles (Coleoptera, Dynastinae) in Panama. Insect Conservation and Diversity 16(1): 147–163. <https://doi.org/10.1111/icad.12613>
- Bickhardt H (1913) H. Sauter's Formosa Ausbeute. Histeridae II. (Col.) (16. Beitrag zur Kenntniss der Histeriden). Entomologische Mitteilungen 2: 166–177. <https://doi.org/10.5962/bhl.part.14989>
- Bili M, Cortesero AM, Mougél C, Gauthier JP, Ermel G, Simon JC, Outreman Y, Terrat S, Mahéo F, Poinso D (2016) Bacterial community diversity harboured by interacting species. PLoS ONE 11(6): e0155392. <https://doi.org/10.1371/journal.pone.0155392>
- Borovec R (2014) Study on Trachyploeini of the Oriental Region (Coleoptera: Curculionidae: Entiminae). Studies and Reports. Taxonomical Series 10(1): 1–39.
- Böving AG, Craighead FC (1930) An illustrated synopsis of the principal larval forms of the order Coleoptera. Entomologica Americana. A Journal of Entomology, New Series, XI(1): 1–351. <https://doi.org/10.5962/bhl.title.6818>
- Bright DEA (2021) Catalog of Scolytidae (Coleoptera): Supplement 4 (2011–2019) with an Annotated Checklist of the World Fauna (Coleoptera: Curculionidae: Scolytidae). Contributions of the C. P. Gillette Museum of Arthropod Diversity, Department of Agricultural Biology, Colorado State University, 654 pp.
- Camacho C, Coulouris G, Avagyan V, Ma N, Papadopoulos J, Bealer K, Madden TL (2009) BLAST+: Architecture and applications. BMC Bioinformatics 10(1): 1–9. <https://doi.org/10.1186/1471-2105-10-421>
- Chimeno C, Morinière J, Podhorna J, Hardulak L, Hausmann A, Reckel F, Grunwald JE, Penning R, Haszprunar G (2019) DNA Barcoding in Forensic Entomology - Establishing a DNA reference library of potentially forensic relevant arthropod species. Journal of Forensic Sciences 64(2): 593–601. <https://doi.org/10.1111/1556-4029.13869>
- Chu H-F (1945) The larvae of the Harpalinae unisetosae (Coleoptera: Carabidae). Entomologica Americana 25(1): 1–71.
- Chung K-F, Shao K-T (2022) Catalogue of life in Taiwan. Web electronic publication. Version 2022. <http://taibnet.sinica.edu.tw>
- Cosandey V (2023) Description of six new species of *Lederina* Nikitsky & Belov, 1982 (Coleoptera: Melandryidae: Melandryinae) from Taiwan. Revue Suisse de Zoologie 130(1): 11–23. <https://doi.org/10.35929/RSZ.0085>
- Costa C, Vanin SA, Casari-Chen SA (1988) *Larvas de Coleoptera do Brasil*. Museu de Zoologia, Universidade de São Paulo, São Paulo, 282 pp. [+ 165 pls] <https://doi.org/10.5962/bhl.title.100233>
- Cuccodorio G (2011) *Megarthus* of Taiwan, with notes on phylogenetic relationship within the genus (Coleoptera: Staphylinidae: Proteininae). Studies and Reports. Taxonomical Series 7(1–2): 25–92.
- Dajoz R (1974) Description de Coléoptères nouveaux de la famille des Cerylonidae. Bulletin du Muséum National d'Histoire Naturelle 238(162): 1059–1067.

- Dajoz R (1979) Coléoptères Cerylonidae nouveaux ou peu connus. Bulletin Mensuel de la Societe Linneenne de Lyon 48(7): 441–452. <https://doi.org/10.3406/linly.1979.10380>
- De Marzo L (2000) Coleotterofauna dei depositi di *Posidonia*: Morfologia larvale in alcune specie caratteristiche (Sphaeridiidae, Histeridae, Ptiliidae, Staphylinidae). Annali del Museo Civico di Storia Naturale. Giacomo Doria 93: 461–471.
- De Marzo L (2002) Larve di coleotteri in detriti vegetali di origine agricola: lineamenti morfologici e presenza stagionale (Polyphaga: 20 famiglie). Entomologica (Bari) 34: 65–131.
- De Marzo L (2007) Note sullo sviluppo preimmaginale in *Drusilla italica* (Bernhauer) (Coleoptera Staphylinidae Aleocharinae). Entomologica (Bari) 39: 211–220.
- De Marzo L (2008) Allestimento della cella pupale e del bozzolo nei Coleotteri: qualche dettaglio etologico (Polyphaga: 7 famiglie). Entomologica (Bari) 40: 91–100.
- De Marzo L (2009) Verifica del numero di età larvali in alcuni stafilinidi (Coleoptera, Staphylinidae). Annali del Museo Civico di Storia Naturale. Giacomo Doria 100: 649–670.
- Fikáček M, Hu F-S, Le M-H, Huang J-P (2023) Can immature stages be ignored in studies of forest leaf litter arthropod diversity? A test using Oxford Nanopore DNA barcoding. Insect Conservation and Diversity. <https://doi.org/10.1111/icad.12702>
- Fitton MG (1976) The larvae of the British genera of Cantharidae (Coleoptera). Journal of Entomology Series B, Taxonomy 44(3): 243–254. <https://doi.org/10.1111/j.1365-3113.1976.tb00015.x>
- Folmer O, Black M, Hoeh W, Lutz R, Vrijenhoek R (1994) DNA primers for amplification of mitochondrial cytochrome c oxidase subunit I from diverse metazoan invertebrates. Molecular Marine Biology and Biotechnology 3: 294–299.
- Giller PS (1996) The diversity of soil communities, the ‘poor man’s tropical rainforest’. Biodiversity and Conservation 5(2): 135–168. <https://doi.org/10.1007/BF00055827>
- Grebennikov VV, Newton AF (2009) Good-bye Scydmaenidae, or why the ant-like stone beetles should become megadiverse Staphylinidae sensu latissimo (Coleoptera). European Journal of Entomology 106(2): 275–301. <https://doi.org/10.14411/eje.2009.035>
- Guéorguiev B (2014) Two new related oodine genera in the Oriental Region, with remarks on the systematic position of the genera *Hololeius* and *Holosoma* (Coleoptera, Carabidae). Deutsche Entomologische Zeitschrift 61(2): 87–104. <https://doi.org/10.3897/dez.61.7754>
- Guéorguiev B, Liang H (2020) Revision of the Palaearctic and Oriental representatives of *Lachnocrepis* LeConte and *Oodes* Bonelli (Coleoptera: Carabidae), with special account on Chinese species. Zootaxa 4850(1): 1–89. <https://doi.org/10.11646/zootaxa.4850.1.1>
- Hajibabaei M, Janzen DH, Burns JM, Hallwachs W, Hebert PDN (2006) DNA barcodes distinguish species of tropical Lepidoptera. Proceedings of the National Academy of Sciences of the United States of America 103(4): 968–971. <https://doi.org/10.1073/pnas.0510466103>
- Hebert PDN, Ratnasingham S, DeWaard JR (2003) Barcoding animal life: Cytochrome c oxidase subunit I divergences among closely related species. Proceedings. Biological Sciences 270(suppl\_1): S96–S99. <https://doi.org/10.1098/rsbl.2003.0025>
- Hebert PDN, Ratnasingham S, Zakharov EV, Telfer AC, Levesque-Beaudin V, Milton MA, Pedersen S, Jannetta P, deWaard JR (2016) Counting animal species with DNA barcodes: Canadian insects. Philosophical Transactions of the Royal Society of London, Series B, Biological Sciences 371(1702): 20150333. <https://doi.org/10.1098/rstb.2015.0333>
- Hendrich L, Morinière J, Haszprunar G, Hebert PDN, Hausmann A, Köhler F, Balke M (2015) A comprehensive DNA barcode database for Central European beetles with a focus on Germany: Adding more than 3500 identified species to BOLD. Molecular Ecology Resources 15(4): 795–818. <https://doi.org/10.1111/1755-0998.12354>
- Hernández-Triana LM, Brugman VA, Nikolova NI, Ruiz-Arrondo I, Barrero E, Thorne L, de Marco MF, Krüger A, Lumley S, Johnson N, Fooks AR (2019) DNA barcoding of British mosquitoes (Diptera, Culicidae) to support species identification, discovery of cryptic genetic diversity and monitoring invasive species. ZooKeys 832: 57–76. <https://doi.org/10.3897/zookeys.832.32257>
- Hinton HE (1942) A revision of the Cerylonini of Borneo (Coleoptera, Colydiidae). Annals & Magazine of Natural History 9(51): 141–173. <https://doi.org/10.1080/03745481.1942.9755474>
- Hisamatsu S (1985) Notes on some Japanese Coleoptera, 1. Transactions of the Shikoku Entomological Society 17: 5–13.
- Ho B-H, Hu F-S, Fikáček M (2022) The dung beetle *Oxyomus* of Taiwan (Coleoptera: Scarabaeidae): Review of the fauna, a new species and its larva associated by DNA barcoding. Zoological Studies (Taipei, Taiwan) 61: e80. <https://doi.org/10.6620/ZS.2022.61-80>
- Hopp PW, Ottermanns R, Caron E, Meyer S, Roß-Nickoll M (2010) Recovery of litter inhabiting beetle assemblages during forest regeneration in the Atlantic forest of Southern Brazil. Insect Conservation and Diversity 3(2): 103–113. <https://doi.org/10.1111/j.1752-4598.2010.00078.x>
- Hoshina H (1999) A taxonomic study on the genera *Dermatohomoeus* and *Colenis* (Coleoptera, Leiodidae) from Japan. Entomological Science 2(3): 413–423.
- Irmeler U (2017) A review of the Neotropical genus *Diochus* Erichson, 1840 (Coleoptera: Staphylinidae: Staphylininae). Contribution to Entomology 67(1): 1–62. <https://doi.org/10.21248/contrib.entomol.67.1.1-62>
- Janke RS, Moog S, Weiss B, Kaltenpoth M, Flórez LV (2022) Morphological adaptation for ectosymbiont maintenance and transmission during metamorphosis in *Lagria* beetles. Frontiers in Physiology 13(979200): 1–15. <https://doi.org/10.3389/fphys.2022.979200>
- Janzen DH, Hallwachs W (2016) DNA barcoding the Lepidoptera inventory of a large complex tropical conserved wildland, Area de Conservacion Guanacaste, northwestern Costa Rica. Genome 59(9): 641–660. <https://doi.org/10.1139/gen-2016-0005>
- Janzen DH, Burns JM, Cong Q, Hallwachs W, Dapkey T, Manjunath R, Hajibabaei M, Hebert PDN, Grishin NV (2017) Nuclear genomes distinguish cryptic species suggested by their DNA barcodes and ecology. Proceedings of the National Academy of Sciences of the United States of America 114(31): 8313–8318. <https://doi.org/10.1073/pnas.1621504114>
- Jeannel R (1941) Un carabique termitophile nouveau de l’Afrique Tropicale. Revue Française d’Entomologie 8(3): 135–146.
- Jeannel R (1942) Faune de France. 40. Coléoptères Carabiques. Deuxième partie. Paul Lechevalier, Paris, 1172 pp.
- Jelínek J (1999) Contribution to taxonomy of the beetle subfamily Nitidulinae (Coleoptera: Nitidulidae). Folia Heyrovskyana 7(5): 251–281.
- Jordal BH, Normark BB, Farrell BD, Kirkendall LR (2002) Extraordinary haplotype diversity in haplodiploid inbreeders: Phylogenetics and evolution of the bark beetle genus *Coccotrypes*. Molecular Phylogenetics and Evolution 23(2): 171–188. [https://doi.org/10.1016/S1055-7903\(02\)00013-1](https://doi.org/10.1016/S1055-7903(02)00013-1)
- Kajtoch Ł (2022) Evolutionary and ecological signals in *Wolbachia*-beetle relationships: A review. European Journal of Entomology 119: 215–226. <https://doi.org/10.14411/eje.2022.023>

- Kajtoch Ł, Kotásková N (2018) Current state of knowledge on *Wolbachia* infection among Coleoptera: A systematic review. *PeerJ* 6: e4471. <https://doi.org/10.7717/peerj.4471>
- Kaszab Z (1964) The zoological results of Gy. Topál's collectings in South Argentina. 13. Coleoptera – Tenebrionidae. *Annales Historico-Naturales Musei Nationalis Hungarici, pars. Zoologica* 56: 353–387.
- Kaszab Z (1979) Die Arten der Gattung *Sivacrypticus* Kaszab, 1964 (Coleoptera, Tenebrionidae). *Annales Historico-Naturales Musei Nationalis Hungarici* 71: 185–204.
- Kaszab Z (1981) Die Gattungen und Arten der Tribus Archeocrypticini (Coleoptera: Tenebrionidae). *Folia Entomologica Hungarica* 52(34): 95–115.
- Klausnitzer B (1997) 51. Familie: Cantharidae. In: Klausnitzer B (Ed.) Die Larven der Käfer Mitteleuropas. 4. Band. Polyphaga Teil 3 sowie Ergänzungen zum 1. bis 3. Band. Goecke & Evers, Krefeld im Gustav Fischer Verlag Jena, Stuttgart, Lübeck, Ulm, Germany, 124–140.
- Kumar S, Stecher G, Tamura K (2016) MEGA7: Molecular Evolutionary Genetics Analysis Version 7.0 for Bigger Datasets. *Molecular Biology and Evolution* 33(7): 1870–1874. <https://doi.org/10.1093/molbev/msw054>
- Lawrence JF (2005) 18.9. Ptilodactylidae. In: Beutel RG, Leschen RAB (Eds) *Handbook of Zoology. Volume IV Arthropoda: Insecta. Part 38 Coleoptera, beetles Vol. 1: Morphology and systematics (Archostemata, Adephaga, Myxophaga, Polyphaga partim)*. Walter de Gruyter, Berlin-New York, 536–542. [567 pp]
- Lawrence JF (2019) Australian Nitidulinae: general review with descriptions of new genera and species (Coleoptera: Nitidulidae). *Zootaxa* 4657(2): 261–290. <https://doi.org/10.11646/zootaxa.4657.2.3>
- Lee C-F, Cheng H-T (2007) The Chrysomelidae of Taiwan I. Sishou-Hills Insect Observation Network Press, Taipei, Taiwan, 199 pp.
- Lee C-F, Cheng H-T, Yu S-F, Tsou M-H, Chen H-J, Lee H (2010) The Chrysomelidae of Taiwan II. Sishou-Hills Insect Observation Network Press, Taipei, Taiwan, 191 pp.
- Lee C-F, Tsou M-H, Cheng H-T, Yu S-F, Chen H-J, Lee H, Chen J-C (2016) The Chrysomelidae of Taiwan III. Sishou-Hills Insect Observation Network Press, Taipei, Taiwan, 199 pp.
- Lindroth CH (1942) *Oodes gracilis* Villa. Eine thermophile Carabide Schwedens. *Notulae Entomologicae* 22: 109–157.
- Liu M, Clarke LJ, Baker SC, Jordan GJ, Burrige CP (2020) A practical guide to DNA metabarcoding for entomological ecologists. *Ecological Entomology* 45(3): 373–385. <https://doi.org/10.1111/een.12831>
- Löbl I (2012) On Taiwanese species of *Baeocera* Erichson (Coleoptera: Staphylinidae: Scaphidiinae). *Zoological Studies (Taipei, Taiwan)* 51(1): 118–130.
- Löbl I (2020) Four new Taiwanese species of *Scaphobaeocera* CSI-KI (Coleoptera, Staphylinidae, Scaphidiinae). *Linzer Biologische Beiträge* 52(1): 327–335.
- Löbl I (2023) New species and records of Scaphidiinae (Coleoptera: Staphylinidae) from mainland China and Taiwan. *Vernate* 42: 135–142.
- Löbl I, Löbl D (2017) *Catalogue of Palaearctic Coleoptera. Archostemata-Myxophaga-Adephaga. Vol. 1. Revised and updated edition*. Brill, Leiden, Boston, 1443 pp. [https://doi.org/10.1163/9789004330290\\_002](https://doi.org/10.1163/9789004330290_002)
- Löbl I, Smetana A (2007) *Catalogue of Palaearctic Coleoptera Volume 4 Elateroidea - Derontoidea - Bostrichoidea - Lymexyloidea - Cleroidea - Cucujoidea*. Apollo Books, Stenstrup, Denmark, 935 pp. <https://doi.org/10.1163/9789004260894>
- Lü L, Cai C-Y, Zhang X, Newton AF, Thayer MK, Zhou H-Z (2020) Linking evolutionary mode to palaeoclimate change reveals rapid radiations of staphylinoid beetles in low-energy conditions. *Current Zoology* 66(4): 435–444. <https://doi.org/10.1093/cz/zoz053>
- Madden MJL, Young RG, Brown JW, Miller SE, Frewin AJ, Hanner RH (2019) Using DNA barcoding to improve invasive pest identification at U.S. ports-of-entry. *PLoS ONE* 14(9): e0222291. <https://doi.org/10.1371/journal.pone.0222291>
- Mann DJ (2006) *Ptilodactyla exotica* Chapin, 1927 (Coleoptera: Ptilodactylidae: Ptilodactylinae) established breeding under glass in Britain, with a brief discussion on the family Ptilodactylidae. *Entomologist's Monthly Magazine* 142: 67–79.
- Mazur S (2007) On new and little known Histerids (Coleoptera: Histeridae) from Taiwan with additional notes on the species composition and zoogeography. *Formosan Entomologist* 27: 67–81.
- McKenna DD, Farrell BD, Caterino MS, Farnum CW, Hawks DC, Maddison DR, Seago AE, Short AEZ, Newton AF, Thayer MK (2015) Phylogeny and evolution of Staphyliniformia and Scarabaeiformia: Forest litter as a stepping stone for diversification of nonphytophagous beetles. *Systematic Entomology* 40(1): 35–60. <https://doi.org/10.1111/syen.12093>
- Meier R, Blaimer BB, Buenaventura E, Hartop E, von Rintelen T, Srivathsan A, Yeo D (2022) A re-analysis of the data in Sharkey et al.'s (2021) minimalist revision reveals that BINs do not deserve names, but BOLD Systems needs a stronger commitment to open science. *Cladistics* 38(2): 264–275. <https://doi.org/10.1111/cla.12489>
- Meierotto S, Sharkey MJ, Janzen DH, Hallwachs W, Hebert PD, Chapman EG, Smith MA (2019) A revolutionary protocol to describe understudied hyperdiverse taxa and overcome the taxonomic impediment. *Deutsche Entomologische Zeitschrift* 66(2): 119–145. <https://doi.org/10.3897/dez.66.34683>
- Merkel O (1988) Novelties of *Sivacrypticus* Kaszab, 1864 and *Enneboeus* Waterhouse, 1878 (Coleoptera, Archeocrypticidae). *Annales Historico-Naturales Musei Nationalis Hungarici* 80: 71–78.
- Miller SE, Hausmann A, Hallwachs W, Janzen DH (2016) Advancing taxonomy and bioinventories with DNA barcodes. *Philosophical Transactions of the Royal Society of London, Series B, Biological Sciences* 371(1702): 20150339. <https://doi.org/10.1098/rstb.2015.0339>
- Nadkarni NM, Longino JT (1990) Invertebrates in Canopy and Ground Organic Matter in a Neotropical Montane Forest, Costa Rica. *Biotropica* 22(3): 286. <https://doi.org/10.2307/2388539>
- Newton AF (1990) Insecta: Coleoptera: Staphylinidae adults and larvae. In: Dindal DL (Ed.). *Soil biology guide*. John Wiley & Sons, New York, 1137–1174. [xviii + 1349 pp]
- Olson DM (1994) The distribution of leaf litter invertebrates along a Neotropical altitudinal gradient. *Journal of Tropical Ecology* 10(2): 129–150. <https://doi.org/10.1017/S0266467400007793>
- Ong U, Hattori T (2019) *Jewel Beetles of Taiwan Vol.1*. Ministry of Beetles, Tainan, Taiwan, 235 pp.
- Ong U, Curletti G, Hattori T (2023) *Jewel Beetles of Taiwan Vol. 2*. Ministry of Beetles, Tainan, Taiwan, 219 pp.
- Owens BE, Carlton CE (2015) “Berlese vs. Winkler”: Comparison of two forest litter coleoptera extraction methods and the Ecoli (Extraction of Coleoptera in Litter) protocol. *Coleopterists Bulletin* 69(4): 645–661. <https://doi.org/10.1649/0010-065X-69.4.645>
- Park SJ, Ahn KJ (2007) Two Pseudoliodinae genera *Dermatohomoeus* Hlisenikowský and *Pseudocolenis* Reitter (Coleoptera: Leioididae: Leioidinae) in Korea with the description of *Pseudocolenis hoshinai*

- new species. *Zootaxa* 1427(1): 49–56. <https://doi.org/10.11646/zootaxa.1427.1.3>
- Paulian R (1941) Les premiers états des Staphyloidea (Coleoptera). Étude de morphologie comparée. Mémoires du Muséum national d'Histoire naturelle 15: 1–361.
- Peng C, Williams RN, Galford JR (1990) Descriptions and key for identification of larvae of *Stelidota* Erichson (Coleoptera: Nitidulidae) found in America North of Mexico. *Journal of the Kansas Entomological Society* 63(4): 626–633.
- Pentinsaari M, Hebert PDN, Mutanen M (2014) Barcoding beetles: A regional survey of 1872 species reveals high identification success and unusually deep interspecific divergences. *PLoS ONE* 9(9): e108651. <https://doi.org/10.1371/journal.pone.0108651>
- Perlman SJ, Hunter MS, Zchori-Fein E (2006) The emerging diversity of *Rickettsia*. *Proceedings of the Royal Society B, Biological Sciences* 273(1598): 2097–2106. <https://doi.org/10.1098/rspb.2006.3541>
- Puthz V (2010) *Edaphus* aus Taiwan (Coleoptera: Staphylinidae) 101. Beitrag zur Kenntnis der Euaesthetinen. *Revue Suisse de Zoologie* 116(2): 265–336. <https://doi.org/10.5962/bhl.part.117785>
- Ratnasingham S, Hebert PDN (2007) BOLD: The Barcode of Life Data System: Barcoding. *Molecular Ecology Notes* 7(3): 355–364. <https://doi.org/10.1111/j.1471-8286.2007.01678.x>
- Sakchoowong W, Jaitrong W, Ogata K, Nomura S, Chanpaisaeng J (2008) Diversity of soil-litter insects: comparison of the pselaphine beetles (Coleoptera: Staphylinidae: Pselaphinae) and the ground ants (Hymenoptera: Formicidae). *Thai Journal of Agricultural Science* 41: 11–18. <https://doi.org/10.1111/j.1479-8298.2008.00281.x>
- Schminke G (1982) Larven und Fortpflanzungsverhalten von *Drusilla canaliculata*, *Zyras humeralis*, *Geostiba circellaris* und *Othius myrmecophilus* (Coleoptera: Staphylinidae). *Drosera* 82(1): 91–100.
- Serri S, Moradi M, Audisio P (2023) First report of an exotic sap beetle, *Phenolia (Lasiodites) picta* (Macleay, 1825) (Coleoptera, Nitidulidae) from Iran with notes on its distribution range and damage on different hosts. *Journal of Insect Biodiversity and Systematics* 9(1): 33–38. <https://doi.org/10.52547/jibs.9.1.33>
- Sharkey MJ, Janzen DH, Hallwachs W, Chapman EG, Smith MA, Dapkey T, Brown A, Ratnasingham S, Naik S, Manjunath R, Perez K, Milton M, Hebert P, Shaw SR, Kittel RN, Solis MA, Metz MA, Goldstein PZ, Brown JW, Quicke DLJ, van Achterberg C, Brown BV, Burns JM (2021) Minimalist revision and description of 403 new species in 11 subfamilies of Costa Rican braconid parasitoid wasps, including host records for 219 species. *ZooKeys* 1013: 1–665. <https://doi.org/10.3897/zookeys.1013.55600>
- Sharkey MJ, Baker A, McCluskey K, Smith A, Naik S, Ratnasingham S, Manjunath R, Perez K, Sones J, D'Souza M, Jacques BS (2023) Minimalist revision of *Mesochorus* Gravenhorst, 1829 (Hymenoptera: Ichneumonidae: Mesochorinae) from Área de Conservación Guanacaste, Costa Rica, with 158 new species and host records for 129 species. *Revista de Biología Tropical* 71(supplement 2): 1–174. <https://doi.org/10.15517/rev.biol.trop.v71iS2.56316>
- Ślipiński SA (1982) New and little known species of the Cerylonidae (Coleoptera). *Polskie Pismo Entomologiczne* 52: 31–58.
- Smetana A (1995) Revision of the tribes Quediini and Tanygnathini. Part III. Taiwan. (Coleoptera: Staphylinidae). Special Publication 6. National Museum of Natural Science, Taichung.
- Solodovnikov AY, Newton AF (2005) Phylogenetic placement of Arrowinini trib.n. within the subfamily Staphylininae (Coleoptera: Staphylinidae), with revision of the relict South African genus *Arrowinus* and description of its larva. *Systematic Entomology* 30(3): 398–441. <https://doi.org/10.1111/j.1365-3113.2004.00283.x>
- Spilman TJ (1978) *Lagria villosa* in Brazil, with new descriptions and illustrations of the larva and pupa (Coleoptera, Lagriidae). *Ciência e Cultura* (São Paulo) 30(3): 342–347.
- Srivathsan A, Lee L, Katoh K, Hartop E, Kutty SN, Wong J, Yeo D, Meier R (2021) ONTbarcoder and MinION barcodes aid biodiversity discovery and identification by everyone, for everyone. *BMC Biology* 19(1): 1–21. <https://doi.org/10.1186/s12915-021-01141-x>
- Staniec B, Pietrykowska-Tudruj E, Wagner GK, Mazur A, Kowalczyk M (2022) Synthesis of current knowledge of the morphology of the larval stages of Paederinae (Coleoptera; Staphylinidae), with a first insight into the mature larva of *Pseudomedon* Mulsant & Rey, 1878, in the light of a new systematic division. *Insects* 13(11): 982. <https://doi.org/10.3390/insects13110982>
- Švec Z (2022) Eight new species of Pseudoliodini (Coleoptera: Leiodidae: Leiodinae) from the East and the Southeast Asia with new morphological, distributional and bionomical data. *Studies and Reports. Taxonomical Series* 18(2): 437–468.
- Tautz D, Arctander P, Minelli A, Thomas RH, Vogler AP (2003) A plea for DNA taxonomy. *Trends in Ecology & Evolution* 18(2): 70–74. [https://doi.org/10.1016/S0169-5347\(02\)00041-1](https://doi.org/10.1016/S0169-5347(02)00041-1)
- Thomson RG (1979) 2.26. Larvae of North American Carabidae with a key to tribes. In: Erwin TL, Ball GE, Whitehead DR, Halpern AL (Eds) *Carabid Beetles. Their Evolution, Natural History, and Classification*. Dr. W. Junk, the Hague, 209–291. [https://doi.org/10.1007/978-94-009-9628-1\\_11](https://doi.org/10.1007/978-94-009-9628-1_11)
- Topp W (1978) Bestimmungstabelle für die Larven der Staphylinidae. In: Klausnitzer B (Ed.). *Ordnung Coleoptera (Larven)*. Dr. W. Junl, The Hague, 304–334.
- Truett GE, Heeger P, Mynatt RL, Truett AA, Walker JA, Warman ML (2000) Preparation of PCR-quality mouse genomic dna with hot sodium hydroxide and tris (HotSHOT). *BioTechniques* 29(1): 52–54. <https://doi.org/10.2144/00291bm09>
- van Emden FI (1942) A key to the genera of larval Carabidae (Col.). *Transactions of the Royal Entomological Society of London* 92(1): 2–99. <https://doi.org/10.1111/j.1365-2311.1942.tb03318.x>
- Viñolas A, Miralles-Nuñez A, Necoechea A (2020) Primeros datos sobre la presencia de *Ptilodactyla exotica* Chapin, 1927 en la Península Ibérica (Coleoptera, Ptilodactylidae). *Revista Gaditana de Entomología* 11: 93–98.
- Weigand H, Beermann AJ, Čiampor F, Costa FO, Csabai Z, Duarte S, Geiger MF, Grabowski M, Rimet F, Rulik B, Strand M, Szucsich N, Weigand AM, Willassen E, Wyler SA, Bouchez A, Borja A, Čiamporová-Zaťovičová Z, Ferreira S, Dijkstra KDB, Eisendle U, Freyhof J, Gadawski P, Graf W, Haegerbaeumer A, van der Hoorn BB, Japoshvili B, Keresztes L, Keskin E, Leese F, Macher JN, Mamos T, Paz G, Pešić V, Pfannkuchen DM, Pfannkuchen MA, Price BW, Rinkevich B, Teixeira MAL, Várбірó G, Ekrem T (2019) DNA barcode reference libraries for the monitoring of aquatic biota in Europe: Gap-analysis and recommendations for future work. *The Science of the Total Environment* 678: 499–524. <https://doi.org/10.1016/j.scitotenv.2019.04.247>
- Wood SL, Bright DE (1992) A catalog of Scolytidae and Platypodidae (Coleoptera), Part 2. Taxonomic Index. *Great Basin Naturalist Memoirs* 13: 1–1553.
- Yao M-C, Lee C-Y, Chiu H-W, Yang E-C, Lu K-H (2011) Application of light traps to monitor population fluctuation of stored-product

- pests in imported brown rice storehouses. *Formosan Entomologist*. 31: 351–366.
- Zamani A, Fric ZF, Gante HF, Hopkins T, Orfinger AB, Scherz MD, Bartoňová AS, Pos DD (2022) DNA barcodes on their own are not enough to describe a species. *Systematic Entomology* 47(3): 385–389. <https://doi.org/10.1111/syen.12538>
- Zhang W-X, Hu F-S, Yin Z-W (2021) Six new species of *Horniella* Raffray from the Oriental region (Coleoptera, Staphylinidae, Pselaphinae). *ZooKeys* 1042: 1–22. <https://doi.org/10.3897/zookeys.1042.66576>
- Zhou H (1996) Population seasonality and larval development of *Lagria hirta* L. (Coleoptera: Lagriidae). *Insect Science* 3(4): 329–337. <https://doi.org/10.1111/j.1744-7917.1996.tb00282.x>
- Zhou H (2001) Reproduction of *Lagria hirta* (Coleoptera: Lagriidae) and its life-history trait correlation. *Environmental Entomology* 30(4): 686–691. <https://doi.org/10.1603/0046-225X-30.4.686>

## Appendix 1. List of identified taxa recorded from Huisun Forest Reserve

Below, we are listing all taxa recorded in the dataset published in this study which are currently identified to genus or species levels. For details about the number of OTUs in the genera listed, the collecting details of all taxa, and their DNA barcodes, please refer to the Suppl. material 2.

**Anthicidae:** *Sapintus plectilis*, *Macrotomoderus* sp.  
**Archeocrypticidae:** *Sivacrypticus taiwanicus*.  
**Bothrideridae:** *Antibothrus* sp. **Cantharidae:** *Maltypus ryukyuanus*. **Carabidae:** *Trichotichnus* sp., *Lebia* sp., *Pentagonica subcordicollis*, *Perigona* cf. *nigriceps*, *Oodes japonicus*, *Rhyzodiastes rimoganensis*, *Trilophus* cf. *alternans*. **Cerambycidae:** *Pterolophia laterialba*. **Cerylonidae:** *Cautomus* sp., *Gyrelon jenpani*, *Thyroderus porcatus*. **Chrysomelidae:** *Ivalia* sp., *Aphthona* sp., *Clavicornaltica* sp., *Trachytetra takizawai*, *Smaragdina nigripennis*, *Xanthonia taiwana*, *Morphosphaera* sp., *Paleosepharia* sp. **Cleridae:** *Omadius zebratus*. **Curculionidae:** *Trachyphloeosoma* sp., *Phaeopholus ornatus*, *Otibazo* sp., *Acallinus* sp., *Seleuca* sp., *Coccotrypes advena*, *Coccotrypes papuanus*, *Coccotrypes longior*, *Orthotomicus* sp., *Microperus* sp., *Hypothenemus eruditus*, *Xyleborinus saxesenii*. **Discolomatidae:** *Aphanocephalus* sp. **Elateridae:** *Adelocera* cf. *shirozui*, *Cardiotarsus* sp., *Ryukyucardiophorus babai*, *Csikia dimatoides*, *Neopsephus* sp. **Endomychidae:** *Mycetina* sp., *Chondria nigropunctata*, *Ectomychus tappanus*. **Erotylidae:** *Cryptophilus* sp., *Neosternus* sp. **Histeridae:** *Anapleus* sp., *Margarinotus curvicollis*, *Tribalus* sp. **Hydrophilidae:** *Anacaena* sp., *Armatus* sp., *Psalitrus* sp. **Lampyridae:** *Luciola kagiana*. **Latrididae:** *Bicava* sp., *Cartodere* sp. **Leiodidae:** *Ptomaphagus* sp., *Agathidium amictum*, *Agathidium pictum*, *Dermatohomoeus* sp. **Lycidae:** *Macrolycus* sp. **Melandryidae:** *Lederina* sp. **Meloidae:** *Epicauta* sp. **Nitidulidae:** *Lasiodites inaequalis*, *Lasiodites pictus*, *Stelidota multiguttata*. **Phalacridae:** gen. sp. **Prionoceridae:** *Idgia* sp. **Ptiliidae:** genn. spp. **Ptilodactylidae:** *Ptilodactyla* sp. **Ptinidae:** *Myrmecoptinus* sp. **Scarabaeidae:** *Oxyomus alligator*, *Rhyparus azumai*, *Onthophagus yangi*. **Scraptiidae:** gen. sp. **Sphindidae:** *Aspidiphorus* sp. **Staphylinidae:** **Aleocharinae:** *Aleochara* sp., *Myrmecocephalus brevisulcus*, *Gyrophanaena* sp., *Drusilla obliqua*, *Orphnebius* sp., *Zyras formosae*. **Euasthetinae:**

*Edaphus* cf. *taiwanensis*, *Stenaesthetus nomurai*. **Mycetoporinae:** *Ischnosoma duplicatum*, *Ischnosoma quadriguttatum*, *Lordithon* sp. **Osoriinae:** *Thoracochirus* sp., *Arpagonus* sp., *Osorius* cf. *huangi*, *Nacaeus* sp. **Oxytelinae:** *Anotylus* cf. *amicus*, *Anotylus* cf. *cimicoides*, *Paraploderus* cf. *thailandicus*. **Paederinae:** *Homaeotarsus* sp., *Astenus* sp., *Hypomedon debilicornis*, *Rugilus japonicus*, *Thinocharis* sp., *Mimopinophilus* sp., *Palaminus* sp. **Proteininae:** *Megarthus* sp. **Pselaphinae:** *Harmophorus* sp., *Cratna* sp., *Physomerinus* sp., *Sathytes rufus*, *Batraxis* sp., *Reichenbachia* sp., *Plagiophorus amygdalinus*, *Morana* sp., *Pseudophanias excavatus*, *Pseudophanias yaimensis*, *Centrophthalmus* sp., *Horniella nantouensis*, *Horniella taiwanensis*, *Labomimus* sp. **Scaphidiinae:** *Baeocera caliginosa*, *Baeocera cooteri*, *Scaphisoma hui*, *Scaphobaeocera* sp., *Scaphoxium* cf. *taiwanum*. **Scydmaeninae:** *Cephennodes taurus* species group, *Cephennomicrus* sp., *Euconnus* sp., *Himaloconnus* sp., *Scydmaenus* sp., *Napoconnus* sp. **Staphylininae:** *Diochus* sp., *Erichsonius* sp., *Hesperopalpus venustus*, *Indoquedius* sp., *Philonthus* sp., *Tolmerinus* sp. **Steninae:** *Stenus* sp. **Tachyporinae:** *Coproporus* cf. *brunnicollis*. **Xantholininae:** gen. sp. **Tenebrionidae:** *Ades* sp., *Derispia* cf. *nanshanchiensis*, *Anaedus spinicornis*, *Lagria scutellaris*, *Stenochinus* sp., *Amarygmus* cf. *taiwanus*. **Zopheridae:** *Pseudotarphius lewisi*.

## Supplementary material 1

### Maximum likelihood tree

Authors: Fang-Shuo Hu, Martin Fikáček, My-Hanh Le

Data type: pdf

Explanation note: The maximum likelihood tree based on all DNA barcode sequences of the leaf litter beetles from the Huisun Forest Reserve, Taiwan.

Copyright notice: This dataset is made available under the Open Database License (<http://opendatacommons.org/licenses/odbl/1.0>). The Open Database License (ODbL) is a license agreement intended to allow users to freely share, modify, and use this Dataset while maintaining this same freedom for others, provided that the original source and author(s) are credited.

Link: <https://doi.org/10.3897/dez.71.112278.suppl1>

## Supplementary material 2

### **The DNA barcodes of the leaf litter beetles from Huisun Forest Reserve and the associated metadata**

Authors: Fang-Shuo Hu, Emmanuel Arriaga-Varela, Gabriel Biffi, Ladislav Bocák, Petr Bulirsch, Albert František Damaška, Johannes Frisch, Jiří Hájek, Peter Hlaváč, Bin-Hong Ho, Yu-Hsiang Ho, Yun Hsiao, Josef Jelínek, Jan Klimaszewski, Robin Kandrata, Ivan Löbl, György Makranczy, Keita Matsumoto, Guan-Jie Phang, Enrico Ruzzier, Michael Schülke, Zdeněk Švec, Dmitry Telnov, Wei-Zhe Tseng, Lan-Wei Yeh, My-Hanh Le, Martin Fikáček

Data type: xlsx

Explanation note: The voucher photos of these specimens are available in the BOLD database and in the Zenodo research archive under <https://doi.org/10.5281/zenodo.10069183>.

Copyright notice: This dataset is made available under the Open Database License (<http://opendatacommons.org/licenses/odbl/1.0>). The Open Database License (ODbL) is a license agreement intended to allow users to freely share, modify, and use this Dataset while maintaining this same freedom for others, provided that the original source and author(s) are credited.

Link: <https://doi.org/10.3897/dez.71.112278.suppl2>

---



# Two new species of the genus *Agramma* (Hemiptera, Heteroptera, Tingidae) from small islands of Japan, with an illustrated key to the Japanese species of the genus

Jun Souma<sup>1</sup>

<sup>1</sup> Shirakami Research Center for Environmental Sciences, Faculty of Agriculture and Life Science, Hirosaki University, Aomori, Japan

<https://zoobank.org/4DB4BB24-7179-4A63-A644-8C4DE86AFC6F>

Corresponding author: Jun Souma (kodokusignal@gmail.com)

Academic editor: Dávid Rédei ♦ Received 20 June 2023 ♦ Accepted 8 January 2024 ♦ Published 30 January 2024

## Abstract

The present study describes two new species of the monocotyledon-feeding lace bugs of the genus *Agramma* Stephens, 1829 (Hemiptera, Heteroptera, Tingidae, Tinginae, Tingini) from small islands of Japan. The first is *A. (A.) izuense* **sp. nov.**, which was recorded as *A. (A.) japonicum* (Drake, 1948) from Hachijo Island, the Izu Islands, in a previous study, and is considered an independent species here based on morphological characteristics and molecular data. The second is *A. (A.) keramense* **sp. nov.**, which has a remarkable spineless head and was discovered from Aka and Geruma islands, Kerama Group, the Ryukyu Islands. Consequently, the following four species of *Agramma* were recognized in Japan: *A. (A.) abruptifrons* Golub, 1990, *A. (A.) izuense* **sp. nov.**, *A. (A.) japonicum*, and *A. (A.) keramense* **sp. nov.** Only dozens of submacropterous morphs were confirmed in these two species in the present study, suggesting that both new species are flightless. In addition, an illustrated key for the identification of the four species from Japan and the host plant relationships of the two new species are provided.

## Key Words

East Asia, host plant, molecular data, new species, phytophagous insect, taxonomy

## Introduction

The true bug family Tingidae (Hemiptera, Heteroptera), known as lace bugs, comprises phytophagous species that are highly host-specific and generally feed on the abaxial side of angiosperm leaves (Schuh and Weirauch 2020). The genus *Agramma* Stephens, 1829 (Tinginae, Tingini), a species-rich Old World taxon with 89 species in three subgenera, includes many species that feed on monocotyledons (cf. Drake and Ruhoff 1965; Péricart and Golub 1996; Aukema et al. 2013; Souma 2020). In Japan, two species belonging to the nominotypical subgenus, namely *A. (Agramma) abruptifrons* Golub, 1990 and *A. (A.) japonicum* (Drake, 1948), have been known mainly from Japan proper (Hokkaido, Honshu, Shikoku, and Kyushu) and its surrounding islands (pertaining to the Palearctic Region) and were reported from *Juncus* sp.

(Juncaceae) and *Carex* spp. (Cyperaceae), respectively (Souma 2020). Many previous studies, both older and newer, have reported several localities for these two species in the four main islands of Japan (Drake 1948; Takeya 1953; Tomokuni 1979; Ichita 1988; Yamada and Tomokuni 2012; Souma 2020; Souma and Hisasue 2022; Souma and Iwata 2022; Nozawa and Okuda 2023; Tago 2023; Yamamoto 2023, etc.). In the small islands surrounding Japan proper, however, only *A. (A.) japonicum* (Drake, 1948) has been recorded from Kunashiri [= Kunashir], Hachijo, Sado and Yakushima islands, which belong to the Palearctic Region (Kerzhner 1978; Tomokuni 1979; Tomokuni and Ishikawa 2002; Souma 2021). Consequently, *Agramma* species on the small islands of Japan have been rather unevenly investigated.

On the other hand, the general habitus of members of the population from Hachijo Island of the Izu Islands,

identified as *A. (A.) japonicum* in the literature, differs from that of *A. (A.) japonicum* described from Sapporo, Hokkaido, Japan proper (cf. Drake 1948; Tomokuni and Ishikawa 2002; Souma 2020). Additionally, an indeterminate species of *Agramma* was collected from Aka and Geruma islands, Kerama Group, the Ryukyu Islands (pertaining to the Oriental region) by the author and his colleague Reo Ito. Therefore, *Agramma* species distributed on the small islands of Japan require a taxonomic study.

In the present study, the population of *A. (A.) japonicum* from Hachijo Island and an indeterminate species from Aka and Geruma islands, the latter having a remarkable spineless head, were considered undescribed species based on careful observation of their morphological characteristics, and the monophyly of the former was supported by molecular data from four gene regions (the COI, COII, 16S, and 28S genes). In conclusion, two new species, namely *A. (A.) izuense* sp. nov. from Hachijo Island and *A. (A.) keramense* sp. nov. from Aka and Geruma islands, were described. In addition, the possibility of flightlessness for the two new species has been suggested, as only submacropterous morphs have been collected so far. An illustrated identification key and photographs of living individuals of all four species of *Agramma* occurring in Japan are provided, and the host plant relationships of the two new species were presented.

## Materials and methods

### Molecular data

A total of 18 operational taxonomic units (OTUs) from four Japanese tingid species were used in the present study (Suppl. material 1). The 16 OTUs consisting of two species of *Agramma*, *A. (Agramma) izuense* sp. nov. and *A. (A.) japonicum*, were used as ingroups because of their strong similarity in terms of morphological characteristics and to judge whether they are independent species or represent geographic variation. The remaining two OTUs consisting of two species, namely *Cochlochila (Physo-dictyon) conchata* (Matsumura, 1913) and *Limnostatua lewisi* (Scott, 1880), were used as outgroups. The genera *Cochlochila* and *Limnostatua* are placed into Tingini as well as *Agramma* but differ from *Agramma* in their morphological characteristics (cf. Drake and Ruhoff 1965; Souma and Ishikawa 2022). Partial sequences of the following gene markers were used for the present analyses: mitochondrial COI (742 bp), COII (765 bp), 16S (361 bp), and nuclear 28S (444 bp). Fragments of each gene were amplified using the following primers: C1-J-2183 (5'CAA CAT TTA TTT TGA TTT TTT GG 3') and TL2-N-3014 (5'TCC AAT GCA CTAATC TGC CAT ATT A 3') (Simon et al. 1994) for COI; C1-J-2798 (5'CCW CGW CGW TAY TCW GAY TAT CC 3') and C2-N-3554 (5'GTT CAT GAR TGW ARD ACA TC 3') (Damgaard and Cognato 2005) for COII; Lace16sF (5'ATG ATT TTT AAA TGG CCG CGT 3') and Lace16sR (5'GAA CTC

TCC AAG AAA ATT ACG CTG T 3') (present study) for 16S; and 28sL (5'CCC GTC TTG AAA CAC GGA CCA A 3') (Muraji and Tachikawa 2000) and Lace28sR (5'TCT GAT CCG AGT CCC ACG GCT 3') (present study) for 28S. All sequences used in the present analyses were newly submitted to GenBank by this study or previously registered to GenBank by Souma (2022).

DNA was extracted using the DNeasy Blood & Tissue Kit (Qiagen, Hilden, Germany). All DNA samples were extracted from the abdomens of the specimens using a nondestructive method. The abdomens were preserved in small polyethylene vials containing 50% glycerin and 50% water solution. The other body parts were preserved as dried specimens and pinned. PCR was performed using the following protocols: initial denaturation at 98 °C for 3 min, denaturation at 98 °C for 10 s, annealing at 50 °C (65 °C in 28S) for 5 s, and extension at 68 °C (72 °C in 28S) for 5 s and 35 cycles (33 cycles in COI), with a final extension at 68 °C (72 °C in 28S) for 3 min. The PCR products were purified using an ExoSAP IT kit (Amersham Biosciences, Amersham, United Kingdom).

The edited sequences used in the present study were compared with related sequences from the National Centre for Biotechnology Information (NCBI) (<http://www.ncbi.nlm.nih.gov>) using the Basic Local Alignment Search Tool (BLAST) algorithm (Altschul et al. 1997).

Sequence alignments were performed using Mega 10.1.8 (Kumar et al. 2018). Gaps were treated as missing data. Six OTUs were used in the analysis of concatenated datasets of COI, COII, 16S, and 28S to estimate the phylogenetic relationship between *A. (A.) japonicum* from three islands of Japan proper (Hokkaido, Honshu, and Kyushu), including the type locality Sapporo (Hokkaido), and *A. (A.) izuense* sp. nov. from Hachijo Island, the Izu Islands (Suppl. material 1). In addition to the six OTUs, 12 OTUs were used in the analyses of the COI datasets to identify the morphological species. The COI dataset of the 18 OTUs contained four OTUs per locality in *A. (A.) izuense* sp. nov. and *A. (A.) japonicum*. The COI, COII, 16S, and 28S sequence datasets were concatenated using Kakusan 4 (Tanabe 2011). The concatenated aligned sequences yielded 2,312 bp. The homogeneity of the base composition of the sequences was tested using the pgttest composition implemented in Phylogears in Kakusan 4. The null hypothesis of homogeneity among the OTUs was rejected for the third codon position of COI. To decrease the saturation and compositional bias, the RY coding dataset of COI for the third codon (Woese et al. 1991) was used for the phylogenetic analyses. The substitution models and partitioning schemes applied in the Bayesian inference analyses were selected using Kakusan 4. Bayesian analyses were performed using MrBayes v.3.2.7 (Ronquist et al. 2012) with two Markov chain Monte Carlo (MCMC) runs of four chains for 2,000,000 generations. The sampled trees and models from the first 1,301,000 generations were discarded as burn-in tree and a majority-rule consensus tree was constructed from the sample trees from the latter 699,000 generations.

Convergence of both runs, visualized using Tracer v.1.6 (Rambaut et al. 2014), was determined to have occurred when the effective sample size (ESS) (Kass et al. 1998) increased above 200. The tree was visualized and edited using Figtree v.1.4.4 (Rambaut 2014) and Adobe Photoshop 2023 ver.24.5, respectively.

To identify the morphological species, the pairwise sequence distances of the COI dataset of 18 OTUs were calculated using the Kimura-two parameter (K2P) model in Mega 10.1.8 (Kumar et al. 2018). In a previous study (Jung et al. 2011), the average interspecific and intraspecific genetic distances of the COI gene in Heteroptera were 6.3% and 0.4%, respectively. Therefore, in the present study, interspecific (intraspecific) genetic distances of more than 9% (0.9%) and less than 3% (0.3%) were treated as large and small, respectively.

## Systematics

The morphological characteristics of the dried specimens were examined, drawn, and measured using a stereoscopic microscope (SZ60; Olympus, Tokyo, Japan) equipped with an ocular grid. To observe the parameres, the pygophores were removed from the body after softening the specimens in hot water. The removed pygophores were immersed in a hot 15% KOH solution for 5 min and then soaked in 99% ethanol for the dissection of the paramere. The parameres were observed after fixing the angles with a gel (Museum Gel Clear, Ready America, California, U.S.A.) placed on the microscope slide. The pygophores and parameres were preserved in small polyethylene vials containing a 50% glycerin and 50% water solution. The polyethylene vials were mounted on the pins with the respective specimens. Photographs of the dried specimens and living individuals were taken using a compact digital camera (Tough TG-6, Olympus, Tokyo, Japan) and digital microscopes (VHX-1100, Keyence, Osaka, Japan; Dino-Lite Premier M, Opto Science, Tokyo, Japan). The image stacks were processed using Adobe Photoshop 2023 ver.24.5 when using Dino-Lite Premier M. The host plants were photographed using a smartphone (iPhone 8, Apple, California, U.S.A.). Morphological terms were assigned according to previous monographs (Takeya 1962; Drake and Davis 1960; Drake and Ruhoff 1965; Schuh and Weirauch 2020).

The type specimens of the new species were deposited at the National Museum of Nature and Science, Ibaraki, Japan (NSMT), the Shirakami Research Center for Environmental Sciences, Faculty of Agriculture and Life Science, Hirosaki University, Aomori, Japan (SIHU), and the Laboratory of Entomology, Faculty of Agriculture, Tokyo University of Agriculture, Kanagawa, Japan (TUA).

Dried specimens of the two known Japanese species of *Agramma*, namely *A. (A.) abruptifrons* and *A. (A.) japonicum*, which were compared with the new species described below, were either recorded in previous studies (Souma 2020, 2021; Souma and Hisasue 2022; Souma

and Iwata 2022; Tago 2023) or newly collected (Suppl. material 3). Newly collected specimens comprising only *A. (A.) japonicum* were deposited at SIHU.

Species distribution records were mapped using SimpleMappr (Shorthouse 2010). Geographical coordinates were obtained from Google Maps (<https://www.google.co.jp/maps>). The map was edited using Adobe Photoshop 2023 ver.24.5.

## Results

### Molecular data

The Bayesian tree of COI, COII, 16S, and 28S genes well supported the monophyly of the clade *A. (A.) izuense* sp. nov. + *A. (A.) japonicum*, *A. (A.) japonicum*, and the clade consisting of the populations of *A. (A.) japonicum* from Honshu and Kyushu (all Bayesian posterior probabilities = 100%) (Fig. 1). The phylogenetic analysis of COI well supported the monophyly of the following taxa and populations (all Bayesian posterior probabilities = 100%): the clade *A. (A.) izuense* sp. nov. + *A. (A.) japonicum*; *A. (A.) izuense* sp. nov.; *A. (A.) japonicum*; and the population of *A. (A.) japonicum* from Kyushu.

The inter- and intraspecific distances of 18 individuals of four lace bug species were generated based on the K2P model of substitution of the partial COI gene (742 bp) (Suppl. material 2). The divergence between the ingroups (*A. (A.) izuense* sp. nov. and *A. (A.) japonicum*) and outgroups (*Cochlochila (Physodictyon) conchata* and *Limnostatus lewisi*) was in the range of 0.1912–0.2198. The interspecific divergence between *A. (A.) izuense* sp. nov. and *A. (A.) japonicum* was in the range of 0.0916–0.1029 and were considered large. As mentioned above, both species, which can also be distinguished based on morphological characteristics (see the identification key), were monophyletic in the Bayesian trees (Fig. 1). Finally, *A. (A.) izuense* sp. nov. and *A. (A.) japonicum* were considered as independent species in the present study.

The intraspecific divergence of the partial COI gene was 0 in *A. (A.) izuense* sp. nov. and 0–0.0262 in *A. (A.) japonicum*. The interpopulation divergence of *A. (A.) japonicum* between Hokkaido, Honshu, and Kyushu were 0.0220 (Hokkaido and Honshu), 0.0248–0.0262 (Hokkaido and Kyushu), and 0.0095–0.0109 (Honshu and Kyushu), and were considered large. In contrast, the intrapopulation divergence within the three islands was 0–0.0013 and was considered small. Furthermore, the Bayesian trees formed separate clades with high posterior probabilities for the three populations of *A. (A.) japonicum* (Fig. 1). However, no morphological differences were found among the specimens from these three islands, and the three populations of *A. (A.) japonicum* were treated as the same species in the present study.

To the best of the author's knowledge (Suppl. material 3) and in accordance with the findings of a previous study (Souma 2020), the submacropterous and macropter-

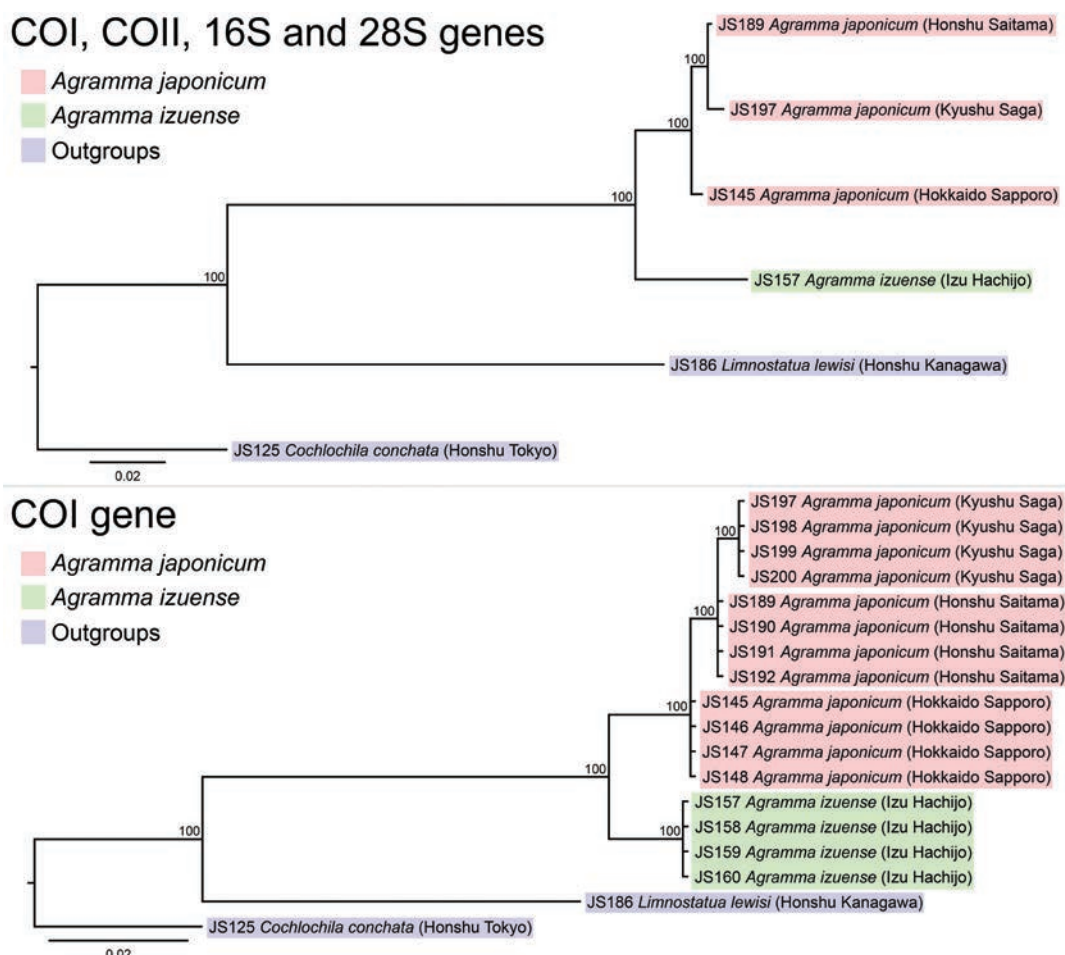


**Figure 1.** Bayesian trees constructed using COI, COII, 16S and 28S genes (2,312 bp) and COI gene (742 bp). Bayesian posterior probabilities are indicated near nodes. Scale bars represent number of expected substitutions per site. Each sample ID is followed by species name and collection locality.

ous morphs of *A. (A.) japonicum* are considered common and rare, respectively. Thus, opportunities for long-distance flight dispersal could be rare in *A. (A.) japonicum*. Although further studies are needed, the hypothesis of the low dispersal ability could explain why the interpopulation and intrapopulation divergences of the partial COI gene in *A. (A.) japonicum* were large and small, respectively.

## Systematics

### Genus *Agramma* Stephens, 1829

Japanese name: Naga-gunbai-zoku

*Agramma* Stephens, 1829: 64. Type species: *Tingis laeta* Fallén, 1807, by monotypy.

**Note.** For synonyms and detailed descriptions of the genus see Péricart (1983), Péricart and Golub (1996) and Souma (2020).

**Remarks.** The genus *Agramma* comprises 88 extant and one fossil species in three subgenera from the Old World. Among them, two species belonging to the nominotypical subgenus, namely *A. (Agramma) abruptifrons*

(Figs 2A, 3A, 4A, 5A, 6A, 7A, 8A, 9A, 10A, B) and *A. (A.) japonicum* (Figs 2D, 3C, 4C, 5E, 6C, 7C, 8C, 9C, 10D), have been known from Japan to date (cf. Souma 2020). Here, two new species of the nominotypical subgenus, namely *A. (A.) izuense* sp. nov. and *A. (A.) kera-mense* sp. nov., are described from Japan. A key to the four species is provided.

### *Agramma (Agramma) izuense* sp. nov.

<https://zoobank.org/23E9D009-B96B-4905-91B8-D783B3BF0ECD>

Figs 2B, C, 3B, 4B, 5B–D, 6B, 7B, 8B, 9B, 10C

Japanese name: Hachijonaga-gunbai

*Agramma nexile* (non Drake, 1948): Tomokuni and Ishikawa (2002: 170) (distribution); Yamada and Tomokuni (2012: 188) (distribution: part); Yamada and Ishikawa (2016: 429) (distribution: part). Misidentifications.

*Agramma japonicum* (non Drake, 1948): Souma (2020: 532) (distribution: part). Misidentification.

**Type series.** *Holotype* (submacropterous ♂, SIHU), “[JAPAN]: Izu Isls., Hachijo Is., Mitsune, Mt. Hachijo-Fuji” [=JAPAN: IZU ISLANDS: Hachijo Island:

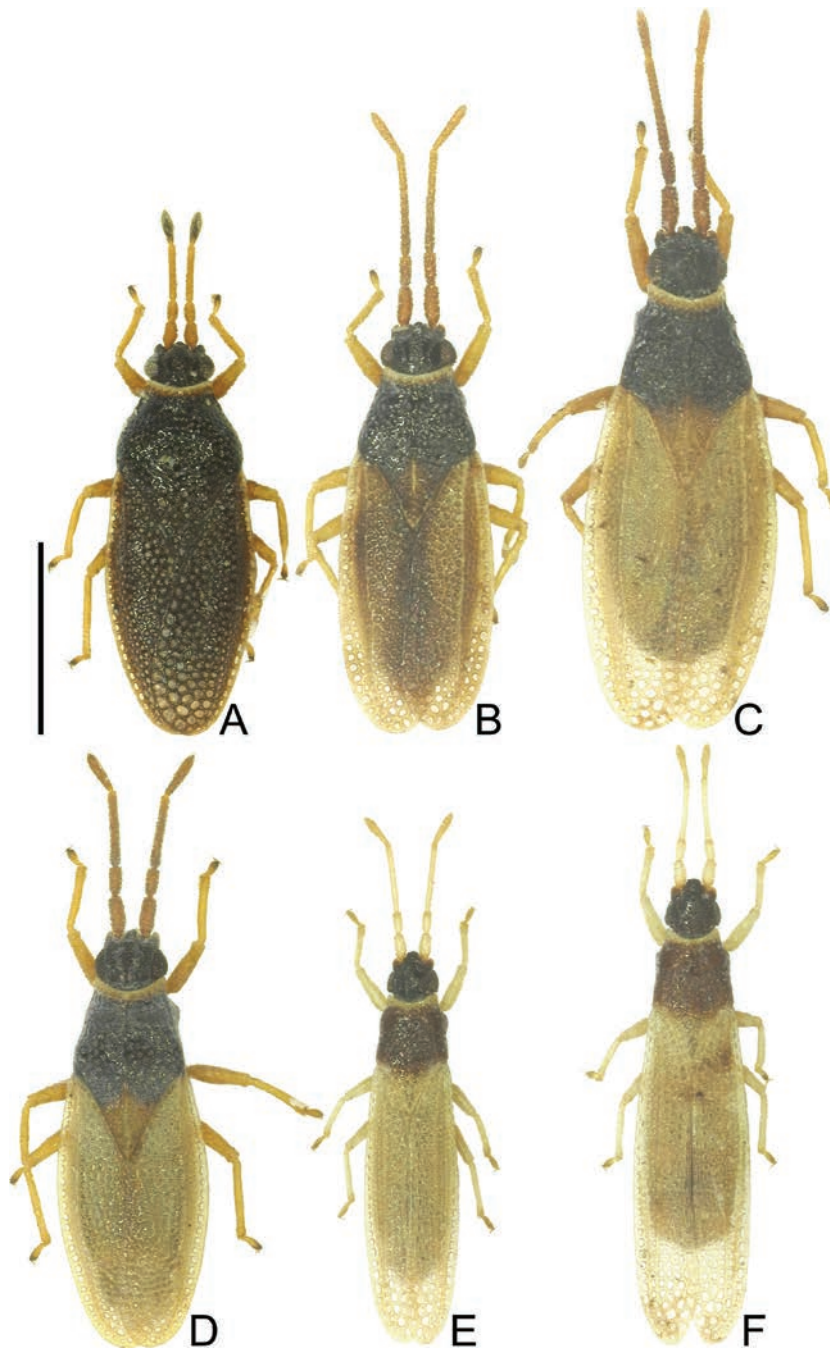


**Figure 2.** Habitus of four *Agramma* species from Japan, dorsal view: A. (*Agramma*) *abruptifrons* from Honshu (A); A. (*A.*) *izuense* sp. nov. from Hachijo Island, Izu Islands, male (B) and female (C); A. (*A.*) *japonicum* from Yakushima Island, Osumi Group, Ryukyu Islands (D); A. (*A.*) *keramense* sp. nov. from Geruma Island, Kerama Group, Ryukyu Islands, male (E) and female (F). Scale bar: 1.0 mm.

Southeastern foothills of Mt. Hachijo-Fuji (approximate coordinates: 33°07'34.5"N, 139°47'10.7"E)], 18.v.2021, leg. J. Souma. **Paratypes** (submacropterous 46 ♂♂ 36 ♀♀), JAPAN: IZU ISLANDS: Hachijo Island: as holotype (submacropterous 8 ♂♂ 4 ♀♀, SIHU); as holotype but 16.v.2021 (submacropterous 3 ♂♂ 6 ♀♀, SIHU); as holotype but 21.v.2021 (submacropterous 6 ♂♂ 10 ♀♀, SIHU); alt. 250–530 m of Mt. Hachijo-Fuji, 4.vii.2001, leg. M. Tomokuni (submacropterous 1 ♂, NSMT); Noboryo Pass, 17.v.2021, leg. J. Souma (submacropterous 9 ♂♂ 3 ♀♀, SIHU; 3 ♂♂ 4 ♀♀, TUA); as above but

5.vii.2001, leg. M. Tomokuni (submacropterous 5 ♂♂ 2 ♀♀, NSMT); Ohkago, 19.v.2021, leg. J. Souma (submacropterous 7 ♂♂ 5 ♀♀, SIHU); Western foothills of Mt. Hachijo-Fuji, 21.v.2021, leg. J. Souma (submacropterous 4 ♂♂ 2 ♀♀, SIHU). Eight specimens collected in 2001 were recorded as “*Agramma nexile* (Drake, 1948)” by the previous study (Tomokuni and Ishikawa 2002).

**Additional material examined. Non-types** (1 nymph, SIHU), JAPAN: IZU ISLANDS: Hachijo Island: as holotype but 16.v.2021. The single nymph recorded above was in poor condition and was thus not described in the present study.

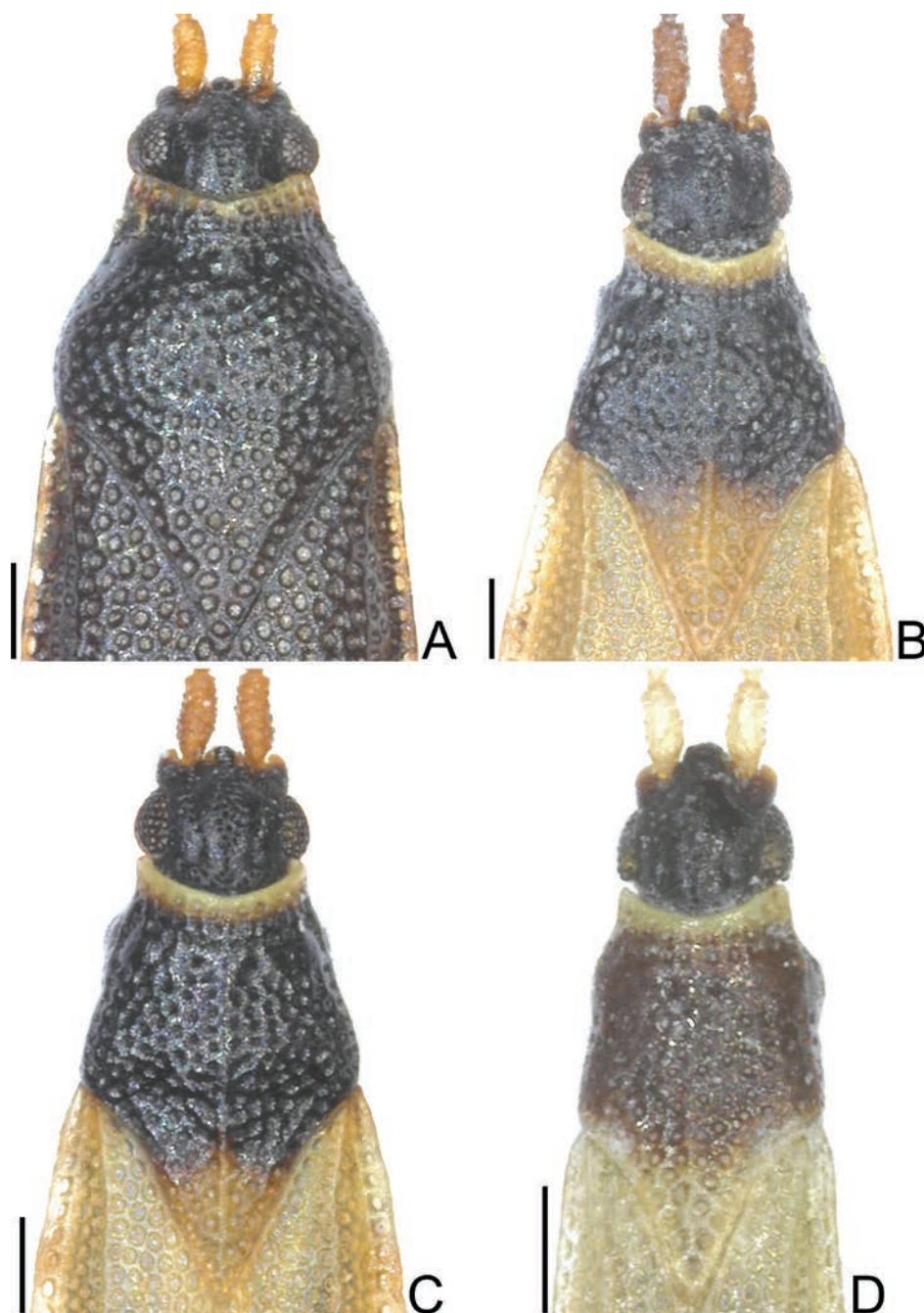


**Figure 3.** Pronota of four *Agramma* species from Japan, dorsal view: A. (*Agramma*) *abruptifrons* (A); A. (*A.*) *izuense* sp. nov. (B); A. (*A.*) *japonicum* (C); A. (*A.*) *keramense* sp. nov. (D). Scale bars: 0.2 mm.

**Diagnosis.** *Agramma* (*Agramma*) *izuense* sp. nov. is recognized among other species of *Agramma* by a combination of the following characters: pubescence on body less than 0.5 times as long as diameter of compound eye; antennal segment IV brown (Fig. 2B, C); posterior process in apical part and hemelytron sometimes irregularly dark (Fig. 5C); thoracic sterna, pygophore and female terminalia black (Figs 4B, 6B, 7B); head with a pair of frontal spines (Figs 3B, 8B); rostrum reaching middle part of mesosternum; pronotum without paranotum; median carina of pronotum distinct on posterior process; anterior margin of hemelytron gently curved outward (Fig. 5B, D); apices of hemelytra separated from each other at rest; R+M

(radiomedial) vein of hemelytron present in apical part, carinate throughout its length; costal area usually with 2 rows of areolae at widest part; discoidal-sutural area with 7–8 rows of areolae at widest part; outer and inner margins of paramere angularly curved in middle part (Fig. 9B); and female terminalia hexagonal in ventral view, with posterior margin protruding posteriad in middle part.

**Description.** *Submacropterous male.* Head, calli, pronotal disc, basal part of posterior process, thoracic pleura, thoracic sterna, sternal laminae, apical part of tarsi and abdomen black; antenna, frontal spine, buccula, rostrum, collar, apical part of posterior process, hemelytron and legs except apical part of tarsi brown; apical part of poste-

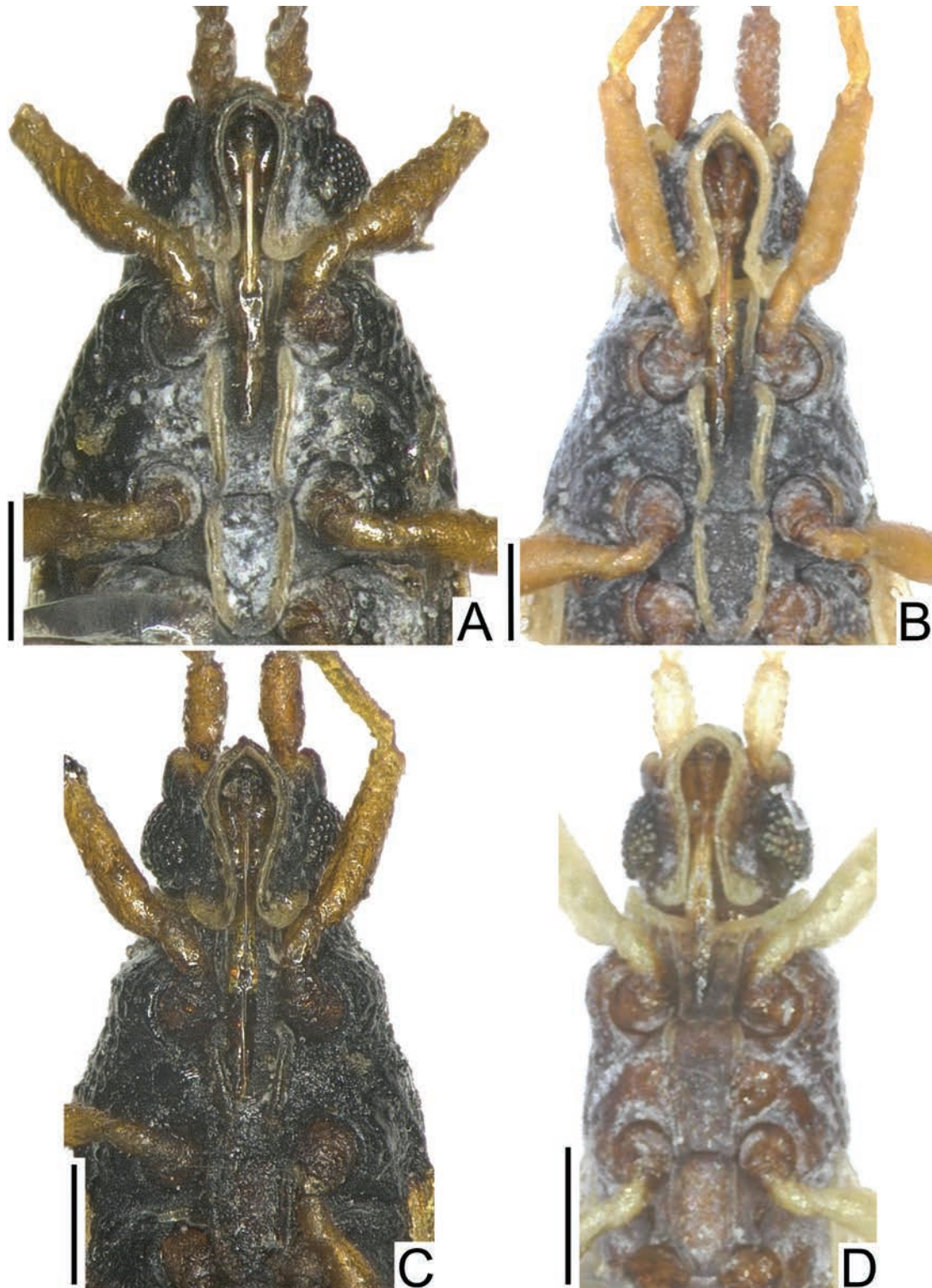


**Figure 4.** Rostra of four *Agramma* species from Japan, ventral view: *A. (Agramma) abruptifrons* (A); *A. (A.) izuense* sp. nov. (B); *A. (A.) japonicum* (C); *A. (A.) keramense* sp. nov. (D). Scale bars: 0.2 mm.

rior process and hemelytron sometimes irregularly dark; compound eyes dark red; pubescence on body yellowish (Figs 2B, 3B, 4B, 5B, C, 6B).

Body (Fig. 2B) oblong; pubescence on body less than 0.5 times as long as diameter of compound eye. Head (Figs 3B, 8B) glabrous, with a pair of frontal spines; frontal spines separated from each other at apices, not

reaching apex of clypeus; antenniferous tubercles obtuse, slightly curved inward; clypeus smooth; vertex coarsely punctate. Compound eye round in dorsal view. Antenna densely covered with pubescence throughout its length and tiny tubercles in segments I to II; segment I cylindrical; segment II cylindrical, shortest among antennal segments; segment III longest among antennal segments;

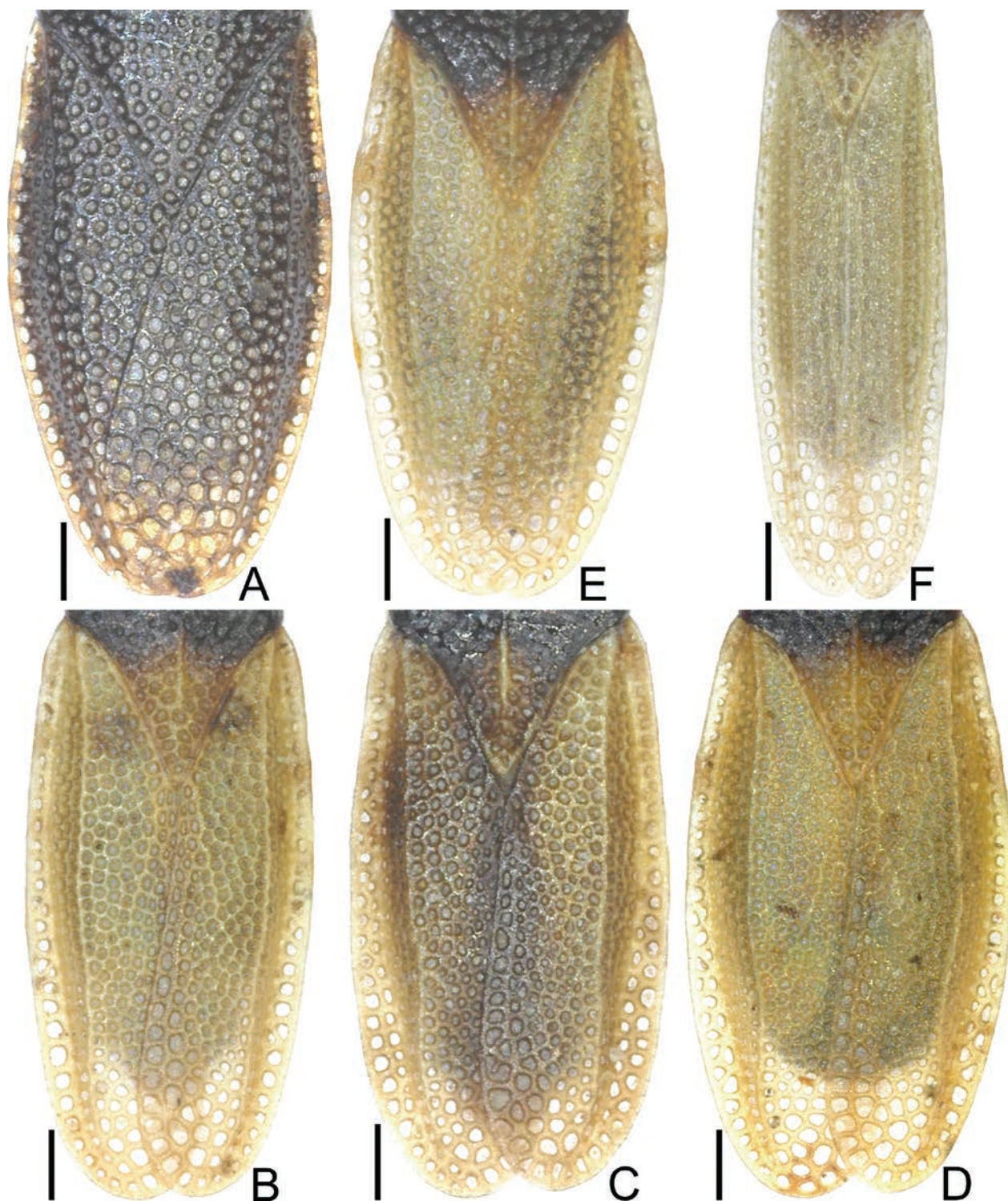


**Figure 5.** Hemelytra of four *Agramma* species from Japan, dorsal view: *A. (Agramma) abruptifrons* (A); *A. (A.) izuense* sp. nov., male (B, C) and female (D); *A. (A.) japonicum* (E); *A. (A.) keramense* sp. nov. (F). Scale bars: 0.2 mm.

segment IV cylindrical, longer than segment I. Bucculae contiguous with each other at anterior ends, with 3 rows of areolae throughout their length. Rostrum (Fig. 4B) reaching middle part of mesosternum.

Pronotum (Figs 3B, 8B) unicarinate, without paranotum. Pronotal disc coarsely punctate. Hood absent. Collar coarsely punctate; anterior margin gently curved inward. Calli smooth. Median carina ridge-like, distinct

on posterior process. Posterior process well-developed, flattened, triangular. Thoracic pleura coarsely punctate. Ostiolar peritreme oblong. Mesosternum (Fig. 4B) as wide as metasternum at widest part. Sternal laminae nearly straight throughout their length. Legs smooth, covered with pubescence.

Hemelytron (Fig. 5B, C), extending beyond apex of abdomen; anterior margin gently curved outward; apices

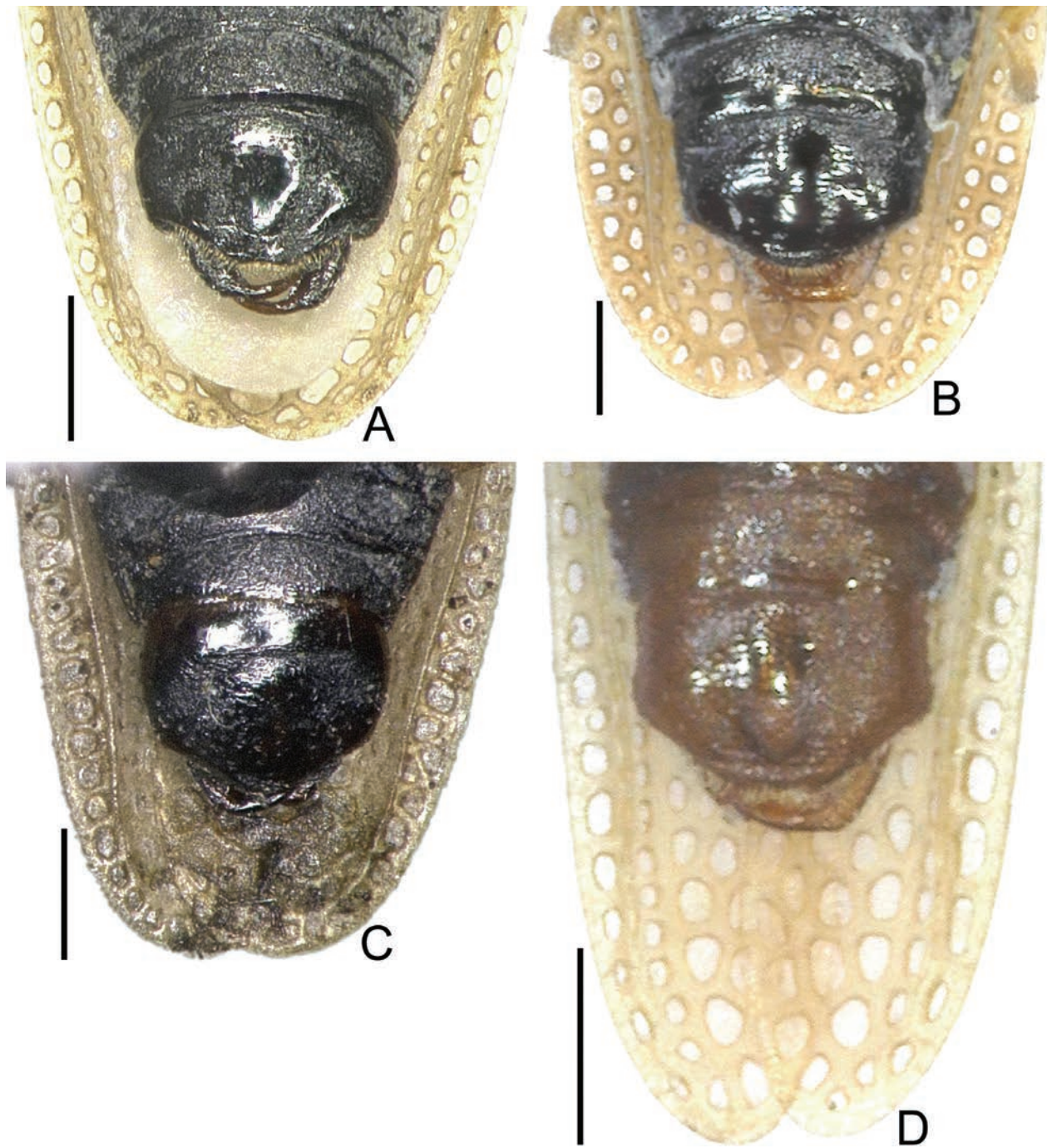


**Figure 6.** Male terminalia of four *Agramma* species from Japan, ventral view: A. (*Agramma*) *abruptifrons* (A); A. (*A.*) *izuense* sp. nov. (B); A. (*A.*) *japonicum* (C); A. (*A.*) *keramense* sp. nov. (D). Scale bars: 0.2 mm.

separated from each other at rest; C (costal) and R+M (radiomedial) veins present, carinate throughout their length; Cu (cubital) vein indistinct; costal area usually with 2 rows of areolae at widest part, rarely with a single row throughout its length; subcostal area with 3–4 rows of areolae at widest part; discoidal-sutural area with 7–8 rows of areolae at widest part; hypocostal lamina with a single row of areolae throughout its length.

Abdomen oblong in dorsal and ventral views. Pygophore (Fig. 6B) compressed dorsoventrally, semicircular in ventral view, covered with pubescence. Paramere (Fig. 9B) slender, expanded in middle part; outer and

inner margins angularly curved in middle part, covered with pubescence in middle part.

Measurements (n = 20). Body length with hemelytra 2.1–2.4 mm; maximum width across hemelytra 0.8–0.9 mm; length of antennal segments I to IV 0.2 mm, 0.1 mm, 0.5 mm, and 0.3 mm, respectively; pronotal length 0.8–0.9 mm; pronotal width across humeri 0.6 mm; hemelytral length 1.4–1.6 mm; maximum width of hemelytron 0.4–0.5 mm.

**Submacropterous female.** General habitus very similar to that of male (Figs 2C, 5D, 7B) except for the following characters: subcostal area of hemelytron wider

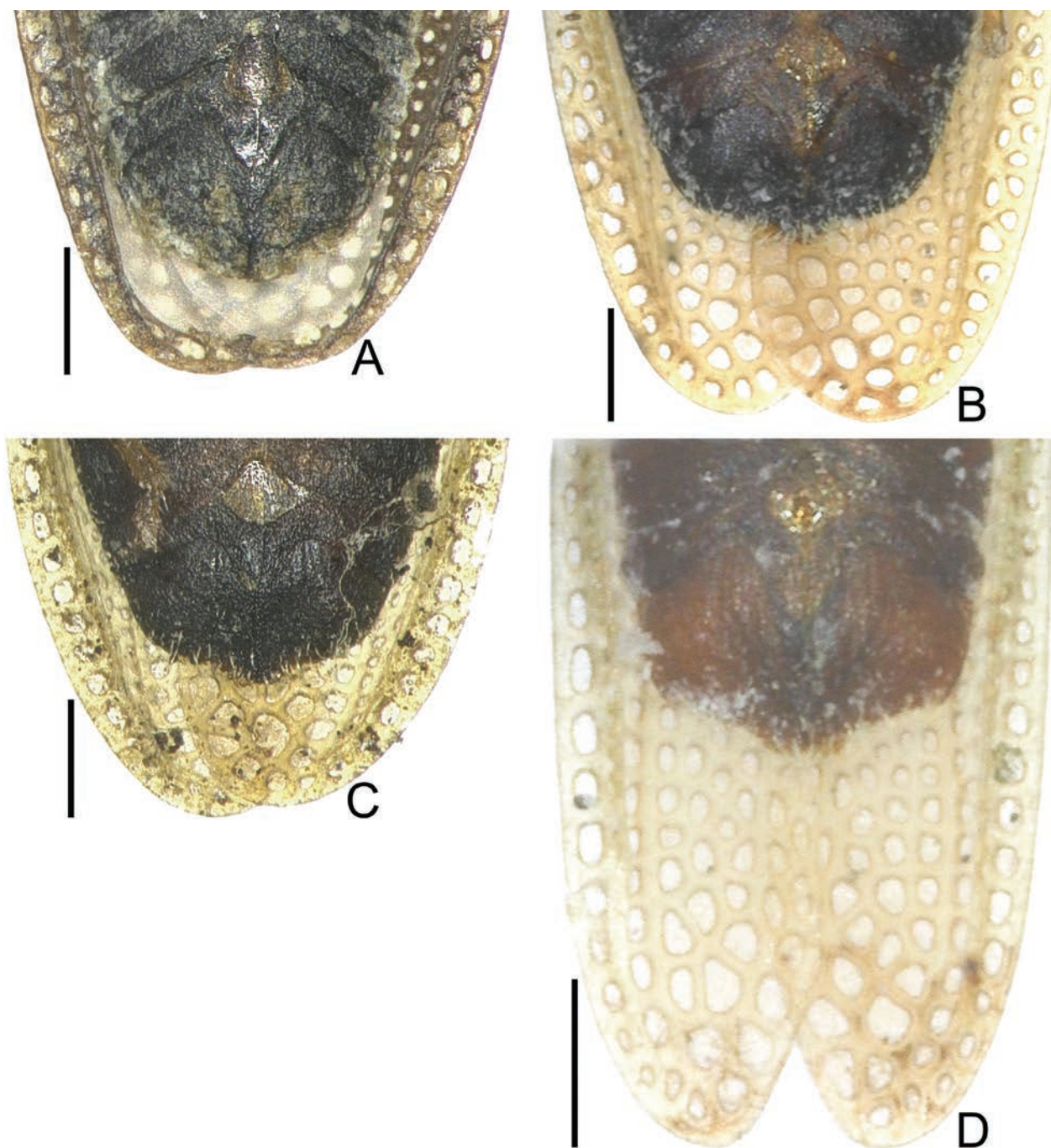


**Figure 7.** Female terminalia of four *Agramma* species from Japan, ventral view: *A. (A.) abruptifrons* (A); *A. (A.) izuense* sp. nov. (B); *A. (A.) japonicum* (C); *A. (A.) keramense* sp. nov. (D). Scale bars: 0.2 mm.

than in male, with 4–5 rows of areolae at widest part; apical part of abdomen hexagonal in ventral view; posterior margin of terminalia protruding posteriad in middle part; and ovipositor with well-developed ovalvula at base.

Measurements ( $n = 20$ ). Body length with hemelytra 2.4–2.6 mm; maximum width across hemelytra 0.9–1.0 mm; length of antennal segments I to IV 0.2 mm, 0.1 mm, 1.5 mm, and 0.3 mm, respectively; pronotal length 0.9–1.0 mm; pronotal width across humeri 0.6–0.7 mm; hemelytral length 1.6–1.8 mm; maximum width of hemelytron 0.5–0.6 mm.

**Remarks.** In a previous study, *Agramma (Agramma) izuense* sp. nov. was misidentified as *A. (A.) japonicum*

(Tomokuni and Ishikawa 2002), because both species are the most similar among the Asian species of the genus *Agramma*. However, the former is easily distinguished from the latter by the following characters: posterior process in apical part and hemelytron sometimes irregularly dark (brown in *A. (A.) japonicum*) (Figs 2B, D, 5C, E); apices of hemelytra separated from each other at rest (close to each other in *A. (A.) japonicum*) (Figs 2C, 5B, D); R+M (radiomedial) vein carinate throughout its length (carinate in basal part and not carinate in apical part in *A. (A.) japonicum*); and costal area usually with 2 rows of areolae at widest part (a single row in *A. (A.) japonicum*). Morphological differences between

the new species and the other two Japanese species are provided in the identification key below.

On the other hand, the new species is similar in general appearance to *A. (A.) ruficorne* (Germar, 1835), which is widely distributed in the Palaearctic Region (Péricart and Golub 1996; Aukema et al. 2013). Nevertheless, *A. (A.) ruficorne* shares the morphological features mentioned in the above paragraph with *A. (A.) japonicum* so that it is easily distinguished from *A. (A.) izuense* sp. nov.

**Distribution.** Japan (Izu Islands: Hachijo Island) (Fig. 12) (Tomokuni and Ishikawa 2002; Yamada and Tomokuni 2012; Yamada and Ishikawa 2016; present study). *Agramma (Agramma) izuense* sp. nov. inhabits the forest floor in the warm-temperate climate of the Izu Islands in the Palaearctic Region.

**Etymology.** The specific epithet refers to its occurrence in the Izu Islands, Japan; an adjective.

**Host plants.** *Carex* sp. (Cyperaceae) (Fig. 11B) (present study). Although the host plant species could not be identified, *Agramma (Agramma) izuense* sp. nov. feeds only on this cyperaceous herb and appears to be monophagous.

**Biology.** *Agramma (Agramma) izuense* sp. nov. feeds on the abaxial surface of the leaves of the abovementioned cyperaceous plant (present study). Dozens of type materials consisting of only submacropterous morphs were collected, suggesting that this new species is flightless. Adults and nymphs were collected in May and July (Tomokuni and Ishikawa 2002; present study).

#### *Agramma (Agramma) keramense* sp. nov.

<https://zoobank.org/5A41CB70-F8B5-4B30-8B29-A0B7CCFB6605>

Figs 2E, F, 3D, 4D, 5F, 6D, 7D, 8D, 9D, 10E–I

Japanese name: Hosonaga-gunbai

**Type series.** *Holotype* (submacropterous ♂, SIHU), “[JAPAN]: the Ryukyus, Okinawa Isls., Aka Is., Aka” [=JAPAN: RYUKYU ISLANDS: Kerama Group: Aka Island: Aka (approximate coordinates: 26°11'43.7"N, 127°17'07.9"E)], 3.xi.2022, leg. J. Souma. *Paratypes* (submacropterous 13 ♂♂ 19 ♀♀), JAPAN: RYUKYU ISLANDS: Kerama Group: Aka Island: as holotype (submacropterous 2 ♂♂ 5 ♀♀, SIHU); as holotype but 4.v.2021, leg. R. Ito (submacropterous 1 ♀, SIHU); as holotype but 5.v.2021, leg. R. Ito (submacropterous 3 ♂♂ 3 ♀♀, SIHU); as holotype but 17.vii.2021, leg. R. Ito (submacropterous 3 ♂♂ 3 ♀♀, SIHU). Geruma Island: Geruma, 3.xi.2022, leg. J. Souma (submacropterous 5 ♂♂ 7 ♀♀, SIHU).

**Additional material examined. Non-types** (7 nymphs), JAPAN: RYUKYU ISLANDS: Kerama Group: Aka Island: as holotype (6 nymphs, SIHU); as holotype but 5.v.2021, leg. R. Ito (1 nymph, SIHU). All 7 nymphs recorded above were in poor condition and are thus not described here.

**Diagnosis.** *Agramma (Agramma) keramense* sp. nov. is recognized among other species of *Agramma* by a combination of the following characters: pubescence on body less than 0.5 times as long as diameter of compound eye; antennal segment IV light brown (Fig. 2E, F); posterior process in apical part and hemelytron light brown (Fig. 5F); thoracic

sterna, pygophore and female terminalia dark brown (Figs 4D, 6D, 7D); head without spine (Figs 3D, 8D); rostrum reaching posterior part of prosternum; pronotum without paranotum; median carina of pronotum indistinct on posterior process; anterior margin of hemelytron nearly straight; apices of hemelytra separated from each other at rest; R+M (radiomedial) vein of hemelytron present in apical part, carinate throughout its length; costal area with a single row of areolae throughout its length; discoidal-sutural area with 5 rows of areolae at widest part; outer and inner margins of paramere gently curved in middle part (Fig. 9D); and female terminalia hexagonal in ventral view, with posterior margin protruding posteriad in middle part.

**Description. Submacropterous male.** Head black; calli, pronotal disc, basal part of posterior process, thoracic pleura, thoracic sterna, sternal laminae and abdomen dark brown; antenna, buccula, rostrum, collar, apical part of posterior process, hemelytron and legs light brown; compound eye dark red; pubescence on body yellowish (Figs 2E, 3D, 4D, 5F, 6D).

Body (Fig. 2E) oblong; pubescence on body less than 0.5 times as long as diameter of compound eye. Head (Figs 3D, 8D) glabrous, without spine; antenniferous tubercles obtuse, slightly curved inward; clypeus smooth; vertex coarsely punctate. Compound eye round in dorsal view. Antenna densely covered with pubescence throughout its length and tiny tubercles in segments I to II; segment I cylindrical, as long as segment II; segment II cylindrical; segment III longest among antennal segments; segment IV cylindrical, longer than segment I. Bucculae contiguous with each other at anterior ends, with 3 rows of areolae throughout their length. Rostrum (Fig. 4D) reaching posterior part of prosternum.

Pronotum (Figs 3D, 8D) without carina, without paranotum. Pronotal disc coarsely punctate. Hood absent. Collar coarsely punctate; anterior margin gently curved inward. Calli smooth. Posterior process well-developed, flattened, triangular. Thoracic pleura coarsely punctate. Ostiolar peritreme oblong. Mesosternum (Fig. 4D) as wide as metasternum at widest part. Sternal laminae nearly straight throughout their length. Legs smooth, covered with pubescence.

Hemelytron (Fig. 5F), extending beyond apex of abdomen; anterior margin nearly straight; apices separated from each other at rest; C (costal) and R+M (radiomedial) veins present, carinate throughout their length; Cu (cubital) vein indistinct; costal area with a single row of areolae throughout its length; subcostal area with 3 rows of areolae at widest part; discoidal-sutural area with 5 rows of areolae at widest part; hypocostal lamina with a single row of areolae throughout its length.

Abdomen oblong in dorsal and ventral views. Pygophore (Fig. 6D) compressed dorsoventrally, semicircular in ventral view, covered with pubescence. Paramere (Fig. 9D) slender, expanded in middle part; outer and inner margins gently curved in middle part, covered with pubescence in middle part.

Measurements (n = 14). Body length with hemelytra 2.2–2.4 mm; maximum width across hemelytra 0.5–0.6 mm;

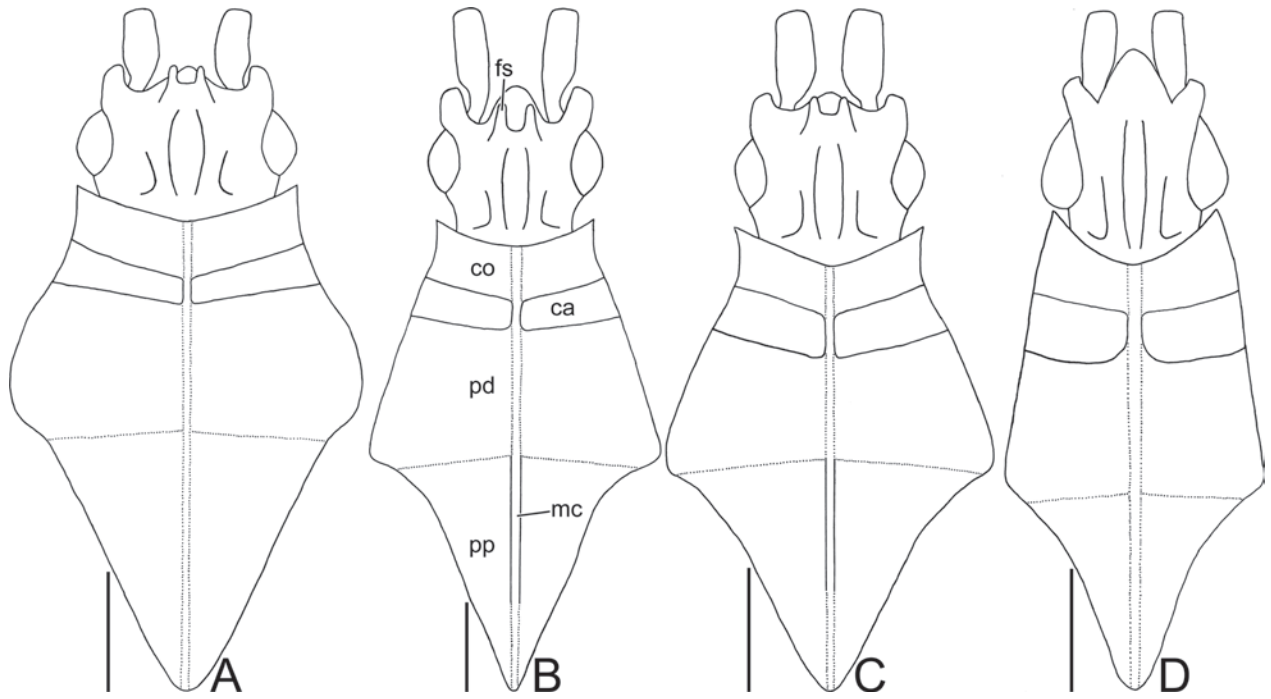


**Figure 8.** Line drawings of pronota of four *Agramma* species from Japan, dorsal view: *A. (Agramma) abruptifrons* (A); *A. (A.) izuense* sp. nov. (B); *A. (A.) japonicum* (C); *A. (A.) keramense* sp. nov. (D). Abbreviations: ca, calli; co, collar; fs, frontal spine; mc, median carina; pd, pronotal disc; pp, posterior process. Scale bars: 0.2 mm.

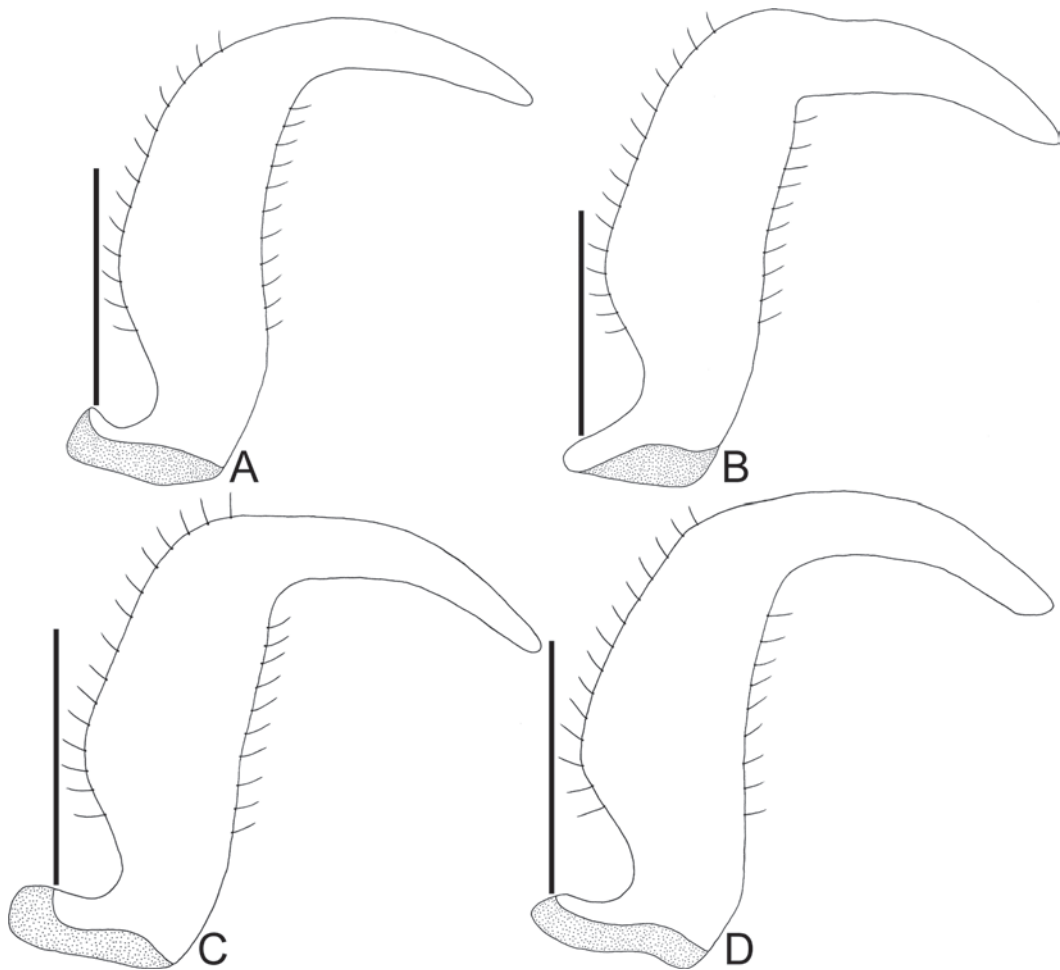


**Figure 9.** Line drawings of parameres of four *Agramma* species from Japan, dorsal view: *A. (Agramma) abruptifrons* (A); *A. (A.) izuense* sp. nov. (B); *A. (A.) japonicum* (C); *A. (A.) keramense* sp. nov. (D). Scale bars: 0.1 mm.

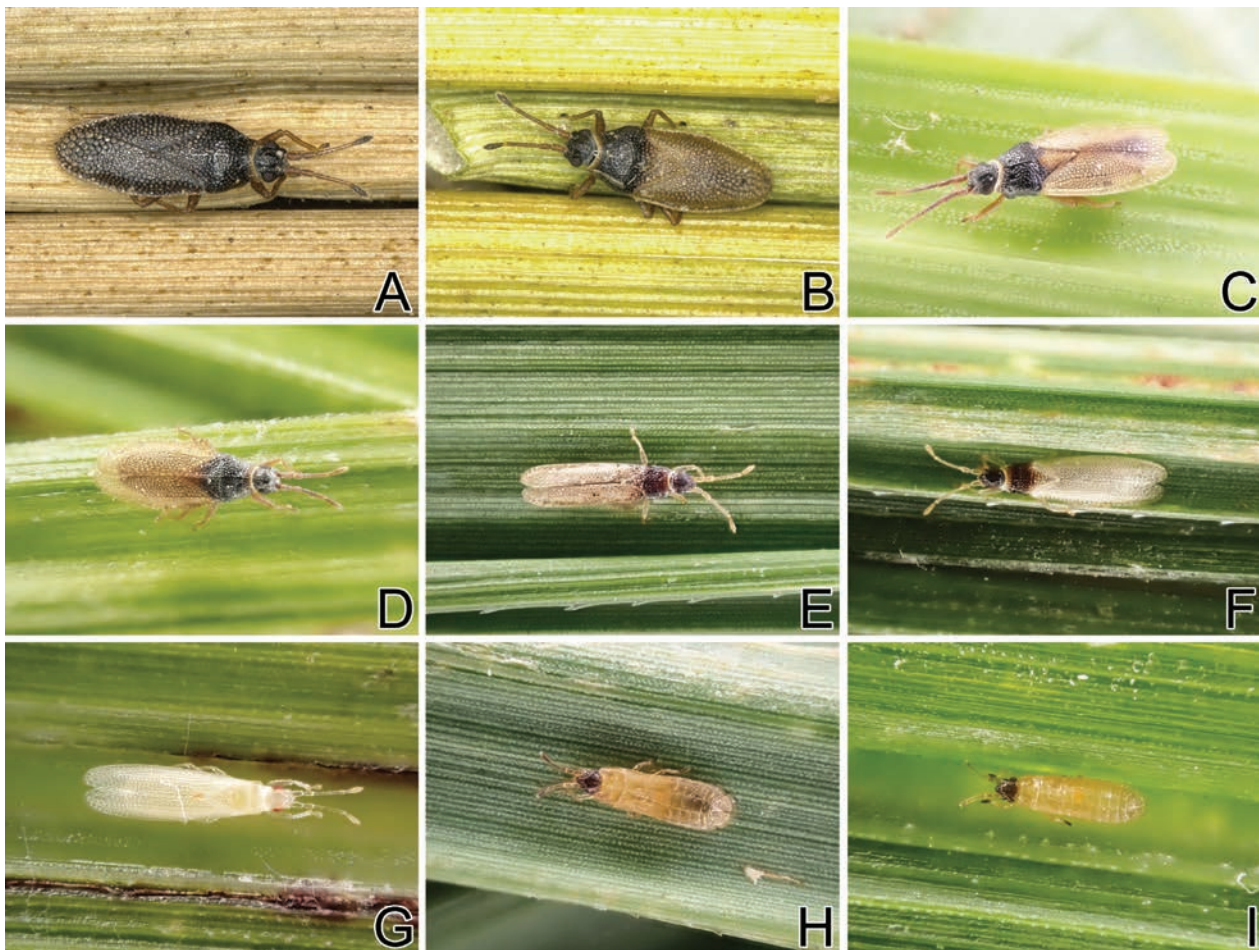


**Figure 10.** Living individuals of four *Agramma* species from Japan: *A. (A.) abruptifrons* from Honshu, female (A) and teneral male (B); *A. (A.) izuense* sp. nov. from Hachijo Island, Izu Islands, female (C); *A. (A.) japonicum* from Honshu, female (D); *A. (A.) keramense* sp. nov. from Aka Island, Kerama Group, Ryukyu Islands, male (E), mature (F) and teneral (G) females, and fifth (H) and fourth (I) instar nymphs.

length of antennal segments I to IV 0.1 mm, 0.1 mm, 0.4 mm, and 0.2 mm, respectively; pronotal length 0.7 mm; pronotal width across humeri 0.4 mm; hemelytral length 1.6–1.7 mm; maximum width of hemelytron 0.3 mm.

**Submacropterous female.** General habitus very similar to that of male (Figs 2F, 7D) except for the following characters: subcostal area of hemelytron wider than in male, with 4 rows of areolae at widest part; apical part of abdomen hexagonal in ventral view; posterior margin of terminalia protruding posteriad in middle part; and ovipositor with well-developed ovivalvula at base.

Measurements ( $n = 19$ ). Body length with hemelytra 2.4–2.5 mm; maximum width across hemelytra 0.6 mm; length of antennal segments I to IV 0.1 mm, 0.1 mm, 0.4 mm, and 0.2 mm, respectively; pronotal length 0.7 mm; pronotal width across humeri 0.4 mm; hemelytral length 1.7–1.8 mm; maximum width of hemelytron 0.3–0.4 mm.

**Remarks.** *Agramma (Agramma) keramense* sp. nov. does not completely match the diagnosis of the genus *Agramma* provided by Souma (2020) because of the lack of spines on the head. However, the new species can be provisionally placed into *Agramma* based on the general similarity.

Among the Asian species of *Agramma*, *A. (A.) keramense* sp. nov. is most similar to *A. (A.) vicinale* (Drake, 1927) in its general habitus. However, based on a comparison between the type materials of the new species and the photographs of the holotype (United States National Museum of Natural History 2023), together with the original description (Drake 1927) of *A. (A.) vicinale*, two main characters were recognized to easily differentiate *A. (A.) keramense* sp. nov. from *A. (A.) vicinale*: head without spine (with a pair of frontal spines in *A. (A.) vicinale*) (Fig. 3D, 8D); and median carina of pronotum indistinct on posterior process (distinct in *A. (A.) vicinale*). Morphological differences between the new species and the three other Japanese species are provided in the identification key below.

**Distribution.** Japan (Ryukyu Islands: Kerama Group: Aka Island, Geruma Island) (Fig. 12). *Agramma (Agramma) keramense* sp. nov. inhabits grasslands in the subtropical climate of Kerama Group of the Ryukyu Islands in the Oriental Region.

**Etymology.** The specific epithet refers to its occurrence in Kerama Group, the Ryukyu Islands, Japan; an adjective.

**Host plants.** Poaceae gen. et sp. indet. (present study) (Fig. 11D). Although the host plant genus and species



**Figure 11.** Monocotyledonous host plants of four *Agramma* species from Japan: *Juncus* sp. (A) from Honshu, damaged by *A. (Agramma) abruptifrons*; *Carex* sp. (B) from Hachijo Island, Izu Islands, damaged by *A. (A.) izuense* sp. nov.; *Carex* sp. (C) from Honshu, damaged by *A. (A.) japonicum*; Poaceae gen. et sp. indet. (D) from Aka Island, Kerama Group, Ryukyu Islands, damaged by *A. (A.) keramense* sp. nov.

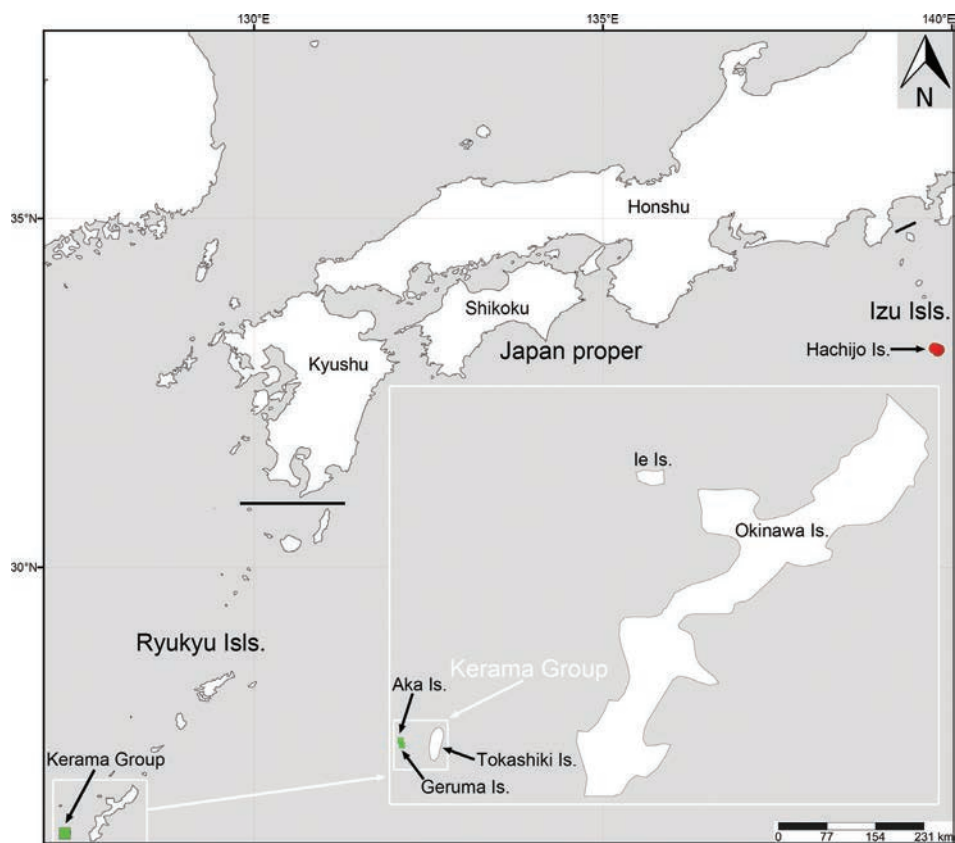


**Figure 12.** Collection sites of two species of *Agramma* from Japan used in present study. Red circles = *A. (Agramma) izuense* sp. nov.; green squares = *A. (A.) keramense* sp. nov.

could not be identified, *Agramma (Agramma) keramense* sp. nov. only feeds on this poaceous herb and appears to be monophagous.

**Biology.** *Agramma (Agramma) keramense* sp. nov. feeds on the abaxial surface of the leaves of the aforementioned

poaceous plant (present study). Dozens of type materials consisting of only submacropterous morphs were collected, suggesting that this new species is flightless. Adults were collected in May, July, and November, whereas nymphs were collected in May and November (present study).

## Key to species of *Agramma* from Japan

- 1 Head without spine (Figs 3D, 8D); rostrum reaching posterior part of prosternum (Fig. 4D); anterior margin of hemelytron nearly straight (Figs 2E, F, 5F); collected from Poaceae (Fig. 11D)..... *Agramma (Agramma) keramense* sp. nov.
- Head with a pair of frontal spines (Figs 3A–C, 8A–C); rostrum reaching middle part of mesosternum (Fig. 4A–C); anterior margin of hemelytron gently curved outward (Figs 2A–D, 5A–E); collected from Cyperaceae or Juncaceae (Fig. 11A–C) ...2
- 2 Antennal segment IV black (Fig. 2A); median carina of pronotum indistinct on posterior process (Figs 3A, 8A); R+M (radiomedial) vein of hemelytron absent in apical part (Fig. 5A); outer and inner margins of paramere gently curved in middle part (Fig. 9A); posterior margin of female terminalia not protruding posteriad in middle part (Fig. 7A); collected from Juncaceae (Fig. 11A)..... *Agramma (Agramma) abruptifrons* Golub, 1990
- Antennal segment IV brown (Fig. 2B, C); median carina of pronotum distinct on posterior process (Figs 3B, C, 8B, C); R+M (radiomedial) vein of hemelytron present in apical part (Fig. 5B, C); outer and inner margins of paramere angularly curved in middle part (Fig. 9B, C); posterior margin of female terminalia protruding posteriad in middle part (Fig. 7B, C); collected from Cyperaceae (Fig. 11B, C)..... 3
- 3 Posterior process in apical part and hemelytron sometimes irregularly dark (Figs 2B, 5C); apices of hemelytra separated from each other at rest (Figs 2C, 5B, D); R+M (radiomedial) vein carinate throughout its length; costal area usually with 2 rows of areolae at widest part; known from Hachijo Island, Izu Islands ..... *Agramma (Agramma) izuense* sp. nov.
- Posterior process in apical part and hemelytron brown (Figs 2D, 5E); apices of hemelytra close to each other at rest; R+M (radiomedial) vein carinate in basal part, not carinate in apical part; costal area with a single row of areolae throughout its length; known from Japan proper and its surrounding islands, and Yakushima Island of the Ryukyu Island ..... *Agramma (Agramma) japonicum* (Drake, 1948)

## Acknowledgements

I sincerely thank the editor (Dávid Rédei, National Chung Hsing University, Taichung, Taiwan) and an anonymous reviewer for their critical comments on this manuscript. I am deeply indebted to Masaaki Tomokuni and Takuya Kiyoshi (NSMT) for loaning valuable materials. I owe my deepest gratitude to Satoshi Maehara (Tochigi, Japan), Masami Nozawa (Saitama, Japan), Kyosuke Okuda (Saitama, Japan), Noriyuki Muro (Tokyo, Japan), and Reo Ito (Oita, Japan) for providing valuable material and information about the collection sites. I am grateful to Takeyuki Nakamura (SIHU), Yu Hisasue (Tokyo, Japan), and Shinya Suzuki (Kyushu University, Fukuoka, Japan) for accompanying me during fieldwork. This study was partially supported by a Grant-in-Aid for JSPS Fellows (JP20J20483) granted to the author from the Japan Society for the Promotion of Science, Tokyo, Japan. I would like to thank Editage (www.editage.com) for the English language editing.

## References

Altschul SF, Madden TL, Schaffer AA, Zhang J, Zhang Z, Miller W, Lipman DJ (1997) Gapped BLAST and PSI-BLAST: A new generation of protein database search programs. *Nucleic Acids Research* 25(17): 3389–3402. <https://doi.org/10.1093/nar/25.17.3389>

Aukema B, Rieger C, Rabitsch W (2013) Catalogue of the Heteroptera of the Palaearctic Region. Vol. 6, Supplement. Netherlands Entomological Society, Amsterdam, Netherland, [xxiv +] 629 pp.

Damgaard J, Cognato AI (2005) Phylogeny and reclassification of species groups in *Aquarius Schellenberg*, *Limnoporus Stål* and *Gerris Fabricius* (Insecta: Hemiptera-Heteroptera, Gerridae). *Systematic Entomology* 31(1): 93–112. <https://doi.org/10.1111/j.1365-3113.2005.00302.x>

Drake CJ (1927) Tingitidae from the Far East and Madagascar (Hemiptera). *Philippine Journal of Science* 34: 307–312.

Drake CJ (1948) New Tingidae from the Orient and other regions (Hemiptera. Heteroptera). *Musée Heude. Notes d'Entomologie Chinoise* 12(15): 173–178.

Drake CJ, Davis NT (1960) The morphology, phylogeny, and higher classification of the family Tingidae, including the description of a new genus and species of the subfamily Vianaidinae (Hemiptera: Heteroptera). *Entomologica Americana* 39: 1–100.

Drake CJ, Ruhoff FA (1965) Lacebugs of the world, a catalog (Hemiptera: Tingidae). *Bulletin of the United States National Museum* 243: [i–viii +] 1–634. [pls. frontis piece + 1–56]

Ichita T (1988) Aomori-ken no Kamemushi (I). *Celastrina* 20: 114–145. [True bugs from Aomori-ken, Honshu, Japan. (I)] [in Japanese]

Jung S, Duwal RK, Lee S (2011) COI barcoding of true bugs (Insecta, Heteroptera). *Molecular Ecology Resources* 11(2): 266–270. <https://doi.org/10.1111/j.1755-0998.2010.02945.x>

Kass RE, Carlin BP, Gelman A, Neal R (1998) Markov chain Monte Carlo in practice: A roundtable discussion. *The American Statistician* 52(2): 93–100.

Kerzhner IM (1978) Poluzhestkokrylye (Heteroptera) Sakhalina i Kuril'skikh ostrovov. [Heteroptera from Sakhalin and the Kuril

- Islands]. Trudy Biologo-Pochvennogo Instituta Dal'nevostochnogo. Otdeleniya Akademii Nauk SSSR. Novaya Seriya 50(153): 31–57. [in Russian]
- Kumar S, Stecher G, Li M, Knyaz C, Tamura K (2018) MEGA X: Molecular evolutionary genetics analysis across computing platforms. *Molecular Biology and Evolution* 35(6): 1547–1549. <https://doi.org/10.1093/molbev/msy096>
- Muraji M, Tachikawa S (2000) Phylogenetic analysis of water striders (Hemiptera: Gerroidea) based on partial sequences of mitochondrial and nuclear ribosomal RNA genes. *Entomological Science* 3(4): 615–626.
- Nozawa M, Okuda K (2023) Saitama-ken kara arata ni kiroku sareru Kamemushi-ru (3). Yosegaki 188: 30–33. [True bugs newly recorded from Saitama Prefecture, Honshu, Japan. (3)] [in Japanese]
- Péricart J (1983) Faune de France 69. Hémiptères Tingidae euro-méditerranéens. Fédération Française des Sociétés de Sciences Naturelles, Paris, France, 620 pp.
- Péricart J, Golub VB (1996) Superfamily Tingoidea Laporte, 1832. In: Aukema B, Rieger C (Eds) Catalogue of the Heteroptera of the Palaearctic Region. Vol. 2, Cimicomorpha I. Netherlands Entomological Society, Amsterdam, Netherlands 3–78.
- Rambaut A (2014) FigTree Ver. 1.4.4. <http://tree.bio.ed.ac.uk/software/figtree/> [Accessed: 2023-5-9]
- Rambaut A, Suchard MA, Xie D, Drummond AJ (2014) Tracer. Version 1.6. <http://beast.bio.ed.ac.uk/Tracer> [Accessed: 2023-5-9]
- Ronquist F, Teslenko M, van der Mark P, Ayres DL, Darling A, Höhna S, Larget B, Liu L, Suchard MA, Huelsenbeck JP (2012) MrBayes 3.2: Efficient bayesian phylogenetic inference and model choice across a large model space. *Systematic Biology* 61(3): 539–542. <https://doi.org/10.1093/sysbio/sys029>
- Schuh RT, Weirauch C (2020) True bugs of the world (Hemiptera: Heteroptera). Classification and natural history (2<sup>nd</sup> edn). Siri Scientific Press, Manchester, UK, 768 pp. [32 pls.]
- Shorthouse DP (2010) SimpleMapp, an online tool to produce publication-quality point maps. <http://www.simplemapp.net> [Accessed: 2023-4-21]
- Simon C, Rati FF, Beckenbach A, Crespi B, Liu H, Flook P (1994) Evolution, weighting, and phylogenetic utility of mitochondrial gene sequences and compilation of conserved polymerase chain reaction primers. *Annals of the Entomological Society of America* 87(6): 651–701. <https://doi.org/10.1093/aesa/87.6.651>
- Souma J (2020) The monocotyledon-feeding lace bugs of the genus *Agramma* from Japan (Hemiptera: Heteroptera: Tingidae). *Acta Entomologica Musei Nationalis Pragae* 60(2): 527–536. <https://doi.org/10.37520/aemnp.2020.035>
- Souma J (2021) Lace bugs from Yakushima Island, Ryukyu Archipelago, Japan (Hemiptera: Heteroptera: Tingidae). *Fauna Ryukyuan* 63: 29–39. [in Japanese with English Summary]
- Souma J (2022) Integrative taxonomy of the Lauraceae-feeding species of the genus *Stephanitis* (Hemiptera, Heteroptera, Tingidae) from Japan. *Deutsche Entomologische Zeitschrift* 69(2): 219–281. <https://doi.org/10.3897/dez.69.89864>
- Souma J, Hisasue Y (2022) Ezonaga-gunbai no Saga-ken kara no hatsu-kiroku. *Pulex* 101: 922. [First record of the lace bug species *Agramma (Agramma) japonicum* (Drake, 1948) (Heteroptera, Tingidae) from Saga Prefecture, Kyushu, Japan] [in Japanese]
- Souma J, Ishikawa T (2022) Taxonomic review of the tingine genera *Cysteochila*, *Hurdchila*, *Physatocheila*, and *Xynotingis* from Japan, with description of a new genus (Hemiptera: Heteroptera: Tingidae). *Zootaxa* 5150(1): 1–42. <https://doi.org/10.11646/zootaxa.5150.1.1>
- Souma J, Iwata Y (2022) First record of the lace bug species *Agramma (Agramma) abruptifrons* Golub, 1990 (Heteroptera, Tingidae) from Kanto District, Honshu, Japan. *Rostria* 67: 48–49. [in Japanese]
- Stephens JF (1829) The nomenclature of British insects; being a compendious list of such species as are contained in the Systematic Catalog of British insects. Baldwin, London, UK, 68 pp.
- Tago T (2023) Saitama-ken ni okeru Hime-mizugiwa-kamemushi to Tatami-gunbai no kiroku. Yosegaki 188: 43–45. [Distributional records of *Micracanthia hasegawai* (Cobben, 1985) (Heteroptera, Saldidae) and *Agramma abruptifrons* Golub, 1990 (Heteroptera, Tingidae) from Saitama Prefecture, Honshu, Japan] [in Japanese]
- Takeya C (1953) Notes on the Tingidae of Shikoku, Japan (Hemiptera). *Transactions of the Shikoku Entomological Society* 3(7): 167–176. [pl. 6]
- Takeya C (1962) Taxonomic revision of the Tingidae of Japan, Korea, the Ryukyus and Formosa Part 1 (Hemiptera). *Mushi* 36(5): 41–75.
- Tanabe AS (2011) Kakusan4 and Aminosan: Two programs for comparing nonpartitioned, proportional, and separate models for combined molecular phylogenetic analyses of multilocus sequence data. *Molecular Ecology Resources* 11(5): 914–921. <https://doi.org/10.1111/j.1755-0998.2011.03021.x>
- Tomokuni M (1979) Records of the family Tingidae collected by Dr. Kintaro Baba in Niigata Prefecture (Hemiptera). *Transactions of the Entomological Society* 50: 135–138. [in Japanese]
- Tomokuni M, Ishikawa T (2002) Hemiptera (Insecta) of Hachijo Island, the Izu Islands, Japan. *Memoirs of the National Science Museum* 38: 169–178. [in Japanese with English summary]
- United States National Museum of Natural History (2023) *Serenthia vicinalis* Drake, 1927. <http://n2t.net/ark:/65665/3b360c0d7-d7ee-4624-b2e7-11534c1d8d5f> [Accessed: 2023-6-4]
- Woese CR, Achenbach L, Rouviere P, Mandelco L (1991) Archaeal phylogeny: Reexamination of the phylogenetic position of *Archaeoglobus fulgidus* in light of certain composition-induced artifacts. *Systematic and Applied Microbiology* 14(4): 364–371. [https://doi.org/10.1016/S0723-2020\(11\)80311-5](https://doi.org/10.1016/S0723-2020(11)80311-5)
- Yamada K, Ishikawa T (2016) Family Tingidae. In: Hayashi M, Tomokuni M, Yoshizawa K, Ishikawa T (Eds) Catalogue of the insects of Japan Volume 4 Paraneoptera. Touka-shobo, Fukuoka, Japan, 429–435. [in Japanese]
- Yamada K, Tomokuni M (2012) Family Tingidae Laporte, 1832. In: Ishikawa T, Takai M, Yasunaga T (Eds) A field guide to Japanese bugs. Terrestrial heteropterans III. Zenkoku Noson Kyoiku Kyokai, Publishing Co., Ltd., Tokyo, Japan, 180–213. [pl. 2–13] [in Japanese]
- Yamamoto M (2023) Tatami-gunbai *Agramma abruptifrons* Golub, 1990 no Shiga-ken kara no saishu-kiroku. *Kamemushi News* 70: 2. [A distributional record of *Agramma abruptifrons* Golub, 1990 (Heteroptera, Tingidae) from Shiga Prefecture, Honshu, Japan] [in Japanese]

## Supplementary material 1

### **Sample IDs and GenBank Accession numbers for 18 individuals of four tingid species used for DNA extraction**

Authors: Jun Souma

Data type: xlsx

Copyright notice: This dataset is made available under the Open Database License (<http://opendatacommons.org/licenses/odbl/1.0>). The Open Database License (ODbL) is a license agreement intended to allow users to freely share, modify, and use this Dataset while maintaining this same freedom for others, provided that the original source and author(s) are credited.

Link: <https://doi.org/10.3897/dez.71.108270.suppl1>

## Supplementary material 3

### **Newly collected specimens of *Agramma (Agramma) japonicum* from Japan deposited at SIHU**

Authors: Jun Souma

Data type: xlsx

Copyright notice: This dataset is made available under the Open Database License (<http://opendatacommons.org/licenses/odbl/1.0>). The Open Database License (ODbL) is a license agreement intended to allow users to freely share, modify, and use this Dataset while maintaining this same freedom for others, provided that the original source and author(s) are credited.

Link: <https://doi.org/10.3897/dez.71.108270.suppl3>

## Supplementary material 2

### **Pairwise genetic divergence (Kimura-two parameter) for 18 individuals of four tingid species based on partial sequences of mitochondrial COI gene**

Authors: Jun Souma

Data type: xlsx

Copyright notice: This dataset is made available under the Open Database License (<http://opendatacommons.org/licenses/odbl/1.0>). The Open Database License (ODbL) is a license agreement intended to allow users to freely share, modify, and use this Dataset while maintaining this same freedom for others, provided that the original source and author(s) are credited.

Link: <https://doi.org/10.3897/dez.71.108270.suppl2>



# Integrated taxonomy, biology and biogeography of the Afrotropical genus *Xyloctonus* (Coleoptera, Curculionidae, Scolytinae)

Bjarte H. Jordal<sup>1</sup>

<sup>1</sup> Department of Natural History, University Museum of Bergen, University of Bergen, P.O. 7800, NO-5020 Bergen, Norway

<https://zoobank.org/E85152C0-2B48-4B15-A49F-776D7CD4CBA4>

Corresponding author: Bjarte H. Jordal (bjarte.jordal@uib.no)

Academic editor: Harald Letsch ♦ Received 23 November 2023 ♦ Accepted 8 February 2024 ♦ Published 1 March 2024

## Abstract

The peculiar Afrotropical bark beetle genus *Xyloctonus* Eichhoff, 1872 is revised and its biology described. Several unusual morphological features reflect adaptations to predator avoidance as they are highly exposed during mating externally on tree trunks and branches. Observations invariably indicate that males and females abandon the nest under bark at an early stage of progeny, the males already before eggs hatch, potentially engaging in subsequent additional matings. Most species have a clear preference for host plants in the plant family Sapotaceae. Although the genus is broadly distributed in forested parts of Africa, Madagascar and Mauritius, most species are found in the eastern part of this range. A Bayesian biogeographical analysis revealed a possible origin of the genus in Madagascar in the early Eocene, with subsequent colonisation of the southern African region in late Eocene. This contrasts with the closely-related xyloctonine genus *Ctonoxylon* Hagedorn, 1910, which is of western Congolian ancestry and more recently reached Madagascar multiple times during late Miocene. Two new species are described: *Xyloctonus magnus* **sp. nov.** from Madagascar and *X. genieri* **sp. nov.** from Burkina Faso. Synonyms are proposed for *X. subcostatus* Eggers, 1939 (= *X. striatus* Eggers, 1939) and *X. scolytoides* Eichhoff, 1872 (= *X. latus* Eggers, 1922). Identification to species is provided in a key illustrated with photographs of most species.

## Key Words

bark beetles, Bayesian Binary MCMC, phylogeny, Reconstruct Ancestral State in Phylogenies, taxonomy

## Introduction

Xyloctonini are a characteristic group of tropical bark beetles in the weevil subfamily Scolytinae. It includes five genera: *Glostatus* Schedl, 1939, *Cryphalomimus* Eggers, 1927, *Ctonoxylon* Hagedorn, 1910 and *Xyloctonus* Eichhoff, 1872 are all Afrotropical, whereas *Scolytomimus* Blandford, 1895 is restricted to the Indo-Malayan and Australian Regions. A recent revision of *Glostatus* placed this genus in a separate subtribe Glostatina Jordal, 2023 and also revealed a rather chaotic taxonomy for this group of beetles. *Ctonoxylon* and *Xyloctonus* are, on the other hand, taxonomically stable groups at the generic level and their morphology leaves little doubt about their affinity (Jordal 2023). The peculiar look of *Xyloctonus* (Figs 1, 2) and the other genera in subtribe Xyloctonina is most strikingly expressed in the rounded and inflated shape of the

pronotum, a deep groove on the anterior side of the pro-tibiae and the impressed lateral sclerites of the metathorax for reception of femur and tibiae (Menier 1974). Such highly-specialised features led some authors to place these weird beetles in their own subfamily Xyloctoninae (Hopkins 1915; Schedl 1961b) or family Xyloctonidae (Eichhoff 1878). Observations on their biology are few and anecdotal, but all species are true bark beetles with likely narrow host plant preferences (Schedl 1961b).

Both *Ctonoxylon* and *Xyloctonus* are broadly Afrotropical. However, *Xyloctonus* has one-third of the species endemic to Madagascar, whereas *Ctonoxylon* until recently did not have any species verified from this island (Wood and Bright 1992). The predominantly Congolian affinities of *Ctonoxylon* may explain its scarce presence on Madagascar, whereas the largely Zambesian distribution of African *Xyloctonus* could have facilitated a closer

connection with this island. A biogeographical analysis of *Xyloctonini* and outgroups is, therefore, presented to test these hypotheses, using reconstruction of ancestral areas in a Bayesian framework.

Rather few publications have dealt with the taxonomy of *Xyloctonus* (see Eggers (1939); Schedl (1953); Menier (1974)) and, generally, very little is known about morphological variation, behaviour and geographical distribution. The taxonomy and biology are, therefore, revised, including an identification key and photographic illustrations. Two new species are described and two other species synonymised which leaves the total number of species at 15 (Table 1). Recent fieldwork has provided new host and country records which, together with observations on their behaviour, will contribute to a better understanding of distribution and ecology.

**Table 1.** Currently valid species of the genus *Xyloctonus* Eichhoff, 1872 and their known distribution.

<i>Xyloctonus aethiops</i> Schedl, 1953	Madagascar
<i>Xyloctonus bimarginatus</i> Eggers, 1939	Democratic Republic of the Congo
<i>Xyloctonus biseriatus</i> Schedl, 1953	Madagascar
<i>Xyloctonus genieri</i> Jordal, sp. nov.	Burkina Faso
<i>Xyloctonus maculatus</i> Schedl, 1965	South Africa
<i>Xyloctonus magnus</i> Jordal, sp. nov.	Madagascar
<i>Xyloctonus mauritanus</i> Menier, 1974	Mauritius
<i>Xyloctonus niger</i> Schedl, 1938	Uganda
<i>Xyloctonus opacus</i> Schedl, 1957	Rwanda
<i>Xyloctonus pubifer</i> Schedl, 1965	Zambia, South Africa
<i>Xyloctonus punctipennis</i> Eggers, 1939	Somalia
<i>Xyloctonus quadricinctus</i> Schedl, 1941	Ghana, Tanzania
<i>Xyloctonus quadridens</i> Schedl, 1953	Madagascar
<i>Xyloctonus scolytoides</i> Eichhoff, 1872	Tropical Africa, incl. South Africa
<i>Xyloctonus subcostatus</i> Eggers, 1939	Guinea, Burkina Faso, Democratic Republic of the Congo, Sudan, Tanzania, Mozambique

## Material and methods

Eggers (1939) often used the informal term type and co-type. The purpose of these terms was clearly holotype (see Wood and Bright (1992)) and paratype. Specimens studied are deposited in the following museum collections:

<b>CAS</b>	California Academy of Sciences, San Francisco, USA.
<b>CMNC</b>	Canadian Museum for Nature, Ottawa, Canada (Genier coll).
<b>RBINS</b>	Royal Belgian Institute of Natural Sciences, Brussels, Belgium.
<b>RMCA</b>	Musee Royal de l'Afrique Centrale, Tervuren, Belgium.
<b>MNHN</b>	Museum National d'Histoire et Naturelle, Paris, France.
<b>MZH</b>	Finnish Museum of Natural History, Helsinki, Finland.

<b>NHMUK</b>	The Natural History Museum, London, UK.
<b>NHMW</b>	Naturhistorisches Museum, Vienna, Austria.
<b>USNM</b>	National Museum of Natural History, Washington D.C., USA.
<b>UWCP</b>	Museum of Natural History, University of Wrocław (Wanat coll).
<b>ZMHB</b>	Museum für Naturkunde der Humboldt-Universität, Berlin, Germany.
<b>ZMUB</b>	University Museum of Bergen, Norway.

Specimens collected by the author were dissected from recently dead wood and lianas identified by local plant experts. Careful removal of bark allows for reconstruction of family structures and brood size. It was noted if a nuptial chamber was present inside the entrance and whether the direction of the egg tunnel (gallery) was parallel or transverse to the wood grain as this is often a species specific trait. The stage of development (larvae, pupae, teneral adults) was noted for each observation and if one or both parents were still present.

External morphological characters were studied in a Leica MZ16 and photographs made with Leica LAS software on a Leica M205 C stereomicroscope. Internal morphological characters were dissected and reported in a previous paper (Jordal 2023).

Biogeographical analyses were based on a new time-calibrated phylogenetic tree as the basis for reconstructing ancestral areas. The molecular data used to reconstruct the time tree were mitochondrial COI and nuclear 28S and EF-1 $\alpha$ , as described in a recent publication (Jordal 2023). Approximate clade ages were estimated in Beast 1.10.4 (Drummond and Rambaut 2007), with the xml file prepared in Beauti. Rates were calibrated with time estimates from a previous analysis of Scolytinae, based on 18 genes (Pistone et al. 2018) and given a normal distribution with five standard deviations to accommodate for uncertainties in these estimates. Nodes used for calibration included the root which combined taxa from Ipini, Hypoborini and Micracidini at 88 Ma, Micracidini without *Leiomicracis* at 79 Ma and the Neotropical micracidine clade at 65 Ma. These particular nodes had relatively small differences between stem and crown ages and estimates were robust across different studies (Jordal and Cognato 2012; Pistone et al. 2018; Jordal 2021a, b). Published estimates on the *Xyloctonini* lineages were excluded to avoid potential bias in the new estimate using a much larger ingroup sample.

Ancestral areas were reconstructed in RASP (Yu et al. 2020) using 1 million iterations of the Bayesian Binary MCMC (BBM) method, based on the new time-tree reconstructed in Beast. The preferred model F81 allows different frequencies of areas in the dataset which better accommodate the small samples of species from Madagascar and southern Africa compared to the Congolian and Zambesian regions. Due to the highly-restricted distribution of most species of *Xyloctonini*, the maximum number of occupied areas was set to 2. Areas were generally defined as the biogeographic regions (realms) of the

world, with the target area Afrotropics (Ethiopian region) divided further into statistically-defined regions *sensu* Linder et al. (2012): Madagascar, Congolian (= Shaba, Congolian and Guinean clusters), Zambesian and southern African (= Namib, Kalahari, Cape and Natal clusters) regions, which are the only relevant areas for the *Xyloctonini* taxa treated here.

## Results

### Phylogenetics and Afrotropical biogeography of *Xyloctonini*

The recent phylogenetic study of *Xyloctonini* resulted in a monophyletic group of five *Xyloctonus* species which were maximally supported as sister to *Scolytomimus* Blandford 1895 (fig. 1 in Jordal (2023)). The distinctness of *Xyloctonus* is also supported morphologically (fig. 2 in

Jordal (2023)), in particular by the symmetrically rounded and flat antennal club with two or three procurved sutures and the genus connects with *Scolytomimus* by the steeply rising venter meeting a short elytral declivity (Figs 1, 2). These two genera share with *Cryphalomimus* a carinated shape of the elytral interstriae (Figs 1–5) and, together with *Ctonoxylon*, all four genera have deeply-grooved protibiae for reception of the tarsi and a large and scoop-like manubrium of the aedeagal tegmen (Jordal 2023).

A new Beast analysis of the molecular data showed similar relationships between genera (Fig. 6), with *Glostatus* separated from the other four genera. Within *Xyloctonus* the two South African taxa *X. maculatus* and *X. latus* were nested within the Malagasy clade, as opposed to the previously published MrBayes analysis (fig. 1 in Jordal (2023)).

Reconstructions of possible ancestral areas revealed contrasting patterns for the three xyloctonine genera with multiple species sampled (Fig. 6). On the basis of



**Figures 1–5.** Posterior view of elytral declivity in **1.** *Xyloctonus quadridens*; **2.** *X. maculatus*; **3.** *X. subcostatus* (paratype of *X. striatus*); **4.** *X. pubifer*; **5.** *X. scolytoides* (paralectotype of *X. latus*). Black arrows points at the shallow furrow on the posterior side of the metatibiae, similar to mesotibiae. White arrow points to the impression of the metaventricle which receives the metafemur. Yellow arrows point at elytral interstriae 9, which in Figs 1–4 runs to the elytral sutures and blocks interstriae 1–8 from reaching elytral apex; in *X. scolytoides* (Fig. 5) all interstriae reach the posterior margin of the elytra.

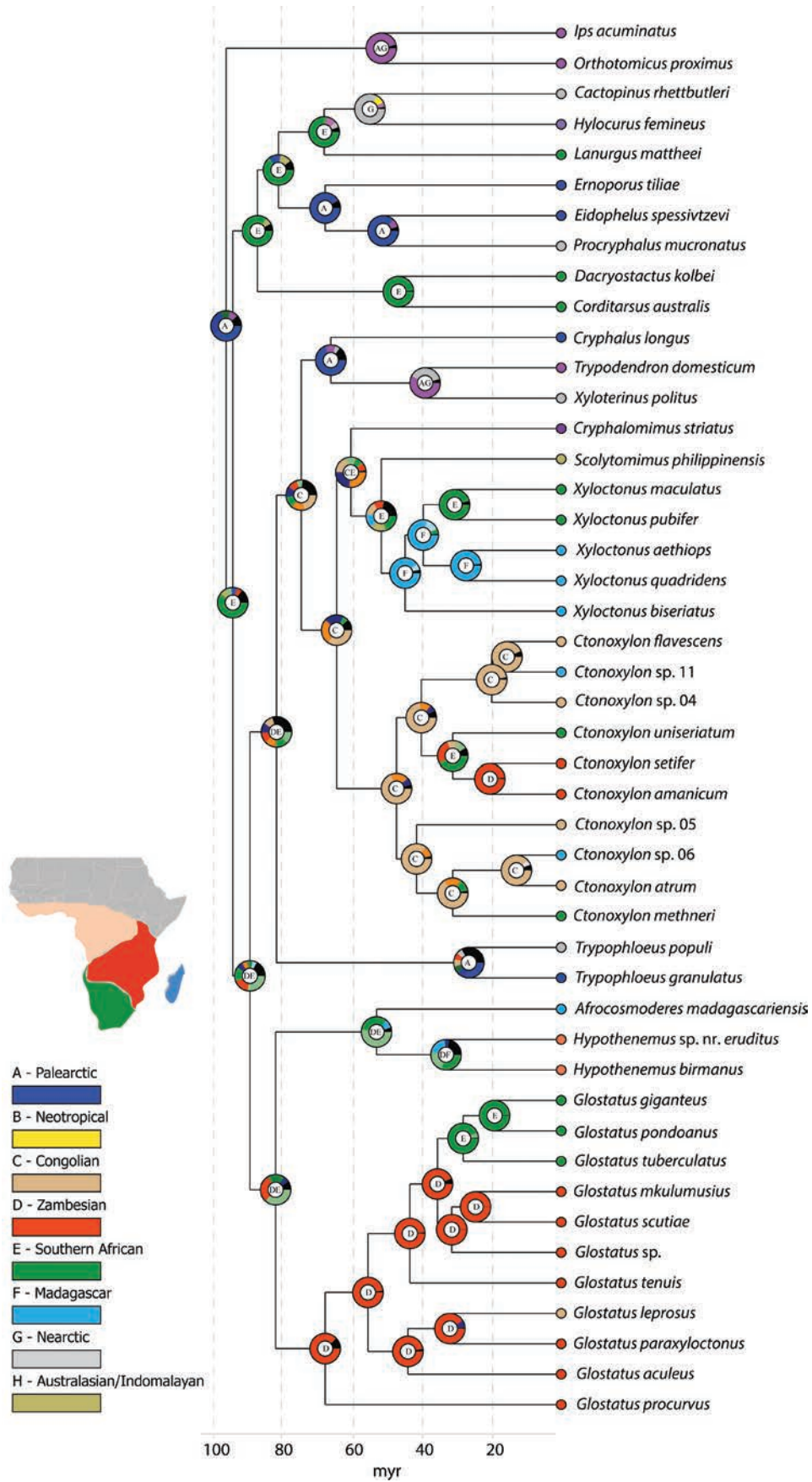


**Figure 6.** Reconstruction of ancestral geographic areas in RASP using the BBM method on a Beast estimated time-tree. The most likely ancestral area is noted by a letter in centre of each pie diagram, with alternative states coloured according to their likelihood proportions. The map inserted shows the approximate extent of relevant Afrotropical subregions *sensu* Linder et al. (2012).

this dataset, *Xyloctonus* was inferred to have originated in Madagascar 52–45 Ma. The southern region of Africa was thereafter reached from Madagascar no later than 31 Ma. *Ctonoxylon* indicated a Congolian ancestry some 64–47 Ma, with more recent expansions to the Zambesian and southern African regions. Colonisation of Madagascar occurred twice and no earlier than 13 and 16 Ma, possibly much later, as these were single species with rather similar morphology to their continental sister species (Jordal, in prep.). *Glostatus* is not part of the core *Xyloctonini* and is not found on Madagascar (Jordal 2023); its inferred ancestry in the Zambesian region was strongly supported and occurred some 82–68 Ma, with a more recent expansion to the southern parts of Africa not earlier than 35 Ma.

## Taxonomy

### *Xyloctonus* Eichhoff, 1872

**Type species.** *Xyloctonus scolytoides* Eichhoff, 1872 (by monotypy).

**Diagnosis.** Eyes divided, except broadly emarginated in *X. maculatus* and *X. genieri* sp. nov. Antennal scapus longer than the 6-segmented funiculus; club flat, outline round, with three, or more rarely two, strongly procurved sutures marked by dense white or golden setae (Figs 22, 40). Pronotum spherical in both lateral and frontal view, lateral margins carinate; anterior half asperate, with either two or four raised teeth along anterior margin. Scutellar shield (scutellum) slightly detached from elytra; interstriae carinate (only declivity in *X. aethiops*), interstitial carinae either reaching posterior margin or more often disrupted by a curved interstriae 9 that reaches elytral suture near apex; declivity short and gently sloping (steep and longer in *X. maculatus*). Metanepisternum, metaventricle and first ventricle usually with split setae, trifid or occasionally plumose setae often present near mesoventricle. Ventricle 3–5 usually steeply rising to meet elytra. Procoxae contiguous; protibiae with deep furrow of anterior face to receive tarsi; other tibiae with distinct, but shallower furrow on its posterior face. Proventriculus with posterior plate strongly reduced, anterior plate with partially open and indistinct median suture, plate covered by simple obtuse tubercles. Male genitalia with large complex intromittent organ (basal sclerites), apophyses (penis apodemes) as long as penis body; tegmen open dorsally, ventrally with a large scoop-shaped manubrium; spiculum gastrale as simple thin curved rod.

**Differential diagnosis.** This genus differs from *Scolytomimus* by the distinct procurved sutures in the antennal club and by the irregular impression around the scutellar shield. It is further distinguished from *Cryphalomimus* and *Ctonoxylon* by the 6-segmented antennal funicle, a rather short, oblique elytral declivity and the symmetrically procurved sutures in the antennal club.

### The *emarginatus* group

Two species are included in this group, defined by having all interstriae reaching the apical margin of the elytra (Fig. 5). One of the taxon names used in the past was ‘*emarginatus*’, now a synonym of *scolytoides*, describing this condition (see *bimarginatus* group below).

### *Xyloctonus scolytoides* Eichhoff, 1872

Figs 7, 8, 10, 11, 13, 14

*Xyloctonus scolytoides* Eichhoff 1872: 134.

*Xyloctonus emarginatus* Eggers, 1939: 16, synonymy by Menier, 1974.

*Xyloctonus latus* Eggers, 1939: 14, syn. nov.

**Type material.** **Syntypes** of *X. scolytoides*: [South Africa] Port Natal [-29.87, 30.97], Dej. [RBINS]. **Paratype** of *X. emarginatus*: [Democratic Republic of the] Congo, Ituri, Djugu, 13.VIII.1931, leg. J. Lebrune [RMCA]. Lectotype of *X. latus*: [Ethiopia] Abyssinia, 8000 feet alt. IX–X 1926, Dr. H. Scott [NHMUK]; and paralectotype, same data [NHMW].

**Diagnosis.** Length 2.1–2.6 mm, 1.9–2.1× as long as wide, colour light to very dark brown; antennal club with two visible procurved sutures; frons with fine setae; anterior margin of pronotum with two raised teeth (Figs 7, 10); all elytral interstriae carinate, reaching posterior elytral margin; striae and interstitial punctures moderately deep; scutellar shield impressed in middle, appearing bilobed; elytral suture with bulgy locking mechanism behind scutellar shield; setae on lateral metaventricle mainly bifid or trifid, anteriorly more plumose.

**Distribution.** Burkina Faso (new country record), Ghana, Ivory Coast, Nigeria, Cameroon, Democratic Republic of the Congo, Uganda, Sudan, Ethiopia, Tanzania, Zambia, South Africa.

**New records.** Burkina Faso, Bale, Boromo [11.755, -2.929], 250 m alt. F. Genier, leg., 10.8.2006, light trap; Comoe, Foret de Boulon [10.343, -4.510], 270 m alt., F. Genier leg., 9.7.2006, flight intercept trap, light trap and Malaise trap; Kompienga, 15 km E Nadiagou [11.113, 0.909], 155 m alt., F. Genier leg., 25.8.2005, flight intercept trap, light trap and Malaise trap; Loroum, Toulfe [13.873, -1.950], 300 m alt., F. Genier leg., 16.7.2006, light trap; Nahouri, Foret de Nazinga [11.045, -1.420], 310 m alt., F. Genier leg., 27.7.2006, light trap and Malaise trap; Passore, 8 km SE Yako [12.928, -2.216], 320 m alt., F. Genier leg., 7. 8. 2006, light trap; Sanguie, Foret de Sorobouli [11.893, -2.799], 270 m alt., F. Genier leg., 13.7.2005 and 28.7.2006, light trap; Ouagadougou, 03.11.1973, R. Linnavouri [MZH]; Bobo Dioulasso, 03.11.1973, R. Linnavouri [MZH]; Nigeria, Kano-Wudil, 17.05.1973, R. Linnavouri [MZH]; Serti [7.51, 11.36], 29. March 1970, coll. J.T. Medler; Cameroon, 35 km S Garoua [9.01, 13.34], 30 March 1972, at black light, JA Gruwell; Tanzania, W. Usambara, Kwai, 1600 m, P. Weiss [ZMHB]; South Africa,

Mpumalanga, Telperion Reserve, 1450 m alt. [-25.735, 28.985], 08.12.2019, beating, M. Wanat leg. [1, UWCP]; Gauteng, Pretoria, Wapadrand, 1540 m alt. [-25.847, 28.384], 09.12.2019, beating, M. Wanat leg. [1, UWCP].

**Biology.** This species is the only species in the genus that is frequently and broadly collected. It is found feeding and breeding in many host plants, such as *Butyrospermum parkii*, *Madhuca latifolia*, *Mimusops caffra* (all in Sapotaceae), *Olea capensis* (Oleaceae), *Garcinia* (Clusiaceae) and *Acacia* (Fabaceae) (see Schedl (1961b)). It is notable that the majority of records are from Sapotaceae which is by far the most typical host plant family for the genus.

**Comments.** The lectotype of *X. latus* is identical, except for some of the setae on upper lateral part of the metaventrite which tend to be trifid or pentafid over a larger area rather than the typical trifid setae in the *X. scolytoides* types.

### *Xyloctonus niger* Schedl, 1938

Figs 9, 12, 15

*Xyloctonus niger* Schedl, 1938 d: 452.

**Type material. Syntypes:** Uganda, Entebbe [0.04, 32.42], 11-II-1938, P. Chandler [NHMUK, NHMW].

**Diagnosis.** Length 2.5 mm, 2.1× as long as wide, colour black, shiny; antennal club with two visible procurved sutures; frons glabrous; anterior margin of pronotum with two raised teeth clearly longer than broad; all elytral interstriae carinate to posterior elytral margin; striae and interstitial punctures very shallow making walls of carinae rather smooth and shiny; scutellar shield a rounded button, clearly detached from the surrounding elytra; elytral suture with bulgy locking mechanism behind scutellar shield; setae on lateral metaventrite bifid.

**Distribution.** Uganda.

**Biology.** Known from the two collections in Uganda; the non-type series were dissected from *Tabernaemontana holzkii* (Apocynaceae) (see Menier (1974)).

**Comments.** This species is very similar to *X. scolytoides*, but can be distinguished by the smooth and shiny interstitial carinae which is not indented along the carina wall, the glabrous frons and the consistently bifid setae on the lateral part of the metaventrite.

### The *bimarginatus* group

All species (except *X. opacus* and *X. punctatus*) have interstriae 9 curved and continued to the elytral suture such that none of the interstriae 1–8 reaches the apical margin (Figs 1–4); thereof the name ‘*bimarginatus*’. In the two deviant species, the gap between the ninth interstriae and the apical margin nearest apex is so tight that interstriae 1–3 apparently reach the apical margin (Fig. 20). Nine species have exactly two raised teeth at the anterior margin of the pronotum, whereas another group of six species have four raised teeth along the anterior margin of the pronotum.

### Species with two-spined pronotum

#### *Xyloctonus opacus* Schedl, 1957

Figs 16, 19, 22

*Xyloctonus opacus* Schedl, 1957: 43.

**Type material. Holotype:** Ruanda [Rwanda], Ihembe, 29-VIII-1952, Dr. Schedl [RMCA].

**Diagnosis.** Length 1.9–2.1 mm, 1.9–2.0× as long as wide, colour black, dull; antennal club with one visible procurved suture; frons finely pubescent; anterior margin of pronotum with two raised teeth; elytral interstriae 1–3 continue to posterior elytral margin, interstriae 4–8 terminate in the transverse interstriae 9 that merge with apical margin at level of interstriae 3; scutellar shield rough, weakly impressed in middle; elytral suture straight (mesal locking mechanism normal).

**Distribution.** Rwanda.

Previous reports from Madagascar (Schedl 1977) are *X. biseriatus* [NHMW].

**Biology.** Collected from *Chrysophyllum* (Sapotaceae) branches about 2–8 cm in diameter (Schedl 1961b). Egg tunnels were cut transversely to the grain and the number of larvae ranged between 14 and 44 (n = 4).

#### *Xyloctonus punctipennis* Eggers, 1939

Figs 17, 20, 23

*Xyloctonus punctipennis* Eggers, 1939: 16.

**Type material. Holotype:** Somalia, Basso Ganana [-0.6, 41.7], VII–VIII-93, V. Bottago [USNM].

**Diagnosis.** Length 1.8–2.4 mm, 2.0–2.1× as long as wide, colour brown, shiny; antennal club with two visible procurved sutures; frons with scant fine setae; anterior margin of pronotum with two raised teeth; elytral interstriae 1–3 continue to posterior elytral margin, interstriae 4–8 terminate in the transversely curved interstriae 9 that merge with the apical margin at level of interstriae 3; scutellar shield smooth, weakly impressed in middle; elytral suture with bulgy locking mechanism near scutellar shield.

**Distribution.** Somalia.

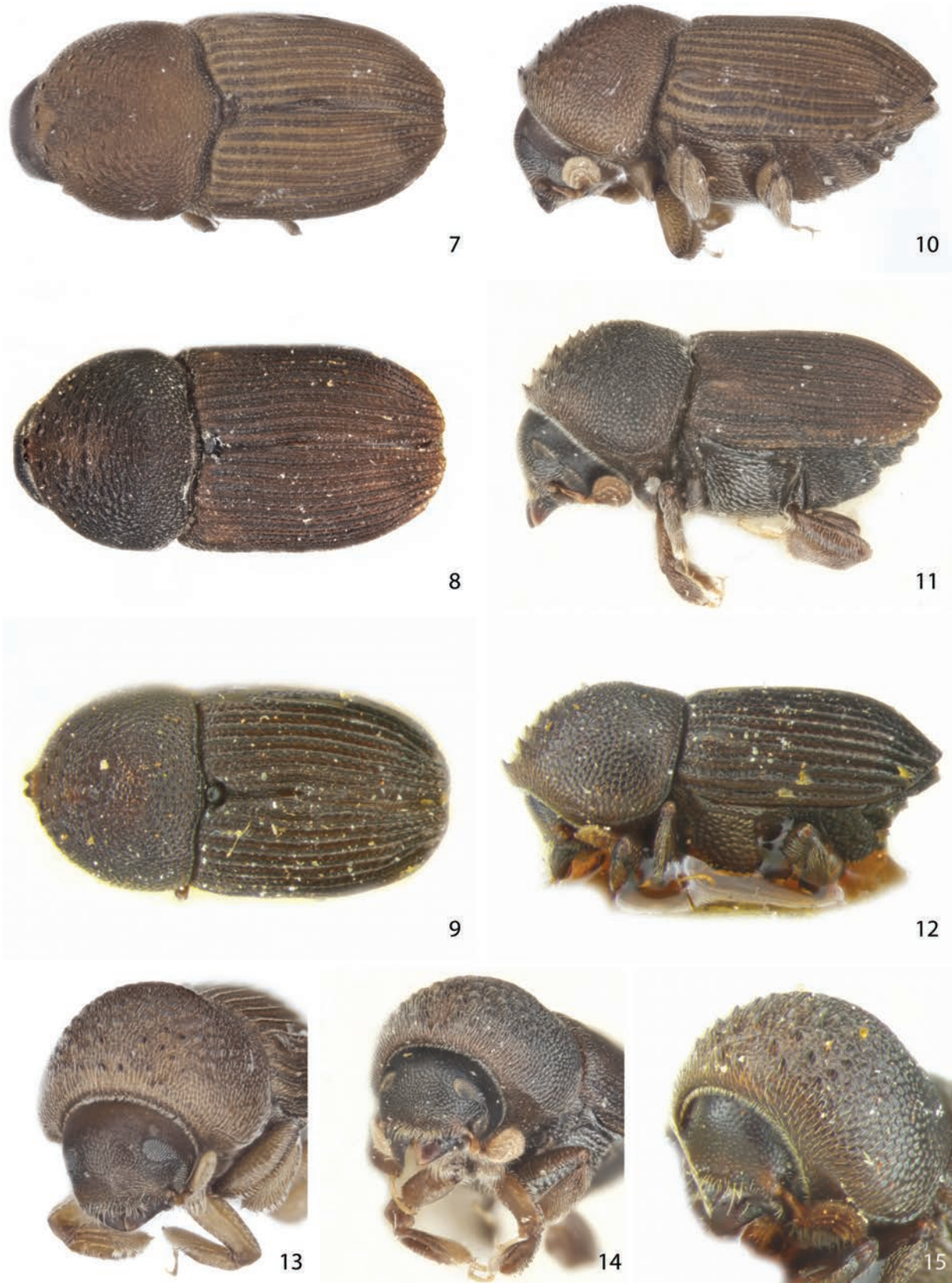
#### *Xyloctonus biseriatus* Schedl, 1953

Figs 18, 21, 24

*Xyloctonus biseriatus* Schedl, 1953: 76.

**Type material. Lectotype:** Madagascar, Region de l’Androy Ambovombe, Dr J. Decorse, 1901, 1 au 15 dec, 00 [MNHN]. **Paralectotype:** Madagascar sud, Fort Dauphin, Allaud, 1900 – I [MNHN].

**Diagnosis.** Length 1.5–2.0 mm, 1.8–1.9× as long as wide, colour black, dull; antennal club with two visible procurved sutures; frons glabrous; anterior margin

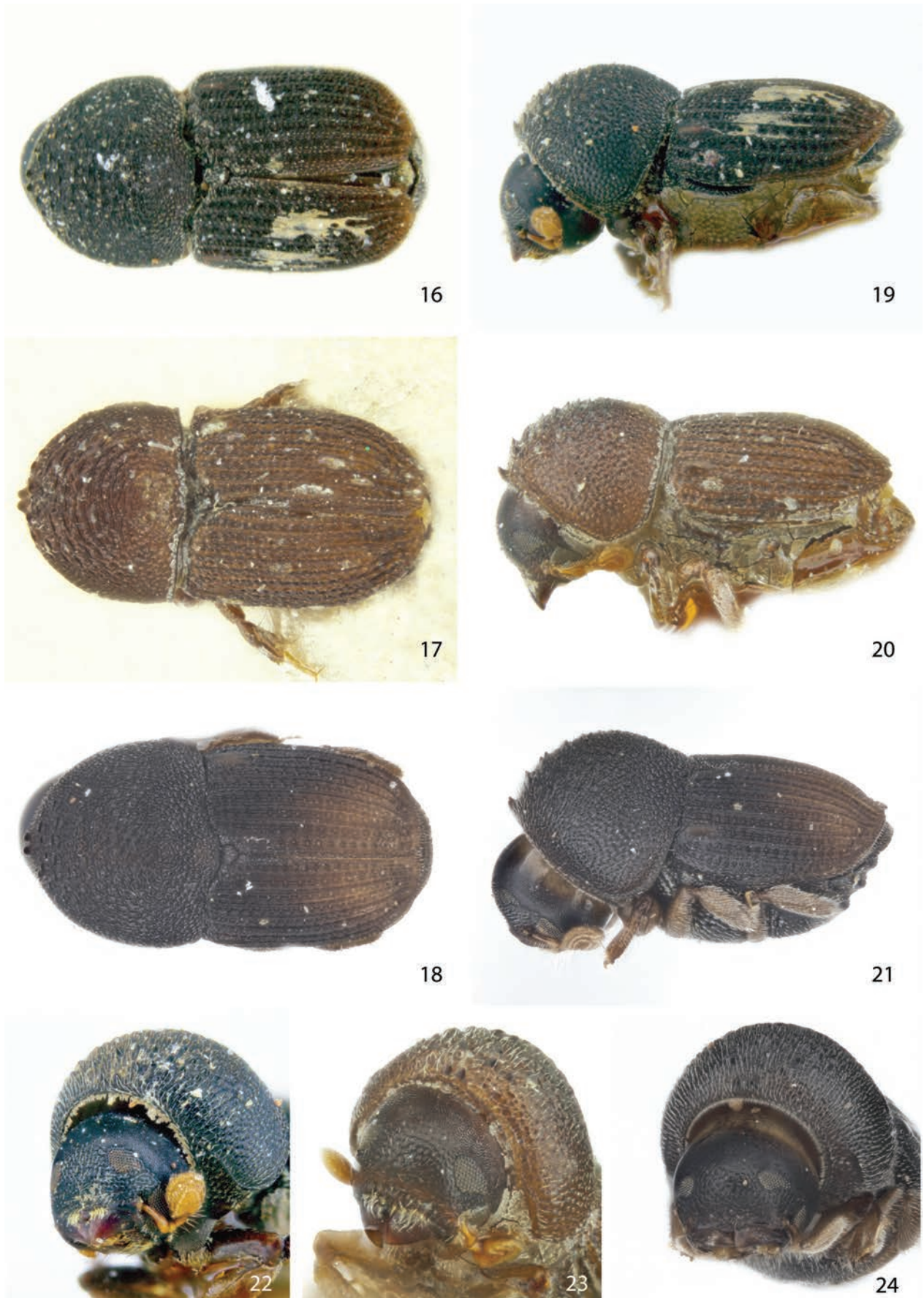


**Figures 7–15.** Dorsal, lateral and front view of *X. scolytoides* (7, 10, 13); paralectotype of *X. latus* (synonym of *X. scolytoides*) (8, 11, 14); holotype of *X. niger* (9, 12, 15).

of pronotum with two raised teeth; elytral interstriae 9 curves before apex and continues transversely to elytral suture; spaces between striae punctures with elongate ele-

vation that mimics a dashed line; scutellar shield slightly impressed in middle; elytral suture straight.

**Distribution.** Madagascar.



**Figures 16–24.** Dorsal, lateral and front view of holotype of *X. opacus* (16, 19, 22); paratype of *X. punctipennis* (17, 20, 23); *X. biseriatus* (18, 21, 24).

**New records.** Madagascar, Ankarafantsika NP [-16.264, 46.828], 200 m alt. ex. *Diospyros* branch, 8 May 2015, B. Jordal, leg. [ZMUB]; Reserve speciale de l'Ankarana, 22.9 km SW Anivorano [-12.93, 49.16], B. Fischer [CAS].

**Biology.** Previously collected in dry forests in the south of Madagascar and the new record from further north was also from a dry forest type. Specimens were collected twice from thin branches of *Diospyros* (Ebenaceae), about 3 cm in diameter. The egg tunnel was cut in the phloem and inner bark layers, transverse to the grain of wood. About 30–40 young teneral and larvae were produced per brood (Table 2). Parents were not present at late larval stage. Colonisation densities were high, with only an average of 0.5 cm distance between egg tunnels.

### *Xyloctonus pubifer* Schedl, 1965

Figs 25, 28, 31

*Xyloctonus pubifer* Schedl, 1965a: 365.

**Type material. Holotype:** South Africa, Port Elisabeth [-33.76, 25.45] [NHMW].

**Diagnosis.** Length 2.8–2.9 mm, 1.8–1.9× as long as wide, colour dark brown; frons finely pubescent; anterior margin of pronotum with two tiny, raised teeth; elytra with dense, fine micro-setae, interstitial and stria punctures dense and similarly sized; elytral interstriae 9 curves before apex and continues to elytral suture; scutellar shield impressed in middle, bilobed, with bifid, short setae; elytral suture straight.

**Distribution,** South Africa, Zambia.

**New records.** South Africa, Western Cape Province, Natures Valley [-33.965, 23.562], 8 Nov. 2007, ex. *Sideroxylon inerme*, B. Jordal, leg. [ZMUB]; Eastern Cape Province, Van Stadens Resort, beating 18.11.2013, M. Wanat leg. [UWCP].

**Biology.** Collected multiple times in this study, from the bark layer of *Sideroxylon inerme* (Sapotaceae). Females were found alone with larvae, the male was not observed, but presumably left their progeny at an earlier stage as observed in other species of the genus. Brood production ranged from 20–27 (n = 3). Flight times were observed in July and August in Zambia (Beaver and Löytyniemi 1985) and estimated to be early October in South Africa, based on expected developing time for the larvae collected in this study.

### *Xyloctonus mauritianus* Menier, 1974

*Xyloctonus mauritianus* Menier, 1974: 662.

**Type material. Holotype,** male: Mauritius, Corps de garde [-20.26, 57.45], 20. V. 1934, J. Vinson [MNHN].

**Diagnosis.** Length 2.1–2.3 mm, 1.9× as long as wide, colour brown, elytra maculated; antennal club with one clearly visible and one faint procurved suture; anterior margin of pronotum with two raised teeth; scutellar shield impressed in middle, with two bulbs at anterior corners; elytral interstriae 9 curves before apex and continues to elytral suture; elytral suture straight.

**Distribution.** Mauritius.

### *Xyloctonus subcostatus* Eggers, 1939

Figs 26, 27, 29, 30, 32, 33

*Xyloctonus subcostatus* Eggers, 1939: 15.

*Xyloctonus striatus* Eggers, 1939: 18, syn. nov.

**Type material. Holotype:** Deutsch Ost Afrika [Tanzania], Bez. Tabora, Ngulu [-3.72, 32.46], vi. 1911, sammler W. Methner [USNM]. **Paratypes** of *X. striatus*: Mozambique, Sangadzé, Moulima [-17.4, 35.0], sur *Acacia*, 1928, P. Lesne [MNHN, NHMW].

**Diagnosis.** Length 1.7–2.8 mm, 2.0× as long as wide, colour brown; antennal club with two visible procurved sutures; male vertex with a simple pars stridens (Fig. 32); anterior margin of pronotum with two raised teeth; pronotum slightly narrower than elytra; elytral interstriae 9 curves above the posterior margin of elytra and continues to elytral suture; interstriae lightly punctured; scutellar shield broad, slightly impressed in middle, roughly punctured; elytral suture with bulgy locking mechanism; setae on lateral upper part of metaventrite bifid.

**Distribution.** Mozambique, Tanzania, Sudan, Democratic Republic of the Congo (new country record) Guinea, Burkina Faso (new country record).

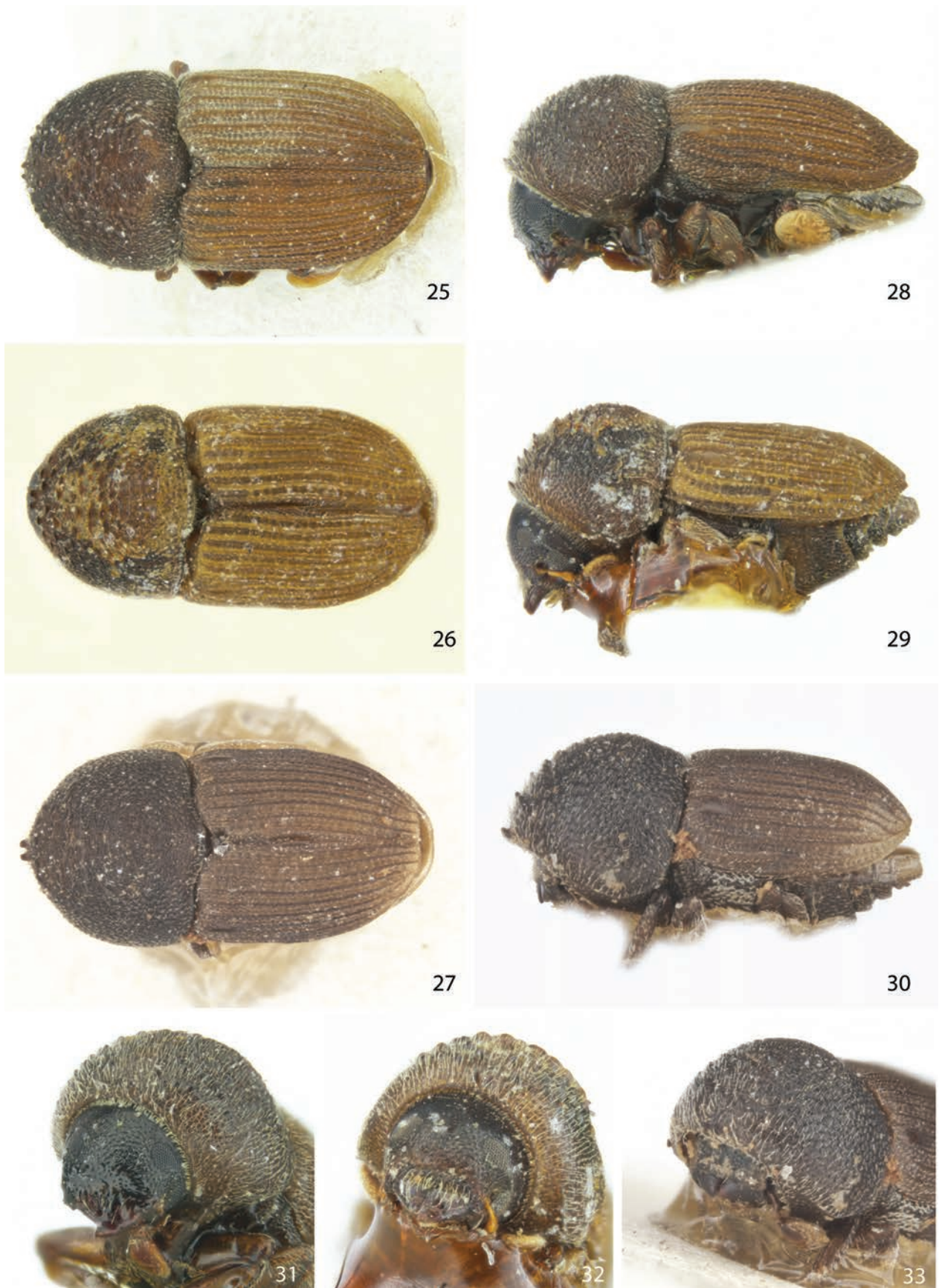
**New records.** Burkina Faso, Comoe, Foret de Boulon, 270 m alt., 10.343, -4.510, 9.7.2006, F. Genier leg. [2, Genier coll.]; Democratic Republic of the Congo, Moba, 780 m alt., -7.030, 29.763, 01.10.1953, H. Bomans leg. [1, RMCA].

A specimen from the Democratic Republic of Congo [RMCA] was erroneously identified by Schedl as *X. scolytoides*.

**Biology.** Collected from an *Acacia* (Fabaceae) branch (identified as *X. striatus*). Two males were collected by a

**Table 2.** Summary of reproduction in species of *Xyloctonus* published in: (1) this paper; (2) Schedl (1977); (3) Schedl (1961b).

Species	Host family	Diam. (cm)	Egg tunnel direction	Brood size	male leave	female leave
<i>Xyloctonus aethiops</i> <sup>1,2</sup>	Phyllanthaceae	1–4	longitudinal	21–40	egg	larvae
<i>Xyloctonus biseriatus</i> <sup>1</sup>	Ebenaceae	2–4	transverse	30–40	egg or larvae	larvae
<i>Xyloctonus pubifer</i> <sup>1</sup>	Sapotaceae	10–20	transverse	20–27	egg	pupae
<i>Xyloctonus maculatus</i> <sup>1</sup>	Sapotaceae	10–20	transverse	12–21	egg	larvae
<i>Xyloctonus opacus</i> <sup>3</sup>	Sapotaceae	5–14	transverse	14–41	?	larvae
<i>Xyloctonus quadridens</i> <sup>1</sup>	Sapotaceae	1–20	transverse	30–50	?	?



**Figures 25–33.** Dorsal, lateral and front view of holotype of *X. pubifer* (25, 28, 31); paratype of *X. subcostatus* (26, 29, 32); paratype of *X. striatus* (synonym of *X. subcostatus*) (27, 30, 33).

Malaise trap in Burkina Faso, in a dry bushland. The records from south-eastern parts of the Democratic Republic of the Congo, Sudan and Guinea are also from very dry forests below 1000 m altitude. Although present on one of Eggers 'co-types' (paratypes), the male pars stridens is here reported for the first time.

**Comments.** Paratypes ('co-types') of *X. striatus* are identical to *X. subcostatus*, except elytral interstriae 9 is a little less separated from the elytral apex.

### *Xyloctonus bimarginatus* Eggers, 1939

Figs 34, 37, 40

*Xyloctonus bimarginatus* Eggers, 1939: 17.

**Type material. Holotype:** [Democratic Republic of the] Congo, Kundelungu [-10.25, 27.60], leg. Mme Tinaut [RMCA].

**Diagnosis.** Length 2.2–2.6 mm, 1.9–2.0× as long as wide, colour brown, shiny; antennal club with two clearly-visible procurved sutures, a third and fainter suture near the margin; frons with scant fine setae, vertex in males with pars stridens; anterior margin of pronotum with two raised teeth; elytral interstriae 9 curves before apex and continues to elytral suture, in dorsal view apical margin of elytra extending beyond margin of interstriae 9, finely serrated; scutellar shield impressed in middle, bilobed; elytral suture with bulgy locking mechanism.

**Distribution.** Democratic Republic of the Congo.

**Comments.** Only known from the type. It is not unlikely that *X. subcostatus* is the same species. However, the type differs by having a longer flange at the elytral apex, in dorsal view extending beyond interstriae 9. It also has coarser punctures along the wall of the interstitial carinae.

### Species with four-spined pronotum

#### *Xyloctonus maculatus* Schedl, 1965

Figs 35, 38, 41

*Xyloctonus maculatus* Schedl, 1965b: 113.

**Type material. Paratype:** South Africa, Cape Province, Port Elisabeth [-33.7, 25.6], VIII. 1960, ex *Sideroxylon inerme*, leg. J.S. Taylor [NHMW].

**Diagnosis.** Length 1.7–2.2 mm, 2.1–2.2× as long as wide, colour light to dark brown, with small, dark spots on elytra; antennal club with two visible procurved sutures; eyes not divided, but deeply emarginated; anterior margin of pronotum with four raised teeth, median pair longest; elytral interstriae 9 curves before apex and continues to elytral suture; scutellar shield rounded, with two tiny pits at anterior corners; elytral suture straight; elytral declivity long, nearly vertical; venter nearly straight.

**Distribution.** South Africa.

**New records.** South Africa, Western Cape Province, Natures Valley [-33.965, 23.562], 8 Nov. 2007, ex *Sideroxylon inerme*, B. Jordal, leg. [ZMUB].

**Biology.** Exclusively recorded from *Sideroxylon inerme* (Sapotaceae). Fallen trees were crowded with males running on the surface in search of females sitting in newly-excavated tunnel openings. Mating occurred at the entrance with only the posterior part of the female exposed. There was no nuptial chamber. Egg galleries were dense and males were guarding the entrance as long as the female was accessible.

#### *Xyloctonus genieri* sp. nov.

<https://zoobank.org/0977F970-815A-409A-B00F-94EDD3140070>

Figs 36, 39, 42

**Type material. Holotype:** Burkina Faso, Comoe, Forêt de Boulon [10.343, -4.510], 270 m alt., F. Genier leg., 10.7.2006, in Malaise trap [CMNC].

**Diagnosis.** Eyes emarginated, not divided. Antennal club with one faint procurved suture. Anterior margin of pronotum with four equally-sized, raised teeth.

**Description.** Length 1.6 mm, 2.1× as long as wide; colour black. **Frons** convex, transversely impressed just above epistoma, surface finely rugose, vestiture scant. Eyes deeply sinuate, broadly emarginated. Antennal funiculus 6-segmented, club finely pubescent, basal suture procurved, others not visible. **Pronotum** coarsely asperate on anterior two-thirds, asperities transversely elongated; anterior margin with four raised teeth. **Scutellar shield** subquadrate, with four small tubercles. **Elytral striae** reticulated, punctures shallow, irregular; interstriae carinated throughout; interstriae 9 reaching elytral suture; elytral suture straight. **Metaventricle** and nearby sclerites and ventrite I with bifid setae.

**Distribution and biology.** Only known from the type locality in a very dry bushland, collected in a Malaise trap.

**Etymology.** Named after the coleopterist François Génier who collected the type specimen in Burkina Faso.

#### *Xyloctonus aethiops* Schedl, 1953

Figs 43, 45, 47, 48

*Xyloctonus aethiops* Schedl, 1953: 77.

*Xyloctonus stenographus* Schedl, 1961a, synonymy by Menier (1974).

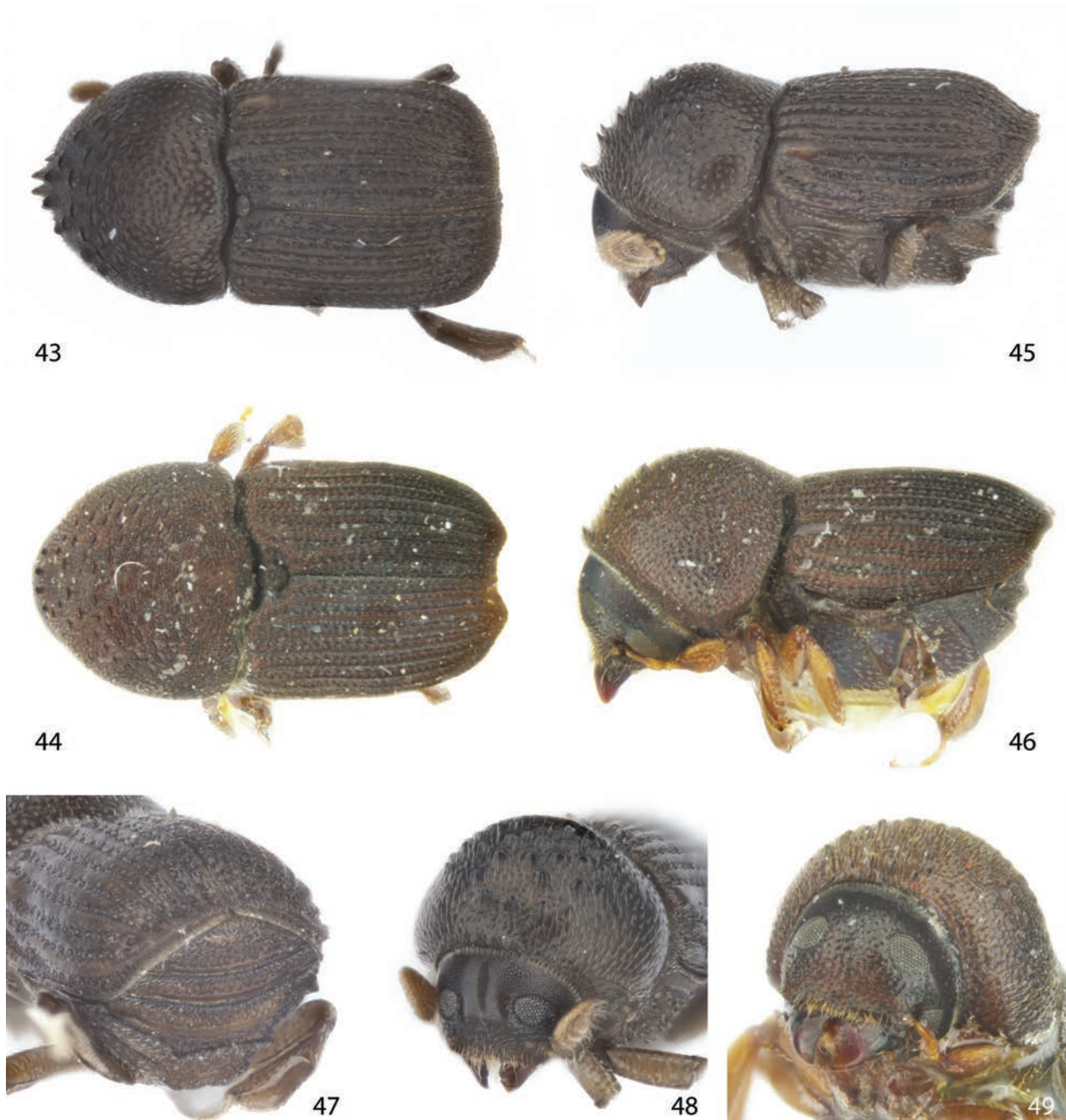
**Type material. Lectotype, X. aethiops:** Madagascar, Ankorika [-12.24, 49.36], K. E. Schedl, 1951 [MNHN].

**Holotype of X. stenographus:** Madagascar, Perinet [-18.93, 48.41], 28. XI. 1952, Dr. K. E. Schedl [MNHN].

**Diagnosis.** Length 1.3–1.6 mm, 2.0× as long as wide, colour dark brown; vertex with faint (false) pars stridens; antennal club with two visible procurved sutures; anterior margin of pronotum with four raised teeth, median teeth longest; elytral interstriae 9 curves before apex and continues to elytral suture; elytral



Figures 34–42. Dorsal, lateral and front view of *X. bimarginatus* (34, 37, 40); *X. maculatus* (35, 38, 41); *X. genieri*, holotype (36, 39, 42).



**Figures 43–49.** Dorsal, lateral and front view declivity and venter with strong spines, of *X. aethiops* (43, 45, 47, 48); *X. quadricinctus*, holotype (44, 46, 49).

interstriae elevated, flattened, carinated on and near declivity only; scutellar shield transversely oval; elytral suture straight. Ventricle I swollen on median third of its posterior margin, ventrite II with four spines along the posterior margin.

**Distribution.** Madagascar.

**New record.** Madagascar, Andasibe, Mantadia National Park [-18.861, 48.447], 900 m alt. 15 May 2015, ex *Uapaca* twig, B. Jordal, leg. [ZMUB].

**Biology.** Two collections from known host were both in the same plant family Phyllanthaceae: *Wielandia mimosoides* (originally in *Savia*) (Schedl 1977) and *Uapaca* sp. This is the only *Xyloctonus* that cut their egg

tunnels parallel to the grain of the wood. Three broods with larvae were dissected from a thin twig of 1 cm thickness and were without parents present. Brood size ranged between 21 and 28 (n = 3).

***Xyloctonus quadricinctus* Schedl, 1941**

Figs 44, 46, 49

*Xyloctonus quadricinctus* Schedl, 1941: 387.

**Type material.** *Holotype*: [Tanzania] Usambara, Derema 850 m alt., 7.10.1891, Conradt S. [NHMW].

**Diagnosis.** Length 2.1 mm, 2.0× as long as wide, colour dark brown; antennal club with three visible procurved sutures; anterior margin of pronotum with four equally-long raised teeth; elytral interstriae 9 curves before apex and continues to elytral suture; scutellar shield rounded, tuberculate; elytral suture straight.

**Distribution.** Ghana, Nigeria, Tanzania.

**Biology.** It has been collected from a Sapotaceae tree, *Gambeya albida* in Ghana (see Schedl (1961b)). Nothing else is known about its biology.

### *Xyloctonus quadridens* Schedl, 1953

Figs 50, 52, 54

*Xyloctonus quadridens* Schedl, 1953: 77.

**Type material. Syntypes:** Madagascar, Mt. D'Ambre, 1930, Sicard leg. [MNHN].

**Diagnosis.** Length 1.9–2.2 mm, 1.8–1.9× as long as wide, colour black, dull; antennal club with two visible procurved sutures, a third suture intergrades with the apical margin of club; anterior margin of pronotum with four raised teeth; elytral interstriae 9 curves before apex and continues to elytral suture; scutellar shield rugose, slightly impressed in middle; elytral suture straight; male profemur with tiny spine on its ventral side.

**Distribution.** Madagascar.

**New records.** Madagascar, Andasibe, Mantadia National Park [-18.861, 48.447], 900 m alt. 15 and 16 May 2015, ex *Labramia bojeri* log, B. Jordal, leg. [ZMUB]; Reserve speciale de l'Ankarana, 22.9 km SW Anivorano, B. Fischer [CAS].

**Biology.** The collection from *Labramia bojeri* (Sapotaceae) is the first known host for this species. Egg tunnels were cut transversely to the grain. Broods were old and only fully sclerotised adults were found.

Counts of larval mines ranged between 30 and 50 (n = 4).

**Comments.** According to Menier (1974), the male should have a pars stridens on its vertex. However, none of the males at hand had this feature, despite the unique presence of a femoral spine (n = 4).

### *Xyloctonus magnus* sp. nov.

<https://zoobank.org/55896893-5EB7-41E2-A7B8-6F301C1E18C8>

Figs 51, 53, 55

**Type material. Holotype:** Madagascar, Anjozorobe 11 km SE [-18.43, 47.94], Malaise trap, BLF2375, B. Fischer, leg. [CAS].

**Diagnosis.** Largest species in the genus, 3.4 mm long; scutellar shield longitudinally elongated as a heart-shaped scoop; sutural side of interstriae 1 with dense fine trifid setae.

**Description.** Length 3.4 mm, 1.9× as long as wide, colour dark brown. **Frons** impressed just above epistoma, nearly glabrous. Antennal club with one strongly procurved suture, others faint; funiculus 6-segmented. Upper and lower eye parts widely separated, roughly punctured between. **Pronotum** very broad, broader than elytra; anterior margin with four raised teeth, median pair slightly longer, asperities near summit as fine granules, intermixed with shiny punctures. **Scutellar shield** elongated, densely pilose, narrowly impressed to form a heart-shaped scoop. **Elytral** striae with transversely elongated punctures, spaced by longitudinally raised ridges, the whole stria appearing as a dashed line. Elytral interstriae 9 curves before apex and continues to elytral suture; elytral suture straight. **Metaventricle** and surrounding sclerites, including ventrite I, with mainly trifid setae.

**Distribution.** Madagascar.

**Biology.** One specimen was taken in a Malaise trap.

**Etymology.** Based on the Latin masculine adjective *magnus*, meaning large, referring to the body size of the species.

## Identification key to the species of *Xyloctonus*

- 1 Elytral interstriae 9 terminates near lateral margin, interstriae 1–8 all reaching apical margin (Fig. 5)..... 2
- Interstriae 9 reaching at least to interstriae 3, usually to the elytral suture, cutting off interstriae 1–8 which do not reach apical margin (Figs 3, 4) ..... 3
- 2 Frons glabrous; pronotal teeth at the anterior margin longer than broad; elytral carinae smooth and shiny; punctures very shallow; colour shiny black (Uganda)..... *X. niger*
- Frons finely pubescent; pronotal teeth at anterior margin as long as broad; elytral interstriae with fine short setae on each side of deeply-punctured interstitial carinae; strial punctures deep; colour matt brown to dark brown (Afrotropical)..... *X. scolytoides*
- 3 Anterior margin of pronotum with four raised teeth (Figs 35, 36)..... 4
- Anterior margin with two raised teeth (Figs 16–18)..... 9
- 4 Eyes sinuate, not divided (Figs 41, 42) ..... 5
- Eyes completely divided, sometimes with a line of scattered ommatidia partly connecting them ..... 6
- 5 Elytra lightly coloured with dark spots; declivity steeply sloping (South Africa) ..... *X. maculatus*
- Elytra uniformly dark; declivity gently sloping (Burkina Faso) ..... *X. genieri* sp. nov.
- 6 Elytral interstriae on disc flattened, carinate near elytral apex; ventrite II with four spines along the posterior margin; body length < 1.7 mm (Madagascar)..... *X. aethiops*
- Interstriae sharply carinate throughout; posterior margin of ventrites without longer spines; body size > 1.8 mm..... 7

- 7 Pronotal teeth along anterior margin spaced by more than width of a tooth (Fig. 44); elytral apex more broadly and deeply attenuated, apical tip of each elytron positioned between interstriae 3 and 4 (Ghana, Tanzania)..... *X. quadricinctus*
- Pronotal teeth at margin nearly contiguous (Figs 50, 51); elytral apex shallowly attenuated with tip of each elytron positioned between interstriae 2 and 3..... 8
- 8 Large species, length 3.4 mm; epistomal hair-like setae prominent, pointing forwards; scutellar shield longer than broad; ventral sclerites with mainly trifid setae (Madagascar)..... *X. magnus* sp. nov.
- Smaller, length < 2.4 mm; epistomal hair largely recumbent, pointing downwards; scutellar shield broader than long; ventral sclerites with mainly bifid setae (Madagascar)..... *X. quadridens*
- 9 Elytral interstriae 9 discontinued at the level of interstriae 3, interstriae 1–3 continue to apical margin..... 10
- Elytral interstriae 9 continues to interstria 1 with a clear gap between interstriae 9 and apical margin, all interstriae 1–8 discontinued before apical margin..... 11
- 10 Elytra appearing shiny; elytral suture with bulgy locking mechanism near scutellar shield (Fig. 17) (Somalia).....
- Elytra appearing dull, reticulate, particularly inside punctures; elytral suture straight throughout (Fig. 16) (Rwanda)....
- ..... *X. punctipennis*
- 11 Elytral striae with longitudinal tubercle between transversely oval punctures which appears like a straight dashed line (Madagascar)..... *X. biseriatus*
- Elytral striae with round punctures, without the dashed line pattern..... 12
- 12 Elytral suture straight; pronotal asperities near summit as broad irregular ridges; interstriae with fine setae on each side of the interstitial carina ..... 13
- Elytral suture with bulgy locking mechanism, pronotal asperities not much broader than tall; interstitial setae barely visible ..... 14
- 13 Pronotal teeth at anterior margin longer than broad, striae punctures large, in a single row; body length 2.0–2.2 mm (Mauritius)..... *X. mauritanus*
- Pronotal teeth at margin not longer than broad; striae punctures small, in two confused rows; body length > 2.7 mm (South Africa, Zambia) ..... *X. pubifer*
- 14 Apical rim of elytra extends far beyond the transverse interstriae 9, forming a lip (Figs 34, 37) (Democratic Republic of the Congo)..... *X. bimarginatus*
- Elytral interstriae 9 near elytral apex approximately at the same level as elytral apex (Burkina Faso and Guinea to Sudan, south-eastern Democratic Republic of the Congo, Mozambique, Tanzania)..... *X. subcostatus*

## Discussion

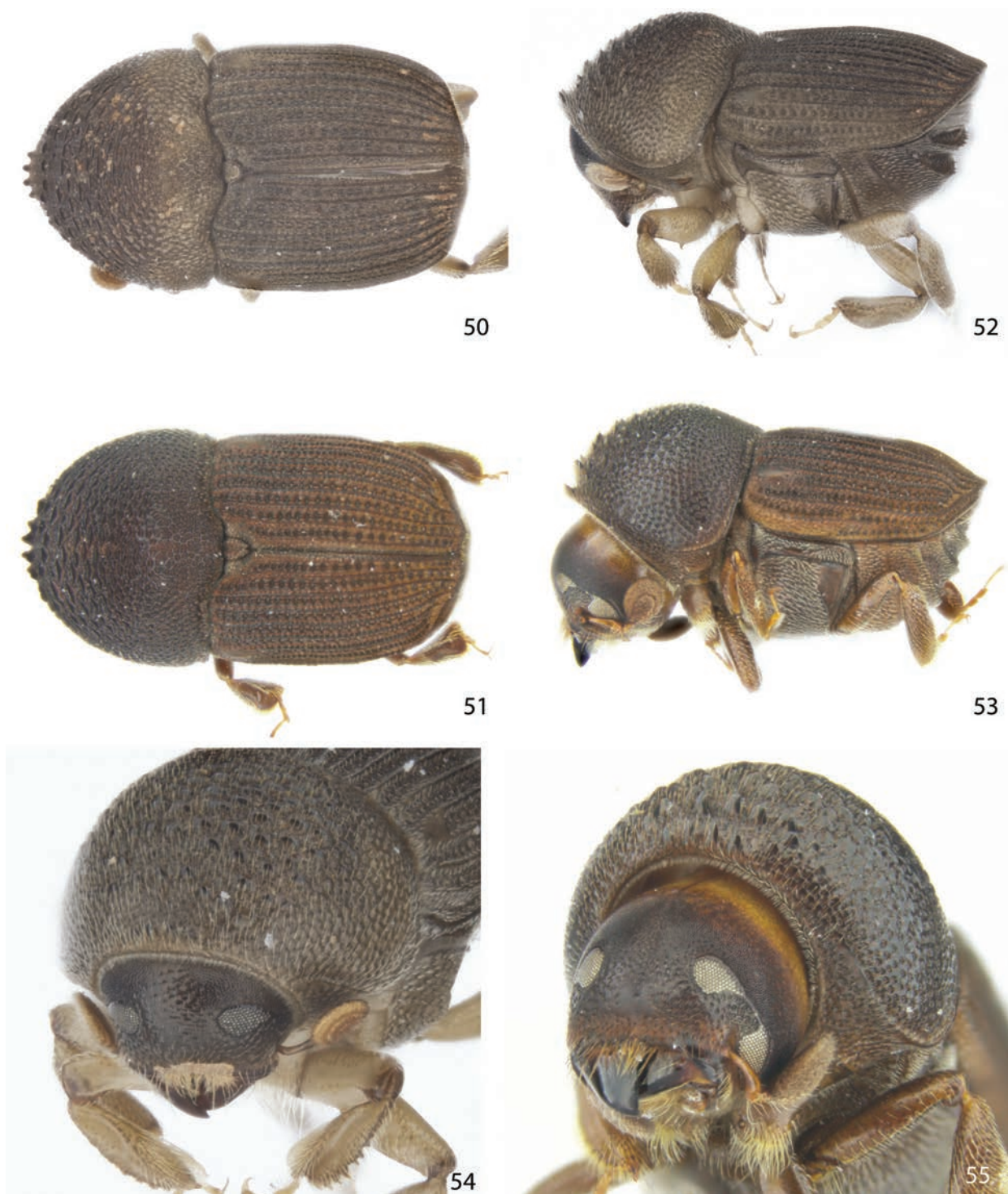
### Biology

*Xyloctonus* species are easily recognised by their compact morphology which reflects a likely adaptation to avoid predators. When disturbed, they easily fall off the branch or trunk after retracting their tarsi into deep grooves on their tibiae, particularly the protibiae. The legs are, furthermore, strongly flattened and the metatibiae and femur fit into a depression of the metanepisternum and metaventricle, which is carinated along its front edge. Observing their mating behaviour in the field reveals fast running of males on the bark to find a colonising female, with which he mates in the tunnel opening. He will, thereafter, guard the opening to prevent further access to the female by other males. This is a very exposed situation that increases the risk of being taken by predatory insects such as ants or even by insectivore birds. These beetles have an impressive reaction speed and fall off the log extremely quickly. Species in *Xyloctonus* and other *Xyloctonina* are, therefore, amongst the most specialised with morphologies deviant from the average bark beetle body shape (Schedl 1961b).

Both males and females stay only for a short time with their broods (Table 2). Males usually leave before the eggs

are hatching and females at some undetermined time later, but usually well before the young tenerals appear. The rather aggressive mating behaviour observed in males of several species seems connected to the external location of mating which involves a high risk of predation. It is likely that the early escape from the egg gallery provides further opportunities for mating and perhaps compensates for the high predation risk during mate search. This behaviour was most clearly demonstrated by *X. maculatus* which may establish a new nest on the same log. Limited parental care with the potential for multiple matings is perhaps also motivated by the generally low brood sizes compared to the average for bark beetles (Browne 1961), although low brood size could also be a consequence of limited parental care.

The low number of known host plants, restricted to a handful of plant families, indicates a high level of host specialisation in this genus. Six of the ten species with known host records were taken from plants in Sapotaceae. Mono- and oligophagy are typical for bark beetles as opposed to the broader range of host plants used by ambrosia beetles (Beaver 1979; Hulcr et al. 2007). The few host plants recorded are not a serendipitous artefact from rare collecting events as multiple collections over time and from localities far from each other were from the same host (Schedl 1957, 1961b, 1977; this study). Five of



Figures 50–55. Dorsal, lateral and front view of male *X. quadridens* (50, 52, 54); *X. magnus*, holotype (51, 53, 55).

the six species reported in this study were collected multiple times in one field work session, suggesting that these species are not extremely rare, although *X. scolytoides* is the only one collected more than four times.

### Plastic dimorphism

A stridulatory apparatus is sometimes present, but varies in size and distinctness. Menier (1974) reported the pres-

ence of a stridulatory file in the upper frons of male *X. quadridens*, which was not observed in the new material. The males of this species have a spine on the ventral side of the femur, but, nevertheless, there was no pars stridens present in any of the new specimens collected. Multiple series of *X. subcostatus* also indicated that at least some males exhibit a pars stridens, previously not reported. Somewhat intermediate is *X. aethiops* which has a partially developed and likely a false pars stridens, a feature not seen in the type material of this species. One should not

exclude the possibility that cryptic species may exist and which differ in their stridulatory apparatus. However, such cryptis seems less likely given their otherwise identical morphology. To firmly conclude on these matters, DNA from multiple populations is needed to test this hypothesis.

## Biogeography

Restricted use of host plants is associated with limited geographical distributions and high endemism in nearly all species of *Xyloctonus*. Amongst the 15 currently-recognised species, only four have a broad distribution including two or more biogeographical regions. However, only one of these have trustworthy records from both western and eastern to southern parts of Africa. The core distribution is in the Zambesian region and four species are found endemic to Madagascar and one on Mauritius. Unfortunately, many of the older samples from the Zambesian region were unsuitable for DNA sequencing and, therefore, limited the biogeographical inference in the BBM analysis. It was, nevertheless, clear that *Xyloctonus* differs strongly from *Ctonoxylon* which unequivocally demonstrated a Congolian ancestry, with much more recent and repeated colonisations of Madagascar and the southern parts of Africa.

It is likely that broader sampling of *Xyloctonus* will further confirm a single ancient colonisation of Madagascar during the Eocene. This was a favourable time to colonise the island due to the trade winds blowing primarily in an eastern direction (Yoder and Nowak 2006; Ali and Huber 2010; Jordal 2021b; Ali and Hedges 2022), but examples of colonisations in the opposite direction are found in, for example, xyleborine (Eliassen and Jordal 2021) and micracidine beetles (Jordal 2021b). The opposite pattern is apparently the norm for *Ctonoxylon* which revealed three independent colonisations with subsequent speciation during the mid- or late Miocene. Each of the two undescribed Malagasy species and one that did not provide DNA data, are all fairly similar to, but distinct from, the African mainland sister species (unpublished manuscript). It is, therefore, possible that these have colonised Madagascar even more recently than that which the dated phylogeny indicates.

It appears more and more clear that insects are not influenced by historical trade winds to the same degree as in non-volant animals (Crottini et al. 2012; Samonds et al. 2012). On the other hand, one needs to keep in mind that most insect groups never managed to settle on Madagascar, for example, *Glostatus* which is found in rather similar ecological niches on the African continent (Jordal 2023). This genus shows a strong core distribution in the Zambesian region (see Fig. 6), with one or few dispersal events towards the southern part of Africa. This pattern is reminiscent of the one for *Ctonoxylon*, whereas *Xyloctonus* may have colonised southern Africa from Madagascar, a pattern known from several scolytine beetle groups (Jordal 2013; Eliassen and Jordal 2021; Jordal 2021b). With

a steady increase in biogeographic data for Afrotropical scolytine beetles, it seems clear that patterns are variable and not particularly correlated with trade winds. A similar pattern is found in plants with windborne seeds, telling us that prevailing wind systems possibly vary more than postulated (Ali and Huber 2010; Ali and Hedges 2022).

## Acknowledgements

The author thanks, in particular, the staff at the California Academy of Sciences and François Génier at CMNC for samples containing new taxa. Additionally, many thanks to the curators at the institutions listed for access to other unidentified material and loan of type specimens. Collecting and export permits for Madagascar were kindly facilitated by MICET and granted by Direction generale de l'environnement et des forets 2012, 2015 and 2018. Permit for collecting and research in the Cape Provinces of South Africa 2006 was granted by Cape Nature no. AAA-004-00062-0035.

## References

- Ali JR, Hedges SB (2022) A review of geological evidence bearing on proposed Cenozoic land connections between Madagascar and Africa and its relevance to biogeography. *Earth-Science Reviews* 232: 104103. <https://doi.org/10.1016/j.earscirev.2022.104103>
- Ali JR, Huber M (2010) Mammalian biodiversity on Madagascar controlled by ocean currents. *Nature* 463(7281): 653–656. <https://doi.org/10.1038/nature08706>
- Beaver RA (1979) Host specificity of temperate and tropical animals. *Nature* 281(5727): 139–141. <https://doi.org/10.1038/281139a0>
- Beaver RA, Löyttyneimi K (1985) Bark and ambrosia beetles (Coleoptera: Scolytidae) of Zambia. *Revue de Zoologie Africaine* 99: 63–85.
- Blandford WFH (1895) Scolytidae. *Biologia Centrali-Americana. Coleoptera* 4: 81–96.
- Browne FG (1961) The biology of Malayan Scolytidae and Platypodidae. *Malayan Forest Records* 22: 1–255.
- Crottini A, Madsen O, Poux C, Strauß A, Vieites DR, Vences M (2012) Vertebrate time-tree elucidates the biogeographic pattern of a major biotic change around the K–T boundary in Madagascar. *Proceedings of the National Academy of Sciences of the United States of America* 109(14): 5358–5363. <https://doi.org/10.1073/pnas.1112487109>
- Drummond AJ, Rambaut A (2007) BEAST: Bayesian evolutionary analysis by sampling trees. *BMC Evolutionary Biology* 7(1): 214–214. <https://doi.org/10.1186/1471-2148-7-214>
- Eggers H (1927) Neue Borkenkäfer (Ipidae, Col.) aus Afrika (Nachtrag III). *Revue de Zoologie et de Botanique Africaines* 15: 172–199.
- Eggers H (1939) Die afrikanische Gattung *Xyloctonus* Eichh. (Col. Ipidae). *Revue de Zoologie et de Botanique Africaines* 32: 14–18.
- Eichhoff WJ (1872) Neue exotische Tomiciden Arten. *Berliner Entomologische Zeitschrift* 15(2–3): 131–137. <https://doi.org/10.1002/mmnd.18710150203>
- Eichhoff WJ (1878) Ratio, descriptio, emendatio eorum Tomicinorum qui sunt in Dr. Medin. Chapuiss et autoris ipsius collectionibus et quos praeterea recognovit. Vol. 8, Societe Entomologique de Liege, Memoires, Liege, 1–581.

- Eliassen J, Jordal BH (2021) Integrated taxonomic revision of Afrotropical *Xyleborinus* (Curculionidae: Scolytinae) reveals high diversity after recent colonization of Madagascar. *Insect Systematics and Diversity* 5(3): 1–39. <https://doi.org/10.1093/isd/ixab011>
- Hagedorn JM (1910) Diagnosen bisher unbeschriebener Borkenkäfer. *Deutsche Entomologische Zeitschrift* 1910(1): 1–13. <https://doi.org/10.1002/mmnd.4801910101>
- Hopkins AD (1915) Contributions toward a monograph of the Scolytid beetles. II. Preliminary classification of the superfamily Scolytoidea. United States Department of Agriculture, Technical Series 17: 165–232.
- Hulcr J, Mogia M, Isua B, Novotny V (2007) Host specificity of ambrosia and bark beetles (Col., Curculionidae: Scolytinae and Platypodinae) in a New Guinea rainforest. *Ecological Entomology* 32(6): 762–772. <https://doi.org/10.1111/j.1365-2311.2007.00939.x>
- Jordal BH (2013) Deep phylogenetic divergence between *Scolytoplatypus* and *Remansus*, a new genus of Scolytoplatypodini from Madagascar (Coleoptera, Curculionidae, Scolytinae). *ZooKeys* 352: 9–33. <https://doi.org/10.3897/zookeys.352.6212>
- Jordal BH (2021a) Molecular and morphological revision of Afrotropical Hypoborini (Coleoptera: Curculionidae: Scolytinae) revealed novel bark beetle taxa with narrow geographical distributions. *European Journal of Entomology* 118: 90–110. <https://doi.org/10.14411/eje.2021.011>
- Jordal BH (2021b) A phylogenetic and taxonomic assessment of Afrotropical Micracidini (Coleoptera, Scolytinae) reveals a strong diversifying role for Madagascar. *Organisms Diversity & Evolution* 21: 245–278. <https://doi.org/10.1007/s13127-021-00481-4>
- Jordal BH (2023) Glostatina, a new xyloctonine subtribe for *Glostatus* (Coleoptera: Curculionidae), based on clear genetic and morphological differences. *European Journal of Entomology* 120: 199–232. <https://doi.org/10.14411/eje.2023.025>
- Jordal BH, Cognato AI (2012) Molecular phylogeny of bark and ambrosia beetles reveals multiple origins of fungus farming during periods of global warming. *BMC Evolutionary Biology* 12(1): 133. <https://doi.org/10.1186/1471-2148-12-133>
- Linder HP, de Klerk HM, Born J, Burgess ND, Fjeldså J, Rahbek C (2012) The partitioning of Africa: Statistically defined biogeographical regions in sub-Saharan Africa. *Journal of Biogeography* 39(7): 1189–1205. <https://doi.org/10.1111/j.1365-2699.2012.02728.x>
- Menier JJ (1974) Les Scolytidae Africaines — Première note de révision du genre *Xyloctonus* (Col.). *Société Entomologique de France. Annales* 19: 653–666. <https://doi.org/10.1080/21686351.1974.12278175>
- Pistone D, Gohli J, Jordal BH (2018) Molecular phylogeny of bark and ambrosia beetles (Curculionidae: Scolytinae) based on 18 molecular markers. *Systematic Entomology* 43(2): 387–406. <https://doi.org/10.1111/syen.12281>
- Samonds KE, Godfrey LR, Ali JR, Goodman SM, Vences M, Sutherland MR, Irwin MT, Krause DW (2012) Spatial and temporal arrival patterns of Madagascar’s vertebrate fauna explained by distance, ocean currents, and ancestor type. *Proceedings of the National Academy of Sciences of the United States of America* 109(14): 5352–5357. <https://doi.org/10.1073/pnas.1113993109>
- Schedl KE (1938) New records of African Scolytidae and Platypodidae (Col.). 54<sup>th</sup> Contribution. *Annals & Magazine of Natural History* 2(11): 450–458. <https://doi.org/10.1080/00222933808526873>
- Schedl KE (1939) Scolytidae und Platypodidae. 59 Beitrag, I. Zur synonymie der Borkenkäfer. *Revue de Zoologie et de Botanique Africaines* 32: 379–387.
- Schedl KE (1941) Neue afrikanische Gattungen und Arten. *Revue de Zoologie et de Botanique Africaines* 34: 379–424.
- Schedl KE (1953) Fauna Madagascariensis, III. Institut Scientifique de Madagascar, Memoires. Ser E 8: 67–106.
- Schedl KE (1957) Scolytoidea nouveaux du Congo Belge, II. Mission R. Mayne - K.E. Schedl 1952. *Musee Royale du Congo Belge Tervuren, Ser 8. Sciences Zoologiques* 56: 1–162.
- Schedl KE (1961a) Fauna Madagascariensis, IV. 188 contribution. Institut Scientifique de Madagascar, Memoires. Ser E 12: 127–170.
- Schedl KE (1961b) Scolytidae und Platypodidae Afrikas. Band I (part). Familie Scolytidae. *Revista de Entomologia de Moçambique* 4: 335–742.
- Schedl KE (1965a) Interessante und neue Scolytoidea aus Afrika. *Revista de Entomologia de Moçambique* 8: 349–379.
- Schedl KE (1965b) South African bark and timber beetles. *Journal of the Entomological Society of Southern Africa* 28: 110–116.
- Schedl KE (1977) Die Scolytidae und Platypodidae Madagaskars und einiger naheliegender Inselgruppen. *Mitteilungen der Forstlichen Bundes-Versuchsanstalt Wien* 119: 1–326.
- Wood SL, Bright DE (1992) A catalog of Scolytidae and Platypodidae (Coleoptera). Part 2: Taxonomic index. *Great Basin Naturalist Memoirs* 13: 1–1553.
- Yoder AD, Nowak MD (2006) Has vicariance or dispersal been the predominant biogeographic force in Madagascar? Only time will tell. *Annual Review of Ecology, Evolution, and Systematics* 37(1): 405–431. <https://doi.org/10.1146/annurev.ecolsys.37.091305.110239>
- Yu Y, Blair C, He XJ (2020) RASP 4: Ancestral state reconstruction tool for multiple genes and characters. *Molecular Biology and Evolution* 37(2): 604–606. <https://doi.org/10.1093/molbev/msz257>

# New genus and species of lice in the *Oxylipeurus*-complex (Phthiraptera, Ischnocera, Philoptera), with an overview of the distribution of ischnoceran chewing lice on galliform hosts

Daniel R. Gustafsson<sup>1</sup>, Chunpo Tian<sup>1,2</sup>, Mengjiao Ren<sup>1</sup>, Zhu Li<sup>3</sup>, Xiuling Sun<sup>4</sup>, Fasheng Zou<sup>1</sup>

<sup>1</sup> Guangdong Key Laboratory of Animal Conservation and Resource Utilization, Guangdong Public Library of Wild Animal Conservation and Utilization, Institute of Zoology, Guangdong Academy of Sciences, 105 Xingang West Road, Haizhu District, Guangzhou, 510260, Guangdong Province, China

<sup>2</sup> College of Life Sciences, Shaanxi Normal University, 620 West Chang'an Street, Chang'an District, Xi'an City, 710119, Shaanxi Province, China

<sup>3</sup> Department of Life Sciences, National Natural History Museum of China, 126, Tianqiao South St. Dongcheng District, Beijing, 100050, China

<sup>4</sup> Collections Department, National Natural History Museum of China, 126, Tianqiao South St. Dongcheng District, Beijing, 100050, China

<https://zoobank.org/AFC4DD57-2761-424D-B766-FE9696EFF040>

Corresponding author: Daniel R. Gustafsson (kotatsu@fripost.org)

Academic editor: Viktor Hartung ♦ Received 30 August 2023 ♦ Accepted 31 January 2024 ♦ Published 12 March 2024

## Abstract

Here, we describe a new genus of lice (Phthiraptera, Ischnocera) in the *Oxylipeurus*-complex, parasitising galliform hosts in the genera *Tragopan* Cuvier, 1829. This genus, *Pelecolipeurus* **gen. nov.**, is separated from other members of the complex by the unique shape of the male subgenital plate and stylus, the male genitalia and other characters. The only previously-known species in the genus is *Lipeurus longus* Piaget, 1880, which is here tentatively re-described as *Pelecolipeurus longus* (Piaget, 1880), based on specimens from a non-type host, *Tragopan temminckii* (Gray, 1831). In addition, we describe a new species, *Pelecolipeurus fujianensis* **sp. nov.**, based on specimens from *Tragopan caboti* (Gould, 1857). An overview of the distribution patterns of ischnoceran lice on galliforms is presented, which suggests that host phylogeny, host biogeography and host biotope, as well as elevation of host range, may all be important factors that have structured louse communities on landfowl. We transfer the genus *Afrilipeurus* from the *Oxylipeurus*-complex to the *Lipeurus*-complex and include an emended key to the *Oxylipeurus*-complex.

## Key Words

chewing lice, Galliformes, new genus, *Oxylipeurus*-complex, Phthiraptera

## Introduction

Chewing lice (Phthiraptera) in the *Oxylipeurus*-complex mainly parasitise gamefowl (Galliformes; Price et al. (2003)) and most species are known from Asian galliforms. Traditionally, most of the species have been placed in the one genus, *Oxylipeurus* (e.g. Clay (1938a); Hopkins and Clay (1952); Price et al. (2003)). However, this classification was challenged by, for example, von Kéler (1958) and Carriker (1967), who considered several

groups of *Oxylipeurus* to be sufficiently distinct to form separate genera. Mey (2009) considered several of these genera valid and, since then, a large number of new genus-level taxa within this complex have been established (Gustafsson and Zou 2020a, b, 2023; Gustafsson et al. 2020a, b).

Assessing taxon limits in this complex is difficult, as the overall chaetotaxy and morphology, including that of the male genitalia, are conserved in many genera and species are often delimited by more nebulous characters,

such as head shape, mesosome shape and degree of reticulation of the cuticle (e.g. Gustafsson et al. (2020a)). Moreover, many species are poorly known and have not been fully described or illustrated; the last detailed revisions of the complex were published by Clay (1938a) and von Kéler (1958).

Gustafsson et al. (2020a) tentatively considered *Lipeurus longus* Piaget, 1880, to belong to the genus *Reticulipeurus* Kéler, 1958, based on its placement by Clay (1938a), von Kéler (1958) and Złotorzycka (1966); however, they stated that they had not examined any specimens and that some aspects of the morphology of this species were aberrant for *Reticulipeurus*. Here, we describe this group as a separate genus, *Pelecolipeurus* gen. nov., based on specimens examined from two hosts in China and examination of photos and illustrations of *Lipeurus longus* Piaget, 1880. We tentatively re-describe the only previously-known species (*L. longus*) and add a second species, *Pelecolipeurus fujianensis* sp. nov.

Given that this new genus is the third *Oxylipeurus*-complex genus to be described in recent years from the same host group, we also take this opportunity to summarise what is known about host-associations amongst ischnoceran lice parasitising galliform hosts. Finally, we update the key to the genera of the *Oxylipeurus*-complex previously published by Gustafsson et al. (2020b).

## Materials and methods

Previously, slide-mounted specimens deposited at the National Natural Museum of Natural History, China (NNHM) were examined with a Nikon Eclipse Ni (Nikon Corporation, Tokyo, Japan), with a drawing tube attached for making illustrations. Drawings were scanned, then compiled and edited in GIMP 2.10 ([www.gimp.org](http://www.gimp.org)). Measurements (all in mm) were made from slide-mounted specimens in the digital measuring software ImageJ 1.48v (Wayne Rasband; [imagej.net](http://imagej.net)): AW = abdominal width (at segment V); HL = head length (at mid-line); HW = head width (at widest point of temples); PRW = prothoracic width; PTW = pterothoracic width; TL = total length (at mid-line).

Host taxonomy follows Clements et al. (2022). Terminology for chaetotaxy and other structures of the lice follows Clay (1951), Mey (1994) Gustafsson and Bush (2017) and Gustafsson et al. (2020a). Abbreviations used in the text follow Gustafsson and Bush (2017) and Gustafsson et al. (2020a) and include: *mds* = mandibular seta; *mms* = marginal mesometathoracic setae; *mths* = metathoracic thorn-like seta; *mtrs* = metathoracic trichoid seta; *mts1–3* = marginal temporal setae 1–3; *os* = ocular seta; *pos* = preocular seta; *ps* = paratergal seta; *pst1–2* = parameral setae 1–2; *s1–8* = sensilla 1–8 of dorsal head; *sts* = sternal seta; *vms* = vulval marginal setae; *vss* = vulval submarginal setae.

## Systematics

### PHTHIRAPTERA Haeckel, 1896

Phthiraptera Haeckel, 1896: 703.

### Ischnocera Kellogg, 1896

Ischnocera Kellogg, 1896: 63.

### Philopteridae Burmeister, 1838

Philopteridae Burmeister, 1838: 422.

## *Oxylipeurus*-complex

Included genera:

*Calidolipeurus* Gustafsson et al., 2020b: 2.

*Cataphractomimus* Gustafsson et al., 2020a: 206.

*Chelopistes* Kéler, 1940: 180.

*Virgula* Clay, 1941: 119.

*Eiconolipeurus* Carriker, 1945: 91.

*Epicolinus* Carriker, 1945: 104.

*Gallancyra* Gustafsson & Zou, 2020a: 11.

*Megalipeurus* Kéler, 1958: 327.

*Oxylipeurus* Mjöberg, 1910: 91.

*Pelecolipeurus* gen. nov.

*Reticulipeurus* Kéler, 1958: 332.

Subgenus: *Reticulipeurus* (*Forcipurellus*) Gustafsson & Zou, 2023:497.

Subgenus: *Reticulipeurus* (*Reticulipeurus*) Kéler, 1958: 332.

*Sinolipeurus* Gustafsson et al., 2020a: 229.

*Splendoroffula* Clay & Meinertzhagen, 1941: 343.

*Splendopeurus* Kéler, 1958: 309.

*Talegallipeurus* Mey, 1982: 242.

*Trichodomea* Carriker, 1946: 365.

*Valimia* Gustafsson & Zou, 2020b: 490.

### *Pelecolipeurus* gen. nov.

<https://zoobank.org/FBCCEB4D-7E49-4BFE-88D7-A71559102743>

**Type species.** *Pelecolipeurus fujianensis* sp. nov.

**Diagnosis.** *Pelecolipeurus* gen. nov. keys to *Reticulipeurus* Kéler, 1958, in the key of Gustafsson et al. (2020b). Species of *Pelecolipeurus* can be separated from *Reticulipeurus* and all other members of the *Oxylipeurus*-complex by the following combination of characters: frons rounded to slightly flattened (Figs 3, 17); dorsal pre-antennal suture present, transversal, but not reaching lateral margins of head (Figs 3, 17); *mms* gathered into a single sublateral bunch (Figs 1, 2, 15, 16); male tergopleurites II–VII medianly interrupted and intertergal sclerites absent (Figs 1, 15); male tergopleurites IX–XI fused to form single plate (Figs 1, 15); female

tergopleurites IX–XI fused laterally, but not medianly, forming two distinct plates (Figs 2, 16); male subgenital plate of unique shape, with lateral extensions at base of stylus (Figs 7, 21); stylus subterminal, elongated to reach beyond distal margin of abdomen (Figs 7, 21); female vulval margin narrowly concave, without lateral accessory vulval plates (Figs 8, 22); male genitalia very long, reaching anteriorly to abdominal segment III (Figs 5, 19); denticulate genital sac present in male genitalia (Figs 5, 19); male genitalia symmetrical, with parameres present, mesosome dominated by large gonopore (Figs 6, 20).

**Description. Both sexes.** Male longer than female (Table 1). Head longer than wide, frons rounded to slightly flattened (Figs 3, 17). Dorsal pre-antennal suture present, but often not well-defined and visible as pale band across head; suture not reaching lateral margins of head. Interior thickenings of pre-antennal head present as double, undulating carinae anterior to suture. Head chaetotaxy as in Figs 3, 17; *mds* may be absent in female; *s2* (?) located median to *s1*; *s5* absent; *s6*–*s8* present; *mts3* only temporal mesoseta, but *os* may be longer than *pos* and *mts1*–*2* in males. Antennae sexually dimorphic, with male scape and pedicel elongated and swollen compared to female (cf. Figs 3, 4, 17, 18); male flagellomere I with distal, finger-like extension and intensely scaly inner surface (Figs 3, 17). Temples rounded, somewhat bulging. Thoracic and abdominal segments as in Figs 1, 2, 15, 16. Legs II and III much longer than legs I; coxae I–II close together. Meso- and metasterna fused. Metepisternum long, reaching almost to mesometasternum. Pronotum with lateral and posterior setae; pteronotum with microsetae in antero-lateral corners and short seta submedianly in distal half; *mms* in single sublateral bunch; *mths* and *mtrs* roughly dorsal. Tergopleurites II–VII in both sexes medianly interrupted; male tergopleurites IX–XI fused into a medianly continuous plate; female tergopleurites IX–XI fused laterally, but not medianly (Figs 2, 16). Male subgenital plate with lateral extensions in distal section (Figs 7, 15); stylus slender, elongated, tapering, attached subterminally and extending beyond distal margin of abdomen. Female subgenital plates reduced to near vulval margin; exact extent of these often not clearly visible. Leg chaetotaxy as in Figs 9–14.

**Male.** Male scape, pedicel and flagellomere I modified compared to female. Male genitalia very long (Figs 5, 19), with basal apodeme reaching to at least abdominal segment III, but diffuse anteriorly. Genital sac present, irregularly, but densely denticulate (Figs 6, 20). Distal third of basal apodeme with irregularly thickened lateral margins articulating with parameral heads. Mesosome simple, with central sclerite on ventral surface associated with 2–3 sensilla; three additional sensilla in oblique, distally divergent rows lateral to this sclerite. Gonopore large, dominating mesosome. Parameres short, slender, *pst1* sensilla in distal third, *pst2* microsetae, situated more or less apically.

**Female.** Vulval margin deeply and narrowly concave (Figs 8, 22). Three sets of genital setae: long, slender *vms*,

the more median setae shorter than the more lateral setae; short, slender or lightly stout *vss* in median part of vulval margin; single seta on each side situated further submarginally and apart from *vss*. Subvulval sclerites present, slender and elongated, reaching to vulval margin.

**Host distribution.** Presently known only from tragopans (genus *Tragopan* Cuvier, 1829), Phasianidae, Galliformes. Some specimens from other hosts (see below) may represent stragglers or contaminations.

**Geographical range.** All known species are from China or the Himalayas, corresponding roughly to the combined range of the known hosts.

**Etymology.** The name *Pelecolipeurus* is derived from “*pélekus*”, Greek for “two-headed axe” and the traditional name for long slender lice, *Lipeurus* Nitzsch, 1818. This refers to the shape of the male subgenital plate.

**Remarks.** Gustafsson et al. (2020a) tentatively included *Lipeurus longus* Piaget, 1880, in *Reticulipeurus* Kéler, 1958, following von Kéler (1958) and Złotorzycka (1966). They noted that they had not examined any specimens and that this placement was doubtful, based on the illustrations published by Clay (1938a) and von Kéler (1958). The examined collection at NNHM includes two different species belonging to the same morphological group as *L. longus* and these are sufficiently different morphologically from all other members of the *Oxylipeurus*-complex that the erection of a separate genus is warranted.

Unfortunately, no specimens from the type host of *Lipeurus longus* were found at NNHM and no specimens of this species have been examined from other collections. A lectotype and five paratypes are available at the Natural History Museum, London (NHML), but we had no opportunity to examine or borrow these. A photo of the lectotype female at the NHML homepage (<https://data.nhm.ac.uk/dataset>) confirms that this species belongs to *Pelecolipeurus*, but is insufficiently detailed to compare adequately with the specimens we have examined at the NNHM. Only two modern illustrations of *L. longus* have been published (Clay 1938a; von Kéler 1958), both of which depict the ventral view of the distal end of the male abdomen. Allowing for individual variation and differences in illustration techniques, we cannot separate the specimens illustrated in these publications from specimens we have seen from *Tragopan temminckii* (Gray, 1831) (see below) and these specimens are here tentatively considered conspecific with *L. longus*; however, this will need to be confirmed by comparison with type specimens of *L. longus* and a re-description of this species.

As the type specimens of *L. longus* could not be examined, we select the species that could be examined as the type species of *Pelecolipeurus*.

**Included species.**

*Pelecolipeurus fujianensis* sp. nov. Type host: *Tragopan caboti* (Gould, 1857).

*Pelecolipeurus longus* (Piaget, 1880: 370) [in *Lipeurus*]. Type host: *Tragopan satyra* (Linnaeus, 1758).

**Table 1.** Measurements of the species of *Pelecolipeurus*. Measurements (all in mm) were made in the digital measuring software ImageJ 1.48v (Wayne Rasband; imagej.net): AW = abdominal width (at segment V); HL = head length (at mid-line); HW = head width (at widest point of temples); PRW = prothoracic width; PTW = pterothoracic width; TL = total length (at mid-line).

Species	Host	Sex	N	TL	HL	HW	PRW	PTW	AW
<i>Pelecolipeurus fujianensis</i>	<i>Tragopan caboti</i>	M	20 <sup>1</sup>	4.00–4.41 (4.20)	0.78–0.93 (0.85)	0.50–0.63 (0.57)	0.39–0.58 (0.48)	0.59–0.84 (0.71)	0.63–0.90 (0.77)
		F	30 <sup>2</sup>	3.45–4.05 (3.74)	0.81–0.91 (0.86)	0.55–0.67 (0.61)	0.40–0.58 (0.49)	0.62–0.85 (0.73)	0.69–1.09 (0.89)
<i>Pelecolipeurus longus</i> s. lat.	<i>Tragopan temminckii</i>	M	6	3.56–4.40	0.70–0.90	0.48–0.71	0.41–0.61	0.58–0.80	0.58–0.91
		F	15	3.24–3.94 (3.59)	0.76–0.91 (0.83)	0.55–0.71 (0.63)	0.38–0.57 (0.47)	0.64–0.84 (0.74)	0.80–1.12 (0.96)

<sup>1</sup> N = 15 for TL; N = 18 for AW.

<sup>2</sup> N = 24 for TL; N = 29 for PTW; N = 38 for AW.

### *Pelecolipeurus fujianensis* sp. nov.

<https://zoobank.org/1CEB3DAA-D063-4616-A4A7-703CE2B2544F>

Figs 1–14

**Type host.** *Tragopan caboti* (Gould, 1857) – Cabot's tragopan.

**Type locality.** Fujian Province, China.

**Specimens examined. Type material.** Ex *Tragopan caboti*: CHINA • **Holotype** ♂; Fujian Province; 29 Sep 1990; collector unknown; box E0026199, slide 65 (NNHM) [Male in lower right corner, near where cover glass is broken, marked with black dot on slide]. **Paratypes** 7♂, 9♀, 8 nymphs; Fujian Province; 29 Sep 1990; collector unknown; box E0026199, slides 64–66, 95 (NNHM). 1♂, 3♀; Fujian Province; 16 Dec 1988; collector unknown; box E0026199, slide 68 (NNHM). 1♀, 3 nymphs; Fujian Province, Jianou; 7 Jan 1997; collector unknown; box E0026195, slide 3 (NNHM). 1♂, 2♀, 6 nymphs; Fujian Province, Wuyi Mountain; Dec. 1989; collector unknown; box E0026011, slide 15, box E0026198, slide 74 (NNHM). 11♂, 15♀, 11 nymphs; Zhejiang Province; 8 Dec 1980; collector unknown; box E0026010, slide 76, box E0026199, slides 88–92 (NNHM).

**Diagnosis.** Due to the limited illustrations published for *Pelecolipeurus longus* from the type host (see above), we here compare *P. fujianensis* sp. nov. with the specimens tentatively identified as *P. longus* from *T. temminckii*, which we consider conspecific with the species illustrated by Clay (1938a) and von Kéler (1958). A re-description of *P. longus* from the type host is necessary to determine additional characters separating this species from *P. fujianensis*.

*Pelecolipeurus fujianensis* can be separated from *P. longus* as illustrated by Clay (1938a) and von Kéler (1958) by the following characters: male fused abdominal segment IX–XI with more or less straight lateral margins in *P. longus*, but with concave lateral margins in *P. fujianensis* (Fig. 7); proximal mesosome of *P. longus* with flattened anterior margin, but with medianly pointed anterior end in *P. fujianensis* (Fig. 6); parameres more curved in *P. longus* than in *P. fujianensis* (Fig. 6).

In addition, *P. fujianensis* can be separated from the population from *T. temminckii* described above by the following characters: frons more flattened in *P. longus* s. lat. (Fig. 17) than in *P. fujianensis* (Fig. 3); male sternal plate VI with 2 *sts* of more or less equal length in *P. longus* s. lat. (Fig. 15), but with lateral seta on each side much shorter than median seta on each side in *P. fujianensis*

(Fig. 1); female sternal plate VI with 1 *sts* on each side and sternal plate VII with 3 medium-length setae and up to 2 microsetae on each side in *P. fujianensis* (Fig. 2), but sternal plate VI with 2 *sts* on each side and sternal plate VII without microsetae in *P. longus* s. lat. (Fig. 16); male subgenital plates of different shape (cf. Figs 7, 21) and stylus evenly tapering distally in *P. longus* s. lat. (Fig. 21), but with convex lateral margins in distal half in *P. fujianensis* (Fig. 7); female subgenital plate medianly continuous in *P. longus* s. lat. (Fig. 22), but medianly interrupted in *P. fujianensis* (Fig. 8); proximal mesosome with flattened to slightly concave anterior margin in *P. longus* s. lat. (Fig. 20), but with pointed anterior margin in *P. fujianensis* (Fig. 6); ventral sclerite of mesosome and shape of gonopore and distal mesosome also differ between species (cf. Figs 6, 20). Male antennal characters may be more similar in these two species than illustrated here (Figs 3, 17), as their shape is affected by mounting. However, scape appears to be broader and the distal process of flagellomere I appears to be longer in *P. fujianensis* (Fig. 3) than in *P. longus* s. lat. (Fig. 17).

**Description. Both sexes.** Head shape and structure as in Fig. 3; frons gently rounded. No prominent reticulation on head. Marginal carina of moderate width, not widening posteriorly. Dorsal pre-antennal suture prominent, not reaching marginal carina laterally. Head chaetotaxy as in Fig. 3; most dorsal sensilla visible as microsetae in most examined specimens. Antennae sexually dimorphic. Thoracic and abdominal segments and chaetotaxy as in Figs 1, 2.

**Male.** Antennae as in Fig. 3; scape, pedicel and flagellomere I swollen and modified in shape compared to female; scape with slight process in proximal third; flagellomere I with prominent distal projection and restricted rugose area, which does not extend to proximal bulbous process of segment. Abdominal chaetotaxy as in Fig. 9; inner ventral *ps* present on segments V–VIII; median *sts* on sternite VI much longer than lateral *sts*. Subgenital plate, stylus and terminalia as in Fig. 7; stylus broadening in distal half, not tapering evenly. Genitalia as in Figs 5, 6. Proximal mesosome with narrow median point, widening distally. Ventral sclerite small, roughly rounded-rectangular, with minute postero-lateral extensions; 1 sensillum on each side associated with sclerite; 3 sensilla on each side lateral to ventral sclerite, forming distally divergent rows. Distal mesosome oval, dominated by large oval gonopore. Parameres curved slightly medianly, with median and lateral fingers of parameral head roughly equal in size. Measurements as in Table 1.

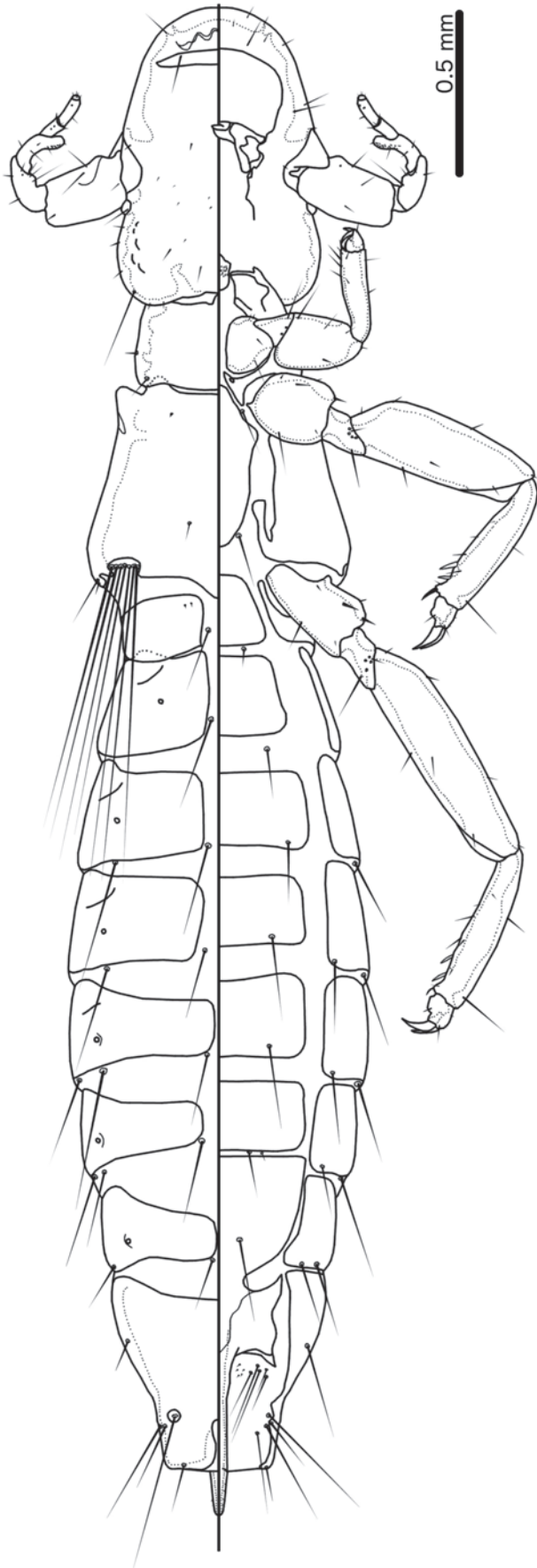


**Figure 1.** *Pelecolipeurus fujianensis* sp. nov. ex *Tragopan caboti* (Gould, 1857). Male habitus, dorsal and ventral views.

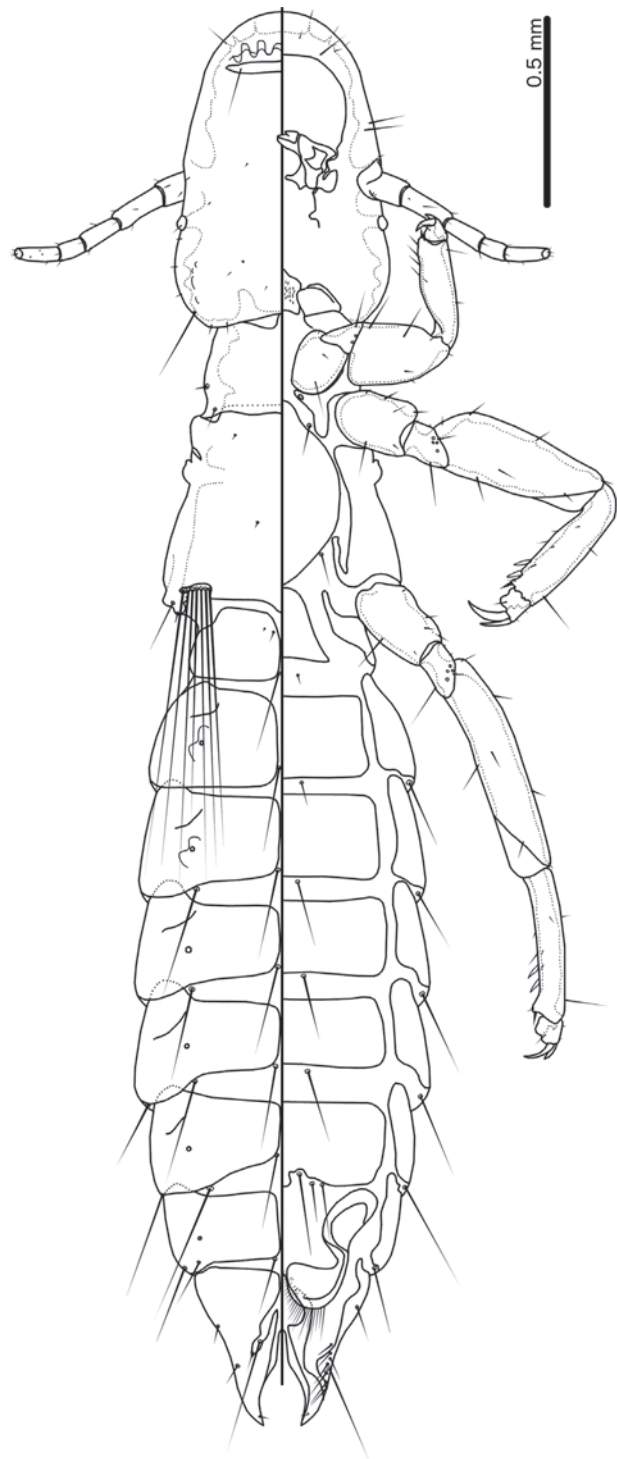
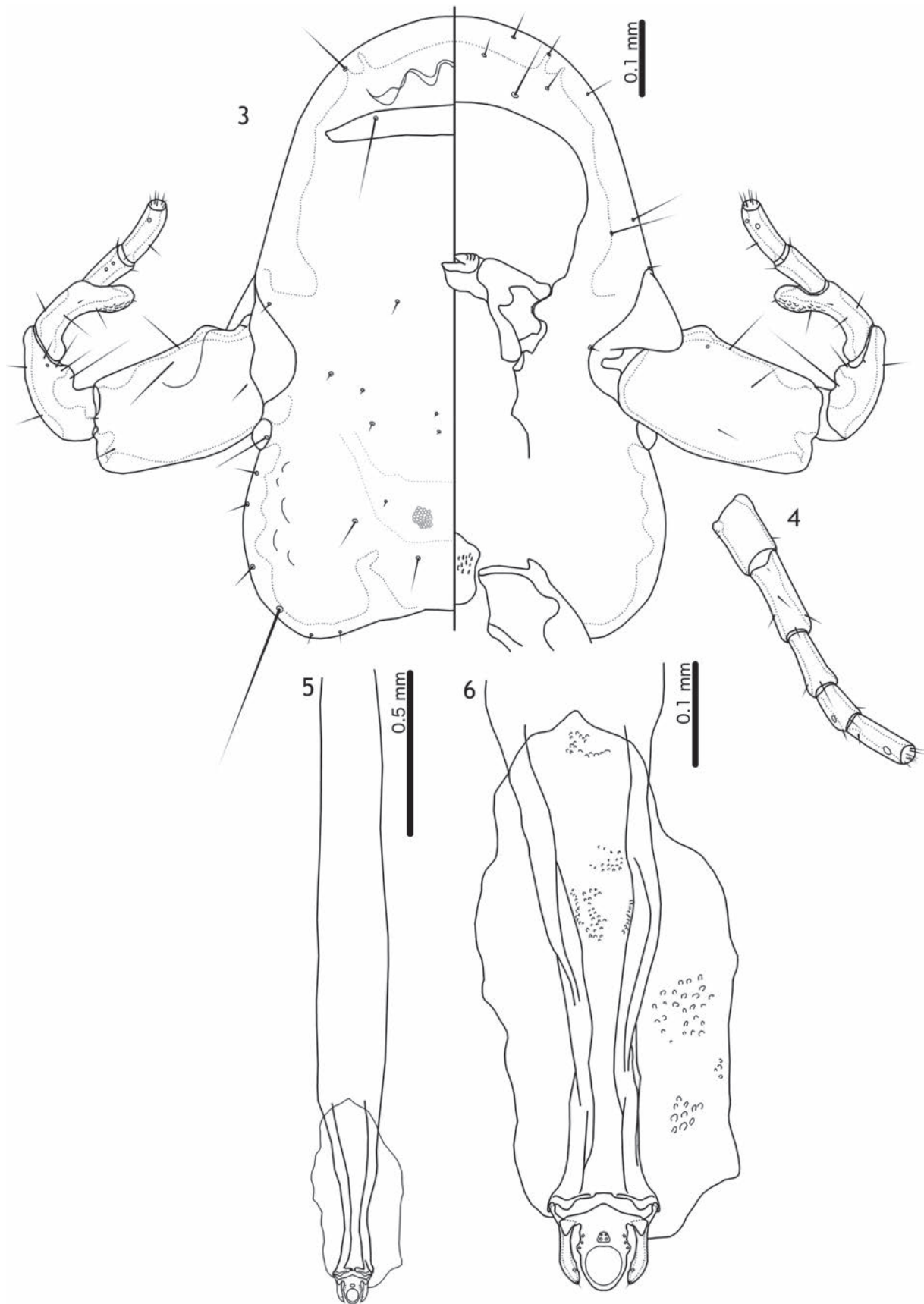


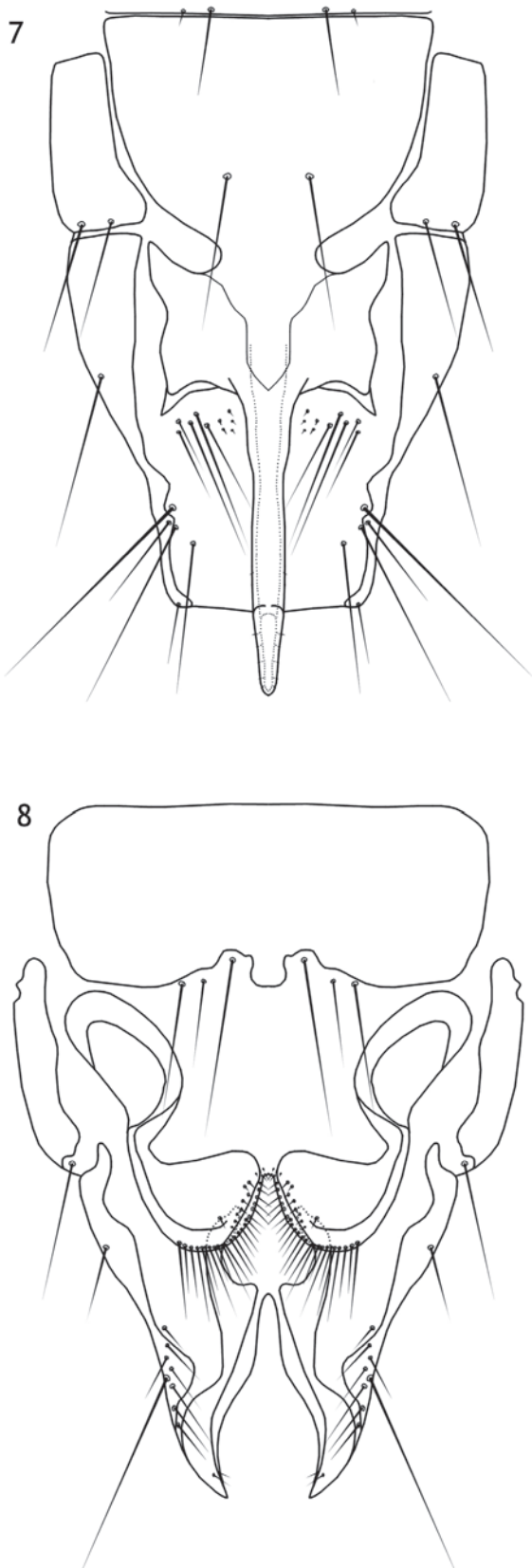
**Figure 2.** *Pelecolipeurus fujianensis* sp. nov. ex *Tragopan caboti* (Gould, 1857). Female habitus, dorsal and ventral views.

**Female.** Antennae as in Fig. 4. Abdominal chaetotaxy as in Fig. 2; sternal plate VI with 1 *sts* on each side. Subgenital plate, vulval margin and terminalia as in Fig. 8; subgenital plate divided medianly. Vulval margin with 17–23 medium-length, slender *vms* and 6–10 short, slender *vss* on each side; median *vms* shorter than lateral *vms*. Measurements as in Table 1.

**Etymology.** The specific name is derived from the type locality.



**Figures 3–6.** *Pelecolipeurus fujianensis* sp. nov. ex *Tragopan caboti* (Gould, 1857). **3.** Male head, dorsal and ventral views; **4.** Female antenna, ventral view; **5.** Male genitalia, ventral view; **6.** Distal male genitalia, ventral view.



**Figures 7, 8.** *Pelecolipeurus fujianensis* sp. nov. ex *Tragopan caboti* (Gould, 1857). **7.** Male subgenital plate and abdominal segments VIII–XI, ventral view; **8.** Female subgenital plate and abdominal segments VIII–XI, ventral view.

***Pelecolipeurus longus* (Piaget, 1880), comb. nov.**

Figs 15–22

*Lipeurus longus* Piaget, 1880: 370.

*Oxylipeurus longus* (Piaget), 1880; Clay, 1938a: 171.

*Reticulipeurus longus* (Piaget, 1880); Kéler, 1958: 332.

**Type host.** *Tragopan satyra* (Linnaeus, 1758) – satyr tragopan.

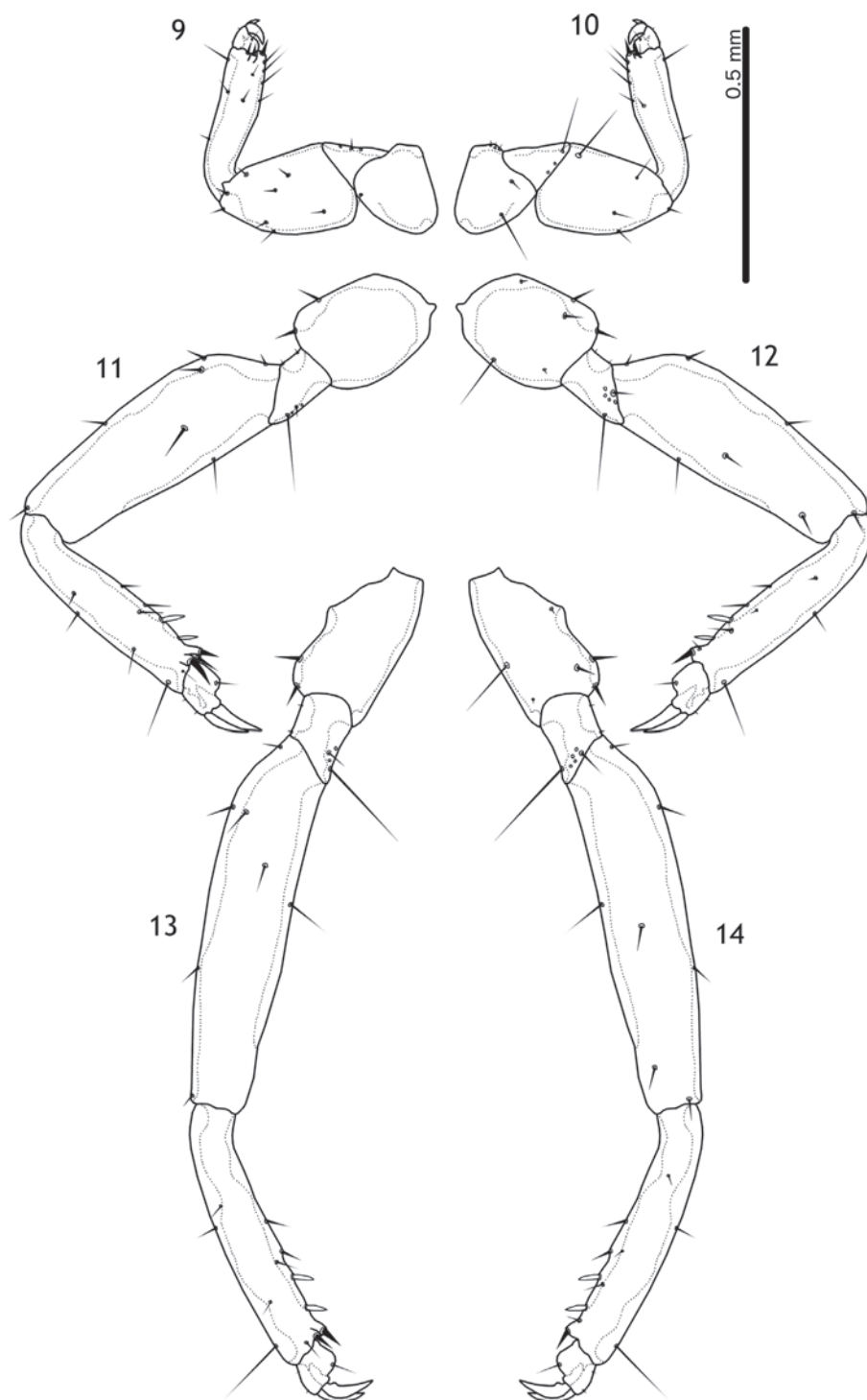
**Type locality.** The Hague, Netherlands (captive bird; host is limited to the Himalayas).

**Other hosts.** *Tragopan temminckii* (Gray, 1831) – Temminck’s tragopan [tentative]. *Tragopan melanocephalus* (Gray, 1829) – western tragopan [uncertain; Clay 1938a: 172].

**Specimens examined.** Ex *Tragopan temminckii*: CHINA • 2♂, 2♀; Shanghai, Shanghai Zoo; 12 Sep. 1988; Shi Xinquan leg.; box E0026199, slides 73–76 (NNHM). 5♀; Beijing, Beijing Zoo; 10 Oct 1973; collector unknown; box E0026199, slides 78–82 (NNHM). 4♂, 6♀; Sichuan Province, Beichuan; 4 May 1984; collector unknown; box E0026199, slides 84–87 (NNHM). Ex *Crossoptilon auritum* [straggler?]: CHINA • 1♀; no locality; 30 Oct 1990; collector unknown; box E0026199, slide 67 (NNHM). Ex *Lophura nycthemera fokiensis* [straggler?]: CHINA • 1♂; Fujian Province; Dec 1990; collector unknown; box E0026199, slide 71 (NNHM). Ex *Tragopan* sp.: CHINA • 1♀; no collection data; box E0026199, slide 83 (NNHM).

**Diagnosis.** Both specimens from *T. temminckii* and those illustrated from the type host by Clay (1938a) and von Kéler (1958) can be separated from *P. fujianensis* sp. nov. by the following characters: male fused abdominal segment IX–XI with more or less straight lateral margins in *P. longus*, but with concave lateral margins in *P. fujianensis* (Fig. 7); proximal mesosome of *P. longus* with flattened anterior margin, but with medianly pointed anterior end in *P. fujianensis* (Fig. 6); parameres more curved in *P. longus* than in *P. fujianensis* (Fig. 6). Specimens from *T. temminckii* can be further separated from *P. fujianensis* by the characters listed under this species above, but examination of specimens from the type host of *P. longus* is necessary to establish whether the population on this host can also be separated from *P. fujianensis* by the same characters and whether the populations on *T. satyra* and *T. temminckii* are conspecific.

**Description (of specimens from *Tragopan temminckii*).** **Both sexes.** Head shape, structure and reticulation pattern as in Fig. 17; frons somewhat flattened. Marginal carina of moderate width, widening posteriorly. Dorsal pre-antennal suture prominent, reaching to or nearly to marginal carina laterally. Head chaetotaxy as in Fig. 17; many dorsal sensilla very small and difficult to see. Antennae sexually dimorphic. Thoracic and abdominal segments and chaetotaxy as in Figs 15, 16.



**Figures 9–14.** *Pelecolipeurus fujianensis* sp. nov. ex *Tragopan caboti* (Gould, 1857). **9.** Male leg I, dorsal side; **10.** Male leg I, ventral side; **11.** Male leg II, dorsal side; **12.** Male leg II, ventral side; **13.** Male leg III, dorsal side; **14.** Male leg III, ventral side.

**Male.** Antennae as in Fig. 17; scape, pedicel and flagellomere I swollen and modified in shape compared to female; scape with seemingly hyaline, broad process in proximal third; flagellomere I with intensely rugose surface and intensely rugose bulbous process near proximal base. Abdominal chaetotaxy as in Fig. 15; inner ventral *ps* absent on all tergopleurites; *sts* on sternite VI of about equal length. Subgenital plate, stylus and terminalia as in Fig. 21; stylus tapering more or less evenly towards distal

end. Genitalia as in Figs 19, 20. Proximal mesosome flattened to slightly concave, with short, stout antero-lateral extensions bent slightly anteriorly. Ventral sclerite inverse V-shaped, with up to 3 sensilla on each side associated with its distal margin; 3 sensilla on each side lateral to ventral sclerite, forming distally divergent rows. Distal mesosome rounded rectangular, dominated by large, roughly rounded-trapezoidal gonopore. Parameres roughly parallel; *pst1–2* as in Fig. 20. Measurements as in Table 1.

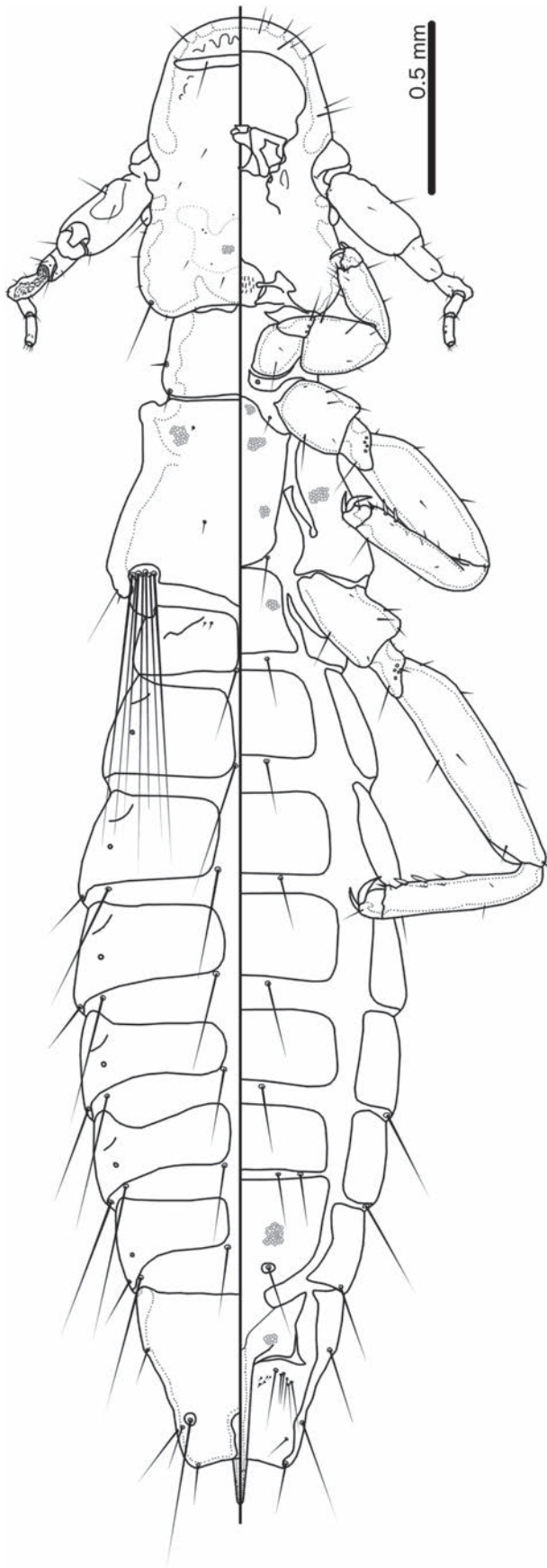


**Figure 15.** *Pelecolipeurus* cf. *longus* (Piaget, 1880) ex *Tragopan temminckii* (Gray, 1831). Male habitus, dorsal and ventral views.

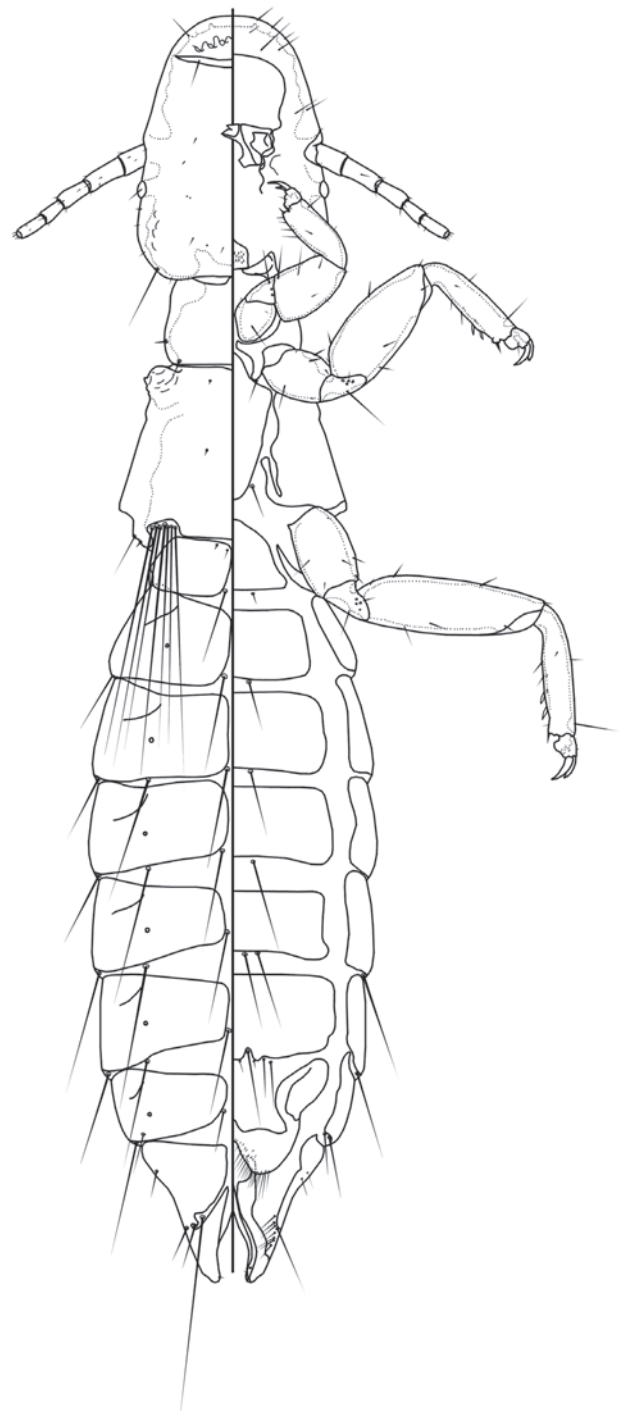
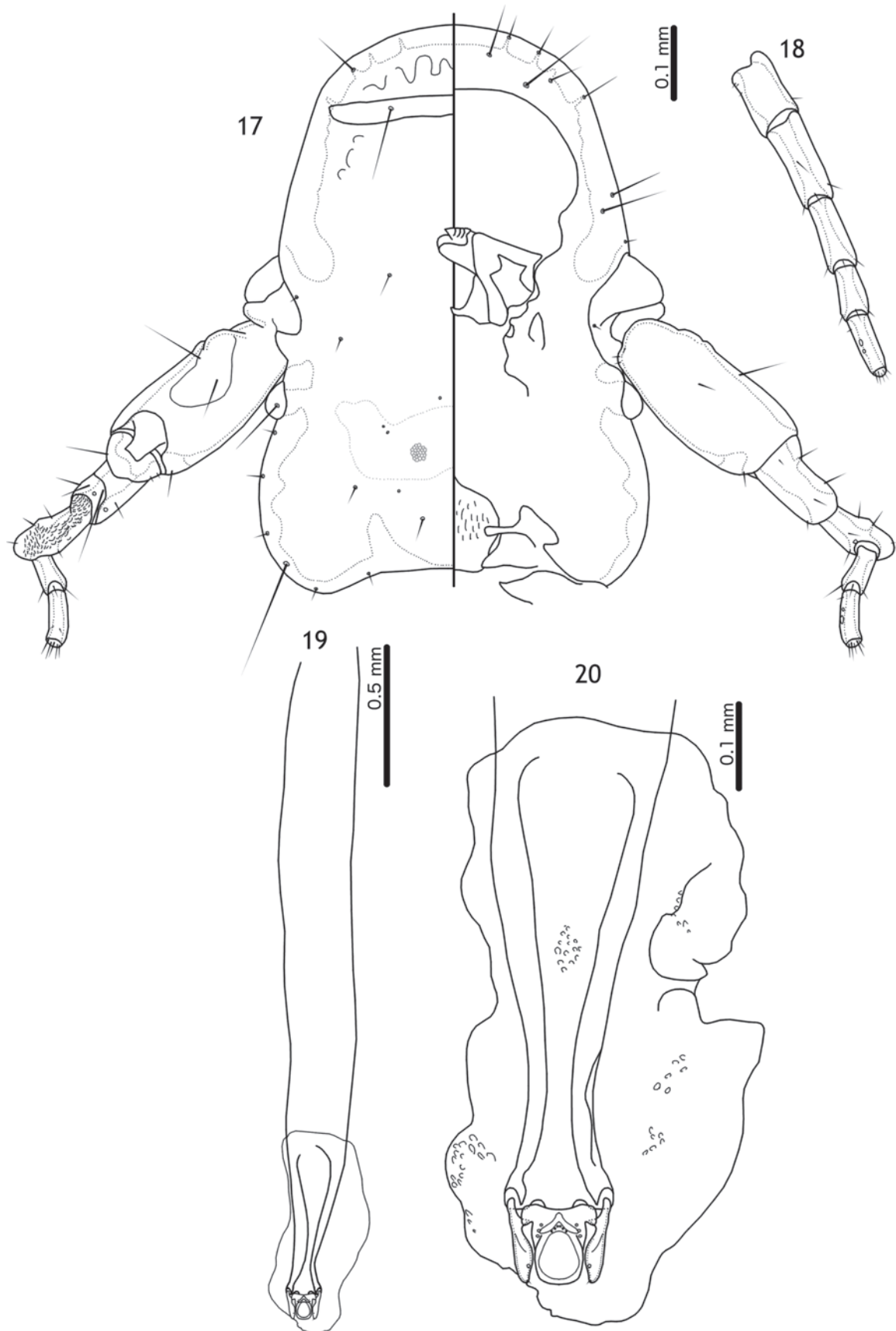


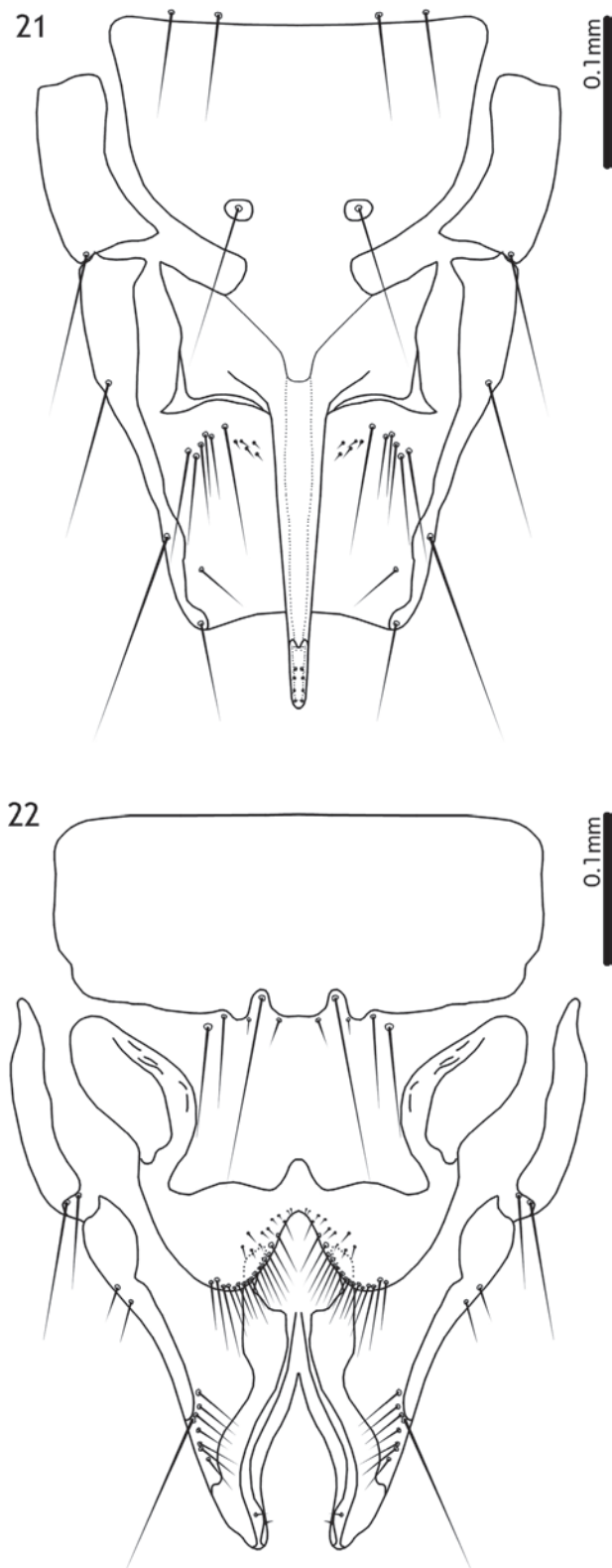
**Figure 16.** *Pelecolipeurus* cf. *longus* (Piaget, 1880) ex *Tragopan temminckii* (Gray, 1831). female habitus, dorsal and ventral views.

**Female.** Antennae as in Fig. 18. Abdominal chaetotaxy as in Fig. 16; sternal plate VI with 2 *sts* on each side. Subgenital plate, vulval margin and terminalia as in Fig. 22; subgenital plate continuous medianly. Vulval margin with 17–22 medium-length, slender *vms* and 8–12 short, slender *vss* on each side; median *vms* shorter than lateral *vms*. Measurements as in Table 1.

**Remarks.** We have not seen any specimens of *L. longus* from the type host. The original illustrations (Piaget



**Figures 17–20.** *Pelecolipeurus* cf. *longus* (Piaget, 1880) ex *Tragopan temminckii* (Gray, 1831). **17.** Male head, dorsal and ventral views; **18.** Female antenna, ventral view; **19.** Male genitalia, ventral view; **20.** Distal male genitalia, ventral view.



**Figures 21, 22.** *Pelecolipeurus cf. longus* (Piaget, 1880) ex *Tragopan temminckii* (Gray, 1831). **21.** Male subgenital plate and abdominal segments VIII–XI, ventral view; **22.** Female subgenital plate and abdominal segments VIII–XI, ventral view.

1880; figs 8, 8a, 8b) are insufficiently detailed to establish its identity beyond placing it in *Pelecolipeurus*. Clay (1938a: 171, figs 33b, 35a) and Kéler (1958: fig. 34) illustrated the male terminalia and male genitalia of this species, confirming our placement of *L. longus* in the new genus *Pelecolipeurus*. Kéler (1958: 327–333) provided some additional morphological details, but did not consider it possible to separate this species from *Reticulipeurus*, even subgenerically. Złotorzycka (1966) placed *P. longus* in *Reticulipeurus*; this was followed tentatively by Gustafsson et al. (2020a), but they did not examine any specimens and noted that the species may need to be moved to a separate genus.

Piaget (1880) treated specimens from both hosts as conspecific. Specimens of *Pelecolipeurus* from *Tragopan temminckii* are similar to *P. longus* (Piaget, 1880) as illustrated by Clay (1938a) and Kéler (1958), but published illustrations and descriptions (Piaget 1880; Clay 1938a; von Kéler 1958) are insufficient to establish the status of these populations adequately. As in illustrations of *L. longus*, the male specimens from *T. temminckii* have largely flat lateral margins of abdominal segment IX–XI, suggesting they are conspecific. However, Clay's illustration of the male mesosome of *L. longus* (Clay 1938a: fig. 35a) indicates that there may be differences in the shape of the mesosome between *L. longus* and specimens we have examined. In our previous experience with Clay's illustrations in this publication (e.g. Gustafsson et al. (2020a)), details such as these are not always reliable when compared to specimens examined by Clay, presumably due to limitations of the microscopy and illustration techniques of the time. Clay (1938a: 172) stated that she had also examined specimens from *T. temminckii* and *Tragopan melanocephalus* and that it was "impossible to say whether [*P. longus*] normally occurs on these two hosts or whether Piaget's specimens are stragglers".

A photo of the lectotype female of *P. longus* is available online at the NHML's homepage (<https://data.nhm.ac.uk/dataset>). In this photo, the distal claspers of the abdomen are more attenuated than illustrated here and the sclerotisations following the vulval margin may be narrower, but this is not clear in the photo. Moreover, these characters may be affected by mounting or be subject to individual variation within the *Oxylipeurus*-complex and cannot be used alone as reliable indicators of species identity. Other characters, such as vulval chaetotaxy, cannot be seen in the photo. A re-examination of the lectotype and the six paralectotypes of *P. longus* will be necessary to establish the identity of specimens from *T. temminckii* (and other hosts) listed here, but, unfortunately, we were not able to either examine the specimen at the NHML, nor borrow this specimen.

We presently consider populations from both *T. satyra* and *T. temminckii* to be conspecific, but note that *P. longus* from the type host is in need of re-description and that such a re-description may warrant the recognition of the specimens described here as a separate species.

## Discussion

Galliforms have some of the most diverse chewing louse faunas of any bird orders. Price et al. (2003) recognised 21 genera of lice from galliform hosts, whereas Mey (2009) recognised a total of 64 genera from the same hosts. Including the new genus described here, an additional eight genera of lice have been described from galliform hosts since 2009, all except two in the *Oxylipeurus*-complex (Mey 2010, 2013; Gustafsson and Zou 2020a, b, 2023; Gustafsson et al. 2020a, b, 2023). In the checklist of Price et al. (2003), lice on galliform hosts represent almost 10% (21 of 212) of all avian louse genera accepted as valid; if genera accepted by Mey (2009) and those described from other host groups since 2003 are added (in total 49 genera; for example, Mey (2004); Gustafsson and Bush (2017); Gustafsson et al. (2020a, b)), this would imply that over 23% (72 of 302) of the known louse genera occur on galliform hosts, despite Galliformes itself comprising ~ 2.66% of bird diversity (290 of 10906 spp.; Clements et al. (2022)).

Clearly, the diversity of lice on galliform hosts is disproportionate to the diversity of host species in this group. The reasons for this over-diversity are unclear. Galliformes constitutes an ancient lineage of birds, with fossil records going back to perhaps the late Cretaceous (Clarke 2004; Agnolin et al. 2006). However, age itself does not necessarily indicate that a host group should have a diverse louse fauna. For instance, the closely-related anseriforms comprise 180 species (~ 1.65% of bird diversity; Clements et al. (2022)), but are only parasitised by 11 (Price et al. 2003) or 14 (Mey 2009) louse genera, constituting 3.61% or 4.61% of louse genera, respectively; note that taxonomic richness of lice is lower in diving than in non-diving birds (Felsö and Rózsa 2006), which may affect this comparison.

Probably, as more becomes known of the lice of galliform hosts, clear patterns may emerge in the distribution of these louse genera that could explain the unexpectedly high diversity of lice on landfowl. However, some patterns are already dimly visible in the known distribution of lice on these hosts. In Table 2, we list the distribution of ischnoceran lice parasitising galliforms, roughly following the classification of Mey (2009), but with some modifications, based on our own examinations of specimens (DRG, unpublished data). It should be noted that no characters are known that can consistently separate the *Goniodes*- and *Goniocotes*-complexes as currently circumscribed (Gustafsson et al. 2021) and Johnson et al. (2011) found both complexes to be paraphyletic. The structure of the male genitalia may ultimately be useful for defining the *Goniocotes*-complex, but this complex is likely nested inside the *Goniodes*-complex as defined by Price et al. (2003; as *Goniodes*), Mey (2009) and here.

Each of the groups of lice included in Table 2 show different patterns of distribution and the Ischnocera of galliform hosts include both generalist genera occurring over several of the major radiations and genera that are more

restricted. Of particular interest are the lice of tragopans and allies (genera *Lophophorus* Temminck, 1813, *Tetraophasis* Elliot, 1871 and *Tragopan*). These three genera together form a monophyletic clade, with no close relatives (Meng et al. 2008; Bao et al. 2010; Liu et al. 2014; Wang et al. 2014, 2017; Kimball et al. 2021). We here refer to this group as the “tragopan group” for simplicity.

### *Oxylipeurus*-complex

The *Oxylipeurus*-complex is widely distributed across galliforms, being absent only from numidid hosts (Table 2); the genus *Afrilipeurus* Mey, 2010, was originally described from species known from numidid hosts, but this genus appears to be a member of the *Lipeurus*-complex (see below) and only superficially similar to lice in the *Oxylipeurus*-complex. Amongst the genera within the *Oxylipeurus*-complex, most are restricted to certain host groups.

There is a clear division in the *Oxylipeurus*-complex between genera occurring mainly on New World host groups and those occurring mainly on Old World host groups. With the exception of *Chelopistes lervicola* (Clay, 1941), all members of the genera *Chelopistes* Kéler, 1940, *Eiconolipeurus* Carriker, 1945, *Epicolinus* Carriker, 1945, *Labicotes* Kéler, 1940, *Trichodomedea* Carriker, 1946 and *Valimia* Gustafsson & Zou, 2020b, are found only on New World hosts. In contrast, the genera *Megalipeurus* Kéler, 1958, *Pelecilipeurus* gen. nov., *Calidolipeurus* Gustafsson et al., 2020b, *Cataphractomimus* Gustafsson et al., 2020a, *Gallancyra* Gustafsson & Zou, 2020a, and *Sinolipeurus* Gustafsson et al., 2020a, are only found on Old World hosts. The genera *Oxylipeurus* Mjöberg, 1910 and *Talegallipeurus* Mey, 1982, are exclusively known in Australia and Wallacea. That leaves only one cosmopolitan genus, *Reticulipeurus* Kéler, 1958, which is known both in the Old and New Worlds.

*Reticulipeurus* also has wider host associations than most other genera in this complex, being known from both Cracidae and Phasianidae II–III. However, the species known from Phasianidae III belong to a different subgenus (Gustafsson and Zou 2023). The species from cracid hosts have not been revised in recent years and may represent a separate radiation. *Reticulipeurus*, as currently understood, may represent a plesiomorphic morphotype, from which other, morphologically more distinct, groups of *Oxylipeurus*-complex lice, have evolved. If not, the distribution of *Reticulipeurus* on two distinct host groups – mainly Asian phasianids and almost entirely Neotropical cracids – requires further study to understand.

Similarly, Gustafsson et al. (2020a) noted that the widely distributed genus *Megalipeurus* slightly differs morphologically amongst different host groups and may also represent several distinct lineages. Most other genera are more restricted: *Eiconolipeurus* and *Epicolinus* on odontophorid hosts, *Labicotes* on cracid hosts, *Trichodomedea* on cracid and odontophorid hosts and *Calidolipeurus*, *Gallancyra* and *Valimia* being known from one

**Table 2.** Distribution of ischnoceran lice across different galliform hosts. The host groupings are based on Kimball et al. (2021); host taxonomy follows Clements et al. (2022). Associations are based on Mey (2006, 2009, 2010, 2013), Gustafsson and Zou (2020a, b, 2023), Gustafsson et al. (2020a,b, 2023) and here; note that the *Goniodes*-, *Goniocotes*- and *Lipeurus*-complexes have not been comprehensively revised since Clay (1938a, 1940) and von K ler (1940) and some of these taxa may not form meaningful groups. In *Goniocotes* Burmeister, 1838 (sensu Price et al. (2003)), four morphologically distinct groups are denoted by Roman numerals; due to the lack of detail in original descriptions of many species in this genus, it is not possible to assess whether these groups represent distinct genera or just well-marked species groups. In *Goniodes* Nitzsch, 1818 (sensu Price et al. (2003)), nine morphologically distinct groups are denoted by Arabic numerals; if *Goniodes* is divided as suggested by Mey (2009), these groups would represent separate genera for which no genus name has ever been published. Note that Price et al. (2003) used a more conservative classification, in which all genera were placed as synonyms of *Goniocotes*, *Goniodes*, *Lipeurus* Nitzsch, 1818 and *Oxylipaurus* Mj berg, 1910, except for *Pachyskelotes* K ler, 1940 and *Passonomedeia* Carriker, 1944. Some genera treated as synonyms of *Goniodes* by Price et al. (2003) are probably closer to *Goniocotes* (see Mey (1997)), based on the morphology of the male genitalia. Conversely, it seems likely that *Pavoniocotes* Gustafsson et al., 2023 and the groups denoted *Goniocotes* III–IV here are more closely related to the *Goniodes*-complex than to the *Goniocotes*-complex. For ease of reference, the position of these species follows Price et al. (2003); these genera are marked with an asterisk (\*) in the list. A few species of *Goniodes* cannot be identified from their available illustrations and descriptions and are here entered as “unknown”.

Host group and genus	<i>Oxylipaurus</i> -complex	<i>Goniocotes</i> -complex	<i>Goniodes</i> -complex	<i>Lipeurus</i> -complex	Other genera
<b>Megapodiidae</b>					
<i>Aepyodius</i>	<i>Oxylipaurus</i>		<i>Homocerus</i> *, <i>Weelahia</i> *	<i>Megathellipeurus</i>	<i>Megapodiella</i>
<i>Alectura</i>	<i>Oxylipaurus</i>		<i>Homocerus</i> *, <i>Weelahia</i> *	<i>Megathellipeurus</i>	
<i>Eulipoa</i>					
<i>Leipoa</i>			<i>Leipoiella</i> *, <i>Megatheliella</i> *	<i>Megathellipeurus</i>	<i>Megapodiella</i>
<i>Macrocephalon</i>		<i>Goniocotes</i> I		<i>Megathellipeurus</i>	
<i>Megapodius</i>	<i>Oxylipaurus</i> , <i>Talegallipeurus</i>		<i>Euligoniodes</i> *, <i>Lobicrotaphus</i> *, <i>Maleoicus</i> *	<i>Malaulipeurus</i>	
<i>Talegalla</i>	<i>Talegallipeurus</i>		<i>Homocerus</i> *, <i>Maleophilus</i> *	<i>Lipeuroides</i> , <i>Megathellipeurus</i>	<i>Megapodiella</i>
<b>Cracidae</b>					
<i>Aburria</i>	<i>Labicotes</i>				
<i>Chamaepetes</i>	<i>Labicotes</i> , <i>Trichodomeida</i>				
<i>Crax</i>	<i>Labicotes</i> , <i>Reticulipeurus</i> , <i>Trichodomeida</i>				
<i>Mitu</i>	<i>Reticulipeurus</i> , <i>Trichodomeida</i>				
<i>Nothocrax</i>					
<i>Oreophasis</i>	<i>Trichodomeida</i>				
<i>Ortalis</i>	<i>Reticulipeurus</i> , <i>Trichodomeida</i>				
<i>Pauxi</i>	<i>Reticulipeurus</i> , <i>Trichodomeida</i>				
<i>Penelope</i>	<i>Reticulipeurus</i> , <i>Trichodomeida</i>				
<i>Penelopina</i>	<i>Labicotes</i> , <i>Trichodomeida</i>				
<i>Pipile</i>					
<b>Numididae</b>					
<i>Acryllium</i>		<i>Goniocotes</i> II		<i>Lipeurus</i>	
<i>Agelastes</i>			<i>Stenocrotaphus</i>	<i>Lipeurus</i>	
<i>Guttera</i>		<i>Goniocotes</i> II	<i>Clayarchigoniodes</i> , <i>Stenocrotaphus</i>	<i>Afrilipeurus</i> , <i>Lipeurus</i>	
<i>Numida</i>		<i>Goniocotes</i> I, <i>Goniocotes</i> II	<i>Clayarchigoniodes</i> , <i>Stenocrotaphus</i>	<i>Lipeurus</i> , <i>Numidilipeurus</i>	
<b>Odontophoridae</b>					
<i>Callipepla</i>	<i>Epicolinus</i>		Genus 8, Unknown		<i>Colinicola</i>
<i>Colinus</i>	<i>Epicolinus</i>		<i>Solenodes</i> ?*, Genus 8	<i>Lipeurus</i>	<i>Colinicola</i> , <i>Cuclotogaster</i> <i>Colinicola</i>
<i>Cyrtonyx</i>					
<i>Dactylortyx</i>	<i>Eiconolipeurus</i> , <i>Trichodomeida</i>				
<i>Dendrortyx</i>	<i>Eiconolipeurus</i> , <i>Epicolinus</i> , <i>Trichodomeida</i>				
<i>Odontophorus</i>	<i>Eiconolipeurus</i> , <i>Trichodomeida</i>		<i>Passonomedeia</i>		
<i>Oreortyx</i>			Genus 8		<i>Colinicola</i>
<i>Philortyx</i>					<i>Colinicola</i>
<i>Ptilopachus</i>			<i>Solenodes</i> *		<i>Cuclotogaster</i>
<i>Rhynchortyx</i>			Genus 8		
<b>Phasianidae I</b>					
<i>Afropavo</i>		<i>Goniocotes</i> III, <i>Goniocotes</i> IV	<i>Archigoniodes</i>	<i>Lipeurus</i>	
<i>Alectoris</i>		<i>Goniocotes</i> I	<i>Solenodes</i> *, Genus 6		<i>Cuclotogaster</i>
<i>Ammoperdix</i>			<i>Oulocrepis</i>		<i>Cuclotogaster</i>
<i>Argusianus</i>			<i>Pachyskelotes</i> , Unknown		
<i>Bambusicola</i>			<i>Oulocrepis</i>		

Host group and genus	<i>Oxylipeurus</i> -complex	<i>Goniocotes</i> -complex	<i>Goniodes</i> -complex	<i>Lipeurus</i> -complex	Other genera
<i>Campocolinus</i>					
<i>Coturnix</i>			<i>Astrocodes</i>		<i>Cuclotogaster</i>
<i>Francolinus</i>		<i>Goniocotes I</i>		<i>Lipeurus</i>	<i>Cuclotogaster</i>
<i>Galloperdix</i>	<i>Megalipeurus</i>	<i>Goniocotes I</i>			
<i>Gallus</i>	<i>Gallancyra</i>	<i>Goniocotes I</i>	<i>Oulocrepis, Stenocrotaphus</i>	<i>Lipeurus, Numidilipeurus</i>	<i>Cuclotogaster, Lagopoecus</i>
<i>Haematortyx</i>					
<i>Margaroperdix</i>			<i>Oulocrepis</i>		<i>Cuclotogaster</i>
<i>Ophrysia</i>					
<i>Ortygornis</i>			<i>Stenocrotaphus</i>		<i>Cuclotogaster</i>
<i>Pavo</i>		<i>Goniocotes I, Pavoniocotes</i>	<i>Goniodes, Genus 1</i>	<i>Lipeurus</i>	
<i>Peliperdix</i>					<i>Cuclotogaster</i>
<i>Perdicula</i>					<i>Cuclotogaster</i>
<i>Polyplectron</i>	<i>Megalipeurus</i>			<i>Lipeurus</i>	
<i>Pternistis</i>		<i>Goniocotes I</i>	<i>Oulocrepis, Stenocrotaphus</i>	<i>Lipeurus</i>	<i>Cuclotogaster</i>
<i>Rheinardia</i>				<i>Lipeurus</i>	
<i>Scleroptila</i>		<i>Goniocotes I</i>	<i>Oulocrepis, Genus 6</i>		<i>Cuclotogaster, Lagopoecus</i>
<i>Synoicus</i>			<i>Astrocodes</i>		
<i>Tetraogallus</i>			<i>Oulocrepis</i>		<i>Cuclotogaster</i>
<i>Tropicoperdix</i>	<i>Megalipeurus</i>			<i>Lipeurus</i>	
<b>Phasianidae II</b>					
<i>Bonasa</i>			<i>Oulocrepis</i>		<i>Lagopoecus</i>
<i>Canachites</i>					
<i>Catreus</i>			<i>Oulocrepis</i>		
<i>Centrocercus</i>			<i>Oulocrepis</i>		<i>Lagopoecus</i>
<i>Chrysolophus</i>	<i>Reticulipeurus</i>		<i>Oulocrepis</i>	<i>Lipeurus</i>	
<i>Crossoptilon</i>	<i>Reticulipeurus</i>	<i>Dictyocotes</i>	<i>Genus 5</i>	<i>Lipeurus</i>	<i>Lagopoecus</i>
<i>Dendragapus</i>			<i>Oulocrepis</i>		<i>Lagopoecus</i>
<i>Falcipectus</i>					
<i>Ithaginis</i>	<i>Reticulipeurus</i>		<i>Oulocrepis</i>		<i>Lagopoecus</i>
<i>Lagopus</i>			<i>Oulocrepis</i>		<i>Lagopoecus</i>
<i>Lerwa</i>	<i>Chelopistes</i>				<i>Lerwoecus</i>
<i>Lophophorus</i>	<i>Cataphractomimus</i>	<i>Dictyocotes</i>	<i>Margaritenes, Genus 2</i>	<i>Lipeurus</i>	<i>Lagopoecus</i>
<i>Lophura</i>	<i>Reticulipeurus</i>	<i>Goniocotes I</i>	<i>Oulocrepis</i>	<i>Lipeurus</i>	<i>Cuclotogaster</i>
<i>Lyrurus</i>					<i>Lagopoecus</i>
<i>Meleagris</i>	<i>Chelopistes, Valimia</i>	<i>Goniocotes I</i>		<i>Lipeurus</i>	
<i>Perdix</i>		<i>Goniocotes I</i>	<i>Solenodes*</i>	<i>Lipeurus</i>	<i>Cuclotogaster</i>
<i>Phasianus</i>	<i>Reticulipeurus</i>	<i>Goniocotes I</i>	<i>Oulocrepis, Solenodes*</i>	<i>Lipeurus</i>	<i>Cuclotogaster, Lagopoecus</i>
<i>Pucrasia</i>	<i>Reticulipeurus</i>		<i>Oulocrepis</i>		
<i>Rhizothera</i>	<i>Reticulipeurus</i>			<i>Lipeurus</i>	
<i>Symaticus</i>	<i>Reticulipeurus</i>	<i>Goniocotes I</i>	<i>Oulocrepis</i>	<i>Lipeurus</i>	<i>Lagopoecus</i>
<i>Tetrao</i>	<i>Reticulipeurus</i>		<i>Oulocrepis</i>		<i>Lagopoecus</i>
<i>Tetraophasis</i>	<i>Sinolipeurus</i>	<i>Dictyocotes</i>	<i>Genus 4</i>		
<i>Tetrastes</i>					<i>Lagopoecus</i>
<i>Tragopan</i>	<i>Cataphractomimus, Pelecolipeurus, Sinolipeurus</i>	<i>Dictyocotes</i>	<i>Genus 3</i>		<i>Lagopoecus</i>
<i>Tympanuchus</i>			<i>Oulocrepis</i>		<i>Lagopoecus</i>
<b>Phasianidae III</b>					
<i>Arborophila</i>	<i>Megalipeurus, Reticulipeurus</i>	<i>Goniocotes I</i>	<i>Astrodes, Kelerigoniodes</i>		<i>Cuclotogaster, Galliphilopterus</i>
<i>Caloperdix</i>	<i>Megalipeurus</i>	<i>Goniocotes I</i>		<i>Lipeurus</i>	
<i>Melanoperdix</i>				<i>Lipeurus</i>	
<i>Rollulus</i>	<i>Calidolipeurus</i>		<i>Astrodes</i>	<i>Lipeurus</i>	
<i>Xenoperdix</i>					

host genus each. The perplexing distribution of the genus *Chelopistes* was discussed in detail by Mey (2006).

Notably, the genera in the tragopan group are hosts to three genera of *Oxylipeurus*-complex that are, so far, not known from hosts outside that clade (*Cataphractomimus*, *Pelecolipeurus*, *Sinolipeurus*). The distribution of lice in these genera on the hosts of this radiation is summarised in Table 3. In at least one case, lice from all three genera

are known from the same host species, echoing the radiation into three congeneric species of the genus *Valimia* on the same host species (Gustafsson and Zou 2020b). To date, there is no example of all three genera occurring on the same host individual. However, data from any galliform host are rather limited, not least because many birds in this radiation are protected. Examinations of birds in, for example, rescue centres may be necessary to establish

**Table 3.** Known distribution of *Oxylipeurus*-complex lice on *Tragopan* spp., *Tetraophasis* spp. and *Lophophorus* spp. These three host genera form a monophyletic clade with no close relatives (Meng et al. 2008; Bao et al. 2010; Liu et al. 2014; Wang et al. 2014, 2017; Kimball et al. 2021). Dashes (“---”) indicate that no species of lice in this genus has, so far, been described from this host. Records suspected to be stragglers or contaminations (see *Pelecolumeurus longus*) are not listed here.

Host species	<i>Cataphractomimus</i> Gustafsson et al., 2020a	<i>Pelecolumeurus</i> gen. nov.	<i>Sinolipeurus</i> Gustafsson et al., 2020a
<i>Lophophorus impejanus</i> (Latham, 1790)	<i>Cataphractomimus burmeisteri</i> (Taschenberg, 1882)	---	---
<i>Lophophorus lluyssii</i> Geoffroy Saint-Hilaire, 1866	<i>Cataphractomimus mirapelta</i> Gustafsson et al., 2020a	---	---
<i>Lophophorus sclateri</i> Jerdon, 1870	<i>Cataphractomimus impervius</i> Gustafsson et al., 2020a	---	---
<i>Tetraophasis obscurus</i> (Verreaux, 1869)	---	---	<i>Sinolipeurus tetraophasis</i> (Clay, 1938)
<i>Tetraophasis szechenyii</i> Madarasz, 1885	---	---	---
<i>Tragopan blythii</i> (Jerdon, 1870)	---	---	---
<i>Tragopan caboti</i> (Gould, 1857)	---	<i>Pelecolumeurus fujianensis</i> sp. nov.	---
<i>Tragopan melanocephalus</i> (Gray, 1829)	<i>Cataphractomimus himalayensis</i> (Rudow, 1869)	<i>Pelecolumeurus longus</i> (Piaget, 1880)?	---
<i>Tragopan satyrus</i> (Linnaeus, 1758)	<i>Cataphractomimus ceratormis</i> (Eichler, 1958)	<i>Pelecolumeurus longus</i> (Piaget, 1880)	---
<i>Tragopan temminckii</i> (Gray, 1830)	<i>Cataphractomimus junae</i> Gustafsson et al., 2020a	<i>Pelecolumeurus longus</i> (Piaget, 1880)?	<i>Sinolipeurus sichuanensis</i> Gustafsson et al., 2020a

whether the three *Oxylipeurus*-complex genera on hosts in the tragopan group ever co-occur on the same host individual and, if so, if they then partition the plumage amongst them.

### *Goniocotes*-complex

Lice in the *Goniocotes*-complex are conspicuously absent from both the mainly New World host radiations, Odontophoridae and Cracidae, as well as from all New World genera in the other host radiations. The sole exception is the turkey, which is sometimes parasitised by *Goniocotes gallinae* (Linnaeus, 1758), normally found on domestic chicken. *Goniocotes gallinae* never seems to be reported from wild turkey in their native range (e.g. Hightower et al. (1953); Kellogg et al. (1969); Nelder and Reeves (2005); Cruz et al. (2013); Camacho-Escobar et al. (2014)) and this host association is likely based only on domestic birds which have been in contact with domestic chicken. Based on current knowledge, the *Goniocotes*-complex would, thus, seem to be an exclusively Old World radiation.

Based on the structure of the male genitalia, lice of the *Goniodes*-complex, listed from megapodiid hosts in Table 2, are likely more closely related to *Goniocotes* than to *Goniodes*. Mey (1997) circumscribed the genera on megapodiid hosts as a distinct group, but excluded the one known *Goniocotes* species from this group. If this group is considered part of the *Goniodes*-complex (as by, for example, Price et al. (2003)), it must be considered an aberrant group within this genus. The only known *Goniocotes* species from a megapodiid host may, as Mey (1997) pointed out, be evidence either of a secondary infestation or of a relict association.

*Goniocotes sensu lato* is widely distributed across Old World landfowl (Table 2) and do not show any obvious

patterns of distribution. At least six morphologically different groups can be found within *Goniocotes*, but the relationship between these groups is unclear. Only one of these groups, *Goniocotes I*, is widely distributed across Numididae and Phasianidae I–III. The poorly-known *Goniocotes II* group is only known from numidid hosts, where it may overlap in distribution with species in *Goniocotes I*. *Goniocotes III–IV* are only known from the Congo peafowl and both groups are poorly known and may not be closely related to the rest of *Goniocotes* (see Clay (1938b)). A fifth group, only known from peafowl, was recently described as the genus *Pavoniocotes* Gustafsson et al., 2023.

The distribution patterns of the sixth group, previously called *Dictyocotes* Kéler, 1940, mirrors that of the three *Oxylipeurus*-complex genera summarised in Table 3, being found mainly on hosts in the tragopan group. However, some species of *Dictyocotes* are also known from hosts in the genus *Crossoptilon* Hodgson, 1838, another high-altitude group of birds, mainly distributed in and around China. The presence of a mesosome in the male genitalia in this group, as well as other morphological characters, suggests that *Dictyocotes* should be separated from *Goniocotes*; this will be discussed in more detail elsewhere (DRG, in prep.).

### *Goniodes*-complex

The *Goniodes*-complex is by far the most diverse of the ischnoceran louse groups known from galliform hosts and almost half (28 of 60; 46.7%) of the groups identified in Table 2 belong to this complex. Of these, at least eight currently have no genus-level name and, with the exceptions of *Pachyskelotes* Kéler, 1940 and *Passonomedea* Carriker, 1944, all were treated as members of a highly polytypic *Goniodes* by Price et al. (2003). To discuss the

distribution of morphologically distinct groups within this complex, we here follow Mey (2009) in resurrecting numerous older names within this complex and use the numbers 1–8 to denote some groups that have no available genus names. We deviate from Mey (2009) only in considering *Zlotoryzckella* Eichler [in Eichler and Vasjukova 1981], 1981, as a synonym of *Oulocrepis* Kéler, 1940. Note that, as some species in this complex have never been adequately described or illustrated, the exact limits of these proposed genera and groups is in some cases tentative. A small number of species are so poorly described that they are noted as “Unknown” genera in Table 2 and not discussed further here.

*Goniodes*-complex lice are unknown from cracid hosts and if the *Goniodes*-complex genera parasitising megapodiid hosts discussed above are moved to the *Goniocotes*-complex, no *Goniodes*-complex lice would be known from members of this host family either. Otherwise, lice in the *Goniodes*-complex occur across all major radiations of galliforms. However, only three groups within this complex could reasonably be said to be widely distributed: *Oulocrepis* Kéler, 1940, *Solenodes* Kéler, 1940 and *Stenocrotaphus* Kéler, 1940. The remaining genera and groups in this complex are known only from single host families or even single host genera (Table 2). *Stenocrotaphus* is mainly known from numidid hosts and African and South Asian francolins and spurfowl, but has, secondarily, also become established on chicken.

*Oulocrepis* is more widely distributed, occurring on many different host genera in Phasianidae I–II. Morphological variation, above all, in the male genitalia in this group is large (see, for example, Clay (1940)) and, above all, the type species (*Goniodes dissimilis* Denny, 1842) is somewhat different from all other species in the group with regards to head shape and male genitalia; however, other characters, such as female genitalia, indicate a close relationship. The genus as circumscribed here seems to be established on hosts in different geographical regions, from the Arctic to Sub-Saharan Africa and, in many cases, seems to occur on the same host species as other *Goniodes*-complex lice.

*Solenodes* is a widely distributed group, which as circumscribed here, occurs on hosts from Odontophoridae and Phasianidae I–II. Notably, most of the hosts of species in *Solenodes* are associated with drier grasslands. The male genitalia of this group are more reminiscent of those of the *Goniocotes*-complex than those of any other group of *Goniodes*-complex lice; however, as these genitalia are much reduced in complexity, it is possible that the group is artificial and, in reality, comprises several different lineages. Several species here placed in this genus are poorly described and illustrated and a revision of the group is needed to establish its limits.

The tragopan group of birds is collectively parasitised by four *Goniodes*-complex genera, of which only one presently has a proposed name: *Margaritenes* Kéler, 1940; the others are here referred to as Genera 2–4. Amongst these, only Genus 2 and Genus 3 appear to be

closely related, sharing similarities in the structure of the male antennae and a unique fusing of the pteronotum and tergopleurite II. Potentially, as these species are studied in more detail, further similarities may be found, but, at present, there seems to be nothing to indicate that all four genera are part of the same radiation within the *Goniodes*-complex.

### *Lipeurus*-complex

Lice in the *Lipeurus*-complex are the most morphologically homogeneous amongst the groups of ischnoceran lice occurring on galliforms. Lice in this complex are unknown from all New World hosts, except the turkey, which is parasitised by *Lipeurus caponis* (Linnaeus, 1758) naturally found on domestic chicken. Two genera in this complex are known from numidid hosts only (but secondarily established on domestic chicken) and three genera are unique to the Megapodiidae (Table 2). Based on the structure of the tergopleurites, female genitalia, male subgenital plate, abdominal chaetotaxy and other characters, it seems likely that *Afrilipeurus* belongs in this complex (see below); thus, three different genera occur on numidid hosts, although only two genera are known to occur on the same host genus. As with the *Goniodes*- and *Oxylipeurus*-complexes, the *Lipeurus*-complex genera known from megapodiid hosts are unique to that radiation, highlighting the distinction of the louse fauna on megapodes.

No *Lipeurus*-complex species have been described from any species of *Tetraophasis* or *Tragopan* and the only species of the genus *Lipeurus* known from *Lophophorus* spp. needs verification and may represent a contamination. As both *Lipeurus*- and *Oxylipeurus*-complex lice are of the wing louse ecomorph, it is conceivable that the multitude of *Oxylipeurus*-complex lice on hosts in the tragopan group have prevented *Lipeurus*-complex lice from establishing themselves there. However, the louse fauna of many members of the tragopan group remain poorly known and the absence of *Lipeurus*-complex species on these hosts needs verification. Moreover, the mechanisms of interspecific competition in lice are poorly known and cases are known where the same host species is parasitised by multiple louse species of the same ecomorph (e.g. head lice on common blackbird; Oslejskova et al. (2020)).

### Other ischnoceran genera

Several smaller groups of ischnoceran louse genera are also known from galliform hosts. Of these, *Megapodiella* Emerson & Price, 1972, is only known from megapodiid hosts, *Colinicola* Carriker, 1946, only from odontophorid hosts, *Lerwoecus* Mey, 2006, only from *Lerwa lerwa* (Hodgson, 1833) and *Galliphilopterus* Emerson & Elbel, 1957, only from *Arborophila brunneopectus* Blyth,

1855. It should be noted that *Colinicola* may be polytypic, based on the structure of the male genitalia and other characters, but this has no major implications for the distribution of this genus. The remaining two genera, *Cuclotogaster* Carriker, 1936 and *Lagopoecus* Waterston, 1922, are more widely distributed.

*Cuclotogaster* is known from hosts in Odontophoridae and Phasianidae I–III; however, the species from New World odontophorid hosts needs verification and may be an introduction following the European colonisation of the Americas. Otherwise, *Cuclotogaster* is absent from all New World hosts, despite being widely distributed in the Old World. Species of *Cuclotogaster* from *Arborophila* spp. are morphologically different from other species, with much narrowed male genitalia and possibly some differences in the tergopleurites and the female genitalia; these characters are poorly studied. The genus has not been thoroughly revised since Clay (1938a) and the overall variation in *Cuclotogaster* is poorly known. Notably, most known hosts are in Phasianidae I and are associated with drier, open country (e.g. savannah, grassland). Species occurring on hosts outside this radiation also often share the same kind of habitat, suggesting that host-switching between sympatric host species may have occurred.

In contrast, the genus *Lagopoecus* is mainly known from hosts in the Phasianidae II radiation, with a few species known from hosts in Phasianidae I; at least the association with domestic fowl may be due to straggling in domestic settings. Species of *Lagopoecus* occur in both the Old and New World and are often associated with more boreal or mountain- or forest-dwelling hosts, but exceptions are known (Table 2). In general, *Lagopoecus* occurs on lowland hosts in the boreal area, but seems more restricted to mountain-dwelling hosts further south and is largely absent south of the Equator.

Galliforms in the tragopan group are parasitised by lice in the genus *Lagopoecus*, but no species of *Cuclotogaster* are known from these hosts. The *Lagopoecus* species parasitising *Lophophorus* spp. are morphologically distinct, lacking the dorsal pre-antennal suture, but species known from *Tragopan* spp. are not similar to these and do not appear to be closely related. The genus *Lagopoecus* has not been comprehensively reviewed since Clay (1938a) and the patterns of variation are poorly known. Nevertheless, based on our current knowledge, there is nothing to suggest that the *Lagopoecus* species on tragopan group hosts form a unique radiation within this genus.

## Contrasting and overlapping patterns

It is clear from this brief overview that no single factor can be used to explain distribution patterns amongst the Ischnocera that parasitise galliform hosts. Overall, both host phylogeny, host biogeography and host ecology appear to influence the known host associations in the groups included in Table 2. Moreover, in some cases, it

is not clear which factors are most important, as several factors overlap.

Undoubtedly, host phylogeny is an important factor structuring host associations in louse communities on galliforms. For instance, there appears to be little overlap between the lice of megapodiid hosts and other landfowl (Table 2), likely reflecting that megapodiids are the sister group of all other galliforms (Kimball et al. 2021). Similarly, many of the groups of lice occurring on nummid hosts do not occur on other host groups naturally (but some have spread to, for example, domestic chicken in domestic settings). Numerous smaller groups are also limited to one or a few closely-related genera, especially in the *Goniodes*-complex.

There is also a distinct difference between most of the New World and Old World galliforms, with *Trichodomea* being shared by two New World host families, but absent on all Old World hosts and most *Cuclotogaster* and *Goniocotes* being absent from New World hosts despite being widely distributed across the Old World. Notably, African odontophorids are not parasitised by the same lice as New World members of this family, but by *Cuclotogaster*, which is widely distributed on other African hosts.

Contrasting with the large-scale biogeographical pattern, some patterns may have more to do with host biotope than with faunal regions. For instance, even if *Cuclotogaster* is largely limited to hosts in Phasianidae I, the genus also occurs on some members of Phasianidae II that occur in less forested areas, such as *Phasianus* Linnaeus, 1758 and *Perdix* Brisson, 1760 (Table 2). Similarly, *Oulocrepis* is found across both these radiations, often on birds that inhabit more open, grassy areas; *Solenodes* and *Stenocrotaphus* also appear to be distributed mainly on hosts in the same type of biotope and include at least some species in other host radiations.

Notably, some patterns cannot easily be explained and may be due to gaps in our knowledge or on incorrect classification of known species. It is, for instance, curious that the widely-distributed genus, *Reticulipeurus*, should occur on both Old World phasianids and New World cracids, despite all other ischnoceran lice on cracids being specific to the New World. Based on published data, there are no obvious morphological differences between the species on these host groups, although the species of cracids have not been revised in recent decades and few detailed illustrations have been published. The distribution of the genus *Megalipeurus* is also difficult to understand, but the genus is morphologically heterogeneous and a revision of the group may reveal that the current circumscription is artificial (Gustafsson et al. 2020a).

It is worth noting that elevation may influence distribution patterns. Several distinct genera and groups are known only or mainly to infest high-elevation hosts, such as *Lerwoecus* and many of the unnamed groups within the *Goniodes*-complex. In contrast, low-elevation hosts are often parasitised by more widely-distributed louse genera (e.g. *Lipeurus*, *Oulocrepis*, *Goniocotes* I).

## Lice of the tragopan group

Most relevant to the taxa described here are those found in the tragopan group, all of which are high-elevation birds within Phasianidae II (Kimball et al. 2021). With the exception of an unconfirmed *Lipeurus* species occurring on one of the species of *Lophophorus*, all of the typically low-elevation groups of Ischnocera are absent from hosts in the tragopan group. However, the diversity of lice in this group is considerable. Despite comprising only ten species in three genera, the species in this group are collectively hosts to at least three *Oxylipeurus*-complex genera (Table 3), as well as a morphologically distinct group of *Lagopoecus*, four genera within the *Goniodes*-complex and almost all the known species of *Dictyocotes*. With the exception of *Dictyocotes*, all these genera and groups are unique to hosts in the tragopan group. This pattern may also be mirrored in the Amblycera. Price and Beer (1964) considered *Colpocephalum tetraophasis* Price & Beer, 1964, “rather unique”, but did not detail in what way; *Amysrsidea impejani* Scharf [in Scharf and Price], 1983, was also described as having some distinct morphological characters, rare for the genus.

Possibly, the relevant factors structuring these host associations are a mixture of host phylogeny – all the hosts, except *Crossoptilon* are closely related – and habitat factors – all the hosts including *Crossoptilon* are high-elevation birds. The overlap in range varies between species pairs, but, in at least some cases, the hosts in these genera co-occur and may even forage together (Madge and McGowan 2002). More data are needed from all hosts in the genera *Lophophorus*, *Tetraophasis* and *Tragopan*, as well as from other high-altitude galliforms, to evaluate the louse community parasitising these hosts and their relationship to related lice on other galliforms.

Future collections may also help determine the extent to which the three genera of *Oxylipeurus*-complex lice on *T. temminckii* co-occur on the same host population. All three species are known from Sichuan Province, China, but from different collection events and areas within this Province. The co-occurrence of three congeneric species of lice in the *Oxylipeurus*-complex was recently reported from turkey (Gustafsson and Zou 2020b) and cases such as these could give insights into the process of microhabitat partitioning in chewing lice and potentially into the process of higher-level radiation of lice on hosts.

## Emended key to the *Oxylipeurus*-complex

Here, we update the genus-level key to the *Oxylipeurus*-complex previously published by Gustafsson et al. (2020b) and emended by Gustafsson and Zou (2023) after the description of the subgenus *Reticulipeurus* (*Forcipurellus*). We here remove the genus *Afrilipeurus* from this complex, based on the justification below and include the genus *Pelecolipeurus*.

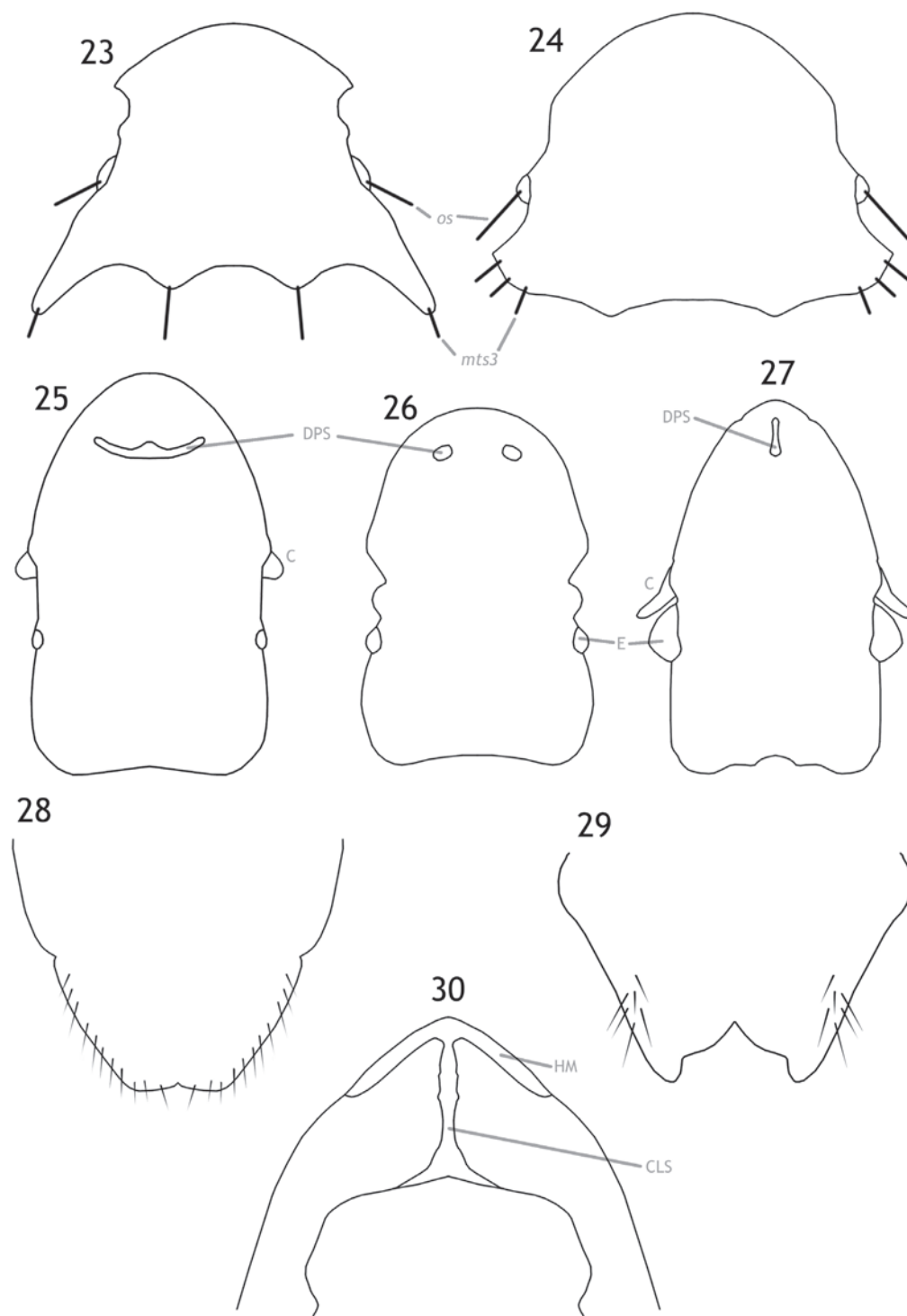
- 1 Broad-headed, with width of head similar to, or wider than, length of head; temples with elongated “horns” (Fig. 23) or with prominent lateral bulges (Fig. 24) ..... 2
- Slender-headed, with head clearly longer than wide; temples generally rounded, never with prominent bulging (Fig. 25) ..... 3
- 2 Temporal setae *mts1–2* macrosetae (Fig. 24) ..... *Trichodomedea* Carriker, 1946
- Temporal setae *mts1–2* microsetae (Fig. 23) ..... *Chelopistes* Kéler, 1939
- 3 Dorsal pre-antennal suture present (Fig. 25) ..... 4
- Dorsal pre-antennal suture absent or, if present, only visible around aperture of *ads* and not extending medianly (Fig. 26) ..... 10.
- 4 Dorsal pre-antennal suture as median, elongated oval, not expanded laterally (Fig. 27); female terminalia with marginal mesosetae distributed more or less equally around distal margin (Fig. 28); eye very large (Fig. 27) and pre-ocular nodus absent ..... *Calidolipeurus* Gustafsson et al., 2020b
- Dorsal pre-antennal suture transversal, normally reaching apertures of *ads* (Fig. 25); female terminalia with marginal setae gathered in the same area (Fig. 29); eye not very large (Fig. 26) and pre-ocular nodus present ..... 5
- 5 Clypeo-labral suture present (Fig. 30); stylus expanded distally, with small “hooks” on lateral margins (Fig. 31) ..... *Gallancyra* Gustafsson & Zou, 2020a
- Clypeo-labral suture absent; stylus differing in shape, but never with lateral “hooks” ..... 6
- 6 Dorsal pre-antennal suture with postero-lateral elongations (“epistomal suture” sensu von Kéler (1958)) extending towards preantennal nodi (Fig. 32); hyaline margin present (Fig. 32) ..... *Splendoroffula* Clay & Meinertzhagen, 1941
- Dorsal pre-antennal suture without such extensions (Fig. 25); hyaline margin absent (Fig. 25) ..... 7
- 7 Dorsal postantennal suture present (Fig. 33); male genitalia asymmetrical, with mesosome much reduced (Fig. 34) ..... *Oxylipeurus* Mjöberg, 1910
- Dorsal postantennal suture absent (Fig. 25); male genitalia symmetrical, with prominent mesosome (variable in shape) ..... 8

- 8 Coni elongated (Fig. 27); male mesosome with prominent V-... or Y-shaped thickening in distal half (Fig. 35); proximal margin of mesosome with rounded lateral lobes (Fig. 35); frons convergent to median point in most species ..... *Megalipeurus* Kéler, 1958
- Coni short (Fig. 25); male mesosome without thickening in distal half; proximal margin of mesosome variable, but never with rounded lateral lobes; frons rounded to flattened (Fig. 25)..... 9
- 9 Male abdominal segments IX+X and XI with prominent postero-lateral extensions (“claspers” sensu Carriker (1945)) (Fig. 36)..... *Eiconolipeurus* Carriker, 1945
- Male abdomen without such structures..... 12
- 10 Stylus of male subgenital plate about as long as rest of subgenital plate (Fig. 37); male genitalia much elongated, with mesosome comprising < 1/10 of total length (Fig. 38)..... *Pelegolipeurus* gen. nov
- Stylus of male subgenital plate < 1/4 of length of subgenital plate; male genitalia shorter, with mesosome comprising ~ 1/5 of total length ..... 11
- 11 Female with prominent “claspers” formed by extensions of abdominal segment XI (Fig. 39); female vulval margin deeply emarginated, with lateral sections forming rounded lobes that have subparallel median margins and median sections convex (Fig. 39); male stylus terminal (Fig. 40)..... *Reticulipeurus (Forcipurellus)* Gustafsson & Zou, 2023
- Female without such claspers (Fig. 41); female vulval margin variably concave, but either with no section of the margin forming lobes or without median section being convex (Fig. 41); male stylus subterminal (Fig. 42)..... *Reticulipeurus (Reticulipeurus)* Kéler, 1958
- 12 Frons convergent to median point (similar to Fig. 33)..... *Talegallipeurus* Mey, 1982
- Frons rounded to flattened (Figs 25, 26)..... 13
- 13 Male parameres strongly S-curved (Fig. 43); stylus arising centrally on abdominal segment IX+X (Fig. 44)..... *Sinolipeurus* Gustafsson et al., 2020
- Male parameres not S-curved (Fig. 45); stylus varying in shape, but always arising terminally or subterminally on subgenital plate (Figs 40, 42) ..... 14
- 14 Male genitalia simple, with parameres fused to basal apodeme and mesosome much reduced (Fig. 46)..... *Epicolinus* Carriker, 1945
- Male genitalia with parameres articulating with basal apodeme, and mesosome not reduced (Fig. 47) ..... 15
- 15 Lateral margins of postantennal head with secondary, ventral carina between antennal socket and site of *mts2* or *mts3* (Fig. 48); area between margin of head and secondary carina, densely reticulated, in some species, including ventral surface of eye (Fig. 48); male parameres with *pst1–2* situated close together apically (Fig. 49); female subgenital plate divided medianly and without lateral accessory vulval plates (Fig. 50)..... *Valimia* Gustafsson & Zou, 2020b
- Lateral margins of postantennal head without secondary carina and without extensive ventral reticulation; male parameres with *pst1–2* separated and only *pst2* apical (Fig. 51); female subgenital plate medianly continuous and with lateral accessory vulval plates present (Fig. 52)..... *Cataphractomimus* Gustafsson et al., 2020

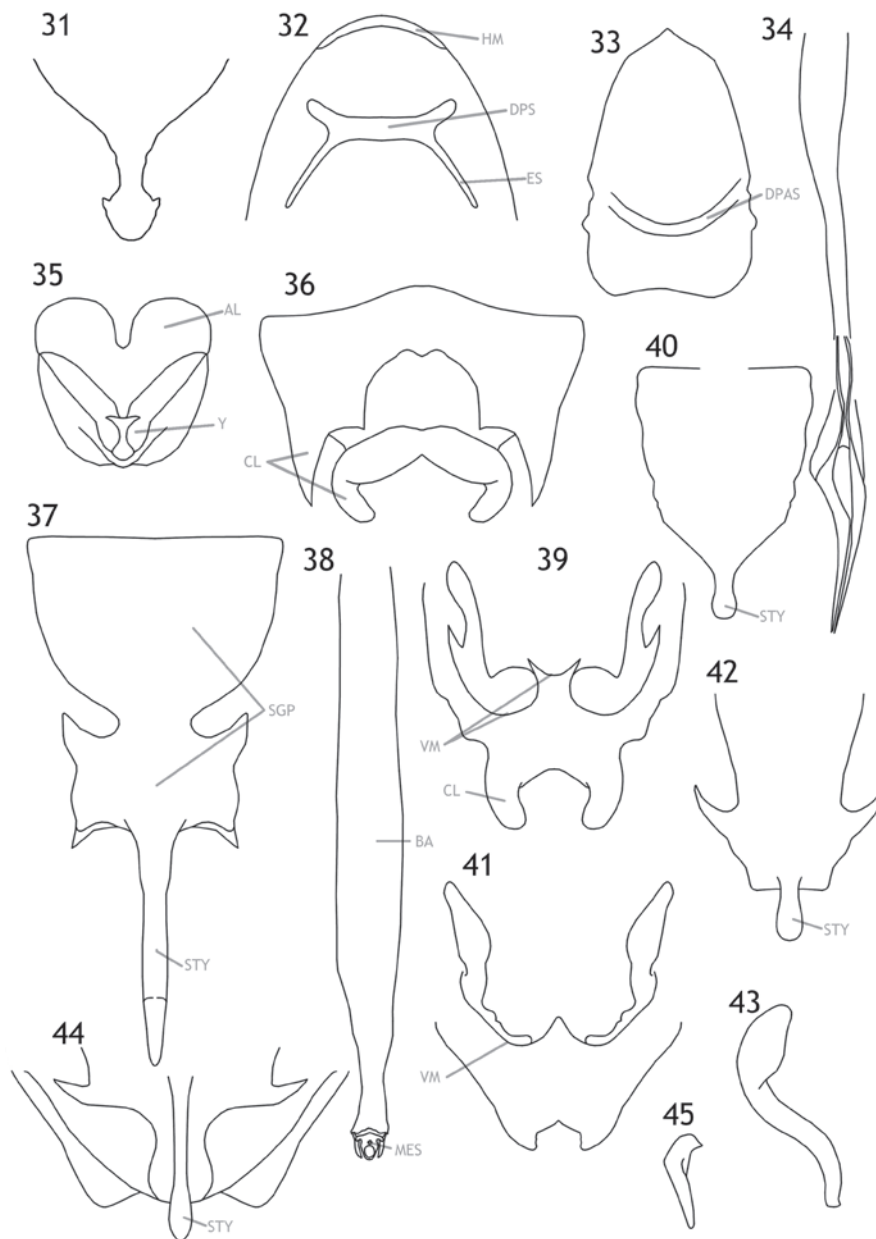
## Removal of *Afrilipeurus*

We believe it is justified to remove the genus *Afrilipeurus* from the *Oxylipeurus*-complex and, instead, place it in the *Lipeurus*-complex, where it is probably closely related to *Numidilipeurus* Tendeiro, 1955, which occurs on the same host group. This is based on the following morphological comparisons:

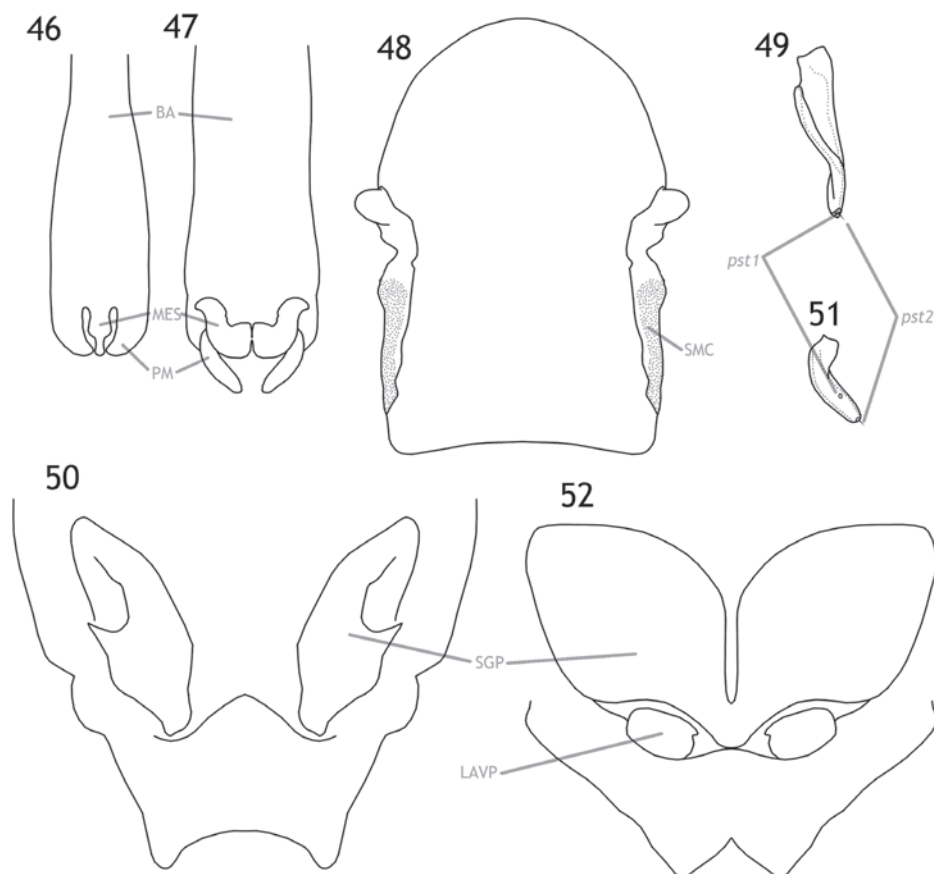
1. Amongst slender-bodied *Oxylipeurus*-complex genera, abdominal chaetotaxy consists of only *sutural setae* and *principal post-spiracular setae* dorsally and only one *sternal seta* on each side on segments II–V ventrally. In the *Lipeurus*-complex, multiple *sternal setae* per segment are the norm and, in the genus *Numidilipeurus*, both multiple *sternal setae* and *tergal posterior setae* are present on tergopleurites II–VIII. *Afrilipeurus* has multiple *sternal setae* and *tergal posterior setae* present on segments II–VIII.
2. Tergopleurites are medianly divided in all *Oxylipeurus*-complex genera except *Talegallipeurus* Mey, 1982, in which tergopleurites VII–IX+X are apparently medianly continuous; moreover, intertergal plates are absent in all *Oxylipeurus*-complex genera. In *Lipeurus* and *Numidilipeurus*, tergal plates are medianly continuous and intertergal plates are common in males, but do not occur in all species. In *Numidilipeurus*, intertergal plates are present on at least male segments III–V. *Afrilipeurus* has medianly continuous tergopleurites and intertergal plates on male segments III–IV.
3. Female genitalia lack distally convergent rows of *vulval oblique setae* in the *Oxylipeurus*-complex and this set of setae is often reduced to one or a few short setae on the posterior margin of abdominal segment VII. In *Numidilipeurus*, these setae are numerous (> 5 per side) and form roughly convergent rows on the ventral side of segments VII–IX+X, which is the same as in *Afrilipeurus*.



**Figures 23–30.** Key characters of the *Oxylipeurus*-complex. **23.** Outline of head and temporal macrosetae (cut off distally) of male *Chelopistes meleagridis* (Linnaeus, 1758), redrawn from Kéler (1939); **24.** Outline of head and temporal macrosetae (cut off distally) of female *Trichodomedea setosus* Carriker, 1946, redrawn from original description; **25.** Outline of head and dorsal preantennal suture of male *Reticulipeurus (Reticulipeurus) mesopelios* (Nitzsch [in Giebel], 1866), redrawn from Gustafsson et al. (2020a); **26.** Outline of head and dorsal preantennal suture of male *Cataphractomimus junae* Gustafsson et al., 2020, redrawn from original description; **27.** Outline of head, dorsal anterior suture and conus of *Calidolipeurus megalops* (Piaget, 1880), redrawn from Gustafsson et al. (2020b); **28.** Female terminalia of *Calidolipeurus megalops* (Piaget, 1880), redrawn from Gustafsson et al. (2020b); vulval margin, lateral macrosetae and subvulval plates not illustrated; **29.** Female terminalia of *Reticulipeurus (Reticulipeurus) mesopelios* (Nitzsch [in Giebel], 1866), redrawn from Gustafsson et al. (2020a); vulval margin, lateral macrosetae and subvulval plates not illustrated; **30.** ventral view of pre-antennal area in *Gallancyra dentata* (Sugimoto, 1934), redrawn from Gustafsson and Zou (2020a). Figures 23–26 and 29–30 reproduced from Gustafsson et al. (2020b), with kind permission of the European Journal of Taxonomy. Abbreviations used: C = conus; CLS = clypeo-labral suture; DPS = dorsal pre-antennal suture; E = eye; HM = hyaline margin; *mts3* = marginal temporal seta 3; *os* = ocular seta. Figures not to scale.



**Figures 31–45.** Key characters of the *Oxylipeurus*-complex. **31.** Outline of stylus in *Gallancyra dentata* (Sugimoto, 1934), redrawn from Gustafsson and Zou (2020a); **32.** Outline of preantennal area and dorsal pre-antennal suture of *Splendoroffula ampullacea* Kéler, 1955, redrawn from von Kéler (1958); **33.** Outline of head and dorsal post-antennal suture of *Oxylipeurus inaequalis* (Piaget, 1880), redrawn from Mey (1990); original drawing asymmetrical; **34.** Male genitalia of *Oxylipeurus inaequalis* (Piaget, 1880), redrawn from Mey (1990); some details left out for clarity; **35.** ventral view of mesosoma of *Megalipeurus sinensis* Gustafsson et al., 2020a, redrawn from original description; **36.** dorsal view of male terminalia of *Eiconolipeurus melanotis* Carriker, 1945, redrawn from original description; setae not illustrated; **37.** Male subgenital plate and stylus of *Pelecolipeurus fujianensis* sp. nov., redrawn from Fig. 7 and simplified somewhat for clarity; **38.** Male genitalia of *Pelecolipeurus fujianensis* sp. nov., redrawn from Fig. 5 and simplified somewhat for clarity; **39.** Female terminalia and vulval margin of *Reticulipeurus (Forcipurellus) formosanus* (Uchida, 1917), redrawn from Gustafsson and Zou (2023); chaetotaxy and other detail omitted for clarity; **40.** Male subgenital plate of *Reticulipeurus (Forcipurellus) formosanus* (Uchida, 1917), redrawn from Gustafsson and Zou (2023); **41.** Female terminalia and vulval margin of *Reticulipeurus (Reticulipeurus) reevesi* (Clay, 1938), redrawn from Gustafsson et al. (2020a); chaetotaxy and other detail omitted for clarity; **42.** Male subgenital plate of *Reticulipeurus (Reticulipeurus) mesopelios* (Nitzsch [in Giebel], 1866), redrawn from Gustafsson et al. (2020a); **43.** Outline of male paramere of *Sinolipeurus tetraophasis* (Clay, 1938), redrawn and simplified from Gustafsson et al. (2020a); **44.** Outline of male terminalia and stylus of *Sinolipeurus tetraophasis* (Clay, 1938), redrawn and simplified from Gustafsson et al. (2020a); **45.** Outline of male paramere of *Reticulipeurus (Reticulipeurus) ithaginis* (Clay, 1938), redrawn and simplified from Gustafsson et al. (2020a). Figures 31–36 reproduced from Gustafsson et al. (2020b), with kind permission of the European Journal of Taxonomy. Abbreviations used: AL = anterior lobes; BA = basal apodeme; CL = “claspers”; DPAS = dorsal post-antennal suture; DPS = dorsal pre-antennal suture; ES = epistomal suture; HM = hyaline margin; MES = mesosoma; SGP = subgenital plate; STY = stylus; VM = vulval margin; Y = Y-shaped thickening. Figures not to scale.



**Figures 46–52.** Key characters of the *Oxylipeurus*-complex. **46.** Distal section of male genitalia of *Epicolinus clavatus* (McGregor, 1917), redrawn from Carriker (1945); **47.** Distal section of male genitalia of *Cataphractomimus mirapelta* Gustafsson et al., 2020a, redrawn from the original description, with some simplification for clarity; **48.** Outline of male head of *Valimia polytrapezia* (Burmeister, 1838), with post-antennal ventral carina and densely reticulated area marked with grey dots; other characters omitted; **49.** Male paramere of *Valimia corpulenta* (Clay, 1938), redrawn from Gustafsson and Zou (2020b); **50.** Outline of ventral view of female terminalia of *Valimia polytrapezia* (Burmeister, 1838); **51.** Male paramere of *Cataphractomimus mirapelta* Gustafsson et al., 2020a, redrawn from the original description; **52.** Outline of ventral view of female terminalia of *Cataphractomimus impervius* Gustafsson et al., 2020a, redrawn and simplified from the original description. Figs 46, 48, 50, 52 reproduced from Gustafsson et al. (2020b), with kind permission of the European Journal of Taxonomy. Abbreviations used: BA = basal apodeme; LAVP = lateral accessory vulval plates; MES = mesosome; PM = parameres; *pst1–2* = parameral setae 1–2; SGP = subgenital plate; SMC = secondary marginal carina. Figures not to scale.

4. *Marginal temporal seta 1* is at least a mesoseta in *Afrilipeurus* and *Numidilipeurus*, but always a microseta in the *Oxylipeurus*-complex.
5. Despite considerable variation amongst genera, the male terminalia in the *Oxylipeurus*-complex are rather uniform in their basic structure, with a generally rounded ano-genital opening, anterior to which may be a transverse sclerotisation that may be continuous with the subgenital plate; several setae of varying length are situated anterior to this opening and a maximum of one seta on each side (typically none) is situated on the ventral side of the poorly-sclerotised areas postero-lateral to the ano-genital opening. Even in genera such as *Pelecolipeurus*, where the ano-genital opening is not clearly visible, its position can be judged by the distribution of setae and the anterior sclerotisation and this structure appears to be found even in the genus *Labic-*

*otes* Kéler, 1940, in which the stylus is absent. The terminalia of the *Lipeurus*-complex males are more variable, but do not include a transverse sclerotisation and the non-sclerotised areas distal to the subgenital plate may form a longitudinal groove, with multiple setae on each side; this is, for instance, the case in some *Numidilipeurus*. In *Afrilipeurus*, there is no transverse sclerotisation and there are multiple small setae on each side lateral to a longitudinal groove.

6. The female subgenital plate is never extended much distal to the row of *sternal setae* of segment VII in the *Oxylipeurus*-complex, but is extended distal to this row in *Lipeurus*-complex and in *Afrilipeurus*.

For these reasons, we here exclude *Afrilipeurus* from the *Oxylipeurus*-complex and transfer it to the *Lipeurus*-complex, where it is probably close to *Numidilipeurus*.

## Acknowledgements

Most of the Phthiraptera specimens in the collection of the National Natural History Museum of China were accumulated over the years by the late researcher Liu Sikong and these specimens provided the type specimens for comparison and additional research materials for this study, for which we express our gratitude. This research was funded by the Introduction of Full-Time High-Level Talent Fund of the Institute of Zoology, Guangdong Academy of Sciences (grant GIABR-GJRC201701), the National Natural Science Foundation of China (grants 31961123003, 32001098), the Foreign Young Talent Plan (QN20200130012) and the Pearl River Talent Recruitment Program of Guangdong Province (Grant 2019QN01N968). These agencies had no influence over the design and execution of this study. We are very grateful for the comments and suggestions made by two reviewers, which helped improve this manuscript.

## References

- Agnolin FL, Novas FE, Lio G (2006) Neornithine birds coracoid from the Upper Cretaceous of Patagonia. *Ameghiniana* 43: 245–248. [http://www.scielo.org.ar/scielo.php?pid=S0002-70142006000100019&script=sci\\_arttext](http://www.scielo.org.ar/scielo.php?pid=S0002-70142006000100019&script=sci_arttext)
- Bao X, Liu N, Qu J, Wang X, An B, Wen L, Song S (2010) The phylogenetic position and speciation dynamics of the genus *Perdix* (Phasianidae, Galliformes). *Molecular Phylogenetics and Evolution* 56(2): 840–847. <https://doi.org/10.1016/j.ympev.2010.03.038>
- Blyth E (1855) Report of curator, Zoological Department, for April meeting, 1855. *Journal of the Asiatic Society of Bengal* 24(3): 252–281. <https://www.biodiversitylibrary.org/bibliography/51678>
- Burmeister H (1838) Mallophaga Nitzsch. In: *Handbuch der Entomologie. Zweiter Band. Besondere Entomologie. Zweite Abteilung. Lauskerfe. Gymnognatha. (Zweiter Hälfte; vulgo Neuroptera). Theod. Chr. Fried. Enslin, Berlin* 2(1): 418–443. <https://phthiraptera.myspecies.info/content/mallophaga-nitzsch>
- Camacho-Escobar MA, Arroyo-Ledezma J, Ávila-Serrano NY, Jeréz-Salas MP, Sánchez-Bernal EI, García-López JC (2014) Ectoparasites and their damage in backyard turkeys in Oaxaca's coast, Mexico. *European Journal of Veterinary Medicine* 7: 1–18. <https://phthiraptera.myspecies.info/node/94847>
- Carriker Jr MA (1936) Studies in Neotropical Mallophaga, Part I.—Lice of the tinamous. *Proceedings. Academy of Natural Sciences of Philadelphia* 88: 45–218. <https://phthiraptera.myspecies.info/content/studies-neotropical-mallophaga-part-i-lice-tinamous>
- Carriker Jr MA (1944) Studies in Neotropical Mallophaga – No. IV. New genera and species. *Boletín de Entomología Venezolana* 3: 65–104. [+ 6 pls] <https://phthiraptera.myspecies.info/content/studies-neotropical-mallophaga-iv-new-genera-and-species>
- Carriker Jr MA (1945) Studies in Neotropical Mallophaga (V). The lipeuroid forms of the New World “Galliformes”. Part 2. *Revista Brasileira de Biologia* 5: 91–112. <https://phthiraptera.myspecies.info/content/studies-neotropical-mallophaga-v-lipeuroid-forms-new-world-galliformes-part-2>
- Carriker Jr MA (1946) [1945] Studies in Neotropical Mallophaga (VII). *Goniodes* and allied genera from gallinaceous hosts. *Revista de la Academia Colombiana de Ciencias Exactas, Físicas y Naturales* 6: 355–399. <https://phthiraptera.myspecies.info/content/studies-neotropical-mallophaga-vii-goniodes-and-allied-genera-gallinaceous-hosts>
- Carriker Jr MA (1967) Posthumous papers of Melbourne A. Carriker, Jr. V. New species of *Colinicola*, *Passonomedeia*, *Eiconolipeurus*, and *Oxylipeurus* (Mallophaga: Philopteridae) from Neotropical gallinaceous hosts. *Bulletin - United States National Museum* 248: 46–55. <https://phthiraptera.myspecies.info/content/posthumous-papers-melbourne-carriker-jr-v-new-species-colinicola-passonomedeia-eiconolipeurus>
- Clarke JA (2004) Morphology, phylogenetic taxonomy, and systematics of *Ichthyornis* and *Apatornis* (Avialae: Ornithurae). *Bulletin of the American Museum of Natural History* 286: 1–179. [https://doi.org/10.1206/0003-0090\(2004\)286<0001:MPTASO>2.0.CO;2](https://doi.org/10.1206/0003-0090(2004)286<0001:MPTASO>2.0.CO;2)
- Clay T (1938a) Revision of the genera and species of Mallophaga occurring on gallinaceous hosts. – Part I. *Lipeurus* and related genera. *Proceedings of the Zoological Society of London, Series B* 108: 109–204. [14 pls] <https://phthiraptera.myspecies.info/content/revision-genera-and-species-mallophaga-occurring-gallinaceous-hosts-part-i-lipeurus-and-rela>
- Clay T (1938b) New species of Mallophaga from *Afropavo congensis* Chapin. *American Museum Novitates* 1008: 1–11. <https://phthiraptera.myspecies.info/content/new-species-mallophaga-afropavo-congensis-chapin>
- Clay T (1940) Genera and species of Mallophaga on gallinaceous hosts. – Part II. *Goniodes*. *Proceedings of the Zoological Society of London* 1940(1–2): 1–120. <https://phthiraptera.myspecies.info/content/genera-and-species-mallophaga-occurring-gallinaceous-hosts-part-ii-goniodes>
- Clay T (1941) A new genus and species of Mallophaga. *Parasitology* 33(1): 119–129. <https://doi.org/10.1017/S0031182000024318>
- Clay T (1951) An introduction to a classification of the avian Ischnocera (Mallophaga): Part I. *Transactions of the Royal Entomological Society of London* 102: 171–194. [+1 pl] <https://doi.org/10.1111/j.1365-2311.1951.tb00746.x>
- Clay T, Meinertzhagen R (1941) Mallophaga miscellany. — No. 2. *Annals and Magazine of Natural History (Series 11)* 7: 329–346. <https://phthiraptera.myspecies.info/content/mallophaga-miscellany-no-2>
- Clements JF, Schulenberg TS, Iliff MJ, Roberson D, Fredericks TA, Sullivan BL, Wood CL (2022) The eBird / Clements checklist of birds of the world: v2021. <http://www.birds.cornell.edu/clementschecklist/download/> [accessed 3 March 2022]
- Cruz MI, Figueroa CJA, Quintero MMT, Alcalá CY (2013) Ectoparasitos de aves en explotaciones de traspatio (*Gallus gallus domesticus*, y *Meleagris gallopavo*) de una region del sur de México. *Revista Ibero-Latinamericana de Parasitología* 72: 185–189. <https://phthiraptera.myspecies.info/node/94851>
- Cuvier G (1829) Le règne animal distribué d’après son organisation, pour servir de base à l’histoire naturelle des animaux et d’introduction à l’anatomie compare. Tome 1. Déterville, Paris, France, [xxxviii+] 584 pp. <https://doi.org/10.5962/bhl.title.1964>
- Denny H (1842) *Monographia anoplurorum Britanniae*. Henry G. Bohn, London, United Kingdom, [xxvi+] 262 pp. <https://phthiraptera.myspecies.info/content/monographia-anoplurorum-britanniae-or-essay-british-species-parasitic-insects>
- Eichler W (1958) *Notulae Mallophagologicae*. XX. Neue Federlingsformen in meiner Federlingsbearbeitung der “Neuen Brehm-Bücherei”.

- Naturwissenschaftliches Museum Nachrichten, Aschaffenburg, Deutschland 58: 59–64. <https://phthiraptera.myspecies.info/content/notulae-mallophagologicae-xx-neue-federlingsformen-meiner-federlingsbearbeitung-der-neuen-br>
- Eichler W, Vasjukova TT (1981) Mallophagen von *Tetrao parvirostris* (Phthiraptera, Mallophaga). Deutsche Entomologische Zeitschrift, Neue Folge 4/5: 231–237. <https://phthiraptera.myspecies.info/content/mallophaga-tetrao-parvirostris-phthiraptera-mallophaga>
- Elliot DG (1871) A monograph of the Phasianidae or family of the pheasants. Vol. 1. Published by the author, New York, United States. [unpaginated] <https://digitalcollections.nypl.org/collections/a-monograph-of-the-phasianidae-or-family-of-the-pheasants/#/?tab=about>
- Emerson KC, Elbel RE (1957) New species and records of Mallophaga from gallinaceous birds of Thailand. Proceedings of the Entomological Society of Washington 59: 232–243. <https://phthiraptera.myspecies.info/content/new-species-and-records-mallophaga-gallinaceous-birds-thailand>
- Emerson KC, Price RD (1972) A new genus and species of Mallophaga from a New Guinea bush fowl. Pacific Insects 14: 77–81. <https://phthiraptera.myspecies.info/content/new-genus-and-species-mallophaga-new-guinea-bush-fowl>
- Felsö B, Rózsa L (2006) Reduced taxonomic richness of lice (Insecta: Phthiraptera) in diving birds. The Journal of Parasitology 92(4): 867–869. <https://doi.org/10.1645/GE-849.1>
- Gould J (1857) *Ceriornis caboti*. Proceedings of the Zoological Society of London 25: 161–162. <https://www.biodiversitylibrary.org/bibliography/44963>
- Gray JE (1829) The animal kingdom: arranged in conformity with its organization. Volume the third. G.B. Whittaker, London, United Kingdom, 690 pp. [+ 24 pls] <https://www.biodiversitylibrary.org/bibliography/45021>
- Gray JE (1831) Illustrations of Indian zoology; chiefly selected from the collection of Major-General Hardwicke. Vol. 1. Treuttel, Wurtz, Treuttel, Jun. & Richter, London, United Kingdom. [unpaginated] <https://doi.org/10.5962/bhl.title.95127>
- Gustafsson DR, Bush SE (2017) Morphological revision of the hyperdiverse *Brueelia*-complex (Insecta: Phthiraptera: Ischnocera: Philopteridae) with new taxa, checklists and generic key. Zootaxa 4313(1): 1–443. <https://doi.org/10.11646/zootaxa.4313.1.1>
- Gustafsson DR, Zou F (2020a) *Gallancyra* gen. nov. (Phthiraptera: Ischnocera), with an overview of the geographical distribution of chewing lice parasitizing chicken. European Journal of Taxonomy 685(685): 1–36. <https://doi.org/10.5852/ejt.2020.685>
- Gustafsson DR, Zou F (2020b) Descriptions of three congeneric species of chewing lice of the *Oxylipeurus*-complex (Insecta: Phthiraptera: Philopteridae) from the turkey, *Meleagris gallopavo*, including a new genus and a new species. Zootaxa 4801(3): 488–512. <https://doi.org/10.11646/zootaxa.4801.3.4>
- Gustafsson DR, Zou F (2023) Species of *Reticulipeurus* Kéler, 1958 (Phthiraptera, Ischnocera, *Oxylipeurus*-complex) parasitic on species of *Arborophila*, with description of a new subgenus and three new species. Zootaxa 5284(3): 496–520. <https://doi.org/10.11646/zootaxa.5284.3.3>
- Gustafsson DR, Lei L, Chu X, Zou F (2020a) Review of Chinese species of the *Oxylipeurus*-complex (Phthiraptera: Philopteridae), with description of two new genera and five new species. Zootaxa 4742(2): 201–255. <https://doi.org/10.11646/zootaxa.4742.2.1>
- Gustafsson DR, Lei L, Zou F (2020b) *Calidolipeurus*, new genus for *Lipeurus megalops* Piaget, 1880 (Phthiraptera: Ischnocera: *Oxylipeurus*-complex), with a redescription of the type species and a preliminary key to the *Oxylipeurus*-complex. European Journal of Taxonomy 686(686): 1–15. <https://doi.org/10.5852/ejt.2020.686>
- Gustafsson DR, Tian C, Zou F (2021) New species of ischnoceran chewing lice (Phthiraptera: Philopteridae) from Chinese birds. Zootaxa 4990(2): 305–328. <https://doi.org/10.11646/zootaxa.4990.2.6>
- Gustafsson DR, Grossi AA, Ren M, Zou F (2023) The Gonioididae (Phthiraptera: Ischnocera) of peafowl (Aves: Galliformes: *Pavo*), with description of a new genus. Journal of Natural History 57(17–20): 996–1048. <https://doi.org/10.1080/00222933.2023.2226375>
- Haeckel E (1896) Systematische Phylogenie. 2. Theil. Systematische Phylogenie der wirbellosen Thiere (Invertebrata). Verlag von Georg Reimer, Berlin, 720 pp. <https://doi.org/10.1515/9783111443935>
- Hightower BG, Lehman VW, Eads RB (1953) Ectoparasites from mammals and birds on a quail preserve. Journal of Mammalogy 54(2): 268–271. <https://doi.org/10.1093/jmammal/34.2.268>
- Hodgson BH (1833) A description of *Perdix lerwa*. Proceedings of the Zoological Society of London 1: 107. <https://www.biodiversitylibrary.org/bibliography/44963>
- Hodgson BH (1838) On a new species of pheasant from Tibet. Journal of the Asiatic Society of Bengal 7(2): 863–865. <https://www.biodiversitylibrary.org/bibliography/51678>
- Hopkins GHE, Clay T (1952) A check list of the genera and species of Mallophaga. British Museum (Natural History), London, United Kingdom, 362 pp. <https://doi.org/10.5962/bhl.title.118844>
- Johnson KP, Weckstein JD, Meyer MJ, Clayton DH (2011) There and back again: switching between host orders by avian body lice (Ischnocera: Gonioididae). Biological Journal of the Linnean Society. Linnean Society of London 102(3): 614–625. <https://doi.org/10.1111/j.1095-8312.2010.01612.x>
- Kellogg VL (1896) New Mallophaga, I,— with special reference to a collection made from maritime birds of the Bay of Monterey, California. Proceedings of the California Academy of Sciences (2<sup>nd</sup> series) 6: 31–168. [14 pls] <https://phthiraptera.myspecies.info/content/new-mallophaga-i-special-reference-collection-made-maritime-birds-bay-monterey-california>
- Kellogg FE, Prestwood AK, Gerrish RR, Doster GL (1969) Wild turkey ectoparasites collected in the southeastern United States. Journal of Medical Entomology 6(3): 329–330. <https://doi.org/10.1093/jmedent/6.3.329>
- Kimball RT, Hosner PA, Braun EL (2021) A phylogenomic supermatrix of Galliformes (Landfowl) reveals biased branch lengths. Molecular Phylogenetics and Evolution 158: 107091. [10 pp.] <https://doi.org/10.1016/j.ympev.2021.107091>
- Liu F, Ma L, Yang C, Tu F, Xu Y, Ran J, Yue B, Zhang X (2014) Taxonomic status of *Tetraophasis obscurus* and *Tetraophasis szechenyii* (Aves: Galliformes: Phasianidae) based on the complete mitochondrial genome. Zoological Science 31(3): 160–167. <https://doi.org/10.2108/zsj.31.160>
- Madge S, McGowan P (2002) Pheasants, partridges & grouse. Including buttonquail, sandgrouse and allies. Christopher Helm, London, United Kingdom, 488 pp.
- Meng Y, Dai B, Ran J, Li J, Yue B (2008) Phylogenetic position of the genus *Tetraophasis* (Aves, Galliformes, Phasianidae) as inferred from mitochondrial and nuclear sequences. Biochemical Systematics and Ecology 36(8): 626–637. <https://doi.org/10.1016/j.bse.2008.01.007>
- Mey E (1982) Zur Taxonomie und Biologie der Mallophagen von *Tallegalla jobiensis longicaudus* A.B. Meyer, 1891 (Aves, Megapodiidae). Reichenbachia, Staatliches Museum für Tierkunde in Dresden

- 20(29): 223–246. <https://phthiraptera.myspecies.info/content/zur-taxonomie-und-biologie-der-mallophagen-von-talegalla-jobien-sis-longicaudus-b-meyer-1891->
- Mey E (1990) Zur Taxonomie der auf Großfußhühnern (Megapodiidae) schmarotzenden *Oxylipeurus*-Arten (Insecta, Phthiraptera, Ischnocera: Lipeuridae). Zoologische Abhandlungen Staatliches Museum für Tierkunde Dresden 46: 103–116. <https://phthiraptera.myspecies.info/content/zur-taxonomie-der-auf-gro%C3%9Ffu%C3%9Fh%C3%BChner-megapodiidae-schmarotzenden-oxylipeurus-arten-insecta-ph>
- Mey E (1994) Beziehungen zwischen Larvenmorphologie und Systematik der Adulti bei den Vogel-Ischnozeren (Insecta, Phthiraptera, Ischnocera). Mitteilungen aus dem Zoologischen Museum in Berlin 70(1): 3–84. <https://doi.org/10.1002/mmnz.19940700102>
- Mey E (1997) Die Gonioididen (Insecta, Phthiraptera, Ischnocera) der Großfußhühner (Megapodiidae). Rudolstädter Naturhistorische Schriften 8: 19–44. <https://phthiraptera.myspecies.info/content/die-gonioididen-insecta-phthiraptera-ischnocera-der-gro%C3%9Ffu%C3%9Fh%C3%BChner-megapodiida>
- Mey E (2004) Zur Taxonomie, Verbreitung und parasitophyletischer Evidenz des *Philoaterus*-Komplexes (Insecta, Phthiraptera, Ischnocera). Ornithologischer Anzeiger 43: 149–203. <https://phthiraptera.myspecies.info/content/zur-taxonomie-verbreitung-und-parasitophyletischer-evidenz-des-philoaterus-komplexes-insecta>
- Mey E (2006) Rätselhaftes Vorkommen zweier Federklingsarten (Insecta, Phthiraptera, Ischnocera) auf dem Haldenhuhn *Lerwa lerwa* (Galliformes, Phasianidae)? In: Hartmann M, Weipert J (Eds) Biodiversität und Naturlandschaft in Himalaya II. Erfurt, Germany, 534 pp. <https://phthiraptera.myspecies.info/content/puzzling-occurrence-two-chewing-lice-species-insecta-phthiraptera-ischnocera-snow-partridge>
- Mey E (2009) Die Mallophagen (Insecta, Phthiraptera: Amblycera & Ischnocera) der Galloanseres (Aves) – ein Überblick. Beiträge zur Jagd- und Wildforschung 34: 151–187. <https://phthiraptera.myspecies.info/node/68807>
- Mey E (2010) *Afrilipeurus novum* genus pro *Oxylipeurus vincenti* v. Kéler (Insecta, Phthiraptera, Ischnocera, Philopteridae s.l.) vom Kräuselhauben-Perlhuhn *Guttera pucherani* (Hartlaub). Rudolstädter Naturhistorische Schriften 16: 99–110.
- Mey E (2013) Chewing lice (Insecta, Phthiraptera) off Bruijn's brush-turkey *Aepyodius bruijnii* from New Guinea (Aves, Galliformes, Megapodiidae). Contributions to Entomology 62: 313–323. <https://doi.org/10.21248/contrib.entomol.63.2.313-323>
- Mjöberg E (1910) Studien über Mallophagen und Anopluren. Arkiv för Zoologi 6(13): 1–296. [5 pls] <https://doi.org/10.5962/bhl.part.26907>
- Nelder MP, Reeves WK (2005) Ectoparasites of road-killed vertebrates in northwestern South Carolina, USA. Veterinary Parasitology 129(3–4): 313–322. <https://doi.org/10.1016/j.vetpar.2004.02.029>
- Nitzsch CL (1818) Die Familien und Gattungen der Thierinsekten (insecta epizoica); als Prodromus einer Naturgeschichte derselben. Magazin der Entomologie 3: 261–316. <https://phthiraptera.myspecies.info/content/die-familien-und-gattungen-der-thierinsekten-insecta-epizoica-als-prodromus-einer-naturgesch>
- Oslejskova L, Kounkova S, Gustafsson DR, Resendes R, Rodrigues P, Literak I, Sychra O (2020) Insect ectoparasites from wild passerine birds in the Azores Islands. Parasite 27: 64. [6 pp.] <https://doi.org/10.1051/parasite/2020063>
- Piaget E (1880) Les Pédiculines. Essai monographique. E.J. Brill, Leiden, the Netherlands, [xxxix +] 714 pp. <https://phthiraptera.myspecies.info/content/les-p%C3%A9diculines-essai-monographique>
- Price RD, Beer JR (1964) Species of *Colpocephalum* (Mallophaga: Menoponidae) parasitic upon the Galliformes. Annals of the Entomological Society of America 57(4): 391–402. <https://doi.org/10.1093/aesa/57.4.391>
- Price RD, Hellenenthal RA, Palma RL, Johnson KP, Clayton DH (2003) The Chewing lice: world checklist and biological overview. Illinois Natural History Survey Special Publication 24, [x +] 501 pp. <https://phthiraptera.myspecies.info/content/chewing-lice-world-checklist-and-biological-overview-0>
- Rudow F (1869) Beitrag zur Kenntniss der Mallophagen oder Pelzfresser. Neue exotische Arten der Familie *Philoaterus*. Inaugural-Dissertation zur Erlangen der Doctorwürde bei der philosophischen Facultät der Universität zur Leipzig. Wilhelm Plötz, Halle, Germany, 47 pp. <https://phthiraptera.myspecies.info/content/beitrag-zur-kenntniss-der-mallophagen-oder-pelzfresser-neue-exotische-arten-der-familie-phil>
- Scharf WC, Price RD (1983) Review of the *Amysrsidea* in the subgenus *Argimenopon* (Mallophaga: Menoponidae). Annals of the Entomological Society of America 76(3): 441–451. <https://doi.org/10.1093/aesa/76.3.441>
- Taschenberg O (1882) Die Mallophagen mit besonderer Berücksichtigung der von Dr. Meyer gesammelten Arten. Nova Acta Academiae Caesareae Leopoldino-Carolinae Germanicae Naturae Cursorium 64: 1–231. [+ 7 pls] <https://doi.org/10.5962/bhl.title.82513>
- Temminck CJ (1813) Histoire naturelle generale des pigeons et des gallinaces. Tome 2. J.C. Sepp & fils, Amsterdam, Netherlands, 477 pp. [+ 3 pls] <https://doi.org/10.5962/bhl.title.64844>
- von Kéler S (1940) [1939] Baustoff zu einer Monographie der Mallophagen. II. Teil: Überfamilie der Nirmoidea (1) Die Familien Trichophlopteridae, Gonioididae, Heptapsogastridae. Nova Acta Leopoldiana (Neue Folge) 8: 1–254. [+ 4 pls] <https://phthiraptera.myspecies.info/content/baustoffe-zu-einer-monographie-der-mallophagen-i-teil-%C3%BCberfamilie-trichodectoidea>
- von Kéler S (1958) The genera *Oxylipeurus* Mjöberg and *Splendoroffula* Clay and Meinertzhagen (Mallophaga). Deutsche Entomologische Zeitschrift, Neue Folge 5: 300–347. <https://phthiraptera.myspecies.info/content/genera-oxylipeurus-mj%C3%B6berg-and-splendoroffula-clay-and-meinertzhagen-mallophaga>
- von Linnaeus C (1758) Systema naturae per Regna Tria Naturae, Secundum Classes, Ordines, Genera, Species, cum Characteribus, Differentiis, Synonymis, Locis. 10<sup>th</sup> edn. Salvius, Stockholm, Sweden. [iv+] 824 pp. <https://linnean-online.org/119965/>
- Wang N, Kimball RT, Braun EL, Liang B, Zhang Z (2014) Assessing phylogenetic relationships among Galliformes: a multigene phylogeny with expanded taxon sampling in Phasianidae. PLoS ONE 8(5): e64312. <https://doi.org/10.1371/journal.pone.0064312>
- Wang N, Hosner PA, Liang B, Braun EL, Kimball RT (2017) Historical relationships of three enigmatic phasianid genera (Aves: Galliformes) inferred using phylogenomic and mitogenomic data. Molecular Phylogenetics and Evolution 109: 217–225. <https://doi.org/10.1016/j.ympev.2017.01.006>
- Waterston J (1922) A new genus of Ischnocera (Mallophaga). Entomologist's Monthly Magazine 3: 159. <https://phthiraptera.myspecies.info/content/new-genus-ischnocera-mallophaga-1>
- Zlotorzycza J (1966) Systematische Bemerkungen über der Gattung *Reticulipeurus* Kéler mit Beschreibung von *R. tetraonis minor* ssp. n. (Mallophaga, Lipeuridae). Polskie Pismo Entomologiczne 36: 111–115. <https://phthiraptera.myspecies.info/content/systematische-bemerkungen-%C3%BCber-die-gattung-reticulipeurus-k%C3%A9ler-mit-beschreibung-von-r-tetra>



# *Et latet et lucet*: Discoveries from the Phyletisches Museum amber and copal collection in Jena, Germany

Brendon E. Boudinot<sup>1,2,3</sup>, Bernhard L. Bock<sup>1</sup>, Michael Weingardt<sup>1</sup>, Daniel Tröger<sup>1</sup>, Jan Batelka<sup>4</sup>, Di Li<sup>1,5</sup>, Adrian Richter<sup>1,6</sup>, Hans Pohl<sup>1</sup>, Olivia T. D. Moosdorf<sup>1,2</sup>, Kenny Jandausch<sup>1,7</sup>, Jörg U. Hammel<sup>8</sup>, Rolf G. Beutel<sup>1</sup>

1 Friedrich-Schiller-Universität Jena, Institut für Zoologie und Evolutionsforschung, Erbertstraße 1, 07743 Jena, Germany

2 National Museum of Natural History, Smithsonian Institution, 10th & Constitution Ave. NW, Washington, DC, USA

3 Senckenberg Naturmuseum Frankfurt, Senckenberganlage 25, 60325 Frankfurt, Germany

4 Department of Zoology, Faculty of Science, Charles University, Viničná 7, 128 43 Praha 2, Czech Republic

5 Department of Entomology, China Agricultural University, 100193 Beijing, China

6 Okinawa Institute of Science and Technology Graduate University, 1919-1 Tancha, Onna son, 904-0495, Japan

7 Institute for Anatomie I, Jena University Hospital, Teichgraben 7, 07743 Jena, Germany

8 Institute of Materials Physics, Helmholtz-Zentrum Hereon, Max-Planck-Straße 1, 21502 Geesthacht, Germany

<https://zoobank.org/050A157B-D712-4094-B4FA-E605151001EA>

Corresponding authors: Brendon E. Boudinot ([boudinotb@gmail.com](mailto:boudinotb@gmail.com), [brendon.boudinot@senckenberg.de](mailto:brendon.boudinot@senckenberg.de));

Bernhard L. Bock ([bernhard-leopold.boock@uni-jena.de](mailto:bernhard-leopold.boock@uni-jena.de)); Michael Weingardt ([michael.weingardt@uni-jena.de](mailto:michael.weingardt@uni-jena.de))

Academic editor: Sonja Wedmann ♦ Received 8 September 2023 ♦ Accepted 8 January 2024 ♦ Published 19 April 2024

## Abstract

As the only direct records of the history of evolution, it is critical to determine the geological source of biota-bearing fossils. Through the application of synchrotron-radiation micro-computed tomography (SR- $\mu$ -CT), Fourier-transformed infrared-spectroscopy (FT-IR), visual evaluation of ultraviolet fluorescence (UV-VS), radiocarbon dating (<sup>14</sup>C quantification), and historical sleuthing, we were able to identify and sort 161 (83 Baltic amber, 71 Copal and 7 Kauri gum pieces) individually numbered and largely mislabeled pieces of East African Defaunation resin (~145 years old) and copal (~390 years old), as well as Baltic amber (~35 million years old) from the Phyletisches Museum collection. Based on this collection, we define two new species: †*Amphientomum knorrei* Weingardt, Bock & Boudinot, **sp. nov.** (Psocodea: Amphientomidae, copal) and †*Baltistena nigrispinata* Batelka, Tröger & Bock, **sp. nov.** (Coleoptera: Mordellidae, Baltic amber). For selected taxa, we provide systematic reviews of the fossil record, including: Amphientomidae, for which we provide a key to all species of *Amphientomum*, extant and extinct, and recognize the junior synonymy of *Am. ectostriolatum* Li, 2002 (an unjustified emendation) under *Am. ectostriolate* Li, 1999 (**syn. nov.**); the fossil ant genus †*Yantaromyrmex* and the clades Dorylinae, Plagirolepidini, *Camponotus*, *Crematogaster*, and *Pheidole* (Formicidae); the Nevrothidae (Neuroptera); and *Doliopygus* (Coleoptera: Curculionidae: Platypodinae). We synonymize *Palaeoseopsis* Enderlein, 1925 with *Amphientomum* Pictet, 1854, **syn. nov.** and transfer one species from *Amphientomum*, forming *Lithoseopsis indentatum* (Turner, 1975), **comb. nov.** To prevent the uncritical usage of unidentifiable fossils attributed to *Camponotus* for macroevolutionary analysis, we transfer 29 species to the form genus †*Camponotites* Steinbach, 1967, which we consider to be most useful as *incertae sedis* in the Formicinae. We treat †*Ctt. ullrichi* (Bachmayer, 1960), **comb. nov.** as unidentifiable hence invalid **stat. nov.** We also transfer †*Ca. mengei* Mayr, 1868 and its junior synonym †*Ca. igneus* Mayr, 1868 to a new genus, †*Eocamponotus* Boudinot, **gen. nov.**, which is *incertae sedis* in the Camponotini. Concluding our revision of *Camponotus* fossils, we transfer †*Ca. palaeopterus* (Zhang, 1989) to *Liometopum* (Dolichoderinae), resulting in †*L. palaeopterus* **comb. nov.** and the junior synonymy of †*Shanwangella* Zhang, 1989, **syn. nov.** under *Liometopum* Mayr, 1861. Because the type specimens of the genera †*Palaeosminthurus* Pierce & Gibron, 1962, **stat. rev.** and †*Pseudocamponotus* Carpenter, 1930 are unidentifiable due to poor preservation, we consider these taxa unidentifiable hence invalid **stat. nov.** To avoid unsupported use of the available fossils names attributed to *Crematogaster* for divergence dating calibration points, we transfer three species to a new collective taxon that is *incertae sedis* in Myrmicinae, †*Incertogaster* Boudinot, **gen. nov.**, forming †*In. aurora* (LaPolla & Greenwalt, 2015), †*In. praecursor* (Emery, 1891), **comb. nov.**, and †*In. primitiva* (Radchenko & Dlussky, 2019), **comb. nov.** Finally, we transfer †*Ph. cordata* (Holl, 1829) back to *Pheidole*, and designate a neotype from our copal collection based on all available evidence. All new species plus the neotype of †*Ph. cordata* are depicted with 3D cybertypes from our  $\mu$ -CT scan data. We introduce the convention of a

double dagger symbol (‡) to indicate fossils in copal or Defaunation resin, as these may yet be extant. To further contextualize our results, we provide a discussion of amber history and classification, as well as the Kleinkuhren locality, to which multiple specimens were attributed. We conclude with conspecti on key biological problems and increasing potential of  $\mu$ -CT for phylogenetic paleontology.

## Key Words

ants, barklice, best practices, digitization, lacewings, micro-computed tomography ( $\mu$ -CT), morphology, museomics, phenomics, taxonomy

## 1. Introduction

“*Et latet et lucet Phaethontide condita gutta, ut videatur apis nectare clusa suo.*”  
 “Caught in a[n] [amber tear] drop of Phaethontide a bee is hidden and shines, so that it may be seen that she is buried in her own nectar.”

– (Mart. 4.32), Marcus Valerius Martialis  
 (between 38 and 41 AD – 102 and 104 AD)

The Phyletisches Museum in Jena, Germany, was founded by the famous and notorious zoologist Ernst Haeckel, who laid the foundation stone in 1907 and donated the museum to the University of Jena in 1908. Today, the collection of the *Jugendstil* or Art Nouveau building contains about 750,000 specimens, of which insects represent approximately two thirds, while the remainder is divided among the other animal classes and phyla, with vertebrates forming a large and valuable proportion. Since its founding, the museum has accumulated material from notable scientific figures, including Haeckel’s successor Ludwig Plate (1862–1937), Richard Semon (1859–1918), Wilhelm Kükenthal (1861–1922), Jürgen Harms (1885–1956), Otto Wohlbered (1870–1945), and Dietrich Starck (1908–2001), among others (see Uschmann 1959; von Knorre 1983).

The paleontological collection of the Phyletisches Museum contains more than 30,000 objects, split into historical and contemporary sets. The historical part is marked with the acronym PMJ P and was acquired after the closure of the geoscientific institutes of Jena University in 1968 and represents a “closed collection”. All other fossils bear the acronym PMJ Pa, and specimens are still added to this contingent. In addition to type material, these collections also contain other historically valuable objects, such as the so called “*Goethe-Stier*” (the holotype of *Bos primigenius taurus* Bojanus, 1827; von Knorre and Beutel 2018) and an elephant skull that was used by von Goethe for his “*Zwischenkieferstudien*” (“studies on the *os intermaxillare*”) (Valentini 1714; Matuschek 2020). The museum also possesses a small amber collection, containing for instance important fossils of Strepsiptera, including members of the stem group and the most ancestral species of the order (Pohl et al. 2005, 2021; Pohl and Beutel 2016).

While reorganizing material and cleaning storage spaces following the closure of the museum in 2020 due to the COVID-19 pandemic, we made a surprising discovery: Another amber collection, which had been lost for several decades. In total, this collection consisted of 161 pieces, of which 76 were unlabeled. The remaining material was labeled as East African copal (“Ost-Afrika”; 3 pieces), amber from Samland (51 pieces from “Bernsteinwerke Königsberg”, 14 from Samland, and 1 piece from “Kleinkuhren”), or stated as possibly coming from Samland (“Samland?”, 15 pieces), as well as one piece from “Ostseestrand” (Baltic Sea beach). As we processed the material and started making identifications, we found a number of potential new records from specimens directly labeled as Baltic amber, with profound evolutionary implications, particularly for the Formicidae. As the new records accumulated, we became skeptical of the labeling and pursued multiple approaches to resolve the sources of the “amber” pieces in this rediscovered fossil collection of the Phyletisches Museum.

The objectives of our present study, therefore, were to: (1) Identify the source or sources of the fossils; (2) identify the insect inclusions as finely as possible; (3) provide taxonomic treatments within the realms of our expertise; and (4) to contextualize this historically overlooked collection more broadly. Toward these ends, we implemented a battery of qualitative and quantitative tests of the fossil matrices, we investigated the historical records from and associated with the Phyletisches Museum, and we applied synchrotron-radiation micro-computed tomography (SR- $\mu$ -CT) and traditional light microscopy methods to interrogate the fine-scale structure of the fossil insects in a comparative framework. Consequently, we report the results of our taphonomic investigation and key historical findings, and we provide revisionary systematic treatments for select taxa of Psocodea, Formicidae, Neuroptera, and Coleoptera.

## 2. Materials and methods

**Note on convention:** We introduce the double dagger symbol (‡) to indicate taxa that are known only from copal or Defaunation resin, to distinguish it from the single dagger (†), which is used to indicate taxa known only from amber.

## 2.1. Fossil specimens

All fossil pieces from the rediscovered *Bernsteinsammlung* (amber collection) of the Phyletisches Museum were provided with unique specimen identifiers. The identifiers are in the “Inv.-Nr. Pa.” series, which corresponds to the older accessions of the museum (von Knorre and Beutel 2018). The amber pieces were stored in three drawers in the attic of the museum and have been untouched for around 50 years. Presumably, due to the strong temperature and humidity fluctuations, the overall condition was quite poor with the fossils having brittle, deteriorated surfaces (Bisulca et al. 2012). Some of the pieces were found to be coated with an unknown type of varnish, which emitted a distinct smell during grinding. Other specimens were unconventionally glued to cardstock. We infer that the glue was some sort of epoxy, as this was commercially available in the late 1940s (Chen et al. 2019), and that the pieces were likely glued by E. Uhlmann sometime after acquisition (see section 3.1.1 below). We observed that the epoxy had “eaten” its way into the amber over time, resulting in dissolved surfaces. We removed the epoxy completely through careful grinding.

## 2.2. Specimen preparation

To facilitate the identification of inclusions, all amber specimens were manually ground and polished. Grinding was done with waterproof single silicon carbide abrasive paper (Robert Bosch GmbH, Robert-Bosch-Platz 1, 70839 Gerlingen, Germany) soaked in water (Sadowski et al. 2021). Initial sandpaper grain size was chosen for each specimen individually, depending on condition and on the distance of the inclusions to the surface. In general, we used the following grain size steps: 180, 400, 500, 1000, 1200, and 2000. Whenever possible, we made an effort to generate flat surface windows for viewing. Grinding was performed with sandpaper over a glass plate in one hand and the amber piece in the other hand. Amber pieces and glass plate were cleaned with water between every grain size step.

We experimented with different polishes such as chalk and Peek Polish (Peek Polish International, 51 Waterloo Road London NW2 7TX, United Kingdom). As the latter contains residual petroleum (Peek Premium Polish Paste Safety Data Sheet), it was used very cautiously but produced good results. Finally, we found that excellent results could be achieved by using the toothpaste Colgate® Sensation White Aktivkohle Zahnpasta (Colgate-Palmolive, 300 Park Avenue New York, NY, United States). A dab of toothpaste placed on microfibre cloth with a small amount of water was used to polish the amber pieces on all sides, until most of the remaining small scratches were no longer visible. To finish a single piece took up to three hours, as constant control under a desktop-mounted magnifying glass was mandatory to prevent grinding off inclusions.

To isolate specific inclusions, some amber specimens were cut into smaller pieces using a Dremel® 3000 (Robert Bosch GmbH, Dremel, 1800 W. Central Rd., Mt. Prospect,

Illinois, U.S.) with a thin saw blade (0.1 mm) attachment. As the Dremel’s minimum speed is 10000/min, which was too fast for freehand amber cutting, we used a defective Proxxon FBS 240/E (Proxxon Inc., 130 US Hwy 321 SW, Hickory, NC 28602 USA) to create guiding cuts. The lowest revolution rate of the Proxxon is given as 5000/min, but the one that we used had a markedly lower speed. With the guiding cuts done, the faster Dremel® could be used safely. This process required very straight cuts to prevent the blade from bending and getting caught in the amber, which would occasionally cause breaking or splintering. Alternatively, we also used a hardwood saw (Heckenrose 3 fein, Augusta-Heckenrose, Werkzeugfabriken GmbH & Co KG, Rudolf-Diesel-Straße 36, 71154 Nufringen, Germany) of 0.3 mm, in this case with the tool fixed in place and the amber pulled over the blade. After polishing and cutting, the specimens were carefully dried using a microfiber cloth.

The final curatorial step was to store the fossils in individually shaped moulds of PE-Foam (SV-Schaumstoffe GmbH, Junkerstraße 10, 82178 Puchheim, Germany) in insect drawers. A slit was cut into the foam above each object, into which the matching label was inserted. A small note was placed under each amber piece (Museumspapier altweiß mit Alkalipuffer, Klug Conservation, Zollstraße 2, 087509 Immenstadt, Germany) with the corresponding inventory number.

## 2.3. Establishing the material origin of the fossils

As most of the specimens in the three PMJ Pa drawers lacked reliable collection information, we undertook a series of tests to determine whether the fossils had the properties of amber or copal. Specifically, we evaluated melting behavior, autofluorescence, hardness, solubility, and density. All tests were compared between the PMJ Pa material and known samples, which were either from Ethiopian, Baltic, or Burmese ambers. As the Ethiopian pieces were a loan from MAIG (Museum of Amber Inclusions, University of Gdańsk, Gdańsk, Poland), we did not sample these destructively.

To confirm that our specimens were products of plant resin rather than artefacts in plastic material, we heated a needle and attempted to insert it into the test samples to test melting behavior. We checked fluorescence using a handheld LED UV flashlight and a 6 pi LED special UV lamp with a 120° angle of radiation. To test hardness, we scratched the test pieces either against our fingernails or *vice versa*. For the solubility test, we used a Dremel disc saw with a diamond blade to cut small pieces from the test samples, which we then placed in 99.5% Acetone; after a few minutes, we removed the samples and pressed them between our fingers. For the density test, we filled two dishes with fresh water, and added salt to saturation to one of them, after which we placed known and unknown samples in both liquids. Finally, we sent a representative sample of 10 specimens that were either labeled as “copal” or “amber” to the International Amber Association (IAA; Gdańsk, Poland) for UV fluorescence and Fourier-transformed infrared spectroscopy (FT-IR) (Table 1).

**Table 1.** Specimens tested at the IAA, their expected sources, results of the FT-IR analysis, and the color of each resin piece. Four specimens (**bold**) conformed to expectations based on the provided label data.

PMJ Pa	Expected source	Result	Color	Notable inclusion
5806	Baltic (succinite)	Copal <i>sensu lato</i>	Yellow	Mantodea
5807	Baltic (succinite)	Copal <i>s. l.</i>	Yellow	Formicidae: <i>Lepisiota</i>
5808	Baltic (succinite)	Copal <i>s. l.</i>	Yellow	Formicidae: <i>Dorylus</i>
5809	Baltic (succinite)	Copal <i>s. l.</i>	Yellow	Psocodea: <i>Amphientomum</i>
5824	Baltic (succinite)	Copal <i>s. l.</i>	Yellow	Formicidae: <i>Crematogaster</i>
<b>5825</b>	<b>Copal</b>	Copal / (Kauri gum?) <sup>1</sup>	Yellow	Psocodea: Archipsocidae
5827	Baltic (succinite)	Copal <i>s. l.</i>	Yellow	Formicidae: <i>Pheidole</i> , <i>Dorylus</i>
5830	Copal	Succinite	Orange	Brachycera, Auchenorrhyncha
<b>5855</b>	<b>Baltic (succinite)</b>	Succinite	Orange	Diptera: Tipulomorpha
<b>5871</b>	<b>Baltic (succinite)</b>	Succinite	Orange	Archaeognatha
<b>5858</b>	<b>Baltic (succinite)</b>	Succinite	Orange	Diptera: Tipulomorpha
5884	Baltic (succinite)	Copal <i>s. l.</i>	Yellow	Formicidae: <i>Dorylus</i>
5889	Baltic (succinite)	Copal <i>s. l.</i>	Yellow	Formicidae: <i>Pheidole</i>

<sup>1</sup> The IAA results suggest that this specimen may be from Kauri gum. Without additional evidence, we provisionally recognize that this specimen is not amber and is of uncertain source.

## 2.4. Microscopy

Specimens were examined at the Phyletisches Museum primarily with a Zeiss Stemi SV 11 stereomicroscope and a Zeiss Axioskop compound microscope. For the stereomicroscope a maximum magnification of 40× was used. For the light microscope we used the magnifications 50×, 100× and 200×.

## 2.5. Photography

To remove minute scratches, the amber pieces selected for photography were polished in three successive steps with ST5000, ST7000 wet abrasive paper (Starcke, Melle, Germany), and Peek polish (Tri-Peek International, Saffron Walden, United Kingdom) or Colgate® Sensation White Aktivkohle Zahnpasta (Colgate-Palmolive, 300 Park Avenue New York, NY, United States).

For overview photographs, stacks of partially focused images were taken of the amber pieces with a Canon EOS R5 equipped with a Canon EF 100 mm f/2.8L Macro IS USM lens (Canon, Krefeld, Germany), which was mounted on a Kaiser copy stand. For focus bracketing, the internal camera software was used. The scene was illuminated with a Euromex LE.5211-230 cold light source for stereomicroscopy (Euromex, Papenkamp, Netherlands) equipped with three gooseneck lamps to adjust light conditions and prevent reflections. Underneath the camera a blurred glass plate was positioned over a black sprayed Kapa® box. The amber pieces were placed on the glass plate in a petri dish filled with distilled water as suggested by Sadowski et al. (2021). The amber was held in place with UHU Patafix (UHU, Bühl, Germany). Some pieces were photographed without water to obtain a better spatial impression.

For shots of details from single embedded specimens, a Canon Eos 7D Mark II (Canon, Krefeld, Germany) equipped with a Mitutoyo M Plan Apo 10 microscopic

lens (Mitutoyo, Kawasaki, Japan) was used. To perform stack shots, the camera was mounted on a StackShot macro rail (Cognisys, Traverse City, USA). Two flashlights (Yongnuo Photographic Equipment, Shenzhen, China) illuminated the scene. The amber pieces were placed on a cover slip. Plasticine was used to level the surface. A drop of glycerine was placed on the surface of the amber piece, and the glycerine was then covered by an additional cover slip. Additional detail images were taken at the Museum für Naturkunde Berlin (MfN), where manual stacks were taken using a Zeiss Axioscope 5 with a Zeiss Achromat S 1,0 FWD 63 (Carl Zeiss AG, Oberkochen, Germany), mounted with a Canon EOS 80D (Canon, Krefeld, Germany) via a T2-T2 1,6× SLR tube.

All photographs were developed with Adobe Lightroom classic (v.11.5) (Adobe, San Jose, USA). The images (option: standard) were denoised with Topaz DeNoise AI (Topaz Labs, Dallas, USA). Zerene Stacker 1.04 (Zerene Systems LLC, Richland, USA) was used to fuse the images (option: align & stack all (PMax).

## 2.6. Micro-computed tomography

Nine specimens (Table 2) were scanned using synchrotron radiation (SR-μ-CT) at the Imaging Beamline P05 (IBL) (Haibel et al. 2010; Greving et al. 2014; Wilde et al. 2016) operated by the Helmholtz-Zentrum Hereon at the storage ring PETRA III (Deutsches Elektronen Synchrotron—DESY, Hamburg, Germany). A photon energy of 18 keV and a sample to detector distances of 30–50 mm were used. Projections were recorded using a 50 MP CMOS camera system with an effective pixel size of 0.46 μm. 4001 projections were recorded for each tomographic scan at equal intervals between 0 and π, with an exposure time of 350 ms. When specimens were too large to fit into the field of view in the z-axis, we scanned overlapping sections and subsequently stitched them together. Tomographic reconstruction was done by applying a transport of intensity

**Table 2.** Specimens scanned at DESY; data available as Suppl. material 1.

Specimen ID	Taxon name	Stage/sex
PMJ Pa 5827_a	Coleoptera: Platypodinae: <i>Doliopygus</i> cf. <i>serratus</i>	Adult male
PMJ Pa 5870	Coleoptera: Mordellidae: † <i>Baltistena nigrispinata</i> Batelka, Tröger & Bock, <b>sp. nov.</b>	Adult, sex indet.
PMJ Pa 5821 <sup>1</sup>	Hemiptera: Auchenorrhyncha: Cixiidae	Adult female
PMJ Pa 5884	Hymenoptera: Formicidae: <i>Dorylus nigricans molestus</i> (Gerstäcker, 1859)	Adult worker
PMJ Pa 5809	Psocodea: ‡ <i>Amphientomum knorrei</i> Weingardt, Bock & Boudinot, <b>sp. nov.</b>	Adult female
PMJ Pa 5825	Psocodea: Archipsocidae	Adult female
PMJ Pa 5889	Hymenoptera: Formicidae: ‡ <i>Pheidole cordata</i> (Holl, 1829)	Adult soldier
PMJ Pa 5874 <sup>2</sup>	Neuroptera: † <i>Palaoneurorthus</i> sp.	Adult male
PMJ Pa 5896 <sup>3</sup>	Arachnida: Salticidae	Adult, sex indet.

<sup>1</sup> Not analyzed further; no taxonomic expertise.

<sup>2</sup> Not analyzed further; poor preservation.

<sup>3</sup> Not analyzed further; specimen not visible in scan files.

phase retrieval and using the filtered back projection algorithm (FBP) implemented in a custom reconstruction pipeline (Moosmann et al. 2014) using MATLAB (Math-Works) and the Astra Toolbox (Palenstijn et al. 2011; van Aarle et al. 2015, 2016). For further processing, raw projections were binned two times resulting in an effective pixel size of the reconstructed volume of 0.913  $\mu\text{m}$ . For segmentation and visualization, the 32-bit .tif image sequences were converted to 8-bit files and downsampled twofold with Fiji (Schindelin et al. 2012), resulting in an effective pixel (voxel) size of 1.826  $\mu\text{m}$ .

## 2.7. <sup>14</sup>C dating of samples

Two samples, PMJ Pa 5809 (‡*Amphientomum knorrei* Weingardt, Bock & Boudinot, sp. nov.) and PMJ Pa 5884 (*Dorylus nigricans molestus*) were dated using <sup>14</sup>C analysis, as recommended by Delclòs Martínez et al. (2020). Amber pieces with a mass of 5 mg (PMJ Pa 5809), 6 mg (PMJ Pa 5884) and 5 mg (PMJ Pa 5889) were cut off and sent to Beta Analytic (4985 S.W. 74<sup>th</sup> Court, Miami, FL, USA 33155). Dating analyses resulted in estimated age ranges with certain likelihoods. The age range with the highest likelihood was chosen (Table 3). Based on our identifications of the copal inclusions and the history of the collections, East Africa was selected as the geographic reference for dating. We chose the psocodean as taxonomic work on the group is challenged, with presently only a handful of specialists working on them (e.g., Mockford 2018). We also chose the putative Baltic *Dorylus* due to its potential evolutionary and biogeographic implications.

**Table 3.** <sup>14</sup>C-dating results based on the testing by Beta Analytic. The maximum age of the estimated range is listed.

<sup>14</sup> C-dated	Specimen contained	Results	Maximum age in years
PMJ Pa 5809	‡ <i>Amphientomum knorrei</i>	390 +/-30 BP	565
PMJ Pa 5884	<i>Dorylus nigricans molestus</i>	50 +/-30 BP	145
PMJ Pa 5889	‡ <i>Pheidole cordata</i> , Lepidoptera indet	720 +/- 30 BP	746

## 2.8. Data segmentation and rendering

$\mu$ -CT-image stacks were segmented and 3D-reconstructed using Amira 6.0.1 (Thermo Fisher Scientific) and Dragonfly 2022.1 (Object Research Systems). Image (tif) stacks and isosurfaces were exported with the Amira macro “Multi-Export” (Engelkes et al. 2018). The isosurfaces were reduced and smoothed with following parameters: It-Total: 5; smooth: iteration: 4, lambda: 0.6; reduction: 0.7. Tiffs were volume rendered in VGStudio Max 2.0 (Volume Graphics) using the option Phong reflection model. The isosurfaces were further smoothed (modifier: smooth and option shade smooth) with Blender 3.2.0 (Blender Foundation). The 3D-Models were uploaded to the 3D repository Sketchfab (URL: <https://sketchfab.com>) using the free blender plugin: Sketchfab for Blender 1.5.0 (URL: <https://github.com/sketchfab/blender-plugin/releases/tag/1.5.0>).

## 2.9. Image plates

Image plates were compiled using Adobe Photoshop (v. 24.1.0) (Adobe, San Jose, USA). Lettering was added with Adobe Illustrator (v. 27.2).

## 2.10. Repositories

Specimens evaluated in the present study, and also for the use of comparison to each other, were from the following collections:

<b>BEBC</b>	Brendon E. Boudinot research collection, Frankfurt am Main, Germany
<b>MAIG</b>	Museum of Amber Inclusions, University of Gdansk, Poland.
<b>PMJ</b>	Phyletisches Museum Jena, Germany.
<b>MNHB</b>	Museum für Naturkunde Berlin, Germany.
<b>MWC</b>	Michael Weingardt research collection, Jena, Germany.
<b>SMNS</b>	Staatliches Museum für Naturkunde Stuttgart, Germany.
<b>USNM</b>	U.S. National Museum of Natural History, Washington, D. C., U.S.A.

## 2.11. Data availability

The raw scan data will be made available at MorphoSource upon acceptance.

## 3. Results

### 3.1. Fossil sources

#### 3.1.1. Fossil provenance

**Collector.** Unknown.

**Date.** Unknown. It is likely that the 161 fossil pieces in the collection were acquired by the Phyletisches Museum in several batches between 1920 and 1930 (see below).

**Circumstantial evidence.** By the handwriting of the label for specimen PMJ Pa 5827, the date of collection is estimated between 1920 and 1930 (personal communication with Uwe Dathe, Historische Sammlungen ThULB, 15.07.2022 and Alexander Gehler, Geowissenschaftliches Zentrum der Georg-August-Universität, 14.07.2022). The label for specimen PMJ Pa 5827 has two different scripts on each side, which cannot be clearly assigned to any handwriting samples in the museum's archives. Furthermore, the former curator of the museum, Dietrich von Knorre, stated that Eduard Uhlmann (1888–1974) was in charge of the small “Bernsteinsammlung” (amber collection); Uhlmann was a scientific assistant, later conservator at the Phyletisches Museum Jena while it was under the directorship of Ludwig Plate (director from 1909–1935), and later became associate professor (*ao. [außerordentlicher] Professor* 1950) and director of the Phyletisches Museum from 1952 till 1954.

In accordance with the statements above, there are handwritten labels on nine specimens (Pa 5828, 5829, 5836, 5871, 5873, 5874, 5875, 5882, and 5885) which can be assigned to E. Uhlmann and his wife Frida Uhlmann (born Preiss, 1894–1981). This assessment is unambiguous as the Uhlmanns re-sorted numerous drawers in the entomology collection, which were labelled by her (Krogmann et al. 2007). Moreover, von Knorre stated (25.07.2022) that Uhlmann (Fig. 1) bequeathed the small amber collection to him after retirement, which von Knorre later added to the museum's collection. We screened the archives of the Friedrich Schiller University (21.07.2022) and the Phyletisches Museum (21–22.07.2022) but did not discover invoices or personal communication of Uhlmann and Plate. In sum, how exactly the small amber collection found its way into the museum cannot be confidently resolved at present.

**Listed localities.** Of the 161 numbered pieces, 76 lacked locality information and one additional number was associated with human-made beads without further information (Pa 5911; not included in the total count).

Of the remaining 85 pieces, 21 have labels indicating a Baltic origin and three are marked as copal from East Africa, such as Pa 5829, which has a handwritten label stating “Kopalinsect Ost-Afrika Diluvium”. One of the putative Baltic pieces, Pa 5827, has a handwritten label “Fundstück von Kleinkuhren Samland” (Filino), while 15 are marked with “Samland?” and the derivation of 51 of the other presumptive amber specimens is indicated as Samland Bernsteinwerke Königsberg on the labels, with an authentic invoice from the “Preuß. Bergwerks- und Hütten-Akt.-Ges. Zweigniederlassung Bernsteinwerke Königsberg Pr. for 1 M” for Pa 5863. For a discussion of the Samland and Kleinkuhren localities, see also section 4.2.

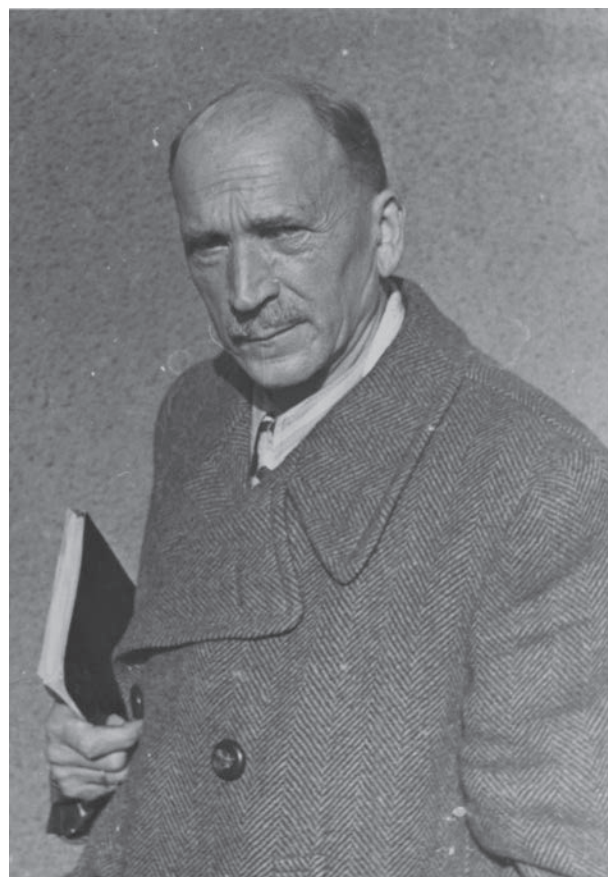


**Figure 1.** Eduard Uhlmann around 1955. Archive of the Phyletisches Museum XXVII.

**Qualitative tests.** Despite the labels, the locality or localities of origin are not as clear as the first impression suggested. As it is not possible to discriminate copal and amber reliably based on the visual appearance alone (e.g., Federman 1990), we conducted a series of qualitative tests (see section 2.3), most of them at the Phyletisches Museum. Overall, the qualitative tests were contradictory and inconclusive. All pieces labelled as amber floated in saltwater and all labelled as copal sunk, apparently confirming the original labels. However, not a single piece in the collection emitted

blue light under UV, while amber specimens of known provenance from the BEBC (burmite, succinite) and MAIG (Ethiopian amber) did. By burning the different samples from the PMJ Pa collection, every piece sized and produced black smoke, as expected for amber. Only one sample (Pa 5809) showed clear white smoke, but burning a larger piece yielded black smoke. Thus, the expected difference—that amber burns and copal melts—was not observed. When only small pieces were left, both copal and amber melted. Most conspicuous was a sweet odor produced by burning a larger piece of copal (from Pa 5809), which clearly distinguished it from true amber. This scent was not detected with smaller pieces, however.

**Quantitative tests.** For quantitative testing, additional small pieces were cut off and sent to the International Amber Association (IAA, 1 Warzywnicza Street, 80-838 Gdańsk, Poland) and checked with the UV/VIS and the FT-IR method (Table 1). The results from these analyses contradicted those from the qualitative tests and showed that all light-yellow pieces were copal, including those with *Dorylus*. In contrast, the darker, orange-colored pieces were true succinite (Baltic amber), including the one with †*Yantaromyrmex*. Finally, the <sup>14</sup>C dating yielded an age of only ~145 years old for the piece containing the *Dorylus*. Therefore, this and other pieces with similar biotic inclusions are identifiable as Defaunation resin (*sensu* Solórzano-Kraemer et al. 2020), while the estimated age for the *Amphientomum*-bearing specimen is ~390 years old.

**Biotic evidence.** Ultimately, our final interpretations of the geological source of the putative amber pieces were based on the combined weight of evidence from the IAA results and the insect inclusions themselves. While it was exciting to consider the possibility that the *Dorylus*, *Lepisiota*, *Pheidole*, and *Crematogaster* ants were first records from Baltic amber, our  $\mu$ -CT scan of the *Dorylus* revealed that it is identifiable as an extant subspecies. Moreover, this subspecies, *Dor. nigricans molestus* (Figs 2A–C, 3, Appendix 1: Fig. A1), was pre-

viously recorded from reliably identified Tanzanian copal by DuBois (1998) (see section 4.2.2 below). Another critical element of biotic evidence was the large piece PMJ Pa 5827, which contained another *Do. n. molestus* as well as a distinctive platypodine beetle (Curculionidae; “ambrosia beetles”, “pinhole borers”). Based on our  $\mu$ -CT rendering of the beetle, Bjarte Jordal (01 Nov 2022) identified it as either *Doliopygus serratus* or *Dol. cf. serratus* (Figs 4A–C, Appendix 1: Fig. A2), which in either case represents bark beetle populations that are extreme generalists, and presently distributed throughout Southern, Central, and West Africa (Beaver and Löyttyniemi 1985). Several other amber pieces from the PMJ Pa contained sweat bees (Meliponini) that closely resembled specimens from known African copal pieces at the SMNS. All these aforementioned fossil pieces were light yellow, while other specimens—without these distinctive taxa—were dark and of a pinkish red color. Among these darker specimens was an ant definitively identifiable as †*Yantaromyrmex geinitzi*, the type species of a Baltic-amber-endemic genus. In section 3.2, we outline the complete list of taxa that we identified in the PMJ Pa collection, as well as the results of investigations on the origin of material compared to the point of starting our investigations.

### 3.2. Fossils of the PMJ Pa amber collection and the origin of material

In Table 4 we provide a list of all specimens sorted taxonomically, including reference to the museum accession numbers.

The initial situation of the material, with a rather chaotic sorting, shows that almost half of the material was without evidence of origin. Around 40% were labelled as Baltic amber, while 3 pieces were labeled as copal (Suppl. material 1). Overall, almost 10% were labelled, but with a question mark, which is not reliable information in any case.

**Table 4.** All identified taxa from the PMJ Pa amber collection.

Taxon	Matrix	PMJ Pa
<b>PLANTAE</b>		
(Trichomes)	Succinite	5872
(Leaf fragments)	first 4 Copal <i>s. l.</i> , 5886 Copal <i>s. l.</i> , all others Succinite	5811, 5820, 5826, 5886, 5839, 5840, 5843, 5848, 5849, 5851, 5855, 5856, 5861, 5862, 5867, 5870, 5883, 5885, 5910
<b>CHELICERATA</b>		
<b>Acari</b>		
(Indet.)	Succinite	5798, 5840, 5854, 5876
<b>Araneae</b>		
Linyphiidae	Copal <i>s. l.</i>	5809
Philodromidae	Succinite	5838
Thomisidae	Succinite	5877
Zodariidae: cf. <i>Trygetus</i>	Copal <i>s. l.</i>	5807
Zodariidae	Succinite	5876
Uncertain: Araneidae, Palpimanidae, Philodromidae, Salticidae, Thomisidae	First two Copal <i>s. l.</i> , others Succinite	5827, 5890, 5843, 5879, 5878, 5881

Taxon	Matrix	PMJ Pa
<b>Opiliones</b>		
(Indet.)	Succinite	5859
<b>HEXAPODA</b>		
(Indet.)	Succinite	5903, 5908
<b>Collembola</b>		
Symphyleona	Succinite	5908
<b>Archaeognatha</b>		
Machilidae	Succinite	5828
(Indet.)	Succinite	5871, 5872
<b>Dictyoptera</b>		
Blattodea	Succinite	5841
Isoptera	first 11 Copal s. l, other Succinite	5794, 5798, 5802, 5803, 5811, 5815, 5818 5819, 5822, 5826, 5827, 5848, 5871
Mantodea	Copal s. l	5806
<b>Hemiptera</b>		
Aphididae	Succinite	5860, 5885
Anthocoridae	Copal s. l	5827
Cicadellidae	Copal, Succinite, Succinite	5827, 5847, 5852
Cixiidae	Copal s. l	5821
Issidae	Copal s. l	5821
Psyllidae	Copal s. l	5798
Coccoidea	Succinite	5856
Fulgoroidea	Copal s. l	5793
Aleyroidea	Copal s. l	5822
(Auchenorrhyncha)	Copal s. l	5809
<b>Psocodea</b>		
Amphientomidae:	Copal s. l	5908
‡ <i>Amphientomum knorrei</i> sp. nov.		
Archipsocidae	Kauri gum?	5825
Liposcelididae	Copal s. l	5827
<b>Thysanoptera</b>		
(Indet.)	Copal s. l	5820, 5822
<b>Hymenoptera</b>		
Anthophila: Apinae	Copal s. l	5795, 5807, 5814, 5816, 5817, 5826, 5892
Anthophila: Apinae: Meliponini	Copal s. l	5796, 5798, 5800, 5806, 5815, 5822, 5824, 5888, 5893
Anthophila: (indet.)	Copal s. l	5793, 5810, 5894
Bethylidae	Copal s. l	5823
Braconidae: Cheloninae	Copal s. l	5896
Braconidae: (indet.)	Copal s. l	5823
Chalcidoidea	Copal s. l	5816, 5819, 5820, 5821
Formicidae: <i>Camponotus</i>	Copal s. l	5829
Formicidae: † <i>Ctenobethylus</i>	Succinite	5851, 5874, 5893, 5903
Formicidae: <i>Crematogaster</i>	Copal s. l	5824
Formicidae: <i>Dorylus n. molestus</i>	Copal s. l	5808, 5827, 5884
Formicidae: Ponerini: cf. <i>Hypoponera</i>	Copal s. l	5819
Formicidae: <i>Lepisiota</i>	Copal s. l	5807
Formicidae: ‡ <i>Pheidole cordata</i>	Copal s. l	5827, 5889
Formicidae: † <i>Yantaromyrmex geinitzi</i>	Succinite	5856
Formicidae: Dolichoderinae	Copal s. l	5817, 5821
Ichneumonidae	Succinite	5869
Platygastroidea: Platygastridae	Copal s. l	5889
Platygastroidea: Scelionidae <i>sensu lato</i>	Copal s. l, Succinite	5809, 5836
Platygastroidea: (indet.)	Copal s. l, Succinite, Succinite	5821, 5846, 5877
(Aculeata)	Copal s. l	5822, 5890
(Parasitica)	Copal s. l	5808, 5891
(Indet.)	Succinite	5843
<b>Neuroptera</b>		
Nevrorthidae: † <i>Palaeoneurorthus</i>	Succinite	5874
<b>Coleoptera</b>		
Cantharidae	Succinite	5863
Chrysomelidae: Bruchinae?	Copal s. l	5827
Chrysomelidae: Alticini?	Copal s. l	5810
Chrysomelidae?	Copal s. l	5892
Curculionidae: <i>Doliopygus</i> cf. <i>serratus</i>	Copal s. l	5827
Curculionidae: Platypodinae	Copal s. l	5798, 5805, 5807, 5812, 5814, 5816, 5819
Elateridae	Succinite	5851, 5866

Taxon	Matrix	PMJ Pa
Mordellidae: † <i>Baltistena nigrispinata</i> <b>sp. nov.</b>	Succinite	5870
Staphylinidae	Copal s. l, Succinite	5828, 5861
Bostrichoidea?	Succinite	5836, 5883
Staphylinoidea? (Polyphaga)	Succinite Copal s. l, Succinite, Copal s. l	5851 5819, 5885, 5891
<b>Diptera</b>		
Ceratopogonidae	Succinite, last one Copal s. l	5848, 5863, 5864, 5889
Chloropidae	Succinite	5836
Dolichopodidae	Succinite	5837
Mycetophilidae	Succinite, last Copal s. l	5848, 5885, 5901, 5890
Sciaridae	Succinite,	5851, 5864
Phoridae	Copal s. l	5808, 5823, 5827
Psychodidae	Copal s. l	5896
Sciaroidea	Copal s. l, Succinite	5809, 5840
(Tipulomorpha)	Succinite	5855, 5858
(Brachycera)	First 7 Copal s. l, all other Succinite	5795, 5807, 5811, 5815, 5822, 5827, 5830, 5836, 5839, 5844, 5846, 5849, 5853, 5854, 5857, 5862, 5865, 5867, 5868, 5871
(Muscomorpha)	Copal s. l	5797, 5799, 5809, 5891
(Calyptrata)	Copal s. l	5586
(Nematocera)	first 5 Copal s. l, all following Succinite	5808, 5827, 5830, 5891, 5895, 5836, 5837, 5839, 5844, 5846, 5854, 5857, 5858, 5861, 5862, 5870, 5871, 5872, 5874, 5877, . . . 5897, 5902, 5903, 5909
(Indet.)	first three Copal s. l, other Succinite	5821, 5892, 5896, 5843, 5882, 5898, 5905
<b>Lepidoptera</b>		
(Indet.)	first 3 Copal s. l, last Succinite	5797, 5804, 5889, 5842,
<b>Trichoptera</b>		
Annulipalpia	Succinite	5850, 5875
Integripalpia	Succinite	5863
(Indet.)	Succinite, Copal s. l	5845, 5891
<b>Amphimesenoptera</b>		
(Indet.)	Succinite	5903

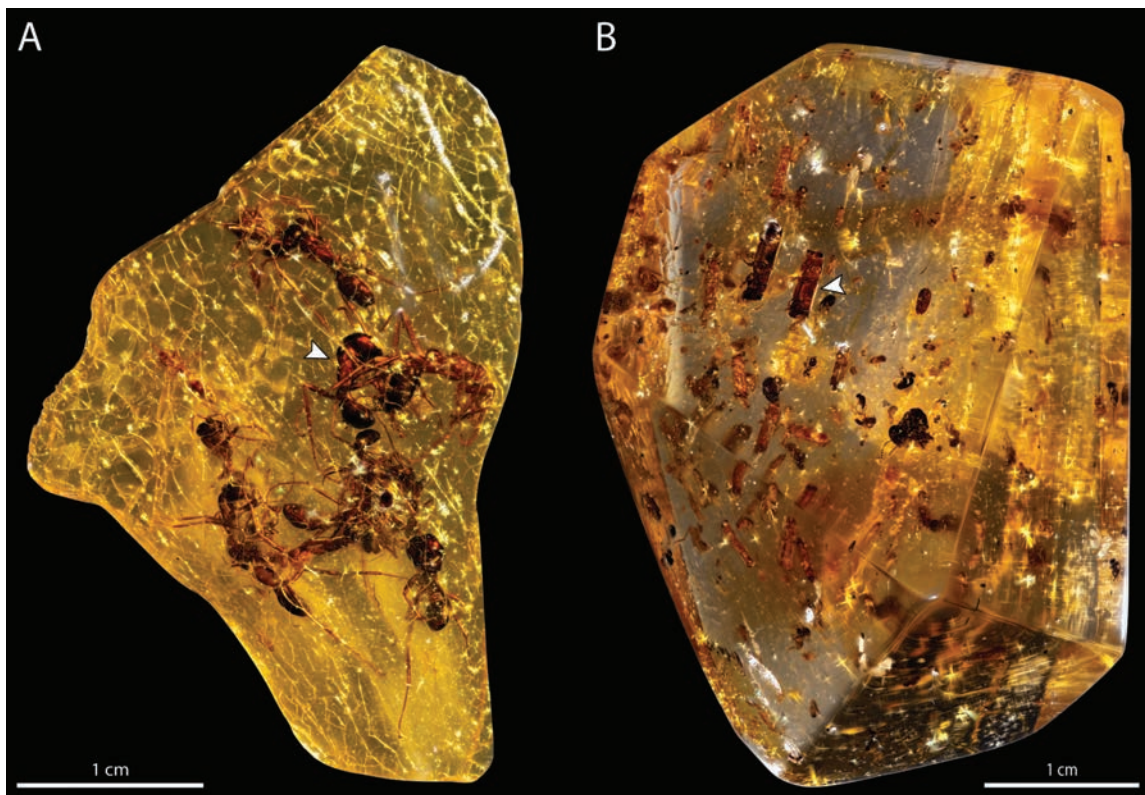


**Figure 2.** Overview photo of a select piece of Defaunation resin (**A**) and a piece without dating analysis performed (**B**). **A.** Piece PMJ Pa 5884,  $^{14}\text{C}$  dated as about ~145 years old, with inclusions of several *Dorylus nigricans molestus* workers; **B.** piece PMJ Pa 5827 with the inclusion of the scanned *Doliopygus* cf. *serratus* as well as another *Do. n. molestus* worker. Arrows mark scanned specimens.

After identification, provenance research and chemical analysis the origin of most of the material could be solved confidently. One of the biggest surprises was that 7 pieces are of Kauri origin. Now, more than half of the material is of clear Baltic origin. The biggest switch was from pieces without evidence and the 3 pieces labelled as copal, as with 44% a sizable number in the collection is indeed East-African copal (Suppl. material 2).

### 3.3. Systematic entomology

#### 3.3.1. Order Psocodea: Synopsis of higher taxa in the PMJ Pa

Mostly families represented by material in the PMJ Pa are reviewed below. The identification of PMJ Pa material was based on the keys of Smithers (1990), with Taylor (2013) for the amphientomid. Specific details about the fossil deposits and their ages in this and other synopsis header sections are drawn from Paleobio (2022); we have included these for the geological information and to ease future divergence-dating phylogenetic analysis. Taxonomic information was drawn in part from the Psocodea Species File Version 5.0 (Johnson et al. 2023) database.

##### 3.3.1.1. Family Amphientomidae Enderlein, 1903. [Note 1] Amphientominae Enderlein, 1903 amber species:

###### I. Genus *Amphientomum* Pictet, 1854. [Note 2].

A. Oise amber [France, Le Quesnoy; Eocene, Ypresian, 56.0–47.8 Mya].

1. †*Am. parisiense* Nel, Prokop, De Ploeg & Millet, 2005.

B. Baltic ambers [Eocene, 37.8–33.9 Mya].

2. †*Am. (Amphientomum) leptolepis* Enderlein, 1905. [Note 3].

3. †*Am. (Amphientomum) paradoxum* Pictet, 1854. [Type species!]

4. †*Am. (Palaeoseopsis) colpolepis* Enderlein, 1905.

C. African resin [ca. 390 ± 30 years].

5. †*Am. knorrei* Weingardt, Bock & Boudinot, sp. nov. [Note 4].

###### II. Genus *Lithoseopsis* Mockford, 1993.

D. Mexican amber [Miocene, 23.0–16.0].

1. †*Li. elongata* (Mockford, 1969).

###### III. Genus †*Proamphientomum* Vishnyakova, 1975.

E. Taimyr amber [Russia; Cretaceous, 85.8–83.5 Mya].

1. †*Pr. cretaceum* Vishnyakova, 1975.

Amphientomidae amber species *incertae sedis*:

###### IV. Genus †*Arcantipsocus* Azar, Nel & Néraudeau, 2009.

F. Charentese amber [France; Cretaceous, 105.3–99.6 Mya].

1. †*Ara. courvillei* Azar, Nel & Néraudeau, 2009. [Note 5].

**Note 1.** As part of our ongoing psocodean revisionary investigations, we provide an extended discussion of *Amphientomum* (see below).

**Note 2.** A list of all extinct and extant *Amphientomum* species is provided in Table 5. With the addition of the new species described herein, there are 20 species attributed to this genus (Johnson et al. 2023), of which four are extinct; it is unknown if the species described herein is still extant.

**Note 3.** The species †*Am. leptolepis* might be a variant of †*Am. paradoxum*, as these two taxa are distinguished by only a few characters (Enderlein 1911). Specifically, †*Am. leptolepis* is differentiated from †*Am. paradoxum* by the following: (1) fore wing with very long and slender scales; (2) sides of the scales parallel; and (3) the count of ctenidiobothria on the hind basitarsus is 36 (vs. 29–34 in †*Am. paradoxum*) (Enderlein 1911). It should be noted that the description of †*Am. leptolepis* was based on two specimens (Enderlein 1911, p. 295) and no additional information on this species was published since then, to the best of our knowledge. Overall, we consider the scale shape as not fully reliable, yet we retain the species status of these two taxa pending more detailed study.

**Note 4.** We describe this new species from African resin in the PMJ Pa collection. See section 3.1.1.1.4 below for our treatment of this taxon.

**Note 5.** Mockford et al. (2013) synonymized †*Arcantipsocidae* Azar, Nel & Néraudeau, 2009 with *Amphientomidae*, arguing that a dark, thickened pterostigma is a homoplastic feature across the order Psocodea, thus cannot be relied upon singly for placement in Psocomorpha. They left †*Arcantipsocus* unplaced within the family but further recognized features that the genus shares with modern *Amphientomidae*, *i.e.*, the hindwing venation and the shape of maxillary palps, head, and forewings.

##### 3.3.1.2. Family Liposcelididae Broadhead, 1950

Liposcelidinae Broadhead, 1950 amber and copal species:

###### I. Genus *Liposcelis* Motschulsky, 1852.

A. Baltic ambers [Eocene, 37.8–33.9 Mya].

1. †*Li. atavus* Enderlein, 1911.

B. Mexican amber [Miocene, 23.0–16.0].

2. †*Li. sp.* [Note 1]. [f].

C. Zanzibar copal [Pleistocene?].

3. †*Li. resinata* (Hagen, 1865).

Embidosocinae Broadhead, 1950 amber species:

###### II. Genus *Belaphopsocus* Badonnel, 1955.

D. Dominican amber [Miocene, 20.4–13.8 Mya].

1. †*Bs. dominicus* Grimaldi & Engel, 2006.

###### III. Genus *Belaphotroctes* Roesler, 1943.

B. Mexican amber [Miocene, 23.0–16.0].

1. †*Bt. ghesquierei* Badonnel, 1949.

E. Zhangpu amber [Miocene, 16.0–13.8].

1. †*Bt. grimaldii* Engel & Wang, 2022.

###### IV. Genus *Embidosocus* Hagen, 1866.

F. Oise amber [France, Le Quesnoy; Eocene, Ypresian, 56.0–47.8 Mya].

1. †*Em. eocenicus* Nel, de Ploeg & Azar, 2004.

A. Baltic ambers [Eocene, 37.8–33.9 Mya].

2. †*Em. pankowskiorum* Engel, 2016.

G. Bitterfeld amber [Eocene, 38.0–33.9 Mya].

3. †*Em. saxonicus* Günther, 1989.

Liposcelididae amber species *incertae sedis*:

II. Genus †*Cretoscelis* Grimaldi & Engel, 2006.

H. Kachin amber [Myanmar; Cretaceous, 99.6–93.5 Mya].

1. †*Csc. burmitica* Grimaldi & Engel, 2006.

**Note 1.** Mockford (1969) recognized a species of *Liposcelis* from Mexican amber that he left undescribed as insufficient structural detail, *i.e.*, cuticular microsculpture and chaetotaxy, was observable.

3.3.1.3. Family Archipsocidae Pearman, 1936

Archipsocinae Pearman, 1936 amber species:

I. Genus *Archipsocopsis* Badonnel, 1948.

A. Mexican amber [Miocene, 23.0–16.0].

1. †*Ari. antiqua* (Mockford, 1969).

II. Genus *Archipsocus* Hagen, 1882.

B. Baltic ambers [Eocene, 37.8–33.9 Mya].

1. †*Aru. puber* Hagen, 1882.

3.3.2. Taxon description (Psocodea)

**Family Amphientomidae Enderlein, 1903**

**Subfamily Amphientominae Enderlein, 1903**

**Genus *Amphientomum* Pictet, 1854**

= *Amphicetomum* Hagen, 1859.

= *Palaeoseopsis* Enderlein, 1925 syn. nov. (Type species: †*Am. colpolepis* Enderlein, 1905 by original designation.).

**Type species.** †*Am. (Amphientomum) paradoxum* Pictet, 1854.

**Remarks.** Pictet (1854) first described the genus from Baltic amber. Enderlein (1905, 1911) defined several character states that define the genus *Amphientomum*. These include a large body size, a relatively small ocellar area where the distance between the ocelli is short, a lack of spur sensilla on the maxillary palpomeres, an elongated and narrow fourth maxillary palpomere, labial palps with two articles, antennal flagellum with secondary annulation, presence of a complete R1 vein in the hindwing, and perhaps more surprisingly the occurrence of only 13 flagellomeres (Enderlein 1911, p. 333). The number of antennomeres might be an oversight by Enderlein (1911), as Hagen (1882) had already described the number of articles (15) correctly. In his revision of Pearman's (1936) phylogenetic system of Psocoptera, Roesler (1944) provided morphological characters to define previously established groupings including the Amphientomidae. In so doing, Roesler designated the previously established genus *Palaeoseopsis* Enderlein, 1925 as a subgenus of *Amphientomum*. As such, *Am. (Palaeoseopsis)* is supposed to differ from *Am. (Amphientomum)* by the open basiradial cell, the lack of the basal section of Rs in the hindwing, and the emarginate scale tips (Ender-

lein 1925; Roesler 1944). Badonnel (1955) went a step further and proposed that the subgenus *Palaeoseopsis* can be removed entirely but did not follow through on this action. It should be noted that an open basiradial cell in the hindwing occurs in all species of the genus that are outside the subgenus *Am. (Amphientomum)*, as in most species only a short spur vein of the basal section of Rs is present or the basal section of Rs is entirely missing. Phylogenetic studies on this genus are lacking and the monophyly of the subgenera *Am. (Palaeoseopsis)* and *Am. (Amphientomum)* is therefore questionable, as they are neither supported by morphological apomorphies, nor by molecular data. We therefore formalize the synonymy of *Amphientomum* and *Palaeoseopsis* j. syn., syn. nov. The diagnostic characters of the genus *Amphientomum* are as follows after the identification key by Taylor (2013): presence of wings, the vein M in the hindwing simple, presence of three ocelli, the lateral ocelli closer to each other than to compound eyes, the vein R1 reaching the wing margin in the hindwing, and the distal section of the vein Sc in the forewing present. See also the Remarks section for †*Am. knorrei* sp. nov.

**Note.** The term sulcus is used here when an external line or furrow corresponds with an internal ridge, *i.e.*, a strengthening ridge (Girón et al. 2023). If no internal ridge is present but a narrow zone of weakness, we use the term suture (e.g., frontal suture). The typical coronal suture (part of the ecdysial suture) of other insects corresponds with an internal ridge in adult psocids and is therefore here classified as a coronal sulcus. The frontal sutures (part of ecdysial suture) are similarly developed as in other insects, without an internal strengthening ridge. The term epistomal sulcus is used as synonym of the frontoclypeal line.

‡***Amphientomum knorrei* Weingardt, Bock & Boudinot, sp. nov.**

<https://zoobank.org/600FA627-5659-486A-AF36-3F808852EB09>

**Etymology.** We dedicate this species to Dietrich von Knorre, whose lifework was to establish and curate the collection of the Phyletisches Museum. Besides being a natural conservationist and a dedicated teacher of students, von Knorre was the curator of the Museum from 1969 till 2003, during which time he dealt with nearly every item in the entire collection. In addition to his more than 270 publications (Köhler 2019), he has done meticulous research on the history of an immense number of objects and has become the museum's "living archive". With the newly discovered specimen bearing his name, we want to express our gratitude for his continuous support and contributions to the Phyletisches Museum.

**Type materials. Holotype.** PMJ Pa 5809, Copal (East African?). Female. Interactive cybertype: Appendix 1: Fig. A3.

**Paratypes.** None.

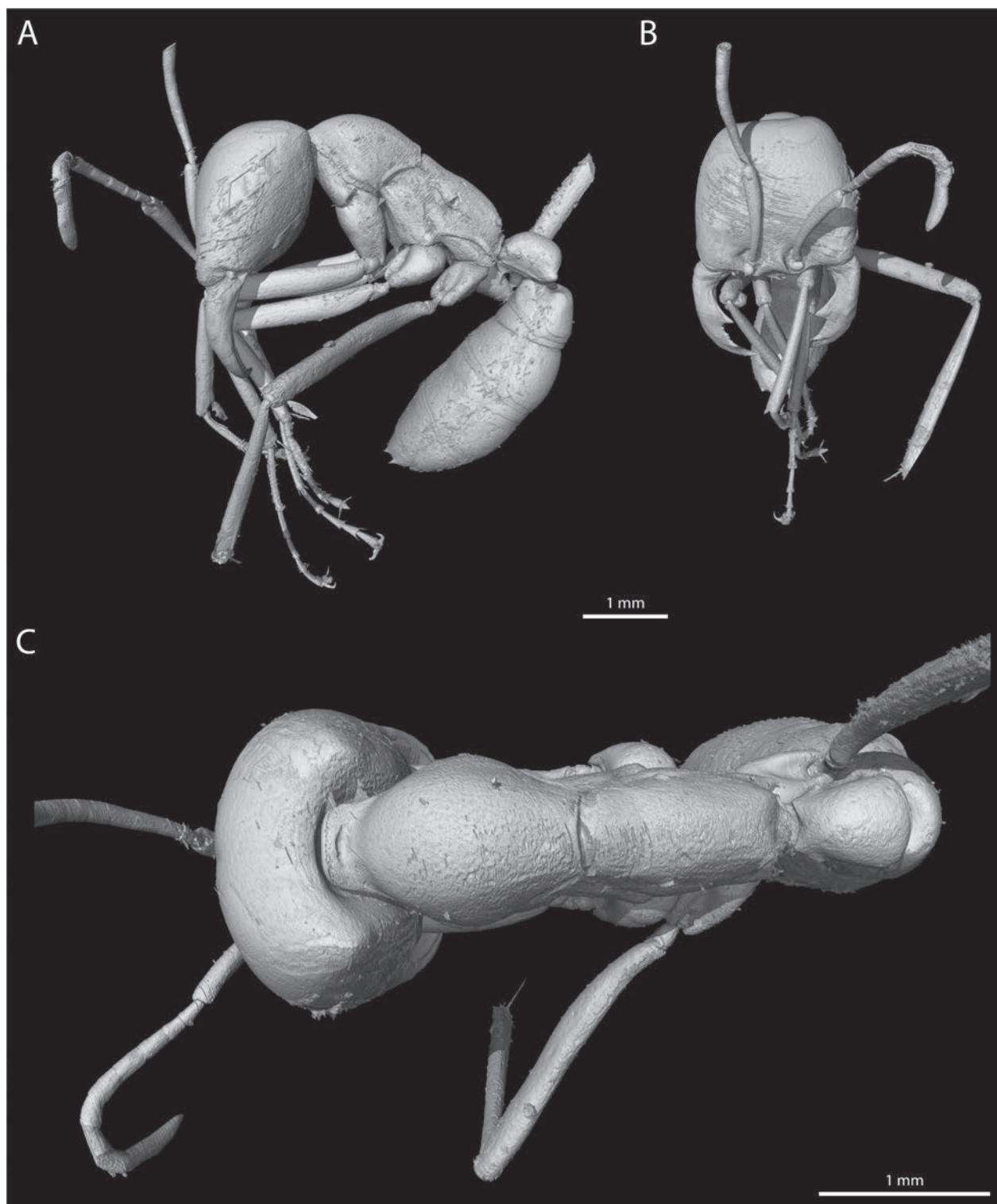


**Figure 3.** A–C. 3D reconstruction of *Dorylus nigricans molestus* (Formicidae: Dorylinae) preserved in piece PMJ Pa 5884. **A.** Habitus lateral; **B.** Habitus frontal; **C.** Habitus dorsal. See section 4.2.1 below for diagnostic remarks.

**Diagnosis.** Macropterous. Wings and body covered with scales. Scales apically straight or medially incised. Epistomal sulcus complete and corresponding epistomal ridge wide. Genae long. Vertex narrow and rounded. Three ocelli of similar size present, forming an isosceles triangle. Lateral ocelli closer to each other than to compound eyes. Compound eyes large and their upper mar-

gin reaching uppermost margin of vertex. Antenna with 15 articles. Flagellomeres with secondary annulation. Maxillary palps with four articles, a minute basal article and a long and cylindrical last palpomere that is rounded distally. No conical sensillum visible on second maxillary article. Tip of lacinia with long lateral region bearing several rounded denticles, and a shorter truncated median

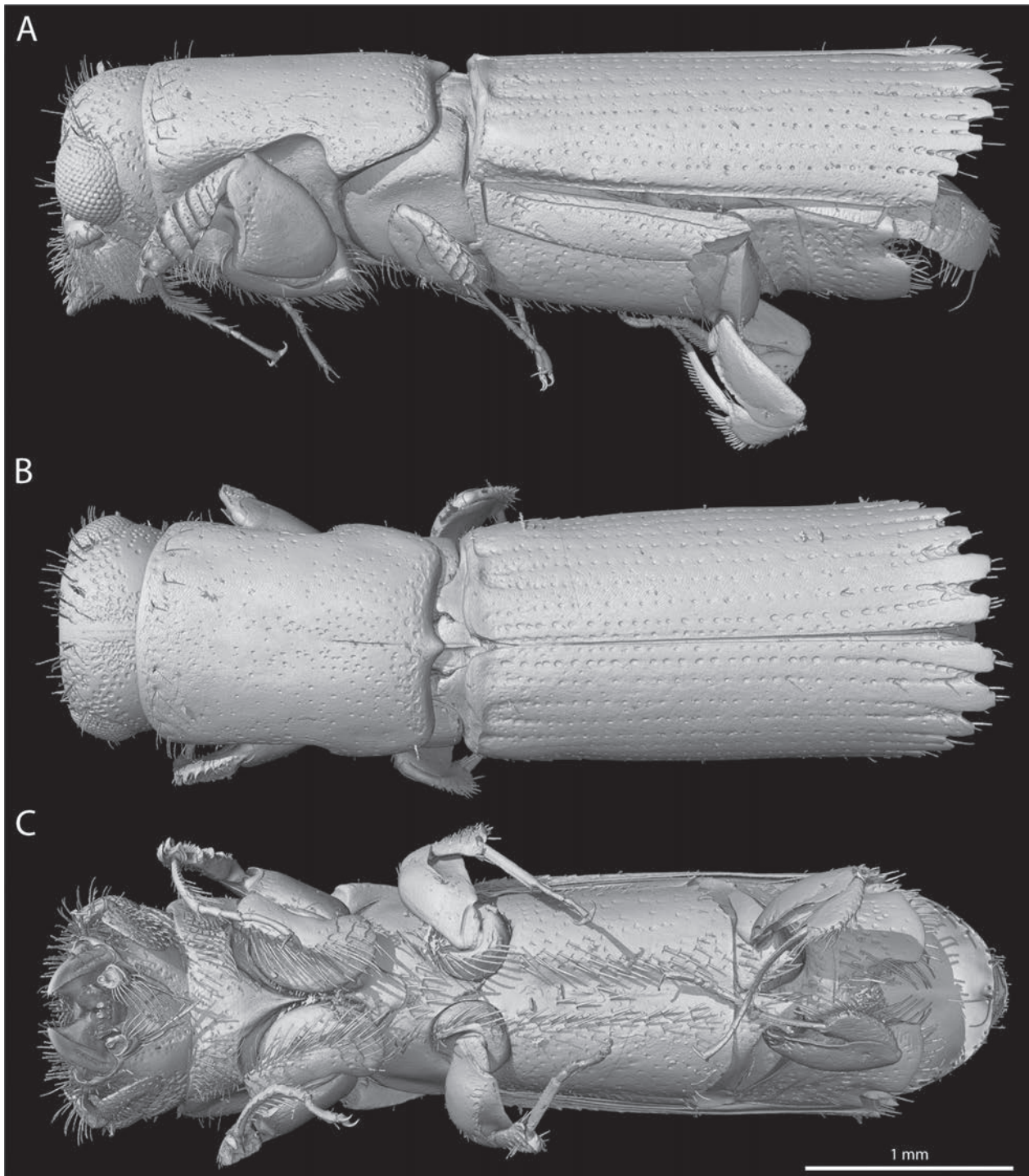


**Figure 4.** 3D reconstruction of *Doliopygus* cf. *serratus* (Curculionidae: Platypodinae) preserved in piece PMJ Pa 5827. **A.** Habitus lateral; **B.** Habitus dorsal; **C.** Habitus ventral.

tine. Water-vapor absorption-apparatus on hypopharynx present. Labial palps with 2 articles, the basal one short and small, the distal one large, round and flattened. Pronotum strongly reduced, barely visible dorsally as mesonotum exceeds its height. All tarsi with 3 articles. First tarsomere of hind leg very long, with 24 ventral ctenid-iobothria. Claws with 1 minute preapical tooth and small ventral subapical microtrichia. Pulvilli absent. Metacoxal interlocking mechanism present. Profemur with at least

27 small spines. Tibiae with horizontal rings of brown scales. Protibia equipped with only 1 distinct apical spur. Mesotibia with 3 long apical spurs. Metatibia with 6 (3 long and 3 short) apical spurs. Unique scale patterning on forewing present, differentiating it from related species. Anteroproximal region of forewing densely covered with dark brown scales. Distal part of Sc in forewing present, closing pterostigma proximally. Rs and M connected by cross vein in forewing. Areola postica of triangular shape

and distinctly longer than high. CuP and A1 do not fuse at forewing margin. Tip of R1 vein of hindwing reaching anterior wing margin. Proximal section of Rs in hindwing absent, basiradial cell open. Hindwing with simple M vein. Conspicuous color patterning on abdomen with pale spots on darker brown patches. Clunium unmodified. Epiproct and paraproct simple, the latter with inconspicuous sensorium. Subgenital plate simple and rounded apically with long setae. T-shaped sclerite not visible. Valvulae largely hidden by subgenital plate, but all three pairs present and external valve bilobed.

**Description. Measurements** (in mm): Body length: 3.7. Head length: 1.4 (labrum–vertex). Head width: 1.2 (between compound eyes). Length of antennae: 2.21. Length of scape: 0.10. Length of pedicel: 0.10. Length of flagellomeres: f1 = 0.29, f2 = 0.27, f3 = 0.23, f4 = 0.26, f5 = 0.18, f6 = 0.15, f7 = 0.11, f8 = 0.12, f9 = 0.09, f10 = 0.10, f11 = 0.06, f12 = 0.09, f13 = 0.07. Length of maxillary palpomeres: I = 0.06, II = 0.24, III = 0.14, IV = 0.22. Length of thorax: 0.90. Length of forewings: 3.9. Width of forewings: 1.4 (largest width). Length of hindwings: 2.8. Width of hindwings: 1.0. Length of hindlegs: F = 0.93, T = 1.54, t1 = 1.03, t2 = 0.15, t3 = 0.15. Length of abdomen: 2.2. Length of subgenital plate: 0.78. Length of epiproct: 0.24. Length of paraproct: 0.3.

**Note.** Different measurements based on photos or renders result from the strong curvature of different body parts. Therefore, we used the 3D reconstructions for most measurements and the photos for measuring the length of metatarsomeres and the forewing.

**Indices** (measured from dorsal, after Lienhard 1998): IO/D: 1.21. PO/D: 0.73.

**Coloration.** Head capsule dark brown. Postclypeus with few small darker spots. Labrum brown, slightly darker than rest of head. Antennal flagellum light brown to middle brown, becoming brighter distally. Maxillary palpomeres dark brown with apical regions of articles 2 and 3 lighter in coloration. Labial palpomeres light brown with dark spot on central area of flattened surface of palpomere 2. Compound eyes light brown, with darker circular areas of pigmentation. Ocelli dark brown, but median ocellus slightly brighter. Thorax slightly darker in color than head. Legs brown, less strongly pigmented apically. Forewing membrane of light brown tone, brighter towards apex. Hindwing almost hyaline, slightly more yellowish to brownish towards base. Wing veins in light brown to brownish tone or almost hyaline. Abdomen with conspicuous pattern of pale ocher patches surrounded by dark brown areas. Subgenital plate nearly uniformly dark brown, but lateral base paler. Ovipositor valves light brown with slight yellowish tint. Scales light brown to dark brown, with tips generally darker than base. Color patterns of head, compound eyes and abdomen possibly faded and with artifacts, due to non-ideal preservation in resin and subsequent suboptimal storage.

**Head capsule.** The head is distinctly higher than wide and anteroposteriorly flattened, thus appearing almost scale shaped. In dorsal view it appears wider than long.

The vertex (Figs 5A, 6B, 7A, ve) is narrow and rounded, while the frontal area is relatively large (Figs 5A, 6A, 7A, B, fr). In frontal view, the dorsal margin of the vertex is almost straight with only a very slight concave impression laterad the median line. Three ocelli (Fig. 6A, oc) are placed flat on the frons and vertex without a cuticular elevation, closer to each other than the lateral ocelli to the compound eyes. The median ocellus is slightly smaller than the lateral ones. The ovoid and relatively large compound eyes are not extending over the upper margin of the head, with a wide distance between them. The circumocular ridge (Figs 8A, B, 9, cor) is well-developed and wide, forming an oval that is slightly curved inwards on its posterior side. Externally, a conspicuous coronal sulcus (Fig. 6B, cs) is discernable, corresponding with the well-developed internal median coronal ridge (Figs 8B, 9, cr). The frontal sutures are present but indistinct. The external epistomal sulcus (Figs 5A, 6A, 7A, B, 10A, eps) is complete and semi-oval, with the postclypeus (Figs 5A, 6A, 7A, B, 10A, pcl) extending ventrally over the ventral genal margin. The large postclypeus is not strongly convex or bulging but rather scale-like. It is approximately twice as long as the frons. Two slit-like impressions begin on the ventral end of the postclypeus slightly laterad the midline and run in an acute angle approximately towards the postclypeal midlength where they obliterate. The internal epistomal ridge (Figs 8A, B, 9, epr) is wide (epistomal ridge in sagittal section longer than half of the length of the entire postclypeus, Fig. 8A, B). The anteclypeus (Figs 6A, 7A, B, 10A, acl) is relatively small and more than 4 times as wide as long, wider proximally than the ventral margin of the postclypeus and enveloping parts of it. The anterior tentorial pits (Fig. 7A, B, atp) are visible directly at the ventral margin of the epistomal ridge, almost adjacent to the anterior mandibular articulation. The posterior tentorial pits dorsad the insertion of the maxillary stipes to the head capsule are slit-like (visible in  $\mu$ CT scan). The well-developed tentorium is composed of large anterior (Figs 9, 11I, ata) and posterior arms (Figs 9, 11I, pta), a narrow corpotentorium (Figs 9, 11I, ct) and thin dorsal arms (Figs 9, 11I, dta). The anterior arms are anteriorly twisted and do not fuse with each other posteriorly. The very thin dorsal arms are not entirely preserved. The right dorsal arm is ending before it reaches the antennal insertion, while the left arm is almost completely missing in the specimen. The corpotentorium is compact and short and the posterior arms straight and thick. A well-developed postoccipital ridge (Fig. 9, por) and external postocciput form the posteriormost cephalic region. The head is posteriorly open, i.e., no genal-, hypostomal- or postgenal bridge or gula is developed but the posteroventral closure of the head is formed by the weakly sclerotized postmentum (Fig. 9, pom).

**Head appendages.** The lobe-shaped labrum (Figs 6A, 7A, B, 10B, 11A, B, lb) is approximately 2-times as wide as long and covered with long setae (likely sensilla) (Fig. 10B). It is narrower at its base and apex and widest at about midlength. A median notch is missing,

and the distal margin evenly rounded. The labral nodes are absent and epipharyngeal sensilla are not visible. A median transverse epipharyngeal fold (Fig. 11B, eptf) is present on the middle region of the epipharynx. The antennal insertions are located in a fovea (Fig. 7A, B, gef), which partly separates the genal region from the frontal region. The genal area is almost twice as long as the frontal area. The internal genal ridge below the fovea is straight (Figs 8A, 9, ger) and increases in thickness posteriorly. It starts shortly behind the posterior end of the ridge enclosing the antennal foramen and ends at the posterior genal region. It corresponds externally with the straight genal sulcus (Fig. 7A, B, ges). The antennae have 15 articles. The barrel-shaped scape and pedicel are approximately as long as wide. All flagellomeres display a secondary annulation (Fig. 5F). The last flagellomere is relatively short and pointed apically. The entire flagellum is very thin and thread-like, with the flagellomeres approximately 1/3 as wide as the pedicellus. The setae on the flagellum are long and thin, slightly thicker and longer on the lateral surface compared to the medial side. The basal portion of the flagellomeres is only faintly differentiated (Fig. 5F), and a proper collar is not developed (see Seeger 1975). The mandibles (Figs 7A, B, 9, 11C, D, md) are subtriangular with similar lengths of the mesal and lateral edges. They are not elongated and of the “outer margin rounded, and posterior margin not hollowed” type (Yoshizawa 2002). The lateral edge is convex over its entire length. The molar region (Fig. 11C, D, mo) is asymmetric, with a distal molar tooth (Fig. 11C, D, mot) on the left mandible. The right mandible has a proximal tooth-like extension (Fig. 11C, D, pmdt). The inner mandibular rim has no distinct features differentiating it from mandibles of other psocids. It is thickest on its median side and becomes narrower laterad. The lateral side of the mandibular rim between the posterior condyle (Fig. 11C, D, pcmd) and anterior socket (Fig. 11C, D, asmd) (primary and secondary mandibular joints) widens. Two apical teeth (incisivi) are present, the apical one (Fig. 11C, D, inc1) longer and wider than the subapical one (Fig. 11D, inc2). Slightly proximad of the incisivi a blade-like projection is present, a convex cutting edge (Fig. 11C, D, mdce). A postmola is not discernible. The apodeme of the mandibular adductor (Fig. 9, amdad), at least partially preserved, inserts on the medial base of mandible. The maxilla lacks a cardo. The stipes (Fig. 7B, st) is oval and represents the main body of the maxilla, together with the apical palpifer (Fig. 7B, ppf). The galeae (Fig. 7A, B, ga) are relatively flat and located between the mandibular concavity anteriorly and the hypopharynx posteriorly (visible in  $\mu$ CT-scan). The tip of the lacinia (Figs 11F, 12I, lc) is long and bears several rounded denticles. It is bent laterad apically. The inner tine is short and bent slightly inwards distally. The outer tine is distinctly longer and higher. The lacinial gland is not preserved or not present. The maxillary palps (Figs 6A, 11E, mxp) consist of four articles. The second article is the longest, ca. 1.3 times as long as the fourth and ca. 2 times as long as the third.

The first article is extremely short and only  $\frac{1}{4}$  as long as the third. Several long setae (likely sensilla) are located on each palpomere except for the glabrous first one. The second maxillary palpomere lacks a conical sensillum. The fourth palpomere is conical and has a rounded apex. The hypopharynx (Fig. 9, hy) is equipped with the anterior sitophore (Figs 9, 11G, sit) and the paired posterior salivary sclerites (Figs 9, 11H, sas). A triangular median extension of the sitophore (Fig. 11G, mesit) is present proximad the mortar, which is (Fig. 11G, mor) is oval and embedded in the sitophore like in a sclerotized block. The oral arms of the sitophore are present but indistinct in the  $\mu$ CT-scan. The paired salivary sclerites are lateral elements of the posterior hypopharynx, ovoid and bowl-shaped. They bear a long apodeme (Fig. 11H, asas) which is long and curved inwards at its internalmost apex. A furrow runs longitudinally (Fig. 11H, lfsas) across each salivary sclerite. The tubular filaments between the sitophore and salivary sclerites are not visible (a resolution of 2  $\mu$ m is not sufficient for visualizing the very thin tubular filaments, which have a diameter of ca. 3  $\mu$ m in a large psocid (von K ler 1966) and connect the longitudinal furrow of the posterior salivary sclerites with the anterior hypopharyngeal mortar), but are likely developed, as the water-vapor absorption apparatus functionally depends on their presence. The labium is composed of a thin-walled and weakly sclerotized postmentum (Fig. 9, pom) and a thicker-walled prementum (Fig. 9, prm). A median furrow separates symmetrical premental halves (see Fig. 11J). The labial palps (Fig. 11J, lap) have two articles. Palpomere 1 (Fig. 11, lap1) is short and narrow, and palpomere 2 (Fig. 11, lap2) plate-like, large and rounded, and displays a darkly pigmented field. The second palpomere bears many long setae (likely sensilla), that are concentrated on the margin. The short and rounded paraglossae (Figs 6A, 11J, pgl) are inserted between the palps. The glossae (Figs 6A, 11J, gl) are probably represented by lobe-shaped structures, almost fused medially, with only a faint medial dividing line. Remnants of soft tissue are visible in the head, which are likely vestiges of the central nervous system, retinulae and possibly the mandibular adductor muscle, as well as other cephalic muscles.

**Thorax.** The cervical region is not exposed. The laterocervical sclerite is indistinctly visible as a thin bar-shaped sclerite, but scarcely discernible from the cervical membrane in the renders. The prothorax is strongly reduced. The pronotum (Fig. 8A, B, prn) is very short and bar-shaped, and the propleurae (Appendix 1: Fig. A3) are continuous with it laterally. The relatively large episternum is located dorsad the small preepisternum (Appendix 1: Fig. A3) and separated from it by an external furrow (Appendix 1: Fig. A3). The mesothorax exceeds the height of the pronotum (Figs 6B, 7A, B, 8A, B). The mesonotum (Figs 6B, 7A, B, 9A, B) is strongly enlarged and dorsally densely covered with scales (Figs 5A, 6B). A prophragma is not developed or extremely reduced. The mesonotum consists of an anterior semicircular part of the scutum,



**Figure 5. A–H.** Photography of †*Amphientomum knorrei* sp. nov. preserved in piece PMJ Pa 5809. **A.** Habitus in dorsofrontal view; **B.** Habitus in ventrocaudal view; **C.** Right metafemur and -tibia in posterior view, rings of brown scales on metatibia; **D.** Distal portion of left hindleg with claw, arrow indicates preapical tooth; **E.** Basitarsomere of hindleg, arrows indicate ctenidiobothria; **F.** Right antennal flagellum, flagellomere 5, arrows indicate secondary annulation; **G.** Scales, arrow indicates scale type III; **H.** Tip of right hindwing with scales, arrows indicate scale type I and II.

larger paired lateral scutal lobes, and a posterior triangular scutellum (Fig. 6B). The anterior scutal portion is separated from the lateral lobes by the lateral parapsidal sulci (Fig. 6B), which correspond with internal parapsidal ridges

(Fig. 8A, B, parr). The postnotum is located posteroventrad the scutellum as a bar-shaped short sclerite (Fig. 6B). The mesophragma (Fig. 8A, B, msp) is wide and strongly developed. The scutoscutellar suture (Fig. 6B) is present,



**Figure 6.** A–C. 3D-reconstruction of †*Amphientomum knorrei* sp. nov. **A.** Habitus in frontal view; **B.** Habitus in dorsal view; **C.** Habitus in ventral view. Abbreviations: acl = anteclypeus, cs = coronal sulcus, gl = glossa, lap = labial palp, lb = labrum, mxp = maxillary palp, oc = ocellus, pcl = postclypeus, pgl = paraglossa.

albeit somewhat weakly developed. The metathorax is distinctly shorter than the mesothorax. The anterior and lateral lobes of the scutum are not separated by an external furrow, whereas a distinct scutoscutellar line delimits the small, rounded scutellum. The metaphragma (Fig. 8A, B, mtp) is wide but smaller than the mesophragma. As the pleural elements of the specimen appear asymmetric on

both sides and as there are many artifacts in the 3D-model, we will not describe this thoracic region in detail. The external sternal elements of each thoracic segment are not discernible from surrounding membranous regions. The profurcae (Fig. 8A, B, prf) are only indistinctly recognizable, whereas the meso- and metafurcae (Fig. 8A, B, msf, mtf) are distinctly visible as distally widened and

flattened arms. Spinae of the meso- and metathorax are absent. The three pairs of coxae are adjacent medially. The profemur bears at least 27 ventral spines (Fig. 10C). The protibia bears one, and the mesotibia three apical spurs. The metatibia displays three short and three long apical spurs. All tarsi are 3-segmented. Metatarsomere 1 bears 24 ctenidiobothria (Fig. 5E). Tarsomere 1 of the foreleg and hindleg are almost 3 times as long as the respective tarsomeres 2 and 3 combined. The very long metatarsomere 1 reaches ca.  $\frac{3}{4}$  of the length of the metatibia. Mesotarsomere 1 is approximately twice as long as mesotarsomeres 2 and 3 combined. Two apical ventral spurs are inserted on tarsomeres 1 and 2 of each pair of legs. The symmetrical claws are equipped with a single small preapical tooth (Fig. 5D) and several ventral microtrichia proximad this structure. Pulvilli are absent. The mirror and rasp substructures of the Pearman's organ are absent. A distinct ball-shaped cuticular projection (Fig. 12A, B, hcp) on the inner side of the left metacoxa is visible, fitting with a cup-shaped emargination (Fig. 12A, B, hce) on the inner side of the right metacoxa. The legs, especially the femora and tibiae, are densely covered with scales. Several closely placed somewhat irregular rings of these surface structures are inserted on the metafemur (Fig. 5C).

**Forewing.** Wing with three types of scales. First type long, parallel-sided, straight and with a straight apex (Fig. 5H). Second type long (slightly to distinctly shorter than type one), parallel-sided to subparallel and straight, emarginate with a median notch (Fig. 5H). Third type short, broad, parallel-sided from  $\frac{2}{5}$  to apex of scale, and converging in the basal  $\frac{1}{5}$ , with a straight and finely frayed apex (Fig. 5G). The wing scales display a longitudinal striation except for type I where this is not visible. The scale patterning is very distinct, with an increased density at the wing base, differentiating it from related species (Figs 5A, B). The proximal Sc vein is very short and ends freely in the wing membrane. A line of dark scales follows approximately this vein. R1 merges at  $\frac{2}{3}$  of the wing length with the anterior margin. A short and anteriorly bent distal Sc vein closes the pterostigma. This triangular cell displays a strongly acute angle between Sc and R1 and is wide (600  $\mu\text{m}$ ) but very low (110  $\mu\text{m}$ ). The base of Rs forms an obtuse angle with the distal portion of this vein. The basal vein of Rs is almost transparent, and dorsally bears a patch of dark scales. The veins R2+3 and R4+5 are convex almost over their whole length, and M1 is curved distally. M2 is almost straight. M3 is concave distally. The origins of all three M veins are placed close to each other, almost forming a fork. The specimen displays a slight asymmetry in the base of the three M veins. On the right forewing, they originate from a common stem, while M1+M2 are connected in left one but both separated from the base of M3. A conspicuous acuminate lobe is present between M1 and M2, and a short cross vein between Rs and M (90  $\mu\text{m}$ ). The areola postica is relatively wide and low and forms a triangle with an acute angle between CuA1 and CuA2. CuP and A1 join the posterior wing margin at a distance from each other

(Fig. 10D). The course of the very faint vein A1 is almost invisible due to the coupling of the fore- and hindwing on both sides. The vein A2 is indistinct.

**Hindwing.** Type I and II scales are present (Fig. 5H). No closed cell is present in the hindwing (Figs 5A, B). R1 and CuA are ending at approximately  $\frac{2}{3}$  of the total wing length, the former on the anterior margin and the latter on the posterior margin. Only one M vein is present. The common veins R2+3 and R4+5 are slightly shorter than half the length of M. R2+3 end anteriorly on the margin in the last  $\frac{1}{5}$  of the wing length. R4+5 ends almost directly on the wing apex, and M almost at the same length as R2+3 but on the posterior margin. Rs is bent anteriorly where it forms a cross vein with R1 in other *Amphientomum* species, but any trace of this cross vein is lacking. CuA is curved at its distal end. The distance between CuA and CuP is approximately equivalent with the length of Rs. A1 is curved and ends on the basal posterior wing margin. The margin of the apical half is covered with long scales and setae, the latter more densely anteriorly.

**Abdomen.** The abdomen is strongly bent towards the thorax (Figs 5A, B, 7A, B). The external segmentation of the abdomen is only partially visible, as some segmental borders are very faint or deformed as an artefact. However, it seems to follow the general pattern in Psocodea (Badonnel 1934) without any conspicuous modifications. The clunium (Fig. 10E, clu), the epiproct (Figs 8B, 10E, epp) and the paraproct (Figs 8B, 10E, pap) are unmodified, the latter covered with long setae and bearing an indistinct sensorium. The apex of the subgenital plate is simple and covered by long setae. The subgenital plate largely covers the ovipositor valves, thus only the tips are exposed (Figs 5B, 6C, 7C). The external valve (Fig. 10F, exv) is bilobed, the dorsal portion wider but not as long as the ventral portion, which is pointed apically. The dorsal valve (Figs 7C, 10F, dov) is almost tubular and apically rounded. The ventral valve (Fig. 10F, vev) is barely discernible but present as an elongated tube.

**Remarks.** “Die Art und Weise der Lagerung und Erhaltung der Stücke im Bernstein erlaubt den Schluß, daß diese Art wesentlich wilder und beweglicher gewesen sei als die übrigen Psocen, dabei aber zugleich weniger derb gebaut. Daß bei den sichtlich starken Anstrengungen der Thiere, dem Harz zu entgehen, das Schuppenkleid oft stark abgerieben wurde, ist leicht begreiflich und durch mitunter massenhaft danebenliegende Schuppen bewiesen. Aber auch die Endglieder der Fühler sind mitunter beim Vordrängen des Thieres abgetrennt, und die obere Membran der Flügel ist zuweilen von der offenbar fester dem Harz anhängenden unteren Membran getrennt, und beim Vordrängen des Thieres in regelmäßige kleine Querfalten gebracht.” – Hermann Hagen's (1882) commentary about the preservation of *Amphientomum* specimens in Baltic amber.

‡*Amphientomum knorrei* Weingardt, Bock & Boudinot, sp. nov. (Troctomorpha: Amphientometae: Amphientomidae) represents the first record of this family and genus in East African copal ( $^{14}\text{C}$  date:  $\sim 390 \pm 13$  years

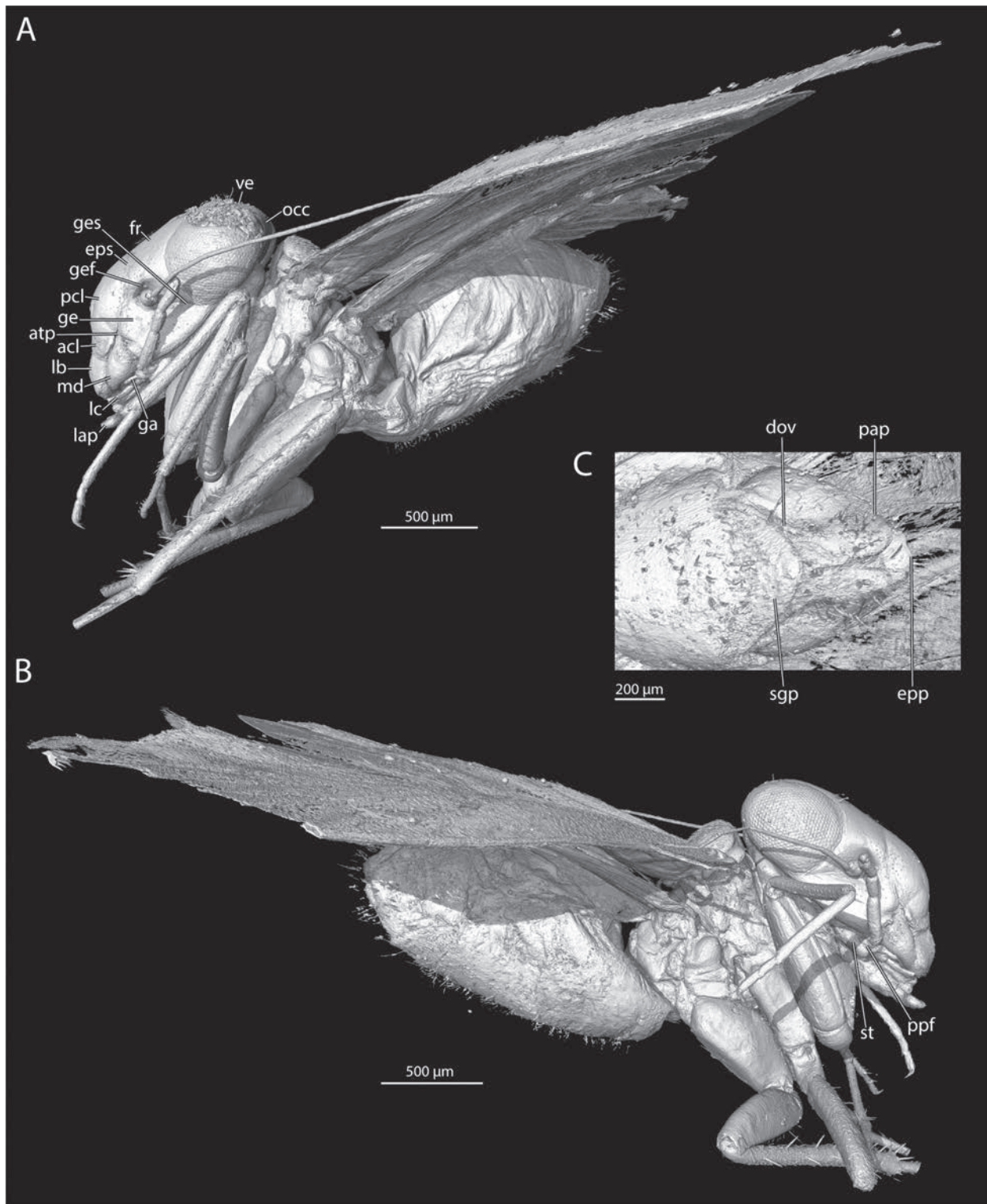


**Figure 7.** A–C. 3D-reconstruction of †*Amphientomum knorrei* sp. nov. **A.** Habitus in left lateral view; **B.** Habitus in right lateral view; **C.** Subgenital plate in ventral view. Abbreviations: acl = anteclypeus, atp = anterior tentorial pit, dov = dorsal valve, epp = epiproct, eps = epistomal sulcus, fr = frons, ga = galea, ge = gena, gef = genal fovea, ges = genal sulcus, lap = labial palp, lb = labrum, lc = lacinia, md = mandible, occ = occiput, pap = paraproct, pcl = postclypeus, ppf = palpifer, sgp = subgenital plate, st = stipes, ve = vertex.

old) and may still be extant in East Africa. The genus *Amphientomum* is known from the lowermost Eocene amber of Oise in France and is at least 56.0–47.8 Mya (Nel et al. 2005) old. In total, 20 species are described including the new one presented here (Table 5). Today

they occur in countries of Western (Ivory Coast, Nigeria), Central (Angola, Republic of the Congo) and Eastern Africa (Madagascar, Tanzania) (Lienhard 2016; Johnson et al. 2023), and one additional species is described from China (Li 1999, 2002). Four species are known from the

fossil record, two, as previously listed, were described by Enderlein (1905), and one by Pictet (1854) from Baltic amber. Additionally, one species was described from French Eocene Oise amber by Nel et al. (2005). The subfossil described here is a female, as the subgenital plate and the apical tips of the valvulae are visible. It differs from all other described species of *Amphientomum* by its characteristic forewing scale pattern.

Only one species has been assigned to *Amphientomum* outside of Africa and Eurasia, *Am. indentatum* Turner, 1975, from an extant population in Jamaica. However, this species is definitely misplaced, as several features of it are not compatible with the currently accepted diagnostic character repertoire of *Amphientomum* (see Taylor 2013 for an identification key of the genera of Amphientomidae), i.e., the lateral ocelli are widely spaced and close to the compound eyes, and the hind wing vein R1 does not reach the wing margin. Given these characters, the species in fact matches with *Lithoseopsis* Mockford, 1993 (Mockford 1993; Taylor 2013). Taylor (2013) proposed a smoothly rounded distal forewing margin as a diagnostic character of this genus. In contrast, *Am. indentatum* displays a characteristic indentation at the tip of the forewing, as reflected by the species name. However, the tips are not acuminate as in ‡*Am. knorrei* sp. nov., similar to other species in *Lithoseopsis* (see Taylor 2013). Based on these observations, we propose a new taxonomic combination: *Lithoseopsis indentatum* (Turner, 1975) comb. nov. By excluding *L. indentatum* from the genus *Amphientomum*, this is now restricted to the Afrotropics and Palearctic (see Table 5). The number of described species of *Lithoseopsis* is hereby increased to 12 (Johnson et al. 2023). Broadhead and Wolda (1985) mentioned the occurrence of three different species of the subgenus *Amphientomum* (*Palaeoseopsis*) in Panama. However, they remain undescribed and no details besides the collecting information are known. It is conceivable that these specimens do not belong to *Amphientomum*, similar to the previously stated case.

As the basal section of Rs is absent in the hindwing of ‡*Am. knorrei* sp. nov. (Fig. 13A), the species can be assigned to the subgenus *Amphientomum* (*Palaeoseopsis*) in the system of Roesler (1944). The shape of scales is arguably not a good diagnostic feature, as several types of scale shapes can occur in a single specimen. Emarginate scales are present in ‡*Am. knorrei* sp. nov. (type II scales, Fig. 5H), a diagnostic character of the subgenus *Am. (Amphientomum)* after Roesler (1944), but there are also scales with an evenly truncated (type I scales, Fig. 5H) or a frayed (type III scales, Fig. 5G) apical edge, a diagnostic criterium for *Am. (Palaeoseopsis)*. On the other hand, Enderlein (1911) introduced evenly truncated scales as diagnostic character for *Am. (Amphientomum)*, while scales with a median notch are characteristic for *Am. (Palaeoseopsis)*. It is likely that Roesler (1944, p. 138) was mistaken in the characterization of both subgenera. As the polarity of the presence or absence of the basal section of Rs in the hindwing is unknown, the subgenus

*Am. (Palaeoseopsis)* is possibly not monophyletic. All species except for †*Am. leptolepis* and †*Am. paradoxum*, both described from Baltic amber, have a reduced basal section of Rs in the hindwing (Table 5). Several species, such as *Am. loebli* and *Am. pauliani* (Table 5), also have a vestigial basal section of Rs, but it is never fused with R1. Given these problematic definitions, we synonymize *Palaeoseopsis* under *Amphientomum* syn. nov. and consequently remove the subgeneric rank from *Amphientomum* pending future study.

**Table 5.** All currently described species of the genus *Amphientomum*. It is uncertain whether ‡*Am. knorrei* sp. nov. is extant. The type species of *Palaeoseopsis* is bolded and that of *Amphientomum* is bolded and in cells with grey shading.

#	Taxon	Authors	Distribution
<b>I</b>	† <i>Am. colpolepis</i>	<b>(Enderlein, 1905)</b>	<b>Baltic amber</b>
II	‡ <i>Am. knorrei</i>	Weingardt, Bock & Boudinot, 2024 sp. nov.	East African copal
III	† <i>Am. leptolepis</i>	Enderlein, 1905	Baltic amber
<b>IV</b>	† <i>Am. paradoxum</i>	<b>Pictet, 1854</b>	<b>Baltic amber</b>
V	† <i>Am. parisiense</i>	Nel, Prokop, De Ploeg & Millet, 2005	French Oise amber
1	<i>Am. acuminatum</i>	Smithers, 1964	Madagascar
2	<i>Am. Aelleni</i>	Badonnel, 1959	Republic of the Congo
3	<i>Am. annulicorne</i>	Badonnel, 1967	Madagascar
4	<i>Am. annulitibia</i>	Smithers, 1999	Tanzania
5	<i>Am. dimorphum</i>	Badonnel, 1967	Madagascar
6	<i>Am. ectostriolate</i>	Li, 1999	China
7	<i>Am. flexuosum</i>	Badonnel, 1955	Angola, Nigeria
8	<i>Am. hieroglyphicum</i>	Badonnel, 1967	Madagascar
9	<i>Am. loebli</i>	(Badonnel, 1979)	Ivory Coast
10	<i>Am. mimulum</i>	Badonnel, 1967	Madagascar
11	<i>Am. montanum</i>	Badonnel, 1967	Madagascar
12	<i>Am. pauliani</i>	Smithers, 1964	Madagascar
13	<i>Am. punctatum</i>	Badonnel, 1967	Madagascar
14	<i>Am. simile</i>	Badonnel, 1967	Madagascar
15	<i>Am. striaticeps</i>	Badonnel, 1967	Madagascar

Several characters of ‡*Am. knorrei* sp. nov. resemble features of *Am. acuminatum*, like the shape of the apex of the lacinia (see Fig. 12 for comparison of all available *Amphientomum* species), the apical lobe of the forewing (see Figs 13, 14 for comparison of all available *Amphientomum* species), as well as the claw with a single preapical tooth. Consequently, this species from Madagascar (Smithers 1964; Badonnel 1967) might be closely related with ‡*Am. knorrei* sp. nov. It differs from it by smaller size (body length = 2.1 mm, forewing length = 2.75 mm), the lower number of ctenidiobothria on the first tarsomere of the hindleg (21–22), the scale pattern on the forewings, and also the facial markings. As the origin of our piece of resin with the psocid inclusion is not fully clarified, the geographical distribution of ‡*Am. knorrei* sp. nov. remains uncertain. That the specimen is enclosed in East African copal imported to Germany during colonial times is suggested by several syninclusions, for instance the *Dorylus* in our present collection. The countries of origin of such pieces of resin are Tanzania, Mozambique, and

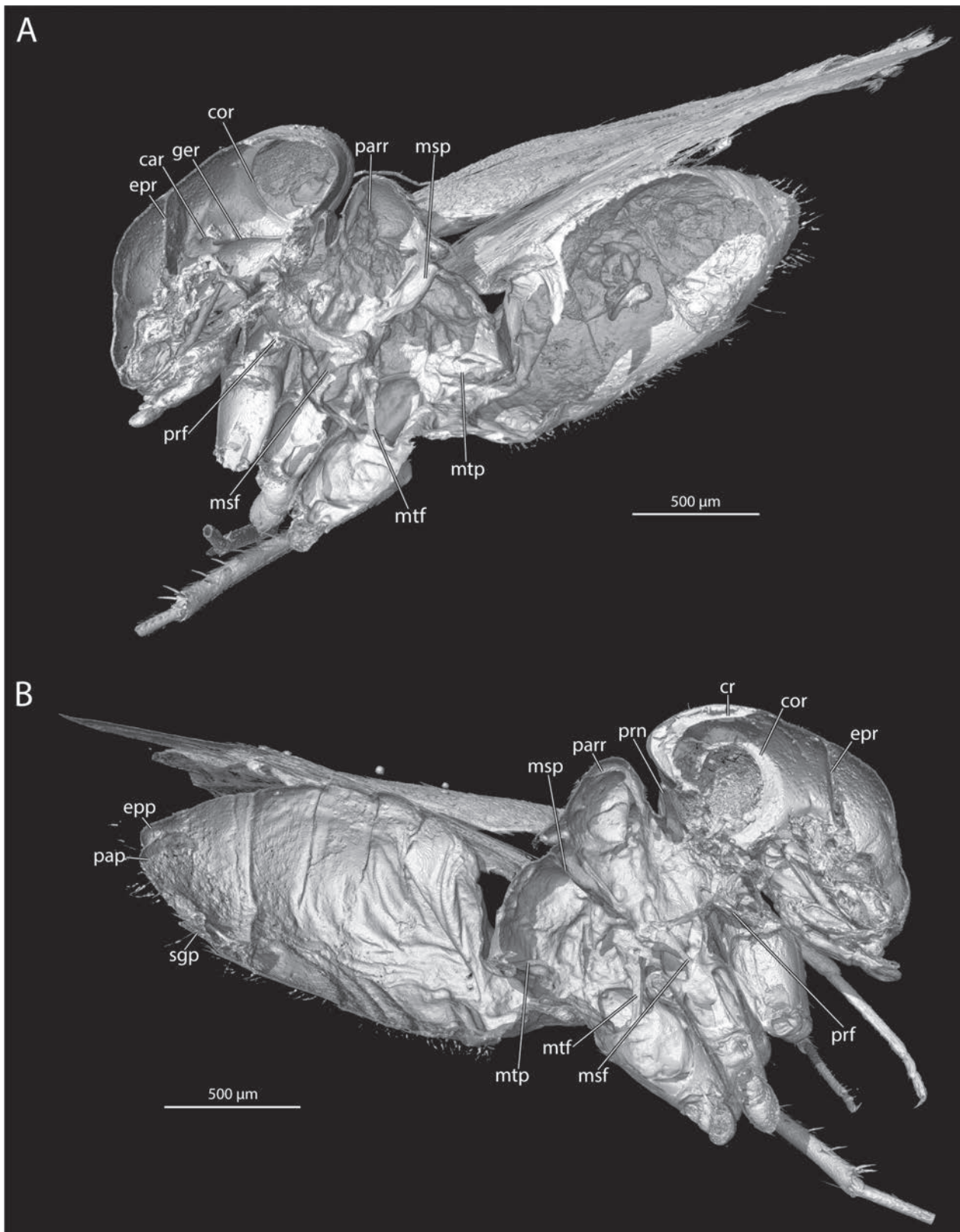


**Figure 8. A–B.** 3D-reconstruction of †*Amphientomum knorrei* sp. nov. **A.** Internal view from left side, sagittal cut; **B.** internal view from right side, sagittal cut. Abbreviations: car = circumantennal ridge, cor = circumocular ridge, cr = coronal ridge, epp = epiproct, epr = epistomal ridge, fl = foreleg, ger = genal ridge, hl = hindleg, lap = labial palp, lc = lacinia, ml = midleg, msf = mesofurca, msp = mesophragma, mtf = metafurca, mtp = metaphragma, pap = paraproct, parr = parapsidial ridge, prf = profurca, prn = pronotum, sgp = subgenital plate.

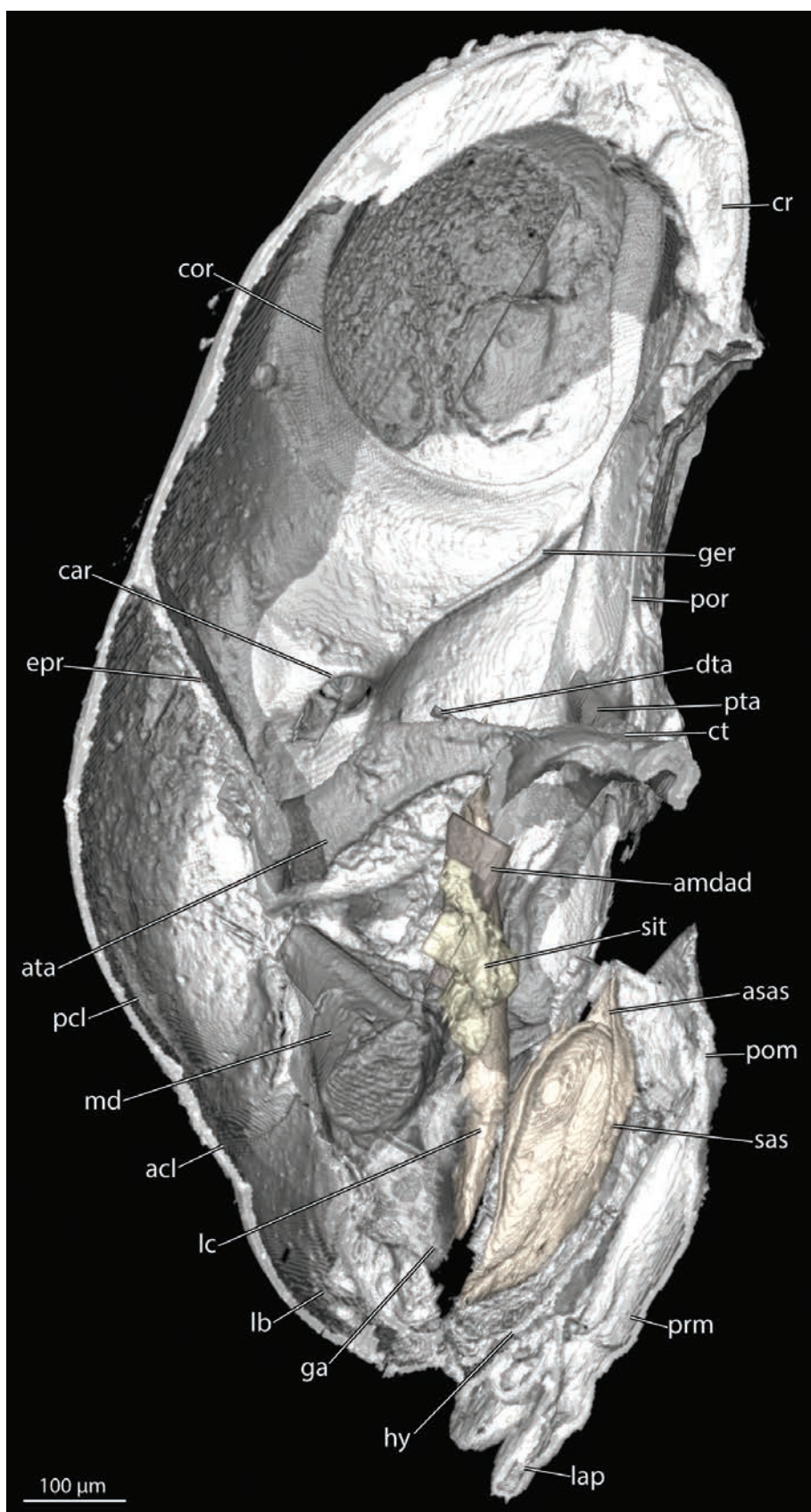


**Figure 9.** 3D-reconstruction of †*Amphientomum knorrei* sp. nov. Internal view of head from left side, sagittal cut. Abbreviations: acl = anteclypeus, amdad = apodeme of mandibular adductor, asas = apodeme of salivary sclerite, ata = anterior tentorial arm, car = circumantennal ridge, cor = circumocular ridge, cr = coronal ridge, ct = corpotentorium, dta = dorsal tentorial arm, epr = epistomal ridge, ga = galea, ger = genal ridge, hy = hypopharynx, lap = labial palp, lb = labrum, lc = lacinia, md = mandible, pcl = postclypeus, pom = postmentum, por = postoccipital ridge, prm = prementum, pta = posterior tentorial arm, sas = salivary sclerite, sit = sitophore.

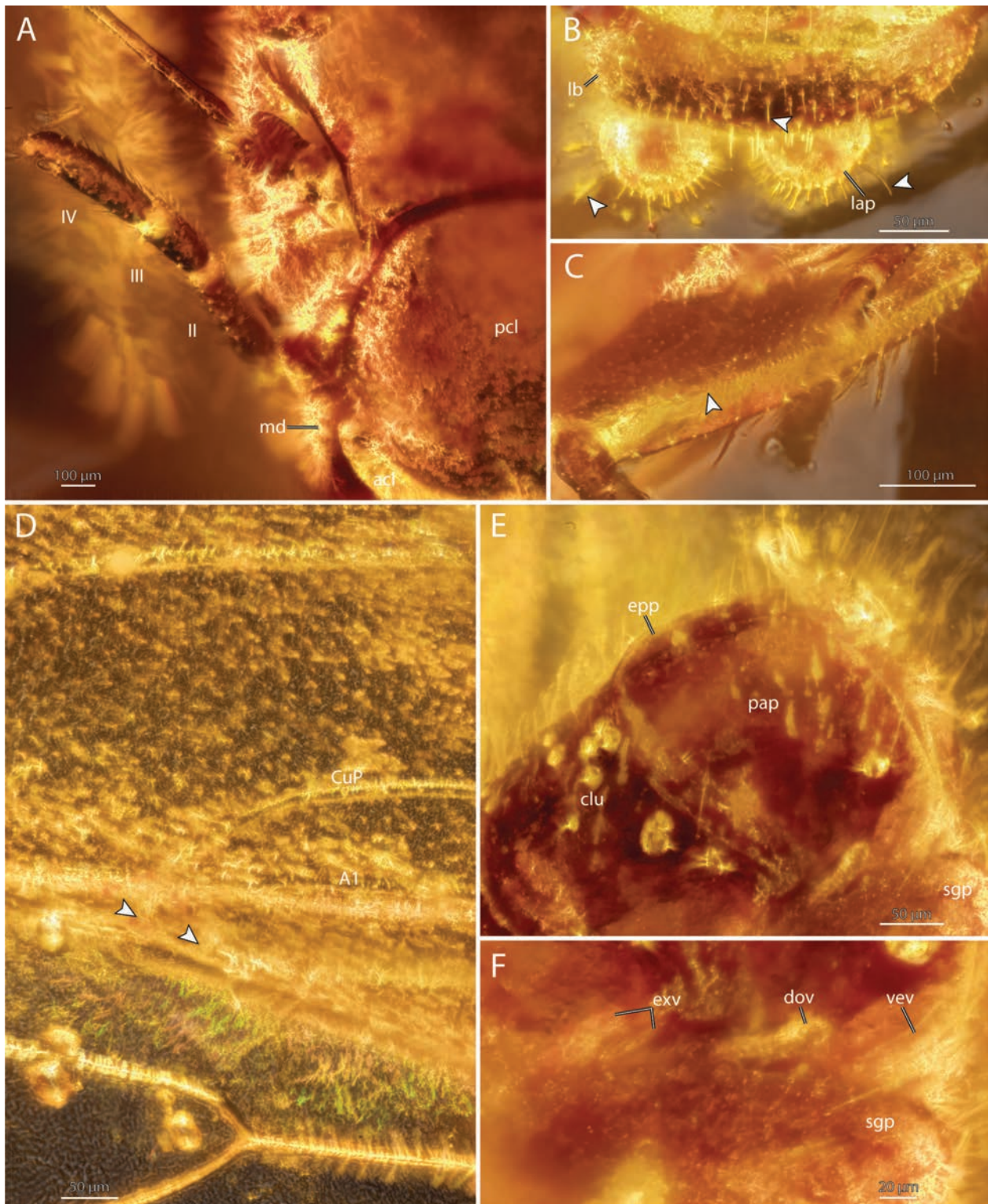


**Figure 10.** A–F. Photography of ♂ *Amphiptomum knorrei* sp. nov. **A.** Right maxillary palp and right portion of head in frontal view, numbers indicate maxillary palp article; **B.** Labrum and labial palps in dorsally inclined frontal view; **C.** Right foretibia in frontal view; **D.** Left fore- and hindwing in dorsal view, arrows indicate where the vein CuP and A1 meet the posterior forewing margin; **E.** Details of paraplect and clunium from lateral view; **F.** Details of ovipositor from ventrolateral view. Abbreviations: clu = clunium, dov = dorsal valve, epp = epiproct., exv = external valve, lap = labial palp, lb = labrum, md = mandible, pap = paraplect, pcl = postclypeus, vev = ventral valve.

Madagascar (Delclòs Martínez et al. 2020). It is therefore likely that *Am. acuminatum* and †*Am. knorrei* sp. nov. have a common distribution in East Africa, while the exact distribution of both species is still unclear.

Finally, an unsolved nomenclatorial issue concerning *Amphientomum ectostriolate* Li, 1999 requires clarification. In the Psocodea Species File (Johnson et al. 2023, date: 2023 August 17) the year of publication for this species is incorrectly listed as *Am. ectostriolate* Li, 2002 and the species *Am. ectostriolatis* Li, 1999 mistakenly listed as a valid taxon. We contend that the name should be *Am. ectostriolate* Li, 1999 based on the following reasoning: (1) The protonym, *Am. ectostriolatis*, was established and illustrated in the monograph on the Chinese Psocoptera (p. 199) by Li (2002); (2) the spelling was later emended by Lienhard (2003) to *Am. ectostriolate* Li, 1999, justifi-

ably so by Articles 19 and 34 of the ICZN (1999), with this emendation considered to be the original spelling by section 32.2; and (3) the name *Amphientomum ectostriolatum* Li, 2002 should be considered an unjustified emendation by Article 33, as the author spelled the name this way in the figure legend and twice in the text, indicating an intended name change, hence this name is available but should be a junior synonym of *Am. ectostriolate* syn. nov.

### ***Amphientomum ectostriolate* Li, 1999**

*Am. ectostriolatis* Li, 1999; original spelling; justifiably emended to *ectostriolate* by Lienhard, 2003: p. 699.  
= *Am. ectostriolatum* Li, 2002 [available unjustified emendation by Li, 2002], syn. nov.

## Identification key for all species of *Amphientomum* Pictet, 1854

The present key is modified after Badonnel (1967) using information from Enderlein (1911), Badonnel (1955, 1979), Smithers (1964, 1999), Li (1999, 2002), and Nel et al. (2005). Note that the species *Amphientomum aelleni* Badonnel, 1959 is excluded from the key as only the nymphal stage is described. This species, however, can be identified using an illustration of the unique coloration pattern of the head (Badonnel 1959, p. 763, fig. 1).

- 1 (A) Species only known from the fossil record. (B) Rs in forewing at a right angle to R1 ..... 2
- (A) Extant species or subfossil. (B) Rs in forewing at an obtuse angle (proximal angle) or almost a right angle to R1 ..... 5
- 2 (A) In Eocene French Oise amber. (B) Basal section of Sc in forewing long, more than half the length of R1 .....  
..... †*Am. parisiense* Nel, Prokop, De Ploeg & Millet, 2005
- (A) In Eocene Baltic amber. (B) Basal section of Sc in forewing short, less than half the length of R1 ..... 3
- 3 (A) Scales with an apicomedial notch. (B) Basal section of Rs missing in hindwing ..... †*Am. colpolepis* Enderlein, 1905
- (A) Scales apically straight. (B) Basal section of Rs present in hindwing ..... 4
- 4 (A) Scales short and broad, tapering proximally. (B) Tarsomere 1 of hindleg with 29–34 ctenidiobothria .....  
..... †*Am. paradoxum* Pictet, 1854
- (A) Scales long and narrow, parallel-sided over entire length. (B) Tarsomere 1 of hindleg with 36 ctenidiobothria .....  
..... †*Am. leptolepis* Enderlein, 1905
- 5(1) (A) Rs in forewing almost at right angle to R1. (B) Distributed in China ..... *Am. ectostriolate* Li, 1999
- (A) Angle between Rs and R1 in forewing distinctly obtuse (proximal angle). (B) Recorded from Africa ..... 6
- 6 (A) Proximal half of antennal flagellum with 4 white rings separated by three black-brown rings. (B) Additionally: proximal 2/3 of femora dark brown; tibiae with three dark brown rings; forewings very wide in relation to their length, their posterior margin strongly arched in the apical half ..... *Am. annulicorne* Badonnel, 1967
- (A) Antennal flagellum almost uniformly brown, without alternating white and dark rings. (B) Other characters variable ..... 7
- 7 (A) Compound eyes elevated or apparently raised above dorsal margin of vertex (frontal view) ..... 8
- (A) Compound eyes on same level as dorsal margin of vertex (frontal view) ..... 10
- 8 (A) Dorsal margin of vertex straight (frontal view). (B) In frontal view, lateral sides of dorsal margin curved downwards, so that compound eyes appear elevated above the rest of the dorsal margin ..... *Am. loebli* (Badonnel, 1979)
- (A) Dorsal edge of vertex distinctly concave (frontal view). (B) In frontal view, compound eyes thus strongly prominent laterally ..... 9
- 9 (A) Legs pale. (B) Proximal halves of fore- and midfemora brown but apices pale; outer margin of proximal halves pale like distal half. (C) Hindfemora with single brown median spot. (D) Tibiae pale, with faint rings. (E) Maxillary palps pale brown, darkening distally. (F) Larger laterodorsal spots on vertex not composed of small dots .....  
..... *Am. montanum* Badonnel, 1967
- (A) Legs dark. (B) Proximal halves of all femora with brown apices; remaining areas yellow. (D) Tibiae with three distinct brown rings. (E) Maxillary palps dark brown. (F) Larger laterodorsal spots on vertex formed by small dots .....  
..... *Am. dimorphum* Badonnel, 1967
- 10 (A) Vertex and frons divided transversely by three or four parallel brown stripes, which extend across compound eyes. (B) Legs pale with few smaller brown patches ..... 11
- (A) No transverse brown stripes on head. (B) Legs brown or pale with extensive brown bands ..... 12

- 11 (A) Forewing strongly convex at level of areola postica. (B) Areola postica smaller, shorter than the next distal section of vein M. (C) Claws with one row of small spines proximad the distalmost preapical tooth ..... *Am. striaticeps* Badonnel, 1967  
 – (A) Forewing weakly convex at level of areola postica. (B) Areola postica larger, longer than the next distal section of vein M. (C) Claws with one row of distinct teeth proximad distalmost preapical tooth ..... *Am. simile* Badonnel, 1967
- 12 (A) Forewing almost uniformly brown, apical third paler. (B) Body color chocolate brown ..... 13  
 – (A) Distinct patterns of contrasting light and dark patches on forewing. (B) Body color variable ..... 14
- 13 (A) Forewing rounded apically. (B) Forewing posterior margin only slightly flexed distally. (C) Head brown with some diffuse spotting between compound eyes and close to ocelli. (D) Femora uniformly dark brown; scales with double striation. (E) Common base of parameres wide ..... *Am. pauliani* Smithers, 1964  
 – (A) Forewing apex pointed. (B) Forewing posterior margin distinctly flexuous. (C) Head uniquely patterned with series of darker dots with various size and horizontal stripes. (D) Femora dark brown on proximal 2/3 or 3/4, with yellow brown apex. (E) Common base of parameres very narrow ..... *Am. punctatum* Badonnel, 1967
- 14 M2 and M3 in forewing strongly curved posteriad at their apical third ..... 15  
 – M2 and M3 in forewing parallel or only slightly curved ..... 16
- 15 (A) Frontal area of head crossed by three distinctive transverse chocolate brown bands. (B) Anterior end of phallosome frame close to basal plate more rounded ..... *Am. flexuosum* Badonnel, 1955  
 – (A) Head without distinctive transverse brown bands. (B) Anterior phallosomal curvature variable .....  
 ..... *Am. annulitibia* Smithers, 1999
- 16 (A) Hindwing R1 interrupted shortly before costa. (B) Forewing without apical lobe. (C) Forewings with unique pattern: anterior and apical margin with several vertical stripes and patches of scales, and basal half almost completely covered with scales. (D) Tibiae uniformly brown ..... *Am. mimulum* Badonnel, 1967  
 – (A) Hindwing R1 reaches costa. (B) Forewing with apical lobe. (C) Forewings without this unique pattern. (D) Tibiae with rings of brown scales ..... 17
- 17 (A) Forewing without large brown patch covering most of anal area. (B) Forewing in its apical 1/3 anteriorly with crescent shaped white patch bordered by brown area. (C) Femora not completely brown. (D) Common base of parameres wide and short ..... *Am. hieroglyphicum* Badonnel, 1967  
 – (A) Forewing with broad zone of dark scales from distal 1/3 of M + Cu to edge of anal area. (B) Forewing without crescent shaped white patch and brown border. (C) Femora completely brown. (D) Common base of parameres wide and fairly long (unknown for *Am. knorrei*, as no male described!) ..... 18
- 18 (A) Head yellowish brown. (B) Vertex with irregular vertical lines parallel to compound eyes and coronal sulcus. (C) Metabasitarsus with 21–22 ctenidiobothria. (D) Anteroproximal region of forewing with or without sparse vestiture of scales ..... *Am. acuminatum* Smithers, 1964  
 – (A) Head dark brown. (B) Vertex without irregular vertical lines. (C) Metabasitarsus with 24 ctenidiobothria. (D) Anteroproximal region of forewing densely covered with dark brown scales ... †*Am. knorrei* Weingardt, Bock & Boudinot sp. nov.

### 3.3.1.3. Further considerations of *Amphientomum*

Several hypotheses on relationships between species of *Amphientomum* have been proposed. According to Badonnel (1979), *Am. flexuosum* and *Am. loebli* are sibling species (= *espèce voisine*), but differ in details of coloration, the reduction of the basal section of Rs in the forewing of *Am. loebli*, and by the presence of a sclerite of the subgenital plate in this species, which is lacking in *Am. flexuosum* (Badonnel 1979). Moreover, both species differ in size and the number of femoral spines (Badonnel 1979), but whether these differences are stable and statistically significant is presently unclear. Both species occur in West Africa and western Central Africa (Angola, Ivory Coast, Nigeria). Additionally, Smithers (1999) proposed that *Am. annulitibia* is likely closely related to *Am. flexuosum*, but noted that it differs in the shape of the anterior margin of the phallosome and in the coloration of the head.

There are few studies on the ecology and faunistics of the East African Psocodea, including for instance the family Amphientomidae (Broadhead and Richards 1982; Georgiev 2022a). One species whose description is based

on a single nymph from a Congolese cave might indicate weak trogliphilic tendencies (Badonnel 1959). As Badonnel (1959) already discussed, a detailed study on the morphology of nymphal stages of Amphientomidae is needed before the specimen can be reliably placed in a genus. Several genera and the subfamily Tineomorphinae can nevertheless be excluded from the list of potential taxa based on the presence of profemoral spines and the shape of the lacinia (Badonnel 1959), while the genus *Amphientomum* seems to be the most likely taxon based on the few described characters that the nymph shares with species of *Amphientomum*. Several species of the genus are known to be attracted by light traps (Badonnel 1979; Smithers 1999).

A character of special interest is the coxal interlocking device described here for the new species (Fig. 15A, B). It consists of a hemispherical outgrowth on the right metacoxa, which fits into a corresponding cavity on the opposite side. A similar device was described by Pearman (1935) for the amphientomine genera *Syllysis* and *Nephax*, but never before for a species of *Amphientomum*. It is conceivable that the interlocking device is part of a jumping mechanism, but there are no observational data for amphientomids

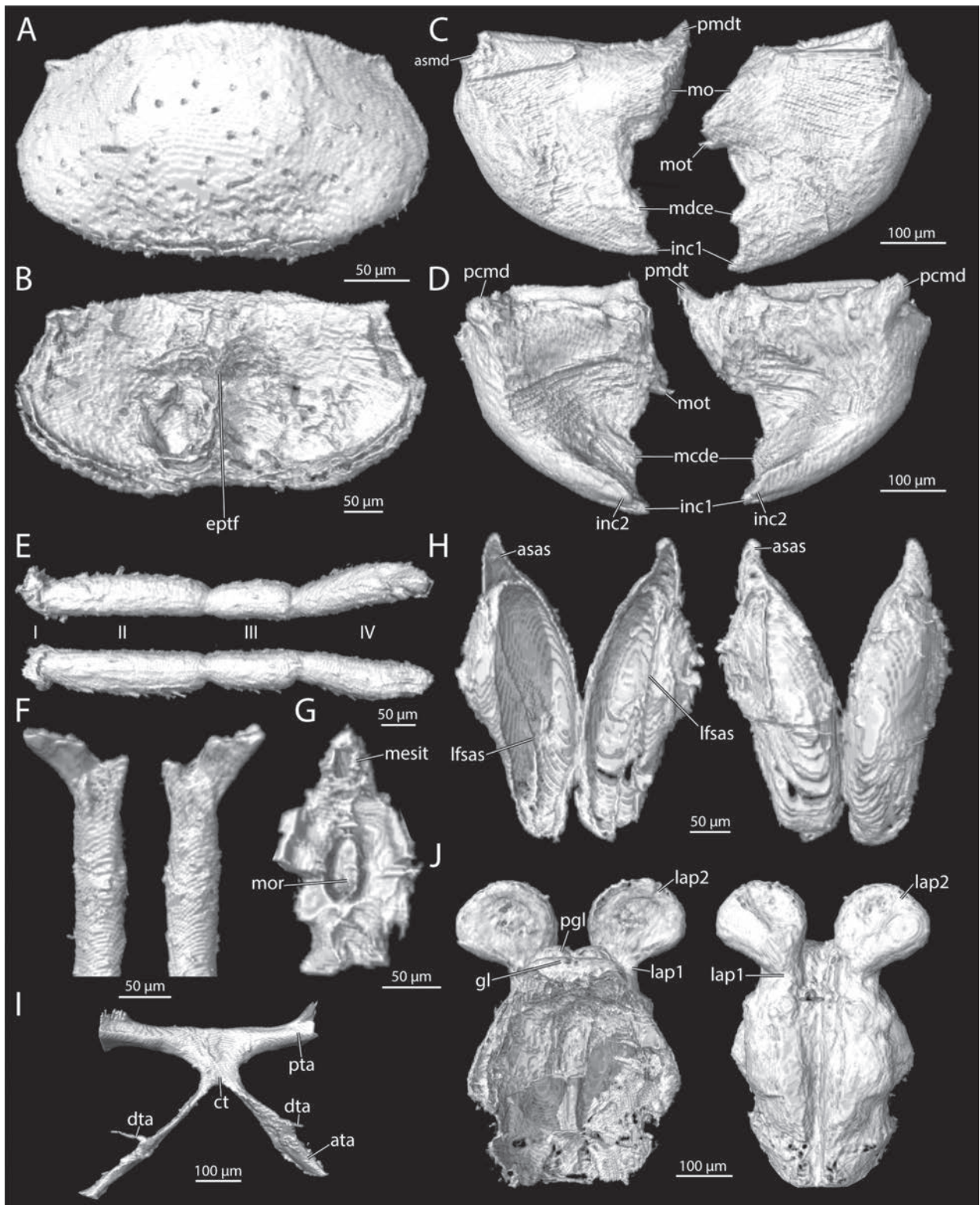


**Figure 11.** A–J. 3D-reconstruction of †*Amphientomum knorrei* sp. nov. **A.** Labrum in anterior view; **B.** Labrum in posterior view; **C.** Mandibles in anterior view; **D.** Mandibles in posterior view; **E.** Maxillary palps, top left palp, bottom right palp, numbers indicate palp article; **F.** Laciniae in anterior view; **G.** Sitophore; **H.** Salivary sclerites in anterior (right) and posterior (left) view; **I.** Tentorium in dorsal view; **J.** Labium in anterior (left) and posterior (right) view. Abbreviations: asmd = anterior socket of mandible, asas = apodeme of salivary sclerite, ata = anterior tentorial arm, ct = corpotentorium, dta = dorsal tentorial arm, eptf = epipharyngeal transverse fold, gl = glossae, inc1/2 = incisivi 1 and 2, lap1/2 = labial palp article 1 and 2, lfsas = longitudinal furrow of salivary sclerite, mdce = mandibular cutting edge, mesit = median extension of sitophore, mo = mola, mor = mortar, mot = molar tooth, pcmd = posterior condyle of mandible, pgl = paraglossa, pmtd = proximal mandibular tooth, pta = posterior tentorial arm.

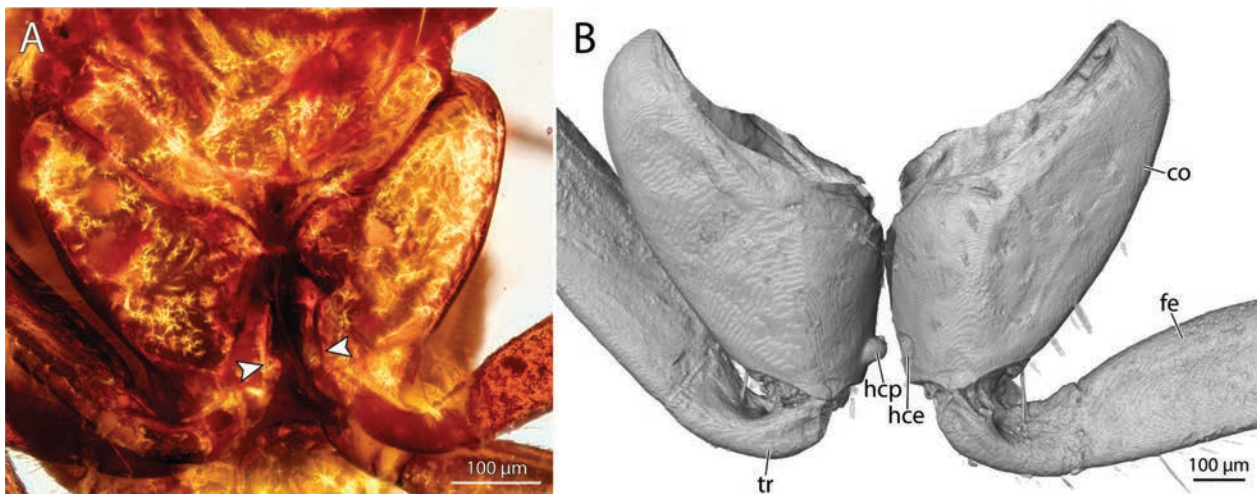


**Figure 12.** A. Photography of †*Amphientomum knorrei* sp. nov., posterior view of hindcoxae, arrows indicate the interlocking mechanism; B. 3D-reconstruction of †*Amphientomum knorrei* sp. nov., posterior view of hindcoxae. Abbreviations: co = coxa, fe = femur, hce = hindcoxal emargination, hcp = hindcoxal projection, tr = trochanter.

that would support this hypothesis. Interestingly, another interlocking device has been described for species of Lepidopsocidae, in this case on the mesocoxae but with a similar arrangement of a hemispherical protuberance on the right and a cavity on the left side, and involvement in jumping was also suggested in this case (Menon 1938; Ramesh et al. 2020). The occurrence of these devices on different segments represents a remarkable case of parallel evolution in the Psocodea. The evolutionary background still requires clarification.

A candidate homolog for the coxal interlocking device is the Pearman's organ, a unique structure of Psocodea, which consists of a mirror and rasp on the inner side of the metacoxae in most psocids (Mockford 2018). It can be missing (e.g., Pachytroctidae, Sphaeropsocidae, and likely in Liposcelididae, where the metacoxae are distinctly separated; Yoshizawa and Lienhard 2010; Mockford 2018) or certain substructures can be reduced (e.g., Amphientomidae with only the mirror part; Weidner 1972; but see discussion above and Mockford 1993 for a different view on the presence of the rasp in the family). We were unable to observe any rasping structures on the metacoxae in †*Am. knorrei* sp. nov. It is possible that the structure was in fact present but is indistinct due to artifacts and the quality of preservation of our specimen. As the mirror was also not visible in the SR- $\mu$ -CT scan and photographs or using light microscopy (maximal resolution 200 $\times$ ), it appears plausible that this interlocking device represents a modification of the Pearman's organ, especially due to the functional requirement of intercoxal contact. Pearman (1935) proposed the same hypothesis on the origin of this device in other Amphientomidae. Smithers (1999) described the "tympaanum" of the metacoxae of *Am. annulitibia* Smithers, 1999, with a thick and strongly raised edge but without an illustration. Nevertheless, it is conceivable that a similar structure is present in this species (described as inconspicuous by Smithers 1999), and that the device is more strongly

developed in †*Am. knorrei* sp. nov. In any case, the device described here differs from the mesocoxal interlocking mechanism observed in Lepidopsocidae, which probably represents a non-homologous neof ormation.

The lack of a robust phylogeny of Amphientomidae impedes the systematic placement of new species. As many genera are only defined by diagnostic characters and not apomorphies (e.g., Taylor 2013), the possibility of non-monophyly of these groups cannot be excluded and paraphyly may even be widespread in the family. It is therefore important for future research to establish a robust phylogeny of amphientomids, based on molecular data and morphological apomorphies. Badonnel (1967) explicitly mentioned that the use of different characters would lead to different systematic placements of his newly described species. This underlines the lack of morphological support for groupings in the family. Badonnel also commented on the minimal variability of the genitalia in *Amphientomum*, as only the basal common shaft of the parameres and the spermapore sclerite are suitable for diagnostic purposes. Mockford (2018) supported this observation, stating that external genitalia of both sexes are uniform throughout the entire amphientomids, with a y-shaped phallosome and three ovipositor valves, with a bilobed external valve (V3) fused over a part of its length with the dorsal valve (V2). The shape of the forewings can also be used as a diagnostic feature (Badonnel 1967), but sexually dimorphic wing shapes in a single species have to be considered (Badonnel 1967). The shape of the lacinia is an important diagnostic feature (Badonnel 1967) and is displayed together with the wing venation in Figs 13–15 for all species of *Amphientomum* with available data. As a phylogenetic analysis and a detailed study of type material would be beyond the scope of this study, we refrain from providing an updated diagnosis of *Amphientomum* or the subgenus *Amphientomum (Palaeoseopsis)*. However, our study is a first step towards a phylogenetic investigation of the genus.

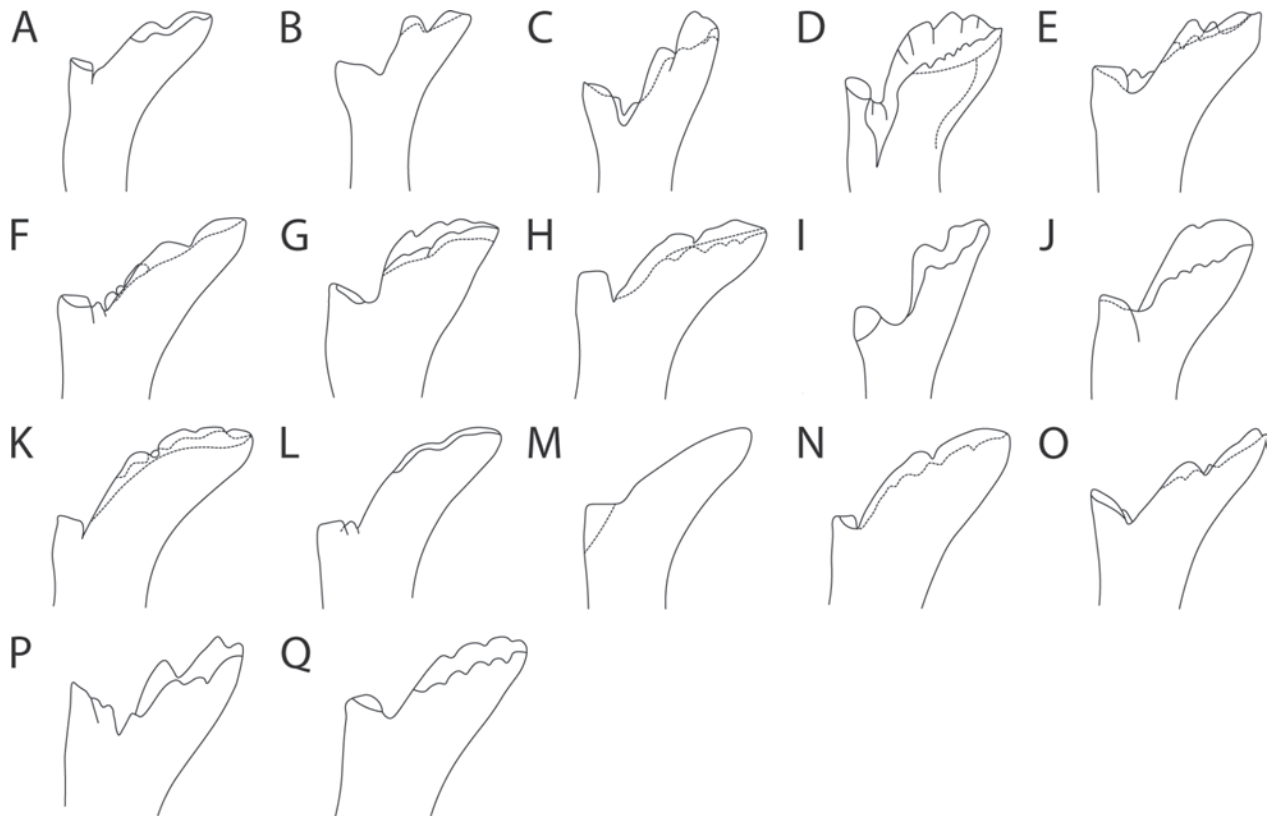


**Figure 13. A–Q.** Schematized drawings of all available laciniae of *Amphientomum* species from the literature and of ‡*Amphientomum knorrei* sp. nov. (Amphientomidae: Amphientominae) preserved in piece PMJ Pa 5809. The laciniae are not up to scale, and the orientation of the lacinia was flipped at 180° for **C, E, H, J–L, N–P** from the original drawings, only the apical portions of the laciniae are shown. **A.** *Am. acuminatum*, male; **B.** *Am. aelleni*, nymph; **C.** *Am. annulicorne*, female; **D.** *Am. annulitibia*; **E.** *Am. dimorphum*, sex not specified; **F.** *Am. dimorphum*, sex not specified; **G.** *Am. flexuosum*, female; **H.** *Am. hieroglyphicum*; **I.** ‡*Am. knorrei* sp. nov., female, redrawn after 3D render; **J.** *Am. loebli*, female; **K.** *Am. mimulum*, sex not specified; **L.** *Am. montanum*, female; **M.** *Am. pauliani*, male; **N.** *Am. punctatum*, male; **O.** *Am. simile*, female; **P.** *A. simile*, female; **Q.** *Am. striaticeps*, female. Figures modified from the following: **A, C, E, F, H, K, L, N, O, P, Q** after Badonnel (1967); **D** after Smithers (1999); **B** after Badonnel (1959); **G** after Badonnel (1955); **J** after Badonnel (1979); **M** after Smithers (1964).

#### 3.3.1.4. Additional observations and remarks for Psocodea in the PMJ Pa collection

A single apterous liposcelidid trapped in the large piece of resin PMJ Pa 5827 together with many other syninclusions is slightly deformed and almost transparent (Fig. 16C). It is a nymph, as only 8 antennomeres are visible, and the specimen is only ca. 0.9 mm long. As no external metafemoral tubercle is visible, it is likely that the single specimen belongs to the subfamily Embidopsocinae. To assign it to a genus of this subfamily and to make sure that the tubercle on the metafemur is indeed absent, further trimming and cutting of the amber piece would be necessary for higher magnification. However, as many syninclusions could be affected by this we refrained from further processing. As the specimen is miniscule, we could not observe other taxonomically relevant characters (Lienhard 1991), for instance the number of tarsomeres. Even though we do not assign the specimen to a genus, we could verify that the last maxillary palpomere is conical, and not enlarged as

in *Belapha* Enderlein, 1917, *Belaphopsocus* Badonnel, 1955, *Belaphotroctes* Roesler, 1943 or *Troctulus* Badonnel, 1955 (Lienhard 1991). This makes a placement in these genera unlikely.

Additionally, one single macropterous specimen of the family Archipsocidae is present in the resin piece PMJ Pa 5825 (see Figs 16A, B, 17A, B, 18A, B, Appendix 1: Fig. A4). The presence of large wings indicates that this individual is a female (Mockford 1993). As the genital region is deformed and blocked by a large air bubble, it is unclear whether ovipositor valvulae are present or not. The visible, apically flattened and very wide subgenital plate resembles the homologous structure of *Archipsocopsis* (Mockford 1993, fig. 248; Georgiev 2022b, fig. 30). The results of the FT-IR analysis (IAA) suggest that the resin containing the archipsocid belongs to a kauri-type (see SI: Report No 41995\_17022023), a tree species today only occurring in New Zealand (Steward and Beveridge 2010). This suggests that the specimen might be part of the fauna of this country and the first possible record of the family in this region (Lienhard 2016). That

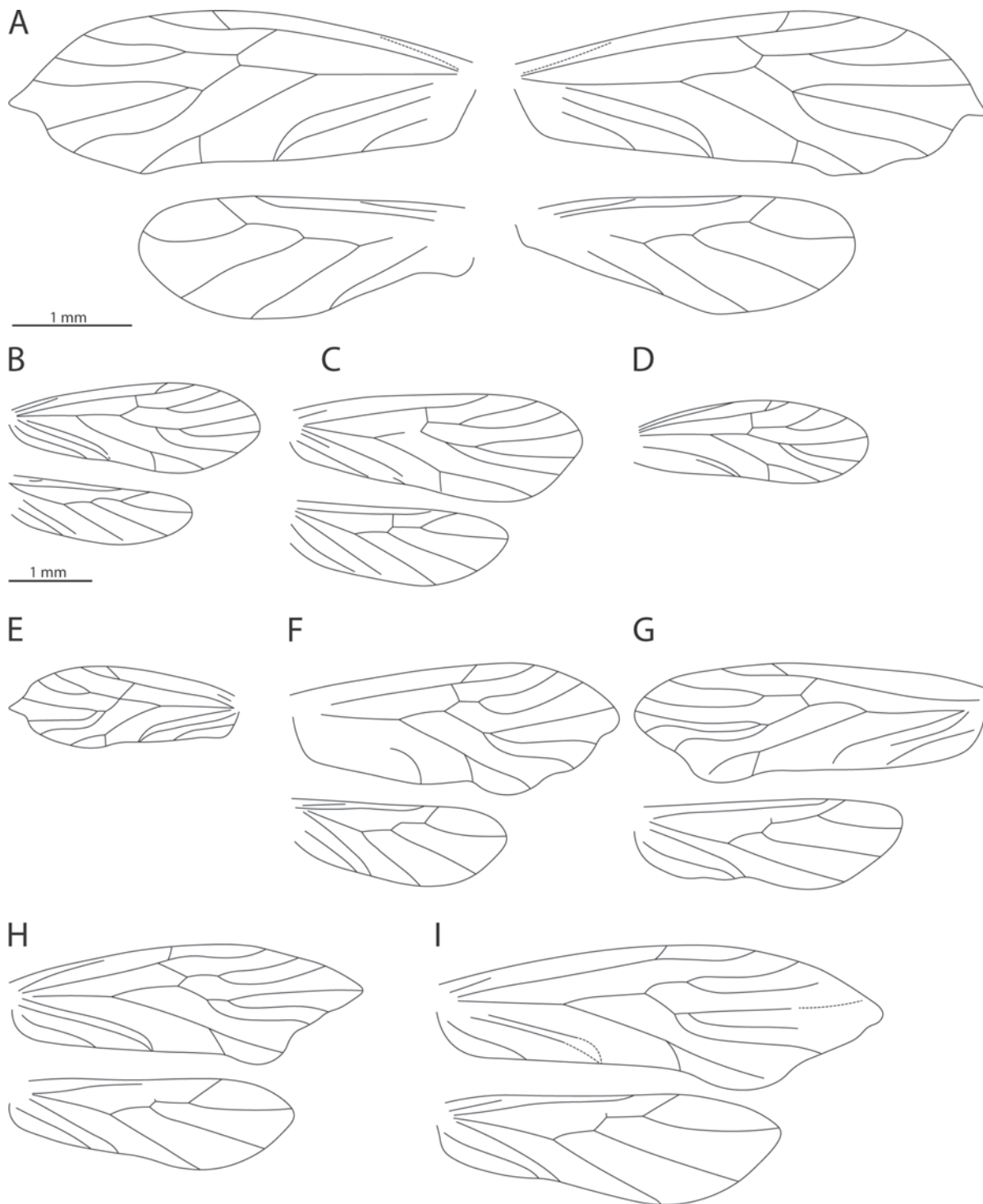


**Figure 14.** A–I. Schematized drawings of all available fore- and hindwings of *Amphientomum* species from the literature and of ‡*Amphientomum knorrei* sp. nov. (Amphientomidae: Amphientominae) preserved in piece PMJ Pa 5809. The same scale bar was used for B–I. A. ‡*Am. knorrei* sp. nov., female; B. †*Am. colpolepis*; C. †*Am. paradoxum*, female; D. †*Am. parisiense*; E. *Am. acuminatum*; F. *Am. annulicorne*, female; G. *Am. annulitibia*, male; H. *Am. dimorphum*, female; I. *Am. dimorphum*, male. Figures modified from the following: B, C after Enderlein (1911); D after Nel et al. (2005); E after Smithers (1964); F, H, I after Badonnel (1967); G after Smithers (1999).

the specimen belongs to the genus *Archipsocopsis* is tentatively suggested by the shape of the subgenital plate. As further confirmation is required, we treat it here as *Archipsocidae* gen. et sp. indet. We briefly characterize

this specimen as follows: Female. Head large and globular, with comparatively small compound eyes. Antennae relatively short and with relatively thick flagellum. Three ocelli present but indistinct. Macropterous. Fore

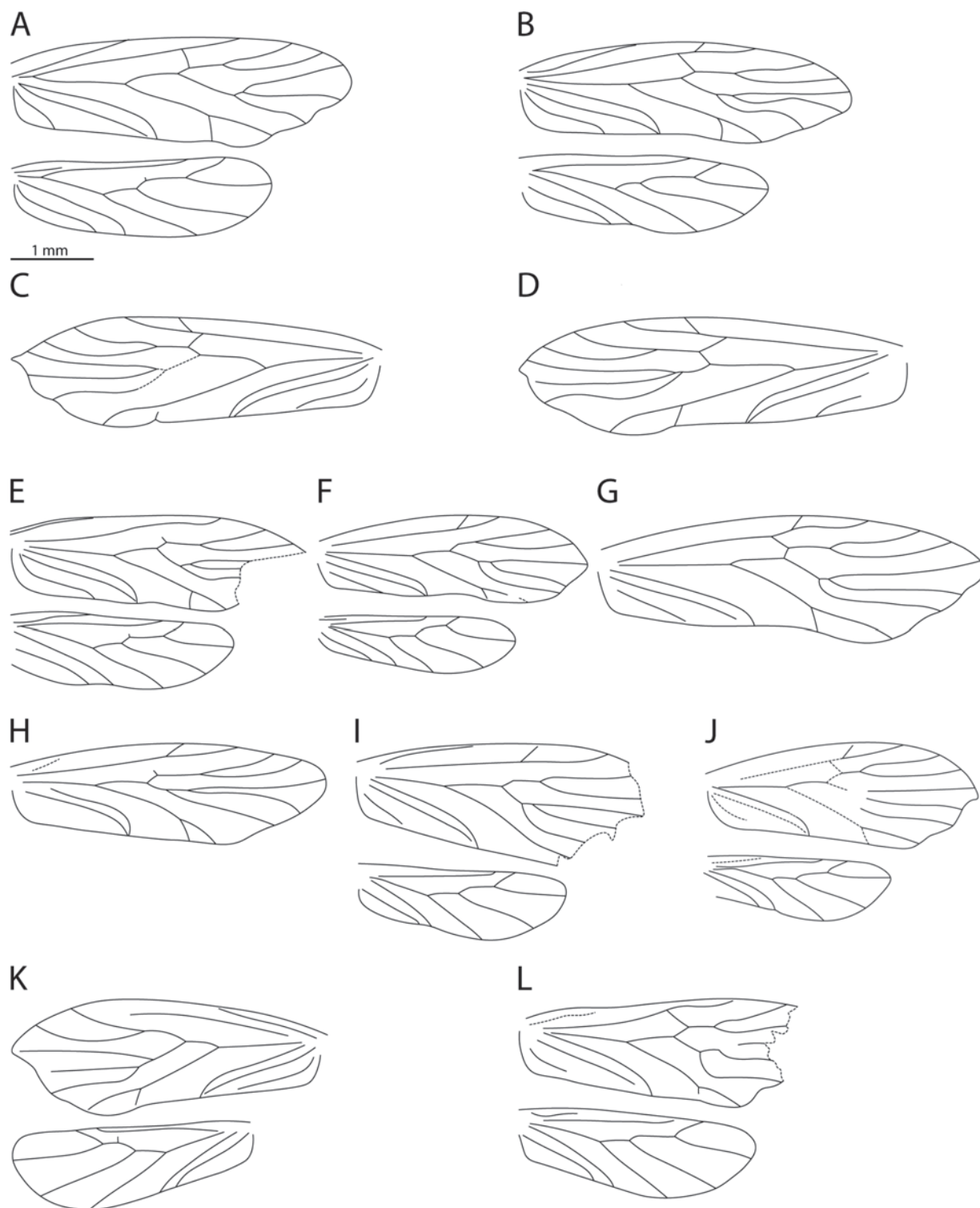


**Figure 15.** A–L. Schematized drawings of all available fore- and hindwings of *Amphientomum* species from the literature. The same scale bar was used for A–L. **A.** *Am. ectostriolate*, **B.** *Am. flexuosum*; **C.** *Am. hieroglyphicum*, female; **D.** *Am. hieroglyphicum*, male; **E.** *Am. loebli*, female; **F.** *Am. mimulum*, male; **G.** *Am. montanum*, female; **H.** *Am. pauliani*; **I.** *Am. punctatum*, male; **J.** *Am. punctatum*, female; **K.** *Am. simile*, female; **L.** *Am. striaticeps*, female. Figures modified from the following: **A** after Li (2002); **B** after Badonnel (1955); **C, D, F, G, I, J, K, L** after Badonnel (1967); **E** after Badonnel (1979); **H** after Smithers (1964).

wings and hind wings completely developed. Tarsi with two articles. Ovipositor seemingly entirely missing. Subgenital plate wide and flattened posteriorly. Body length: 1.46 mm. Forewing length: 1.71 mm. Hindwing length: 1.45 mm.

### 3.3.2. Order Hymenoptera: Subfamilial and tribal synopsis of fossil Formicidae in the PMJ Pa collection

In this section, we review the fossil record of each subfamily of ants that occurs in the Phyletisches Museum

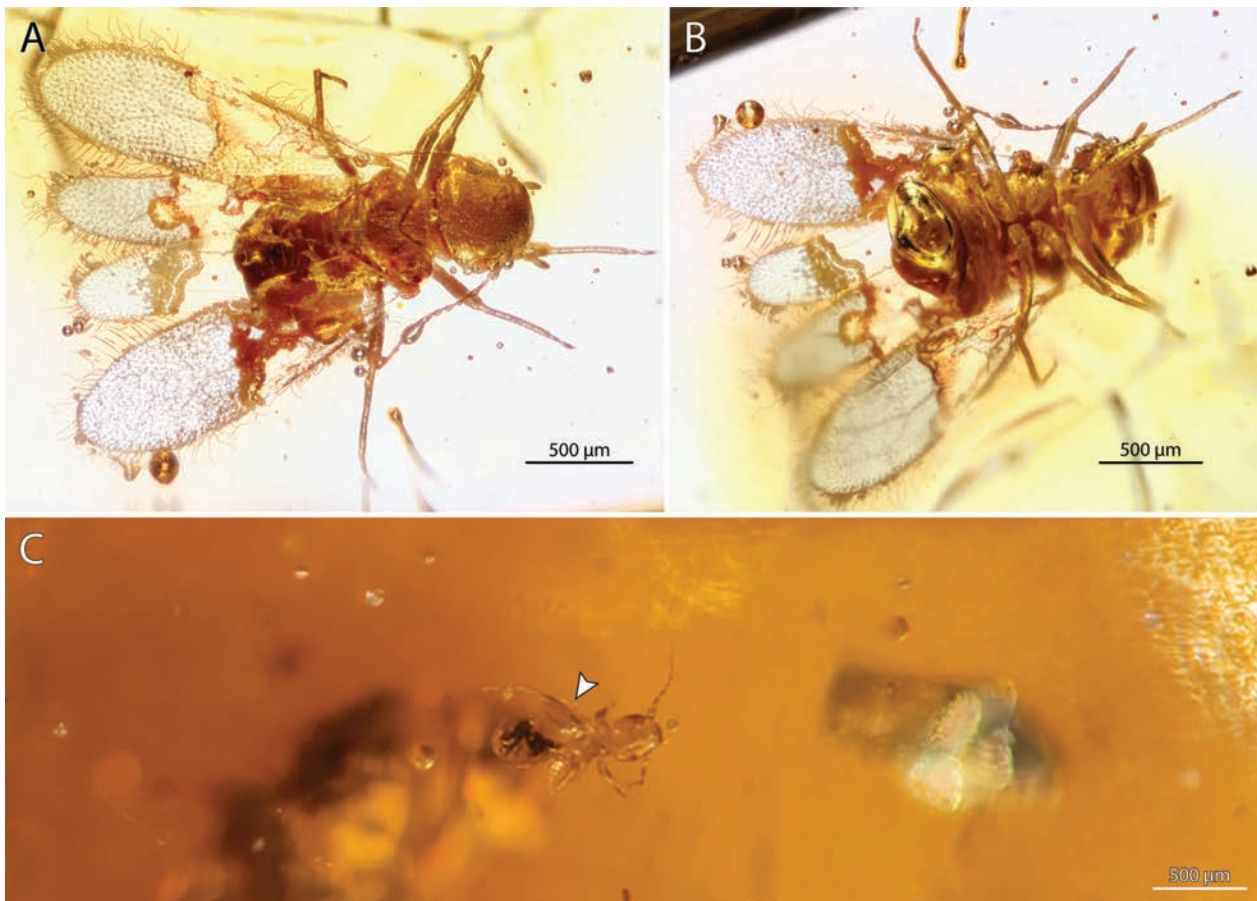


**Figure 16.** **A, B.** Photography of Archipsocidae gen. et sp. indet. preserved in piece PMJ Pa 5825. **C.** Photography of Liposcelididae gen. et sp. indet. Preserved in piece PMJ Pa 5827. **A.** Habitus in dorsal view; **B.** Habitus in ventral view; **C.** Habitus in ventral view, arrow indicates right hindfemur.

amber collection, with the exception of Formicinae, for which our review is restricted to the tribes Plagiolepidini and Camponotini. See section 3.3.1 for details about deposit and age source information.

### 3.3.2.1. Subfamily Dorylinae Leach, 1815

Amber fossils: Identifiable to species:

- A. Baltic ambers [Eocene, 37.8–33.9 Mya].
- I. Genus †*Procerapachys* Wheeler, 1915. [Note 1].
    1. †*Pr. annosus* Wheeler, 1915. [w, m]. [Type species of genus].
    2. †*Pr. favosus* Wheeler, 1915. [w].
    3. †*Pr. sulcatus* Dlussky, 2009. [w].
  - II. Genus *Acanthostichus* Mayr, 1887.
    5. †*A. hispaniolicus* de Andrade, 1998b. [w].
  - III. Genus *Cylindromyrmex* Mayr, 1870.
    6. †*Cy. antillanus* de Andrade, 1998a. [q].
    7. †*Cy. electrinus* de Andrade, 1998a. [q].
    8. †*Cy. inopinatus* de Andrade, 1998a. [q].
  - IV. Genus *Neivamyrmex* Borgmeier, 1940.
    9. †*N. ectopus* Wilson, 1985. [w]. [see Wilson 1985b].
- Copal fossils: Identifiable to species:
- C. East African copal [Holocene, 145 years based on our <sup>14</sup>C analysis; < 36 Kya more generally, based on Solórzano-Kraemer et al. 2020].

V. Genus *Dorylus* Fabricius, 1793.

10. *D. nigricans molestus* (Gerstäcker, 1859). [w]. [See section 4.2.1; Fig. 3].

D. Colombian copal [Pleistocene(?); DuBois 1998].

- VI. Genus *Neivamyrmex* Borgmeier, 1940.
11. *N. iridescens* Borgmeier, 1950. [w].

**Note 1.** After the morphological and phylogenomic revision of the Dorylinae by Borowiec (2016, 2019), the generic identities of the species attributed to †*Procerapachys* are uncertain. Ongoing work by multiple research groups will resolve at least some of these questions. At least one specimen in the BEBC is meaningfully identifiable as *Lioponera* (unpubl. data).

### 3.3.2.2. Subfamily Dolichoderinae Forel, 1878

3.3.2.2.1. Genus †*Yantaromyrmex* Dlussky & Dubovikoff, 2013 [Note 1]

Amber fossils: Identifiable to species:

- A. Baltic ambers [Eocene, 37.8–33.9 Mya].
1. †*Y. constrictus* (Mayr, 1868). [w].
  2. †*Y. geinitzi* (Mayr, 1868). [w, q, m]. [Note 2].
  3. †*Y. intermedius* Dlussky & Dubovikoff, 2013. [w].
  4. †*Y. mayrianum* Dlussky & Dubovikoff, 2013. [w].
  5. †*Y. samlandicus* (Wheeler, 1915). [w].

**Note 1.** †*Yantaromyrmex* is an extinct genus of ants that is endemic to ambers from Baltic sources. The genus is of unknown phylogenetic affiliation with other Dolichoderinae, although it has been hypothesized to be close to the so-called “DNAPPTOFI” clade of the Leptomyrmecini (sensu, Ward et al. 2010; Boudinot et al. 2016), more specifically, as an ancestor of the clade containing *Anonychomyrma* and *Iridomyrmex* (Dlussky and Dubovikoff 2013). Addressing this hypothesis is outside the scope of the present study, so we retain the placement of this fossil in Leptomyrmecini and note explicitly that this is an uncertain and untested relationship.

**Note 2.** The PMJ Pa specimen identified as †*Y. geinitzi* (PMJ Pa 5856) was identified using the key of Dlussky and Dubovikoff (2013).

### 3.3.2.3. Subfamily Formicinae Latreille, 1802

#### 3.3.2.3.1. Tribe Plagiolepidini Forel, 1886

Amber and copal fossils: Identifiable to species:

##### I. Genus *Lepisiota* Santschi, 1926.

A. African copal [Holocene, < 36 Kya (Solórzano-Kraemer et al. 2020)].

1. †*Le. cf. canescens* [w]. [Note 1].

##### II. Genus *Plagiolepis* Mayr, 1861.

B. Baltic amber [Eocene, 37.8–33.9 Mya].

2. †*Pl. klinsmanni* Mayr, 1868. [w].

• Wheeler, 1915: 101 (m); Dlussky, 2010a: 65 (“ergatoid” q).

3. †*Pl. kuenowi* Mayr, 1868. [w].

= †*Pl. balticus*: Dlussky, 2010a: 69.

• Dlussky, 2010a: 70 (q).

4. †*Pl. singularis* Mayr, 1868. [q].

5. †*Pl. solitaria* Mayr, 1868. [m].

6. †*Pl. squamifera* Mayr, 1868. [w].

7. †*Pl. wheeleri* Dlussky, 2010. [w].

C. Rovno amber [Ukraine; Eocene, 38.0–33.9 Mya].

8. †*Pl. minutissima* Dlussky & Perkovsky, 2002. [m].

D. Saxonian (Bitterfeld) amber [Germany; Eocene (Priabonian), 38.0–33.9 Mya].

9. †*Pl. paradoxa* Dlussky, 2010. [m].

E. Sicilian amber [Italy; Oligocene, 11.6–5.3 Mya].

10. †*Pl. labilis* Emery, 1891. [w].

##### III. Genus *Acropyga* Roger, 1862.

F. Dominican amber [Miocene, 20.4–13.8 Mya].

11. †*Acropyga glaesaria* LaPolla, 2005. [q, m].

Species inquirendae:

##### II. Genus *Plagiolepis*.

G. Uncertain [Cenozoic?].

(1.) †*Pl. succini* André, 1895. [Note 2].

**Note 1.** This specimen (PMJ Pa 5807) may be the first fossil or sub-fossil *Lepisiota* recorded to date. The specimen is dark, has the bituberculate form of the propodeum associated with *L. canescens*, and lacks spines on the petiolar node. *Lepisiota* is also the third genus (of nine) from the Plagiolepidini to be recovered from fossil-bearing sediments, the other two being *Acropyga* and *Plagiolepis*.

Ants of this tribe were formerly lumped with the *Prenolepis* genus group of the Lasiini (see Bolton 2003; Boudinot et al. 2022a).

**Note 2.** As reported by Dlussky (2010a, b), there is considerable uncertainty about the generic identity and geological origin of the fossil(s) described as †*Pl. succini* by André (1895). In André’s own words (paraphrased, p. 83), “despite its great size for [*Plagiolepis*], this species resembles [*Anoplolepis*] *custodiens* [F. Smith]”, with the following diagnostic note (also paraphrased): “but it is distinguished by its size and the thicker and less elongate antennae”. Dlussky (2010a, b) was unable to find the specimen(s) originally described by André and speculated that the taxon may be from East African copal, *i.e.*, misidentified as Baltic amber. This species should, therefore, be continued to be considered of uncertain status until the original or additional material becomes available.

#### 3.3.2.3.2. Tribe Camponotini Forel, 1878

**Overview.** The Camponotini is a comparatively diverse tribe of Formicinae with > 1950 valid species attributed to eight extant genera (Bolton 2023), which have received revisionary attention subsequent to the major phylogenomic study of Blaimer et al. (2015) (see Ward et al. 2016; Ward and Boudinot 2021). Because this clade represents a major radiation of ants (e.g., Rafiqi et al. 2020), fossils are particularly important for understanding and modeling the tempo and mode of formicine evolution. The diversity of fossils attributed to this tribe, moreover, necessitates this overview. Prior to the present study, Camponotini contained two monotypic and valid fossil genera (†*Chimaeromyrma brachycephala* Dlussky, 1988, †*Pseudocamponotus elkoanus* Carpenter, 1930), one monotypic fossil genus that is a synonym of *Camponotus* Mayr, 1861 (†*Palaeosminthurus juliae* Pierce & Gibron, 1962), one fossil species attributed to *Polyrhachis* (†*Po. annosus* Wappler et al., 2009), and 29 valid and 5 invalid fossil species placed in *Camponotus* itself (Bolton 2023).

Based on our assessment of all 38 of these fossil species plus the three species attributed to the *Camponotus*-like form taxon †*Camponotites* Steinbach, 1967, we propose the following revision to the fossil record of Camponotini below. In brief, we transfer one species out of the subfamily Formicinae to *Liometopum* (I), we recognize one as yet unidentified copal specimen of *Camponotus* (II) and one fossil species of *Polyrhachis* (III), we leave †*Chimaeromyrma* and †*Pseudocamponotus incertae sedis* in Camponotini (IV, VII), we transfer one Baltic fossil species from *Camponotus* to †*Eocamponotus* gen. nov. (V), we revive †*Palaeosminthurus* and consider it unidentifiable while transferring it out of Camponotini as *incertae sedis* in Formicinae (VI), and finally, we transfer 29 fossil species from *Camponotus* to the form genus †*Camponotites*, which we treat as a catch-all that is *incertae sedis* in Camponotini (VIII). We also provide detailed annotations for our synopsis of fossil Camponotini (see the “Notes”).

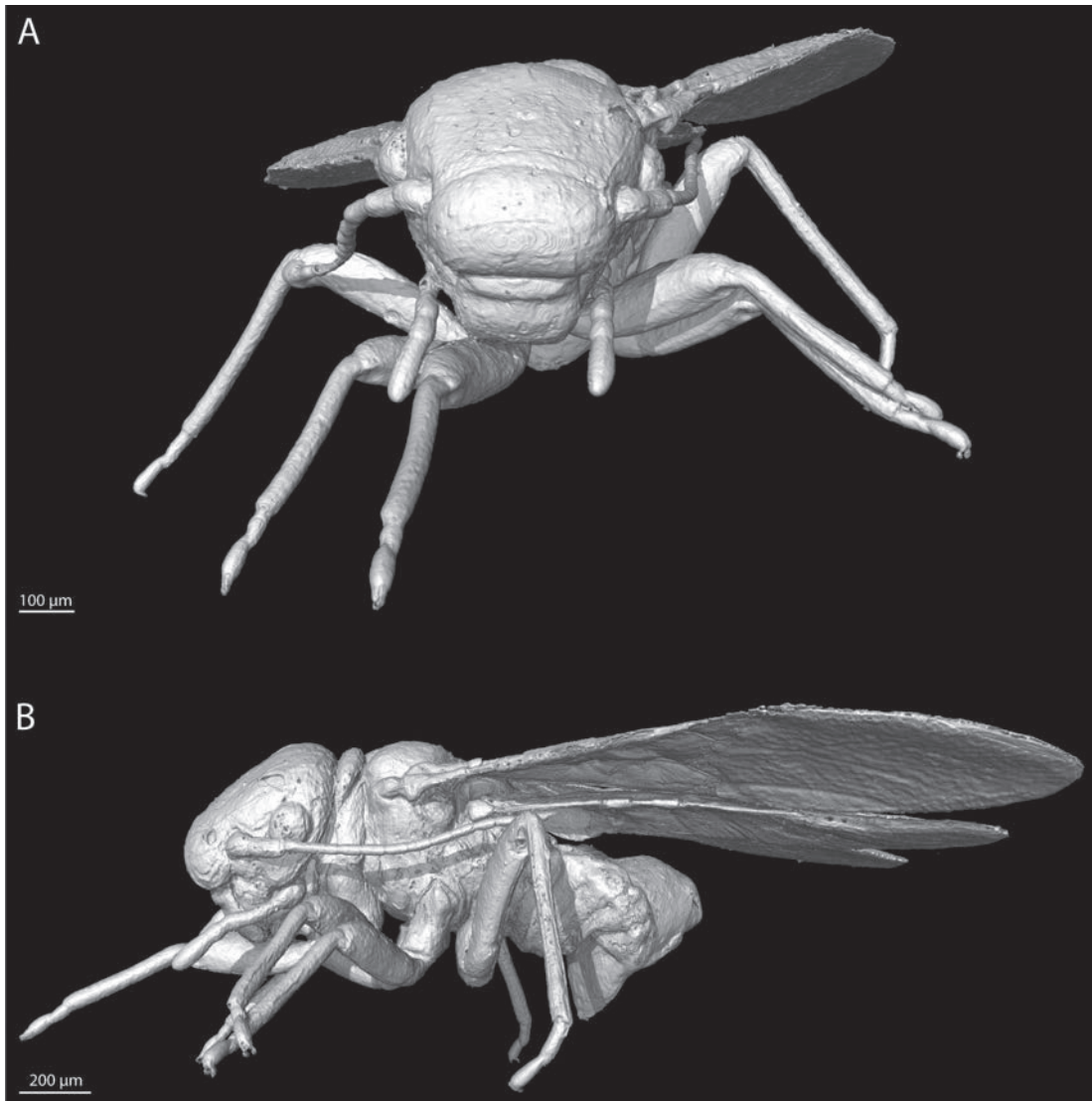


**Figure 17. A, B.** 3D-reconstruction of Archipsocidae gen. et sp. indet. **A.** Habitus in frontal view; **B.** Habitus in lateral view.

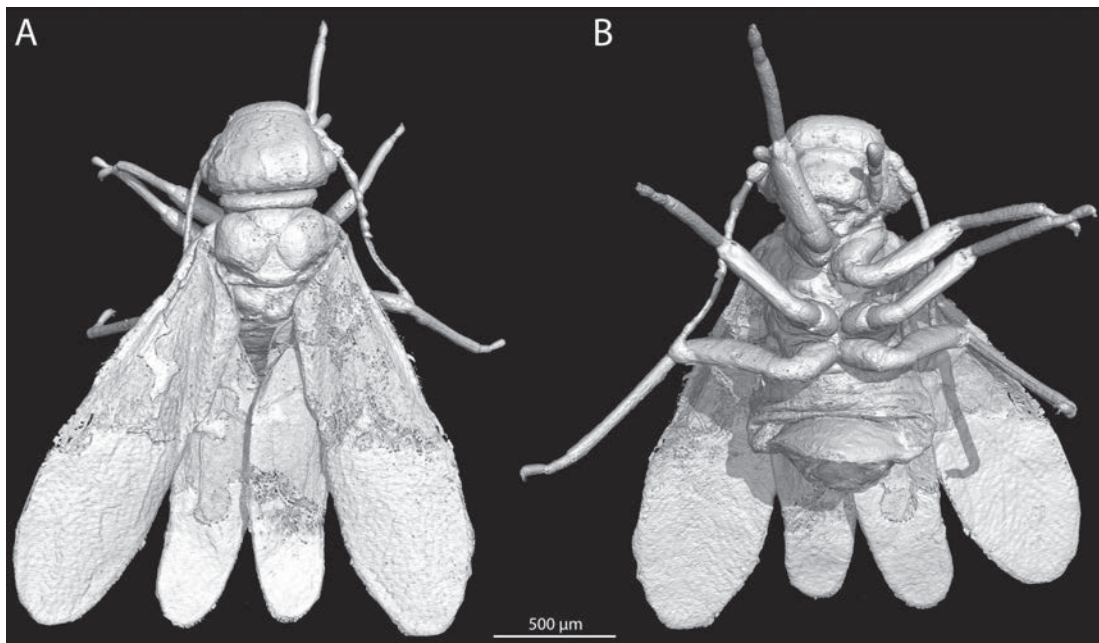


**Figure 18. A, B.** 3D-reconstruction of Archipsocidae gen. et sp. indet. **A.** Habitus in dorsal view; **B.** Habitus in ventral view.

Finally, we point out that all future studies on fossils that may possibly be associated with *Camponotus* or Camponotini should critically evaluate the morphological evidence for placement in any of the extant genera particularly in reference to Ward et al. (2016) for workers and Ward and Boudinot (2021) for workers and alates (the wing venation characters apply equally to males and queens). A recent work which ignored these studies is Takahashi and Aiba (2023), which misidentified multiple specimens as *Camponotus*. If a species name must be given to a fossil that cannot be placed in any of the extant genera of Camponotini based on synapomorphies, we strongly encourage authors to place these fossils in the form genus †*Camponotites* so that uncertainty is explicitly recognized and to prevent the propagation of errors in macroevolutionary analysis.

I. Transferred to *Liometopum* (Dolichoderinae):

Compression fossil:

A. Shanwang formation [China, Linqu County; Miocene (Burdigalian), 20.4–16.0 Mya].

a. *Liometopum* Mayr, 1861.

= †*Shanwangella* Zhang, 1989. Syn. nov.

(1.) †*L. palaeopterum* (Zhang, 1989). Comb. nov. [q]. [Note 1].

= †*S. palaeoptera* Zhang, 1989.

• Combination in *Camponotus*: Hong and Wu 2000: 19.

II. Genus *Camponotus* Mayr, 1861, subgenus indet. [Note 2].

Copal fossil: Identifiable to species:

B. East African copal [Holocene, < 36 Kya (Solórzano-Kraemer et al. 2020)].

1. *Ca.* sp. THIS STUDY. [w]. [Note 3].

III. Genus *Polyrhachis* Smith, F., 1857.

Compression fossil:

C. Varvara formation [Miocene, 7.2–5.3 Mya].

1. †*Po. annosus* Wappler et al., 2009. [Note 4].

IV. Genus †*Chimaeromyrma* Dlussky, 1988, *incertae sedis* in tribe.

Amber fossil:

D. Sakhalin amber [Eocene, 47.8–41.3 Mya].

1. †*Ch. brachycephala* Dlussky, 1988. [Note 5].

V. Genus †*Eocamponotus* Boudinot, gen. nov. [Note 6].

Type species: †*Eo. mengei* (Mayr, 1868) by original designation.

Amber fossils: Identifiable to species:

E. Baltic ambers [Eocene, 37.8–33.9 Mya].

1. †*Eo. mengei* (Mayr, 1868). [w]. Comb. nov. [Note 7].

= †*Eo. igneus* (Mayr, 1868). Comb. nov.

• Synonymized by Wheeler (1915): 138.

VI. Genus †*Palaeosminthurus* Pierce & Gibron, 1962 stat. rev., *incertae sedis* in Formicinae, unidentifiable hence invalid stat. nov.:

Phosphatized fossil:

F. Barstow formation, Calico member [USA, California; Miocene (Hemingfordian), 20.4–16.0 Mya].

(–) †*Pa. juliae* Pierce & Gibron, 1962. [m]. Comb. rev.; unidentifiable, hence invalid, stat. nov. [Note 8].

= Formerly unresolved junior homonym of *Camponotus juliae* Emery, 1903.

• Transferred to Formicidae: Najt, 1987: 152.

• Status as species: Bolton, 1995b: 311.

• Transferred to *Camponotus*: Snelling, R.R. pers. comm. to Bolton, B. 2004, in Bolton (2023).

VII. Genus †*Pseudocamponotus* Carpenter, 1930, *incertae sedis* in tribe, unidentifiable hence invalid stat. nov.

Compression fossil:

G. Elko formation [Eocene, 37.2–28.4 Mya].

(–) †*Ps. elkoanus* Carpenter, 1930. [q]. Unidentifiable, hence invalid, stat. nov. [Note 5].

VIII. Genus †*Camponotites* Steinbach, 1967, *incertae sedis* in Formicinae. [Note 9].

Amber fossil: Unidentifiable at neontological genus level:

H. Fushun amber [China, Liaoning, Jijuntun formation; Eocene (Lutetian), 47.8–41.3 Mya].

(1.) †*Ctt. tokunagai* (Naora, 1933). [q?]. Comb. nov. [Note 10].

Compression fossils: Unidentifiable at neontological genus level: [Note 11].

I. Green River formation [USA, Colorado; Eocene, 50.3–46.2 Mya].

(2.) †*Ctt. vetus* (Scudder, 1877). [q?]. Comb. nov. [Note 12].

J. Bouldnor formation, Bembridge Marls member [Great Britain; Eocene (Priabonian), 38.0–33.9 Mya].

(3.) †*Ctt. cockerelli* (Donisthorpe, 1920). [m]. Comb. nov.

= †*Leucotaphus cockerelli* Donisthorpe, 1920.

• Combination in *Camponotus*: Dlussky and Perfilieva 2014: 417.

K. Florissant formation [USA, Colorado; Eocene, 37.9–33.9 Mya].

(4.) †*Ctt. fuscipennis* (Carpenter, 1930). [q]. Comb. nov.

(5.) †*Ctt. microcephalus* (Carpenter, 1930). [q]. [Note 13]. Comb. nov.

(6.) †*Ctt. petrifactus* (Carpenter, 1930). [w]. Comb. nov.

L. Brunstatt, horizon d2 [France; Early Oligocene, 33.9–28.4 Mya].

(7.) †*Ctt. compactus* (Förster, 1891). [q]. Comb. nov.

(8.) †*Ctt. vehemens* (Förster, 1891). [m]. Comb. nov.

• Théobald, 1937: 218 (w, q, m).

= Senior synonym of †*Ca. miserabilis* Förster, 1891: Théobald, 1937: 218.

M. Creek near Bechlejovice [Czechia; Oligocene (Rupelian), 33.9–28.1].

(9.) †*Ctt. novotnyi* (Samšínák, 1967). [q]. Comb. nov.

N. Rott formation [Germany, Orsberg; Oligocene: 28.4–23.0 Mya].

(10.) †*Ctt. lignitus* (Germar, 1837). [q]. Comb. nov.

= †*Formica lignitum* Germar, 1837.

• Combination in *Camponotus*: Mayr, 1867: 51.

- O. Niveau du gypse d'Aix Formation [France; Oligocene (Chatthian), 28.1–23.0 Mya].
- (11.) †*Ctt. longiventris* (Théobald, 1937). [q, m]. Comb. nov.
- (12.) †*Ctt. theobaldi* (Özdikmen, 2010). [m]. Comb. nov.
- Replacement name for †*Ca. saussurei* Théobald, 1937.
- (13.) †*Ctt. penninervis* (Théobald, 1937). [m]. Comb. nov.
- A. Shanwang formation (see above).
- (14.) †*Ctt. ambon* (Zhang, 1989). [q?]. Comb. nov.
- (15.) †*Ctt. ampullosus* (Zhang, 1989). [q?]. Comb. nov.
- (16.) †*Ctt. curviansatus* (Zhang, 1989). [q]. Comb. nov.
- (17.) †*Ctt. gracilis* (Zhang, 1989). [m?]. Comb. nov.
- (18.) †*Ctt. longus* (Zhang, 1989). [q]. Comb. nov.
- (19.) †*Ctt. microthoracus* (Zhang, 1989). [q]. Comb. nov.
- (20.) †*Ctt. plenus* (Zhang, 1989). [q]. Comb. nov.
- (21.) †*Ctt. shanwangensis* (Hong, 1984). [q]. Comb. nov.
- (22.) †*Ctt. pictus* (Zhang et al., 1994) [q]. [Note 14]. Comb. nov. • Previously junior primary homonym of *Ca. ligniperda pictus* Forel, 1886.
- (23.) †*Ctt. xiejiaheensis* (Hong, 1984). [m]. Comb. nov.
- TYPE SPECIES of †*Rabidia* Hong, 1984.
  - Combination in *Oecophylla*: Zhang, 1989: 297.
  - Combination in †*Camponotites* Dlussky et al., 2008: 616.
- P. Radoboj [Croatia; Miocene (Sarmatian), 12.7–11.6 Mya].
- (24.) †*Ctt. heracleus* (Heer, 1849). [m]. Comb. nov. = †*Formica heraclea* Heer, 1849.
- Combination in *Camponotus*: Mayr, 1867: 52.
  - Also described as new by Heer, 1850: 116.
- (25.) †*Ctt. induratus* (Heer, 1849). [m]. Comb. nov. = †*Formica indurate* Heer, 1849.
- Dlussky and Putyatina 2014: 249 (m, q).
  - Combination in *Camponotus*: Mayr, 1867: 52.
  - Also described as new by Heer, 1850: 116.
- (26.) †*Ctt. oeningensis* (Heer, 1849). [q]. Comb. nov. = †*Formica obesa oeningensis* Heer, 1849.
- Combination in *Camponotus* and raised to species: Cockerell, 1915: 486.
- Q. Joursac [France; Miocene, 11.6–7.2].
- (27.) †*Ctt. obesus* (Piton, 1935). [q?]. [Note 15]. Comb. nov.
- R. Montagne d'Andance Saint-Bauzile, Privas [France, Ardèche; Miocene (Turolian), 8.7–5.3 Mya].
- (28.) †*Ctt. crozei* (Riou, 1999). [q]. Comb. nov.
- S. Brunn-Vösendorf [Austria; Miocene (Messinian), 7.2–5.3 Mya]
- (–.) †*Ctt. ullrichi* (Bachmayer, 1960). [wing]. Comb. nov.; unidentifiable, hence invalid, stat. nov. [Note 16].

- T. Willerhausen clay pit [Germany; Pliocene (Piacenzian), 3.6–2.6 Mya].
- (29.) †*Ctt. silvestris* Steinbach, 1967. [q].
- †*Camponotites* Steinbach, 1967 TYPE SPECIES.
  - Redescribed: Dlussky et al. 2011: 452.
- (30.) †*Ctt. steinbachi* Dlussky et al., 2011. [q].

**Note 1.** The species †*Ca. palaeopterus* (Zhang, 1989) was originally attributed to its own genus, †*Shanwangella* Zhang, 1989 before being placed in *Camponotus* by Hong and Wu (2000). The fossil cannot be attributed to Formicinae at all, however, due to the presence of cross vein 2rs-m, which never occurs in Formicinae; this crossvein encloses the second submarginal cell of the wing. Because the specimen has 2rs-m, lacks postpetiolation of abdominal segment III, and does not have cinctation of abdominal segment IV (= presence of transverse sulci), we transfer the species to Dolichoderinae. Therein, the specimen is recognizable as an alate of *Liometopum* given its large size (discal and submarginal cells ~ 1 mm long), its massive gaster, and details of the venation. †*Liometopum palaeopterus* comb. nov. was discovered in Shanwang in the Shandong Province, reasonably within the current distribution of the extant species *L. sinense* Wheeler, 1921 (Del Toro et al. 2009). Moreover, it is plausible that the fossil represents an ancestral population given that *L. sinense* is the only species currently known from China, at least to present knowledge. Unfortunately, gynes and males are unknown for the extant species. The unusual head and antennae of †*L. palaeopterus* comb. nov. are here interpreted as preservational artefacts.

**Note 2.** *Camponotus* and the tribe Camponotini more broadly is one of the most challenging taxonomic puzzles in the Formicidae, and not merely due to the massive size of these taxa (1084 valid species and 411 valid subspecies are currently attributed to *Camponotus* at the date of writing, Bolton 2023). Although some genera in the tribe are reasonably identifiable based on external morphology (e.g., Ward et al. 2016), others, such as the fundamental distinction between *Colobopsis*—which is sister to all other Camponotini—and the hyperdiverse *Camponotus* is challenging even with extant material in hand and under the microscope (Ward and Boudinot 2021). For these reasons, we substantially revise the fossil system of *Camponotus* in order to meet the twin aims of: (1) cleaning up the useless species names attributed to *Camponotus*, and (2) discouraging uncritical use of these fossils for macroevolutionary analysis (e.g., Klimeš et al. 2022). Toward these aims, we have: (a) provided a new genus name for †*Camponotus mengei*, †*Eocamponotus* gen. nov., as this fossil cannot be confidently placed in *Camponotus* yet; (b) transfer red 29 fossil taxa from *Camponotus* to the form genus †*Camponotites*, which we treat as *incertae sedis* in Formicinae; and (c) transfer red one species out of the Formicinae altogether.

**Note 3.** The minor worker specimen (PMJ Pa 5829) is difficult to identify, given the limited resources available. We attempted to identify the specimen using Emery's (1925) key to Old World *Camponotus* subgenera, Brian Taylor's

*Ants of Africa* website (Taylor 2022), and AntWeb (2022). Ultimately, we were unable to obtain a satisfying identification. In mesosomal form and postcephalic setation, the specimen resembles *Camponotus* (*Myrmacraphe*) *furvus* Santschi, 1911 but it differs in head shape and by having shorter palps. In Taylor's key, the specimen runs to *C. acvapimensis* Mayr, 1862, yet it differs in mesosomal form. We therefore conservatively consider the specimen unidentified.

**Note 4.** †*Polyrhachis annosa* neatly meets the expectations for *Polyrhachis* as it clearly has lateral petiolar spines, which is synapomorphic condition of the genus. Based on the limited preservation, we do not have confidence that this species will be placeable either in the stem or crown of the genus based on morphology. However, given that the Varvara formation is young, being dated at between 7–5 Myo, we do not think that it is defensible to place this fossil in a separate genus. We therefore leave this species in *Polyrhachis* with the hope that future phylogenetic work will resolve the polarity of petiolar spines within the genus.

**Note 5.** The monotypic genera †*Chimaeromyrma* and †*Pseudocamponotus* have been treated as *incertae sedis* in Camponotini, for which we see no specific morphological evidence to question these otherwise harmless placements. We choose to retain †*Chimaeromyrma brachycephala* Dlussky, 1988 as a valid genus and species as it is possible that the identification of this amber fossil may be refined through the application of  $\mu$ -CT at some point in the future. As for †*Pseudocamponotus elkoanus* Carpenter, 1930, we doubt that this fossil will ever be identifiable given the lack of wing venation and very limited preservation of the single known specimen. Given that there is insufficient preservation to confidently place the species to tribe, we consider †*Ps. elkoanus* to be unidentifiable, hence invalid stat. nov. We do not synonymize †*Pseudocamponotus* with †*Camponotites*, however, as the former would take priority and we prefer the latter name as the form genus, given that it has the proper suffix (-tites) to indicate paleontological uncertainty.

**Note 6.** We erect the genus †*Eocamponotus* gen. nov. for †*Camponotus mengei* and its junior synonym †*Ca. igneus* as, although these fossils are sufficiently preserved for species diagnosis, formal combined-evidence analysis failed to support a relationship with any particular genus of the Camponotini (Boudinot et al. 2022a). In so doing, we aim to preclude the usage of this fossil in macroevolutionary analysis as a calibration point for the genus *Camponotus*. At most, this fossil species can be used as a calibration for the Camponotini; whether as a stem or crown calibration point, however, is much less certain, and a conservative approach would be for the stem of the tribe.

**Note 7.** We briefly note that †*Ca. mengei* was described alongside †*Ca. igneus* by Mayr (1868), and that the latter was accepted in a number of articles until Wheeler (1915) concluded that the latter is a subjective synonym of the former based on an examination of 103 *Camponotus* specimens and Mayr's types of †*Ca. mengei*. Wheeler reported that the type specimens of †*Ca. igneus* were in the collection of Franz Anton Menge, which is presumably in Gdańsk, Po-

land. The valid species was originally considered to be a *Ca. (Tanaemyrmex)* but was recently suggested by Radchenko and Perkovsky (2021) to be *Ca. (Camponotus)* due particularly to the form of its clypeus, and the shapes of the head and mesosoma, without further specification. Reevaluation of the morphological affinities of this species is necessary.

**Note 8.** †*Ctt. juliae* (Pierce & Gibron, 1962) comb. nov. is represented by a single male that was phosphatized in a calcareous nodule in the Calico member of the Miocene-aged Barstow formation in the Mojave Desert of California. The taxonomic history of this fossil is unusual. In its original description in Pierce and Gibron (1962), the fossil was classified as a new species of a new genus representing a new family of symphypleonan Collembola: †*Palaeosminthurus juliae* (†*Palaeosminthuridae*). These names went unnoticed for more than two decades, until the collembolist Dr Judith Najt (see Deharveng et al. 2017) observed that the preserved head, scape, thorax, and leg remnants of the fossil belong to a hymenopteran, which she identified as *Camponotus* (see Najt 1987). Subsequently, Roy R. Snelling examined the fossil, presumably at the Los Angeles County Museum, and concluded that the taxon is a junior synonym of *Camponotus festinatus* (Buckley, 1866) (Snelling 2006), an identification that was communicated to Barry Bolton in 2004 but went unpublished by the time of Roy Snelling's death in 2008. Bolton provisionally accepted this hypothesis in his taxonomic catalog (Bolton 2023). Here, after critical consideration of the available morphological evidence, we exclude the species from *Camponotus*, and revive the genus †*Palaeosminthurus* stat. rev., which we consider to be *incertae sedis* in Formicinae and unidentifiable hence invalid stat. nov. Specifically, we attempted to run the specimen through the male-based key to all Nearctic genera of Smith (1943) and that of Boudinot for all New World formicine genera (see section 3.7.H of Boudinot 2020); there is simply too little structural detail preserved to render a meaningful identification of this fossil. Unless a method like laminar  $\mu$ -CT may be applied successfully, we anticipate that this fossil will remain unidentifiable at the genus and tribal levels among the Formicinae.

**Note 9.** Here, we recognize the form taxon †*Camponotites* to which we transfer 29 species. †*Camponotites* should be categorically precluded from usage as calibration points for macroevolutionary analysis of the Formicinae or Formicidae. A balance for retaining and actively using this form genus is that the fossils in this taxon may be useful for paleogeographic study, so invalidation of this name may result in loss of paleostratigraphic information. Future work involving direct re-examination of these fossils is necessary to determine some of the taxa now placed in †*Camponotites* may perhaps be placed with more confidence among the genera of Camponotini—such as †*Ctt. novotnyi* (Samšić, 1967) comb. nov. as this fossil is quite well preserved and clearly displays the major synapomorphy of the Camponotini, namely that the antennal sockets are separated posteriorly from the posterior clypeal margin. For this example, however,

the remainder of the specimen is too poorly preserved to allow the fossil to be meaningfully associated with any extant genus of the Camponotini.

**Note 10.** From the illustration provided in the original description, it is not possible to confidently identify the specimen as a member of *Camponotus*. We retain this species as *incertae sedis* in the genus to encourage future work on the fossil, if possible.

**Note 11.** All of these fossils could be considered unidentifiable to species, hence invalid, but are here treated as *incertae sedis* in *Camponotus* to highlight their existence. Critically, because of the lack of morphological information, it is possible that a number of these taxa belong to other genera of Camponotini (see Ward et al. 2016 and Ward and Boudinot 2021). Reexamination of the original material is necessary in all cases.

**Note 12.** While it may be tempting to use †*C. vetus* as a calibration for *Camponotus* or the Camponotini, it cannot be confidently attributed to any living genus, subgenus, or species group due to insufficient morphological information.

**Note 13.** The generic placement of †*Ca. microcephalus* is dubious and should be confirmed through direct examination of type and additional material.

**Note 14.** Although †*Camponotus pictus* Zhang et al., 1994 is a junior primary homonym of *Ca. ligniperda pictus* Forel, 1886, we transfer this species to the form taxon †*Camponotites*, rendering a *nomen novum* unnecessary.

**Note 15.** The compression-fossil taxon †*Ca. obesus* is represented by fragments of the mesosoma, legs, and metasoma, all of which are preserved in a dorso-antrolateral oblique view. These remains are suggestive of *Camponotus* but otherwise cannot be identified meaningfully. Identification, in this case, is primarily driven by the rough similarity and absence of other ~14 mm long ants with an apparently rounded mesosoma in modern Western Europe.

**Note 16.** Bachmayer (1960) described †*Ctt. ullrichi* based on a single forewing from a Miocene-aged deposit in Austria. This ~10.3 mm long wing cannot be attributed to *Camponotus* or the Camponotini because free M diverges from Rs+M proximal to 2r-rs by more than twice the length of that cross vein. In Camponotini, free M diverges at or distal to 2r-rs (see Char. 499 on p. 293 of Boudinot et al. 2022b; also, Ward and Boudinot 2021). Because only Myrmelachistini in Formicinae have the split of Rs+M well proximal to 2r-rs, and as these ants are minuscule, we would prefer to consider the taxon *incertae sedis* in Formicidae. However, as this would necessitate the recognition of another “trashbin” form taxon, we elect to place the fossil in †*Camponotites* and to consider it unidentifiable, hence subjectively invalid stat. nov.

#### Genus †*Eocamponotus* Boudinot, gen. nov.

<https://zoobank.org/031A69F6-4431-4C53-9898-73728761C2C6>

**Type species.** †*Eo. mengei* (Mayr, 1868) by original designation.

**Note.** *Incertae sedis* in Camponotini.

3.3.2.4. Subfamily Myrmicinae Lepeletier de Saint-Fargeau, 1835

3.3.2.4.1. Genus *Crematogaster* Lund, 1831

I. Species retained in *Crematogaster*.

Copal fossil: Identifiable to species:

A. African copal [Holocene, < 36 Kya (Solórzano-Kraemer et al. 2020)].

1. *Cre. sp.* THIS STUDY. [w].

II. Fossils excluded from *Crematogaster*:

Genus †*Incertogaster* Boudinot, gen. nov., *incertae sedis* in Myrmicinae. [Note 1].

Type species: †*Inc. primitiva* (Radchenko & Dlussky, 2019), by original designation.

B. Kishenehn formation [USA, Montana; 47.8–41.3 Mya].

(1.) †*In. aurora* (LaPolla & Greenwalt, 2015). [q]. [Note 2]. Comb. nov.

C. Rovno amber [Ukraine; Eocene, 38.0–33.9 Mya].

(2.) †*In. praecursor* (Emery, 1891). [m]. [Note 3]. Comb. nov.

D. Sicilian amber [Italy; Oligocene, 11.6–5.3 Mya].

(3.) †*In. primitiva* (Radchenko & Dlussky, 2019). [m]. [Note 3]. Comb. nov.

**Note 1.** We erect the explicit catchall taxon †*Incertogaster* gen. nov., into which we place †*In. aurora* comb. nov., †*In. praecursor* comb. nov., and †*In. primitiva* comb. nov. We do so in order to recognize that these latter two species are not meaningfully placeable in *Crematogaster* based on their preserved morphologies, and that †*In. aurora* requires renewed attention. We choose †*In. primitiva* as the type species as the specimen of †*In. praecursor* examined by Emery is likely lost (see, e.g., Boudinot et al. 2016), and as the compression fossils require revised scrutiny and may be placeable in other genera, whether extant or extinct.

**Note 2.** †*Crematogaster aurora* is the oldest fossil attributed to the genus and is the most difficult to critique due to its highly suggestive but incomplete preservation. While we are uncertain about the placement of the fossil in *Crematogaster* due to the apparently axial postpetiolar helcium (*i.e.*, located at about mid-height of AIV rather than atop AIV) and the unknown antennomere count, the specimen does indeed lack a vertically oriented petiolar node, at least as preserved. To prevent the use of this fossil for divergence dating analysis while the preserved anatomy is reevaluated, we transfer the species forming †*In. aurora* comb. nov. We hope that additional specimens may be found, or the known specimens are subjected to documentation using advanced techniques. One of the authors (BEB) examined both the type and the paratype of †*In. aurora* at the USNM and observed that the paratype differed substantially, having (possibly) antennal scrobes but more importantly a lateromedially narrow postpetiole that was anteriorly attached to abdominal segment IV (metasomal III). Additionally, this specimen possibly had a 2–3-merous antennal club. Altogether, this raises doubt about the attribution of the paratype to †*In. aurora*, which remains of uncertain identification at present.

**Note 3.** The amber-preserved males described by Emery as †*In. praecursor* comb. nov. and Radchenko & Dlussky as †*In. primitiva* comb. nov. are unlikely to be representatives of either the stem or crown of the genus *Crematogaster* and are *incertae sedis* in the Myrmicinae within †*Incertogaster*. Both specimens have 13-merous antennae, while all *Crematogaster* males examined by the lead author have antennae that are 10–12-merous (Bolton 2003, p. 286; BEB, unpubl. data). Other diagnostic features include the short scape, which is  $\leq 2 \times$  the length of the pedicel, the pedicel shape, which is globular rather than cylindrical, and the mandibles, which are reduced or otherwise vestigial; the anterodorsal position of the postpetiolar helcium on abdominal segment IV can be difficult to discern. Unfortunately, Emery did not illustrate the wings or the face of †*Cr. praecursor*, so the fossil may need to be considered unidentifiable, hence subjectively invalid, if the specimen does not resurface. †*Crematogaster primitiva*, on the other hand, is well illustrated; its scapes are about  $4 \times$  the length of the pedicels, and the pedicels are not swollen or globular in shape. The mesosoma of this fossil (PMJ Pa 5824) is large and the mesoscutum is impressed, as in many *Crematogaster*, but the long and strongly nodiform petiole also contradict placement in that genus. At present, we cannot confidently attribute †*Cr. primitiva* to any valid generic taxon.

#### Genus †*Incertogaster* Boudinot, gen. nov.

<https://zoobank.org/C309774E-AD72-4AD1-81D5-A13DDA867614>

**Type species.** †*Inc. primitiva* (Radchenko & Dlussky, 2019), by original designation.

**Note.** *Incertae sedis* in Myrmicinae.

#### 3.3.2.4.2. Genus *Pheidole* Westwood, 1839

Amber/copal species: Identifiable to species:

- A. Mexican amber [Miocene, 23.0–16.0 Mya].
  1. †*Ph. pauchil* Varela-Hernández & Riquelme, 2021. [w].
  2. †*Ph. anticua* Casadei-Ferreira et al., 2019. [w].
  3. †*Ph. primigenia* Baroni Urbani, 1995. [w].
  4. †*Ph. tethepa* Wilson, 1985. [w]. [see Wilson 1985a].
- C. East African copal *sensu lato* [Holocene, < 36 Kya (Solórzano-Kraemer et al. 2020)].
  5. †*Ph. rasnitsyni* Dubovikoff, 2011. [w]. [Note 1].
- D. East African copal or Defaunation resin [Holocene, < 36 Kya (Solórzano-Kraemer et al. 2020)].
  6. †*Ph. cordata* (Holl, 1829). [w, s]. [Note 2].
    - = †*Formica cordata* Holl, 1829.
    - Neotype here designated (specimen Pa 5889).

Compression fossil species: *Species inquirenda*.

- E. Florissant formation [USA, Colorado; Eocene, 37.9–33.9 Mya].
  - (1.) †*Ph. tertiaria* Carpenter, 1930. [q]. [Note 3].

**Note 1.** Similar to the recent description of a *Dorylus* from putative Baltic amber (see section 4.2.1), the species †*Ph. rasnitsyni* was initially interpreted as an Eocene fossil (Dubovikoff 2011) but later reidentified as copal based on reevaluation of the material (Dubovikoff pers. comm. in Perkovsky 2016).

**Note 2.** We designate one soldier (= major) from the PMJ Pa collection (PMJ Pa 5889, copal,  $^{14}\text{C}$ -dated: ~700 years old) as the neotype of the †*Ph. cordata*, and tentatively associate a minor worker (PMJ Pa 5827) with this name although we do not recognize this as a secondary type. See section 3.3.2.6.1 for elaboration and Casadei-Ferreira et al. (2019) for a recent review of this taxon.

**Note 3.** Given the single photograph available for this species, which is otherwise reported from two specimens (Carpenter 1930), we consider †*Ph. tertiaria* in need of revised study, and strongly recommend against its use in divergence dating analysis until definitive synapomorphies of *Pheidole* may be documented. Most notably would be the occurrence of cross vein 2rs-m, which encloses the second submarginal cell and is otherwise absent from other Myrmicinae with the exception of various Myrmicini and Pogonomyrmecini.

#### 3.3.2.4.2.1. *Pheidole* taxon treatment

##### †*Pheidole cordata* (Holl, 1829)

Figs 19–21, Appendix 1: Fig. A5

**Neotype.** PMJ Pa 5889, *designated here*. Figs 19A–D, 20A–D, 21B, D, F.

**Locality and horizon.** East African copal (IAA results for PMJ Pa 5889: copal (Table 1);  $^{14}\text{C}$ -dating for PMJ Pa 5889: ~700 years old).

**Syninclusions.** Platygastridae, Ceratopogonidae, and Lepidoptera.

**Preservation.** The cuticle is preserved as a distinct layer as seen in the SR- $\mu$ -CT scan data. Most of the soft tissues are absent, except for parts of the digestive tract and some musculature, such as parts of the mandibular adductor (0 md1) and some muscles of the legs. The endoskeleton of the head and mesosoma is distinctly preserved and can be meaningfully used for future comparative anatomy.

**Paraneotypes.** None.

**Diagnosis.** The species, represented by the major worker, is identifiable as a member of the *Ph. megacephala* species group by (1) the presence of the conspicuous ventral convexity of the postpetiolar sternum (Fig. 19A; e.g., Salata and Fisher 2020). It differs from *Ph. megacephala* (Fabricius, 1793), *Ph. megatron* Fischer & Fischer, 2013, and *Ph. spinosa* Forel, 1891 by (2) the well-developed inner hypostomal teeth (Fig. 20B; e.g., Salata and Fisher 2022). Among the *megacephala* group species more broadly (e.g., Fischer et al. 2012), it differs in having (3) facial rugosity that extends to the posterior margin of the occipital lobes (Fig. 20A, note: among type specimens of the group imaged on AntWeb, this condition also occurring in *Ph. megacephala impressifrons* Wasmann, 1905, which has a

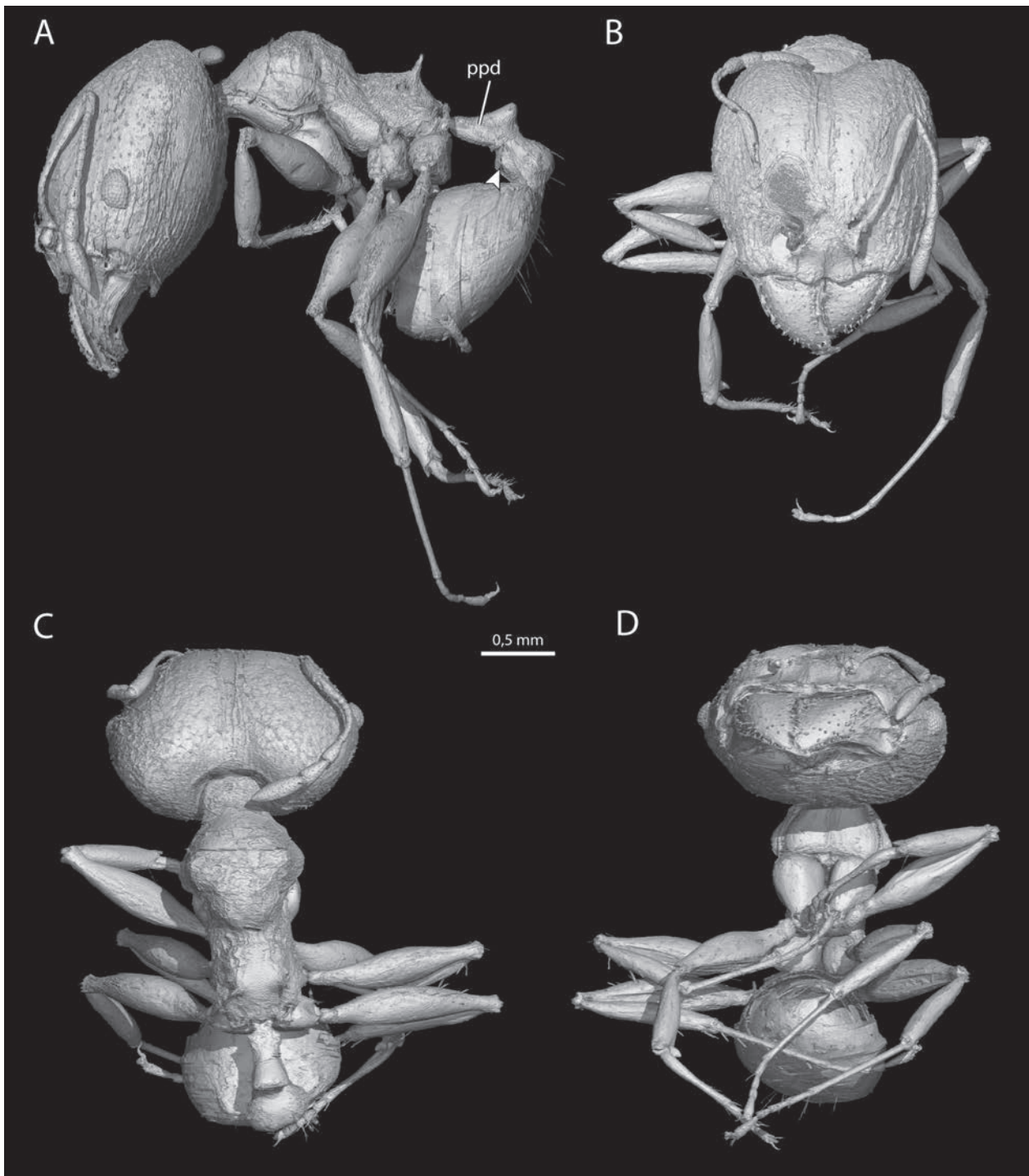


**Figure 19.** A–D. 3D-reconstruction of the neotype of †*Pheidole cordata* A. Habitus in lateral view; B. Habitus in frontal view; C. Habitus in dorsal view; D. Habitus in ventral view. Abbreviation: ppd = propodeum.

more angular bulge of the postpetiolar sternum). See the description below for further conditions.

**Description.** *Measurements* (in mm; abbreviations follow Salata and Fisher 2022): EL = 0.152; HL = 1.290; HW = 1.230; MTL = 0.673; PNW = 0.618; PPW = 0.324; PSL = 0.202; PTW = 0.172; SL = 0.714; WL = 1.110.

*Indices* (also following Salata and Fisher 2022): CI = 95.3; MTI = 54.7; SI = 58.0; PNI = 50.2; PPI = 26.3; PSLI = 16.4. Note: Measurements taken from cross-sectional projections in DragonFly using the reregistration and ruler tools.

**Head.** In full-face view (Figs 19B, 20A), the head is subcordate, with the lateral margins widest somewhat beyond head midlength and with the posterior portions of the lateral margins converging posterad to the occipital lobes. In lateral view (Fig. 19A), the head is subovate. The antennal scrobes are indistinct. The occipital lobes are rugose, with shagreened interspaces. The inner hypostomal teeth are well-developed; they are distant from the outer teeth, which are also well-developed (Fig. 20B). The median hypostomal tooth is indistinct.

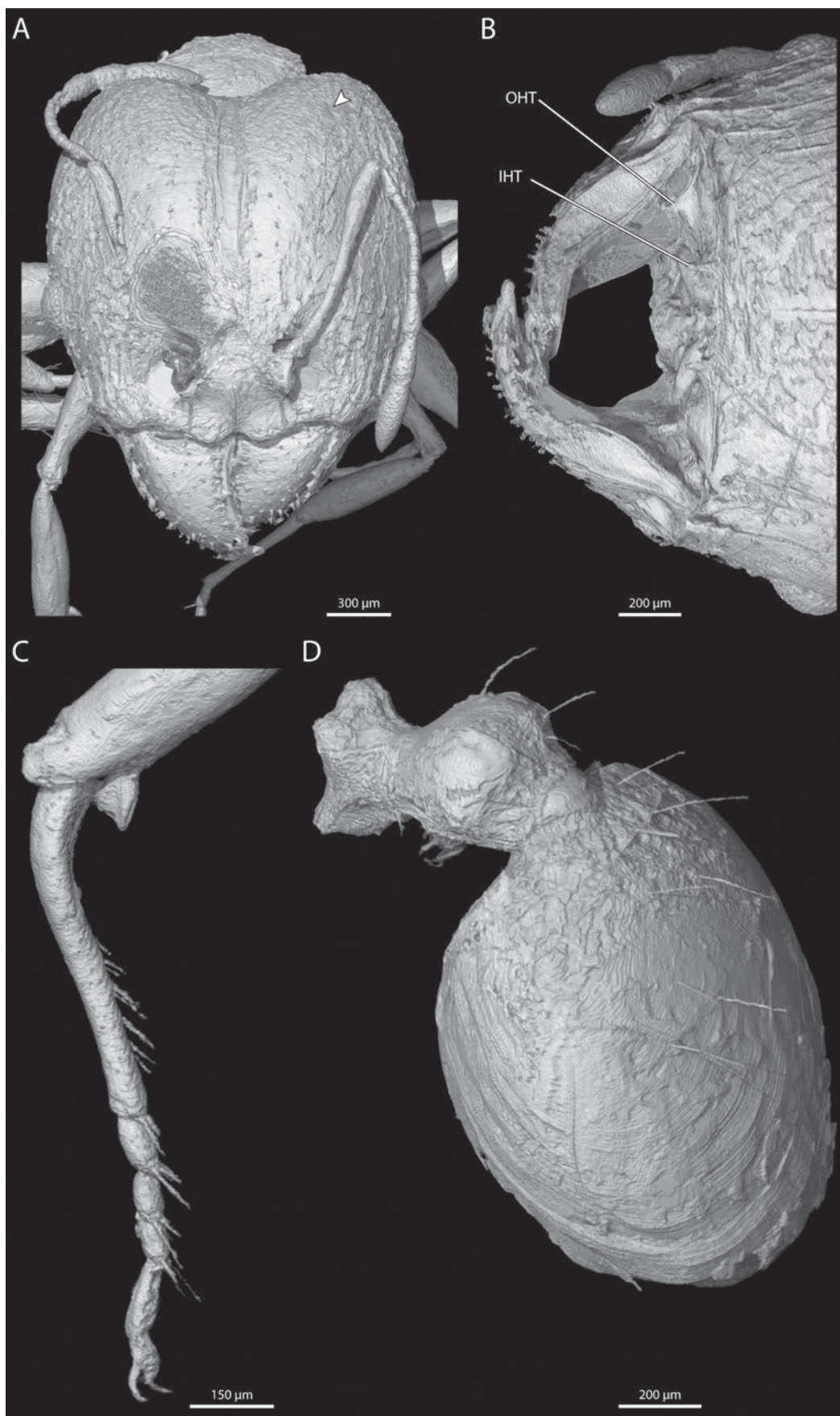


**Figure 20.** A–D. 3D-reconstruction of the neotype of †*Pheidole cordata* preserved in piece PMJ Pa 5889. **A.** Details of head in frontal view, arrow indicates occipital lobe; **B.** Detail of mouthparts in ventral view; **C.** Details of foreleg in lateral view; **D.** Details of metasoma in dorsolateral view. Abbreviations: IHT = inner hypostomal tooth, OHT = outer hypostomal tooth.

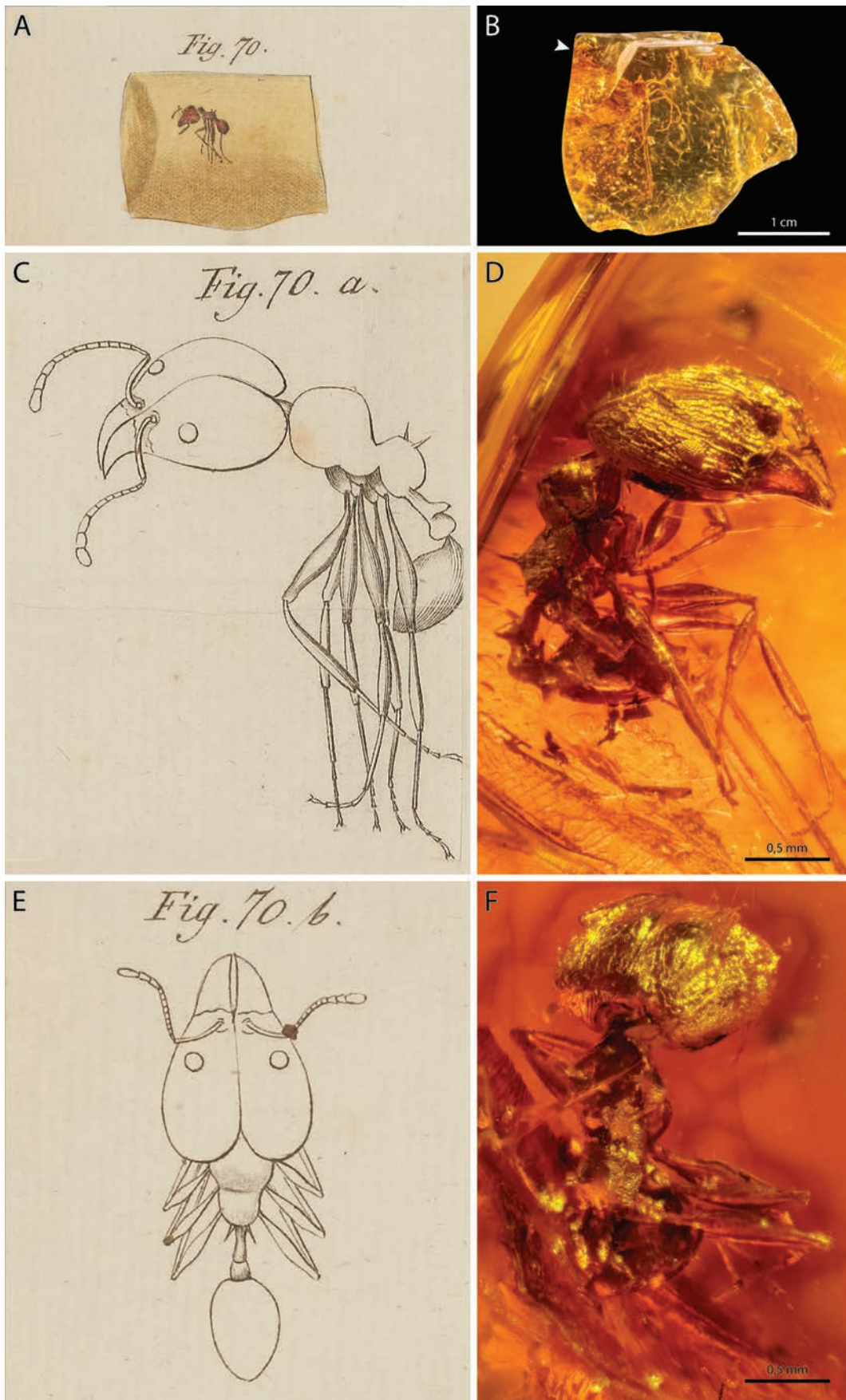


**Figure 21.** A, C, E. Copper lithographs by Schweigger (1819), which Holl (1829) named †*Formica cordata*. B, D, F. Photographs of the neotype of ‡*Pheidole cordata* A. Overview of the amber piece; B. Overview of the amber piece, arrow indicates the inclusion; C. Habitus in lateral view; D. Habitus in ventrolateral view; E. Habitus in dorsal view; F. Habitus in dorsolateral view.

**Mesosoma.** The humeral tubercle of the pronotum is weakly developed. The mesonotal bulge is distinct but not pronounced. The metanotum is only weakly indicated by a slight angularity of the promesonotal profile in lateral view. The propodeal spines are moderately long, with a wide base and acute tip (Fig. 19A).

**Metasoma.** The bulge of the postpetiolar sternum is rounded anteriorly. The first gastral tergum (ATIV) appears to be shagreened at its base (Fig. 20D).

**Setation.** Length and stature of setation uncertain, although density measurable in the scans based on the distinct occurrence of the setiferous punctation.

**Coloration.** Not clearly visible; appears brownish/red-dish.

**Remarks on the neotype.** Designation of the soldier in piece PMJ Pa 5889 as the neotype of †*Ph. cordata* meets the requirements of article 75 of the ICZN (1999), as follows. 75.3.1. The identity of this taxon is in severe need of clarification, as it has vexed systematists for nearly two centuries (e.g., Mayr 1868; Casadei-Ferreira et al. 2019) and may mistakenly be used for evolutionary inference, such as an Eocene-aged calibration for divergence dating based on the assumption that it is from Baltic amber, as recorded by, e.g., Bolton (1995, p. 319) and Bolton (2003). 75.3.2, –.3. Diagnostic remarks and description are provided above. 75.3.4. The original material is known to be lost (Casadei-Ferreira et al. 2019). It is unclear if the material sent by Schweigger ever made it to the MfN Berlin in the first half of the 19<sup>th</sup> century; see p. 111 of Schweigger (1819) and elsewhere for his stated intent to have the specimens identified there. Further, Holl (1829, p. 140) indicates that he defined his species †*Formica cordata* based on the observations of Schweigger and Mayr (1868, p. 18) explicitly states that he had not seen the material referred to by Holl. 75.3.5. The neotype matches the best available evidence. More specifically, the first author of the present work directly examined a physical print of the original illustrations by Schweigger (1819, figs 70, 70a, 70b on plate 8 therein; Fig. 21A, C, E), which were used by Holl (1829) to designate the species. Based on this, that author observed clearly illustrated 3-merous antennal clubs, which would rule out other Afrotropical Myrmicinae (Fisher and Bolton 2016). The illustrations further show attributes of *Pheidole*, including a massive head, high and domed promesonotum, low and spined propodeum, and long petiolar peduncle with a short node. Mayr (1868) was uncertain about the size of the original material, which is unknowable at this point and irrelevant for the present designation. Therefore, we interpret the fossil as *Pheidole* based on the available evidence (Fig. 21B, D, F), which is restricted to the examined copper plate due to loss of the original material. 75.3.6. The designated neotype does come from the original type locality and horizon as much as is practicable, given that Schweigger (1819): (a) knew about copal (pp. 103, 104 therein) and East African copal was available around that time (e.g., Smith 1868, see section 4.3.2 below); (b) he was uncertain about the provenance of the two specimens

eventually named †*Ph. cordata* by Holl (1829), as stated in the text; and (c) he pointed out that the species he examined resembled a taxon possibly from Africa (“Diese Bildung findet sich an Ameisen südlicher Länder.”, pp. 119 therein). Regarding the type locality further, although we cannot be absolutely certain that the specific fossil is from East African or Malagasy copal *sensu lato*, the syninclusion of a *Pheidole* minor from the PMJ Pa collection with *Dorylus* (PMJ Pa 5827), which has never been recorded from Madagascar, strongly implies that the material was from the mainland of the African continent. 75.3.7. The neotype is permanently preserved in and available for study at the Phyletisches Museum, Jena.

We have taken this action to resolve a suite of problems associated with the name †*Ph. cordata*, as recently reviewed by Casadei-Ferreira et al. (2019), who, after much consideration, concluded by placing this fossil *incertae sedis* in Myrmicinae. We fully agree with Casadei-Ferreira et al. (2019) that this fossil needs to be disposed of in order to avoid its uncritical use in systematic or evolutionary study and inference. By placing the name †*Ph. cordata* back in *Pheidole*, we alleviate the need for treating this taxon in the next revision of the fossil record of Myrmicinae, particularly as the specific epithet will be paired with the genus *Pheidole*, unless it were returned to *Formica*, to which it certainly cannot belong. Further, by designating a neotype we permanently fix this name to a known specimen that is both preserved in perpetuity in the PMJ Pa collection and is available for global evaluation via the cyber-type data. Finally, there is no possibility beyond egregious error for this taxon to be used as an Eocene calibration for *Pheidole* as the neotype is from <sup>14</sup>C-dated copal (copal *sensu lato*).

**Remarks on Afrotropical *Pheidole*.** It is widely appreciated among myrmecologists working on *Pheidole* that the genus is in severe need of revision both globally and in the Afrotropical region (Wilson 2003; Fischer et al. 2012; Sarnat et al. 2015), which is also the particular case for the *megacephala* species group (Fischer et al. 2012; Salata and Fisher 2022). While we would strongly prefer to not provide a one-off description of a *Pheidole* due to this complicated problem, we accept this as necessary and acceptable only in order to resolve the problem of †*Ph. cordata*, which is otherwise an irksome thorn-in-the-side bestowed upon generations of us by the well-meaning cataloging work of Holl (1829).

Although †*Ph. cordata* as typified here cannot be included in barcoding or phylogenomic datasets given its poor soft tissue preservation, it is our hope that the SR-μ-CT data may allow the confident and quantitative placement of this species among the species allied to *Ph. megacephala* via a dedicated revision of this species group. As noted in our diagnosis above, the neotype of †*Ph. cordata* (PMJ Pa 5889) is most similar to *Ph. megacephala impressifrons*, being most starkly distinguished from this form by the form of the postpetiolar sternum in lateral view. Notably, the form of the medial hypostomal teeth has not been recorded for the various forms of *Ph. megacephala* and similar species (e.g., Fischer et al. 2012). Whether the newly typified

species †*Ph. cordata* is extant is an open question; it is plausible that the historical habitat has been destroyed, hence this species may be considered a candidate Lazarus taxon. Further exploration of known Afrotropical copal *sensu lato* and extant myrmecofauna will be of considerable value.

### 3.3.3. Order Neuroptera: Synopsis of Nevrorthidae

#### 3.3.3.1. Family Nevrorthidae Nakahara, 1915. [Note 1]

##### I. Genus †*Balticoneurorthus* Wichard, 2016.

A. Baltic ambers [Eocene, 37.8–33.9 Mya].

1. †*Ba. elegans* Wichard, 2016. [m].

##### II. Genus †*Cretarhopalis* Wichard, 2017.

B. Kachin amber [Myanmar; Cretaceous, 99.6–93.5 Mya].

1. †*Crh. patrickmuelleri* Wichard, 2017. [f].

##### III. Genus †*Electroneurorthus* Wichard, Buder & Caruso, 2010.

A. Baltic ambers [see above].

1. †*El. malickyi* Wichard, Buder & Caruso, 2010. [f].

##### IV. Genus †*Girafficervix* Du, Niu & Bao, 2023.

C. Daohugou shale [China; Jurassic, 166.1–157.3 Mya].

1. †*G. baii* (Du, Niu & Bao, 2023). [l].

##### V. Genus †*Palaeoneurorthus* Wichard, 2009.

A. Baltic ambers [see above].

1. †*Pa. bifurcatus* Wichard, 2009. [m].

2. †*Pa. eoacaenus* Wichard, 2016. [m].

3. †*Pa. groehni* Wichard, Buder & Caruso, 2010. [m].

4. †*Pa. hoffeinsorum* Wichard, 2009. [m]. [Type species!].

##### VI. Genus †*Proberotha* Krüger, 1923.

A. Baltic ambers [see above].

1. †*Pr. dichotoma* Wichard, 2016. [f].

2. †*Pr. eoacaenus* Krüger, 1923. [m, f]. [Type species!].

##### VII. Genus †*Rhopalis* Pictet, 1854.

A. Baltic ambers [see above].

1. †*Rh. relictata* Pictet, 1854. [f, m]. (See also: Wichard et al. 2010.)

##### VIII. Genus †*Sisyronneurorthus* Nakamine, Yamamoto, Takahashi & Liu, 2023.

B. Kachin amber [see above].

1. †*S. aspoecorum* Nakamine et al., 2023. [f].

**Note 1.** Six of the eight fossil genera of Nevrorthidae are monotypic. For those two genera that have more than one species attributed to them, the type species is indicated.

#### 3.3.3.2. Genus *Palaeoneurorthus* Wichard, 2009

##### Genus *Palaeoneurorthus* Wichard, 2009

**Type species.** †*Palaeoneurorthus hoffeinsorum* Wichard, 2009.

**Diagnosis.** This genus can be characterized by the forewing with costal cross veins almost all simple, the cross veins 3rp3+4-rp2 present in forewings and absent in hindwings, the flattened male sternum 9 with tongue-like tip and the needle-like male gonapophyses 9.

**Note.** One male specimen in the amber collection (PMJ Pa 5874) is a member of Nevrorthidae. It was assigned to the genus *Palaeoneurorthus* based on our examination (Fig. 22A). We briefly characterize this specimen below:

##### †*Palaeoneurorthus* sp.

**Description.** Body length ca. 3.0 to 4.0 mm; forewing length 7.5–7.8 mm, hindwing length 6.4–6.8 mm.

**Head.** Ocelli absent. Antenna slenderly filiform, with slightly enlarged scapus, smaller pedicellus, and 30 flagellomeres. Maxillary palps and labial palps not visible.

**Wings** (Fig. 22B, C). Elliptical, translucent. Forewing venation with trichosors present among marginal forks of RA, RP, MA, MP, CuA and CuP; all costal cross veins simple. Sc and RA almost parallel to margin, connected basally and subdistally by two and one cross veins, respectively. RP with three main branches. MA fused with RP at proximal 1/3 of wing, distally branched. MP proximally separated into two main branches, with each branch bifurcated distad. Cu branching near wing base; CuA with seven pectinate branches; CuP sinuate, simple, forked distad. A simple. Most cross veins present at base, middle and distal 1/3. Hindwing venation: Basal part of the hindwing not visible. Trichosors present among marginal forks of RA, RP, MA, MP, CuA and CuP; costal cross veins on proximal 2/3 not visible, distal 1/3 simple. Sc and RA almost parallel to margin, subcostal cross veins absent. RP with two main branches. MA fused with RP at wing proximal 1/3, distally forked. MP with two main branches, one branch bifurcated distally and the other proximally, respectively. Cu branching near wing base; CuA with ten pectinate branches, CuP straight, simple. A not visible. Only two rows of cross veins visible, present at middle and distal 1/3, respectively. In forewings the cross vein 3rp3+4-rp2 present; in hindwings cross vein rp3+4-rp2 absent.

**Abdomen** (Fig. 22D, E). Visible part of abdominal segment 9 annular. Sternum 9 not visible. Robust gonocoxites 9 (= “gonocoxa” in Boudinot 2018) strongly incurved, with broad base, apically tapering, with strongly sclerotized, claw-like gonostyli 9 (= “stylus” in Boudinot, 2018), which are directed ventromedially. Ventrolateral lobes (= gonapophyses 9, “penital sclerites” in Boudinot 2018) consist of two needle-shaped projections, which are distinctly spaced; dorsal projection slightly longer than ventral one, both pointed apically. Ectoproct (= “proctiger” in Boudinot 2018) broad, slightly convex at middle and distinctly protruding on both sides in dorsal view.

**Remarks.** There are four described species belonging to *Palaeoneurorthus*, which are all known from Baltic ambers (Wichard 2009, 2016, Wichard et al. 2010). Among the four species of *Palaeoneurorthus* with males described our collection shares similarities with *P. eoacaenus* in having the set of two needle-like projections of gonapophyses 9, and the ventral projection of gonapophyses 9 being shorter than the dorsal one longer. However, based on our examination, the ventral projection of gonapophyses 9 is slightly

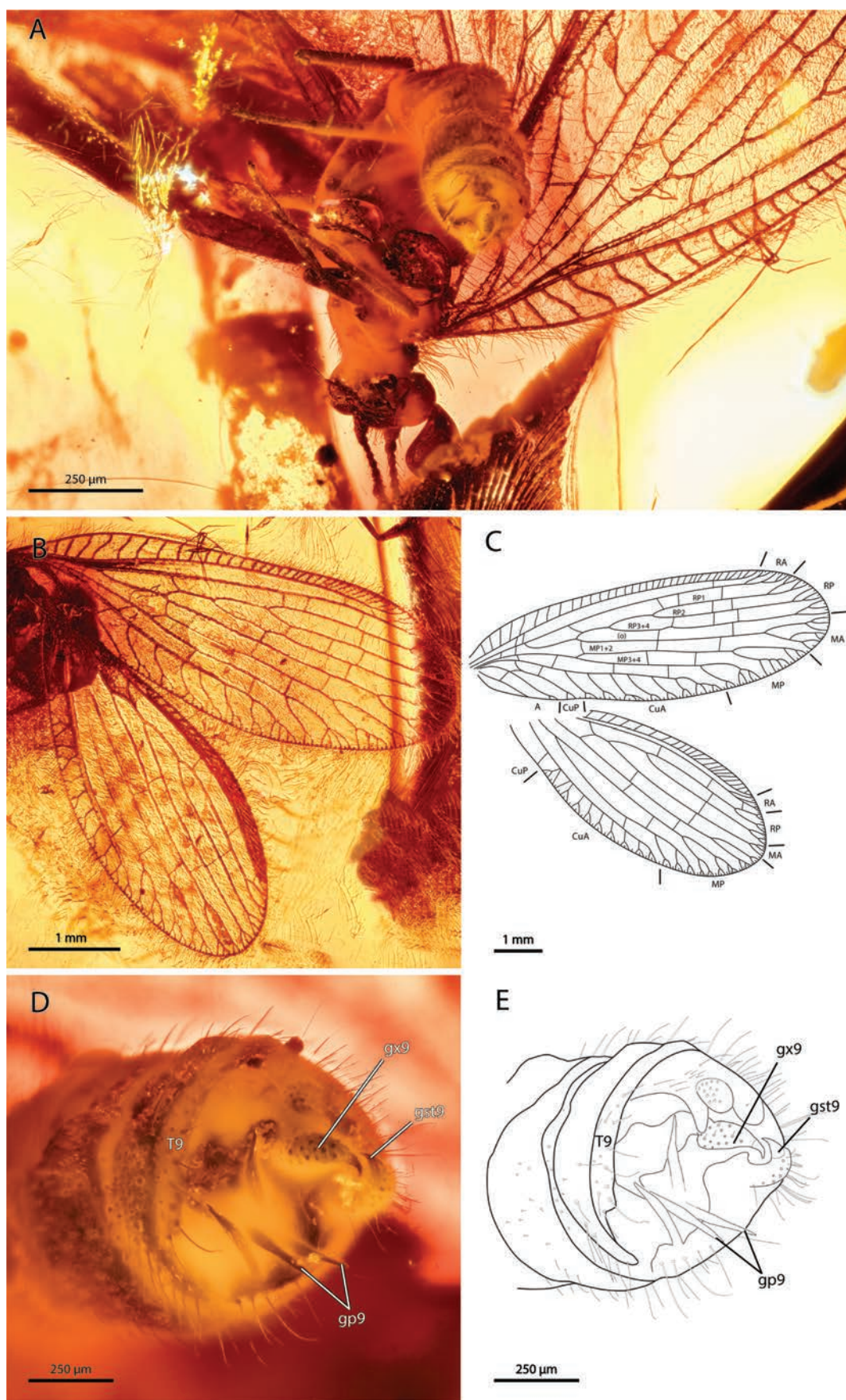


**Figure 22.** †*Palaeoneurorthus* sp. (Nevrorthidae) preserved in piece PMJ Pa 5874. **A.** Overview; **B.** Wing venation; **C.** Wing venation drawing; **D.** Genitalia; **E.** Genitalia drawing. Abbreviations: e = ectoproct, gp9 = gonapophyses 9, gst9 = gonostyli 9, gx9 = gonocoxites 9, T9 = tergum 9.

shorter than the dorsal one (Fig. 22C), whereas the dorsal projection is almost five times longer in *P. eoacenus* (Wichard 2016: fig. 6f). That the sternum 8 and the base of gonapophyses 9 are not visible impedes a further comparison. Thus, we currently treat this amber as *Palaeoneurorthus* sp.

### 3.3.4. Order Coleoptera

#### 3.3.4.1. Synopsis of fossil *Doliopygus* (Platypodinae)

##### 3.3.4.1.1. Genus *Doliopygus* Schedl, 1939

Copal taxa:

- A. East African “copal” [Holocene, 0.0–0.0 Mya].
  1. *D. crinitus* Chapuis, 1865. [Note 1].
  2. *D. tenuis* Strohmeier, 1912. [Note 1].
- B. Defaunation resin or copal (possible East African) [Holocene, 0.0–0.0 Mya].
  3. *D. cf. serratus* HERE. [Note 2].

**Note 1.** *Doliopygus crinitus* and *D. tenuis* were identified by Schedl (1939) from East African copal as species of *Crossotarsus*, with this original material presumably associated with the material misidentified as Baltic amber by F. Smith (e.g., Smith 1868; Grimaldi et al. 1994; O’Hara et al. 2013; see Note 2 of *Dorylus* above).

**Note 2.** We do not have the expertise to confidently identify the  $\mu$ -CT scanned specimen to species level, thus we appreciate the identification suggested by Bjarte Jordal. *Doliopygus* is known to be paraphyletic (Jordal 2015), with *D. serratus* being close to *D. chapuisi* (B. Jordal, pers. comm. 9 Nov 2022). Given the objective of the present manuscript, the tentative species identification is sufficient to resolve our uncertainty about the age of the resin matrix.

#### 3.3.4.2. Family Mordellidae Latreille, 1802

##### Family Mordellidae Latreille, 1802

**Note.** We do not provide a taxonomic synopsis of Mordellidae here as the fossil record of the family has been recently treated by Batelka et al. (2023).

#### 3.3.4.2.1. †*Baltistena* (a collective group name established by Batelka et al. 2023)

##### †*Baltistena nigrispinata* Batelka, Tröger & Bock, sp. nov.

<https://zoobank.org/CF6A27EB-FACD-482C-81B1-ECDD3130B529>

**Etymology.** The species name *nigrispinata* refers to distinctly black combs on metatibia and tarsomeres contrasting with orange surface of the cuticle.

**Type materials.** *Holotype*. PMJ Pa 5870, Baltic amber. Sex indeterminable. *Cybertype*: Appendix 1: Fig. A6.

**Paratypes.** None.

**Differential diagnosis.** The species belong to the subgroup of Mordellistenini with emarginated or dilated pen-

ultimate pro- and mesotarsomere *sensu* (Ermisch 1950). To this possible clade belong twelve of fourteen of Baltic Mordellistenini so far described (Batelka et al. 2023). In †*B. nigrispinata* sp. nov. the eyes are glabrous without interfacetal (= interommatidial) setae as in †*Palaeostena eocenica* Kubisz from which it differs by lower number of combs on metatibia and metatarsomeres I and II, and by the shape of palpomere IV which is type C1 *sensu* Franciscolo (1957) in †*Palaeostena*. The ultimate maxillary palpomere is securiform as in †*Baltistena korschefskyi* (Ermisch) from which †*B. nigrispinata* sp. nov. differs by the absence of combs on metatarsomere III and by the comb formula. The ring of short black scale-like setae on the tip of pygidium is similar to that in †*Baltistena brevispina* Batelka, Rosová & Prokop and in †*Palaeostena eocenica*. The metakatepisternum is fused early with the metaven-trite in the middle of its posterior edge, which has so far only been observed in †*Palaeostena eocenica* among the Eocene Mordellistenini, while the other four species described by Batelka et al. (2023) have a separate and discernible metakatepisternum that is elongate and extends to the metanepisternum. Based on the shape of the body, the glabrous eyes, the shape of the metakatepisternum, and the setae on the cauda, †*B. nigrispinata* sp. nov. most closely resembles †*Palaeostena eocenica*. Also, while adding the species into the key provided by Batelka et al. (2023) it is coupled with †*Palaeostena eocenica* and †*Baltistena amplicolis* (Ermisch). From the last species, †*B. nigrispinata* sp. nov. differs by the comb formula, the shape of the ultimate maxillary palpomere, and the length of antennomeres III and IV, combined compared to antennomere V.

This set of characters observed for †*B. nigrispinata* sp. nov. supports the hypothesis that the species of Baltic Eocene Mordellidae formed a characteristic fauna that was much different from extant European representatives (Batelka et al. 2023).

**Description.** Head subglobular, frons continuously convex, hind margin of eye at posterior margin of head, elytra convex, pygidium long, metacoxa broad, comb formula 3//2/1/0/0. Habitus in lateral view (Fig. 23A, Fig. 24A).

Main diagnostic characters as defined by Franciscolo (1967) and Batelka et al. (2023): Right antenna well visible, left antenna (Fig. 23B) visible from basal part of antennomere II, antennomeres subcylindrical, slightly compressed, without any lateral projections, antennomeres III–IV slightly widening towards apex (Fig. 24B), length ratios of antennomeres as follows: ?-1.4-1.0-1.25-1.6-1.4-?-?-1.6-2.0; antennomere XI regularly rounded at apex; antennae densely covered by erect or semierect sensilla from antennomere III. Maxillary palpomere I small, palpomere II prolonged, widest at apex, palpomere III short, triangular, palpomere IV long, securiform of *Mordella*-type (Franciscolo 1957: fig. 6\_A1) (Fig. 24C). Eyes finely faceted; Eyes glabrous without interfacetal setae. Scutellar shield continuously rounded (Franciscolo 1957: fig. 9\_type10) (Fig. 24D). Basal side of pronotal disc widely convex in central part (Fig. 24E). Elytra 3.2 × as long as pronotal disc. Form of protarsi indiscernible. Structure of

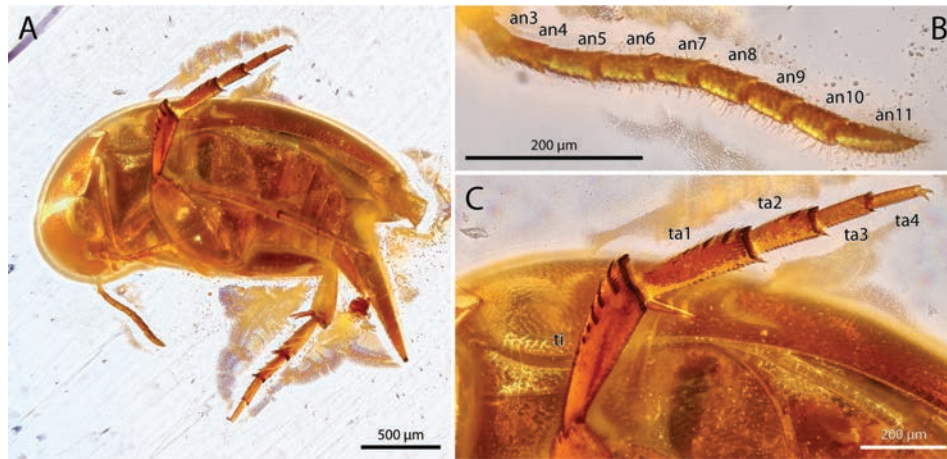


**Figure 23.** A–C. Holotype of †*Baltistena nigrispinata* Batelka, Tröger & Bock, sp. nov. (Mordellidae) preserved in piece PMJ Pa 5870. A. Habitus; B. Left antenna; C. Right metathoracic leg. Abbreviations: an3–an11 = antennomeres 3–11, ta1–4 = tarsomeres 1–4.

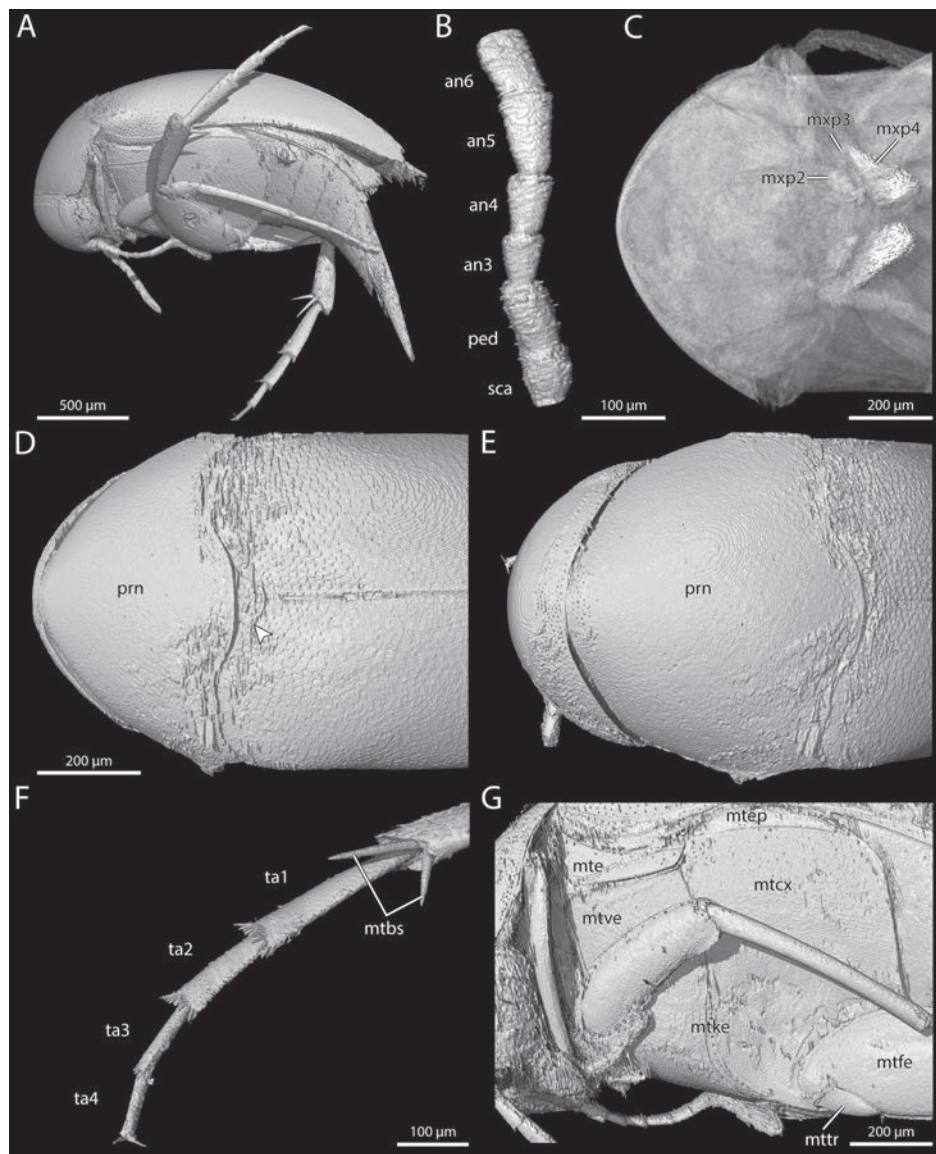


**Figure 24.** A–F. 3D reconstruction of the holotype of †*Baltistena nigrispinata* Batelka, Tröger & Bock, sp. nov. (Mordellidae). A. Habitus in lateral view; B. Antennomeres I–VI; C. Maxillary palpomeres; D. Habitus dorsally (scutellar shield pointed by arrow); E. Pronotal disc; F. Metatibial spurs; G. Thorax laterally. Abbreviations: an3–an6 = antennomeres 3–6, mtbs = metatibial spurs, mtcx = metacoxa, mtfe = metafemur, mte = metanepisternum, mtep = metepimeron, mttr = metatrochanter, mtke = metakatepisternum, mtve = metaventrite, mxp2–4 = maxillary palpomeres 2–4, ped = pedicel, prn = pronotum, sca = scape, ta1–4 = tarsomeres 1–4.

protibia indiscernible. Mesotarsomeres I – III cylindrical, tarsomere I  $6.1 \times$  as long as wide; tarsomeres II and III  $5.0 \times$  as long as wide; tarsomere IV excised almost to middle region; tarsomere V about  $3.0 \times$  as long as wide. Mesotibia very slightly shorter than metatarsomeres combined. Metatibia (Fig. 23C) with three distinct lateral combs of scale-like setae including preapical comb, combs do not reach middle of metatibia; preapical comb runs parallel with apical fringe of setae, remaining two combs slightly oblique; few isolated patches of scale-like setae inserted posterior to last dorso-lateral comb. Metatibia with two spurs, outer spur shorter than inner one (Fig. 24F). Metatarsomeres (Fig. 23C) I–IV with row of spiniform setae consisting ventrally of 12 to 17 short, strong setae, formula: 17/14/12/15; metatarsomere I with two black and short lateral combs of scale-like setae and three isolated patches of black setae; metatarsomere II with one short lateral comb of scale-like setae and one black isolated seta, metatarsomeres III – IV without combs; length ratio of metatarsal segments 2.2-1.2-1-1. Pygidium long and straight,  $2.4 \times$  as long as hypopygium. Metanepisternum long and narrow, lower corner of posterior edge rounded, anterior edge  $3 \times$  as long as posterior edge, ventral edge  $7.5 \times$  as long as posterior edge (Fig. 24G). Metakatepisternum restricted to ventral part of thorax, fused with median portion of posterior edge of metaventrite (Fig. 24G). Pretarsal claws long and straight, with 2 indistinct teeth on ventral edge. Tip of pygidium with ring of short black scale-like setae. Lengths in mm: pronotal disc = 0.46, elytra = 1.29, mesotibia = 0.46, metatarsomere I = 0.38, pygidium = 0.73, body without head = ca. 2.

## 4. Discussion

### 4.1. Geological provenance of the rediscovered PMJ Pa amber collection

Between the taxonomic and color qualities of the resin pieces, coupled with the IAA results (Table 1), we were able to sort the fossils into Baltic amber and African copal categories to our satisfaction. Initially, the conflict among the qualitative tests and the results from the IAA confounded us. After considering these results, the true significance of the biotic inclusions, however, became clear, resolving the conundrum of fossil source. From our perspective, it was deeply surprising to find specimens interpreted as copal from the IAA tests that were directly labelled as from “Samland Kleinkuhren” in the PMJ Pa collection, especially as there are no reports, to our knowledge, that copal has been found in the Samland Peninsula (See also 4.2.2.). While we were initially skeptical that labels and objects might have been mixed in the small PMJ Pa collection, this seems to be the most likely scenario. We note that von Knorre kept the collection as it was given to him, thus the collection has not been seen and processed until now. The evidence from the PMJ Pa amber collection clearly shows a shift in source, especially from “without” to a confidently assigned one and simply false labeling could be

resolved, and thus presents in a small scale what it might look like in another, larger collection.

At the bottom line, the scenario we encountered with this collection illustrates two critical points: (1) the importance of the correct labeling of any specimen, further underscoring the value of accurate corresponding information for contemporary and future research (King 1975; Corado 2005; Donovan and Riley 2013); and (2) the necessity of skepticism for fossils, even when having label data, as it was only the combination of biotic and chemical data that allowed us to draw confident conclusions about “amber” provenance in the present study. While the chemical or biotic evidence alone may have been sufficient, our uncertainty was not resolved until we had both lines of evidence, which clearly showed the inadequacy of the qualitative tests that have been supposed to differentiate between amber and copal.

### 4.2. Historical conspectus

To arrive at a more comprehensive understanding of the Phyletisches Museum amber collection and the materials contained therein, it was necessary to review the historical literature on amber in general (section 4.2.1) and on the Kleinkuhren locality in particular (section 4.2.2).

#### 4.2.1. From the amber road to the 19<sup>th</sup> century

In antiquity, Tacitus (circa 56–120 AD) correctly concluded that amber was a tree resin: “*sucum tamen arborum esse intellegas, quia terrena quaedam atque etiam volucris animalia plerumque interlucent, quae implicata humore mox durescente materia*” (that it is a tree sap, however, can be seen from the fact that some crawling, but also flying animals are often visible between, which get into the liquid and are then trapped when the material hardens) Tac. Ger. 45.6 The Baltic Sea has been a source of amber well before the time of Tacitus, as amber from this region has been found in neolithic burial sites (Singer 2016). There exists much older evidence for the use of amber, such as in the cave of Isturitz, dating back to 34,000 years ago (King 2022), but only a brief outline with a focus on Baltic amber shall be given here as full-length books have been published on the subject from various perspectives (e.g., Brost and Dahlstrom 1996; Grimaldi 1996; King 2022).

Through the so called “Amber Road”, an ancient trade route, amber was exported from Europe to Asia, the Mediterranean Sea and Egypt (Singer 2008, 2016). Amber might have reached Egypt directly by sea or via Syria, of which the famous Quatna lion would be proof (Mukherjee et al. 2008). In the neolithic era the first use of amber was certainly due to superstition and so the transparent, flammable and, when rubbed, fragrant material was attributed with protective properties. It was worn by the living as jewels or donated as precious grave goods (Andrée 1951; Frondel 1968; Larsson 2010; Vijande Vila et al. 2015). The scientific use of inclusions played a subordinate role during antiquity, despite a few correct inferences that amber is a

tree resin and is originally liquid, for example, Tacitus (see above), Aristotle (*Meteorology* 4.10), or Pliny the Elder (Plin. Nat. 37.11). Nevertheless, the “amber effect” was already known by Plato, which is the oldest mention of the fact that rubbed amber attracts lightweight objects placed near it (Assis 2010). With this only applying to amber, our present terms “electric” and “electricity” are derived from the Ancient Greek ἤλεκτρον (*ēlektron*) (Andrée 1951).

Considerable time passed until inclusions became demonstrably more important for science, from the Bronze Age via ancient scholars up to the 16<sup>th</sup> century. As early as in the beginning of 14<sup>th</sup> century, the paternoster makers used amber for their necklaces (Buchholz 1961; Hinrichs 2007). Amber as jewellery and art is still widely appreciated today (Pileckaitė 2001; Goldenberg 2004; Sado 2022) and one of the most famous goldsmiths in the last century was Toni Koy (1896–1990). Written evidence for the beginning of a scientific use was provided by scholars, such as medical doctors and pharmacists, or affluent persons interested in natural history.

One of the first scientific records, found in Gessner (1565)–[1566], is about the mineral collection of Johannes Kentmann (p. 22–24), who listed in his order “*Succina gravida*” few insects in amber, for example “5. *Eiufdem coloris, in quo formica. Darin ein omeiß.*”, i.e., an ant is within. In his work he used the system of minerals published by Agricola (1546) and was in fact one of the first scholars to put it into practice. A comparable scientific collection of that time was owned by Michele Mercati, an Italian polymath (cf. Hinrichs 2007), whose work was published posthumously in 1717 (Mercati 1717; King 2022). Amber was an attractive object in the so-called *Wunderkammern* (cabinets of curiosities), where it was valued more for its beauty than for scientific reasons. Probably one of the best-known wonder chambers is the famous “*Grünes Gewölbe*” in Dresden (Germany), while the most famous and mysterious is the *Bernsteinzimmer* of Königsberg, which was established by the Prussian king Frederick I in 1701 and the following years, and vanished in 1944, in the turmoil of war. The possible survival and whereabouts of this assembly of amber remain a mystery.

In 1742 Nathanael Sendel published his “*Historia Succinorum*” on the Dresdner amber collection of Augustus the Strong (Augustus II, “August der Starke”) and his son Friedrich August II. In this remarkable work, which largely deals with animals enclosed in amber as shown in part one “*Historia insectorum succino conditorum*” (Sendel 1742), he laid the foundation of modern amber research (Wichard and Wichard 2008). Even if Sendel erroneously assumed that amber was formed by soil in so-called “Gagat-Veins”, as well as some inaccurate species determinations (Greven and Wichard 2010), the merit of this work is undisputed, due in part to the 13 rich lithographs by Christian Friedrich Boetius (1706–1782). Another breakthrough in amber research was achieved by Georg Carl Berendt with his “*Die Insekten im Bernstein*”. Berendt was clearly ahead of his time, as he concluded “[...] *die Art ist verschwunden. Dass sie ausgestorben*

*sei, lässt sich nicht behaupten [...] wahrscheinlich ist sie durch das veränderte Klima nur verdrängt [...]*” ([...] the species disappeared. It cannot be said it is extinct [...] it has probably only been displaced by the changing climate [...]) (Berendt 1830, pp. 37). The issue of climate change is today more relevant than ever (Flannery 2009, Tollefson 2022), and amber inclusions can provide valuable evidence (Słodkowska 2013; Penney 2010; Penney et al. 2013; Solórzano-Kraemer et al. 2020). Moreover, Berendt was aware of the importance of inclusions for the study of earth’s history, and he saw evidence against the constancy of species (Berendt 1830, pp. 5 and 6; Hinrichs 2007). With Berendt a modern state of amber research was reached, with a broad knowledge of insects, and cooperation between researchers with different taxonomic expertise. Furthermore, Berendt already distinguished between copal and true amber and was aware of the true origin of amber as a fossilized resin of a pine tree. Regardless of the theoretical basis of the time, new species were constantly described and the total number of described species from amber surely exceeds 4860 (Briggs 2018; Ross 2021), most of them being insects.

Far fewer specimens have been reported from copal, with a total of only about 120 species from these resins reported or described from East Africa and Madagascar (Solórzano-Kraemer et al. 2020), for example. Copal has been and still is largely undervalued as a scientific resource (Penney 2010; Penney and Preziosi 2013), although it has great potential for the study of recent biodiversity (Delclòs Martínez et al. 2020; Solórzano-Kraemer et al. 2020, 2022). Indeed, the young age of copal inclusions renders them ideal for documenting the loss of biodiversity, particularly since the colonial and industrial eras. Solórzano-Kraemer et al. (2020) recognized amber as > 2.58 Mya, Pleistocene and Holocene copals as between 2.58–0.0117 Mya and 0.0117 Mya–1760 AD, and Defaunation resin as younger than 1760 AD. Faced with the dual threats of global climate change and global deforestation, the intensive study of copal and Defaunation resin along with extant taxa may be our best and last chance to understand our contemporary biotic communities before it is too late.

Symington Grieve wrote in his book about the great auk in 1885:

*“The following pages have been written in the hope of interesting some in the story of an extinct bird. The whole history of the Great Auk is a sad one – the continued slaughters of the helpless victims culminating in the final destruction of the race on the skerry, named Eldey, off the coast of Iceland, excites to pity. The last of the Great Auks has lived and died. The race was blotted out before naturalists, when too late, discovered it was gone. Regrets are now useless – the living Garefowl is extinct.”*

This happened, because of human influence, as it did for at least another 14 vertebrate species in the last 200 years (Piper 2009). One of the most well-known examples of anthropogenic extinction is the marsupial

Thylacine (*Thylacinus cynocephalus*), which was hunted relentlessly to the margins of extinction, till the last one died in 1936 at Hobart Zoo (Brook et al. 2023). Another famous and quite recent event of extinction, not only through hunting, but also due to habitat loss it that of the passenger pigeons (*Ectopistes migratorius*). Who would have thought that a bird, so common that flock size easily exceeded millions of individuals (Wright 1911), could go extinct? Of course, one key factor was that they were hunted as a food resource, the other on the deforestation, as due to their high specialization in tree nuts, they were not able to find enough food anymore (Guiry et al. 2020). These extinct species, victims of human activities, are today highly valued objects in museums, be it for display, teaching or scientific research.

Humans' fatal impact on environment extinction is progressing at an alarming rate, with a lot of species going extinct without ever being noticed (McKinney 1999; Régnier et al. 2015). Therefore, copal and Defaunation resin are not only a short window to the past, but they should also be a warning, of what is to come. Defaunation resin in particular is not only amenable to  $\mu$ -CT analysis, as conducted here (Figs 3, 4, 6–11, 17), but also to genomic study, at least in some cases (Modi et al. 2021). With so many recent and near recent taxa to describe, let alone true amber fossils, it is imperative that we recognize the value of all biological specimens preserved in collections.

#### 4.2.2. The Samland and Kleinkuhren localities

Samland, or the Kaliningrad Peninsula of today, is located on the south-eastern shore of the Baltic Sea, which has been part of the Soviet Union and Russia since 1945.

One direct locality (PMJ Pa 5827) from the collection is given as *Kleinkuhren* (in German), today known as Filino, which is located on the north-western tip of Samland. Most specimens contained in the piece were to be very untypical (see sect. 3.1.1. Biotic evidence) for the region of origin on the label, which drove us to further investigate on these localities.

Since the earliest written records of the region, the practice of “*Bernsteingrüberey*” (amber mining or fishing) has been exercised by the inhabitants of the coast of Samland, which they also used to earn their living (Weber 1740; Hildt 1803). In 1861, Karl Mayer described the “faunula of Kleinkuhren”, with 35 specimens to be found in the marine sandstone (Mayer 1861). According to these findings, he assigned the layer to the Rupelian (33.9 and 27.82 Ma). Noetling and A. von Koenen, came to the same conclusion some years later (Meyer 1914). The age of these sediments was questioned, however, and more recent investigations suggest that it is distinctly older, about 48 Ma (Ritzkowski 1997). Nevertheless, Perkovsky et al. (2007) pointed out that the results of Kaplan et al. (1977) are more reliable and suggested 37.7 Ma (Perkovsky et al. 2007), which in retrospect is closer to Mayer. The age estimations of all these researchers clearly indicate that no copal occurs in the sediments of the

Samland region. Additionally, we were not able to find any report that copal has ever been found in the region of Kaliningrad-Oblast or its shores.

With the localities “Samland?” or “Samland, Bernsteinwerke Königsberg” and one with an original invoice (see section 3.1.1 above) the question when the collection was acquired could be further clarified. The Preußischen Bergwerks-Hütten-Aktiengesellschaft (Preussag) was founded on December the 13<sup>th</sup> in 1923; only a few years later they joined forces to form a manufacturing company known as “Staatliche Bernstein-Manufaktur GmbH” (SBM) in 1926 (Erichson and Tomczyk 1998). In 1929, the VEBA (Vereinigte Elektrizitäts- und Bergwerks-AG, Berlin) was established for the uniform financing of the state economic enterprises (Winkler 2019). This indicates that Pa 5863 was purchased between 1923 and 1929. It was not uncommon that amber was sold to entomologists, which was advertised in a timely manner (Königsberg-Pr. 1937). Today, the amount of amber harvested from the Samland peninsula per year was 500 tons in the first decades of the 20<sup>th</sup> century (Causey 2011).

#### 4.3. Biological conspectus

The primary data that can be captured from fossil organisms ranges from preserved anatomy—whether from sclerites or soft tissue (e.g., Pohl et al. 2010; Boudinot et al. 2022c; Richter et al. 2022)—to chemical composition (e.g., Trueman 2013; Barden et al. 2017; McCoy et al. 2017), with the two sources of information being nearly indistinguishable depending on the tools used and the scale of comparison (e.g., Modi et al. 2021; Jiang et al. 2022). In order to maximize the biological value of fossils, it is essential to identify the geological source unambiguously and to critically evaluate the plausible phylogenetic affinities of the inclusions. While the former requires the tracking or retracing of stone provenance often coupled with chemical tests (e.g., section 3.1.1 above and 4.3.2 below), the latter depends on: (1) the phylogenetic stability of the taxonomic system in question; (2) the quality of anatomical information obtained from the specimen; and (3) the availability of comparable information from extant taxa. In best case scenarios, both the phylogeny and phenotypic affinities of the fossils may be evaluated jointly (e.g., Klopstein and Spasojevic 2019; Mongiardino Koch and Thompson 2021; Boudinot et al. 2022a) or in sequence, which nearly always requires substantial revision of fossil interpretations (e.g., Fikáček et al. 2020; Boudinot et al. 2022d; Schädel et al. 2022). A special issue of contemporary paleontological phylogenetics is to produce a classification that is both robust and systematically organizes diagnostic information, allowing future works to place fossils with certainty, or at least explicit uncertainty. Below, we highlight both issues via discussion of the Psocodea (section 4.3.1), which are grossly understudied anatomically, and *Dorylus* (section 4.3.2), which have been plagued by taphonomic uncertainty for

over a century. We conclude this section with a consideration of broader issues and methods for paleoentomology (section 4.3.3).

#### 4.3.1. The case of barklice (“Psocoptera”), an underestimated and undeservedly spurned group

The barklice, or the psocopteran grade of the order Psocodea, are in a twilight zone of phylogenetic paleontology, as fossil material is very abundant from the present through the Mesozoic, yet the extant taxa are grossly understudied anatomically (Yoshizawa 2002; Mockford 2018; Kawata et al. 2022). Moreover, only the sub- and infraordinal relationships have been resolved via molecular systematics (de Moya et al. 2021), with the exception of a few families (Mockford 1999; Yoshizawa and Johnson 2008). As a consequence, a well-founded system to place fossils is lacking. The morphological assumptions of prior generations of taxonomists are largely untested, hence still dominant in the process of taxonomic determination and evolutionary inference. This is in addition to being problematic for understanding Psocodea for their own sake. This reduces the phylogenetic key role of the group as either sister to the Holometabola or the Condylgnatha (Misof et al. 2014), which are issues of crucial importance to broader insect phylogenetics and evolutionary history.

Two extinct taxa directly highlighting the present difficulties of psocodean systematics are †*Arcantipsocus* and †*Paramesopsocus*, both originally placed in new, nominal families (Azar et al. 2008, 2009), and now considered to belong to Amphientomidae and Electrentomidae, respectively (Mockford et al. 2013). In both cases, the authors relied on the cladistic analysis of Yoshizawa (2002) for morphological characters. Azar et al. (2008, 2009) recognized that the taxonomic sampling of Yoshizawa (2002) was focused on Psocomorpha. Nevertheless, they placed their fossils using the characters of that study as the matrix was the most comprehensive that was available. As a consequence, both paleontological studies attributed the fossils to Psocomorpha, with overreliance on the thick pterostigma and presence of the nodus, which were considered as autapomorphies of the suborder (Yoshizawa 2002). By studying an expanded sample of fossil and extant taxa, Mockford et al. (2013) recognized that these characters are homoplastic among the suborders, and that other, less prominent features reasonably place †*Paramesopsocus* near Amphientomidae and †*Arcantipsocus* within this family. Even though this is certainly an improvement, these placements have yet to be incisively scrutinized using adequate data sets and analytical methods.

Both examples underline the problems with placing fossils into insufficiently founded systems, where relationships are often not supported by well-defined apomorphies, or where assumptions have yet to be tested. A specific problem in psocodean systematics is the almost exclusive use of characters of wing venation and genitalia, while most other body parts or organs are understudied and neglected during investigations. In a comparative sense,

it is surprising that the shape and presence or absence of sclerites (except for genital structures) are very rarely used in systematic research on Psocodea, in contrast to other groups or insects (see, e.g., Pohl and Beutel 2005; Beutel et al. 2011). They are often the best-preserved characters in amber fossils besides the wings and might provide many phylogenetically informative features. It is conceivable that the missing access to new technologies may impede scientific progress in this field. Moreover, many fossils are simply not sufficiently preserved for detailed observation. With our present work, we hope to ignite interest in a more thorough morphological analysis of extant and fossil Psocodea, particularly using modern morphological methods such as  $\mu$ -CT and computer rendering, which can reveal rich morphological data from limited material (Figs 7–11).

#### 4.3.2. The case of *Dorylus*, a long historical arc

Ants of the genus *Dorylus* dominate Old World tropical ecosystems above and below ground, where they occur, and have long fascinated and challenged systematists working on ants (Gotwald 1995; Borowiec 2016; Boudinot et al. 2021). As such, the geological age and paleogeographic distribution of their crown clade is of considerable interest. Any fossils potentially attributable to *Dorylus* are thus of substantial evolutionary importance. In the present study, we identified one such species represented by dozens of individual specimens preserved in resins labeled as “Baltic amber” from the PMJ Pa collection (Figs 2, 3). The temptation to accept this assumption as a conclusion was powerful, yet we struggled to make sense of the initial qualitative tests. We therefore sent samples of the resin matrix for FT-IR, which contradicted the hypothesis that these specimens were from Eocene-aged succinite. Still not satisfied, we subjected one quality exemplar of this *Dorylus* species to SR- $\mu$ -CT scanning and 3D reconstruction (Appendix 1: Fig. A1).

With our  $\mu$ -CT data, we were able to identify the PMJ Pa *Dorylus* as belonging to the extant subspecies *Dorylus nigricans molestus*, based on the key to subgenera from Gotwald (1982) and the key to the *D. nigricans* species group (former *Anomma*) of Santschi (1912). Specifically, the fossil has 11-merous antennae with flagellomeres that are longer than wide, the terminal abdominal tergum has well-defined ridges around its central depression, the spines of the frontal carinae and posterolateral corners of the head are lacking, the petiole widens posteriorly as seen in dorsal view, and the ventral posterolateral corners of the node angular and produced, rather than rounded. Coupled with the identification of the synincluded platypodine as a member of an extant metapopulation, we were forced to reject the succinite hypothesis. Subsequent  $^{14}\text{C}$  analysis resulted in an estimated age of  $\sim 145$  years for the *D. n. molestus*-bearing piece, squarely falling in the category of Defaunation resin. Although these specimens are not as ancient as we were led to believe by the original labels, they may yet be of systematic value: To resolve the species boundaries of this complex, a comprehensive

revision of *Dorylus nigricans* integrating sequence and morphological data is necessary (see Wilson and Brown 1953 on subspecies in myrmecology and Borowiec 2019 for further consideration in the context of Dorylinae).

The PMJ Pa *D. n. molestus* are far from the first positive subfossil members of *Dorylus* and the first false positive *Dorylus* from Baltic amber. Alongside the doryline *Neivamyrmex iridescens* from Colombian copal, DuBois (1998) previously reported *D. n. molestus* from confirmed East African copal *sensu lato*. Over a century before, F. Smith (1868) had identified a *Dorylus* (“being either *Anomma rubella* or a closely related species”, p. 184) from what he assumed to be Baltic amber, but which was later determined to be East African copal (Grimaldi et al. 1994; O’Hara et al. 2013). Notably, “*Anomma rubella*” is currently considered to be *Dor. nigricans rubellus* (Savage, 1849), which suggests that the imperfect F. Smith may have handled material quite similar to, if not from the same source, as that of the PMJ Pa and those cited by DuBois (1998). Even more recently, Solórzano-Kraemer et al. (2022) figured multiple unidentified *Dorylus* specimens from Holocene copal (= Defaunation resin) from Tanzania (their fig. 11e, f), while the unavailable name †*Dissumulodorylus perseus* was provided for specimens of putative Baltic origin (Sosiak et al. 2022), which were later revealed via FT-IR to be sub-fossil resin by those authors (Sosiak et al. 2023a, b). Although moot due to unavailability, which we maintain, key structural details for species-level identification were not visible in their scans even after refined segmentation (Dubovikoff and Zharkov 2023). The work of Sosiak et al. (2022, 2023a, b) is an exemplary demonstration of biological hypothesis testing, and further underscores the necessity for a critical approach to the use of “amber” fossils for systematics and evolutionary influence.

#### 4.3.3. Fossil evaluation: Further pitfalls

The two direct examples arising from the main part of this study illustrate the dual difficulties and importance of correctly identifying fossil provenance (section 4.3.2) and placing fossils in systems, when robust phylogenetic and anatomical documentation is lacking (section 4.3.1). With the deep and expanding backlog of amber fossils from Eocene Baltic and other sources (e.g., Peris et al. 2016; Delclòs et al. 2023), a true flood has become available with the intensive exploration of Burmese Kachin amber (e.g., Ross 2019, 2021; Boudinot 2020; Boudinot et al. 2020; Peris and Rust 2020; Pohl et al. 2021; Beutel et al. acc. pend. minor revision), all of which necessitates critical care in the treatment of anatomical information from these and other fossils, including adpression fossils, which may be older but are usually less well-preserved (e.g., Boudinot et al. 2022b). In addition to inadequacy of the phylogenetic system (point 1, section 4.3.1), insufficient morphological documentation (point 2, section 4.3.1), and failure to compare fossils to extant taxa (or absence of comparable information; point 3, section 4.3.1), we recognize three more shortcomings that, in variable

combination, may lead to problematic inferences: (4) lack of taxonomic and evolutionary context, e.g., no keys, character lists or data matrices are provided; (5) inexpert knowledge of potentially related extant groups; and (6) inadequate phylogenetic evaluation. Because the literature is rapidly being filled with incautious conclusions, which are hard to correct, we find it unfortunately necessary to outline these issues and some examples so as to encourage finer comparative attention to detail.

The erroneous conclusions of two examples may have been emolliated via taxonomic specialist contribution (e.g., Li et al. 2022; see also Vitali 2019). Critical reevaluation of a putative mordellid larva from Cretaceous amber (Zippel et al. 2022) found that the insect in question is a sawfly (Batelka and Engel 2022), possibly belonging to the family Blasticomidae (Rasnitsyn and Müller 2023), while putative “triungulins” of Strepsiptera (Schwarz et al. 2005) were eventually correctly placed based on piecemeal reconstruction of fine structures (Beutel et al. 2016, Batelka et al. 2019) with the final clarification provided by Pohl et al. (2018), wherein the first true strepsipteran primary larva enclosed in amber was identified. A third example, that of the putative new beetle family †Ptismidae (Kirejtshuk et al. 2016), was recognized as a synonym of the scirtiform family Clambidae after it was shown that this taxon was defined based on symplesiomorphies and gross rather than specific, structural similarities (Cai et al. 2019). As in many “high throughput” studies on amber fossils, the documentation and interpretation of morphological features were insufficient.

Beyond problems of nomenclature and systematics, lack of precise observation and identification may also lead to evolutionary misinterpretations that may have ramifying consequences for paleoecology. For example, there are presently only few events of pollination documented in the fossil record of the Cretaceous and Cenozoic and these should be taken with caution (e.g., Peña-Kairath et al. 2023). A new species of the cucujoid family Kateretidae was described by Tihelka et al. (2021), who suggested that the beetle was feeding on angiosperm pollen and was acting as a pollinator, thus seemingly revealing a very early event on beetle-angiosperm interaction. However, it was shown by Bao et al. (2022) that the pollen in question was in fact of gymnosperm origin and not ingested by the beetle via careful documentation and experimental replication of pollinivory.

An apparent and frequent problem in insect paleoentomology are fossil placements based more-or-less on intuition (e.g., Kirejtshuk et al. 2016; Kirejtshuk 2020), rather than arguments in the sense of synapomorphies or formal phylogenetic analyses based on maximum parsimony (MP) or Bayesian inference (BI). The placement of adpression fossils was formally evaluated by Fikáček et al. (2020) and Boudinot et al. (2022d), using morphological data sets and phylogenetic topologies based on comprehensive molecular data sets. A similar approach was recently applied to minute myxophagan beetles in Burmese amber (Fikáček et al. 2023). The characters were analyzed

in a Bayesian framework under different schemes of constraints, also using phylogenetic patterns based on molecular phylogenies. It is still a common practice in paleoentomology to erect and shift extant or extinct taxa without adequate analyses or at least phylogenetic arguments in the sense of apomorphies (e.g., Kirejtshuk 2020). However, this approach leads to random taxonomic and phylogenetic changes, lacks a solid basis, and does not help to understand the evolution of beetles and other groups (e.g., Fikáček et al. 2020; Boudinot et al. 2023).

#### 4.4. Technological Conspectus: Phenomics

A key technology transforming the study of insect anatomy and evolution is micro-computed tomography ( $\mu$ -CT), which allows for the non-destructive, replicable, quantitative sampling of structures at the submicron scale either preserved or in motion, in the case of x-ray kinematics (or cineradiography, e.g., van de Kamp et al. 2015; Wulff et al. 2017). The non-invasive generation of phenomic data further allows for the evaluation of complex functional interactions, such as for the metasoma of Scorpiones (Günther et al. 2021) and copulation in Strepsiptera (Peinert et al. 2016; Jandausch et al. 2023), Hymenoptera (Semple et al. 2021), and Lepidoptera (Zlatkov et al. 2023). For the purposes of paleoentomology,  $\mu$ -CT has profound advantage as beam penetrance allows for the discovery of biological inclusions in opaque amber (Lak et al. 2008), phosphatized nodules (van de Kamp et al. 2018), and even Triassic coprolites (Qvarnström et al. 2021). In a pair of studies on Cretaceous stem ants (Boudinot et al. 2022c; Richter et al. 2022), it was discovered that soft tissue may be preserved in spectacular detail, including a nearly complete cephalic muscle set, glands, and elements of the central nervous system, and the utility of  $\mu$ -CT was demonstrated for revisionary systematics and phylogenetic character discovery. That  $\mu$ -CT is especially valuable for character discovery and phylogenetic hypothesis testing was also demonstrated in a study on the prosternum of extant Hymenoptera (Boudinot et al. in prep.), which expanded the available anatomical variables of this structure from 11 to 124. This study further showed potential for  $\mu$ -CT as a tool for museomics, as a century-old specimen produced high-quality scan data, complementing genome capture from preserved material (e.g., Blaimer et al. 2016). Although relatively time-consuming, even simple surface renders may be highly informative (e.g., Garcia et al. 2019; Jałoszyński et al. 2020), especially for rare taxa or irreplaceable specimens (e.g., Simonsen and Kitching 2014) and when used as one prong of a multi-modal approach for phenotype documentation, alongside green-fluorescent light for fossils (e.g., Clarke et al. 2018; Boudinot et al. 2020, 2022c), and SEM, CLSM, and manual histology for extant taxa (e.g., Richter et al. 2019, 2023; see also Friedrich and Beutel 2008, Friedrich et al. 2014).

Even though the loss of information and amount of artefacts are usually very low, some aspects must be taken

into account: (a) depending on fixation considerable deformation can occur, as for instance tissue preserved in ethanol can shrink through dehydration, depending on time and tissue properties up to a loss of 60% of the original volume (Hedrick et al. 2018; Leonard et al. 2022); (b) imaging contrast can be distinctly improved by iodine-staining (Metscher 2009) but this can demineralize specimens immersed for a longer time span (Early et al. 2020); (c) stained specimens can be de-stained very efficiently using thiosulfate solution, but this can increase calcium solubility and cause decalcification (Mataic and Bastani 2006; see Callahan et al. 2021 for a de-staining protocol); (d) desktop micro-CT scanners are still expensive and energy consuming, and not accessible for all scientists; (e) the post-processing of the data can be very time consuming; and (f) in the case of most synchrotron-scanned resin pieces a dark band occurs where the beam passed (e.g., Pohl et al. 2019; Sadowski et al. 2021), consequently thus it is also preferable that the piece should be carefully documented with photographs before scanning. Care should always be taken not to use an excessive level of energy of synchrotron radiation, as this can be destructive or leave behind an irreversible brownish band to the amber. The documentation of structural details can be enhanced by isolating individual structures of a certain specimen through physical preparation, or using an intact specimen; the target focal areas can be cleaned with chloroform (Ammar et al. 2015). Moreover, appropriate cleaning can distinctly reduce artifacts and thus accelerate the further processing. This can be further optimized with AI, for instance by using Biomedisa (Lösel et al. 2020).

Another major advantage of  $\mu$ -CT data is that they can be made available to the community in suitable databases. A specimen gone through the three steps mentioned above can be distributed to scientists or the public in various forms. The data accessibility is crucial in different ways, but especially so for museum material and type specimens (Faulwetter et al. 2013), with cybertypes having use even beyond classificatory purposes (e.g., Naumann et al. 2020). For many active researchers, access to type material is often very difficult (Orr et al. 2020). Shipping is expensive and bears an enormous risk of damage or even losing specimens. In most cases, the scientific benefit and the entitlement of scientists to study the fauna of their country outweighs this risk (Dupérré 2020). However,  $\mu$ -CT data can be made available electronically and thus open a new dimension of making specimens accessible, in the ideal case even including surface textures and color (Ijiri et al. 2018). Even though digital information can never fully replace the physical type specimens (Rogers et al. 2017), it is a highly efficient way to facilitate revisions and also to stimulate scientific inquiry and discussion in different contexts. Even if technical resources are limited, this can be extended using models from platforms like Sketchfab (Epic Games, Cary, North Carolina, USA) or MorphoSource (MorphoSource.org). In our study as well as in previous contributions (Aibekova et al. 2022; Tröger et al. 2023; Weingardt et al. 2023), these options were used to visualize complex

3-dimensional structures in an easily accessible way to contribute to a better understanding of insect morphology.

A final aspect of  $\mu$ -CT data that confers unique advantage is for museums- and classroom-based pedagogy (e.g., Shelmerdine et al. 2018). School children and students can examine, disassemble, and assemble a wide variety of objects which enhances the understanding of complex 3D objects. The risk of damage is negligible compared to real specimens or wax models. This has been successfully demonstrated with the neurocranium of the mud-shark *Squalus acanthias* at the Institute of Zoology and Evolutionary Research of the Friedrich Schiller University (Jena, Germany) (Moritz pers. comm., 2022). 3D reconstructions are further advantageous as they can be scaled, which facilitates the visualization of structures or even entire animals which are otherwise hardly accessible. In the current project EntomonVR (Saqalaksari et al. 2023) demonstrated new opportunities to study and enhance the understanding of insect morphology in an engaging and appealing way. A less expensive way to present  $\mu$ -CT results as 3D printed models was used in the exhibition of the Phyletisches Museum, where a copulating pair of leaf beetles (*Neocrepidodera ferruginea*) is on display, which was magnified forty times and airbrushed. With the above mentioned combination, a multisensory approach in museums can be boosted, as it is possible to conserve valuable objects, while allowing visitors to simultaneously handle an authentic copy (Wilson et al. 2017; Ziegler et al. 2020). This includes the option to make objects tangible for visually impaired visitors (Neumüller et al. 2014). The use of CT-scans to create highly realistic enlarged models of different organisms is now gaining great momentum, as for instance demonstrated by 10TONS (<https://www.10tons.dk/>) or Julia Stoess (<https://www.insektenmodelle.de/de/>).

## 5. Conclusion

The only direct documentation of the history of evolution in the dimension of time is the fossil record, for which the highest fidelity of preservation is afforded by exuded resins that may fossilize over the course of millions of years, thus forming amber. To be useful for biodiversity studies, it is critical that the source of inclusion-bearing resins be identified, as the difference in age between true amber and copal or Defaunation resin may profoundly influence ecological, biogeographical, and evolutionary inferences. The rediscovered amber collection of the Phyletisches Museum allowed us to starkly demonstrate this crux, as several pieces labeled as Baltic amber would have represented new generic records for the ant fauna of the Eocene, including the widespread and dominant genera *Crematogaster*, *Dorylus*, *Lepisiota*, and *Pheidole*. Through chemical (FT-IR, UV-VIS,  $^{14}\text{C}$ ), systematic (anatomical SR- $\mu$ -CT reconstruction), and historical investigation, we were able to not only correct the historical mislabeling of these and all other specimens in the amber collection, but to also review and revise the fossil record of *Amphientomum*

and the Amphientomidae (Psocodea), several clades of Formicidae (Camponotini, *Crematogaster*, Dorylinae, *Pheidole*, Plagiolepidini, †*Yantaromyrmex*), the Nevrorthidae (Neuroptera), and two beetle genera (*Doliopygus*, Platypodinae; †*Baltistena*, Mordellidae). With respect to fossil resin provenance, we found that the study of historical records is highly useful where these exist, and that the generally recommended qualitative tests for amber identity fail spectacularly when benchmarked against quantitative tests, particularly FT-IR. In brief, when new records of taxa that are millions to tens of millions years older than the oldest known representative, great care should be taken to ensure that label data accurately reflect the source of the fossil material. With the rediscovered *Bernsteinsammlung*, the Phyletisches Museum is now known to comprise Defaunation resin, copal, and succinite (true Baltic amber) as well as Kachin amber. The biological value of subfossil material should not be overlooked.

## Conflicts of interest

The authors declare no conflict of interest. The funders had no role in the design of the study; in the collection, analyses, or interpretation of data; in the writing of the manuscript; nor in the decision to publish the results.

## Author contributions

Conceptualization: BEB, BLB. Methodology: BEB, BLB, MW, DT, KJ, JUH, HP. Software: JUH. Validation: BEB, BLB. Investigation: BEB, BLB, MW, DT, KJ, JUH, DL, OTDM, JB, AR. Resources: JUH. Data Curation: BEB, BLB, MW, JUH, JB. Writing, original draft: BEB, BLB, DT, MW, JB, DL. Writing, review & editing: RGB, AR, HP. Visualization: MW, DT, BLB. Supervision: RGB, HP. Project administration: BEB, BLB. Funding acquisition: BEB, DT, MW, AR.

## Funding

This research was funded by the following.

- Boudinot: the Alexander von Humboldt Stiftung via a research fellowship (2020–2022) and a Peter S. Buck research fellowship at the Smithsonian Institute (2023).
- Richter: the Evangelisches Studienwerk Villigst eV via a scholarship (2020–2022).
- Förderverein Phyletisches Museum Jena e. V.
- Research of Jan Batelka was financed from operational program „Grant Schemes at CU“ (reg. no. CZ .02.2.69/0.0/0.0/19\_073/0016935).
- Tröger: scholarship of the Deutsche Bundesstiftung Umwelt (DBU) (2022–)
- Weingardt: Landesgraduiertenstipendium (2023–), Honours Programme University of Jena 2021–2022

## Data availability statement

The original  $\mu$ -CT datasets of †*Amphientomum knorrei* Weingardt, Bock & Boudinot, sp. nov. (PMJ Pa 5809), Archipsocidae gen. et sp. indet (PMJ Pa 5825), †*Baltistena nigrispinata* Batelka, Tröger & Bock, sp. nov. (PMJ Pa 5870), *Doliopygus* cf. *serratus* (PMJ Pa 5827), *Dorylus nigricans molestus* (PMJ Pa 5884), and the neotype of †*Pheidole cordata* (PMJ Pa 5889) are databased and assigned a unique identifier at the Phyletisches Museum (Jena, Germany) and additionally available at the data repository MorphoSource (URL: <https://www.morphosource.org/projects/000547325?locale=en>) with the reference numbers: 000549407 (†*Amphientomum knorrei* Weingardt, Bock & Boudinot, sp. nov.), 000549379 (Archipsocidae gen. et sp. indet.), 000549353 (*Dorylus nigricans molestus*), 000549006 (†*Baltistena nigrispinata* Batelka, Tröger & Bock, sp. nov.), 000548650 (*Doliopygus* cf. *serratus*), 000552612 (†*Pheidole cordata* Holl 1829, neotype).

## Acknowledgments

We thank: Dietrich von Knorre and Matthias Krüger for sharing their profound knowledge of the whole PMJ collection; the International Amber Association (IAA) Gdańsk, Poland for chemical analysis; Brian Fisher, Michele Esposito, and Barry Bolton for AntWeb and AntCat; Charles Lienhard, Lulan Jie, Gurusamy Ramesh, Alexander Rasnitsyn, Christian Schmidt, and Dmitry Vassilenko for sharing Psocodea literature; Vincent Perrichot for loaning Ethiopian amber material; Feiyang Liang for confirming the genus identification of *Amphientomum* and providing additional information on amphientomid genitalia; Phil Ward and Rodolfo da Silva Probst for discussing the ideal treatment of the camponotine fossils; Alêxandre Ferreira for discussing the Defaunation resin *Pheidole*; Bjarte Jordal for identification of the platypodine, provision of literature, and discussion of *Doliopygus* systematics; Eva-Maria Sadowski, David Ware, and Andreas Abele-Rassuly for the possibility to take photographs at the MfN Berlin; and Jill Oberski for providing comment on a pre-submission version of the MS and for consistent discussion during the construction and revision of the work. We also thank Kazunori Yoshizawa and Phil Ward for their incisive and useful feedback on the manuscript, as well as the editor, Sonja Wedmann; we thank Phil once more for catching an embarrassing blunder, for which we are grateful.

We acknowledge the provision of beamtime related to the proposal BAG-20190010 at PETRA III beamline P05 of DESY, a member of the Helmholtz Association (HGF). We acknowledge the support during the beam times by Hereon team members Fabian Wilde, Julian Moosmann, and Felix Beckmann. This research was supported in part through the Maxwell computational resources operated at Deutsches Elektronen-Synchrotron DESY, Hamburg, Germany. Gunnar Brehm for the loan of his lepiLED. Additional support was provided by the Alexander von Humboldt Stiftung (BEB: 2020–2022; the Japan Society for the

Promotion of Science (AR: 2023–), the Smithsonian Institution (BEB: 2023), Landesgraduiertenstipendium (MW: 2023–), the Honours Programme from University of Jena (MW: 2021–2022), the Evangelisches Studienwerk Villigst eV (AR: 2020–2022), the Deutsche Stiftung für Umwelt (DT 2022–), the Grant Schemes at Charles University (JB: reg. no. CZ.02.2.69/0.0/0.0/19\_073/0016935), Susanne & Jens Wurdinger and the Förderverein Phyletisches Museum e.V.. We are very grateful to the Smithsonian's Biodiversity Heritage Library and the librarians who kindly permitted us to examine an original book (Schweigger 1819) and scanned the pages: Leslie Overstreet and Erin Rushing. Last but not least, we thank the Museum für Naturkunde (Berlin) for waiving the publication costs of our article.

## References

- Aarle WV, Palenstijn WJ, de Beenhouwer J, Altantzis T, Bals S, Batenburg KJ, Sijbers J (2015) The ASTRA Toolbox: A platform for advanced algorithm development in electron tomography. *Ultramicroscopy* 157: 35–47. <https://doi.org/10.1016/j.ultramic.2015.05.002>
- Aarle WV, Palenstijn WJ, Cant J, Janssens E, Bleichrodt F, Dabrovolski A, de Beenhouwer J, Batenburg KJ, Sijbers J (2016) Fast and flexible X-ray tomography using the ASTRA toolbox. *Optics Express* 24: 25129–25147. <https://doi.org/10.1364/OE.24.025129>
- Agricola G (1546) *De Natura Fossilium*. Libri X, Basel.
- Aibekova L, Boudinot BE, Beutel RG, Richter A, Keller RA, Hita-Garcia F, Economu EP (2022) The skeletomuscular system of the mesosoma of *Formica rufa* workers (Hymenoptera: Formicidae). *Insect Systematics and Diversity* 6: 1–26. <https://doi.org/10.1093/isd/ixac002>
- Ammar E-D, Hentz M, Hall DG, Shatters Jr RG (2015) Ultrastructure of wax-producing structures on the integument of the melaleuca psyllid *Boreioglycaspis melaleucae* (Hemiptera: Psyllidae), with honeydew excretion behavior in males and females. *PLoS ONE* 10: e0121354. <https://doi.org/10.1371/journal.pone.0121354>
- André E (1895) Notice sur les fourmis fossiles de l'ambre de la Baltique et description de deux espèces nouvelles. *Bulletin de la Société Zoologique de France* 20: 80–84.
- Andrée K (1951) *Der Bernstein – Das Bernsteinland und sein Leben*. Kosmos, Stuttgart 95 pp.
- AntWeb (2022) Version 8.77.4. California Academy of Science. <https://www.antweb.org> [last accessed 18 July 2022]
- Assis AKT (2010) *The experimental and historical foundations of electricity*. Apeiron, Montreal, 268 pp. <https://doi.org/10.1007/s11191-010-9318-z>
- Azar D, Hajar L, Indary C, Nel A (2008) Paramesopsocidae, a new Mesozoic psocid family (Insecta: Psocodea “Psocoptera”: Psocomorpha). *Annales de la Société Entomologique de France* 44: 459–470. <https://doi.org/10.1080/00379271.2008.10697581>
- Azar D, Nel A, Néraudeau D (2009) A new Cretaceous psocodean family from the Charente-Maritime amber (France) (Insecta, Psocodea, Psocomorpha). *Geodiversitas* 31: 117–127. <https://doi.org/10.5252/g2009n1a10>
- Bachmayer F (1960) Insektenreste aus den Congerienschichten (Pannon) von Brunn-Vösendorf (südl. von Wien) Niederösterreich. *Sitzungsberichte der Österreichischen Akademie der Wissenschaften. Mathematisch-Naturwissenschaftliche Klasse. Abteilung I* 169: 11–16. [https://doi.org/10.1007/978-3-662-25541-4\\_1](https://doi.org/10.1007/978-3-662-25541-4_1)

- Badonnel A (1934) Recherches sur l'anatomie des Psoques. 241 pp. [80 figs]
- Badonnel A (1948) Psocoptères du Congo Belge (2e note). Revue de Zoologie et de Botanique Africaines 40: 266–322.
- Badonnel A (1949) Psocoptères du Congo Belge (3e note). Bulletin de l'Institut Royal des Sciences Naturelles de Belgique 25: 1–64.
- Badonnel A (1955) Psocoptères de l'Angola. Publicações Culturais da Companhia de Diamantes de Angola 26: 1–267.
- Badonnel A (1959) Un psoque cavernicole du Moyen-Congo. Revue Suisse de Zoologie 66: 761–764. <https://doi.org/10.5962/bhl.part.117922>
- Badonnel A (1967) Insectes Psocoptères. Faune de Madagascar 23: 1–235.
- Badonnel A (1979) Psocoptères de la Côte d'Ivoire (2e note). Revue Suisse de Zoologie 86: 11–22. <https://doi.org/10.5962/bhl.part.82275>
- Bao T, Wedmann S, Grímsson F, Beutel RG, Seyfullah L, Bao L, Jarzembowski EA (2022) Was the kateretid beetle *Pelretes* really a Cretaceous angiosperm pollinator? Nature Plants 8: 38–40. <https://doi.org/10.1038/s41477-021-01044-3>
- Barden P, Herhold HW, Grimaldi DA (2017) A new genus of hell ants from the Cretaceous (Hymenoptera: Formicidae: Haidomyrmecini) with a novel head structure. Systematic Entomology 42: 837–846. <https://doi.org/10.1038/s41477-021-01044-3>
- Baroni Urbani C (1995) Invasion and extinction in the West Indian ant fauna revisited: the example of *Pheidole* (Amber Collection Stuttgart: Hymenoptera, Formicidae. VIII: Myrmicinae, partim). Stuttgarter Beiträge zur Naturkunde. Serie B, Geologie und Palaontologie 222: 1–12.
- Batelka J, Engel MS (2022) The 'first fossil tumbling flower beetle' larva is a symphytan (Hymenoptera). Acta Entomologica Musei Nationalis Pragae 62: 57–59. <https://doi.org/10.37520/aemnp.2022.005>
- Batelka J, Prokop J, Pohl H, Bai M, Zhang W, Beutel RG (2019) Highly specialized Cretaceous beetle parasitoids (Ripiphoridae) identified with optimized visualization of microstructures. Systematic Entomology 44: 396–407. <https://doi.org/10.1111/syen.12331>
- Batelka J, Rosová K, Prokop J (2023) Diversity and morphology of Eocene and Oligocene Mordellidae (Coleoptera). Acta Entomologica Musei Nationalis Pragae 63: 451–478. <https://doi.org/10.37520/aemnp.2023.027>
- Beaver RA, Löyttyniemi K (1985) The platypodid ambrosia beetles of Zambia (Coleoptera: Platypodidae). Revue Zoologique Africaine 99: 113–134.
- Berendt GC (1830) Die Insekten im Bernstein: Ein Beitrag zur Thiergeschichte der Vorwelt. Nicolai, Danzig, 38 pp.
- Beutel RG, Friedrich F, Hörschemeyer T, Pohl H, Hünefeld F, Beckmann F, Meier R, Misof B, Whiting MF, Vilhelmsen L (2011) Morphological and molecular evidence converge upon a robust phylogeny of the megadiverse Holometabola. Cladistics 27: 341–355. <https://doi.org/10.1111/j.1096-0031.2010.00338.x>
- Beutel RG, Zhang WW, Pohl H, Wappler T, Bai M (2016) A miniaturized beetle larva in Cretaceous Burmese amber: Reinterpretation of a fossil "strepsipteran triungulin". Insect Systematics & Evolution 47: 83–91. <https://doi.org/10.1163/1876312x-46052134>
- Beutel RG, Xu Ch-P, Jarzembowski E, Kundrata R, Boudinot BE, McKenna D, Goczał J (acc. pend. minor revision) The evolutionary history of Coleoptera (Insecta) in the late Paleozoic and the Mesozoic. Systematic Entomology [acc. pend. minor rev.].
- Bisulca C, Nascimbene PC, Elkin L, Grimaldi DA (2012) Variation in the deterioration of fossil resins and implications for the conservation of fossils in amber. American Museum Novitates 2012: 1–19. <https://doi.org/10.1206/3734.2>
- Blaimer BB, Brady SG, Schultz TR, Lloyd MW, Fisher BL, Ward PS (2015) Phylogenomic methods outperform traditional multi-locus approaches in resolving deep evolutionary history: A case study of formicine ants. BMC Evolutionary Biology 15(271): 1–14. <https://doi.org/10.1186/s12862-015-0552-5>
- Blaimer BB, Lloyd MW, Guillory WX, Brady SG (2016) Sequence capture and phylogenetic utility of genomic ultraconserved elements obtained from pinned insect specimens. PLoS ONE 11: e0161531. <https://doi.org/10.1371/journal.pone.0161531>
- Bolton B (1995) A new general catalogue of the ants of the world. Cambridge, Mass.: Harvard University Press, 504 pp.
- Bolton B (2003) Synopsis and classification of Formicidae. Memoirs of the American Entomological Institute 71: 1–370.
- Bolton B (2023) AntCat, an Online Catalog of the Ants of the World by Barry Bolton. <https://antcat.org> [accessed 31 October 2023]
- Borgmeier T (1940) Duas notas myrmecológicas. Revista de Entomologia (Rio de Janeiro) 11: 606.
- Borgmeier T (1950) Uma nova espécie do gênero *Neivamyrmex* Borgmeier (Hym. Formicidae). Revista de Entomologia (Rio de Janeiro) 21: 623–624.
- Borowiec ML (2016) Generic revision of the ant subfamily Dorylinae (Hymenoptera, Formicidae). ZooKeys 608: 1–280. <https://doi.org/10.3897/zookeys.608.9427>
- Borowiec ML (2019) Convergent evolution of the army ant syndrome and congruence in big-data phylogenetics. Systematic Biology 68: 642–656. <https://doi.org/10.1093/sysbio/syy088>
- Boudinot BE, Probst RS, Brandão CRF, Feitosa RM, Ward PS (2016) Out of the Neotropics: Newly discovered relictual species sheds light on the biogeographical history of spider ants (*Leptomyrmex*, Dolichoderinae, Formicidae). Systematic Entomology 41: 658–671. <https://doi.org/10.1111/syen.12181>
- Boudinot BE (2018) A general theory of genital homologies for the Hexapoda (Pancrustacea) derived from skeletomuscular correspondences, with emphasis on the Endopterygota. Arthropod Structure & Development 47: 563–613. <https://doi.org/10.1016/j.asd.2018.11.001>
- Boudinot BE (2020) Systematic and Evolutionary Morphology: Case Studies on Formicidae, Mesozoic Aculeata, and Hexapodan Genitalia. University of California, Davis.
- Boudinot BE, Perrichot V, Chaul JCM (2020) †*Camelosphecia* gen. nov., lost ant-wasp intermediates from the mid-Cretaceous (Hymenoptera, Formicoidea). ZooKeys 1005: 21–55. <https://doi.org/10.3897/zookeys.1005.57629.figure13>
- Boudinot BE, Moosdorf OTD, Beutel RG, Richter A (2021) Anatomy and evolution of the head of *Dorylus helvolus* (Formicidae: Dorylinae): Patterns of sex- and caste-limited traits in the sausagefly and the driver ant. Journal of Morphology 282: 1616–1658. <https://doi.org/10.1002/jmor.21410/v2/response1>
- Boudinot BE, Borowiec ML, Prebus MM (2022a) Phylogeny, evolution, and classification of the ant genus *Lasius*, the tribe Lasiini and the subfamily Formicinae (Hymenoptera: Formicidae). Systematic Entomology 47: 113–151. <https://doi.org/10.1111/syen.12522>
- Boudinot BE, Khouri Z, Richter A, Griebenow ZH, van de Kamp T, Perrichot V, Barden P (2022b) Evolution and systematics of the Aculeata and kin (Hymenoptera), with emphasis on the ants (Formicoidea: †@@@idae fam. nov., Formicidae). bioRxiv, 450 pp. <https://doi.org/10.1101/2022.02.20.480183>
- Boudinot BE, Richter A, Katzke J, Chaul JCM, Keller RA, Economo EP, Beutel RG, Yamamoto S (2022c) Evidence for the evolution of eusociality in stem ants and a systematic revision of †*Gerontoformica*

- (Hymenoptera: Formicidae). *Zoological Journal of the Linnean Society* 195: 1355–1389. <https://doi.org/10.1093/zoolinnean/zlab097>
- Boudinot BE, Yan EV, Prokop J, Luo X-Z, Beutel RG (2022d) Permian parallelisms: Reanalysis of †Tshekardocoleidae sheds light on the earliest evolution of the Coleoptera. *Systematic Entomology* 48: 69–96. <https://doi.org/10.1111/syen.12562>
- Boudinot BE, Fikáček M, Liebermann ZE, Kusy D, Bocak L, McKenna DD, Beutel RG (2023) Systematic bias and the phylogeny of Coleoptera—A response to Cai et al. (2022) following the responses to Cai et al. (2020). *Systematic Entomology* 48: 223–232. <https://doi.org/10.1111/syen.12570>
- Briggs DE (2018) Sampling the insects of the amber forest. *Proceedings of the National Academy of Sciences of the United States of America* 115: 6525–6527. <https://doi.org/10.1073/pnas.1807017115>
- Broadhead E (1950) A revision of the genus *Liposcelis* Motschulsky with notes on the position of this genus in the order Corrodentia and on the variability of ten *Liposcelis* species. *Transactions of the Royal Entomological Society of London* 101: 335–388. <https://doi.org/10.1111/j.1365-2311.1950.tb00449.x>
- Broadhead E, Richards AM (1982) The Psocoptera of East Africa — A taxonomic and ecological survey. *Biological Journal of the Linnean Society, Linnean Society of London* 17: 137–216. <https://doi.org/10.1111/j.1095-8312.1982.tb01545.x>
- Broadhead E, Wolda H (1985) The diversity of Psocoptera in two tropical forests in Panama. *Journal of Animal Ecology* 54: 739–754. <https://doi.org/10.2307/4375>
- Brook BW, Sleightholme SR, Campbell CR, Jarić I, Buettel JC (2023) Resolving when (and where) the Thylacine went extinct. *The Science of the Total Environment* 877: 162878. <https://doi.org/10.1016/j.scitotenv.2023.162878>
- Brost L, Dahlstrom A (1996) *The Amber Book*. Mountain Press Pub. Co., Missoula Mt, 134 pp.
- Buchholz H (1961) Ein kurzer Führer durch die Sonderausstellung des Wandernden Museums Schleswig-Holstein. *Bernstein - das Gold des Nordens*. Schmidt & Klaunig, Kiel.
- Buckley SB (1866) Descriptions of new species of North American Formicidae. *Proceedings of the Entomological Society of Philadelphia* 6: 152–172.
- Cai C, Lawrence JF, Yamamoto S, Leschen RA, Newton AF, Ślipiński A, Yin Z, Huang D, Engel MS (2019) Basal polyphagan beetles in mid-Cretaceous amber from Myanmar: Biogeographic implications and long-term morphological stasis. *Proceedings of the Royal Society B, Biological Sciences* 286: 20182175. <https://doi.org/10.1098/rspb.2018.2175>
- Callahan S, Crowe-Riddell JM, Nagesan RS, Gray JA, Davis Rabosky AR (2021) A guide for optimal iodine staining and high-throughput diceCT scanning in snakes. *Ecology and Evolution* 11: 11587–11603. <https://doi.org/10.1002/ece3.7467>
- Carpenter FM (1930) The fossil ants of North America. *Bulletin of the Museum of Comparative Zoology* 70: 1–66.
- Casadei-Ferreira A, Chaul JCM, Feitosa RM (2019) A new species of *Pheidole* (Formicidae, Myrmicinae) from Dominican amber with a review of the fossil records for the genus. *ZooKeys* 866: 117–125. <https://doi.org/10.3897/zookeys.866.35756>
- Causey F (2011) *Amber and the ancient world*. Getty Publications, 144 pp. <https://doi.org/10.1515/etst-2013-0005>
- Clarke DJ, Limaye A, McKenna DD, Oberprieler RG (2018) The weevil fauna preserved in Burmese amber—snapshot of a unique, extinct lineage (Coleoptera: Curculionidae). *Diversity* 11: 1. <https://doi.org/10.3390/d11010001>
- Chapuis F (1865) *Monographie des Platypides*. H. Dessain, Liège, 344 pp. <https://doi.org/10.5962/bhl.title.9204>
- Chen C, Li B, Kanari M, Lu D (2019) 3. Epoxy adhesives. In: Rudawska A (Ed.) *Adhesives and adhesive joints in industry applications*. IntechOpen, 148 pp. <https://doi.org/10.5772/intechopen.86387>
- Cockerell TDA (1915) *British fossil insects*. *Proceedings of the United States National Museum* 49: 469–499. <https://doi.org/10.5479/si.00963801.49-2119.469>
- Corado R (2005) The importance of information on specimen labels. *Ornitologia Neotropical* 16: 277–278.
- De Andrade ML (1998a) Fossil and extant species of *Cylindromyrmex* (Hymenoptera: Formicidae). *Revue Suisse de Zoologie* 105: 581–664. <https://doi.org/10.5962/bhl.part.80052>
- De Andrade ML (1998b) First description of fossil *Acanthostichus* from Dominican amber (Hymenoptera: Formicidae). *Mitteilungen der Schweizerische Entomologische Gesellschaft* 71: 269–274.
- Deharveng L, D’Haese CA, Grandcolas P, Thibaud J-M, Weiner WM (2017) Judith Najt. A life dedicated to Collembola and research support for systematics. *Zoosystema* 39: 5–14. <https://doi.org/10.5252/z2017n1a1>
- Delclòs Martínez X, Peñalver Mollá E, Ranaivosoa V, Solórzano-Kraemer MM (2020) Unravelling the mystery of ‘Madagascar copal’: Age, origin and preservation of a Recent resin. *PLoS ONE* 15: e0232623. <https://doi.org/10.1371/journal.pone.0232623>
- Delclòs Martínez X, Peñalver E, Barrón E, Peris D, Grimaldi DA, Holz M, Labandeira CC, Saupé EE, Scotese CR, Solórzano-Kraemer MM, Álvarez-Parra S, Arillo A, Azar D, Cadena EA, Dal Corso J, Kravčec J, Monleón-Getino A, Nel A, Peyrto D, Bueno-Cebollada CA, Gallardo A, González-Fernández B, Goula M, Jaramillo C, Kania-Kłosok I, López-Del Valle R, Lozano RP, Meléndez N, Menor-Salván C, Peña-Kairath C, Perrichot V, Rodrigo A, Sánchez-García A, Santer M, Sarto i Monteys V, Uhl D, Luis Viejo J, Pérez-de la Fuente R (2023) Amber and the Cretaceous Resinous Interval. *Earth-Science Reviews* 243: 104486. <https://doi.org/10.1016/j.earscirev.2023.104486>
- Del Toro I, Pacheco JA, MacKay WP (2009) Revision of the ant genus *Liometopum* (Hymenoptera: Formicidae). *Sociobiology* 53: 299–369.
- de Moya RS, Yoshizawa K, Walden KK, Sweet AD, Dietrich CH, Kevin PJ (2021) Phylogenomics of parasitic and nonparasitic lice (Insecta: Psocodea): combining sequence data and exploring compositional bias solutions in next generation data sets. *Systematic Biology* 70: 719–738. <https://doi.org/10.1093/sysbio/syaa075>
- Dlussky GM (1988) Ants of Sakhalin amber (Paleocene?). *Paleontologicheskii jurnal [Палеонтологический журнал]* 1988: 50–61. [In Russian]
- Dlussky GM (2009) The ant subfamilies Ponerinae, Cerapachyinae and Pseudomyrmecinae (Hymenoptera, Formicidae) in the Late Eocene ambers of Europe. *Paleontological Journal* 43: 1043–1086. <https://doi.org/10.1134/s0031030109090068>
- Dlussky GM (2010a) Ants of the genus *Plagiolepis* Mayr (Hymenoptera, Formicidae) from Late Eocene ambers of Europe. *Paleontologicheskii jurnal [Палеонтологический журнал]* 2010: 64–73. <https://doi.org/10.1134/s0031030110050096> [In Russian]
- Dlussky GM (2010b) Ants of the genus *Plagiolepis* Mayr (Hymenoptera, Formicidae) from Late Eocene ambers of Europe. *Paleontological Journal* 44: 546–555. <https://doi.org/10.1134/s0031030110050096>
- Dlussky GM, Dubovikoff DA (2013) *Yantaromyrmex* gen. n. – a new ant genus (Hymenoptera: Formicidae) from Late Eocene ambers of

- Europe. *Caucasian Entomological Bulletin* 9: 305–314. <https://doi.org/10.23885/1814-3326-2013-9-2-305-314>
- Dlussky GM, Perkovsky EE (2002) Ants (Hymenoptera, Formicidae) from the Rovno Amber. *Vestnik Zoologii* 36: 3–20. [In Russian]
- Dlussky GM, Perfilieva KS (2014) Superfamily Formicoidea Latreille, 1802. In: Antropov AV, Belokobylskij SA, Compton SG, Dlussky GM, Khalaim AI, Kolyada VA, Kozlov MA, Perfilieva KS, Rasnitsyn AP (Eds) *The Wasps, Bees and Ants (Insecta: Vespida–Hymenoptera) from the Insect Limestone (Late Eocene) of the Isle of Wight, UK*. *Earth and Environmental Science Transactions of the Royal Society of Edinburgh* 104: 410–438. <https://doi.org/10.1017/s1755691014000103>
- Dlussky GM, Putyatina TS (2014) Early Miocene ants (Hymenoptera, Formicidae) from Radoboj, Croatia. *Neues Jahrbuch für Geologie und Paläontologie. Abhandlungen* 272: 237–285. <https://doi.org/10.1127/0077-7749/2014/0409>
- Dlussky GM, Wappler T, Wedmann S (2008) New middle Eocene formicid species from Germany and the evolution of weaver ants. *Acta Palaeontologica Polonica* 53: 615–626. <https://doi.org/10.4202/app.2008.0406>
- Dlussky GM, Karl HV, Brauckmann C (2011) *Camponotites steinbachi* Dlussky, Karl and Brauckmann n. sp., 453–454. In: Dlussky GM, Karl HV, Brauckmann C, Gröning E, Reich M (2011) Two ants (Insecta: Hymenoptera: Formicidae: Formicinae) from the Late Pliocene of Willershausen, Germany, with a nomenclatural note on the genus *Camponotites*. *Palaontologische Zeitschrift* 85: 449–455. <https://doi.org/10.1007/s12542-011-0104-2>
- Donisthorpe H (1920) British Oligocene ants. *Annals & Magazine of Natural History* 6: 81–94. <https://doi.org/10.1080/00222932008632412>
- Donovan SK, Riley M (2013) The importance of labels to specimens: An example from the Sedgwick Museum. *Geological Curators' Group* 509. <https://doi.org/10.55468/GC51>
- DuBois MB (1998) The first fossil Dorylinae with notes on fossil Ecitoninae (Hymenoptera: Formicidae). *Entomological News* 109: 136–142.
- Dubovikoff DA (2011) The first record of the genus *Pheidole* Westwood, 1839 (Hymenoptera, Formicidae) from the Baltic amber. *Russian Entomological Journal* 20: 255–257. <https://doi.org/10.15298/rusentj.20.3.06>
- Dubovikoff DA, Zharkov DM (2023) A comment on: An Eocene army ant (2022) by Sosiak CE et al. *Biology Letters* 19: 20220603. <https://doi.org/10.1098/rsbl.2022.0603>
- Dupérré N (2020) Old and new challenges in taxonomy: What are taxonomists up against? *Megataxa* 1: 59–62. <https://doi.org/10.11646/megataxa.1.1.12>
- Early CM, Morhardt AC, Cleland TP, Milensky CM, Kavich GM, James HF (2020) Chemical effects of diceCT staining protocols on fluid-preserved avian specimens. *PLoS ONE* 15: e0238783. <https://doi.org/10.1371/journal.pone.0238783>
- Emery C (1891) Le formiche dell'ambra Siciliana nel Museo Mineralogico dell'Università di Bologna. *Memorie della Reale Accademia delle Scienze dell'Istituto di Bologna* 1: 141–165. <https://doi.org/10.5962/bhl.title.13914>
- Emery C (1903) Intorno ad alcune specie di *Camponotus* dell'America Meridionale. *Rendiconti delle Sessioni della Reale Accademia delle Scienze dell'Istituto di Bologna (n.s.)* 7: 62–81.
- Emery C (1925) Hymenoptera. Fam. Formicidae. Subfam. Formicinae. *Genera Insectorum* 183: 1–302.
- Enderlein G (1903) Die Copeognathen des indo-australischen Faunengebietes. *Annales Historico-Naturales Musei Nationalis Hungarici* 1: 179–344.
- Enderlein G (1905) Zwei neue beschuppte Copeognathen aus dem Bernstein. *Zoologischer Anzeiger* 29: 39–43.
- Enderlein G (1911) Die fossilen Copeognathen und ihre Phylogenie. *Palaeontographica* 58: 279–360.
- Enderlein G (1917) 5. Beiträge zur Kenntnis der Copeognathen. IV. Zur Kenntnis der Copeognathen des Kongogebietes. *Zoologischer Anzeiger* 49: 254–256.
- Enderlein G (1925) Beiträge zur Kenntnis der Copeognathen IX. *Konowia (Vienna)* 4: 97–108.
- Engel MS (2016) A new species of the booklouse genus *Embidopsocus* in Baltic amber (Psocoptera: Liposcelididae). *Novitates Paleontologicae* 16: 1–9. <https://doi.org/10.17161/np.v0i16.5706>
- Engel MS, Wang B (2022) A new species of embidopsocine barklouse in Langhian amber from Zhangpu, China (Psocoptera: Liposcelididae). *Palaeontology* 5: 487–492. <https://doi.org/10.11646/palaeontology.5.5.10>
- Engelkes K, Friedrich F, Hammel JU, Haas A (2018) A simple setup for episcopic microtomy and a digital image processing workflow to acquire high-quality volume data and 3D surface models of small vertebrates. *Zoomorphology* 137: 213–228. <https://doi.org/10.1007/s00435-017-0386-3>
- Erichson U, Tomczyk L (1998) Die Staatliche Bernstein-Manufaktur Königsberg: 1926–1945. *Eigenverlag des deutschen Bernsteinmuseums, Ribnitz-Damgarten*, 154 pp.
- Ermisch K (1950) Die Gattungen der Mordelliden der Welt. *Entomologische Blätter* 45(46): 1.
- Fabricius JC (1793) *Entomologia systematica emendata et aucta. Secundum classes, ordines, genera, species, adjectis synonymis, locis observationibus, descriptionibus*. Tome 2. C. G. Proft, Hafniae [= Copenhagen], 519 pp. <https://doi.org/10.5962/bhl.title.125869>
- Faulwetter S, Vasileiadou A, Kouratoras M, Dailianis T, Arvanitidis C (2013) Micro-computed tomography: Introducing new dimensions to taxonomy. *ZooKeys* 263: 1. <https://doi.org/10.3897/zookeys.263.4261>
- Federman D (1990) Amber. In: *Modern jeweler's consumer guide to colored gemstones*. Springer, 22–25. [https://doi.org/10.1007/978-1-4684-6488-7\\_4](https://doi.org/10.1007/978-1-4684-6488-7_4)
- Fikáček M, Beutel RG, Cai C, Lawrence JF, Newton AF, Solodovnikov A, Šlipiński A, Thayer MK, Yamamoto S (2020) Reliable placement of beetle fossils via phylogenetic analyses – Triassic *Leehermania* as a case study (Staphylinidae or Myxophaga?). *Systematic Entomology* 45: 175–187. <https://doi.org/10.1111/syen.12386>
- Fikáček M, Yamamoto S, Matsumoto K, Beutel RG, Maddison DR (2023) Phylogeny and systematics of Sphaeriusidae (Coleoptera: Myxophaga): minute living fossils with underestimated past and present-day diversity. *Systematic Entomology* 48: 233–249. <https://doi.org/10.1111/syen.12571>
- Fischer G, Hita Jánoszyński F, Peters MK (2012) Taxonomy of the ant genus *Pheidole* Westwood (Hymenoptera: Formicidae) in the Afro-tropical zoogeographic region: definition of species groups and systematic revision of the *Pheidole pulchella* group. *Zootaxa* 3232: 1–43. <https://doi.org/10.11646/zootaxa.3232.1.1>
- Fisher BL, Bolton B (2016) *Ants of the world. Ants of Africa and Madagascar. A guide to the genera*. Berkeley: University of California Press [ix +] 503 pp. <https://doi.org/10.1525/9780520962996>
- Flannery T (2009) Now or ever: Why we must act now to end climate change and create a sustainable future. *Open Road+ Grove/Atlantic*. <https://doi.org/10.5860/CHOICE.47-4429>

- Forel A (1878) Études myrmécologiques en 1878 (première partie) avec l'anatomie du gésier des fourmis. Bulletin de la Société Vaudoise des Sciences Naturelles 15: 337–392.
- Forel A (1886) Études myrmécologiques en 1886. Annales de la Société Entomologique de Belgique 30: 131–215.
- Förster B (1891) Die Insekten des “Plattigen Steinmergels” von Brunstatt. Abhandlungen zur Geologischen Spezialkarte von Elsass-Lothringen 3: 333–594.
- Franciscolo MF (1957) Coleoptera Mordellidae I. IN: South African Animal Life. Results of the Lund University Expedition in 1950–1951. Almqvist & Wiksells, Uppsala 4: 207–291.
- Franciscolo ME (1967) Coleoptera, Mordellidae: A monograph of the South African genera and species. 3. Tribe Mordellistenini. South African Animal Life: 67–203.
- Friedrich F, Beutel RG (2008) Micro-computer tomography and a renaissance of insect morphology. Developments in X-ray tomography VI, SPIE. <https://doi.org/10.1117/12.794057>
- Friedrich F, Matsumura Y, Pohl H, Bai M, Hörschemeyer T, Beutel RG (2014) Insect morphology in the age of phylogenomics: Innovative techniques and its future role in systematics. Entomological Science 17: 1–24. <https://doi.org/10.1111/ens.12053>
- Fronde JW (1968) Amber Facts and Fancies. Economic Botany 22: 371–382. <https://doi.org/10.1007/bf02908134>
- Garcia FH, Lieberman Z, Audisio TL, Liu C, Economo EP (2019) Revision of the highly specialized ant genus *Discothyrea* (Hymenoptera: Formicidae) in the Afrotropics with X-Ray Microtomography and 3D Cybertaxonomy. Insect Systematics and Diversity 3: 5. <https://doi.org/10.1093/isd/ixz015>
- Georgiev D (2022a) New species of Psocoptera (Insecta) from East Africa. Historia Naturalis Bulgarica 44: 51–62. <https://doi.org/10.48027/hnb.44.072>
- Georgiev D (2022b) New records of Psocoptera from East Sub-Saharan Africa. ZooNotes 12: 1–36. <https://doi.org/10.48027/hnb.44.011>
- Germar EF (1837) Fauna insectorum Europae. Fasciculus 19. Insectorum protogaeae specimen sistens insecta carbonum fossilium. Kümmerle, Halle, 25 pp.
- Gerstäcker A (1859) Monatsberichte der Königlich Preussischen Akademie der Wissenschaften zu Berlin 1858: 261–264. [Untitled. Introduced by: „Hr. Peters berichtete über sein Reisewerk, von dem die Insekten bis zum 64., die Botanik bis zum 34. Bogen gedruckt sind und teilte den Schluss der Diagnosen der von Hrn. Dr. Gerstäcker bearbeiteten Hymenopteren mit.“]
- Gessner C (1565)[-1566] De omni rerum fossilium genere, gemmis, lapidibus, metallis, et huiusmodi, libri aliquot, plerique nunc primum editi. Excudebat Iacobus Gesnerus, Tiguri.
- Girón JC, Tarasov S, González Montaña LA, Matentzoglou N, Smith AD, Koch M, Boudinot BE, Bouchard P, Burks R, Vogt L, Yoder M, Osumi-Sutherland D, Friedrich F, Beutel RG, Mikó I (2023) Formalizing invertebrate morphological data: A descriptive model for cuticle-based skeleto-muscular systems, an ontology for insect anatomy, and their potential applications in biodiversity research and informatics. Systematic Biology 72: 1084–1100. <https://doi.org/10.1093/sysbio/syad025>
- Goldenberg A (2004) Polish amber art. Thesis, Indiana University.
- Gotwald Jr WH (1982) Army ants. In: Hermann HR (Ed.) Social Insects. Vol. 4. Academic Press, New York, 157–254. <https://doi.org/10.1016/b978-0-12-342204-0.50010-3>
- Gotwald Jr WH (1995) Army ants: the biology of social predation. Cornell University Press, Ithaca, New York, [xviii +] 302 pp. <https://doi.org/10.1086/419419>
- Greven H, Wichard W (2010) Schmetterlinge oder Köcherfliegen? Bemerkungen zum Kapitel „De papilionibus “aus der „Historia succinorum” (1742) des Nathanael Sendel. Entomologie Heute 22: 107–150.
- Greving I, Wilde F, Ogurreck M, Herzen J, Hammel JU, Hipp A, Friedrich F, Lottemoser L, Dose T, Burmester H, Müller M, Beckmann F (2014) P05 imaging beamline at PETRA III: first results. In: Stuart RS (Ed.) Proceedings of SPIE - Developments in X-Ray Tomography IX, 9212, San Diego, 92120O-8. <https://doi.org/10.1117/12.2061768>
- Grimaldi DA (1996) Amber: Window to the Past. Harry N. Abrams, 216 pp. <https://doi.org/10.5860/choice.33-5724>
- Grimaldi D, Engel MS (2006) Fossil Liposcelididae and the lice ages (Insecta: Psocodea). Proceedings. Biological Sciences 273: 625–633. <https://doi.org/10.1098/rspb.2005.3337>
- Grimaldi DA, Shedrinsky A, Ross A, Baer NS (1994) Forgeries in fossils in “amber”: History, identification and case studies. Curator 37: 251–274. <https://doi.org/10.1111/j.2151-6952.1994.tb01023.x>
- Guiry EJ, Orchard TJ, Royle TC, Cheung C, Yang DY (2020) Dietary plasticity and the extinction of the passenger pigeon (*Ectopistes migratorius*). Quaternary Science Reviews 233: 106225. <https://doi.org/10.1016/j.quascirev.2020.106225>
- Günther KK (1989) *Empidopsocus saxonicus* sp. n., eine neue fossile Psocoptera-Art aus Sächsischem Bernstein des Bitterfelder Raumes (Insecta: Psocoptera: Liposcelidae). Mitteilungen aus dem Zoologischen Museum in Berlin 65: 321–325. <https://doi.org/10.1002/mmnz.19890650214>
- Günther A, Drack M, Monod L, Wirkner CS (2021) A unique yet technically simple type of joint allows for the high mobility of scorpion tails. Journal of the Royal Society Interface, 18(182): 20210388. Hagen H (1865) Synopsis of the Psocina without ocelli. Entomologist's Monthly Magazine 2: 121–124. <https://doi.org/10.1098/rsif.2021.0388>
- Hagen HA (1866) On some aberrant genera of Psocina. Entomologist's Monthly Magazine 2: 170–172.
- Hagen HA (1882) Ueber Psociden in Bernstein. Entomologische Zeitung 43: 217–237.
- Haibel A, Ogurreck M, Beckmann F, Dose T, Wilde F, Herzen J, Müller M, Schreyer A, Nazmov V, Simon M, Last A, Mohr J (2010) Micro and nano-tomography at the GKSS Imaging Beamline at PETRA III. Developments in X-Ray Tomography VII, Vol. 7804 SPIE. <https://doi.org/10.1117/12.860852>
- Hedrick BP, Yohe L, Linden AV, Dávalos LM, Sears K, Sadier A, Rossiter SJ, Davies KTJ, Dumont E (2018) Assessing soft-tissue shrinkage estimates in museum specimens imaged with diffusible iodine-based contrast-enhanced computed tomography (diceCT). Microscopy and Microanalysis 24: 284–291. <https://doi.org/10.1017/S1431927618000399>
- Heer O (1849) Die Insektenfauna der Tertiärgebilde von Oeningen und von Radoboj in Croatien. Zweiter Theil: Heuschrecken, Florfliegen, Aderflüger, Schmetterlinge und Fliegen. W. Engelmann, Leipzig [vi +] 264 pp.
- Heer O (1850) Die Insektenfauna der Tertiärgebilde von Oeningen und von Radoboj in Croatien. Zweite Abtheilung: Heuschrecken, Florfliegen, Aderflüger, Schmetterlinge und Fliegen. Neue Denkschriften der Allgemeinen Schweizerischen Gesellschaft für die Gesamten Naturwissenschaften 11: 1–264.
- Hildt JA (1803) Magazin der Handels- und Gewerbskunde.

- Hinrichs K (2007) Bernstein, das „Preußische Gold“ in Kunst- und Naturalienkammern und Museen des 16.-20. Jahrhunderts. Diss. Humboldt-Universität.
- Holl F (1829) Handbuch der Petrefactenkunde. Bd. 2 [part]. P. O. Hilschersche Buchhandlung, Dresden, 117–232.
- Hong Y, Wu J (2000) The emendation of *Shanwangella palaeoptera* Zhang and its concerned problems. *Geoscience (Beijing)* 14: 15–20. [in Chinese]
- Ijiri T, Todo H, Hirabayashi A, Kohiyama K, Dobashi Y (2018) Digitization of natural objects with micro CT and photographs. *PLoS ONE* 13: e0195852. <https://doi.org/10.1371/journal.pone.0195852>
- ICZN (1999) International Code of Zoological Nomenclature. 4th edn. The International Trust for Zoological Nomenclature, London, UK. 306 pp. <https://www.iczn.org/the-code/the-code-online/> [accessed: January 2024]
- Jandausch K, van de Kamp T, Beutel RG, Niehuis O, Pohl H (2023) ‘Stab, chase me, mate with me, seduce me’: How widespread is traumatic insemination in Strepsiptera? *Biological Journal of the Linnean Society. Linnean Society of London* 140: 206–223. <https://doi.org/10.1093/biolinnean/blad046>
- Jafoszyński P, Luo XZ, Hammel JU, Yamamoto S, Beutel RG (2020) The mid-Cretaceous †*Lepiceratus* gen. nov. and the evolution of the relict beetle family Lepiceridae (Insecta: Coleoptera: Myxophaga). *Journal of Systematic Palaeontology* 18: 1127–1140. <https://doi.org/10.1080/14772019.2020.1747561>
- Jiang H, Tomaschek F, Muscente AD, Niu C, Nyunt TT, Fang Y, Schmidt U, Chen J, Lönartz M, Mähler B, Wappler T, Jarzembowski EA, Szewo J, Zhang H, Rust J, Wang B (2022) Widespread mineralization of soft-bodied insects in Cretaceous amber. *Geobiology* 20: 363–376. <https://doi.org/10.1111/gbi.12488>
- Johnson KP, Smith VS, Hopkins HH (2023) Psocodea Species File Online. Version 5.0/5.0. <http://Psocodea.SpeciesFile.org> [accessed: July 2023]
- Jordal BH (2015) Molecular phylogeny and biogeography of the weevil subfamily Platypodinae reveals evolutionarily conserved range patterns. *Molecular Phylogenetics and Evolution* 92: 294–307. <https://doi.org/10.1016/j.ympev.2015.05.028>
- van de Kamp T, dos Santos Rolo T, Baumbach T, Greven H (2015) X-ray radiography of a spraying stick insect (Phasmatodea). *Entomologie Heute* 27: 37–44.
- van de Kamp T, Schwermann AH, dos Santos Rolo T, Lösel PD, Engler T, Etter W, Faragó T, Göttlicher J, Heuveline V, Kopmann A, Mähler B, Mörs T, Odar J, Rust J, Tan Jerome N, Vogelgesang M, Baumbach T, Krogmann L (2018) Parasitoid biology preserved in mineralized fossils. *Nature Communications* 9: 3325. <https://doi.org/10.1038/s41467-018-05654-y>
- Kawata A, Ogawa N, Yoshizawa K (2022) Morphology and phylogenetic significance of the thoracic muscles in Psocodea (Insecta: Paraneoptera). *Journal of Morphology* 283: 1106–1119. <https://doi.org/10.1002/jmor.21492>
- Kaplan AA, Grigelis AA, Strelnikova NI, Glikman LS (1977) Stratigraphy and correlation of Palaeogene deposits of South-Western cis-Baltic region. *Sovetskaâ Geologiâ* 4: 30–43.
- King VT (1975) Labels are Important. *Rocks and Minerals* 50: 523–526. <https://doi.org/10.1080/00357529.1975.11762911>
- King R (2022) Amber: From Antiquity to Eternity: Reaktion Books, 272 pp.
- Kirejtshuk AG (2020) Taxonomic review of fossil coleopterous families (Insecta, Coleoptera). Suborder Archostemata: Superfamilies Coleopseoidea and Cupedoidea. *Xiandai Dizhi* 10: 73. <https://doi.org/10.3390/geosciences10020073>
- Kirejtshuk AG, Chetverikov PE, Azar D, Kirejtshuk PA (2016) Ptismidae fam. nov. (Coleoptera, Staphyliniformia) from the lower Cretaceous Lebanese amber. *Cretaceous Research* 59: 201–213. <https://doi.org/10.1016/j.cretres.2015.10.027>
- Klimeš P, Drescher J, Buchori D, Hidayat P, Nazarreta R, Potocký P, Rimandai M, Scheu S, Matos-Maraví P (2022) Uncovering cryptic diversity in the enigmatic ant genus *Overbeckia* and insights into the phylogeny of Camponotini (Hymenoptera: Formicidae: Formicinae). *Invertebrate Systematics* 36: 557–579. <https://doi.org/10.1071/IS21067>
- Klopfstein S, Spasojevic T (2019) Illustrating phylogenetic placement of fossils using RoguePlots: An example from ichneumonid parasitoid wasps (Hymenoptera, Ichneumonidae) and an extensive morphological matrix. *PLoS ONE* 14: e01212942. <https://doi.org/10.1371/journal.pone.0212942>
- Knorre Dv (1983) Die zoologisch-paläontologischen Sammlungen des Phyletischen Museums. Friedrich-Schiller-Universität Jena, Bernd Wilhelmi, Jena.
- Knorre Dv, Beutel RG (2018) Jena: The Palaeontological Collections at the Phyletisches Museum in Jena. *Paleontological Collections of Germany, Austria and Switzerland*, Springer: 339–346. [https://doi.org/10.1007/978-3-319-77401-5\\_33](https://doi.org/10.1007/978-3-319-77401-5_33)
- Köhler UBG (2019) Dr. Dietrich von Knorre - der Malakologe, Museologe und Naturschützer sowie einer der letzten klassischen Zoologen Deutschlands wurde 80 Jahre. *Mitteilung der Deutschen Malakozoologischen Gesellschaft* 100: 49–62.
- Königsberg-Pr. Pd B (1937) Bernstein-Einschlüsse. *Entomologisches Nachrichtenblatt (Troppau)* 1: 3.
- Krogmann L, Knorre Dv, Beutel RG (2007) Die Chalcidoidea-Sammlung von Ferdinand Rudow (1840–1920) im Phyletischen Museum (Jena). *Mitteilungen aus dem Hamburgischen Zoologischen Museum und Institut* 104: 129–140.
- Krüger L (1923) Neuroptera succinica baltica. Die im baltischen Bernstein eingeschlossenen Neuropteren des Westpreußischen Provinzial-Museums (heute Museum für Naturkunde und Vorgeschichte) in Danzig. *Stettiner Entomologische Zeitung* 84: 68–92.
- Lak M, Néraudeau D, Nel A, Cloetens P, Perrichot V, Tafforeau P (2008) Phase contrast X-ray synchrotron imaging: Opening access to fossil inclusions in opaque amber. *Microscopy and Microanalysis* 14: 251–259. <https://doi.org/10.1017/s1431927608080264>
- LaPolla JS (2005) Ancient trophophoresy: a fossil *Acropyga* (Hymenoptera: Formicidae) from Dominican amber. *Transactions of the American Entomological Society* 131: 21–28.
- LaPolla JS, Greenwalt DE (2015) Fossil ants (Hymenoptera: Formicidae) of the Middle Eocene Kishenehn Formation. *Sociobiology* 62: 163–174. <https://doi.org/10.13102/sociobiology.v62i2.163-174>
- Larsson L (2010) A double grave with amber and bone adornments at Zvejnieki in northern Latvia. *Archaeologia Baltica* 13: 80–90.
- Leach WE (1815) Entomology. In: Brewster D (Ed.) *The Edinburgh encyclopedia*. William Blackwood, Edinburgh 9: 57–172. <https://doi.org/10.5962/bhl.title.66019>
- Leonard KC, Worden N, Boettcher ML, Dickinson E, Hartstone-Rose A (2022) Effects of long-term ethanol storage on muscle architecture. *The Anatomical Record* 305: 184–198. <https://doi.org/10.1002/ar.24638>
- Li F (1999) Psocids (Psocoptera) of Fujian Province, China. *Fauna of insects, Fujian Province of China* 3.

- Li F (2002) Psocoptera of China. National Natural Science Foundation of China: [xlvii +] 1976 pp. (2 Vols) [1547 figs, 10 pl. at the end of the 2<sup>nd</sup> Vol.].
- Li YD, Ruta R, Tihelka E, Liu ZH, Huang DY, Cai Ch-Y (2022) A new marsh beetle from mid-Cretaceous amber of northern Myanmar (Coleoptera: Scirtidae). *Scientific Reports* 12: 13403. <https://doi.org/10.1038/s41598-022-16822-y>
- Lienhard C (1991) New records and species of *Belaphopsocus* (Psocoptera: Liposcelididae). *The Raffles Bulletin of Zoology* 39: 75–85.
- Lienhard C (1998) Psocoptères euro-méditerranéens. *Faune de France* 83, [XX+] 517 pp. [148 figs, 11 plates]
- Lienhard C (2003) Nomenclatural amendments concerning Chinese Psocoptera (Insecta), with remarks on species richness. *Revue Suisse de Zoologie* 110: 695–721. <https://doi.org/10.5962/bhl.part.80207>
- Lienhard C (2016) Country checklists of the Psocoptera species of the world. Extracted from Lienhard C, Smithers CN (2002) Psocoptera (Insecta) world catalogue and bibliography. *Psocid News I* (Special Issue): 1–123.
- Lösel PD, van de Kamp T, Jayme A, Ershov A, Faragó T, Pichler O, Tan Jerome N, Aadeppu N, Bremer S, Chilingaryan SA, Heethoff M, Kopmann A, Odar J, Schmelzle S, Zuber M, Wittbrodt J, Baumbach T, Heuveline V (2020) Introducing Biomedisa as an open-source online platform for biomedical image segmentation. *Nature Communications* 11: 5577. <https://doi.org/10.1038/s41467-020-19303-w>
- Lund PW (1831) Lettre sur les habitudes de quelques fourmis du Brésil, adressée à M. Audouin. *Annales des Sciences Naturelles* 23: 113–138. <https://doi.org/10.5962/bhl.part.7282>
- Matuschek O (2020) *Goethes Elefanten*. Insel Verlag, Berlin.
- Mayer C (1861) Die Faunula des marinen Sandsteines von Kleinkuhren bei Königsberg. [Publisher not ascertainable]
- Mayr G (1861) Die europäischen Formiciden. Nach der analytischen Methode bearbeitet. C. Gerolds Sohn, Wien, 80 pp. <https://doi.org/10.5962/bhl.title.14089>
- Mayr G (1862) Myrmecologische Studien. Verhandlungen der Kaiserlich-Königlichen Zoologisch-Botanischen Gesellschaft in Wien 12: 649–776.
- Mayr G (1867) Vorläufige Studien über die Radoboj-Formiciden, in der Sammlung der k. k. geologischen Reichsanstalt. *Jahrbuch der Kaiserlich-Königlichen Geologischen Reichsanstalt Wien* 17: 47–62.
- Mayr G (1868) Die Ameisen des baltischen Bernsteins. *Beiträge zur Naturkunde Preussens* 1: 1–102.
- Mayr G (1870) Neue Formiciden. Verhandlungen der Kaiserlich-Königlichen Zoologisch-Botanischen Gesellschaft in Wien 20: 939–996.
- Mayr G (1887) Südamerikanische Formiciden. Verhandlungen der Kaiserlich-Königlichen Zoologisch-Botanischen Gesellschaft in Wien 37: 511–632.
- McCoy VE, Boom A, Kraemer MMS, Gabbott SE (2017) The chemistry of American and African amber, copal, and resin from the genus *Hymenaea*. *Organic Geochemistry* 113: 43–54. <https://doi.org/10.1016/j.orggeochem.2017.08.005>
- McKinney ML (1999) High rates of extinction and threat in poorly studied taxa. *Conservation Biology* 13: 1273–1281. <https://doi.org/10.1046/j.1523-1739.1999.97393.x>
- Mercati M (1717) *Michaelis Mercati Samminiatisensis Metallotheca: Hauptw* (Vol. 1). Salvioni.
- Mataic D, Bastani B (2006) Intraperitoneal sodium thiosulfate for the treatment of calciphylaxis. *Renal Failure* 28: 361–363. <https://doi.org/10.1080/08860220600583781>
- Menon MGR (1938) Coxal interlocking in the Lepidopsocidae and its probable taxonomic value. *Current Science* 7: 66–67.
- Metscher BD (2009) MicroCT for comparative morphology: Simple staining methods allow high-contrast 3D imaging of diverse non-mineralized animal tissues. *BMC Physiology* 9: 1–14. <https://doi.org/10.1186/1472-6793-9-11>
- Meyer E (1914) [Neue Nr. 1186] Germau [Russkoje, Pyeckoe]/Geologische Karte.
- Misof B, Liu S, Meusemann K, Peters RS, Donath A, Mayer C, et al. (2014) Phylogenomics resolves the timing and pattern of insect evolution. *Science* 346: 763–767. <https://doi.org/10.1126/science.1257570>
- Mockford EL (1969) Fossil insects of the Order Psocoptera from Tertiary amber of Chiapas, Mexico. *Journal of Paleontology* 43: 1267–1273.
- Mockford EL (1993) *North American Psocoptera (Insecta)*. CRC Press, New York, 1–455. <https://doi.org/10.1201/9780203745403-1>
- Mockford EL (1999) A Classification of the Psocopteran Family Caeciliusidae (Caeciliidae Auct.). *Transactions of the American Entomological Society* 125: 325–417.
- Mockford EL (2018) Biodiversity of Psocoptera. In: Footitt RG, Adler PH (Eds) *Insect Biodiversity: Science and Society*, Vol. II. 417–456. <https://doi.org/10.1002/9781118945582>
- Mockford EL, Lienhard C, Yoshizawa K (2013) Revised classification of ‘Psocoptera’ from Cretaceous amber, a reassessment of published information. *Insecta Matsumurana (N.S.)* 69: 1–26.
- Modi A, Vergata C, Zilli C, Vischioni C, Vai S, Tagliacuzzi GM, Lari M, Caramelli D, Taccioli C (2021) Successful extraction of insect DNA from recent copal inclusions: Limits and perspectives. *Scientific Reports* 11: 1–8. <https://doi.org/10.1038/s41598-021-86058-9>
- Mongiardino Koch N, Thompson JR (2021) A total-evidence dated phylogeny of Echinoidea combining phylogenomic and paleontological data. *Systematic Biology* 70: 421–439. <https://doi.org/10.1093/sysbio/syaa069>
- Moosmann J, Ershov A, Weinhardt V, Baumbach T, Prasad MS, LaBonne C, Xiao X, Kashef J, Hoffmann R (2014) Time-lapse X-ray phase-contrast microtomography for in vivo imaging and analysis of morphogenesis. *Nature Protocols* 9: 294–304. <https://doi.org/10.1038/nprot.2014.033>
- Mukherjee AJ, Roßberger E, James MA, Pfälzner P, Higgitt CL, White R, Pegg DA, Azar D, Evershed RP (2008) The Qatna lion: Scientific confirmation of Baltic amber in late Bronze Age Syria. *Antiquity* 82: 49–59. <https://doi.org/10.1017/s0003598x00096435>
- Najt J (1987) Le Collembolle fossile *Paleosminthurus juliae* est un Hyménoptère. *Revue Française d’Entomologie* 9: 152–154. [Nouvelle Série]
- Nakahara W (1915) On the Hemerobiinae of Japan. *Annotationes Zoologicae Japonenses* 9: 11–48.
- Nakamine H, Yamamoto S, Takahashi Y, Liu XY (2023) A remarkable new genus of Nevrorthidae (Neuroptera, Osmyloidea) from mid-Cretaceous Kachin amber of northern Myanmar. *Deutsche Entomologische Zeitschrift* 70: 113–120. <https://doi.org/10.3897/dez.70.98873>
- Naumann B, Reip HS, Akkari N, Neubert D, Hammel JU (2020) Inside the head of a cybertype—three-dimensional reconstruction of the head muscles of *Ommatoiulus avatar* (Diplopoda: Juliformia: Julidae) reveals insights into the feeding movements of Juliformia. *Zoological Journal of the Linnean Society* 26: 954–75. <https://doi.org/10.1093/zoolinnean/zlzl109>
- Nel A, de Ploëg G, Azar D (2004) The oldest Liposcelididae in the lowermost Eocene amber of the Paris Basin (Insecta: Psocoptera). *Geologica Acta* 2: 31–36.

- Nel A, Prokop J, de Ploeg G, Millet J (2005) New Psocoptera (Insecta) from the lowermost Eocene Amber of Oise, France. *Journal of Systematic Palaeontology* 3: 371–391. <https://doi.org/10.1017/S1477201905001598>
- Neumüller M., Reichinger A, Rist F, Kern C (2014) 3D printing for cultural heritage: Preservation, accessibility, research and education. 3D research challenges in cultural heritage: a roadmap in digital heritage preservation: 119–134. [https://doi.org/10.1007/978-3-662-44630-0\\_9](https://doi.org/10.1007/978-3-662-44630-0_9).
- O’Hara JE, Raper CM, Pont AC, Whitmore D (2013) Reassessment of *Paleotachina* Townsend and *Electrotachina* Townsend and their removal from the Tachinidae (Diptera). *ZooKeys* 361: 27–37. <https://doi.org/10.3897/zookeys.361.6448>
- Orr MC, Ascher JS, Bai M, Chesters D, Zhu CD (2020) Three questions: How can taxonomists survive and thrive worldwide? *Megataxa* 1: 19–27. <https://doi.org/10.11646/megataxa.1.1.4>
- Özdikmen H (2010) New names for the preoccupied specific and sub-specific epithets in the genus *Camponotus* Mayr, 1861 (Hymenoptera: Formicidae). *Munis Entomology & Zoology* 5: 519–537.
- Palenstijn WJ, Batenburg KJ, Sijbers J (2011) Performance improvements for iterative electron tomography reconstruction using graphics processing units (GPUs). *Journal of Structural Biology* 176: 250–253. <https://doi.org/10.1016/j.jsb.2011.07.017>
- Paleobio DB (2022) The Paleobiology Database: Revealing the History of Life. <https://paleobiodb.org/#/> [accessed: 18 July 2022]
- Pearman JV (1935) Two remarkable amphientomids (Psocoptera). *Stylops* 4: 134–137. <https://doi.org/10.1111/j.1365-3113.1935.tb00576.x>
- Pearman JV (1936) The taxonomy of the Psocoptera: Preliminary sketch. *Proceedings Royal Entomological Society of London (B)* 5: 58–62. <https://doi.org/10.1111/j.1365-3113.1936.tb00596.x>
- Peinert M, Wipfler B, Jetschke G, Kleinteich T, Gorb SN, Beutel RG, Pohl H (2016) Traumatic insemination and female counter-adaptation in Strepsiptera (Insecta). *Scientific Reports* 6: 25052. <https://doi.org/10.1038/srep25052>
- Peña-Kairath C, Delclòs X, Álvarez-Parra S, Peñalver E, Engel MS, Ollerton J, Peris D (2023) Insect pollination in deep time. *Trends in Ecology & Evolution* 38: 749–759. <https://doi.org/10.1016/j.tree.2023.03.008>
- Penney D (2010) Biodiversity of fossils in amber from the major world deposits. Siri Scientific Press.
- Penney D, Preziosi RF (2013) Sub-fossils in copal: An undervalued scientific resource. Paper presented at the Abstracts and Proceedings of the International Amber Researcher Symposium (Deposits—Collections—The Market). Gdansk International Fair Co. Amberif.
- Penney D, Wadsworth C, Green DI, Kennedy SL, Preziosi RF, Brown TA (2013) Extraction of inclusions from (sub) fossil resins, with description of a new species of stingless bee (Hymenoptera: Apidae: Meliponini) in Quaternary Colombian copal. *Paleontological Contributions* 2013: 1–6. <https://doi.org/10.17161/PC.1808.11103>
- Peris D, Rust J (2020) Cretaceous beetles (Insecta: Coleoptera) in amber: the palaeoecology of this most diverse group of insects. *Zoological Journal of the Linnean Society* 189: 1085–1104. <https://doi.org/10.1093/zoolinnean/zlz118>
- Peris D, Ruzzier E, Perrichot V, Delclòs X (2016) Evolutionary and paleobiological implications of Coleoptera (Insecta) from Tethyan-influenced Cretaceous ambers. *Geoscience Frontiers* 7: 695–706. <https://doi.org/10.1016/j.gsf.2015.12.007>
- Perkovsky EE (2016) Tropical and Holarctic ants in Late Eocene ambers. *Vestnik Zoologii* 50: 111–122. <https://doi.org/10.1515/vzoo-2016-0014>
- Perkovsky E, Rasnitsyn A, Vlaskin A, Taraschuk M (2007) A comparative analysis of the Baltic and Rovno amber arthropod faunas: Representative samples. *African Invertebrates* 48: 229–245.
- Pictet FJ (1854) Classe insectes. *Traité de Paléontologie: ou, Histoire Naturelle des Animaux Fossiles Considérés dans Leurs Rapports Zoologiques et Géologiques* 2: 301–405. <https://doi.org/10.5962/bhl.title.13903>.
- Pierce WD, Gibron SJ (1962) Fossil arthropods of California. 24. Some unusual fossil arthropods from the Calico Mountains nodules. *Bulletin of the Southern California Academy of Sciences* 61: 143–151.
- Pilekaić R (2001) Amber jewelry of Sigitas Virpilaitis: Postmodern approach. *Acta Academiae artium Vilnensis. Dailė* 22: 213–218.
- Piper R (2009). *Extinct animals: an encyclopedia of species that have disappeared during human history*, Bloomsbury Publishing USA. <https://doi.org/10.5040/9798400649219>
- Piton L (1935) [New species *Camponotus obesus* attributed to Piton]. In: Piton L, Théobald N (Eds) *La faune entomologique des gisements Mio-Pliocènes du Massif Central*. *Revue des Sciences Naturelles d’Auvergne (n.s.)* 1: 65–104 [pp. 68].
- Pohl H, Beutel RG (2016) †*Kinzelbachilla ellenbergeri*—a new ancestral species, genus and family of Strepsiptera (Insecta). *Systematic Entomology* 41: 287–297. <https://doi.org/10.1111/syen.12158>
- Pohl H, Beutel RG (2005) The phylogeny of Strepsiptera. *Cladistics* 21: 328–374. <https://doi.org/10.1111/j.1096-0031.2005.00074.x>
- Pohl H, Beutel RG, Kinzelbach R (2005) Protoxenidae fam. nov. (Insecta, Strepsiptera) from Baltic amber—A ‘missing link’ in strepsipteran phylogeny. *Zoologica Scripta* 34: 57–69. <https://doi.org/10.1111/j.1463-6409.2005.00173.x>
- Pohl H, Wipfler B, Grimaldi D, Beckmann F, Beutel RG (2010) Reconstructing the anatomy of the 42-million-year-old fossil *Mengea tertiaria* (Insecta, Strepsiptera). *Naturwissenschaften* 97: 855–859. <https://doi.org/10.1007/s00114-010-0703-x>
- Pohl H, Batelka J, Prokop J, Müller P, Yavorskaya MI, Beutel RG (2018) A needle in a haystack: Mesozoic origin of parasitism in Strepsiptera revealed by first definite Cretaceous primary larva (Insecta). *PeerJ* 6: e5943. <https://doi.org/10.7717/peerj.5943>
- Pohl H, Hammel JU, Richter A, Beutel RG (2019) The first fossil free-living late instar larva of Strepsiptera (Insecta). *Arthropod Systematics & Phylogeny* 77: 125–140. <https://doi.org/10.26049/ASP77-1-2019-06>
- Pohl H, Wipfler B, Boudinot BE, Beutel RG (2021) On the value of Burmese amber for understanding insect evolution: Insights from †*Heterobathmilla*—an exceptional stem group genus of Strepsiptera (Insecta). *Cladistics* 37: 211–229. <https://doi.org/10.1111/cla.12433>
- Qvamström M, Fikáček M, Wernström JV, Huld S, Beutel RG, Arriaga-Varela E, Ahlberg PE, Niedźwiedzki G (2021) Exceptionally preserved beetles in a Triassic coprolite of putative dinosauriform origin. *Current Biology* 31: 3374–3381. <https://doi.org/10.1016/j.cub.2021.05.015>
- Radchenko AG, Dlussky GM (2019) First record of the ant genus *Crematogaster* (Hymenoptera: Formicidae) from the Late Eocene European ambers. *Annales Zoologici (Warsaw)* 69: 417–421. <https://doi.org/10.3161/00034541anz2019.69.2.008>
- Radchenko AG, Perkovsky EE (2021) Wheeler’s dilemma revisited: First *Oecophylla-Lasius* syninclusion and other ants syninclusions in the Bitterfeld amber (late Eocene). *Invertebrate Zoology* 18: 47–65. <https://doi.org/10.15298/invertzool.18.1.05>
- Rafiqi AM, Rajakumar A, Abouheif E (2020) Origin and elaboration of a major evolutionary transition in individuality. *Nature* 585: 239–244. <https://doi.org/10.1038/s41586-020-2653-6>

- Ramesh G, Babu R, Subramanian KA (2020) New species of *Soa* Enderlein, 1904 (Psocodea: 'Psocoptera': Lepidopsocidae) from the Western Ghats of India. *Zootaxa* 4881: 383–392. <https://doi.org/10.11646/zootaxa.4881.2.11>
- Rasnitsyn AP, Müller P (2023) Identity of the insect larva described by Zippel et al. (2022) in the mid-Cretaceous Burmese (Kachin) amber (Hymenoptera, Tenthredinoidea, Blasticotomidae = Xyelotomidae, syn. nov.). *Palaeoentomology* 6: 13–16. <https://doi.org/10.11646/palaeoentomology.6.1.4>
- Régnier C, Achaz G, Lambert A, Cowie RH, Bouchet P, Fontaine B (2015) Mass extinction in poorly known taxa. *Proceedings of the National Academy of Sciences of the United States of America* 112: 7761–7766. <https://doi.org/10.1073/pnas.1502350112>
- Richter A, Keller RA, Rosumek FB, Economo EP, Garcia FH, Beutel RG (2019) The cephalic anatomy of workers of the ant species *Wasmannia affinis* (Formicidae, Hymenoptera, Insecta) and its evolutionary implications. *Arthropod Structure & Development* 49: 26–49. <https://doi.org/10.1016/j.asd.2019.02.002>
- Richter A, Boudinot BE, Yamamoto S, Katzke J, Beutel RG (2022) The first reconstruction of the head anatomy of a Cretaceous insect, †*Gerontoformica gracilis* (Hymenoptera: Formicidae), and the early evolution of ants. *Insect Systematics and Diversity* 6: 4. <https://doi.org/10.1093/isd/ixac013>
- Richter A, Boudinot BE, Garcia FH, Billen J, Economo EP, Beutel RG (2023) Wonderfully weird: The head anatomy of the armadillo ant, *Tatuidris tatusia* (Hymenoptera: Formicidae: Agroecomyrmecinae), with evolutionary implications. *Myrmecological News* 33. [https://doi.org/10.25849/myrmecol.news\\_033:035](https://doi.org/10.25849/myrmecol.news_033:035)
- Riou B (1999) Descriptions de quelques insectes fossiles du Miocène supérieur de la Montagne d'Andance (Ardèche, France). *EPHE Biologie et Evolution des Insectes* 11/12: 123–133.
- Ritzkowski S (1997) K-Ar-Altersbestimmungen der bernsteinführenden Sedimente des Samlandes (Paläogen, Bezirk Kaliningrad). *Metalla (Sonderheft)* 66: 19–23.
- Roesler R (1943) Über einige Copeognathengenera. *Stettiner Entomologische Zeitung* 104: 1–14.
- Roesler R (1944) Die Gattungen der Copeognathen. *Stettiner Entomologische Zeitung* 105: 117–166.
- Roger J (1862) Einige neue exotische Ameisen-Gattungen und Arten. *Berliner Entomologische Zeitschrift* 6: 233–254. <https://doi.org/10.1002/mmnd.47918620118>
- Rogers DC, et al. (2017) Images are not and should not ever be type specimens: A rebuttal to Garraffoni & Freitas. *Zootaxa* 4269: 455–459. <https://doi.org/10.11646/zootaxa.4269.4.3>
- Ross AJ (2019) Burmese (Myanmar) amber checklist and bibliography 2018. *Palaeoentomology* 2: 22–84. <https://doi.org/10.11646/palaeoentomology.2.1.5>
- Ross AJ (2021) Supplement to the Burmese (Myanmar) amber checklist and bibliography, 2020. *Palaeoentomology* 4: 57–76. <https://doi.org/10.11646/palaeoentomology.4.1.11>
- Sado A (2022) Amber on Fashion Week. *Bursztynisko. The Amber Magazine* 46: 6.
- Sadowski E-M, Schmidt AR, Seyfullah LJ, Solórzano-Kraemer MM, Neumann C, Perrichot V, Hamann C, Milke R, Nascimbene PC (2021) Conservation, preparation and imaging of diverse ambers and their inclusions. *Earth-Science Reviews* 220: 103653. <https://doi.org/10.1016/j.earscirev.2021.103653>
- Salata S, Fisher BL (2020) *Pheidole* Westwood, 1839 (Hymenoptera, Formicidae) of Madagascar – an introduction and a taxonomic revision of eleven species groups. *ZooKeys* 905: 1–235. <https://doi.org/10.3897/zookeys.905.39592>
- Salata S, Fisher BL (2022) Taxonomic revision of the *Pheidole megacephala* species-group (Hymenoptera, Formicidae) from the Malagasy Region. *PeerJ* 10: e13263. <https://doi.org/10.7717/peerj.13263>
- Samšínák K (1967) *Camponotus novotnyi* sp. n., eine neue tertiäre Ameise aus Böhmen. *Vestník Ustředního Ústavu Geologického* 42: 365–366.
- Santschi F (1911) Nouvelles fourmis du Congo et du Benguela. *Revue Zoologique Africaine (Brussels)* 1: 204–217.
- Santschi F (1912) Fourmis d'Afrique et de Madagascar. *Annales de la Société Entomologique de Belgique* 56: 150–167. <https://doi.org/10.5962/bhl.part.5816>
- Santschi F (1926) Trois notes myrmécologiques. *Annales de la Société Entomologique de France* 95: 13–28. <https://doi.org/10.1080/21686351.1926.12280094>
- Sarnat EM, Fischer G, Guénard B, Economo EP (2015) Introduced *Pheidole* of the world: Taxonomy, biology and distribution. *ZooKeys* 543: 1–109. <https://doi.org/10.3897/zookeys.543.6050>
- Savage TS (1849) The driver ants of western Africa. *Proceedings of the Academy of Natural Sciences of Philadelphia* 4: 195–200.
- Schädel M, Yavorskaya M, Beutel RG (2022) The earliest beetle †*Coleopsis archaica* (Insecta: Coleoptera)—morphological re-evaluation using Reflectance Transformation Imaging (RTI) and phylogenetic assessment. *Arthropod Systematics & Phylogeny* 80: 495–510. <https://doi.org/10.3897/asp.80.e86582>
- Schedl KE (1939) Die Einteilung und geographische Verbreitung der Platypodidae. 56. Beitrag zur Morphologie und Systematik der Scolytidae und Platypodidae. In: Jordan K, Hering EM (Eds) *Verhandlungen, VII. Internationaler Kongress für Entomologie. Vol. 1. Selbstverlage der Internationalen Kongresse für Entomologie, Weimar*, 377–410.
- Schindelin J, Arganda-Carreras I, Frise E, Kaynig V, Longair M, Pietzsch T, Preibisch S, Rueden C, Saalfeld S, Schmid B, Tinevez J-T, White DJ, Hartenstein V, Eliceiri K, Tomancak P, Cardona A (2012) Fiji: An open-source platform for biological-image analysis. *Nature Methods* 9: 676–682. <https://doi.org/10.1038/nmeth.2019>
- Schawaroch V, Kathirithamby J, Grimaldi D (2005) Strepsiptera and triungula in Cretaceous amber. *Insect Systematics & Evolution* 36: 1–20. <https://doi.org/10.1163/187631205788912787>
- Schweigger AF (1819) Beobachtungen auf naturhistorischen Reisen. Anatomisch-physiologische Untersuchungen über Corallen; nebst einem Anhang, Bemerkungen über den Bernstein enthaltend. Reimer, Berlin, 127 pp. <https://doi.org/10.5962/bhl.title.14416>
- Scudder SH (1877) The first discovered traces of fossil insects in the American Tertiaries. *Bulletin of the United States Geological and Geographical Survey of the Territories* 3: 741–762.
- Seeger W (1975) Funktionsmorphologie an Spezialbildungen der Fühlergeißel von Psocoptera und anderen Paraneoptera (Insecta); Psocodea als monophyletische Gruppe. *Zeitschrift für Morphologie der Tiere* 81: 137–159. <https://doi.org/10.1007/bf00301153>
- Semple TL, Vidal-García M, Tatarnic NJ, Peakall R (2021) Evolution of reproductive structures for in-flight mating in thynnine wasps (Hymenoptera: Thynnidae: Thynninae). *Journal of Evolutionary Biology* 34: 1406–1422. <https://doi.org/10.1111/jeb.13902>
- Sendel N (1742) *Historia succinorum corpora aliena involventium et naturae opere pictorum et caelatorum ex regis augustorum cimeliis Dresdae conditis aeri insculptorum conscripta a Nathanaeli Sendelio: apud Io. Fridericum Gleditschium*. <https://doi.org/10.5962/bhl.title.150129>
- Shelmerdine SC, Simcock IC, Hutchinson JC, Aughwane R, Melbourne A, Nikitichev DI, Ong J-I, Borghi A, Cole G, Kingham E, Calder

- AD, Capelli C, Akhtar A, Cook AC, Schievano S, David A, Ourselin S, Sebire NJ, Arthurs OJ (2018) 3D printing from microfocus computed tomography (micro-CT) in human specimens: Education and future implications. *The British Journal of Radiology* 91: 20180306. <https://doi.org/10.1259/bjr.20180306>
- Simonsen TJ, Kitching IJ (2014) Virtual dissections through micro-CT scanning: A method for non-destructive genitalia ‘dissections’ of valuable Lepidoptera material. *Systematic Entomology* 39: 606–618. <https://doi.org/10.1111/syen.12067>
- Singer GG (2008) Amber in the ancient Near East. *Centro de Estudios de Historia del Antiguo Egipto-Universidad Católica Argentina*. Disponible em. [https://www.academia.edu/241848/Amber\\_in\\_the\\_Ancient\\_Near\\_East](https://www.academia.edu/241848/Amber_in_the_Ancient_Near_East) [Acceso em, 1]
- Singer GNG (2016) Amber exchange in the Late Bronze Age Levant in cross-cultural Perspective. Paper presented at the International Conference about the Ancient Roads in San Marino.
- Ślodka B, Kramarska R, Kasiński JR (2013) The Eocene Climatic Optimum and the formation of the Baltic amber deposits. Paper presented at the The international amber researcher symposium. “Amber. Deposits-Collections-The Market”. Gdansk, Poland: Gdansk International fair Co. Amberif.
- Smith F (1857) Catalogue of the hymenopterous insects collected at Sarawak, Borneo; Mount Ophir, Malacca; and at Singapore, by A. R. Wallace. *Journal of the Proceedings of the Linnean Society of London. Zoology* 2: 42–88. <https://doi.org/10.1111/j.1096-3642.1857.tb01759.x> [part]
- Smith F (1868) Explanation of the plate of organic remains found in amber, in Amber; its origin and history, as illustrated by the geology of Samland. *Quarterly Journal of Science* 5: 183–184.
- Smith MR (1943) A generic and subgeneric synopsis of the male ants of the United States. *American Midland Naturalist* 30: 273–321. <https://doi.org/10.2307/2421283>
- Smithers CN (1964) On the Psocoptera of Madagascar. *Revue de Zoologie et de Botanique Africaines* 70: 209–294.
- Smithers CN (1990) Key to the families and genera of Psocoptera (Arthropoda: Insecta). *Technical Reports of the Australian Museum* 2: 1–82. <https://doi.org/10.3853/j.1031-8062.2.1990.77>
- Smithers CN (1999) New species and new records of Psocoptera from Tanzania. *African Entomology* 7: 91–106.
- Snelling RR (2006) Taxonomy of the *Camponotus festinatus* complex in the United States of America (Hymenoptera: Formicidae). *Myrmecologische Nachrichten* 8: 83–97.
- Solórzano-Kraemer MM, Delclòs X, Engel MS, Peñalver E (2020) A revised definition for copal and its significance for palaeontological and Anthropocene biodiversity-loss studies. *Scientific Reports* 10: 19904. <https://doi.org/10.1038/s41598-020-76808-6>
- Solórzano-Kraemer MM, Kunz R, Hammel JU, Peñalver E, Delclòs X, Engel MS (2022) Stingless bees (Hymenoptera: Apidae) in Holocene copal and Defaunation resin from Eastern Africa indicate Recent biodiversity change. *The Holocene* 32: 414–432. <https://doi.org/10.1177/09596836221074035>
- Sosiak CE, Borowiec ML, Barden P (2022) An Eocene army ant. *Biology Letters* 18: 20220398. <https://doi.org/10.1098/rsbl.2022.0398>
- Sosiak CE, Borowiec ML, Barden P (2023a) Retraction: An Eocene army ant. *Biology Letters* 19: 20230059. <https://doi.org/10.1098/rsbl.2023.0059>
- Sosiak CE, Borowiec ML, Barden P (2023b) An invited reply to: A comment on: An Eocene army ant (2022) by Sosiak CE et al. *Biology Letters* 19: 20230140. <https://doi.org/10.1098/rsbl.2023.0140>
- Steward GA, Beveridge AE (2010) A review of New Zealand kauri (*Agathis australis* (D. Don) Lindl.): Its ecology, history, growth and potential for management for timber. *New Zealand Journal of Forestry Science* 40: 33–59.
- Strohmeyer H (1912) Neue Platypodiden aus Deutsch-Ostafrika, Kamerun und Französisch-Kongo. *Entomologische Blätter* 8: 78–86.
- Saqalaksari MP, Talebi AA, van de Kamp T, Haghghi SR, Zimmermann D, Richter A (2023) EntomonVR: a New Virtual Reality Game for Learning Insect Morphology. *bioRxiv*, 25 pp. <https://doi.org/10.1101/2023.02.01.526587>
- Takahashi Y, Aiba H (2023) Winged formicine ant fossils (Hymenoptera, Formicidae) from the Chibanian (Middle Pleistocene) Shiobara Group, Tochigi Prefecture, Japan. *Chishitsugaku Zasshi* 129: 573–578. <https://doi.org/10.5575/geosoc.2023.0023>
- Taylor B (2022) The Ants of (sub-Saharan) Africa (Hymenoptera: Formicidae). Profusely illustrated with original drawings and photographs and Catalogue notes on all ant species described from sub-Saharan Africa. 12<sup>th</sup> edn. <https://antsofAfrica.org/> [accessed: 18 July 2022]
- Taylor CK (2013) The genus *Lithoseopsis* (Psocodea: Amphientomidae) in the Western Australian fauna, with description of the male of *Lithoseopsis humphreysi* from Barrow Island. *Records of the Western Australian Museum* 83: 245–252. <https://doi.org/10.18195/issn.0313-122x.83.2013.245-252>
- Tihelka E, Li L, Fu Y, Su Y, Huang D, Cai C (2021) Angiosperm pollinivory in a Cretaceous beetle. *Nature Plants* 7: 445–451. <https://doi.org/10.1038/s41477-021-00893-2>
- Tollefson J (2022) Climate change is hitting the planet faster than scientists originally thought. *Nature* 28. <https://doi.org/10.1038/d41586-022-00585-7>
- Tröger D, Stark H, Beutel RG, Pohl H (2023) The morphology of the free-living females of Strepsiptera (Insecta). *Journal of Morphology* 284: e21576. <https://doi.org/10.1002/jmor.21576>
- Trueman CN (2013) Chemical taphonomy of biomineralized tissues. *Palaeontology* 56: 475–486. <https://doi.org/10.1111/pala.12041>
- Turner BD (1975) The Psocoptera of Jamaica. *Transactions of the Royal Entomological Society of London* 126: 533–609. <https://doi.org/10.1111/j.1365-2311.1975.tb00860.x>
- Uschmann G (1959) *Geschichte der Zoologie und der zoologischen Anstalten in Jena 1779–1919*, Gustav Fischer Verlag, Jena.
- Varela-Hernández F, Riquelme F (2021) A new ant species of the genus *Pheidole* Westwood, 1839 from Miocene Mexican amber. *Southwestern Entomologist* 46: 75–82. <https://doi.org/10.3958/059.046.0107>
- Valentini MB (1714) *Musei museum, oder, der vollständigen Schaubühne fremder Naturalien: die raresten Naturschätze aus allen bis daher gedruckten Kunstkammern, Reißbeschreibungen und anderen curiosen Büchern enthalten, und benebenst einer neu ausgerichteten Zeug- und Rüstkammer der Natur auch vielen curiosen Kupferstücken vorgestellt sind*. Von D. Michael Bernhard Valentini. <https://doi.org/10.5962/bhl.title.150208>
- Vijande Vila E, Domínguez-Bella S, Cantillo Duarte JJ, Martínez López J, Barrena Tocino A (2015) Social inequalities in the Neolithic of southern Europe: The grave goods of the Campo de Hockey necropolis (San Fernando, Cádiz, Spain). *Comptes Rendus. Palévol* 14: 147–161. <https://doi.org/10.1016/j.crpv.2014.11.004>
- Vishnyakova VN (1975) Psocoptera in Late Cretaceous insect-bearing resins from the Taimyr. *Entomological Review* 54: 63–75.
- Vitali F (2019) Systematic notes on the Cerambycidae (Insecta: Coleoptera) described from Burmese amber. *Palaeontology* 2: 215–218. <https://doi.org/10.11646/palaeontology.2.3.3>

- von Kéler S (1966) Zur Mechanik der Nahrungsaufnahme bei Corrodentien. *Zeitschrift für Parasitenkunde* (Berlin, Germany) 27: 64–79. <https://doi.org/10.1007/BF00261218>
- Wappler T, Dlussky GM, Reuter M (2009) The first fossil record of *Polyrhachis* (Hymenoptera: Formicidae: Formicinae) from the Upper Miocene of Crete (Greece). *Palaontologische Zeitschrift* 83: 431–438. <https://doi.org/10.1007/s12542-009-0035-3>
- Ward PS, Boudinot BE (2021) Grappling with homoplasy: taxonomic refinements and reassignments in the ant genera *Camponotus* and *Colobopsis* (Hymenoptera: Formicidae). *Arthropod Systematics & Phylogeny* 79: 37–56. <https://doi.org/10.3897/asp.79.e66978>
- Ward PS, Brady SG, Fisher BL, Schultz TR (2010) Phylogeny and biogeography of dolichoderine ants: Effect of data partitioning and relict taxa on historical inference. *Systematic Biology* 59: 342–362. <https://doi.org/10.1093/sysbio/syq012>
- Ward PS, Blaimer BB, Fisher BL (2016) A revised phylogenetic classification of the ant subfamily Formicinae (Hymenoptera: Formicidae), with resurrection of the genera *Colobopsis* and *Dinomyrmex*. *Zootaxa* 4072: 343–357. <https://doi.org/10.11646/zootaxa.4072.3.4>
- Weber FC (1740) Das veränderte Rußland: In welchem Die jetzige Verfassung des Geist- und Weltlichen Regiments, Der Kriegs-Staat zu Lande und zu Wasser, Der wahre Zustand der Rußischen Finanzen, die geöffneten Berg-Wercke, die eingeführte Academien, Künste, Manufacturen, ergangene Verordnungen, Geschäfte mit denen Asiatischen Nachbahren und Vasallen, nebst der allerneuesten Nachricht von diesen Völckern, Ingleichen Die Begebenheiten des Czarewizen Und was sich sonst merckwürdiges in Rußland zugetragen; Nebst verschiedenen bisher unbekanntenen Nachrichten vorgestellt werden. 3: Die Regierung der Kayserin Catharina und des Kaysers Petri Secundi und sonst alle vorgefallene Merkwürdigkeiten in sich haltend. 243.
- Weidner H (1972) Copeognatha (Staubläuse). *Handbuch der Zoologie* 4: 2. [Hälfte, Berlin.]
- Weingardt M, Beutel RG, Pohl H (2023) *Xenos vesparum* (Strepsiptera: Xenidae)—A new insect model and its endoparasitic secondary larva. *Insect Systematics and Diversity* 7: 4. <https://doi.org/10.1093/isd/ixad003>
- Westwood JO (1839) An introduction to the modern classification of insects; founded on the natural habits and corresponding organisation of the different families. Volume 2. Part XI. London: Longman, Orme, Brown, Green and Longmans, 193–224. <https://doi.org/10.5962/bhl.title.34449>
- Wheeler WM (1915) [“1914”] The ants of the Baltic Amber. *Schriften der Physikalisch-Ökonomischen Gesellschaft zu Königsberg* 55: 1–142. <https://doi.org/10.5962/bhl.title.14207>
- Wheeler WM (1921) Chinese ants. *Bulletin of the Museum of Comparative Zoology* 64: 529–547.
- Wichard W (2009) Taxonomic names. *Aquatic Insects in Baltic Amber*: 1–335.
- Wichard W, Buder T, Caruso C (2010) Aquatic lacewings of family Nevrothidae (Neuroptera) in Baltic amber. *Denisia* 29: 445–457.
- Wichard W (2016) Overview and descriptions of Nevrothidae in Baltic amber (Insecta, Neuroptera). *Palaediversity* 9: 95–111. <https://doi.org/10.18476/pale.v9.a7>
- Wichard W (2017) Family Nevrothidae (Insecta, Neuroptera) in mid-Cretaceous Burmese amber. *Palaediversity* 10: 1–5. <https://doi.org/10.18476/pale.v10.a1>
- Wichard N, Wichard W (2008) Nathanael Sendel (1686–1757) Ein Wegbereiter der paläobiologischen Bernsteinforschung. *Palaediversity* 1: 93–102.
- Wilde F, Ogurreck M, Greving I, Hammel JU, Beckmann F, Hipp A, Lottermoser L, Khokhriakov I, Lytaev P, Dose T, Burmester H, Müller M, Schreyer A (2016) Micro-CT at the imaging beamline P05 at PETRA III. *AIP Conference Proceedings* 1741: 030035. <https://doi.org/10.1063/1.4952858>
- Wilson EO (1985a) Ants of the Dominican amber (Hymenoptera: Formicidae). 1. Two new myrmicine genera and an aberrant Pheidole. *Psyche* (Cambridge) 92: 1–9. <https://doi.org/10.1155/1985/17307>
- Wilson EO (1985b) Ants of the Dominican amber (Hymenoptera: Formicidae). 2. The first fossil army ants. *Psyche* (Cambridge) 92: 11–16. <https://doi.org/10.1155/1985/63693>
- Wilson EO (2003) *Pheidole* in the New World. A dominant, hyperdiverse ant genus. Cambridge, Mass.: Harvard University Press, [ix + ]794 pp.
- Wilson EO, Brown Jr WL (1953) The subspecies concept and its taxonomic application. *Systematic Zoology* 2: 97–111. <https://doi.org/10.2307/2411818>
- Wilson PF, Stott J, Warnett JM, Attridge A, Smith MP, Williams MA (2017) Evaluation of touchable 3D-printed replicas in museums. *Curator* 60: 445–465. <https://doi.org/10.1111/cura.12244>
- Winkler HJ (2019) Preußen als Unternehmer 1923–1932. In *Preußen als Unternehmer 1923–1932*: de Gruyter. <https://doi.org/10.1515/9783110830682>
- Wright AH (1911) Other early records of the passenger pigeon (concluded). *The Auk* 28: 427–449. <https://doi.org/10.2307/4070951>
- Wulff NC, van de Kamp T, dos Santos Rolo T, Baumbach T, Lehmann GU (2017) Copulatory courtship by internal genitalia in bushcrickets. *Scientific Reports* 7: 42345. <https://doi.org/10.1038/srep42345>
- Yoshizawa K (2002) Phylogeny and higher classification of suborder Psocomorpha (Insecta: Psocodea: ‘Psocoptera’). *Zoological Journal of the Linnean Society* 136: 371–400. <https://doi.org/10.1046/j.1096-3642.2002.00036.x>
- Yoshizawa K, Johnson KP (2008) Molecular systematics of the barklouse family Psocidae (Insecta: Psocodea: ‘Psocoptera’) and implications for morphological and behavioral evolution. *Molecular Phylogenetics and Evolution* 46(2): 547–559. <https://doi.org/10.1016/j.ympev.2007.07.011>
- Yoshizawa K, Lienhard C (2010) In search of the sister group of the true lice: A systematic review of booklice and their relatives, with an updated checklist of Liposcelididae (Insecta: Psocodea). *Arthropod Systematics & Phylogeny* 68: 181–195. <https://doi.org/10.3897/asp.68.e31725>
- Zhang J (1989) Fossil insects from Shanwang, Shandong, China. [In Chinese.]. Jinan, China: Shandong Science and Technology Publishing House, 459 pp.
- Zhang J, Sun B, Zhang X (1994) Miocene insects and spiders from Shanwang, Shandong. [In Chinese.]. Beijing: Science Press, [v + ] 298 pp.
- Ziegler MJ, Perez VJ, Pirlo J, Narducci RE, Moran SM, Selba MC, Hastings AK, Vargas-Vergara C, Antonenko PD, MacFadden BJ (2020) Applications of 3D paleontological data at the Florida Museum of Natural History. *Frontiers of Earth Science* 8: 1–20. <https://doi.org/10.3389/feart.2020.600696>
- Zippel A, Haug C, Müller P, Haug JT (2022) First fossil tumbling flower beetle-type larva from 99 million year old amber. *Palaontologische Zeitschrift* 96: 219–229. <https://doi.org/10.1007/s12542-022-00608-8>
- Zlatkov B, Vergilov V, Pérez Santa-Rita JV, Baixeras J (2023) First 3-D reconstruction of copulation in Lepidoptera: Interaction of genitalia in *Tortrix viridana* (Tortricidae). *Frontiers in Zoology* 20: 22. <https://doi.org/10.1186/s12983-023-00500-4>

## Appendix 1



**Figure A1.** Model 1 of *Dorylus nigricans molestus* (Formicidae: Dorylinae) preserved in piece PMJ Pa 5884. An interactive version of this model is available in the HTML version of this article online and on Sketchfab: URL: <https://sketchfab.com/3d-models/dorylus-sp-94769aba51364c5ab51ec8b92485609a>.

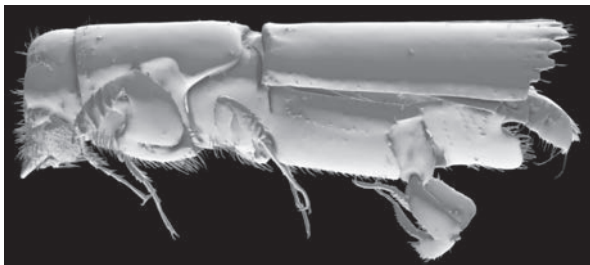


**Figure A2.** Model 2 of *Doliopygus cf. serratus* (Curculionidae: Platypodinae) in piece PMJ Pa 5827. An interactive version of this model is available in the HTML version of this article online and on Sketchfab: URL: <https://sketchfab.com/3d-models/platypodidae-e6d79e10baf6456ea137888f814e0925>.



**Figure A3.** Model 3 of the holotype specimen of  $\ddagger$ *A. knorrei* Weingardt, Bock & Boudinot, sp. nov. (Amphientomidae: Amphientominae) preserved in piece PMJ Pa 5809. An interactive cybertype is available in the HTML version of this article online and on Sketchfab: URL: <https://sketchfab.com/3d-models/amphientomum-knorrei-a7e0f1c0c6234093a384a51c2be48730>.

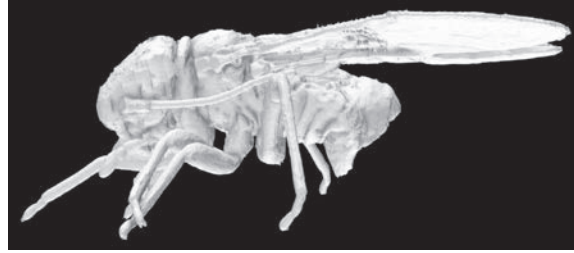


**Figure A4.** Model 4 of Archipsocidae gen. et sp. indet. preserved in kaori gum piece PMJ Pa 5825. An interactive version of this model is available in the HTML version of this article online and on Sketchfab: URL: <https://sketchfab.com/3d-models/archipsocidae-21ac330840f14ab5ac6d50898aba3a4d>.



**Figure A5.** Model 5 of the neotype of  $\ddagger$ *Pheidole cordata* Holl, 1829 preserved in copal piece PMJ Pa 5889. An interactive cybertype is available in the HTML version of this article online and on Sketchfab: URL: <https://sketchfab.com/3d-models/pheidole-cordata-695385c99247469ebb28bc4049b9e301>.



**Figure A6.** Model 6 of the holotype of  $\ddagger$ *Baltistena nigrispinata* Batelka, Tröger & Bock, sp. nov. (Mordellidae) preserved in piece PMJ Pa 5870. An interactive cybertype is available in the HTML version of this article online and on Sketchfab: URL: <https://sketchfab.com/3d-models/baltistena-nigrispinata-0b8819500b854c42b782b42b79c781c4>.

## Supplementary material 1

### **Amber and copal specimens of the Phyletisches Museum collection**

Authors: Brendon E. Boudinot, Bernhard L. Bock, Michael Weingardt, Daniel Tröger, Jan Batelka, Di LI, Adrian Richter, Hans Pohl, Olivia T. D. Moosdorf, Kenny Jandausch, Jörg U. Hammel, Rolf G. Beutel

Data type: docx

Explanation note: Amber and copal specimens of the Phyletisches Museum collection sorted by inventory number with the number of pieces given for each, what source they had according to the label and what source they are after identifying.

Copyright notice: This dataset is made available under the Open Database License (<http://opendatacommons.org/licenses/odbl/1.0>). The Open Database License (ODbL) is a license agreement intended to allow users to freely share, modify, and use this Dataset while maintaining this same freedom for others, provided that the original source and author(s) are credited.

Link: <https://doi.org/10.3897/dez.71.112433.suppl1>

## Supplementary material 2

### **Protocol of the IAA**

Authors: Brendon E. Boudinot, Bernhard L. Bock, Michael Weingardt, Daniel Tröger, Jan Batelka, Di LI, Adrian Richter, Hans Pohl, Olivia T. D. Moosdorf, Kenny Jandausch, Jörg U. Hammel, Rolf G. Beutel

Data type: pdf

Copyright notice: This dataset is made available under the Open Database License (<http://opendatacommons.org/licenses/odbl/1.0>). The Open Database License (ODbL) is a license agreement intended to allow users to freely share, modify, and use this Dataset while maintaining this same freedom for others, provided that the original source and author(s) are credited.

Link: <https://doi.org/10.3897/dez.71.112433.suppl2>

# The obligate fig-pollinator family Agaonidae in Germany (Hymenoptera, Chalcidoidea)

Silvan Rehberger<sup>1</sup>, Jonathan Vogel<sup>2</sup>, Björn Müller<sup>2</sup>, Cristina Vasilita<sup>3</sup>, Lars Krogmann<sup>3</sup>, Stefan Schmidt<sup>4†</sup>, Ralph S. Peters<sup>2</sup>

<sup>1</sup> Feigenparadies, c/o youngbrain GmbH, Sedanstr. 7, 79098 Freiburg im Breisgau, Germany

<sup>2</sup> Leibniz Institute for the Analysis of Biodiversity Change (LIB), Museum Koenig Bonn, Arthropoda Department, Adenauerallee 127, 53113 Bonn, Germany

<sup>3</sup> Stuttgart State Museum of Natural History, Department of Entomology, Rosenstein 1, 70191 Stuttgart, Germany

<sup>4</sup> SNSB-Zoologische Staatssammlung München, Münchhausenstr. 21, 81247 Munich, Germany

<https://zoobank.org/5E0C69D9-51DA-4F91-8FB9-56CC6E26EDD9>

Corresponding author: Ralph S. Peters (r.peters@leibniz-lib.de)

Academic editor: Silas Bossert ♦ Received 20 December 2023 ♦ Accepted 22 April 2024 ♦ Published 27 May 2024

## Abstract

All native and many cultivated fig plants are pollinated by representatives of the family Agaonidae (fig wasps), which are specialised, secondarily phytophagous relatives of parasitoid wasps that evolved an obligate mutualism with fig trees. So far, distribution of Agaonidae in Europe has been limited to southern, mostly Mediterranean areas, for example, in Greece, Croatia, Hungary, Italy, France, Spain and Portugal. Here, we report the first four records of the family for Germany, all in the form of the widespread species *Blastophaga psenes* (Linnaeus, 1758). New verified records are from three States in western and south-western Germany, Baden-Wuerttemberg (Radolfzell at Lake Constance and Sasbach am Kaiserstuhl near Freiburg), Saarland (Saarbrücken) and Northrhine-Westalia (Bochum) and all are based on citizen-scientist observations and collections. The new records are considerably more northern than previously recorded localities and, strikingly, geographically distant from these. All records can be attributed to the presence of large male caprifig trees (*Ficus carica* L. var. *caprificus*), whose three generations of fruits host the development stages of *Blastophaga psenes*. We generated DNA barcode data of specimens from three localities and added them to the national GBOL (German Barcode of Life) database and the international Barcode of Life database (BOLD). The somewhat surprising occurrence of the species/family in Germany might be attributable to increasing temperatures as a result of global warming, but this needs further investigation. Additionally, the presence of fig wasps, assuming it stabilises, could offer new opportunities for fig farming in Germany.

## Key Words

Fig wasps, *Ficus carica*, *Blastophaga psenes*, pollination, first records

## Introduction

All species of the genus *Ficus* (figs) (Moraceae) depend on obligate pollinators of the wasp family Agaonidae (Hymenoptera, Chalcidoidea). There are about 880 accepted species of figs and many more undescribed (POWO 2023), associated with, so far, 640 described species of agaonid

fig wasps, which represent probably about 20–30% of the existing species (van Noort and Rasplus 2023). Numerous additional chalcid wasp species complement the fig system as facultative pollinators, inquilines or parasitoids of other fig-associated wasps. Fig fruits are not only vital food sources in natural environments for many vertebrates and invertebrates, but also commercially important. The

† Deceased.

commercially most important species is *Ficus carica* L., which produces the well-known edible fig fruits. More than 1,200 cultivars of *Ficus carica* are pomologically described (e.g. Condit (1955)). The yearly average worldwide fig production in 2015–2019 was 1,185,768 metric tonnes on 285,513 ha of cultivated area (Ferrara et al. 2022). The close association with fig plants and its striking diversity make Agaonidae a group of special ecological and economic relevance. In Europe, only few species are present. *Blastophaga psenes* (Linnaeus, 1758) is the most widespread, with populations limited to southern, mostly Mediterranean areas, for example, in Greece, Croatia, Hungary, Italy, France, Spain and Portugal. It has not been reported in Germany; the nearest validated records in France are hundreds of kilometres away from the German border (Baud 2008, 2023). Here, we report records of the fig wasp *Blastophaga psenes* from *Ficus carica* trees in four different localities across western and south-western Germany, these being the first records for the Agaonidae family in Germany. All recorded specimens were observed and collected by citizen scientists from the fig enthusiasts' community. Wasps were photographed, identified, DNA-barcoded and vouchered. *Blastophaga psenes* and *Ficus carica* are connected by a complex pollination and reproduction cycle. In order to discuss and understand the background of the records of *B. psenes* reported herein and to link the entomology and the fig community in this interdisciplinary paper, we provide an overview of this complex connection with a little more detail.

*Ficus carica* shows a special type of inflorescence called the syconium, which is built as a fleshy fruit from the stem (Stover et al. 2007). It is urn-shaped and contains multiple flowers, which can only be accessed through a small hole, called the ostiolum. *Ficus carica* is a gynodioecious, but functionally dioecious plant species (Kjellberg and Valdeyron 1990; Aradhya et al. 2010). The caprifig plants, also known as *Ficus carica* L. var. *caprificus*, have bisexual flowers with both fertile male flowers, which spend pollen, and sterile short-styled female flowers, also called gall flowers. They functionally represent the male plant. The function of the gall flowers is to host the eggs laid by *Blastophaga psenes* and then develop the pulpy gall and feed the fig wasp larvae. The fig plants *sensu stricto*, also known as *Ficus carica* L. var. *domestica* (Fruit Fig, Edible Fig) which bear the edible fig fruits, are unisexual and have only fertile long-styled female flowers. They functionally represent the female plant. *Ficus carica* bears – depending on the cultivar – up to three generations of fruits every year. The first generation are the Profichi (male) and Breba (female), which start to grow in spring from the previous year's wood and buds. The second generation are the Mammoni (male) and Fichi (female), also called Main Crop, which start to develop in summer from the newly-grown wood and buds of the same year. Later in the year, male figs grow the Mamme as third generation fruits; these enable the overwintering of *Blastophaga psenes*.

Female fig cultivars are differentiated by their fruit generations into two types: Uniferous cultivars grow mainly Fichi and no or almost no Breba fruits. Biferous cultivars

grow both Breba and Fichi. Female fig cultivars are also differentiated by their ability to grow parthenocarpic fruits (i.e. fruits without pollination). The Smyrna type only grows fruits with pollination. The Common type, sometimes also referred to as the Adriatic type, grows and ripens all fruit generations without pollination, though pollination can occur. The San Pedro type grows ripe Breba without pollination, but ripe Fichi only after pollination. Since *Blastophaga psenes* has, so far, not been present in wide areas of central and western Europe, including Germany, figs are almost exclusively grown as a hobby and not as a commercial fruit. Due to a large number of parthenocarpic Common and San Pedro cultivars, it is possible to grow figs without the pollinator. However, in the main production areas, the so-called caprification has been actively aided for centuries by planting caprifig trees or by hanging male caprifig branches in the fig plantations (Prgomet and Prgomet 2020; Kjellberg et al. 2022). Pollination from caprification results in less fruit dropping, in larger fruits, earlier ripening and also in a better taste. The sole pollinator of *Ficus carica* is *Blastophaga psenes*. After winter, the first generation of *B. psenes* develops in the gall flowers of the Mamme from the year before. The highly-modified wingless male wasps emerge first and inseminate the winged female wasps within the fig. The male wasps help the females to escape from the syconium by chewing narrow tunnels. The female wasps carry some of the omnipresent male pollen of the Mamme flower. The female wasps then reach the next fig trees by active or wind-driven flight and enter the figs through the ostiolum (Kjellberg et al. 1987). In the case of a male syconium (Profichi or Mammoni, in the first or second generation, respectively), the wasp will successfully oviposit into the flowers and the next generation of fig wasps can develop in the gall flowers. In case of a female syconium (Breba or Fichi, in first or second generation, respectively), which includes only long-styled fertile female flowers, the wasps pollinate, but do not oviposit and then die and are digested, presumably by the specific enzyme Ficain. In the Mamme as the third generation of male syconium, *B. psenes* will overwinter.

Both species, *Ficus carica* and *Blastophaga psenes*, rely on a fine-tuned interaction with three fruit and wasp generations, with male and female figs and on perfect timing. The fig trees in central Europe, for example Germany, that are sometimes just ornamental plants, are usually parthenocarpic female trees. Previously, male fig trees were found only occasionally in Germany, but in recent years, their number has been growing (Rehberger 2023). Their presence is a prerequisite for the occurrence and establishment of fig wasps in Germany.

## Methods

### Institutional abbreviations

SMNS – Staatliches Museum für Naturkunde Stuttgart, Germany

ZFMK – Museum Koenig Bonn, Germany

ZSM – SNSB-Zoologische Staatssammlung München, Germany

Fig wasps were collected out of male fig tree fruits at different locations in Germany. They were either immersed in ethanol or died dry and were shipped to ZFMK for DNA barcoding or to ZSM for morphological identification.

## DNA barcoding

At ZFMK, we processed 21 specimens from three locations in Baden-Württemberg (Radolfzell and Kaiserstuhl) and North Rhine-Westphalia (Bochum). We extracted DNA and amplified the CO1 barcode region at the molecular lab of the ZFMK following the protocols described in Jafari et al. (2023). Amplification and subsequent sequencing using forward primer LCO 2198-JJ and reverse primer HCO 2198-JJ (Astrin and Stüben 2008) did not yield any sequences. Alternatively, as forward primer, we used the newly-designed Heloridae-CV-F (primer sequence 5-TATTTGGAATATGAGCAGG-3) (published herein) and, as reverse primer, the HCO 2198-JJ primer. The amplified fragment is 619 bp long. Of the total of 21 specimens, 20 were successfully sequenced. In 18 of these, the barcodes fulfil all necessary criteria (e.g. chromatogram quality,  $\leq 1\%$  ambiguities or disagreements between the contig sequences) to meet the defined GBOL gold standard (see, for example, Jafari et al. (2023)). Accordingly, the sequencing success is 85.7% or 95.2% including the non-gold standard specimens. Sanger sequencing was done by BGI BIO Solutions Co, Ltd. (Hong Kong).

We complemented our sequences with one *Blastophaga psenes* sequence downloaded from BOLD (BOLD sequence ID: GBMIN30266-13) and outgroup sequences downloaded from BOLD (*Pleistodontes* sp., BOLD sequence ID: ASMII11091-22; *Blastophaga silvestriana*, ID: GBAH19865-19; *B. nipponica*, ID: GBAH20335-19;

*B. yeni*, ID: GBAH20406-19). All sequences were aligned with the MUSCLE (v. 3.9.425) algorithm allowing for a maximum of eight iterations (Edgar 2004). For the sole purpose of alpha taxonomical evaluation of conspecificity, we calculated a Neighbour-Joining tree using the Tamura-Nei distance model (Tamura and Nei 1993). We added bootstrap support values, based on 325,235 seed value (Geneious default) and 1,000 replicates. The final tree is rooted with *Pleistodontes* sp. We performed all steps from alignment to tree reconstruction in Geneious Prime 2022.1.1 (Biomatters Ltd.). We uploaded all successfully produced barcode sequences to BOLD (Ratnasingham and Hebert 2007) to the dataset DS-DEBLPSEN; the respective BOLD-IDs are listed in Table 1.

## Results

Confirmed records of *Blastophaga psenes* (those complemented by DNA barcodes marked \*) in order of discovery date are:

1. Radolfzell\*, found by Raphael Gebhard for the first time on 12.05.22 and also in 2023.
2. Saarbrücken, found by Anja Ruppert for the first time on 25.05.2022 and also multiple times in 2023.
3. Sasbach im Kaiserstuhl\*, found by Stephan Rawer and Silvan Rehberger for the first time on 16.08.2022 and also in 2023.
4. Bochum\*, found by Nikolaj Spiegel for the first time on 17.08.2022 and also multiple times in 2023.

Note that we do not give more detailed locality data to prevent vandalism of the respective fig trees. Detailed locality data are available from the authors upon reasonable request.

Localities are on display in Fig. 1. Vouchers are deposited at ZFMK, SMNS and ZSM (Table 1). In addition,

**Table 1.** BOLD-IDs of barcoded specimens, along with specimen IDs and depository information.

Specimen ID	Locality	Sex	BOLD-ID	bp-Length (ambiguities)	Depository
ZFMK-TIS-2637655	Bochum	♀	GBHYG1886-23	619(0)	SMNS
ZFMK-TIS-2637656	Bochum	♀	GBHYG1887-23	619(0)	ZSM
ZFMK-TIS-2637657	Bochum	♀	GBHYG1888-23	619(0)	ZFMK
ZFMK-TIS-2637658	Bochum	♀	GBHYG1889-23	619(0)	ZFMK
ZFMK-TIS-2637659	Bochum	♂	GBHYG1890-23	619(0)	ZFMK
ZFMK-TIS-2637660	Bochum	♂	GBHYG1891-23	619(0)	ZFMK
ZFMK-TIS-2637661	Bochum	♂	GBHYG1892-23	619(0)	ZFMK
ZFMK-TIS-2637662	Bochum	♂	GBHYG1893-23	619(0)	ZFMK
ZFMK-TIS-2637670	Sasbach/Kaiserstuhl	♀	GBHYG1894-23	619(0)	SMNS
ZFMK-TIS-2637671	Sasbach/Kaiserstuhl	♀	GBHYG1895-23	619(0)	ZSM
ZFMK-TIS-2637673	Sasbach/Kaiserstuhl	♂	GBHYG1896-23	619(0)	ZFMK
ZFMK-TIS-2637674	Sasbach/Kaiserstuhl	♂	GBHYG1897-23	619(0)	ZFMK
ZFMK-TIS-2637675	Radolfzell	♂	GBHYG1898-23	619(0)	SMNS
ZFMK-TIS-2637677	Radolfzell	♂	GBHYG1899-23	619(0)	ZSM
ZFMK-TIS-2637679	Radolfzell	♀	GBHYG1900-23	619(0)	ZFMK
ZFMK-TIS-2637680	Radolfzell	♀	GBHYG1901-23	619(0)	ZFMK
ZFMK-TIS-2637681	Radolfzell	♀	GBHYG1902-23	619(0)	ZFMK
ZFMK-TIS-2637682	Radolfzell	♀	GBHYG1903-23	619(0)	ZFMK



**Figure 1.** Map of records of *Blastophaga psenes* in Germany. Base Map Licence: CC BY-SA 3.0, Wikimedia Commons, Author: NordNordWest.

members of the *Ficus carica* Facebook group have recorded observations from 2023 of large numbers of fig wasps entering the ostium or emerging from caprifig fruits in Würzburg, Karlsruhe and Kippenheim near Offenburg. These observations lack detailed species identification and records are not vouchered. However, because of the uniqueness of the wasp and system reported here, we consider these records reliable and valuable and, ergo, also added them to Fig. 1, represented by blue filled triangles. Finally, pollinated Main Crop fruits from cultivars with obligatory pollination, indicating successful pollination, were observed in Riegel am Kaiserstuhl and Freiburg im Breisgau in 2022 and 2023, as well as in Wattenscheid, Essen and in Rheinfelden in 2023. These records do not include observed, identified or vouchered wasps, but are also shown in Fig. 1, represented by blue outlined triangles.

Analyses of DNA barcodes show conspecificity of the specimens with sequences generated herein, as well as with the *B. psenes* sequence added from BOLD, with

a maximum intraspecific difference of 1.1%. There is a notable distance between the specimens from the Kaiserstuhl and the remaining specimens from Bochum and Radolfzell (Fig. 2). The barcode sequences between these two groups differ by 0.6–1.1%. Within the clusters, there is a maximum difference of 0.5%. Morphologically, all specimens from Germany we consider conspecific.

## Discussion

The records of the agaonid *Blastophaga psenes* (Fig. 3) in Germany in 2022 came as a surprise, even more so since records are from four different, disjunct localities, ranging as far north as the City of Bochum in central-western Germany. These unexpected records immediately prompt the question as to why they are now present. Figs do not belong to the autochthonous flora of central Europe, but are considered as archaeophytes for Germany and have

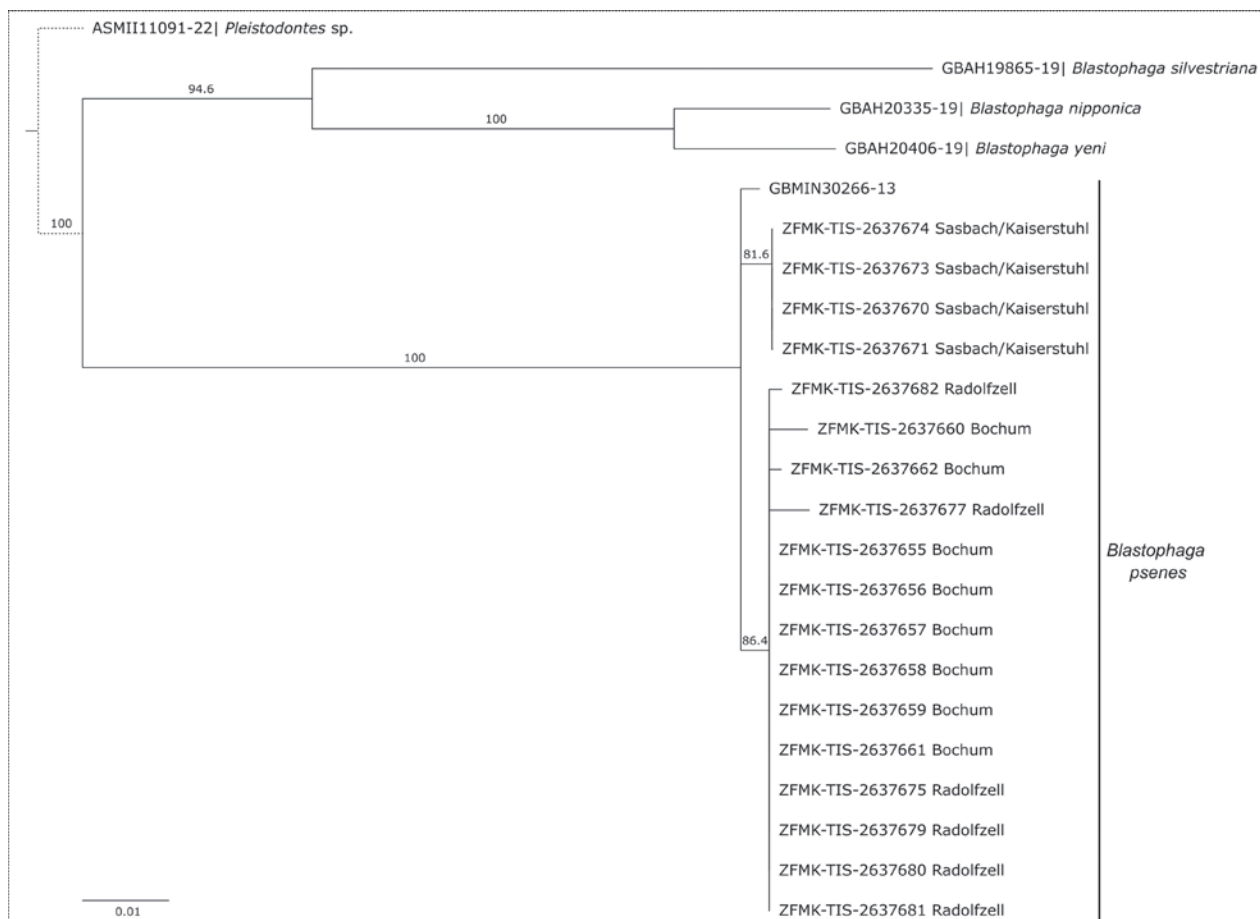


**Figure 2.** NJ tree, based on DNA barcode data for *B. psenes* specimens from three localities in Germany, complemented with one *B. psenes* sequence, three congeneric sequences and one *Pleistodontes* sp. (Agaonidae) sequence accessed via BOLD. The dotted branches that connect *Pleistodontes* sp. are not to scale. The support values (bootstrap with 1,000 replicates) are indicated on the respective branches.

been cultivated in Germany for more than 1,200 years (Gareis 1895; Knörzer 1981). Therefore, a long time has passed with figs present, but without any records of *B. psenes*, i.e. presumably without the species being present, in Germany. The nearest known reproducing populations of *B. psenes* are located in Provence (France), in Tuscany (Italy), in Croatia and in Hungary. In France, *B. psenes* is present only south of the line between Bordeaux and Lyon and only in non-mountainous areas (Baud 2008, 2023). Farmers in northern Italy have observed fig wasps occasionally in the lower warm parts of the valleys in the southern Alps in recent years, but not with stable reproducing populations (pers. comm. 2023). By linear distance, these could be the nearest populations, but the Alps are certainly a barrier for natural range extension of *B. psenes*. The other nearest populations are separated from the newly-recorded sites in Germany by 400 km (France) and 600 km (Hungary and Croatia). The intra-specific differences in DNA barcode sequence (i.e. a maximum of 1.1% between two groups; see results) might indicate that specimens from Kaiserstuhl and from Radolfzell/Bochum have different originating populations. It is possible that small populations were already present

in Germany in previous years, but were overlooked. As outlined in the Introduction, successful reproduction of *B. psenes* depends on a complex chronological interplay with male and female fig trees and their fig fruit generations. All prerequisites must now be fulfilled at various locations in Germany, otherwise the records would not have been possible. Given the complexity of the system, it is unlikely that the records reported herein are the result of an immediate change, suddenly bridging hundreds of kilometres. Unpublished records of fig wasps from the fig hobbyists' community in Alsace (France), Gent (Belgium), The Hague (Netherlands), Graz and Klagenfurt (both Austria) from 2023 indicate a step-by-step change and spread from both western and eastern populations, presumably along the rivers Danube, Rhine and Rhône. It is a task for the future to compare the German populations with those from other regions of Europe in order to reconstruct the origins of range extensions.

Higher mean temperatures as a result of climate change are the first obvious explanation for the new records in Germany, as is well known for many other insect taxa – for example, the fig-associated lepidopteran *Choreutis nemorana* (Hübner, 1799) (de Prins et al. 2014). However, con-



**Figure 3.** *Blastophaga psenes* female (collected in Saarbrücken in 2022), displaying the unique habitus of agaonid wasps.

sidering the highly-specialised obligate mutualism with *Ficus carica*, increased temperature alone cannot explain the occurrence of *B. psenes* in Germany. A necessary, but not sufficient condition for *B. psenes* to reproduce is the presence of male caprifig trees with fruits at all stages of its range extension routes. In recent years, the occurrence of male caprifig trees has significantly increased in central Europe (Rehberger 2023). The plants grow wild along the banks of rivers and lakes, in harbours and adjacent to sewage channels, possibly from seeds distributed by birds or from remains of figs consumed by humans or they are – often unintentionally – cultivated in public parks and also private gardens by people taking wild trees or cuttings with them from their holidays, not knowing that they might not bear eatable fruit. Maybe these occurrences of male caprifig trees allowed both migration and establishment of new populations of *B. psenes*.

At the moment, we do not know whether or not these populations become established. However, since the 2022 generation of the wasps already was the result of a successful reproduction and since more occurrences were recorded in 2023, it is well possible that these populations will establish and even spread further. Statements have to be made with caution, because *B. psenes* has not been known to expand its range, but is known to be difficult to establish in new areas. One of the best known examples is the deliberate introduction of *B. psenes* in southern California for the purpose of cultivating Turkish Smyrna fig cultivars. After many failed attempts with other spe-

cies of *Blastophaga* and also some failures with *B. psenes* they finally succeeded in 1889 (Eisen 1891; Ramirez 1970). After that, no range extension was observed and attempts for introduction in Texas, southern Arizona and Florida failed. In China, *B. psenes* has recently been considered for a local introduction and local domestication, as well as de-novo-domestication of wild pollinators via host-switches (Wang 2023). These activities show the importance of the pollinator for commercial fig production. Both yield and tasting quality of cultivated figs for some cultivars improve with the presence of the specialised pollinator. Cultivars of the Smyrna type fully depend on pollination by fig wasps. Hence, these new records will also be of economic interest because establishment of *B. psenes* in Germany and other regions of western and central Europe might enable future commercial fig farming.

## Conclusion

The multiple records of this extraordinary wasp taxon Agaonidae in Germany are the starting point for more in-depth studies on the details of the extension of the species' range as well as on their potential to fundamentally change fig plant cultivation in central Europe. In our team of citizen and professional scientists, we will curiously monitor the development over the next years and continue to study the story of this intriguing plant-insect-interaction in Europe.

## Acknowledgements

This paper is dedicated to the memory of our co-author, colleague and friend Stefan Schmidt.

We would like to thank Anja Ruppert, Raphael Gebhard, Stephan Rawer and Nikolaj Spiegel and many other people from the *Ficus carica* Facebook-Group for their support in searching for *Blastophaga psenes* populations at male fig trees in their home regions. Song Miaoyu and Huiqin Ma (Agricultural University Beijing, China) provided insights into research concerning *Ficus carica* and *Blastophaga psenes* in China. Don Shaw is acknowledged for linguistic help. We thank Vera Rduch (Museum Koenig Bonn) for her constant help with coordination of the GBOL III: Dark Taxa project. J. Vogel, B. Müller and R.S. Peters are supported by a grant from the Federal Ministry of Education and Research (BMBF), Berlin, Germany (FKZ 16LI1901A), for the project ‘GBOL III: Dark Taxa’.

## References

- Aradhya MK, Stover E, Velasco D, Koehmstedt A (2010) Genetic structure and differentiation in cultivated fig (*Ficus carica* L.). *Genetica* 138(6): 681–694. <https://doi.org/10.1007/s10709-010-9442-3>
- Astrin JJ, Stüben PE (2008) Phylogeny in cryptic weevils: molecules, morphology and new genera of western Palaearctic Cryptorhynchinae (Coleoptera: Curculionidae). *Invertebrate Systematics* 22(5): 503. <https://doi.org/10.1071/IS07057>
- Baud P (2008) Le Figuier – pas a pas. Edisud, Provence.
- Baud P (2023) Fig tree. Edisud, Provence.
- Condit IJ (1955) Fig varieties: A monograph. *Hilgardia* 23(11): 323–538. <https://doi.org/10.3733/hilg.v23n11p323>
- de Prins W, Bagnée JY, Spronck R, Spronck R (2014) *Choreutis nemorana* (Lepidoptera: Choreutidae) well established in Belgium. *Phegea* 42(2): 29–32.
- Edgar RC (2004) MUSCLE: A multiple sequence alignment method with reduced time and space complexity. *BMC Bioinformatics* 5(1): 113. <https://doi.org/10.1186/1471-2105-5-113>
- Eisen G (1891) The Introduction of *Blastophaga Psenes* into California. *Zoe: A Biological Journal* 2: 114–115.
- Gareis K (1895) Die Landgüterverordnung Kaiser Karls des Großen (Capitulare de villis vel curtis imperii). Textausgabe mit Einleitung und Anmerkungen. J. Guttentag, Berlin. <https://doi.org/10.1515/9783112378724>
- Ferrara G, Mazzeo A, Colasuonno P, Marcotuli I (2022) Production and growing regions. In: Sarkhosh A, Yavari A, Ferguson L (Eds) *The Fig – Botany, Production and Uses*. CABI International, 47–92. <https://doi.org/10.1079/9781789242881.0003>
- Jafari S, Müller B, Rulik B, Rduch V, Peters RS (2023) Another crack in the Dark Taxa wall: A custom DNA barcoding protocol for the species-rich and common Eurytomidae (Hymenoptera, Chalcidoidea). *Biodiversity Data Journal* 11(e101998): 1–13. <https://doi.org/10.3897/BDJ.11.e101998>
- Kjellberg F, Valdeyron G (1990) Species-specific pollination: a help or a limitation to range extension? In: di Castri F, Hansen AJ, Debussche M (Eds) *Biological Invasions in Europe and the Mediterranean Basin*. Monographiae Biologicae, vol 65. Springer, Dordrecht. [https://doi.org/10.1007/978-94-009-1876-4\\_23](https://doi.org/10.1007/978-94-009-1876-4_23)
- Kjellberg F, Gouyon P-H, Ibrahim M, Raymond M, Valdeyron G (1987) The stability of the symbiosis between dioecious figs and their pollinators: A study of *Ficus carica* L. and *Blastophaga psenes* L. *Evolution; International Journal of Organic Evolution* 41(4): 693–704. <https://doi.org/10.2307/2408881>
- Kjellberg K, van Noort S, Rasplus J-Y (2022) Fig wasps and pollination. In: Sarkhosh A, Yavari A, Ferguson L (Eds) *The Fig – Botany, Production and Uses*. CABI International, 231–254. <https://doi.org/10.1079/9781789242881.0009>
- Knörzer K-H (1981) Römerzeitliche Pflanzenfunde aus Xanten. *Archaeophysica* 11.
- POWO (2023) Plants of the World Online. Facilitated by the Royal Botanic Gardens, Kew. <http://www.plantsoftheworldonline.org/> [Retrieved 05 December 2023]
- Prgomet Ž, Prgomet I (2020) Smokva (*Ficus carica* L.). *Skink d.o.o., Rovinj*.
- Ramirez BW (1970) Host specificity of fig wasps (Agaonidae). *Evolution; International Journal of Organic Evolution* 24(4): 680–691. <https://doi.org/10.2307/2406549>
- Ratnasingham S, Hebert PDN (2007) Barcoding BOLD: The Barcode of Life Data System ([www.barcodinglife.org](http://www.barcodinglife.org)). <https://doi.org/10.1111/j.1471-8286.2007.01678.x>
- Rehberger S (2023) Faszination Feigen – Paradiesfrüchte in Deutschland. Frühjahrstagung des Pomologen-Verein e.V., Naumburg, Germany. Zenodo, Naumburg. <https://doi.org/10.5281/zenodo.11049333>
- Stover E, Aradhya MK, Ferguson L, Crisosto C (2007) The fig: Overview of an ancient fruit. *HortScience* 42(5): 1083–1087. <https://doi.org/10.21273/HORTSCI.42.5.1083>
- Tamura K, Nei M (1993) Estimation of the number of nucleotide substitutions in the control region of mitochondrial DNA in humans and chimpanzees. *Molecular Biology and Evolution* 10: 512–526. <https://doi.org/10.1093/oxfordjournals.molbev.a040023>
- van Noort S, Rasplus JY (2023) Figweb: figs and fig wasps of the world. <https://www.figweb.org/> [Accessed on 01.08.2023]
- Wang G (2023) Implication of P-A coevolution to the domestication of figs and pollinators [in preparation]. *Proceedings of the VII International Symposium on Fig: Weiyuan, China. Acta horticulturae*.



# Larval morphology of a Palearctic Rutelini, *Parastasia ferrieri* (Coleoptera, Scarabaeidae), with discussions on their feeding habits

Xiao-Yu Sun<sup>1</sup>, Xu-Ming Dong<sup>1</sup>, Lu Jiang<sup>1</sup>

<sup>1</sup> Key Laboratory of Economic and Applied Entomology of Liaoning Province, College of Plant Protection, Shenyang Agricultural University, Shenyang, Liaoning 110866, China

<https://zoobank.org/694FED8F-4B56-4CBD-95E3-DB50230DAED6>

Corresponding author: Lu Jiang (jianglu@syau.edu.cn)

Academic editor: Emmanuel Arriaga Varela ♦ Received 5 October 2023 ♦ Accepted 4 April 2024 ♦ Published 2 July 2024

## Abstract

Rutelini is one of the largest tribes of Rutelinae, widely distributed but primarily in the New World. Recently, both larvae and adults of *Parastasia ferrieri* had been discovered in Liaoning Province of northeastern China from the Palearctic realm. The third-instar larvae of *P. ferrieri* were described using light and scanning electron microscopy in order to discover more morphological characters for larval taxonomy. The larvae of *P. ferrieri* exhibit remarkable features, including four protuberances on labrum, no helus on epipharynx, two scissorial teeth on each mandible, five stridulatory teeth plus a blunt protuberance on each maxilla, and the obtuse claws on the thoracic legs. The correlation between morphological features and feeding habits is briefly discussed.

## Key Words

saproxyllic, shining leaf chafer, SEM, ultramorphology, white grub

## Introduction

Rutelinae, commonly known as shining leaf chafers, are so named due to the bright colors of most of their species and their adults feeding on plant leaves (Jameson and Ratcliffe 2002). Rutelinae encompass more than 4,000 species distributed among 235 genera (Krajčák 2007; Dietz et al. 2023). These species are further categorized into seven tribes: Adoretini, Alvarengiini, Anatistini, Anomalini, Anoplognathini, Geniatini, and Rutelini (Bouchard et al. 2011). On tribal level, in fact, Rutelinae exhibit great diversity on adult morphology, geographical distribution, diurnal/nocturnal rhythms, phototaxis, or even larval feeding habits (Frew et al. 2016; Ślipiński and Lawrence 2019).

Larvae of Rutelinae are commonly referred to as white grubs, exhibiting diverse feeding and living habits at the tribal level (Ritcher 1966; Johnson and Rasmann 2015; Frew et al. 2016). The larvae are described as root-feeding in some Anoplognathini, Geniatini, Adoretini and most of the Anomalini species (Habeck 1963; Ritcher 1966; McQuillan 1985; Fuhrmann 2013; Fang et al. 2018). However, the larval feeding habits remain

generally unknown in Anatistini and Alvarengiini (Pardo-Locarno et al. 2006; Fuhrmann 2013; Rodrigues et al. 2017). Rutelini larvae predominantly exhibit saproxyllic habits, characterized by their consumption of decaying wood, vegetation, roots, or other organic matter (Ritcher 1948), distinguishing them from the majority of other root-attacking larvae in the Anomalini (Ritcher 1966; Zhang 1984). It is unwise to generalize the ecological role of a specific Rutelinae species until their larvae have been accurately identified (Ślipiński and Lawrence 2019). Unfortunately, larval identification has been proven to be extremely challenging, with fewer than 2% of all known species having been described (Newton 1990; Śípek 2010; Lawrence et al. 2011).

The Rutelini encompass approximately a thousand species assigned into 93 genera, with a primary presence in the New World (Jameson 1997; Ślipiński and Lawrence 2019). They exhibit an array of distinctive morphological features, including enlarged mandibles, prominent thoracic horns, expanded hindlegs, and striking metallic coloration (Jameson and Ratcliffe 2002). Notably, Old World Rutelini typically display significant sexual dimor-

phism, with male adults possessing well-developed thoracic horns or mandibles (Jameson 1997; Ślipiński and Lawrence 2019). Regarding their immature stages, the larval morphology of Rutelini has been described for a limited subset, totaling 39 species in 24 genera (Ritcher 1948, 1966; Jameson and Morón 2001; Albertoni et al. 2014; Carvalho et al. 2019; Barria et al. 2020; Barria et al. 2021; Lugo-García et al. 2023).

*Parastasia* is one of the largest genera within Rutelini, comprising approximately 105 species worldwide (Wada 2015; Zhao 2019; Hongsuwong et al. 2022). However, unlike many other Rutelini beetles, the adults of *Parastasia* do not display enlarged structures or vibrant metallic coloration (Zhao 2019). Recently, both larvae and adults of *Parastasia ferrieri* were observed in Liaoning Province of northeastern China, belonging to the Palearctic realm, similar to the previous records in Korea (Kim 2014). Larvae of *P. brevipes* have been morphologically described and reported to feed on dead wood (Ritcher 1966). However, most of the other larvae of *Parastasia* are not adequately described hitherto.

In this study, third instar larvae of *P. ferrieri* were obtained through rearing. Their morphology is described using light and scanning electron microscopy in order to better understand the morphological diversity within the group and help with the identification of larvae in this genus.

## Materials and methods

### Insect collection and rearing

Larvae of *P. ferrieri* were collected from Qipanshan Forest Park in Shenyang City, Liaoning Province of northeastern China, in late October 2019. A total of 13 adult *P. ferrieri* beetles (Fig. 1A, B) were obtained through rearing in the following May. Paired adults were kept in plastic boxes filled with moist, fermented sawdust (Beetle-Password Company, Shenyang, China), and a decayed wood log off-cut was provided to facilitate potential boring and egg-laying. Third instar larvae were collected from the sawdust in the following September.

### Light and scanning electron microscopy

To conduct morphological observations, a total number of ten larvae were fixed in Dietrich's solution (formalin: 95% ethanol: glacial acetic acid: distilled water = 6: 15: 1: 80, v/v), which was heated up to 70 °C and then left to cool naturally for 12 h under a fume hood before being preserved in 75% ethanol (Jiang and Hua 2015).

Photographs were captured using a SONY ILCE-7RM4 digital camera. Scanning electron microscopy (SEM) was employed to examine third instar larvae. These larvae were dissected and examined in 75% ethanol using a Leica EZ4HD Stereoscopic Zoom Microscope. After a two-minute ultrasonic cleaning and two rinses in 75% ethanol, they were prepared for SEM. Dissected organs underwent serial dehydration using graded ethanol, followed by replace-

ment with tertiary butanol. They were then subjected to freeze-drying for 3 hours, sputter-coated with gold, and examined under a Hitachi S-3400N scanning electron microscope (Hitachi, Tokyo, Japan) at 5 kV. Nomenclature for larval morphology follows (Ritcher 1966).

Voucher specimens of both adults (Fig. 1A–E) and larvae (Fig. 1F) were deposited at the Entomological Museum of Shenyang Agricultural University (SYAU).

## Results

### General larval morphology

Larvae are of typically scarabaeiform shape, bearing three pairs of thoracic legs on the C-shaped body (Fig. 1F). The larval trunk is generally white in addition to the yellowish head capsule, thoracic legs and spiracles. The prothoracic spiracles are C-shaped,  $0.41 \pm 0.05$  mm ( $N = 20$ ) in length. Spiracles on the anterior six abdominal segments are similar in sizes, approximate  $0.22 \pm 0.05$  mm ( $N = 20$ ) in length. Whereas, the spiracles on the seventh and eighth abdominal segments are comparative larger,  $0.27 \pm 0.05$  mm ( $N = 20$ ) and  $0.28 \pm 0.05$  mm ( $N = 20$ ) respectively.

### Head

The head capsules are  $3.1 \pm 0.15$  mm ( $N = 10$ ) in width. The larval head displays symmetrical adornment, boasting a total of 14 pairs of setae. These include two pairs aligned vertically on the clypeus, five pairs in the frontal region (comprising two pairs of posterior frontal setae and three pairs of anterior frontal setae), three pairs on the vertex, and four pairs in the genal area (Fig. 2A).

The antenna is elongated and slender, comprising four segments, with the second segment being the longest (Fig. 2C). The basal two segments of the antenna are adorned with one and four setae, respectively. The third segment is smooth, featuring two to four oval dorsal sensory spots. The distal segment of the antenna of conical shape with seven sensilla basiconica at its apex (Fig. 2D).

### Mouthparts

The mouthparts are of a biting-chewing type, consisting of a labrum, a pair of mandibles, and a maxilla-labia complex.

Labrum exhibits symmetry and is slightly wider than it is long. The outer surface of the labrum displays symmetrical features, including four prominent protuberances and seven pairs of setae (Fig. 2B). The distal margin of the labrum is equipped with numerous sensory setae pointed distally (Fig. 3A).

Epipharynx, membranous, situated on inner surfaces of labrum and clypeus. Epipharynx is further divided into distinct functional areas (Fig. 3A), including a heptomeron at the apex, a pair of plegmatium on the lateral margin, nesium in the central portion, and glabrous gymnoparia on

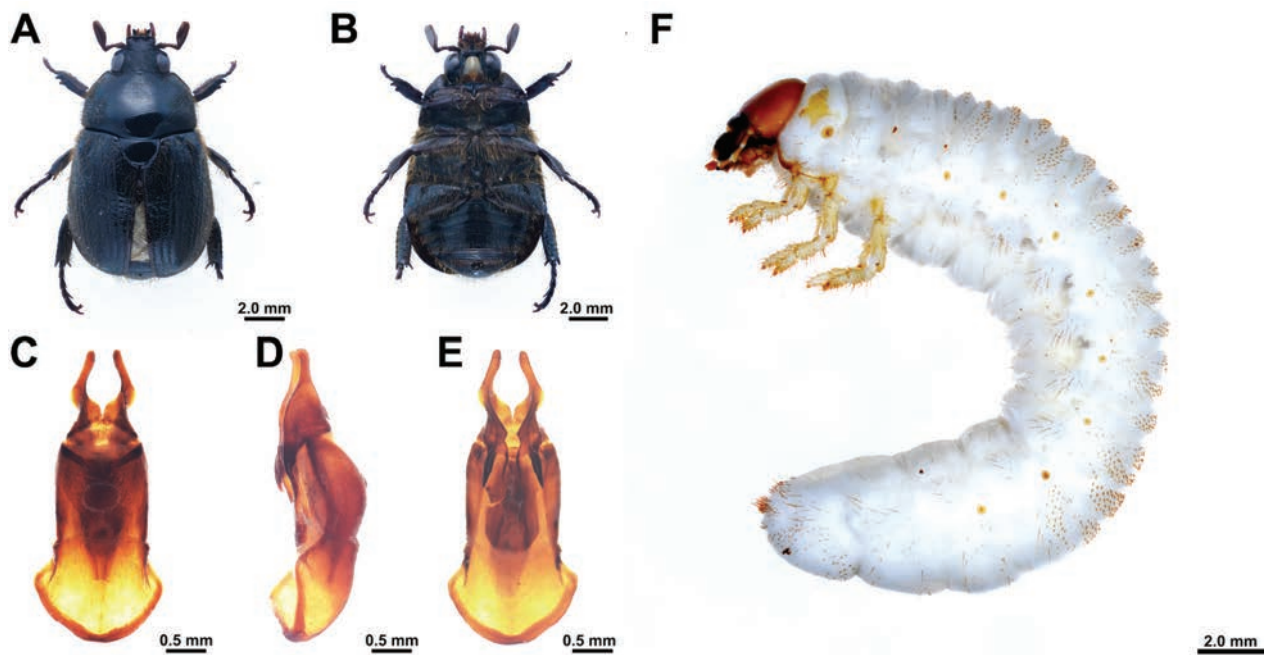


**Figure 1.** Adults and a larva of *Parastasia ferrieri*. **A.** Male adult, dorsal view; **B.** Male adult, ventral view; **C.** Male genitalia, dorsal view; **D.** Male genitalia, lateral view; **E.** Male genitalia, ventral view; **F.** Third instar larva.

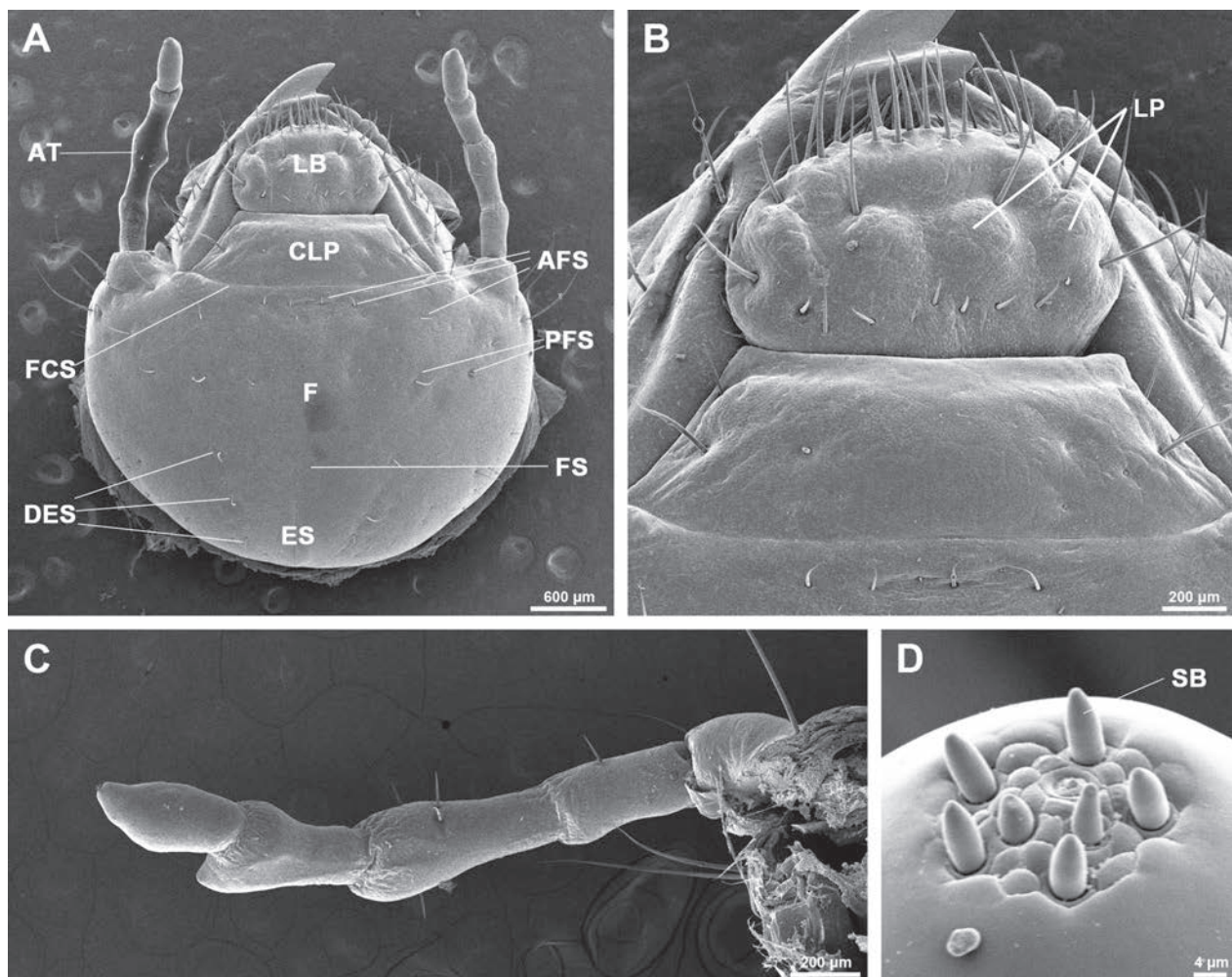


**Figure 2.** Larval head of *Parastasia ferrieri*. **A.** Head; **B.** Labrum; **C.** Antenna; **D.** Sensilla on the apex of antenna. AFS, anterior frontal seta; AT, antenna; CLP, clypeus; DES, dorsoepicranial setae; ES, epicranial stem; F, frons; FCS, frontoclypeal suture; LB, labrum; LP, labral protuberance; PFS, posterior frontal seta; SB, sensillum basiconicum.

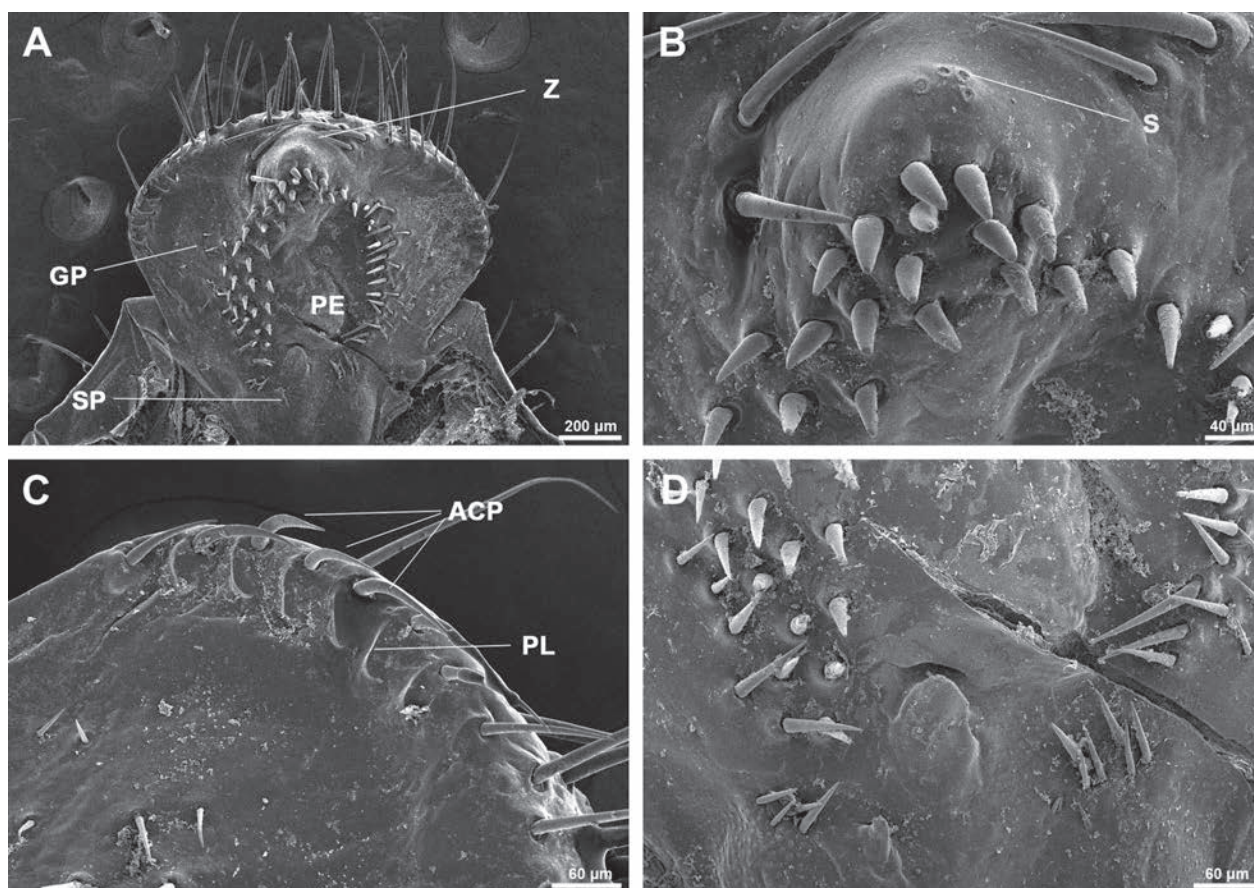


**Figure 3.** Larval epipharynx of *Parastasia ferrieri*. **A.** Epipharynx; **B.** Magnification of heptomerum; **C.** Magnification of plegma; **D.** Basal part of the epipharynx. ACP, acanthoparia; GP, gymnoparia; PL, plegma; PE, pedium; SP, sclerotized plate; S, sensillum; Z, zygum.

both sides (Fig. 3A). The heptomerum exhibits a slight curvature and is composed of four minute sensilla basiconica, lacking helus (Fig. 3B). The plegmatium consists of eight acanthoparia, intricately intertwined with an equal number of plegma (Fig. 3C). The chaetoparia displays asymmetry and is composed of numerous sensilla chaetica, with a higher density on the right side than on the left. Adjacent to the right acanthoparia, the sensory nesium is situated, featuring four micro sensilla basiconica at its apex (Fig. 3D).

The paired mandibles are heavily sclerotized, bearing two anterodorsal setae and a row of 11 setae on the lateral surface (Fig. 4A, B). The paired mandibles each bear a shuttle-shaped stridulatory area on ventral surface (Fig. 4C, D). The mandibular incisor is equipped with two apical teeth curved inward. The molar region exhibits asymmetry, featuring a prominent molar tooth accompanied by an acia on the left and a group of four ridged molar teeth on the right (Fig. 4C, D). The ventral process is relatively narrow on the left mandible (Fig. 4D), while it is generally wider on the right mandible (Fig. 4C).

The maxillae, labia, and hypopharynx are fused together to form a structural complex (Fig. 4E). Each of the paired maxillae comprises a cardo, a stipes, a maxillary palp, and a lobe fused from the galea and lacinia (Fig. 4E). The maxillary stridulatory area comprises a row of five stridulatory teeth and an anterior truncate process (Fig. 4F). The maxillary palp consists of four segments, with

the longest distal segment bearing a digitiform organ on its lateral surface and ten sensilla basiconica on its apex (Fig. 4E). The labia comprise a mentum, a prementum, a pair of two-segmented labial palps, and a sensory glossa (Fig. 4E). Dorsally, the glossa is adorned with numerous sensilla (Fig. 4E). The hypopharynx is specialized, forming a hypopharyngeal sclerome that bears a sclerotized truncate process, two tufts of microtrichia on the left, and a pair of membranous lobes on the lateral margin (Fig. 4F).

### Thoracic legs

Each of the thoracic legs is composed of five segments: coxa, trochanter, femur, tibiotarsus, and a distal single claw (see Fig. 5A, B). The coxa exhibits a long and slender shape. The trochanter possesses a slight curvature. The femur is covered with numerous setae on its surface. The tibiotarsus is originally a fusion of the tibia and tarsus, and it bears medium-sized setae on its dorsal, ventral, and lateral sides. The distal claw is heavily sclerotized, featuring an obtuse distal end and bearing three short setae.

The respiratory plate is composed of numerous minute openings that encircle the oval bulla, along with a slightly curved spiracular slit (refer to Fig. 5B). The prothoracic spiracles are slightly larger than the abdominal ones. The abdominal spiracles are similar in size (see Fig. 1).

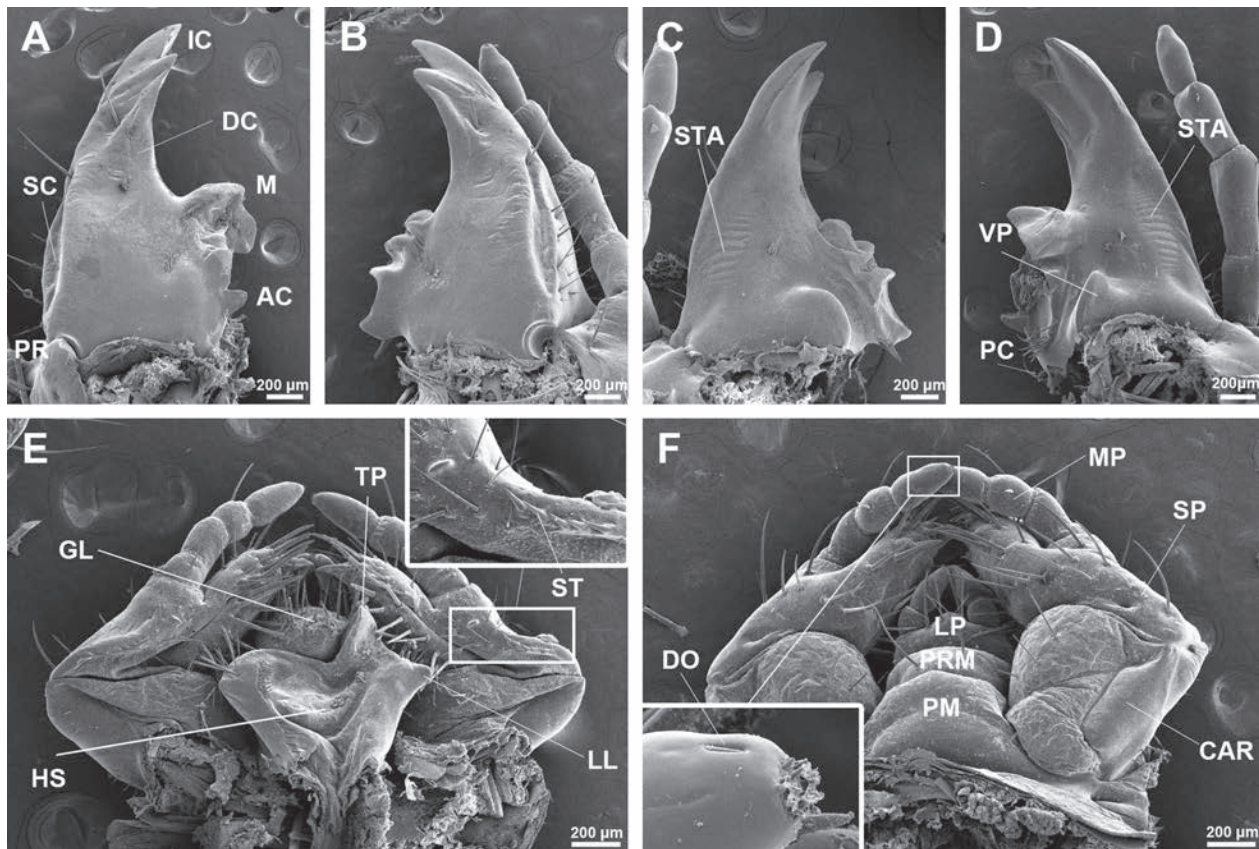


**Figure 4.** Mandibles and maxillae of *Parastasia ferrieri*. **A.** Left mandible, dorsal surface; **B.** Right mandible, dorsal surface; **C.** Right mandible, ventral surface; **D.** Left mandible, ventral surface; **E.** Maxillae and labia, ventral surface, insert showing the magnification of maxillary palpus; **F.** Maxilla, labia, and hypopharynx, dorsal surface. AC, acia; CAR, cardo; DC, dorsal carina; DO, digitiform organ; GL, glossa; HS, hypopharyngeal sclerome; IC, incisor; LL, lateral lobe; LP, labial palp; M, mola; MP, maxillary palp; PC, penicillus; PM, postmentum; PR, precoila; SC, scobis; ST, stridulatory teeth; STA, stridulatory area; SP, stipes; TP, truncate process; VP, ventral process.

## Raster

The raster is furnished with paralleled palidia, each composed of a longitudinal patch of mesal directed pali, surrounding a prominent septula. The palidia are submerged in a large number of setae, which are slightly longer and distributed at the lateral region.

## Discussion

In this study, larvae of *P. ferrieri* were described using scanning electron microscopy for the first time. The larvae of *P. ferrieri* are remarkable for the following structures: bearing four protuberances on labrum; no helus on epipharynx; two scissorial teeth on each mandible; five stridulatory teeth and a blunt protuberance on each maxilla; obtuse claws on thoracic legs, and 12 pairs of pali on raster. By the combination of these characters, larvae of *P. ferrieri* can be readily distinguished from most of the other larvae in Rutelini (Ritcher 1948, 1966; Jameson and Morón 2001; Albertoni et al. 2014; Carvalho et al. 2019; Barria et al. 2020; Barria et al. 2021; Lugo-García et al. 2023).

The labrum exhibits a wide range of morphological features within families or subfamilies of Scarabaeidae

(Ritcher 1966; Grebennikov and Scholtz 2004). The labrum is typically fan-shaped in Passalidae and Lucanidae (Hayes 1929; Qu et al. 2019), trilobed in Aphodiinae, Scarabaeinae, some Cetoniinae, and Pleocomidae (Grebennikov and Scholtz 2004; Li et al. 2019; Dong et al. 2020), or bearing an apical protuberance in some Sericinae (Šípek and Ahrens 2011). In the genus *Apogonia* (Melolonthinae), the labrum forms a dorsal ridge (Jia et al. 2023), while in some Hybosoridae, the labrum possesses serrations (Grebennikov and Scholtz 2004; Grebennikov et al. 2004). The labrum has varying numbers of setae or display glabrous, wrinkled, or humped dorsal surfaces in different lineages (Qu et al. 2019; Jia et al. 2020; Jia et al. 2021; Jia et al. 2023). In this study, the larval labrum of *P. ferrieri* is atypical for the presence of four protuberances on its dorsal surface, which is not mentioned in the congeneric larvae of *P. brevipes* (Ritcher 1966).

Previous comprehensive studies (Ritcher 1966; Zhang 1984; Sawada 1991) have indicated that heli on the epipharynx often serve as valuable taxonomic characteristics for larval identifications in Scarabaeidae (Fang et al. 2018; Jia et al. 2021). In Rutelinae, the larval epipharynx is equipped with two to four heli in Anomalini (Micó et al. 2003), six to eight in Anoplognathini (Neita-Moreno and Morón 2017), six to nine in Adoretini (Fang et al. 2018),

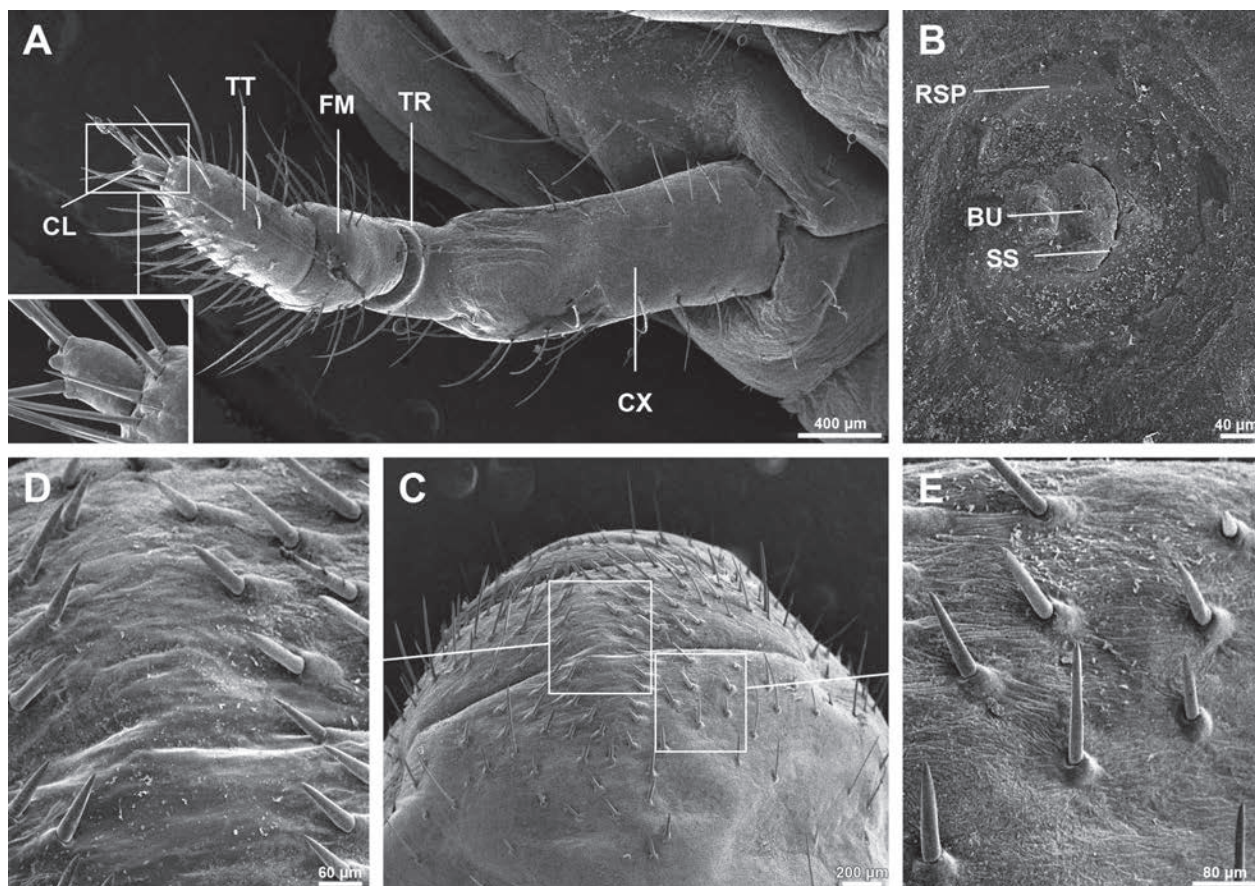


**Figure 5.** Thoracic legs, spiracles and raster of *Parastasia ferrieri*. **A.** Prothoracic leg, lateral view; **B.** Prothoracic spiracle; **C.** Raster; **D.** Magnification of the anterior palidia; **E.** Magnification of the hamate seta. BU, bulla; CL, claw; CX, coxa; FM, femur; RSP, respiratory plate; SS, spiracular slit; TT, tibiotarsus; TR, trochanter.

or entirely absent in Geniatini and Rutelini (Jameson and Morón 2001; Fuhrmann 2013). In this study, the larval epipharynx of *P. ferrieri* is devoid of heli, consistent with previous descriptions in Rutelini (Ritcher 1966; Jameson and Morón 2001; Barria et al. 2020; Barria et al. 2021; Lugo-García et al. 2023).

Mandibles, being the most heavily sclerotized structures on mouthparts, are structurally correlated with feeding habits (Zhang 1984). The larval mandibular incisor typically varies: straight and apically sharp in some wood-consuming species of Lucanidae and Passalidae (Hayes 1929; Katovich and Kriska 2002; Richards and Spencer 2014; Qu et al. 2019), sharp but inwardly curved in dung decomposers within Aphodiinae and Scarabaeinae (Jerath 1960; Edmonds and Halffter 1978; Frolov 2009; Li et al. 2019), or blade-like and specialized to form a cutting edge in phytophagous Melolonthinae (Jia et al. 2020; Jia et al. 2021; Jia et al. 2023). Within Rutelinae, the mandibular incisors are typically blade-like in some phytophagous larvae of Anomalini and Adoretini (Micó et al. 2003; Fang et al. 2018), and are apically sharp and curved in some saproxylic larvae of Rutelini (Jameson and Morón 2001). Within Rutelini, larval mandibles are usually asymmetric, equipped with three teeth on the left and two teeth on the right (Jameson and Morón 2001; Albertoni et al. 2014; Carvalho et al. 2019). In this study,

however, the larval mandibular incisor is symmetric, each bearing two scissor-like teeth, similar to the previously described larvae of *P. brevipes* (Ritcher 1966).

The claws of thoracic legs show considerable morphological diversity across lineages (Zhang 1984). In most species of Melolonthinae and Cetoniinae, the claw is typically curved, sharp, and adorned with paired setae (Sousa et al. 2018; Jia et al. 2020; Jia et al. 2021; Jia et al. 2023). Conversely, it is usually blunt in some wood-decomposing species within Lucanidae (Katovich and Kriska 2002; Qu et al. 2019) and remnant in certain dung-feeding larvae of Geotrupidae (Grebennikov and Scholtz 2004). In Rutelinae, thoracic claws are typically sharp in Adoretini (Fang et al. 2018), Geniatini (Pardo-Locarno et al. 2006; Fuhrmann 2013), and Anomalini (Micó and Galante 2005). However, they display morphological heterogeneity among the pro-, meso-, or metathoracic legs in some species of Rutelini (Carvalho et al. 2019). In this study, the claws of *P. ferrieri* are generally blunt on all three pairs of thoracic legs, congruent with other saproxylic larvae in Lucanidae (Richards and Spencer 2014; Qu et al. 2019).

Rutelinae usually attract attention due to their exquisite adult appearances or the economic losses caused by their larval stages (Jameson and Ratcliffe 2002). In the Palearctic realm, particularly in northeastern China, larvae of Rutelinae are frequently recognized as agricultural pests,

because they mostly belong to the phytophagous Anomaliini or Adoretini (Zhang 1984; Sawada 1991). This scarcity record of *P. ferrieri* may be attributed to their small, nocturnal adults, or the fact that their larvae never attack living organs of crops or trees. Given their significance of biogeographical distribution, the larvae of *P. ferrieri* warrant increased attention for conservation purposes.

## Author contributions

Conceived and designed the experiments: LJ, YYS. Performed the experiments: YYS, XMD. Analyzed the data: YYS and LJ. Wrote the paper: YYS, XMD and LJ.

## Acknowledgements

We are grateful to Ming-Zhi Zhao and Zi Shan for their kind help during our larval collecting and rearing periods. Our special thanks go to Dr. Yuan-Yuan Lu and Dr. Valentina Filippini for their valuable suggestions on our earlier draft. This research was financially supported by the National Natural Science Foundation of China (grant no. 32370470 and 31702036), China Postdoctoral Science Foundation (grant no. 2020M680982), Natural Science Foundation of Liaoning Province (2021-MS-230), Scientific Research Project of Education Department of Liaoning Province (LJKZ0641), Science and Technology Planning Project of Liaoning Province (grant no. 1618214601077) and Scientific Research Foundation for the Introduced Talent of Shenyang Agricultural University (grant no. 880417008).

## References

- Albertoni FF, Fuhrmann J, Ide S (2014) *Lagochile emarginata* (Gyllenhal): Morphology of immature and imago, and biological records (Coleoptera, Scarabaeidae, Rutelinae). *Revista Brasileira de Entomologia* 58(1): 32–46. <https://doi.org/10.1590/S0085-56262014000100007>
- Barria G, Manuel D, Quirós DI, Emmen D (2020) Descripción de los estadios inmaduros de *Rutela sanguinolenta* Waterhouse (Coleoptera: Scarabaeidae: Rutelinae: Rutelini). *Revista Chilena de Entomología* 46(2): 313–319. <https://doi.org/10.35249/rche.46.2.22.2020>
- Barria MD, Quirós DI, Emmen D (2021) Descripción de la larva y pupa de *Pelidnota prolixa* Sharp (Coleoptera: Scarabaeidae: Rutelinae: Rutelini). *Folia Entomologica Mexicana* 7: e0071003. [nueva serie]
- Bouchard P, Bousquet Y, Davies AE, Alonso-Zarazaga MA, Lawrence JF, Lyal CH, Newton AF, Reid CAM, Schmitt M, Ślipiński SA, Smith ABT (2011) Family-group names in Coleoptera (Insecta). *ZooKeys* 88: 1–972. <https://doi.org/10.3897/zookeys.88.807>
- Carvalho T, Duarte P, Fuhrmann J, Grossi P (2019) Description of the last larval instar and pupa of *Chlorota paulistana* Ohaus, 1912 (Coleoptera: Melolonthidae: Rutelinae: Rutelini). *Revista Brasileira de Entomologia* 63(3): 245–249. <https://doi.org/10.1016/j.rbe.2019.05.002>
- Dietz L, Seidel M, Eberle J, Misof B, Pacheco TL, Podsiadlowski L, Ranasinghe S, Gunter NL, Niehuis O, Mayer C, Ahrens D (2023) A transcriptome-based phylogeny of Scarabaeoidea confirms the sister group relationship of dung beetles and phytophagous pleurostict scarabs (Coleoptera). *Systematic Entomology* 48(4): 672–686. <https://doi.org/10.1111/syen.12602>
- Dong X-M, Jia Z-C, Jiang L (2020) Morphological description of the third instar larva of *Lasiotrichius succinctus hananoi* (Sawada) (Coleoptera: Scarabaeidae: Cetoniinae: Trichiini), using scanning electron microscopy. *Microscopy Research and Technique* 84(2): 368–375. <https://doi.org/10.1002/jemt.23594>
- Edmonds WD, Halfiter G (1978) Taxonomic review of immature dung beetles of the subfamily Scarabaeinae (Coleoptera: Scarabaeidae). *Systematic Entomology* 3(4): 307–331. <https://doi.org/10.1111/j.1365-3113.1978.tb00002.x>
- Fang H, Li C, Jiang L (2018) Morphology of the immature stages of *Adoretus tenuimaculatus* Waterhouse, 1875 (Coleoptera: Scarabaeidae: Rutelinae: Adoretini). *Journal of Asia-Pacific Entomology* 21(4): 1159–1164. <https://doi.org/10.1016/j.aspen.2018.09.001>
- Frew A, Barnett K, Nielsen UN, Riegler M, Johnson SN (2016) Below-ground ecology of scarabs feeding on grass roots: Current knowledge and future directions for management in Australia. *Frontiers in Plant Science* 7: 321. <https://doi.org/10.3389/fpls.2016.00321>
- Frolov AV (2009) Larval morphology of *Aphodius sus* (Herbst) and *A. variicolor* Koshantschikov (Coleoptera: Scarabaeidae: Aphodiinae). *Zootaxa* 2169(1): 45–54. <https://doi.org/10.11646/zootaxa.2169.1.4>
- Fuhrmann J (2013) Description of the third larval instar and pupa of *Geniates barbatus* Kirby (Coleoptera: Scarabaeidae: Rutelinae). *Revista Brasileira de Entomologia* 57(1): 40–46. <https://doi.org/10.1590/S0085-56262013000100007>
- Grebennikov VV, Scholtz CH (2004) The basal phylogeny of Scarabaeoidea (Insecta: Coleoptera) inferred from larval morphology. *Invertebrate Systematics* 18(3): 321–348. <https://doi.org/10.1071/IS03013>
- Grebennikov VV, Ballerio A, Ocampo FC, Scholtz CH (2004) Larvae of Ceratocanthidae and Hybosoridae (Coleoptera: Scarabaeoidea): Study of morphology, phylogenetic analysis and evidence of paraphyly of Hybosoridae. *Systematic Entomology* 29(4): 524–543. <https://doi.org/10.1111/j.0307-6970.2004.00257.x>
- Habeck DH (1963) Descriptions of immature stages of the Chinese rose beetle. *Adoretus sinicus* Burmeister (Coleoptera: Scarabaeidae). *Proceedings of the Hawaiian Entomological Society* 18: 251–258.
- Hayes WP (1929) Morphology, taxonomy, and biology of larval Scarabaeoidea. *Illinois Biological Monograph* 12: 1–119. <https://doi.org/10.5962/bhl.title.50108>
- Hongsuwong T, Sanguansub S, Jaitrong WJZ (2022) A new species and a new synonym in the scarab genus *Parastasia* Westwood, 1841 (Coleoptera: Scarabaeidae: Rutelinae), with a key to species from Thailand. *Zootaxa* 5205: 547–562. <https://doi.org/10.11646/zootaxa.5205.6.3>
- Jameson ML (1997) Phylogenetic Analysis of the Subtribe Rutelina and Revision of the *Rutela* Generic Groups (Coleoptera: Scarabaeidae: Rutelinae: Rutelini). Lawrence: University of Kansas.
- Jameson ML, Morón MA (2001) Descriptions of the larvae of *Chlorota cincticollis* Blanchard and *Chasmodia collaris* (Blanchard) (Scarabaeidae: Rutelinae: Rutelini) with a key to the larvae of the American genera of Rutelini. *Coleopterists Bulletin* 55(3): 385–396. [https://doi.org/10.1649/0010-065X\(2001\)055\[0385:DOTLOC\]2.0.CO;2](https://doi.org/10.1649/0010-065X(2001)055[0385:DOTLOC]2.0.CO;2)
- Jameson ML, Ratcliffe BC (2002) Series Scarabaeiformia Crowson 1960 (= Lamellicornia), Superfamily Scarabaeoidea Latreille 1802. In: Arnett RH, Thomas MC, Skelley PE, Frank JH (Eds) *American Beetles*. CRC Press, Boca Raton.

- Jerath ML (1960) Notes on the larvae of nine genera of Aphodiinae in the United States (Coleoptera: Scarabaeidae). *Proceedings of the United States National Museum* 111(3425): 43–94. <https://doi.org/10.5479/si.00963801.111-3425.43>
- Jia Z-C, Lu C, Zhou R-J, Jiang L (2020) Comparative morphology between the white grubs *Pseudosymmachia tumidifrons* and *Brahmina faldermanni* (Coleoptera: Scarabaeidae: Melolonthinae) using scanning electron microscopy. *Zoologischer Anzeiger* 289: 8–17. <https://doi.org/10.1016/j.jcz.2020.08.008>
- Jia Z-C, Fang H, Jiang L (2021) Morphological description of the white grub *Melolontha incana* (Coleoptera: Scarabaeidae: Melolonthinae Melolonthini). *Microscopy Research and Technique* 84(5): 921–928. <https://doi.org/10.1002/jemt.23653>
- Jia Z-C, Dong H, Li Y-T, Zhao X-X, Jiang L (2023) Morphology of a grass-feeding white grub *Apogonia cupreoviridis* (Coleoptera: Scarabaeidae: Melolonthinae: Diplotaxini) using scanning electron microscopy. *Acta Zoologica (Stockholm, Sweden)* 105(2): 225–233. <https://doi.org/10.1111/azo.12460>
- Jiang L, Hua BZ (2015) Morphological comparison of the larvae of *Panorpa obtusa* Cheng and *Neopanorpa lui* Chou & Ran (Mecoptera: Panorpidae). *Zoologischer Anzeiger* 255: 62–70. <https://doi.org/10.1016/j.jcz.2015.02.004>
- Johnson SN, Rasmann S (2015) Root-feeding insects and their interactions with organisms in the rhizosphere. *Annual Review of Entomology* 60(1): 517–535. <https://doi.org/10.1146/annurev-ento-010814-020608>
- Katovich K, Kriska N (2002) Description of the larva of *Nicagus obscurus* (LeConte)(Coleoptera: Lucanidae: Nicaginae), with comments on its position in Lucanidae and notes on the larval and adult habitat. *Coleopterists Bulletin* 56(2): 253–258. [https://doi.org/10.1649/0010-065X\(2002\)056\[0253:DOTLON\]2.0.CO;2](https://doi.org/10.1649/0010-065X(2002)056[0253:DOTLON]2.0.CO;2)
- Kim JI (2014) Insect Fauna of Korea. *Arthropoda: Insecta: Coleoptera: Scarabaeoidea: Pleurosticti*. *The Flora and Fauna of Korea* 12: 1–252.
- Krajčůk M (2007) Checklist of Scarabaeoidea of the world 2. Rutelinae (Coleoptera: Scarabaeidae:Rutelinae) (Animma.X – Supplement 4). Plzen, Czech Republic.
- Lawrence JF, Ślipiński A, Seago AE, Thayer MK, Newton AF, Marvaldi AE (2011) Phylogeny of the Coleoptera based on morphological characters of adults and larvae. *Annales Zoologici* 61(1): 1–217. <https://doi.org/10.3161/000345411X576725>
- Li C, Lu Y, Fang H, Jiang L (2019) Morphology of the third instar larva of *Colobopteris quadratus* (Coleoptera: Scarabaeidae: Aphodiinae) using scanning electron microscopy. *Microscopy Research and Technique* 82(8): 1372–1379. <https://doi.org/10.1002/jemt.23289>
- Lugo-García GA, García AA, Aragón-Sánchez M, Cuate-Mozo VA, Pérez-Torres BC (2023) Description of the larva of *Parachrysinia parapatrica* (Coleoptera: Melolonthidae: Rutelinae: Rutelini) from Puebla, México. *Acta Zoológica Mexicana* 39: 1–6. [nueva serie] <https://doi.org/10.21829/azm.2023.3912620>
- McQuillan PB (1985) The identification of root feeding cockchafer larvae (Coleoptera: Scarabaeidae) found in pastures of Tasmania. *Australian Journal of Zoology* 33(4): 509–546. <https://doi.org/10.1071/ZO9850509>
- Micó E, Galante E (2005) Larval morphology and biology of some European Anomalini (Coleoptera: Scarabaeoidea: Rutelidae: Anomalinae). A phylogenetical approach. *Insect Systematics & Evolution* 36(2): 183–198. <https://doi.org/10.1163/187631205788838519>
- Micó E, Morón MA, Galante E (2003) New larval descriptions and biology of some New World Anomalini beetles (Coleoptera: Scarabaeoidea: Rutelinae). *Annals of the Entomological Society of America* 96(5): 597–614. [https://doi.org/10.1603/0013-8746\(2003\)096\[0597:N-LDABO\]2.0.CO;2](https://doi.org/10.1603/0013-8746(2003)096[0597:N-LDABO]2.0.CO;2)
- Neita-Moreno JC, Morón MA (2017) Description of immature stages of *Platycoelia valida* Burmeister, 1844 (Coleoptera: Melolonthidae: Rutelinae: Anoplognathini). *Revista Brasileira de Entomologia* 61(4): 359–364. <https://doi.org/10.1016/j.rbe.2017.07.002>
- Newton AF (1990) Larvae of Staphyliniformia (Coleoptera): Where do we stand? *Coleopterists Bulletin* 44: 205–210.
- Pardo-Locarno LC, Morón MA, Montoya-Lerma J (2006) Descripción de los estados inmaduros de *Leucothyreus femoratus* Burmeister (Coleoptera: Melolonthidae: Rutelinae: Geniatiini) con notas sobre su biología e importancia agrícola en Colombia. *Folia Entomologica Mexicana* 45: 179–193. <https://doi.org/10.21829/azm.2007.232572>
- Qu Z-F, Jia Z-C, Jiang L (2019) Description of the third instar larva of the stag beetle *Prismognathus dauricus* Motschulsky, 1860 (Coleoptera: Scarabaeoidea: Lucanidae) using electron microscopy. *Micron (Oxford, England)* 120: 10–16. <https://doi.org/10.1016/j.micron.2019.02.001>
- Richards K, Spencer CP (2014) Descriptions and key to the larvae of the Tasmanian endemic genus *Hoplogonus* Parry (Coleoptera: Lucanidae), and comparison with the sympatric *Lissotes rudis* Lea. *Zootaxa* 3884(4): 347–359. <https://doi.org/10.11646/zootaxa.3884.4.4>
- Ritcher PO (1948) Descriptions of the larvae of some ruteline beetles with keys to tribes and species (Scarabaeidae). *Annals of the Entomological Society of America* 41(2): 206–212. <https://doi.org/10.1093/aesa/41.2.206>
- Ritcher PO (1966) *White Grubs and Their Allies: A Study of North American Scarabaeoid Larvae*. Oregon State University Press, Corvallis, Oregon, 220 pp.
- Rodrigues SR, Gomes ES, Morón MA, Fuhrmann J (2017) Description of the third instar and pupa of *Geniates borelli* Camerano and *Anomala testaceipennis* Blanchard (Coleoptera: Scarabaeidae: Rutelinae). *Coleopterists Bulletin* 71(2): 375–388. <https://doi.org/10.1649/0010-065X-71.2.375>
- Sawada H (1991) *Morphological and Phylogenetical Study on the Larvae of Pleurostict Lamellicornia in Japan*. Tokyo University of Agriculture Press, Tokyo, 132 pp.
- Šípek P (2010) *Immature Stages of the Pleurostict Scarab Beetles (Coleoptera: Scarabaeidae: Pleurosticti): Morphology, Biology and Phylogenetic Implication*. Prague: Charles University.
- Šípek P, Ahrens D (2011) Inferring larval taxonomy and morphology in *Maladera* species (Coleoptera: Scarabaeidae: Sericini) using DNA taxonomy tools. *Systematic Entomology* 36(4): 628–643. <https://doi.org/10.1111/j.1365-3113.2011.00582.x>
- Ślipiński A, Lawrence JF (2019) *Australian Beetles Volume 2: Archostemata, Myxophaga, Adepaga, Polyphaga (part)*. CSIRO, Clayton, 769 pp. <https://doi.org/10.1071/9780643097315>
- Sousa R, Fuhrmann J, Kouklík O, Šípek P (2018) Immature stages of three species of *Inca* LePeletier & Serville, 1828 (Coleoptera: Scarabaeidae: Cetoniinae) and morphology of phytophagous scarab beetle pupa. *Zootaxa* 4434(1): 65–88. <https://doi.org/10.11646/zootaxa.4434.1.4>
- Wada K (2015) A new species of the genus *Parastasia* (Coleoptera, Rutelinae) from Northeast India. *Kogane* 17: 87–90.
- Zhang ZL (1984) *Economic Insect Fauna of China, Fascicule 28, Coleoptera: Larvae of Scarabaeoidea*. Science Press, Beijing.
- Zhao M (2019) Notes on the genus *Parastasia* Westwood (Coleoptera: Scarabaeidae: Rutelinae) from China, with description of a new species. *Zootaxa* 4613(2): 240–250. <https://doi.org/10.11646/zootaxa.4613.2.2>

# *Lochetica ramii* sp. nov. – a new species of *Lochetica* Kriechbaumer, 1892 (Hymenoptera, Ichneumonidae, Phygadeuontinae) from Finland, with a key to world species

Juuso Paappanen<sup>1</sup>

<sup>1</sup> *Samoilijantie 3 D 28, 70200 Kuopio, Finland*

<https://zoobank.org/F25F9574-5B1D-4007-8B42-A8C1BD7B6EFF>

Corresponding author: Juuso Paappanen (japaappanen@gmail.com)

Academic editor: D. Zimmermann ♦ Received 22 February 2024 ♦ Accepted 22 May 2024 ♦ Published 18 July 2024

## Abstract

Two tentatively distinct morphological forms belonging to the Darwin wasp genus *Lochetica* Kriechbaumer, 1892 (Hymenoptera, Ichneumonidae) were found to occur in Finland, although only one species is known in Europe. The identity of the two forms were resolved by examining additional museum material, DNA barcoding and revising the relevant types. Both morphology and molecular results support the recognition of a new species, *Lochetica ramii* sp. nov., from Finnish specimens – in addition to *Lochetica westoni* (Bridgman, 1880) already known from Finland. New host associations are given for both species and their ecology is discussed. An identification key is given to the known species of *Lochetica* of the world to facilitate the recognition of the new species.

## Key Words

Parasitoid wasps, Phygadeuontinae, north Europe, Palearctic, saproxylic, identification, key

## Introduction

The Darwin wasp genus *Lochetica* Kriechbaumer, 1892 is a species-poor genus within the megadiverse Ichneumonidae, comprising only four species, all occurring in the Holarctic Region (Yu et al. 2012; Watanabe 2021). Information regarding the life history of the genus *Lochetica* only accounts for one species, *Lochetica westoni* (Bridgman, 1880), which has been associated with the crabronid genus *Passaloecus* Shuckard, 1837 (Barbey and Ferriere 1923; Jonaitis 1981; Kreisch 2000), which nest in above-ground structures such as beetle burrowings in (dead) wood, galls and plant stems (e.g. Blösch (2000)).

For the greater part of the 20<sup>th</sup> century, two species of *Lochetica* have been known: *L. westoni* (Bridgman, 1880) and *Lochetica pimplaria* (Thomson, 1888), until Horstmann (1972) established the synonymy between the two

species. The initial placement of *L. westoni* in a separate genus (*Cecidonomus* Bridgman, 1880) likely maintained their separation for such a long period. Townes (1983) revised the genus and provided the first identification key to the genus describing two new species: *Lochetica farta* from Taiwan and *Lochetica agonia* from the western United States. Watanabe (2021) described *Lochetica japonica* from Japan, which increased the number of species to four. All species, except for *L. westoni*, are known by only a few specimens.

Two tentatively distinct morphological forms of *Lochetica* were recognised to occur in Finland. This prompted the present study with the aim to resolve their identities. Subsequently, a new species of *Lochetica* is here described from Finnish specimens and an identification key for all five known species of *Lochetica* is provided. New host associations are given and the ecology of the genus is discussed.

## Methods

### Specimen data and depositories

The studied material comprises 88 specimens of *Lochetica*, which are deposited in the following collections (later referred by the given abbreviations):

<b>MZH</b>	Natural History Museum, Helsinki, Finland.
<b>MZLU</b>	Lund University Biological Museum, Lund, Sweden.
<b>NCM</b>	Norwich Castle Museum, Norwich, United Kingdom.
<b>KPM-NK</b>	Kanagawa Prefectural Museum of Natural History, Odawara, Kanagawa, Japan.
<b>RJK</b>	Secondary collection of Reijo Jussila, Kuhmo, Finland.

All specimens have been given ID labels by the associated museum. This facilitates later revision of the specimens mentioned in this article. In addition, all but three specimens are deposited in public museums.

### Morphology

Morphological terms follow Broad et al. (2018). The following abbreviations are used in the text:

<b>Tergite</b>	Metasomal tergite.
<b>Temple ratio</b>	The width of the temples, in dorsal view, measured halfway between the posterior ocelli and the occipital carina, divided by the maximum width of the head (in dorsal view).
<b>Ovi-tib ratio</b>	The length of the ovipositor projecting beyond the apex of the metasoma (in <i>Lochetica</i> , equal to the length of the ovipositor sheaths) divided by the length of the hind tibia (measured in outer lateral view).
<b>POL:OOL</b>	The distance between the lateral ocelli divided by the distance between a lateral ocellus and the compound eye.
<b>OD:OOL</b>	The diameter of the lateral ocellus divided by the distance between the lateral ocellus and the compound eye.

The specimens were examined with a common main objective type Olympus SZX16 stereo-microscope with a plan apochromatic objective, using magnifications 7×–115×. Measurements were done with an ocular micrometer, with one eye closed. The length of the body is usually impossible to measure since the body is rarely straight. The fore-wing length has been widely used as a proxy for body size. Here both measures are reported; however, the body length is not an absolute measurement of the specimen, but partly an evaluation on how long the specimen would be if straightened. This is not the ideal method, but

was favoured instead of taking an absolute measurement of the specimen regardless of its posture.

Temple ratio and ovi-tib ratio were statistically compared between the species with the Welch t-test. These analyses, as well as the graphs, were done in R (v. 4.3.2) via the RStudio (v. 12.0-369) software. The package stats (v. 4.3.2) was used to perform the t-tests, the package effsize (0.8.1) was used to calculate the effect sizes and the package beeswarm (0.4.0) was used to produce the graphs.

All morphological examinations, measurements and identifications were done by the author in 2023. Photographs of the types of the *Cecidonomus westoni*, *Phygadeuon pimplarius* and *L. japonica* were examined.

### Photographs

Figs 3, 6, 7 are focus stacks, composed of dozens of individual photographs, taken by the author with the Olympus OM-5 camera with an extended and reversed Schneider Kreuznach Componon S 50mm F/2.8 lens, using the in-camera pixel shift technology (tripod high-res mode). Individual photographs were stacked with the CombineZP (v. 1.0) software using the Quick Align and Do Stack –macros. The photographs of type material deposited in collections other than the MZH, have been taken with various equipment by the corresponding curators.

### Molecular methods

Ten specimens of *Lochetica* were sequenced for the cytochrome oxidase subunit I (COI) marker (the standard barcode region *sensu* Hebert et al. (2003)). The tissue sample used for DNA extraction was a single leg, in most cases one of the middle pair, of each specimen. DNA extraction, PCR and sequencing were carried out by the Canadian Centre for DNA Barcoding, according to the prescribed protocols described in deWaard et al. (2008). The forward primer LepF1 (ATTCAACCAATCATAAAGATATTGG) and the reverse primer LepR1 (TAAACTTCTGGATGTCCAAAAAATCA) were used to amplify the selected marker. The Sanger sequencing protocol was used to obtain the sequence.

In addition to these ten sequences, all public COI sequences assorted to BINs with at least one specimen identified as *Lochetica* were downloaded from the BOLD database (downloaded 26 Nov 2023). These included only three sequences, all from Norwegian specimens.

The resulting combined data of thirteen sequences were aligned with the MUSCLE algorithm (Edgar 2004) within the MEGA XI software (Tamura et al. 2021). The following (default) settings were selected for the alignment, cluster method: UPGMA, gap open penalty: -400, gap extend penalty: 0, min. diag. length (lambda): 24. The alignment was manually examined; however, no further changes were made to the alignment, for example, no sites were removed.

A distance matrix (p-distances) was calculated in R (v. 4.3.2) via the RStudio software (v. 12.0-369), with the package ape (v. 5.7-1). Sites with missing data were de-

leted in pairwise calculations. The resulting matrix was transferred to Microsoft Excel 2013 (v. 15.0.5153.1000), where the distance measures were obtained. The matrix was also used to create a Neighbour-Joining tree with the same package (ape) in R.

## Data sharing

Full data used in this study are available as Suppl. material 1: a spreadsheet file with specimen and morphological data, Suppl. material 2: R script (a simple text file) containing the code to produce the statistical analyses and graphs and Suppl. material 3: aligned sequences in fasta format. The sequences and their associated accession numbers are also available at the GenBank and the BOLD database via the doi: [dx.doi.org/10.5883/DS-LOCH24](https://doi.org/10.5883/DS-LOCH24)

## Results

### Morphological comparison

Comparing the mean ovi-tib ratio between *L. westoni* and *L. ramii* sp. nov. (Fig. 1A) using the Welch t-test, the ratio is larger in *L. westoni* (mean 2.8) than in *L. ramii* sp. nov. (mean 2.1) ( $t = -22.8$ ,  $DF = 71.8$ ,  $p < 0.001$ ; Cohen's

$d = -5.3$ ). There are no overlapping specimens with regards to this character, although the gap is rather small: max. for *L. ramii* sp. nov. is 2.4 and min. for *L. westoni* is 2.6). The *L. japonica* specimens overlap with *L. ramii* sp. nov., but not with *L. westoni*. The ovi-tib ratio of *L. japonica* was not statistically compared to other species due to its small sample size.

Comparing the mean temple ratio between *L. westoni* and *L. ramii* sp. nov. (Fig. 1B) using the Welch t-test, the ratio is larger in *L. ramii* sp. nov. (mean 0.95) than in *L. westoni* (mean 0.88) ( $t = 9.7$ ,  $DF = 64.6$ ,  $p < 0.001$ ; Cohen's  $d = 2.3$ ). There are numerous overlapping specimens with regards to this character (Fig. 1B).

### COI comparison

All specimens yielded long sequences, varying in length from 621 bp to 658 bp. The COI sequences of seven specimens of *L. ramii* sp. nov. and six specimens of *L. westoni* were compared. No sequences for the other three species of *Lochetica* are available. The interspecific distances between the two species range from 7.12% to 8.05%, while the intraspecific distances within the specimens of *L. ramii* sp. nov. and *L. westoni* are 0.00–0.16% and 0.00–0.61%, respectively. The barcode gap is distinct (Fig 2).

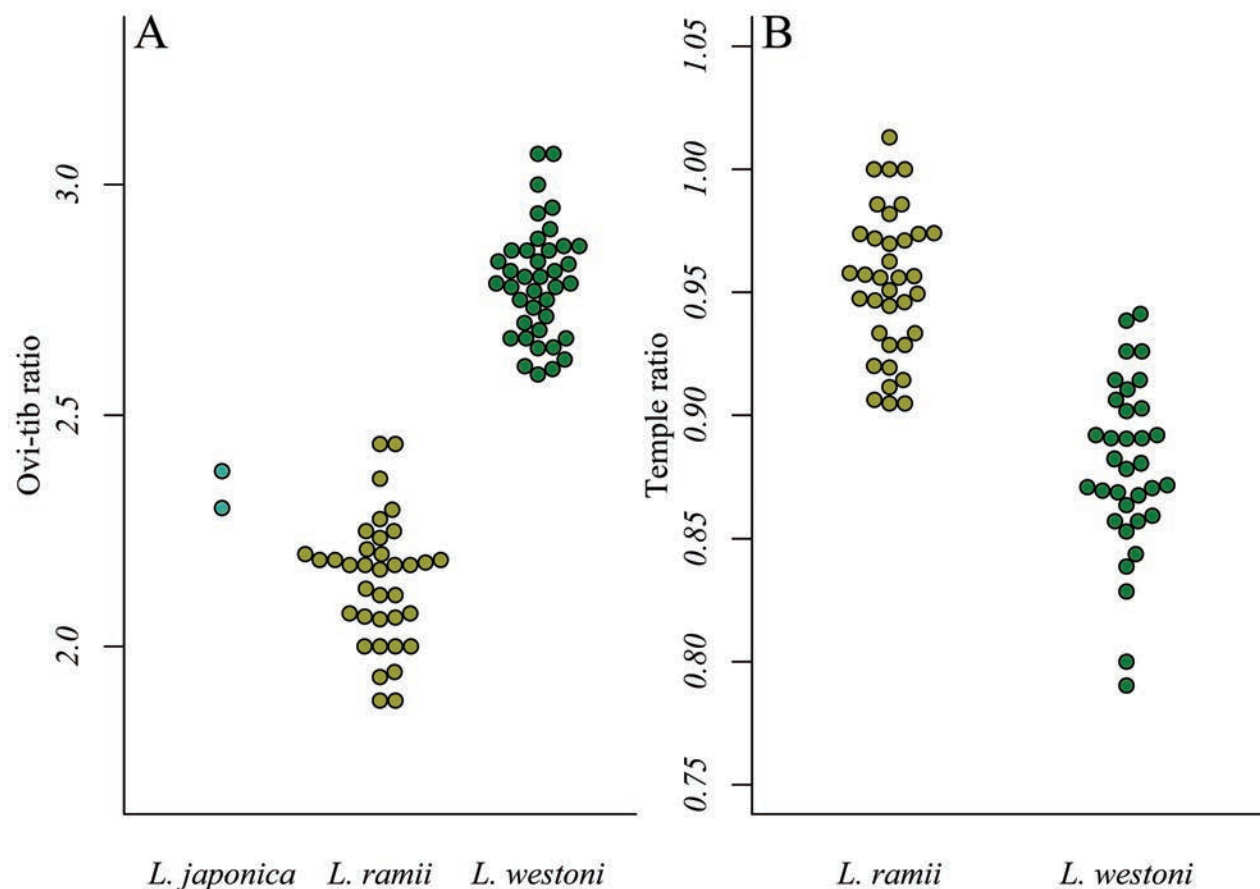


**Figure 1.** Swarmplots comparing the selected morphological ratios of examined females. **A.** Comparison of the relative length of the ovipositor. The data on *Lochetica japonica* Watanabe, 2021 is derived from the original description; **B.** Comparison of the temple ratio (see the Methods section for definition). Each point represents one specimen, the points are moved horizontally to avoid overlap.

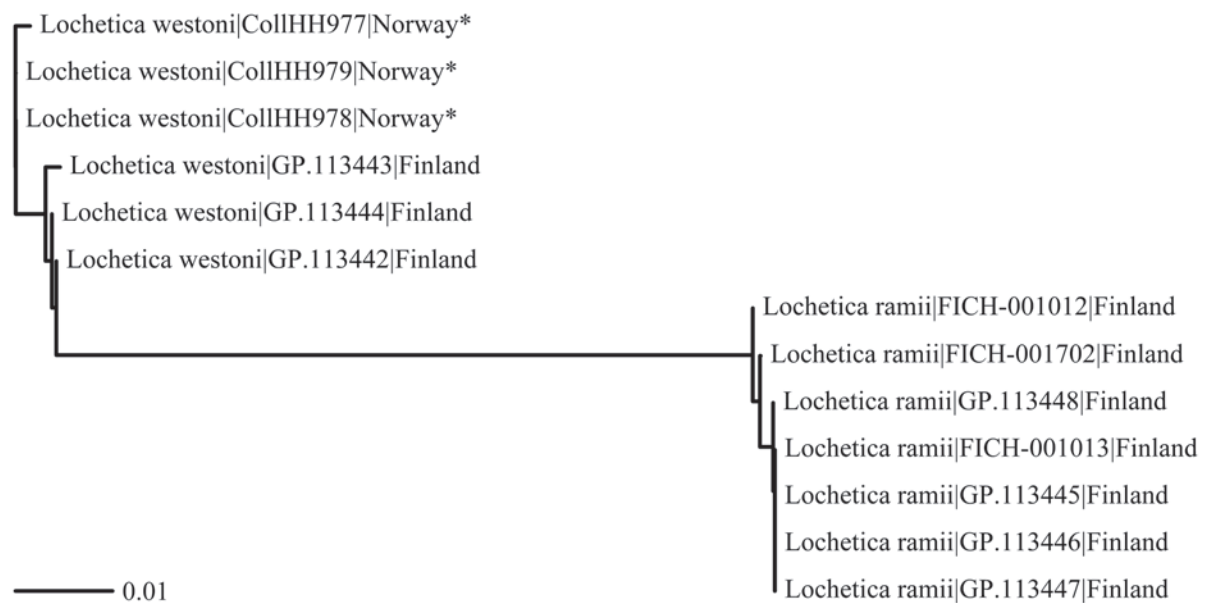


**Figure 2.** A simple Neighbour-Joining phylogenetic tree (p-distance) illustrating the barcode gap between the specimens. The scale bar represents 1% divergence. The ID after the species name refers to the sample ID in the BOLD-database (same as the museum (specimen) ID in Finnish material). The specimens marked with an asterisk (\*) have not been examined.

## Systematics

### Genus *Lochetica* Kriechbaumer, 1892

*Lochetica* Kriechbaumer, 1892: 340.

**Type species.** *Phygadeuon pimplarius* Thomson, 1888. Monotypic.

**Diagnosis.** Dense punctation and hairs across the body surface. The clypeus wide, weakly separated from the face, anterior edge of clypeus and mandibles covered with very dense short hairs. Temples rather wide. Sternaulus long. Propodeum with complete carination and pentagonal area superomedia. Spiracles of first tergite near the middle. The fore wing with a closed areolet, vein 3rs-m is weakly pigmented; vein 2m-cu long, straight, forming acute angle with vein CU, with one short bulla.

### *Lochetica westoni westoni* (Bridgman, 1880)

Figs 3, 4

*Cecidonomus Westoni* Bridgman, 1880: 264. Lectotype designated by Horstmann (1972).

*Phygadeuon pimplarius* Thomson, 1884: 941. Lectotype designation of Townes published by Frilli (1973).

**Material examined.** *Lectotype* of *Cecidonomus westoni* Bridgman, 1880 (photographs examined) UNITED KINGDOM (presumably) • 1 ♀; “from Mr. Weston”; “*Westoni*”; “*lektotypus Cecidonomus westoni* ♀ Bridgm. Horstm. det. 1970”; “J. B. Bridgman coll. Norwich Museum 1895.40.1124”.

**Lectotype** of *Phygadeuon pimplarius* Thomson 1884 (photographs examined) SWEDEN • 1 ♀; “Öke å” [Skåne, Sjöbo, Övedskloster]; [55.684°N, 13.633°E]; “*Lectotypus Phygadeuon pimplarius* Thm. Tow. 58”; MZLU 5385:1.

**Other material.** FINLAND • 38 ♀♀, 5 ♂♂ [MZH]. RUSSIA • 2 ♀♀ [MZH].

**Diagnosis.** The female is distinguished by the long epomia (Fig. 3A), long ovipositor (ovi-tib ratio 2.6–3.1 in examined specimens) (Fig. 4E), almost completely red legs (Fig. 4E), yellow tegulae (Fig. 3F), narrow temples (temple ratio 0.80 to 0.95 in examined material) and strong latero-median carinae of the first tergite (Fig. 3E). The male is distinguished by the yellow tegulae, medially white mandibles, long epomia and, to some extent, the strongly rugose sculpture of mesopleuron and metapleuron (Fig. 3C).

The extent of the red colouration on the metasoma in females varies considerably. In the Finnish specimens, usually only the first tergite is laterally slightly reddish; however, some specimens have extensively red first and second terga. A subspecies *Lochetica westoni rufiventris* Habermehl, 1919 from Algeria (not examined) has the metasoma completely red.

**Distribution.** Most European countries, Turkey, Algeria, Japan (Yu et al. 2012), Russia (Jonaitis 1981) and Georgia (Riedel et al. 2018).

**Ecology.** Both open and forested habitats are used, especially sites with dead wood or other suitable nesting sites for hosts.

The type series has been reared from “galls” (Bridgman 1880), which Morley (1907) later states were the galls of *Cynips Kollari* (= *Andricus kollari* (Hartig,

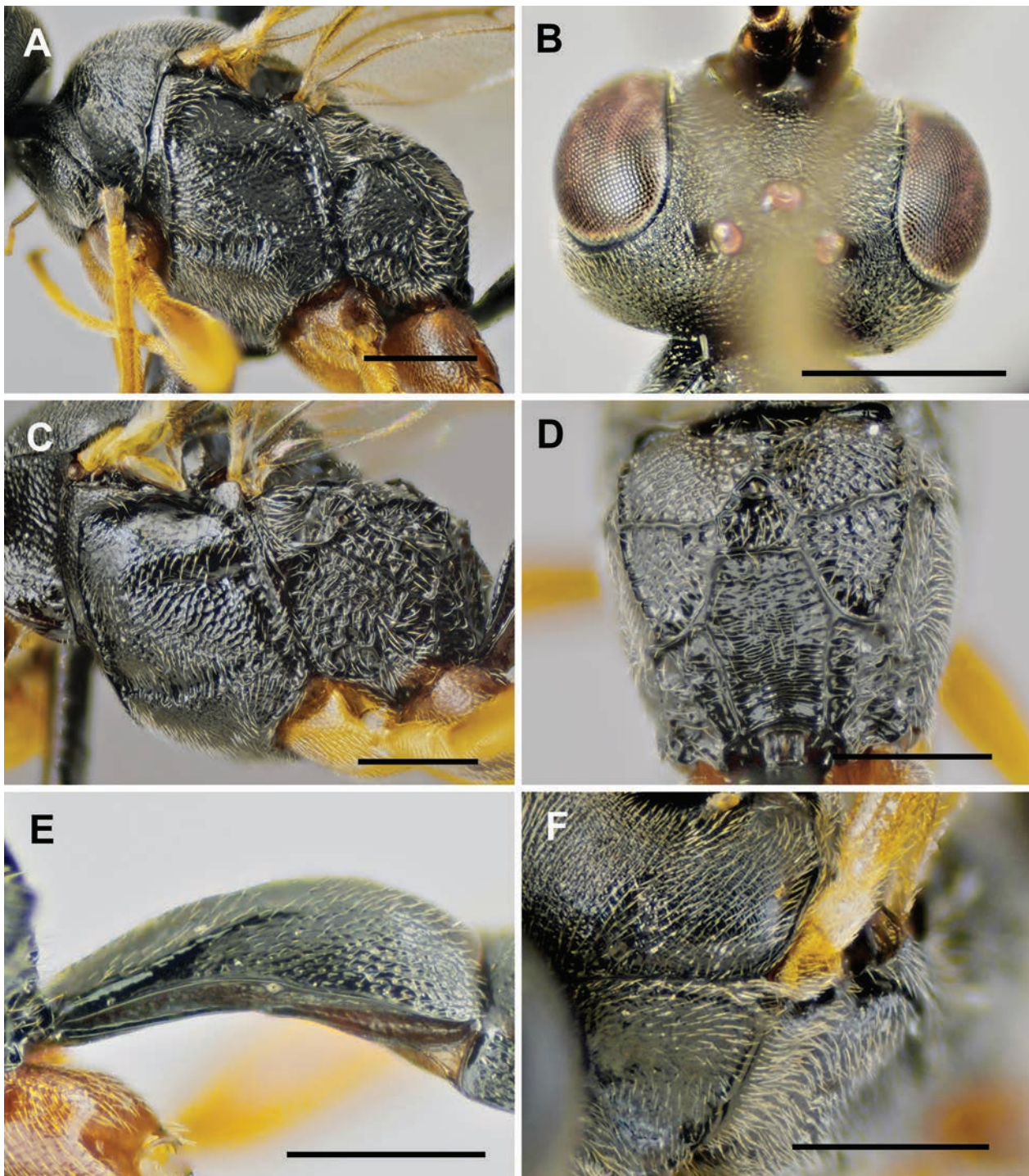


**Figure 3.** *Lochetica westoni* (Bridgman, 1880), a non-type specimen MZH GP.113444 (except for C). **A.** Mesosoma of the ♀ (lateral view); **B.** Head of the ♀ (dorsal view); **C.** Mesopleuron and metapleuron of the non-type ♂ MZH GP.109783 (lateral view); **D.** Propodeum of the ♀ (oblique posterior view); **E.** The first tergite of the ♀ (lateral view); **F.** Tegula of the ♀ (oblique anterolateral view). Scale bars: 0.5 mm.

1843)). *Passaloecus gracilis* (Curtis, 1834) have been recorded to nest in galls of *A. kollari* (Lomholdt 1975). Barbey and Ferriere (1923) reared *L. westoni* from the nests of *Passaloecus gracilis* inside empty beetle burrowings in the bark of *Pinus sylvestris* L. They also state that *L. westoni* overwinters as a larva in a silky cocoon and postulated that the female must oviposit

to the host while the nest is still under construction, since the ovipositor is not long enough to reach the host larvae behind the outer resin plug that encloses the nest. Jonaitis (1981) also reported *Passaloecus gracilis* nesting inside branches as a host and Kreisch (2000) reported the host *Passaloecus insignis* (Vander Linden, 1829).

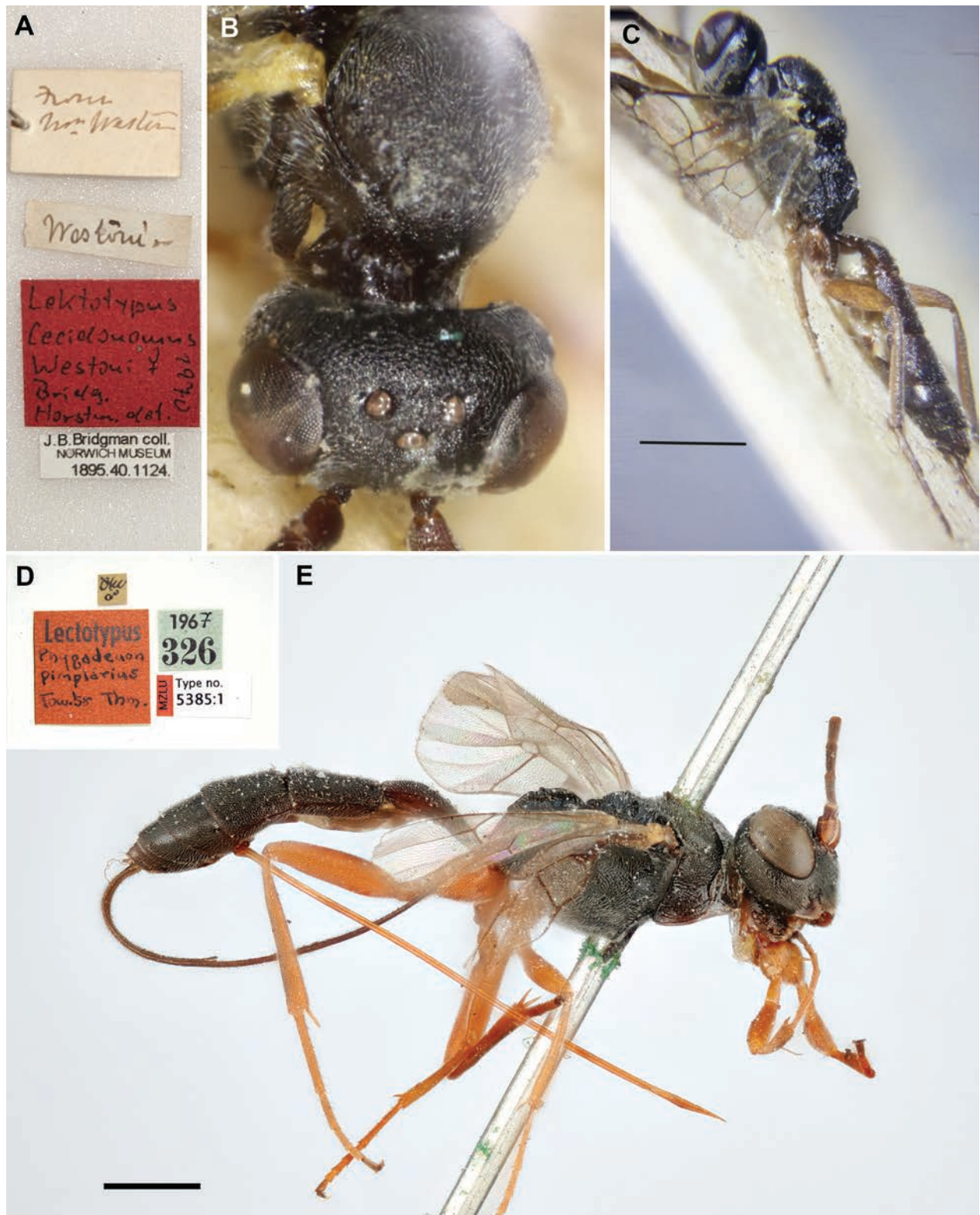


**Figure 4.** A–C. The Lectotype of *Cecidonomus westoni* Bridgman, 1880. Photo credit: Tony Irwin. **A.** Labels; **B.** Head and part of the mesosoma (dorsal view); **C.** Habitus (lateral view); **D–E.** Lectotype of *Phygadeuon pimplarius* Thomson, 1884. Photo credit: Biological Museum, Lund University (MZLU); **D.** Labels; **E.** Habitus (lateral view). Scale bars: 1 mm.

New rearing records published in this study are the following: a male reared from *Passaloecus monilicornis* Dahlbom, 1842 (MZH GP.109784), a female reared from *Passaloecus eremita* Kohl, 1893 (MZH GP.109755) and

a male reared from *Passaloecus borealis* Dahlbom, 1844 (MZH GP.109783). In all cases, no additional information how the host was confirmed were given and no host remains or cocoon were included in the pin. Furthermore,

*P. borealis* is extremely difficult to separate from *Passaloecus turionum*; thus, the record could refer to either of the two species. In addition, one specimen was reared from an unidentified *Passaloecus* larva inside an artificial nest (an *Angelica* L. stem) on the wall of a building (MZH GP.109758).

In conclusion, *L. westoni* utilises most species of the genus *Passaloecus* (recorded from *P. gracilis*, *P. monilicornis*, *P. insignis*, *P. eremita*, *P. borealis/turionum* and *Passaloecus* sp.) nesting in (dead) wood (including buildings and other structures), galls and most likely also plant stems.

### *Lochetica westoni rufiventris* Habermehl, 1919

*Lochetica pimplaria* f. *rufiventris* Habermehl, 1919: 110. Lectotype designated by Horstmann (1991).

**Remarks.** This taxon is known from Algeria and, according to Horstmann (1991), it is distinguished from *L. w. westoni* only by its completely red metasoma. Horstmann considered it a subspecies and, since I have not examined the type or any material from the Mediterranean, his view of the taxon is followed here.

### *Lochetica japonica* Watanabe, 2021

Fig. 5

*Lochetica japonica* Watanabe, 2021: 110, figs 47A–H, fig. 62J, fig 65Q, fig. 66Q.

**Material examined. Holotype** (photographs examined) JAPAN • 1 ♀; Tochigi Pref., Nasushiobara City, Shiobara, Utou-sawa; 22–28 May 2008; T. Matsumura leg.; Malaise-trap; KPM-NK 81989.

**Diagnosis.** The female is distinguished by the long epomia (cf. Fig. 3A), weak latero-median carinae of the first tergite, clearly defined punctation of the body (especially the vertex (Fig. 5E) and the area externa of the propodeum (Fig. 5B)), pronotum with transverse crenulae, wide (developed) temples (Fig. 5E), a shallow transverse depression followed by a low elevation on the vertex (Fig. 5E), almost completely black legs (Fig. 5D) and mandibles (Fig. 5A). The male is unknown.

**Distribution.** Japan (Watanabe 2021).

**Ecology.** Unknown.

### *Lochetica ramii* sp. nov.

<https://zoobank.org/8354C52C-6202-4BA2-B8C0-94EC47B97A50>

Figs 6, 7

**Material examined. Holotype** FINLAND • 1 ♀ (pinned); Sb [Savonia borealis], Kuopio, Mökinoja; “6966126:3529339” [62.7976°N, 27.575°E]; 18 Jun 2021; Juuso Paappanen leg.; “niitty, hirsirakennuksen

seinä” [meadow, on a wall of a log barn]; COI sequence GP.113446; MZH GP.113446.

**Paratypes** (37 ♀♀, 1 ♂) FINLAND • 1 ♀; “Finby” [Särkisalo], [Finnarv, Vedudden]; [60.1143°N, 22.9485°E]; 14 Jul 1950; R. Elfving leg.; MZH GP.109724 • 4 ♀; “Keuruu” [Keuruu]; [62.257°N, 24.708°E]; [1928]; Hellén leg.; MZH GP.109731, MZH GP.109732, MZH GP.109733, MZH GP.109779 • 1 ♀; Aitolahti; [61.5481°N, 23.8825°E]; 13 Jul 1932; V. Saarinen leg.; MZH GP.109725 • 1 ♀; “H:fors” [Helsinki]; [60.1797°N, 24.9393°E]; Hellén leg.; MZH GP.109734 • 1 ♀; Helsinki; [60.1797°N, 24.9393°E]; 11 Sep 1965; V. J. Karvonen leg.; MZH GP.109727 • 1 ♀; Ilomantsi, Koitajoki; 62.93310°N, 31.43978°E; 18 Jun–8 Aug 2023; Juuso Paappanen leg.; ~ 2 years ago dead standing *Picea abies*; [Tereshkin trap]; MZH GQ.7565 • 7 ♀; Ilomantsi, Koitajoki; 62.93390°N, 31.44084°E; 18 Jun.–8 Aug. 2023; Juuso Paappanen leg.; dying ø 39 cm standing *Picea abies*; [Tereshkin trap]; MZH GQ.7566, MZH GQ.7567, MZH GQ.7568, MZH GQ.7569, MZH GQ.7570, MZH GQ.7571, MZH GQ.7572 • 1 ♀; Karjalohja; [60.2609°N, 23.7138°E]; 25 Jul 1969; J. Perkiömäki leg.; MZH GP.109729 • 1 ♀; Kb [Karelia borealis], Ilomantsi, Koitajoki, Palokangas; 6989825:3724830 [62.9419°N, 31.4305°E]; 13 Jun–11 Jul 2022; Seppo Karjalainen & Maarit Similä leg.; [prescribed burn of a *Pinus sylvestris* dominated forest]; MZH GP.109742 • 1 ♀; Kb [Karelia borealis], Ilomantsi, Patvinsuon kansallispuisto, Raanisuo; 7003901:3694317 [63.0855°N, 30.8475°E]; 11 Jul–17 Aug 2022; Seppo Karjalainen & Maarit Similä leg.; COI sequence BOLD sample id GP.113447; MZH GP.113447 • 1 ♀; Kb [Karelia borealis], Joensuu, Kuhasalo; 62.58126°N, 29.73376°E; 14 Aug 2017; Juuso Paappanen leg.; [*Picea abies* dominated forest]; MZH GP.109738 • 1 ♀; Kb [Karelia borealis], Lieksa, Kuikkasuo; 7034335:3673955 [63.3683°N, 30.4779°E]; 18 Aug–17 Sep 2021; Sampsa Malmberg & Maarit Similä leg.; [prescribed burn of a *Pinus sylvestris* dominated forest]; MZH GP.109743 • 1 ♂; Kn [Ostrobothnia kajanensis], Ristijärvi, pappilan peltoaukea; 71571:35582 [64.5074°N, 28.2125°E]; em. 30 Apr. 2008; Reima Leinonen leg.; koivupölkkykasvatus [reared from trap nest (birch wood block)]; COI sequence BOLD sample id FICH-001702; RJK FICH-001702 • 1 ♀; Ok [Ostrobothnia kajanensis], Kuhmo, Elimyssalo, Risulampi; 7122708:3660871 [64.1659°N, 30.3083°E]; 29 Jul–26 Aug 2022; Sampsa Malmberg et al. leg.; [prescribed burn of a *Pinus sylvestris* dominated forest]; COI sequence BOLD sample id GP.113448; MZH GP.113448 • 1 ♀; Ok [Ostrobothnia kajanensis], Paltamo, Itkonpuro; 7147421:526944 [64.45127°N, 27.55991°E]; 9 Jul–27 Jul 2023; I. Immonen & M. Laaksonen leg.; [moist/shaded forest next to a stream]; MZH GQ.7563 • 1 ♀; Ok [Ostrobothnia kajanensis], Talaskangas, Sopenjoki; 7098580:503358 [64.01405°N, 27.06866°E]; 22 Jul–6 Aug 2021; I. Immonen leg.; [moist/shaded forest next to a stream]; MZH GQ.7564 • 1 ♀; Parikkala, [Laurila]; [61.56718°N, 29.51232°E]; 12 Jul 1945; Hellén leg.; MZH GP.109726 • 1 ♀; Sa [Savonia australis], Mäntyharju,



**Figure 5.** The holotype of *Lochetica japonica* Watanabe, 2021. Photo credits: Kyohei Watanabe. **A.** Head (oblique anteroventral view); **B.** Propodeum (oblique posterodorsal view); **C.** Labels; **D.** Habitus (lateral view); **E.** Head and mesoscutum (dorsal view).

Kousa; 68022:34674 [61.327°N, 26.3922°E]; 23 Aug 2019; Juuso Paappanen leg.; *Pinus sylvestris* dominated forest; MZH GP.109741 • 1 ♀; Sa [Savonia australis], Ruokolahti, [Inkilänsaari]; [61.32062°N, 28.75517°E]; 26 Jul 1948; W. Hellén leg.; MZH GP.109735 • 1 ♀; Sb [Savonia borealis], Savonranta; 69077:6026 [62.261°N, 28.9761°E]; 13 Jul–10 Aug 1996; P. Martikainen leg.; dead aspen; Window trap; MZH GP.109730 • 1 ♀; Sb [Savonia borealis], Vieremä, Luvejoki; 63.98762°N, 26.74378°E; 21 Jul–17 Aug 2022; Juuso Paappanen leg.; a large, ~ 2 years ago dead standing *Picea abies* (shaded); MZH GP.109739 • 1 ♀; Ta [Tavastia australis], Vanaja; [60.978°N, 24.562°E]; 1954; Erkki Valkeila leg.; e *Pas-*

*saloeus monilicornis*; MZH GP.109736 • 2 ♀; same as preceding; 1955; MZH GP.109737, MZH GP.109780 • 1 ♀; Tb [Tavastia borealis], Jyväskylä, Kotalamminmäki; 69028:34311 [62.2248°N, 25.6763°E]; 4 Jul 2019; Juuso Paappanen leg.; dying *Picea abies*; COI sequence BOLD sample id GP:113445; MZH GP:113445 • 1 ♀; Tb [Tavastia borealis], Jyväskylä, Roninmäki; 69014:34326 [62.2125°N, 25.7056°E]; 5 Jul–18. Jul 2019; Juuso Paappanen leg.; recently dead standing *Picea abies*; MZH GP.109740 • 1 ♀; V [Regio aboënsis], Nousiainen, Tepastus; 6735:344 [60.6991°N, 24.1525°E]; 4 Jul–8 Jul 2006; Reijo Jussila leg.; RJK FICH-001012 • 1 ♀; V [Regio aboënsis], Turku, Paattinen; 6727:244 [60.5763°N,

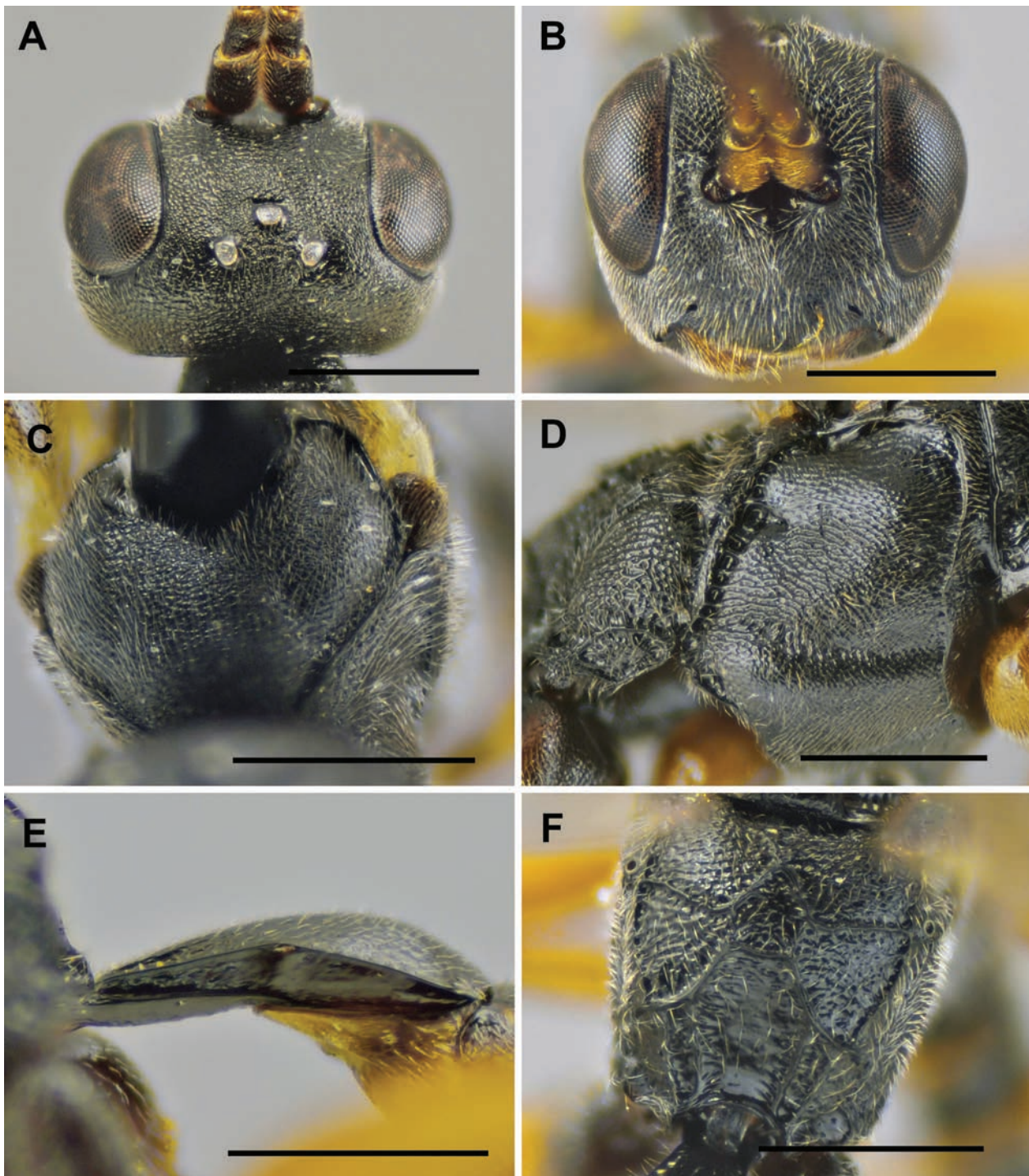


**Figure 6.** *Lochetica ramii* sp. nov. holotype ♀ (except for D). **A.** Head (dorsal view); **B.** Head (anterior view); **C.** Mesoscutum and tegulae (dorsal view); **D.** Mesopleuron of the paratype ♀ MZH GP.113447 (lateral view); **E.** The first tergite; **F.** The propodeum (posterodorsal view). Scale bars: 0.5 mm.

22.3374°E]; 29 Oct 2006; Reijo Jussila leg.; RJK FICH-001013 • 1 ♀; Vihti, Siikajärvi; [60.2882°N, 24.5214°E]; 22 Aug 1965; V. J. Karvonen leg.; MZH GP.109728.

**Comparative diagnosis.** The female differs from *L. japonica* by the vertex uniformly sloping from the ocelli to the occiput, with shallow, almost granulate sculpture (Fig. 6A) (with a shallow transversely orientated depression, low elevation and large, rather deep punctures in *L. japonica* (Fig. 5E)); shallow, transversely

orientated surface sculpture of area externa of propodeum, punctures very weakly discernible (Fig. 6F) (clearly defined deep punctures in *L. japonica* (Fig. 5B)); the pronotal sulcus without transverse crenulae (present in *L. japonica*); predominantly red legs (almost completely black in *L. japonica*); black or dark brown tegulae (Fig. 6C) (yellowish-brown in *L. japonica* (Fig. 5E)); predominantly red mandibles (black with reddish tips in *L. japonica*).

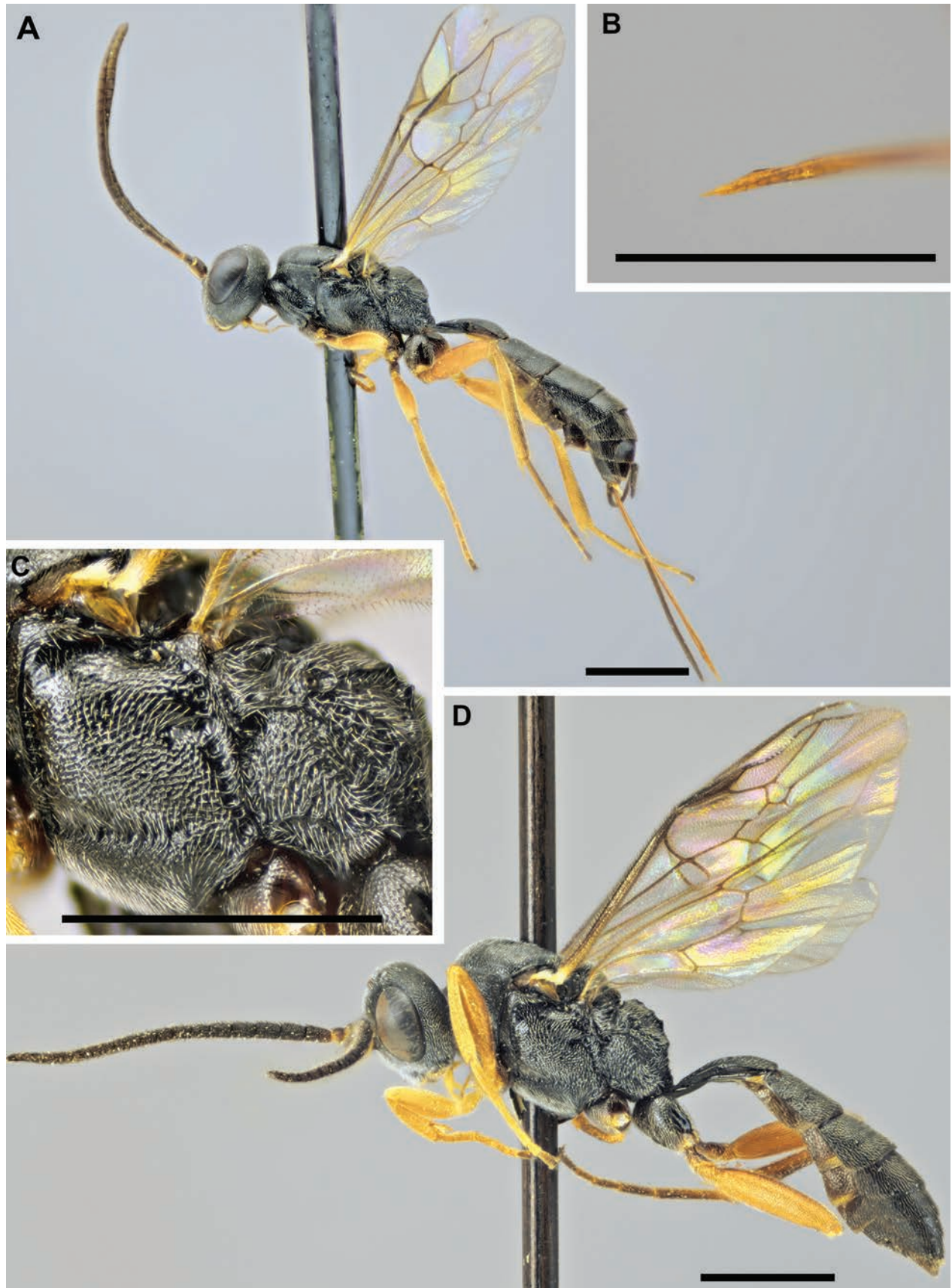


**Figure 7.** *Lochetica ramii* sp. nov. **A.** Holotype ♀ habitus (lateral view); **B.** Tip of the ovipositor of the holotype ♀ (lateral view); **C.** Mesopleuron and metapleuron of the ♂ paratype RJK FICH-001702 (lateral view); **D.** Paratype ♂ habitus RJK FICH-001702 (lateral view). Scale bars: 1 mm.

The female differs from *L. westoni* by the short and weak latero-median carinae of the first tergite, not extending beyond the level of spiracles (Fig. 6E) (strong carinae, extending beyond spiracles in *L. westoni* (Fig. 3E)); shorter and weaker crenulae of the sternaulus (Fig. 6D) (longer and stronger in *L. westoni* Fig. 3A); shorter ovipositor (ovi-tib ratio 1.9–2.4) (2.6–3.1 in *L. westoni*); black or dark brown tegulae (Fig. 6C) (yellow in *L. westoni* (Fig. 3F)). The male differs from *L. westoni* primarily by the black tegulae, contrasting with the pale yellow humeral plates (Fig. 7D, cf. Fig. 6C) (yellow tegulae, similarly coloured to the humeral plates in *L. westoni* (cf. Fig. 3F)). The sculpture of the mesopleuron and metapleuron is somewhat weaker (Fig. 7C) (stronger in *L. westoni* (Fig. 3C)). The trochanters and hind tarsi dorsally darker in *L. ramii* sp. nov.; however, both of the latter characters are rather subtle and possibly become obsolete when more specimens are revealed.

Both sexes are differentiated from *L. agonia* by the long epomia ventrad to pronotal sulcus (cf. Fig. 3A) (absent or short in *L. agonia*) and by the black or dark brown tegulae (Fig. 6C) (yellow (♀) or “ivory” (♂) in *L. agonia*). The females are also distinguished by the weak, but angulate nodus of the ovipositor (Fig. 7B) (very weak and rounded in *L. agonia*).

Female is differentiated from *L. farta* by the area petiolaris of the propodeum having rather weak transverse sculpture concentrated to the sides, usually without sculpture medially (Fig. 6F) (the area petiolaris with very dense transverse sculpture in *L. farta*); strong latero-median longitudinal carina separating the area postero-externa from the area petiolaris (weak in *L. farta*).

**Description. Female** (holotype and paratypes). **Length.** Body length 5.6 mm (4.6–6.3 mm (n = 36)) excluding the ovipositor, fore wing length 3.6 mm (3.2–4.3 mm (n = 37)).

**Head.** Punctuation dense, shallow, individual punctures indistinctly delimited, coalescing, vertex more granulate than punctate (Fig. 6A). Surface moderately matt, covered in dense, short (shorter than diameter of ocellus), white hairs, except clypeus with slightly longer, light brown hairs; hairs very dense on anterior edge of clypeus and mandibles (Fig. 6B); antennae, including scapes, with short hairs only. First flagellar segment without plate sensillae, second with one, remaining with gradually increasing number, being almost absent from posterior side of flagellum. Eyes bare. Occipital carina complete, joining hypostomal carina 0.6× basal length of mandible away from mandibular base. Malar space 0.8× as long as the basal width of mandible. Face very wide, with low central prominence (Fig. 6B). In anterior view, head 0.9× wider than high; in dorsal view, the medial length of head from occipital carina to level of antennal sockets 0.5× maximum width of the head; temple ratio 0.95 (paratypes: 0.9–1.0), POL:OOL 1.1, OD:OOL 0.5 (see Methods section for definitions). Both antennae with 20 flagellar segments (paratypes (n = 35): 20–23), all segments more

than 1.5× longer than wide, decreasing in length towards apex. Width of segments fairly uniform across length of flagellum, increasing only very slightly apically. First flagellar segment 5× as long as wide and 1.3× longer than scape. Scape 1.7× as long as wide. Penultimate (next to last) flagellar segment 1.5× as long as wide. Head predominantly black, mandibles medially red with proximal fourth and teeth black (paratypes: from completely red with only teeth black to about basal third of mandibles black). Maxillary and labial palpi light brown, gradually darker proximally. Anterior side of scapes red (paratypes: from predominantly black with red patches anteriorly to predominantly red with dark spot posteriorly). Anterior side of two proximal flagellar segments red (paratypes: 0 to 4 basal-most segments with red anterior faces). Pedicel with narrow red apical annulus.

**Mesosoma.** Mesoscutum and scutellum moderately densely and shallowly punctate, similarly to head. Notauli not crenulate, weakly impressed, but long, extending to middle of mesoscutum. Posterior half of mesoscutum obscured by pin in the holotype. Scuto-scutellar groove smooth, without crenulae. Pronotum with same superficial punctures as rest of body, with stronger rugosity posteriorly and medially with larger shiny interstices between sculpture (about 2× wider than the punctures); pronotal sulcus without transverse crenulae; epomia not particularly strong, long, extending near posterior margin of pronotum ventrad to pronotal sulcus. Mesopleuron covered with denser, stronger, coalescing punctures, especially dorsad to sternaulus coalescing to form rugose areas (Fig. 6D); Dorsal part ventrad to subtegular ridge, with larger and distinctly shinier interstices between small punctures, interstices about 2× diameter of punctures. Sternaulus long, almost reaching posterior margin of mesopleuron, crenulae rather weak, longest distinctly weaker and only slightly longer than crenulae on mesopleural furrow (Fig. 6D) (paratypes: from short and weak to as highly raised and slightly longer than longest crenulae on mesopleural furrow). Epicnemial carina and posterior transverse carina of mesosternum complete. Mediosternal groove rather deep, not widened posteriorly with uniformly strong crenulae across its length. Metapleuron strongly rugosepunctate, juxtacoxal carina and metapleural carina distinct and complete (Fig. 6D). Sculpture of propodeum shallow, with indistinct transverse rugosity, individual punctures difficult to discern (Fig. 6F) (paratypes: rugosity variable, but never distinctly punctate); densely hairy. Area petiolaris differs in sculpture from rest of propodeum: shiny and sparsely scattered with longer setae, laterally with faint transverse sculpture, which is absent medially (Fig. 6F). Propodeal carination strong and complete; area superomedia slightly longer than wide (as long as wide in a few paratypes), pentagonal with very short, weak, parallel lateral carinae (paratypes: nearly absent lateral carinae in some specimens and less parallel in others); spiracles circular; apophyses not evident, carina somewhat enlarged in this position. Mesosoma 0.7×

length of metasoma. Mesosoma (excl. legs and wings) black, including posterior corner of pronotum and tegulae (paratypes: black in most, but dark brown in a few and reddish-brown in one reared and evidently teneral specimen); humeral plates contrastingly pale yellow (Fig 6C).

**Legs.** Hind femora 3.8× as long as wide. Lengths of tarsal segments in mm from first to fifth: 0.53, 0.27, 0.18, 0.10, 0.02. Claws moderately curved, simple, without teeth, basal lobe or pecten, few longer hairs present at base of claw. Arolium rather small, slightly more than half length of claw. Middle and hind tibiae with two reddish tibial spurs each, subequal in length and very slightly bent at apex. Coxae mainly black, fore and middle coxae with reddish spot on inner side (paratypes: from mostly red with dark patches to black with only small red patches on the inner side of middle coxae). Trochanters black with suffused red colouration, fore trochanters more red than black. Trochantelli, femorae and tibiae red, tibiae with darker outer surface, only weakly in fore leg. Tarsi with mixture of red and dark, with segments darker on outer surface and apically with narrow, indistinct reddish annuli.

**Wings.** The fore wing vein 3rs-m present, weakly pigmented, areolet symmetrical, pentagonal; vein 2m-cu rather long, straight, with one short bulla, forming acute angle with vein CU; vein RS straight; radius anterior (RA) slightly longer than pterostigma; pterostigma 2.8× as long as wide; vein 1cu-a slightly postfurcal relative to M&RS. Nervellus of hind wing intercepted at lower fifth (paratypes: from one fifth to one fourth below middle). Wing veins, including the pterostigma, uniformly dark brown, excluding narrow zone at the base of the wings with pale yellow veins; humeral plates pale yellow.

**Metasoma.** Punctuation generally more well defined than on rest of body. First metasomal tergite with strong punctuation (shiny interstices smaller than diameter of punctures), posterior part with weakly punctured area, interstices several times diameter of punctures. Dorsolateral carinae sharp, complete, with spiracle situated just ventrad to carina (Fig. 6E). Glymmae absent. Latero-median carinae present as faint striae not extending up to level of spiracles (Fig. 6E) (paratypes: varying in length from virtually absent to extending up to level of spiracles as faint striae). Second and third terga with very strong, dense, coalescing punctures, posterior margins of terga with punctures slightly smaller and more superficial. Rest of terga somewhat densely punctulate with shiny interstices distinctly larger than punctures. Metasoma black, except for narrow, translucently brownish posterior margins of first and second terga (paratypes: first tergite from completely black to black with indistinctly delimited red patches laterally; second from completely black to black with anterior fourth red. Terga 1–3 with posterior margins from completely black to black with narrow reddish-brown translucent zones); covered with dense, short, light brown hairs. Thyridia of second metasomal tergite small, shiny, oval and red (black in some paratypes). Unsclerotised parts of metasomal ster-

na more or less brown, except for yellowish sclerite of first sternite. Sclerotised part of first metasomal sternite extends half way up length of sternite and up to level of spiracles on first tergite, suture between it and first tergite straight. First tergite 3.7× wider posteriorly than anteriorly, 1.6× longer than its maximum (posterior) width (paratypes: 1.1–1.7× its width (n = 32)). Second tergite 0.8× as long as wide.

**Ovipositor.** Dorsal valve with weak, but angulate nodus, tip beyond nodus gradually tapering, sharp (Fig. 7B). Lower valves with about five visible teeth (apical-most too small to distinguish), widely spaced, slanted, extending further towards apex ventrally than dorsally. Ovipositor sheaths covered with rather dense black hairs, about as long as diameter of sheaths. Portion of ovipositor projecting beyond metasomal apex 2.2× length of hind tibia, 0.5× length of body and 0.7× length of fore wing (paratypes: 1.9–2.4× length of hind tibia, 0.4–0.6× body and 0.6–0.9× fore wing (n = 36 for all).

**Male** (paratype). **Length.** Body length 4.9 mm, fore wing length 3.5 mm.

**Head.** Mandibles whitish-yellow with black teeth, reddish colouration next to mandibular teeth and mandibular base. Palpi pale reddish-yellow. Malar space 0.8× as long as basal width of mandible. Temple ratio 1.0, POL:OOL 1.3, OD:OOL 0.5. Anterior halves of scapes white, antennae otherwise black, with 21 flagellar segments, conversely to female, apical flagellomeres gradually narrower apically (Fig. 7D). Scape 1.8×, first flagellar segment 1.8× and penultimate flagellar segment 1.4× as long as wide. First flagellar segment 1.2× as long as scape; segments 8 to 12 with tyloidea, very narrow, strongly raised, more so apically, with acute apical end, almost as long as segments, except in 8<sup>th</sup> segment with medially situated tyloid about one fourth of length of segment.

**Mesosoma.** Generally rougher surface sculpture than in female: mesopleuron medially strongly rugose; sternaulus with longer, stronger crenulae than in female, longest crenulae as strong as and longer than crenulae on mesopleural furrow (Fig. 7C); metapleuron and propodeum rugose, no punctures discernible. Propodeal carination is strong, stronger than in female. Tegulae black, contrasting with pale yellow humeral plate. Pterostigmae of the fore wings dark brown. Coxae and hind trochanters mainly black with suffused red colouration, especially evident in fore coxae, about half red, half black; femorae, tibiae, trochantelli, fore- and mid-trochanters and tarsi, except fifth tarsal segment, red; hind tibiae and tarsi dorsally suffused with blackish (Fig 7D). Hind femora 4.2× as long as wide; lengths of hind tarsal segments from first to last in mm: 0.59, 0.30, 0.18, 0.15, 0.14.

**Metasoma.** Latero-median carinae of first tergite long and rather strong, extending beyond level of spiracles. First tergite 1.5× and second tergite 0.7× as long as wide. Genitalia somewhat obscured. Parameres slightly narrowed apically and slightly downcurved, ventral margin slightly concave in lateral view, small parallel-sided gap between two parameres ventrally. Aedeagus not visible.

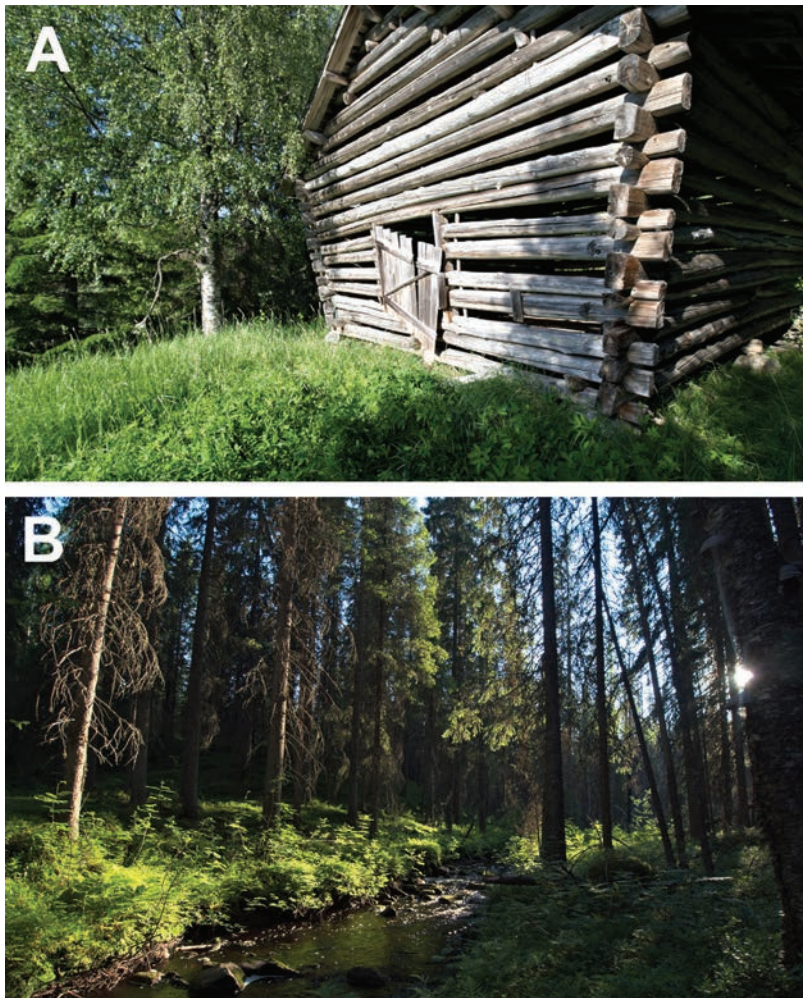


**Figure 8.** Habitats of *Lochetica ramii* sp. nov. **A.** The type locality Mökinoja: an old log barn on the edge of a mesic meadow (the meadow is outside of the frame). **B.** Luvejoki, the habitat of paratype MZH GP.109739 (about 300 m from the exact spot).

**Etymology.** *L. ramii* sp. nov. is my first species description. Thus, I take the opportunity to name the species in the honour of my grandfather Raimo “Rami” Konga (1936–2009) who had a profound impact on the development of my love for nature, which eventually led to the discovery of this species. The specific epithet is to be treated as a noun in the genitive case.

**Distribution.** Finland. Mainly in the Palearctic boreal forest biome *sensu* Olson et al. (2001). In addition, few specimens originate from the northernmost margin of the temperate broadleaf and mixed forest biome.

**Ecology.** The specimens have been collected from both open biotopes (Fig. 8A) and coniferous forests (Fig. 8B). More details are available for each specimen in the Material Examined section. Although both *L. ramii* sp. nov. and *L. westoni* occur frequently in the same habitats (and locations), it seems that *L. ramii* sp. nov. is more common in shaded, usually *Picea abies* L. dominated, forests (such as the one in Fig. 8B), while the opposite seems to be the case in the more exposed habitats. However, more data are needed for reliable comparisons.

Three examined specimens (MZH GP.109737, MZH GP.109736, MZH GP.109780) have been reared from

*Passaloecus monilicornis* Dahlbom, 1842 (Crabronidae). The pins do not include the host remains and the labels do not state how the host was confirmed; however, considering the strong preference of *L. westoni* to parasitise *Passaloecus*, these rearing records are in line with expectations. The holotype was collected together with *Passaloecus monilicornis* and *Passaloecus eremita* on the same wall of a log barn (Fig. 8A).

There are not enough data to postulate whether a smaller subset of *Passaloecus* species is utilised as hosts (opposed to *L. westoni*, which seems to utilise most species) or whether additional genera of cavity-nesting aculeates are used.

## Discussion

The support for the species status of *L. ramii* sp. nov.

Several morphological characters and an ample 7% divergence in COI sequences readily separate the new species from *L. westoni*. However, no sequences were available

for the remaining three species. Colour characters have been partly emphasised to differentiate the new species from the morphologically closest species *L. japonica*. Colour is known to vary geographically between distant populations on many insects, including the Ichneumonidae. Thereby, it is possible that the differences observed are not diagnostic, which could even imply the synonymy between *L. ramii* sp. nov. and *L. japonica*; however, the differences in head structure and surface sculpture of the head and mesosoma, in combination with the differences in colour adequately distinguish the new species from *L. japonica*. Despite several attempts, accessing the types of *L. agonia* and *L. farta* in the collection of the American Entomological Institute failed. The original descriptions are, however, sufficient for the new species to be distinguished from the two by at least two morphological characters. Furthermore, the two species occur in very different regions (western United States and Taiwan) from *L. ramii* sp. nov. (Finland).

The new species is described from a rather large number of specimens. However, as more specimens from a wider geographical area are revealed, the morphological and molecular gap between *L. ramii* sp. nov. and other species of the genus will no doubt become smaller. For example, there were no overlapping specimens of *L. ramii* sp. nov. and *L. westoni* regarding their ovi-tib ratio, but the difference is so small that it is likely that overlapping specimens are likely to surface in the future.

### The males of *Lochetica*

The males of the genus are rarely collected: three of the five species are only known from females and the number of females to males in the studied material is 38 ♀♀:1 ♂ in *L. ramii* sp. nov. and 40 ♀♀:5 ♂♂ in *L. westoni*. The

sole male of *L. ramii* sp. nov. and three of the five males of *L. westoni* were reared. In addition, the reared type series of *Cecidonomus westoni* consisted of 9 ♀♀ and 15 ♂♂ (Bridgman 1880), which demonstrates the different sex ratio opposed to the studied museum material. On the basis of these data, it seems evident that the males are difficult to find other than via rearing. Female-biased sex ratios are not uncommon in Hymenoptera (Quicke 1997 and references therein); however, since rearing seems to produce males and females in a “normal” ratio, the most likely explanation is that the males of *Lochetica* are short-lived and thereby rarely collected other than via rearing. Another contributing factor could be that the males of Phygadeuontinae are usually more difficult to identify and, thus, are more likely to end up in the unsorted parts of collections than the females.

### Future work

The distribution of *L. ramii* sp. nov. in Finland is rather widespread, extending from 60° to 64° in latitude. Thus, it is almost certain that *L. ramii* sp. nov. is also present in the neighbouring countries, but possibly also more widely in Europe and Asia. It is possible it has been previously confused with *L. westoni*, as it has been in Finland.

There are probably numerous species of *Lochetica* yet to be described, even in well-studied regions of the world. Future studies should attempt to examine large amounts of museum material from a wide geographic area – something the scope of this study did not allow. There is also an evident scarcity of information regarding most of the described species of *Lochetica* as well: the hosts and ecology is unknown in three out of five species, the males are unknown in two species and two species are only known from one or two specimens.

### Identification key to the species of *Lochetica* of the world

The keys include all known species of *Lochetica*; however, no specimens of *L. agonia* and *L. farta* have been examined and their characters are based on Townes (1983). Townes (1970) and Horstmann (1978) can be used for the identification of the genus.

♀♀

- 1 The epomia short or absent ventrad to the pronotal sulcus. The ovipositor with a rounded or absent nodus. The legs red and the tegulae yellow..... *Lochetica agonia* Townes, 1983
- The epomia long ventrad to the pronotal sulcus, extending as a weak ruga nearly to the posterior edge of the pronotum (Fig. 3A). The ovipositor with a very small but angulate nodus (Fig. 7B). The colour of the legs and tegulae similar only in *L. westoni*..... 2
- 2 The area petiolaris of the propodeum very densely transversely sculptured. The latero-median longitudinal carina of the propodeum, separating the area postero-externa from the area petiolaris, is weak. The coxae, trochanters and tegulae dark..... *Lochetica farta* Townes, 1983
- The area petiolaris weakly to moderately transversely sculptured, the sculpture concentrated on the sides (Figs 3D, 7B). The latero-median longitudinal carina of the propodeum, separating the area postero-externa from the area petiolaris, is strong (Figs 3D, 7B). Colouration variable..... 3

- 3 The latero-median carinae of the first tergite strong, extending at least to the level of spiracles (Fig. 3E). In dorsal view, the head narrowed behind the eyes (Fig. 3B). The sternaulus with strong crenulae, stronger and longer than the crenulae on the mesopleural furrow (Fig. 3C). The ovipositor about long as the body (ovi-tib ratio more than 2.5). The legs predominantly red (coxae and tarsi sometimes with dark colouration) and the tegulae yellow (Fig. 3F) ..... *Lochetica westoni* (Bridgman, 1880)
- The latero-median carinae of the first tergite weak or absent (Fig. 6E). The head slightly narrowed to widened behind the eyes (dorsal view). The sternaulus with weaker crenulae, not stronger than the ones on the mesopleural furrow (Fig. 6D). The ovipositor about as long as the metasoma or shorter (ovi-tib ratio less than 2.5) (Fig. 7A). Either legs or tegulae mainly black ..... 4
- 4 The mesosoma with shallower, less defined punctures, especially the area externa of the propodeum with punctures weakly, or not, discernible amongst the weak transversely orientated sculpture (Fig. 6F). The vertex uniformly sloping from the ocelli to the occiput; punctation weak and shallow, sculpture almost granulate (Fig. 6A). The pronotal sulcus without transverse crenulae. The tegulae black or dark brown (Fig. 6C). The femorae and tibiae predominantly red (Fig. 7A). The mandibles reddish with black base and teeth (Fig. 6B) ..... *Lochetica ramii* sp. nov.
- The mesosoma with more clearly defined, deep punctation, especially the area externa of the propodeum with dense, clearly defined punctures (Fig. 5B). The vertex with a shallow transverse depression followed by a low elevation; punctures large and rather deep (Fig. 5E). The pronotal sulcus with transverse crenulae. The tegulae light brownish-yellow (Fig. 5E). The legs, including femorae and tibiae predominantly black or dark brown with some suffused reddish colouration (Fig. 5D). The mandibles mainly black (Fig. 5A) ..... *Lochetica japonica* Watanabe, 2021



This key is very tentative. It is based on a very small sample and the males of *L. japonica* and *L. farta* are unknown. The characters in parentheses are of uncertain diagnostic value.

- 1 The epomia short or absent ventrad to the pronotal sulcus. Tegulae “ivory”. The mandibles mostly red. Nearctic ..... *Lochetica agonia* Townes, 1983
- The epomia long ventrad to the pronotal sulcus, extending near the posterior margin of the pronotum, but rather weakly indicated. Tegulae yellow or black. The mandibles mainly white, with blackish or reddish colouration proximally and distally. Palearctic ..... 2
- 2 The tegulae yellow, similar in colour to the adjacent humeral plate (Fig. 3C, cf. Fig. 3F). (mesopleuron and metapleuron with stronger rugosity (Fig. 3C). Trochanters and hind tarsi generally red) ..... *Lochetica westoni* (Bridgman, 1880)
- 3 The tegulae black, contrasting with the pale yellow humeral plate (Fig. 7C, cf. Fig. 6C). (mesopleuron and metapleuron with weaker rugosity (Fig. 7C). The trochanters and hind tarsi darkened dorsally) ..... *Lochetica ramii* sp. nov.

## Acknowledgements

I thank all who gave access to specimens: Juho Paukkunen (Museum of Natural History, Helsinki) loaned the bulk of the material used in this study, Kyohei Watanabe (Kanagawa Prefectural Museum of Natural History) photographed the holotype of *Lochetica japonica*, David Waterhouse and Dr. Tony Irwin (Norwich Museum) photographed the lectotype of *Cecidonomus westoni*, Rune Bygebjerg and Christoffer Fägerström (Lund University Biological Museum) photographed the lectotype of *Phygadeuon pimplarius*, Gergely Várkonyi gave access to the previously barcoded Finnish specimens, including the sole male specimen of *L. ramii*. Many specimens also originated from recent species inventories conducted as part of the Beetles-LIFE and other projects carried out by Metsähallitus (Sampsa Malmberg, Mervi Laaksonen, Eerikki Rundgren). Marko Mutanen gave much needed comments, corrections and suggestions regarding the DNA barcoding sections of this paper and Ika Österblad sent me a crucial piece of literature.

## References

- Barbey A, Ferriere C (1923) Un cas intéressant de parasitologie de l'écorce du pin sylvestre. Bulletin de la Société Vaudoise des Sciences Naturelles 55: 77–81.
- Blösch M (2000) Die Grabwespen Deutschlands. Lebensweise, Verhalten, Verbreitung. Die Tierwelt Deutschlands 71, Goecke & Evers, Keltern, 480 pp.
- Bridgman JB (1880) Three new Ichneumonids. Entomologist 13: 263–265. <https://doi.org/10.5962/bhl.part.27903>
- Broad GR, Shaw MR, Fitton MG (2018) Ichneumonid Wasps (Hymenoptera: Ichneumonidae): their Classification and Biology. Handbooks for the Identification of British Insects 7(12), Royal Entomological Society, 418 pp.
- deWaard JR, Ivanova NV, Hajibabaei M, Hebert PDN (2008) Assembling DNA Barcodes. In: Martin CC, Martin CC (Eds) Environmental Genomics. Methods in Molecular Biology 410, Humana Press. [https://doi.org/10.1007/978-1-59745-548-0\\_15](https://doi.org/10.1007/978-1-59745-548-0_15)
- Edgar RC (2004) MUSCLE: Multiple sequence alignment with high accuracy and high throughput. Nucleic Acids Research 32(5): 1792–1797. <https://doi.org/10.1093/nar/gkh340>

- Frilli F (1973) Studi sugli imenotteri icneumonidi. IV. Il genere *Phygadeuon* s. l. – revisione delle specie descritte da CG Thomson. *Entomologica* 9: 85–117.
- Hebert PD, Cywinska A, Ball SL, DeWaard JR (2003) Biological identifications through DNA barcodes. *Proceedings. Biological Sciences* 270(1512): 313–321. <https://doi.org/10.1098/rspb.2002.2218>
- Horstmann K (1972) Type revision of the species of *Cryptinae* and *Campopleginae* described by J. B. Bridgman (Hymenoptera: Ichneumonidae). *Entomologist* 105: 271–228.
- Horstmann K (1978) Revision der Gattungen der *Mastrina* Townes (Hymenoptera, Ichneumonidae, Hemitelinae). *Zeitschrift der Arbeitsgemeinschaft Österreichischer Entomologen* 30: 65–70.
- Horstmann K (1991) Revision einiger Gattungen und Arten der *Phygadeuontini* (Hymenoptera, Ichneumonidae). *Mitteilungen der Münchner Entomologischen Gesellschaft* 81: 229–254.
- Jonaitis (1981) [in Kasparyan, DR] *Opredeliteli Nasekomich Europeiskoy Chasti SSSR. Pereponchatokrylye*, 3(3). *Opredeliteli po Faune SSSR*, St. Petersburg, 687 pp.
- Kreisch WF (2000) Beobachtungen an Nisthilfen für aculeate Hymenopteren im Kernbereich von Großstädten (Hym.). *Entomologische Nachrichten und Berichte* 44: 229–235.
- Lomholdt O (1975) The *Sphecidae* (Hymenoptera) of Fennoscandia and Denmark. *Fauna Entomologica Scandinavica* 4(1), Scandinavian Science Press, Copenhagen, 452 pp.
- Morley C (1907) *Ichneumons of Great Britain Cryptinae*. *Ichneumonologica Britannica* 2, Plymouth.
- Olson DM, Dinerstein E, Wikramanayake ED, Burgess ND, Powell GV, Underwood EC, D'Amico JA, Itoua I, Strand HE, Morrison JC, Loucks CJ, Allnutt TF, Ricketts TH, Kura Y, Lamoreux JF, Wettengel WW, Hedao P, Kassem KR (2001) *Terrestrial Ecoregions of the World: A New Map of Life on Earth: A new global map of terrestrial ecoregions provides an innovative tool for conserving biodiversity*. *Bioscience* 51(11): 933–938. [https://doi.org/10.1641/0006-3568\(2001\)051\[0933:TEOTWA\]2.0.CO;2](https://doi.org/10.1641/0006-3568(2001)051[0933:TEOTWA]2.0.CO;2)
- Quicke DL (1997) *Parasitic wasps*. Chapman & Hall Ltd, London, 470 pp.
- Riedel M, Diller E, Japoshvili G (2018) The Ichneumonid fauna (Hymenoptera: Ichneumonidae) of Lagodekhi Reserve, Sakartvelo (Georgia), with descriptions of four new species. *Linzer Biologische Beiträge* 50(2): 1447–1507.
- Tamura K, Stetcher G, Kumar S (2021) *MEGA11: Molecular Evolutionary Genetics Analysis Version 11*. *Molecular Biology and Evolution* 38(7): 3022–3027. <https://doi.org/10.1093/molbev/msab120>
- Townes H (1970) The Genera of *Ichneumonidae* part 2. *Memoirs of the American Entomological Institute* 12(2), The American Entomological Institute, Michigan.
- Townes H (1983) Revisions of twenty genera of *Gelini* (Ichneumonidae). *Memoirs of the American Entomological Institute* 35, The American Entomological Institute, Michigan.
- Watanabe K (2021) Taxonomic and zoogeographic study of the Japanese *Phygadeuontinae* (Hymenoptera, Ichneumonidae), with descriptions of 17 new species. *Kanagawa Kenritsu Hakubutsukan Kenkyu Hokoku, Shizen Kagaku* 50: 55–136. [https://doi.org/10.32225/bkpmnh.2021.50\\_55](https://doi.org/10.32225/bkpmnh.2021.50_55)
- Yu DSK, van Achterberg C, Horstmann K (2012) *Taxapad 2012, Ichneumonoidea 2011. Database on flash-drive (version 20120606)*, Ottawa, Ontario, Canada.

## Supplementary material 1

### R script for statistical analyses and graphs

Author: Juuso Paappanen

Data type: R

Explanation note: The script file containing all the code to replicate the statistical analyses and recreate the graphs used in the study. The file is a simple text file, which can be opened in R or in any text editor (e.g. notepad).

Copyright notice: This dataset is made available under the Open Database License (<http://opendatacommons.org/licenses/odbl/1.0>). The Open Database License (ODbL) is a license agreement intended to allow users to freely share, modify, and use this Dataset while maintaining this same freedom for others, provided that the original source and author(s) are credited.

Link: <https://doi.org/10.3897/dez.71.121217.suppl1>

## Supplementary material 2

### Aligned sequences

Author: Juuso Paappanen

Data type: fas

Explanation note: The aligned COI sequences in .fasta format used in the study.

Copyright notice: This dataset is made available under the Open Database License (<http://opendatacommons.org/licenses/odbl/1.0>). The Open Database License (ODbL) is a license agreement intended to allow users to freely share, modify, and use this Dataset while maintaining this same freedom for others, provided that the original source and author(s) are credited.

Link: <https://doi.org/10.3897/dez.71.121217.suppl2>

## Supplementary material 3

### Specimen and morphological data

Author: Juuso Paappanen

Data type: xlsx

Explanation note: A spreadsheet file (MS Excel) containing the data of specimens used in the study. The data includes specimen id, species name, collecting location and date, collector and selected morphological characters.

Copyright notice: This dataset is made available under the Open Database License (<http://opendatacommons.org/licenses/odbl/1.0>). The Open Database License (ODbL) is a license agreement intended to allow users to freely share, modify, and use this Dataset while maintaining this same freedom for others, provided that the original source and author(s) are credited.

Link: <https://doi.org/10.3897/dez.71.121217.suppl3>

# A second species of the genus *Manodactylus* Moser, 1919 (Coleoptera, Scarabaeidae, Melolonthinae, Macroductylini) from the highlands of Colombia

Julián Clavijo-Bustos<sup>1</sup>, María I. Castro-Vargas<sup>2</sup>, Jhon César Neita Moreno<sup>1</sup>

<sup>1</sup> Sección Entomología, Colecciones Biológicas, Centro Colecciones y Gestión de Especies, Instituto de Investigación de Recursos Biológicos Alexander von Humboldt, Villa de Leyva, Boyacá, Colombia

<sup>2</sup> Maestría en Ciencias Agrarias – Entomología, Facultad de Ciencias Agrarias, Universidad Nacional de Colombia sede Bogotá, Bogotá D.C., Colombia

<https://zoobank.org/73CD46B3-AA8E-42CB-8640-3C04D799D1F6>

Corresponding author: Julián Clavijo-Bustos (jclavijo@humboldt.org.co)

Academic editor: Matthias Seidel ♦ Received 17 January 2024 ♦ Accepted 29 May 2024 ♦ Published 30 July 2024

## Abstract

Moser in 1919 described the genus *Manodactylus* for the new species *Manodactylus gaujoni* Moser, 1919, which was described based on specimens of Abbé Gaujon from Loja, Ecuador; a syntype of this species was designated in 2017 as the lectotype. Earlier, *Macroductylus gaujoni* was described by Ohaus in 1909 based on a specimen collected also in highlands of Loja; however, this type specimen is presumably lost. We designate the lectotype as a neotype for *Macroductylus gaujoni* Ohaus, 1909 based on the congruence between the type localities and the diagnostic characters mentioned in the descriptions. Thus, *Manodactylus gaujoni* Moser, 1919 is a junior objective synonym of *Macroductylus gaujoni* Ohaus, 1909, which is presented here in the new combination under the genus *Manodactylus*. Also, a second species of the genus *Manodactylus* is described from the Paramo ecosystem in the Andes of southern Colombia. *Manodactylus paramicola* sp. nov. differs from *M. gaujoni* by the shape of clypeus and punctuation of pronotum and elytra. Diagnosis for the genus and for the species, the description of *M. paramicola* sp. nov., and a distribution map are presented.

## Key Words

distribution, new species, scarab, taxonomy

## Introduction

Moser (1919) described the genus *Manodactylus*, as well as the unique and singular species currently placed in it. The description of *Manodactylus gaujoni* Moser, 1919 was based on an unspecified number of specimens from the southern Andes of Ecuador, in the province of Loja (Moser 1919; Katovich 2008). However, Ohaus (1909) already used the name *Macroductylus gaujoni* Ohaus, 1909 for a species in Loja with similar morphology and from a nearby locality of *Manodactylus gaujoni sensu* Moser (1919) (Fuhrmann and Vaz-de-Mello 2017). The original type series of *Macroductylus gaujoni* Ohaus (1909) has not been found yet, and this

taxonomic and nomenclatural problem is still waiting to be solved (Fuhrmann and Vaz-de-Mello 2017).

Since its description, the genus *Manodactylus* and the single described species remained little-known, and only one new record was presented from the department of Piura in Peru (Saavedra Albuquerque et al. 2015). This new record has not been confirmed until now and a previous study overlooked it (see Fuhrmann and Vaz-de-Mello 2017). In two studies on the tribe Macroductylini, the genus *Manodactylus* was found to be morphologically similar to the genera *Chariodactylus* Moser, 1919 and *Macroductylus* Dejean, 1821 (implied by the identification keys) (Katovich 2008; Fuhrmann and Vaz-de-Mello 2017).

Despite having been redescribed by Katovich (2008) and re-diagnosed by Fuhrmann and Vaz-de-Mello (2017), the generic limits of *Manodactylus* are still not well defined. Hence, we propose complementary characters to the diagnosis of the genus and designate a neotype for *M. gaujoni* Ohaus, 1909 in order to give nomenclatural stability to the species name; also, we describe a second species of *Manodactylus* from the southern Andes of Colombia, and provide a diagnosis for the single previously known species.

## Materials and methods

Type specimens are deposited in the following institutions (curators in parenthesis):

- CEUN** Colección Entomológica de la Universidad de Nariño. Pasto, Nariño, Colombia (G. Castillo, M. Rodríguez).
- CMNC** Canadian Museum of Nature. Ottawa, Canada (R. Anderson, A. B. T. Smith, F. Génier).
- IAvH-E** Sección de Entomología, Colecciones Biológicas del Instituto de Investigación de Recursos Biológicos Alexander von Humboldt. Villa de Leyva, Boyacá, Colombia (J. C. Neita Moreno).
- MFNB** Museum für Naturkunde, Leibniz-Institut für Evolutions- und Biodiversitätsforschung. Berlin, Deutschland (J. Willers, B. Jaeger).

Measurements of the new species were taken using a Mitutoyo NTD12-6" M digital caliper. For transcription of type specimens' labels, a slash '/' indicates different lines, two slashes '/' indicate different labels, and label characteristics are presented between square brackets '[' ]'.

The photographs of habitus were taken with a Canon EOS 5D Mark II camera with a Canon EF 100 mm f/2.8 macro lens, and photographs of male genitalia, mouthparts, and morphological details were taken with a Leica S8APO stereomicroscope with a Leica MC190 HD camera. The distribution map is based on information from the type specimen's labels and literature (Ohaus 1909; Saavedra Albuquerque et al. 2015) and was made on the online software SimpleMapp (Shorthouse 2010). The plates were organized using Photoshop 21.2.0.

## Results and discussion

### Genus *Manodactylus* Moser, 1919

**Type species.** *Manodactylus gaujoni* Moser, 1919 (by monotypy, junior objective synonym of *Manodactylus gaujoni* (Ohaus, 1909), comb. nov.)

**Diagnosis.** Color black, shiny; clypeus trapezoidal; clypeus and frons forming a subpentagonal area, surface with small, coarse, rounded punctures densely and irregularly distributed giving a rugose appearance; frons with a

smooth raised narrow area extending from anterior angles to the vertex, and delimiting the subpentagonal area; eyes small, interocular distance more than six times the dorsal width of the eye; antennae with nine antennomeres; pronotum diamond shaped, strongly wider medially, wider than long, and borders with small, rounded punctures bearing setae of different length; limit between scutellar shield and mesoscutum not evident; elytral base wider than pronotal base; each elytron with five striae between suture and humeral callus, 10 in total, each with a regular row of small, rounded punctures; prosternum with two anterior, longitudinal sulci; metaventricle densely setose medially; femora subequal in length to their respective tibiae; tibiae shorter than their respective tarsi; tarsal claws bifid, and with an acute triangular tooth basally; protibia along the outer edge with two teeth distributed in the apical third; protibia gradually widening from base to apex but narrowing from the inner edge in the apical third, and lacking apical spur; abdomen with intersegmental membrane VII–VIII exposed; abdominal ventrites 2–5 densely setose medially, and ventrite 5 evidently longer than the others; pygidium vertical, strongly convex; phallobase cylindrical, around 2.5 times the length of parameres; parameres fused at the base, short, apically slightly downward curved and with apex rounded.

**Taxonomic remarks.** *Manodactylus* is very similar to *Chariodactylus* and *Macroductylus*, all three genera sharing the trapezoidal clypeus, antennae with nine antennomeres, pronotum strongly wider medially, mesoscutum–scutellar shield limit not evident, prosternum anteriorly with two longitudinal sulci, protibia with two teeth on the outer edge, absence of protibial spur, and internal area of metatarsomere 5 unarmed (Fuhrmann and Vaz-de-Mello 2017). *Manodactylus* also shares with *Macroductylus* the small eyes (interocular distance of more than five times the dorsal width of the eye), and with *Chariodactylus* the pronotum slightly wider than long and the protibia gradually widening from base to apex but narrowing from the inner edge in the apical third.

As suggested in a previous work, a cladistic analysis including these three genera is needed to confirm the validity of these taxa (Fuhrmann and Vaz-de-Mello 2017). However, we prefer to retain each of these genera as valid until this taxonomic issue will be resolved, and propose the following characters to distinguish *Manodactylus* from the other two genera (some of these characters were mentioned by Fuhrmann and Vaz-de-Mello 2017): small eyes (Fig. 5B, D) (large eyes in *Chariodactylus*, interocular distance of less than 3.5 times the dorsal width of the eye), pronotum glabrous (Fig. 5A, C) (setose in *Chariodactylus*) and wider than long (Fig. 5A, C) (longer than wide or as long as wide in *Macroductylus*), and protibia gradually widening from base to apex but narrowing from the inner edge in the apical third (Fig. 4A) (protibia widening near the base but narrowing from the inner edge around the middle of the length in *Macroductylus*).

We identified some other morphological features which are probably useful to distinguish *Manodactylus*

from the other genera, but we were unable to check them in other genera and species from outside of Colombia. Males of both species of *Manodactylus* have the inner angle of the protibia slightly projected downward (Fig. 4B) (kind of similar to the ‘polex’ of some Ochodaeidae species), which is not projected in *Macroductylus* species from Colombia. Also, males of *Manodactylus paramicola* sp. nov. have two mesotibial spurs (Fig. 4D) and one metatibial spur (Fig. 4E), while males of the Colombian species of *Macroductylus* only have two spurs in the apex of mesotibiae.

***Manodactylus gaujoni* (Ohaus, 1909), comb. nov.**

Figs 1, 5A, B

*Macroductylus gaujoni* Ohaus, 1909: 95 (original description).

*Manodactylus gaujoni* Moser, 1919: 44, new junior objective synonym.

**Type material.** *Manodactylus gaujoni* Moser, 1919: lectotype male (MFNB), examined on photos: “Equateur / Loja / Abbé Gaujon” [white printed label] // “LECTOTYPE / *Manodactylus* ♂ / *gaujoni* / Moser 1919 / des. J. Fuhrmann & / F.Z. Vaz.de.Mello. 2014” [red handwritten label]. Lectotype designated by Fuhrmann and Vaz-de-Mello, 2017. *Macroductylus gaujoni* Ohaus, 1909: lectotype male of *Manodactylus gaujoni* Moser, 1919

designated here as the neotype (see under Remarks), with the additional label “NEOTYPE / *Macroductylus gaujoni* / Ohaus, 1909 / Des: Clavijo-Bustos, Castro-Vargas & Neita Moreno, 2024” [red printed label].

**Diagnosis.** *Manodactylus gaujoni* shares with *M. paramicola* sp. nov. the overall appearance, black color, shiny, with bicolored legs; clypeus trapezoidal; clypeus and frons forming a subpentagonal area delimited in the frons by a smooth raised narrow area extending from anterior angles to the vertex; eyes small, interocular distance around six to seven times the dorsal width of the eye; pronotum with micropunctures when viewed under high magnification; and each elytron with five striae between suture and humeral callus, 10 in total, and the interstriae convex.

*Manodactylus gaujoni* can be distinguished from *M. paramicola* sp. nov. by the following characters: body of a more lustrous color, with femora and tarsi reddish-brown, but tibiae dark brown; clypeus only slightly emarginate medially, with borders on each side of medial emargination widely rounded and slightly upturned; the subpentagonal area formed by clypeus and frons flat; the pronotum also with small, rounded, setigerous punctures but only on the borders; each elytral stria shallow, with a regular row of small, rounded punctures distanced by 1–4 times one puncture diameter; interstriae only slightly convex.



**Figure 1.** *Macroductylus gaujoni* Ohaus, 1909, male neotype = *Manodactylus gaujoni* Moser, 1919, male lectotype. A. Dorsal view; B. Ventral view; C. Labels.

**Remarks.** Ohaus (1909: 95) in the brief description of *Macroductylus gaujoni* mentioned that many specimens of Abbé Gaujon from Loja (Ecuador) that were sent to Europe, were collected by the Ecuadorian native Angelo Ordoñez (referred as Angelo Ordonnez by Ohaus, 1909: 95). Ohaus also contacted Angelo Ordoñez and when they both were going to Angelo's house in Loja, Ohaus collected a black specimen of '*Macroductylus*' with long red legs, which he named *Macroductylus gaujoni*. On the other hand, Moser (1919: 44) described the new genus *Manodactylus* declaring it to be similar to *Macroductylus* and with the type species *Manodactylus gaujoni*, whose description was based on specimens of Abbé Gaujon also from Loja. According to Moser (1919), *Manodactylus gaujoni* is characterized by being black with red or reddish-brown femora and tarsi, diagnostic characters that are also visible in the lectotype of *Manodactylus gaujoni* Moser, 1919 (Fig. 1). So far, the type specimen of *Macroductylus gaujoni* Ohaus, 1909 has not been found (Fuhrmann and Vaz-de-Mello 2017) and is presumably lost.

Therefore, we here designate the male lectotype of *Manodactylus gaujoni* Moser, 1919 as the neotype for *Macroductylus gaujoni* Ohaus, 1909. Our proposal is based on the congruence between the type locality of both species, the fact that the Ecuadorian Angelo Ordoñez was presumably involved in the collecting of both type specimens, and the diagnostic color pattern of the specimens mentioned in both descriptions. This will give stability to the species name making both taxa objective synonyms, with *Macroductylus gaujoni* Ohaus, 1909 as the senior synonym. *Macroductylus gaujoni* Ohaus, 1909 is transferred to the genus *Manodactylus*.

It is important to mention that the male paralectotype deposited in SDEI (Senckenberg Deutsches Entomologisches Institut. Müncheberg, Germany) has an Ohaus' label "Macroductylus Gaujoni / Cotype Moser", but also has another label indicating that it belongs to Abbé Gaujon's specimens (as the lectotype and other paralectotypes of *Manodactylus gaujoni* from Moser) (Fuhrmann and Vaz-de-Mello 2017). This possibly suggests that both Ohaus and Moser referred to the same species, and probably a misunderstanding led to the double description of *M. gaujoni*. The simplicity of Ohaus' 'description' might indicate that he used an unpublished name of a species by Moser, or alternatively Moser could have tried to complete Ohaus' description while describing his new genus placing the species. However, available information is not enough to confirm one of these two scenarios. Although, this specimen is the only one having an Ohaus label, we do not consider it to be the lost syntype of *Macroductylus gaujoni* because it was collected by Abbé Gaujon and not by Ohaus as stated in the original description.

**Distribution.** Ecuador, province of Loja; Peru, department of Piura (needs confirmation) (Fig. 6). The type series of *Manodactylus gaujoni* Moser, 1919 is from Loja, Ecuador (Moser 1919). Ohaus (1909) mentioned for *Macroductylus gaujoni* that there is a hill called Hornil-

los, and a road from there goes to 'San Francizco', the highest peak of the Eastern Cordillera visible from Loja and located about 3000 m asl (Ohaus 1909: 95). From this peak, there is a range from west to east, almost reaching the mouth of River Sabanilla in Zamora; this range is narrow, but with some broad points similar to 'San Francizco' (Ohaus 1909: 95).

#### *Manodactylus paramicola* sp. nov.

<https://zoobank.org/A4593819-8F5D-4DD9-A501-BE262E0C1F8A>

Figs 2, 3, 4, 5C, D

**Type material.** *Holotype* male (IAvH-E) labeled: "Pasto (Nar.) / 29 - X - 58" [white printed label, second line handwritten] // "B. Yanguatin / Suelo paramo / Alt. 3500 mts" [white handwritten label] // "Holotypus ♂ / *Manodactylus paramicola* n. sp. / Clavijo-Bustos, Castro-Vargas & Neita Moreno, / 2024" [red printed label] // "Instituto Humboldt / Colombia / IAvH-E-266051" [white printed label with QR code]. **Paratypes:** 2 males (CEUN) labeled like the holotype, except by: "Paratypus ♂ / ..." [yellow printed label]; 1 male (CMNC) labeled: "Colombia, Cauca, San Sebastian, / Valencia, 1°54'0.15"N, 76°40'12.29"W, WGS84, 2950 m, Cap. manual, / 2018-09-07, D. E. Martínez-Revelo" [white printed label] // "Cauca Valencia / 7-sep-18" [white handwritten label], and the same yellow paratype label.

**Description.** Male. Total length: 7.9–9.5 mm (holotype: 9.3 mm), maximum width of pronotum: 3.0–3.6 mm (holotype: 3.5 mm), width at the base of pronotum: 2.0–2.5 mm (holotype: 2.4 mm), width at the base of elytra: 2.8–3.3 mm (holotype: 3.3 mm). Color black, shiny, with rounded micropunctures when viewed under high magnification; antennae with antennomeres 1–6 dark brown and antennomeres 7–9 (antennal club) black; apex of femora, and tibiae and tarsi, dark brown. Body elongate and slender, subparallel. **Head:** Clypeus trapezoidal, anterior border emarginate medially, borders on each side of medial emargination narrowly rounded, slightly angulated and upturned; clypeus and frons forming a subpentagonal concave area, surface with small, coarse, rounded punctures densely and irregularly distributed, separated by less than one time one puncture diameter, giving a rugose appearance, and each puncture bearing a short, slender pale-yellow seta; frons with a smooth raised narrow area extending from anterior angles to the vertex, and delimiting the subpentagonal concave area. Fronto-clypeal suture not well-marked. Vertex smooth medially, laterally with punctures similar to those of the surface of clypeus and frons. Eyes small, interocular distance equal to 6.2 times the dorsal width of the eye. Ocular canthus very short and narrow, dorsally covered with small, coarse, rounded punctures densely and irregularly distributed, each bearing a moderately long, thick reddish-yellow seta. Antennae with nine antennomeres, antennal club equal to the combined length of antennomeres 2–6.

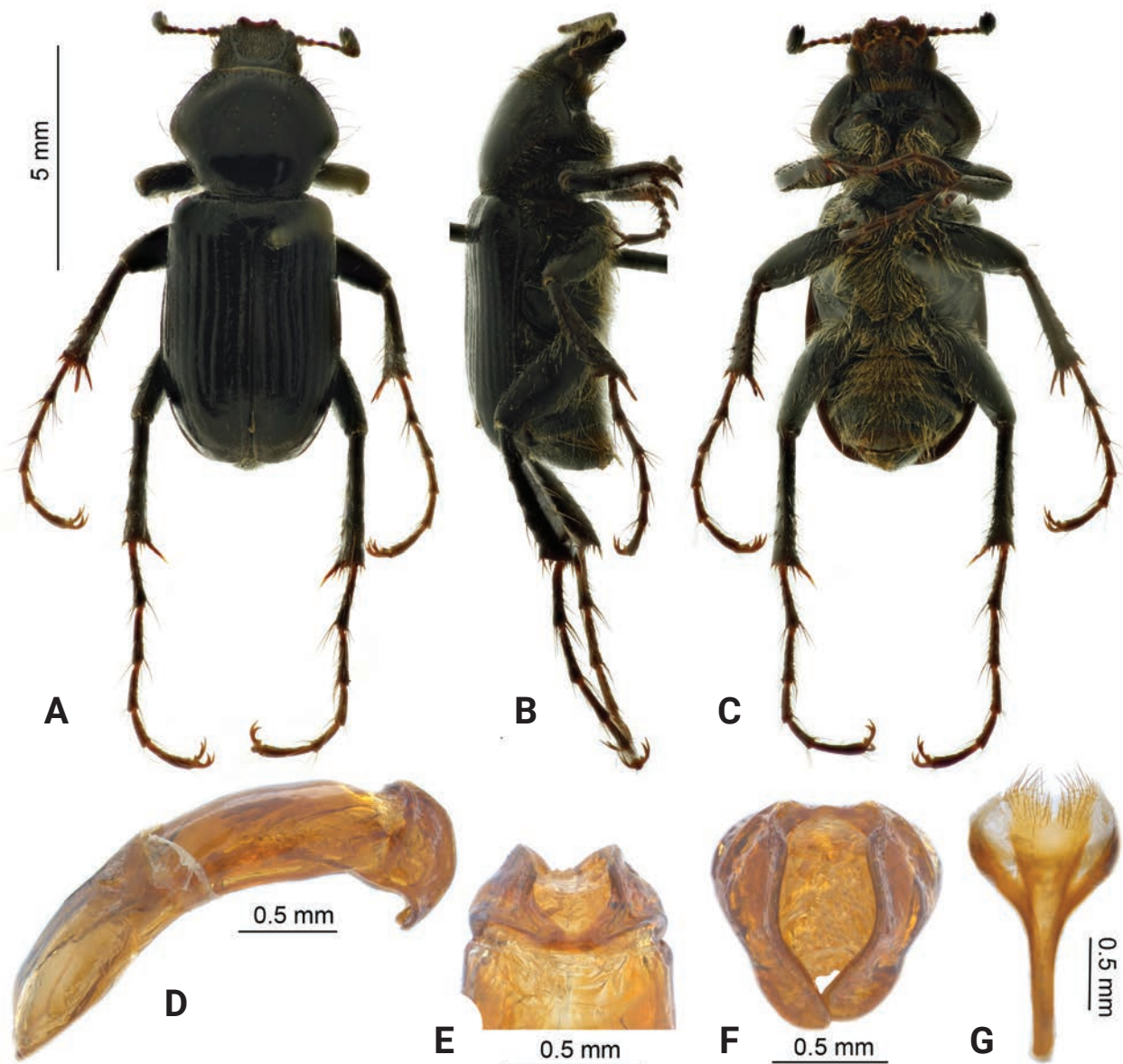


**Figure 2.** *Manodactylus paramicola* sp. nov., male holotype. **A.** Dorsal view; **B.** Lateral view; **C.** Ventral view; **D.** Aedeagus in lateral view; **E.** Parameres in dorsal view; **F.** Parameres in frontal view; **G.** Spiculum gastrale in dorsal view.

**Mouthparts:** Mandibles triangular, sclerotized, molar lobes slightly asymmetric; long setae present in the apical half of outer edge and in the inner edge, in a membranous lobe apically setose; surface of molar lobes with ridges. Maxillae with the cardo projected horizontally; maxillary palps with four palpomeres; lacinia apically membranous, with a tuft of setae; galea with eight teeth and covered of setae apically. Labium with mentum oblong, longer than wide, slightly narrowing anteriorly, anterior edge truncate, ventral surface with large, thick setae; prementum with two labial palps, each with three palpomeres. Labrum with the anterior edge of distal epipharynx slightly emarginate medially; chaetopariae with several rows of long setae, laeotorma and dextiotorma long. **Pronotum:** Pronotal disc convex, diamond shaped, strongly wider medially, and wider than long. Surface medially with few

small, rounded punctures sparsely and irregularly distributed, separated by 3–5 times one puncture diameter, each puncture bearing a short, slender pale-yellow seta. Borders margined, with an irregular row of small, rounded punctures; the row has less punctures over the anterior and posterior borders than over the anterior angles; each puncture on anterior and posterior borders bearing a short, slender pale-yellow seta, otherwise, each puncture bearing a moderately long, thick reddish-yellow seta, and over the anterior angles with few punctures bearing a long, thick reddish-yellow seta. Anterior angles acute, posterior angles rounded. **Scutellum:** Scutellar shield slightly longer than wide; surface laterally with few small, rounded punctures sparsely and irregularly distributed, separated by one to less than one times one puncture diameter, each puncture bearing a short, slender pale-yellow seta. Limit

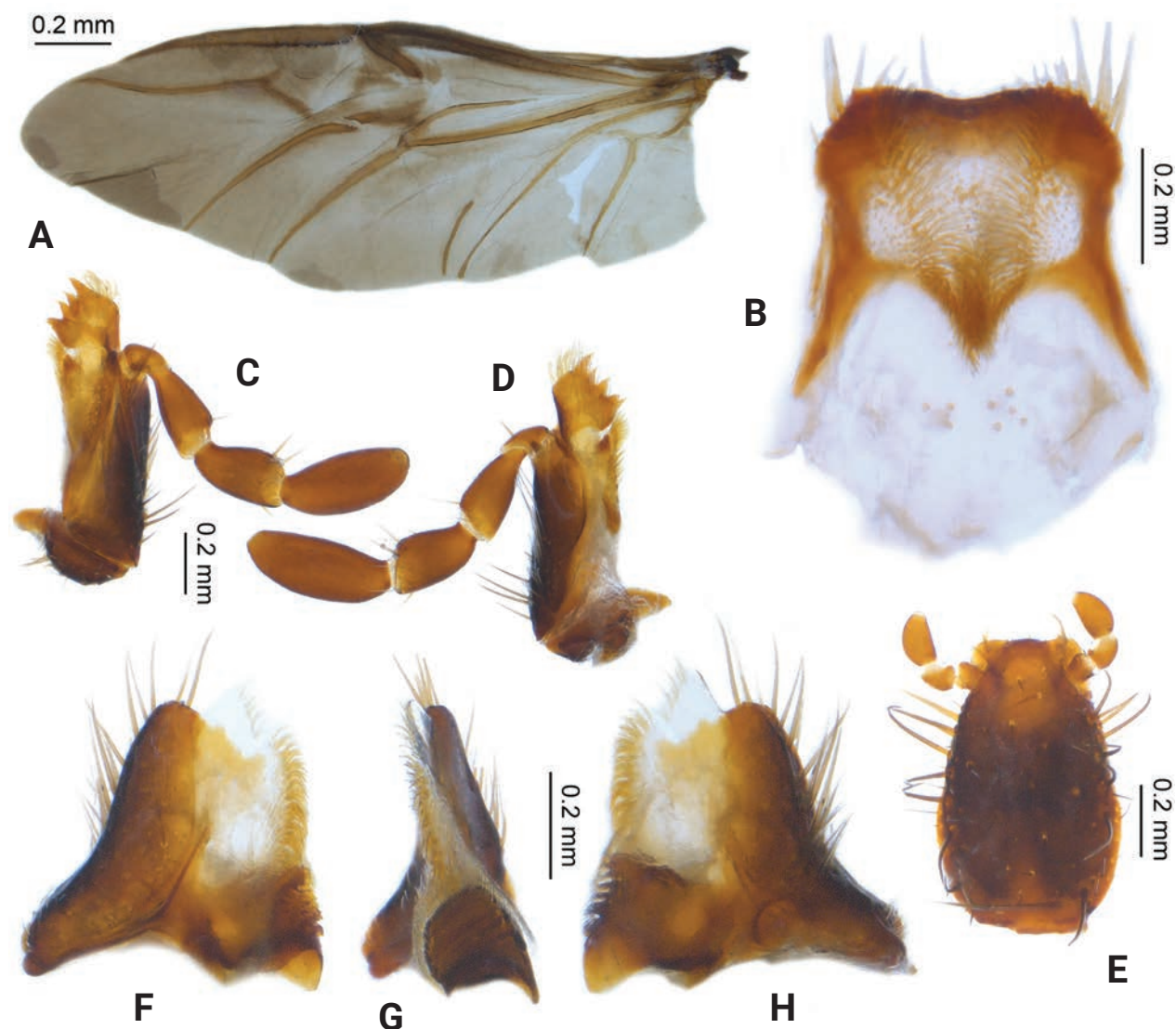


**Figure 3.** *Manodactylus paramicola* sp. nov., male paratype. **A.** Hind wing in dorsal view; **B.** Epipharynx in ventral view; **C.** Left maxilla in ventral view; **D.** Left maxilla in dorsal view; **E.** Labium in ventral view; **F.** Left mandible in dorsal view; **G.** Left mandible in lateral internal view; **H.** Left mandible in ventral view.

between scutellar shield and mesoscutum not evident.

**Hind wings:** Fully developed. **Elytra:** Elytral base wider than pronotal base. Humeral and apical calluses slightly prominent, rounded. Each elytron with five striae between suture and humeral callus, 10 in total, but lateral striae less evident; striae disappearing over the apical declivity; each stria deep, with a regular row of small, rounded punctures distanced by 3–5 times one puncture diameter. Interstriae strongly convex. Surface of interstriae, humeral and apical calluses with scattered, small, rounded punctures. Some punctures in the surface, including some in the striae, bearing a short, slender pale-yellow setae. **Hypomeron:** Hypomeral disc convex. Surface anteriorly smooth, otherwise covered with small, rounded punctures sparsely and irregularly distributed, separated by 5–8 times one puncture diameter; each puncture bearing a moderately long, pale-yellow seta. **Prosternum:** Disc with two anterior, longitudinal sulci. **Mesoventrite:** Disc

flat in the middle. Surface with few small, rounded punctures separated by 1–2 times one puncture diameter, each puncture bearing a short, slender pale-yellow seta. **Mesepimerum and metepisternum:** Surfaces with scattered small, rounded punctures, each puncture bearing a short, slender pale-yellow seta. **Metaventricle:** Disc flat and densely setose in the central area. Surface of central area covered with small, rounded punctures densely and irregularly distributed, separated by less than one time one puncture diameter, each bearing a moderately long, slender pale-yellow seta. Surface of lateral arms similar to that of central area, but with evidently sparser punctures, thus less setose, and smooth externally. **Hind wings:** Apical edge rounded;  $RP_3$  y  $RA_4+RP_1$  apically parallel; MSP projected toward the wing margin;  $MP_{3+4}$  short, not projected apically. **Legs:** Femora subequal in length to their respective tibiae; surface almost completely smooth, with scattered small, rounded punctures, each bearing a short,

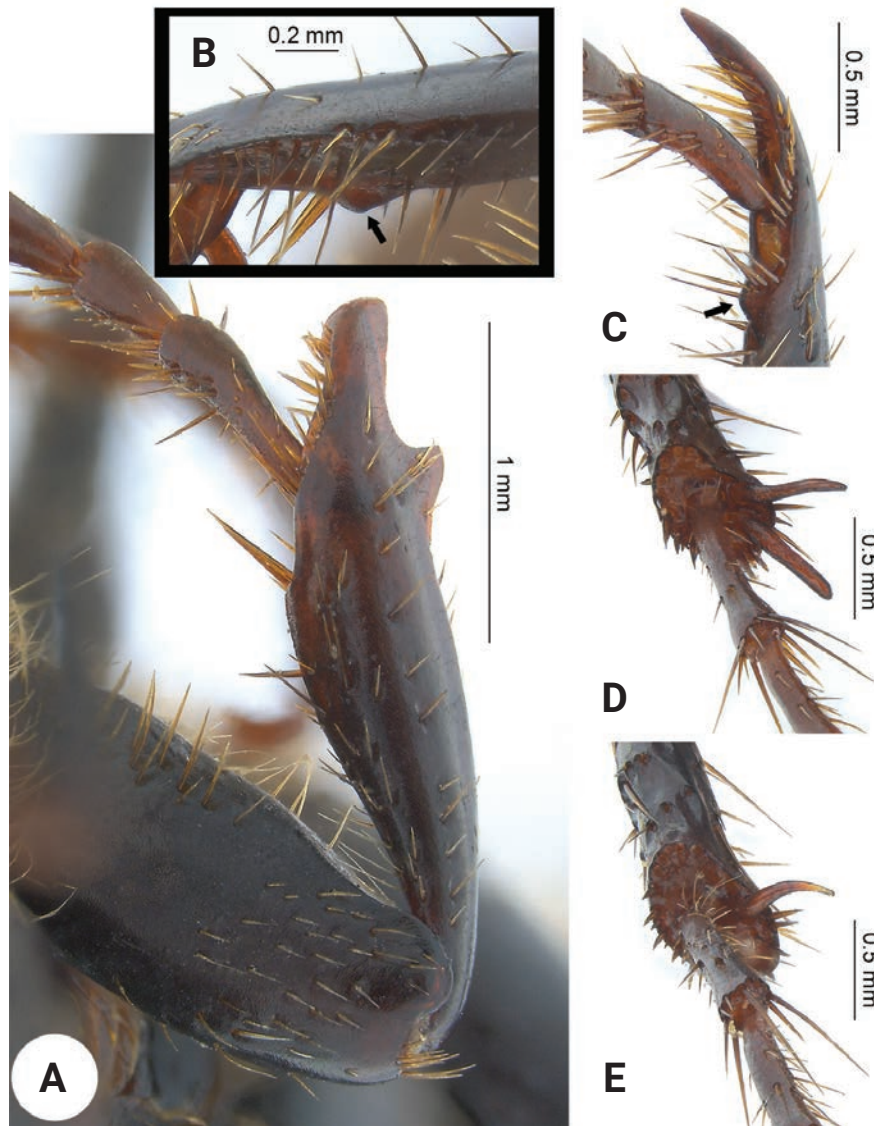


**Figure 4.** *Manodactylus paramicola* sp. nov., male holotype. **A.** Protibia in dorsal view; **B.** Detail of the downward projection of the inner angle of protibia; **C.** Apex of protibia; **D.** Apex of mesotibia; **E.** Apex of metatibia. Black arrows point to downward projection of the inner angle of protibia.

slender pale-yellow seta; anterior and posterior border moderately setose in the basal third. Tibiae shorter than their respective tarsi. Tarsal claws bifid, ventral part slightly thicker, shorter, and more downward curved than dorsal part; each claw over the basal third with an acute triangular tooth. Protibia along the outer edge with two teeth distributed in the apical third, apical tooth larger than basal; inner angle slightly projected downward; protibia gradually widening from base to apex but narrowing from the inner edge in the apical third; surface smooth except for a few scattered punctures and a regular row of small, rounded punctures separated by 2–4 times one puncture diameter, each puncture bearing a short, slender pale-yellow seta; anterior and posterior borders with scattered moderately long, slender pale-yellow setae; lacking apical spur. Protarsomere 1 subequal to the combined length of protarsomeres 2–3, protarsomere 2–4 subequal in length, and protarsomere 5 subequal to the combined

length of protarsomeres 3–4; internal face of protarsomeres with few scattered short to moderately long, thick reddish-yellow seta. Mesotibiae with a more or less evident ventral transverse carina near the apical third of its length; surface with few small, rounded punctures sparsely distributed, each bearing a short or moderately long, thick reddish-yellow seta; apex over the ventral surface with intercalate extremely short and short, thick reddish-yellow spinules; two subequal apical spurs present, the dorsal spur slightly longer than the ventral, both about three quarters of the length of the mesotarsomere 1. Mesotarsomere 1 slightly longer than mesotarsomere 2, mesotarsomere 2 slightly longer than mesotarsomere 3, mesotarsomeres 3 and 4 subequal in length, and mesotarsomere 5 slightly shorter than the combined length of the mesotarsomere 3–4; internal face of mesotarsomeres with a few scattered short to moderately long, thick reddish-yellow seta. Metatibiae surface with a few

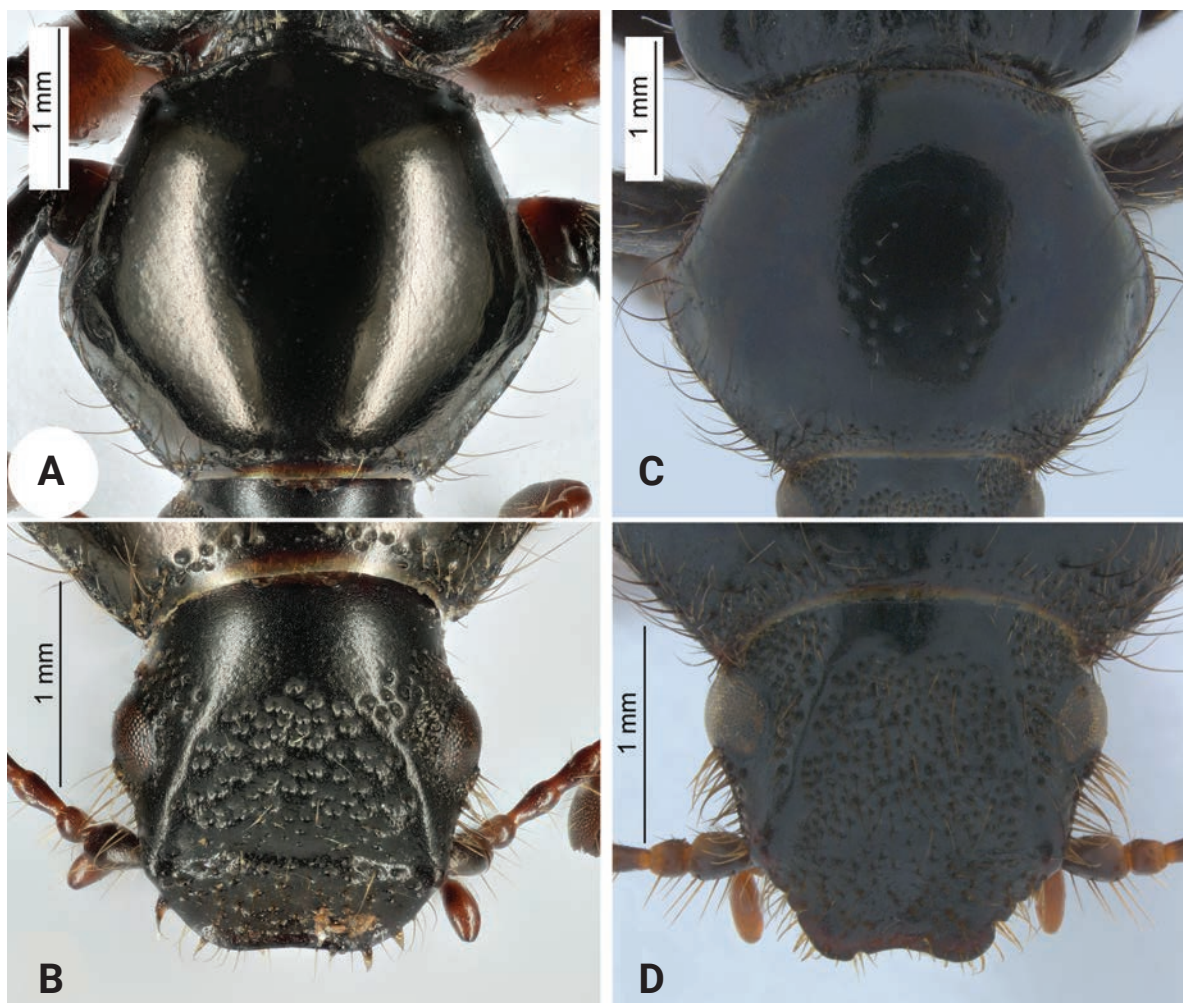


**Figure 5.** *Manodactylus* species. **A, B.** *Macroductylus gaujoni* Ohaus, 1909, male neotype = *Manodactylus gaujoni* Moser, 1919, male lectotype; **C, D.** *Manodactylus paramicola* sp. nov., male holotype. **A, C.** Pronotum in dorsal view; **B, D.** Head in dorsal view.

small, rounded punctures sparsely distributed, each bearing a short or moderately long, thick reddish-yellow seta; apex over the ventral surface with intercalate extremely short and short, thick reddish-yellow spinules; one apical spur present, about a half of the length of the metatarsomere 1. Metatarsomere 1 slightly longer than metatarsomere 2, metatarsomere 2 slightly longer than metatarsomere 3, metatarsomeres 3 slightly longer than metatarsomere 4, and metatarsomere 5 slightly shorter than the combined length of the metatarsomere 3–4; internal face of metatarsomeres with few scattered short or moderately long, thick reddish-yellow seta (thicker than the slender setae mentioned, but not as spine-like setae). **Abdomen:** Abdominal ventrites 2–5 densely setose medially, surface covered with small, rounded punctures densely and irregularly distributed, separated by less than 1 times one puncture diameter, each bearing a moderately long, slender pale-yellow seta, some few bearing longer setae; surface laterally similar, but with evidently sparser punctures, thus sparsely setose; anterior border of each of these ventrites densely setose. Ventrite 5 longer than the others. Ventrite 6 almost smooth, with few small, rounded punctures bearing a long, slender pale-yellow seta; anterior

or border with moderately long, thick reddish-yellow setae. Pygidium vertical, strongly convex; surface with few small, rounded punctures sparsely and irregularly distributed, separated by 2–5 times one puncture diameter, each bearing a short, slender pale-yellow seta; setae convergent over the longitudinal central area, and punctures sparser externally. **Genitalia:** Hemisternite 9 covered with small, rounded punctures densely and irregularly distributed, separated by one time one puncture diameter; anterior edge truncate and slightly emarginate medially. Spiculum lateral arms short, the spiculum gastrale around two times the length of a spiculum lateral arm, and the cranial part with apex rounded. Phallobase cylindrical, 2.5 times the length of parameres. Parameres fused at the base, short, apically curved and slightly downward, with the apex rounded; the inner edge of each paramere sinuous, with an evident, strong indentation in the basal third.

**Female.** Unknown.

**Diagnosis.** *Manodactylus paramicola* shares with *M. gaujoni* the overall appearance (see Diagnosis for *M. gaujoni*). *Manodactylus paramicola* can be distinguished from *M. gaujoni* by having the femora, tibiae, and tarsi very dark brown; clypeus emarginate medially,

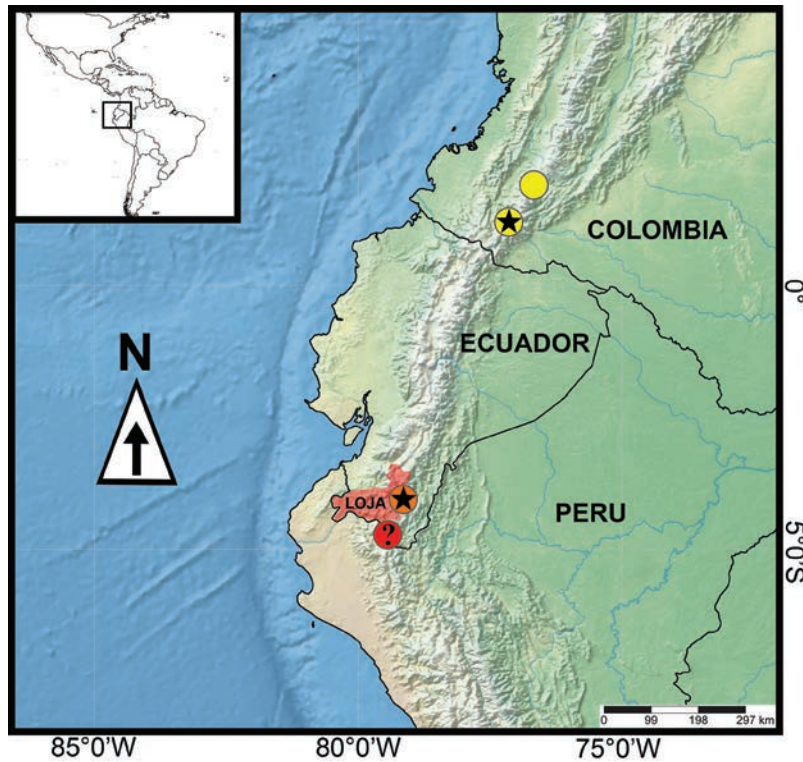


**Figure 6.** Distribution map of *Manodactylus*. *Macroductylus gaujoni* Ohaus, 1909, male neotype = *Manodactylus gaujoni* Moser, 1919, male lectotype. A star is used for approximate holotype locality when possible; '?' to denote unverified records; red color is used for *Manodactylus gaujoni* Moser, 1919; orange color is used for *Macroductylus gaujoni* Ohaus, 1909; yellow color is used for *Manodactylus paramicola* sp. nov.

with borders on each side of medial emargination narrowly rounded, slightly angulated and upturned; the subpentagonal area formed by clypeus and frons concave; the pronotum also with small, rounded, setigerous punctures on the borders but few also present medially in the disc, separated by 3–5 times one puncture diameter; each elytral stria deep, with a regular row of small, rounded punctures distanced by 3–5 times one puncture diameter; and interstriae strongly convex.

**Etymology.** Epithet compound, from the Spanish noun *Páramo* for Paramo ecosystem, and the Latin suffix *-icola* meaning inhabitant. The specific name means 'inhabitant of Paramo', in allusion to the ecosystem where the specimens were collected.

**Distribution.** Colombia, departments of Cauca and Nariño (Fig. 6). Three of the specimens were collected in Pasto, department of Nariño, with the information 'Paramo ground' (*Suelo paramo*) on the label, referring to the ecosystem in which the specimens were found. The fourth specimen was collected in San Sebastián, a small, populated place located less than 10 kilometers from the Páramo de las Papas in the department of Cauca.

## Acknowledgements

Thanks to the curators and staff of the institutions where studied type specimens are deposited, especially to B. Jaeger (MFNB) for supplying photographs of the lecto-

type of *Manodactylus gaujoni* used in this manuscript. Also, we thank the reviewers, A. Ballerio and the editor for comments on previous versions of this manuscript. Special thanks to L. L. Vargas-Longas and W. Bayfield-Farrell for their comments and language revision of the manuscript. Also, we thank Diego E. Martínez R., who collected, and shared with us, a paratype.

## References

- Fuhrmann J, Vaz-de-Mello FZ (2017) Macroductylini (Coleoptera, Scarabaeidae, Melolonthinae): Primary types of type species and taxonomic changes to the generic classification. *European Journal of Taxonomy* 350(350): 1–71. <https://doi.org/10.5852/ejt.2017.350>
- Katovich K (2008) A generic-level phylogenetic review of the Macroductylini (Coleoptera: Scarabaeidae: Melolonthinae). *Insecta Mundi* 23: 1–78.
- Moser J (1919) Beitrag zur Kenntnis der Melolonthiden (Col.). (IX). *Stettiner Entomologische Zeitung* 80: 3–64.
- Ohaus F (1909) Bericht über eine entomologische Studienreise in Südamerika. *Stettiner Entomologische Zeitung* 70: 3–139. <https://doi.org/10.1002/mmnd.48019090312>
- Saavedra Albuquerque D, Vaz de Mello F, Ugaz Cherre A, Pacherra Timaná C (2015) Coleópteros (Coleoptera: Scarabaeidae) de los bosques de niebla, Ramos y Chin Chin, Ayabaca-Huancabamba, Piura-Perú. *INDES* 3(1): 108–116. <https://doi.org/10.25127/indes.20153.138>
- Shorthouse DP (2010) SimpleMapppr, an online tool to produce publication-quality point maps. <https://www.simplemapppr.net>



# Revision of the genus *Kunungua* (Hemiptera, Heteroptera, Miridae) with descriptions of three new species and new generic synonymy

Darya S. Bolshakova<sup>1</sup>, Fedor V. Konstantinov<sup>1,2</sup>

<sup>1</sup> Zoological Institute, Russian Academy of Sciences, Universitetskaya nab. 1, St. Petersburg 199034, Russia

<sup>2</sup> National Museum of Natural History, Bulgarian Academy of Sciences, 1 Tsar Osvoboditel Blvd, 1000 Sofia, Bulgaria

<https://zoobank.org/74733A0A-16A8-4FBB-9690-E822DA98FC4B>

Corresponding author: Fedor V. Konstantinov (fkonstantinov@gmail.com)

Academic editor: Dávid Rédei ♦ Received 11 March 2024 ♦ Accepted 22 May 2024 ♦ Published 31 July 2024

## Abstract

This study provides a taxonomic revision of the genus *Kunungua* Carvalho, 1951 (Hemiptera, Heteroptera, Miridae, Bryocorinae, Eccritotarsini) with the description of three new species, *K. atramentomaculata* sp. nov., *K. gemina* sp. nov., and *K. ornata* sp. nov. Revised diagnoses for the genus and three additional species are given, along with a key to the species. Habitus photographs, illustrations of male genitalic structures, and distributional information are provided for each species. The placement of *Kunungua* within the *Prodromus* group of genera is discussed. The genus *Duducoris* Odhiambo, 1962 is recognised as a new junior subjective synonym of *Prodromus* Distant, 1904, resulting in new combinations for the five species contained in the subsumed genus. *Kunungua pallida* Linnavuori, 1975 is excluded from the genus *Kunungua* and treated as a species of uncertain generic placement.

## Key Words

Central Africa, morphology, taxonomy, distribution

## Introduction

This paper focuses on the small African plant bug genus *Kunungua* Carvalho, 1951 (Hemiptera, Heteroptera, Miridae, Bryocorinae, Eccritotarsini). Bryocorines include more than 1000 species assigned to ca. 200 genera and have a principally tropical distribution, with a relatively few taxa inhabiting temperate regions (Konstantinov et al. 2018). Representatives of the group exhibit fascinating structural diversity not only in general appearance, but also in characters which are generally uniform across other tribes of plant bugs, e.g., in thoracic, pretarsal, and genitalic structures. Four tribes are currently recognised within the subfamily, with Eccritotarsini comprising more than 60 percent of all described species of the Bryocorinae (Konstantinov and Knyshov 2015; Namyatova et al. 2016).

While the majority of eccritotarsine taxa are confined to the New World, the existing data suggest an Oriental origin for this clade (Konstantinov et al. 2018). No at-

tempt has been made to infer phylogenetic relationships within the Eccritotarsini on a global scale. The only cladistic analysis within the group was that of Stonedahl (1988) for a group of six genera from the Indo-Pacific and West Africa. However, according to the results of our preliminary analysis, several apparently monophyletic lineages could be tentatively recognised within the tribe.

One of these groups, which we refer to as the *Prodromus* group of genera, is distinguished by a unique modification of the aedeagus which takes the form of a simple sclerotised tubule. Notably, the outer section (phallosoma) and the inner section (endosoma) of the aedeagus in the genera of *Prodromus* complex lack a clear demarcation. While in other bugs, the endosoma is membranous and eversible, in the genera of the *Prodromus* complex, it remains consistently everted and sclerotised. Additionally, the ductus seminis in this group remains entirely membranous (Konstantinov and Zinovjeva 2016; Konstantinov et al. 2018) and terminates with a secondary gonopore which lacks ornamentation. Some members of this group

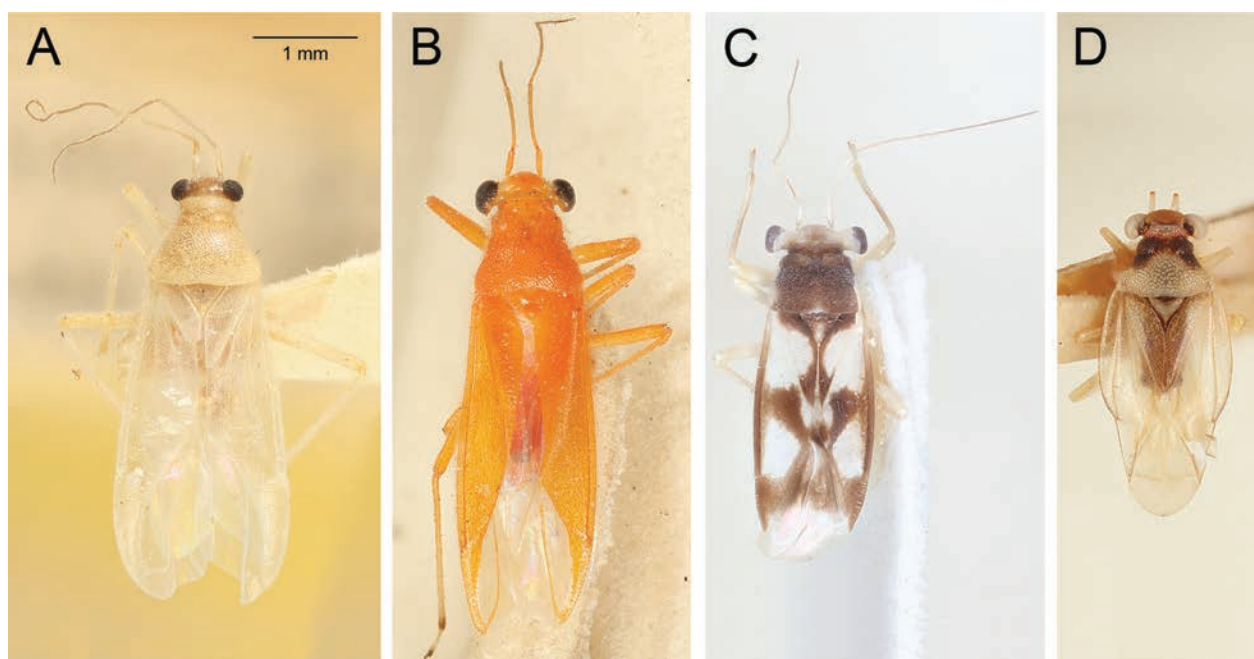


**Figure 1.** Species of *Prodrumus* group, dorsal view. **A.** *Myiocapsus mindanao*, ZISP\_ENT 00013938; **B.** *Stenopterocoris nigricornis*, ZISP\_ENT 00013937; **C.** *Stylopomiris malayensis*, ZISP\_ENT 00013939; **D.** *Zikaniola elegans*, ZISP\_ENT 00013939.

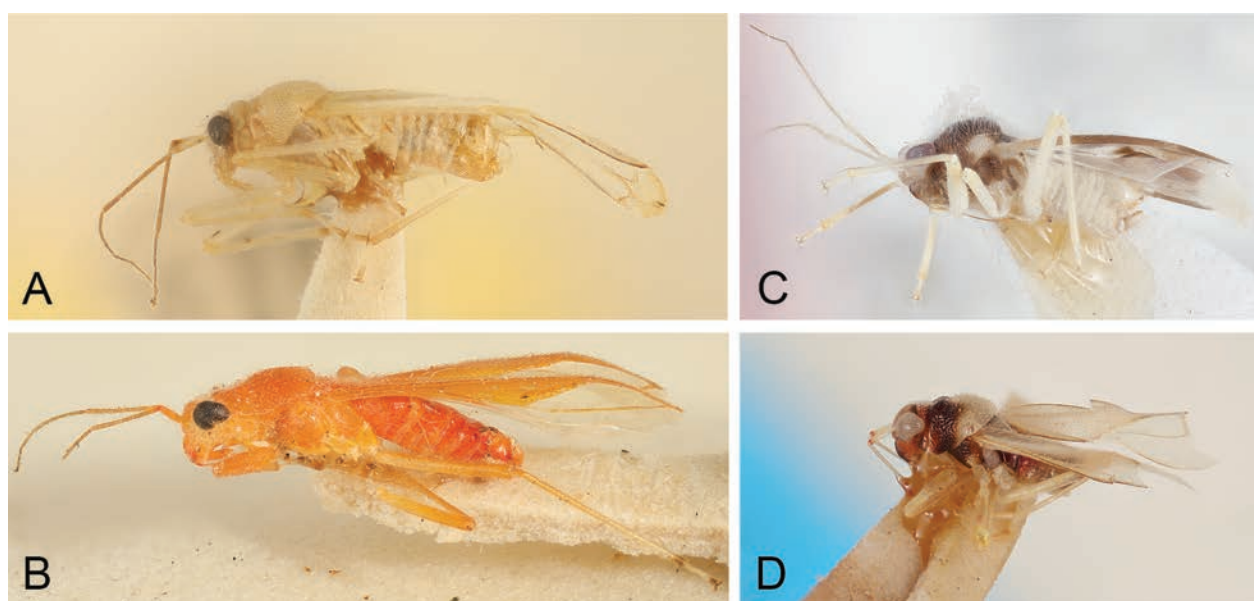


**Figure 2.** Species of *Prodrumus* group species, lateral view. **A.** *Myiocapsus mindanao*, ZISP\_ENT 00013941; **B.** *Stenopterocoris nigricornis*, ZISP\_ENT 00013937; **C.** *Stylopomiris malayensis*, ZISP\_ENT 00013939; **D.** *Zikaniola elegans*, ZISP\_ENT 00013939.

exhibit small, non-retractable membranous lobes at the apex of the aedeagus. In addition, taxa belonging to the *Prodrumus* group typically exhibit substylate eyes, a deeply punctate pronotum, a generally elongated body with long and comparatively thin legs, and a broad head in dorsal view.

The genera comprising the *Prodrumus* group are: *Ambunticoris* Carvalho, 1981 (Konstantinov and Zinovjeva 2016: figs 1–13), *Duducoris* Odhiambo, 1962 (Fig. 3 F–H), *Ernestinus* Distant, 1911 (Yasunaga and Ishikawa 2016: figs 1–7), *Frontimiris* Carvalho, 1981 (Cassis et al. 2016: fig. 1), *Grossicoris* Carvalho, 1973 (Carvalho 1973: fig.

1), *Kunungua* (Fig. 6), *Myiocapsus* Poppius, 1914 (Figs 1A, 2A), *Namyatovia* Yeshwanth & Konstantinov, 2021 (Yeshwanth and Konstantinov 2021: figs 3D–F, 4A–C), *Prodrumus* Distant, 1904 (Fig. 3A–E), *Sinervus* Stål, 1860 (Henry and Howard 2016: figs 1–16), *Sinervaspartus* Henry & Howard, 2016 (Henry and Howard 2016: figs 17–20), *Spartacus* Distant, 1884 (Alvarez-Zapata et al. 2022: fig. 37), *Stenopterocorisca* Carvalho, 1981 (Carvalho 1981: fig. 183), *Stonedahlia* Yeshwanth & Konstantinov, 2021 (Yeshwanth and Konstantinov 2021: fig. 4D–F), *Stylopomiris* Stonedahl, 1986 (Figs 1C, 2C), *Taricoris* Carvalho, 1981 (Carvalho 1981: figs 187, 188), *Thaumastomiris* Kirkaldy,

1902 (Yeshwanth and Konstantinov 2021: figs 9G–J, 10), and *Zikaniola* Carvalho, 1946 (Figs 1D, 2D).

This lineage is broadly distributed, found primarily in tropical regions, extending from the southern part of North America and the Neotropics to the Philippines, New Guinea, and northern Australia. Three genera from this group, *Duducoris*, *Kunungua*, and *Prodromus*, are known to inhabit the Ethiopian Region. Among these, *Duducoris* and *Kunungua* are restricted to this region, while *Prodromus* has a more widespread distribution that includes the Oriental Region.

*Kunungua* was established by Carvalho (1951) to comprise two African species with a wide head and stylate eyes, namely *K. boxi* Carvalho, 1951 from Ghana, the type species of the genus and *K. cinnamomea* Carvalho, 1951 from Congo. Since then, two more species have been described, *K. ukerewensis* Odhiambo, 1962 from Tanganyika and *K. pallida* Linnavuori, 1975, the latter being known from a single female collected in Equatoria, Sudan. No new information regarding the genus has been published since then, spanning nearly half a century.

In this paper, we provide redescriptions for all known *Kunungua* species and descriptions of three new species. We propose the exclusion of *K. pallida* from *Kunungua* due to the presence of a set of characters atypical for the genus and present a key to all *Kunungua* spp. A notable feature for distinguishing *Kunungua* species is their specific colour patterns with distinct bands. Additionally, the shape of the parameres plays a crucial role in distinguishing species that may appear habitually similar.

While working on the updated diagnosis of the genus, a thorough analysis of morphological characters was conducted to distinguish *Kunungua* from the two most closely related genera, viz. *Prodromus* and *Duducoris*. Our results led to the conclusion that *Kunungua* warranted recognition as a separate genus and no distinct differences were observed between *Duducoris* with *Prodromus*. We propose that the former genus be treated as a junior synonym of *Prodromus*. A detailed discussion of this matter and a revised diagnosis for *Prodromus* are also provided.

**Table 1.** Measurements (mm). Abbreviations. Pronot. – width and length of pronotum at base and along midline, respectively, Head length – distance between apex of clypeus and the highest point of vertex, AI – length of antennal segment I, Pr. disc – length of posterior part of pronotum behind calli measured at midline.

Specimens	Width					Length							
	Head	Vertex	Pronot.	Calli	Collar	Head	AI	Pronot.	Pr. disc	Calli	Collar	Body	
<i>Kunungua atramentomaculata</i> sp. nov.													
♀, N = 1	0.95	0.58	1.14	0.61	0.48	0.26	0.45	0.95	0.63	0.18	0.15	4.20	
<i>Kunungua boxi</i> Carvalho, 1951													
♂, N = 1	0.88	0.50	0.92	–	–	–	0.50	1.80	–	–	–	3.53	
♀, N = 1	0.74	0.45	0.86	–	–	–	0.38	1.63	–	–	–	3.20	
<i>Kunungua cinnamomea</i> Carvalho, 1951													
♂, N = 3	Mean	0.91	0.46	1.10	0.56	0.48	0.35	0.45	1.09	0.66	0.27	0.16	3.98
	Min	0.83	0.43	0.99	0.53	0.45	0.33	0.43	0.98	0.56	0.24	0.15	3.50
	Max	0.95	0.48	1.18	0.60	0.50	0.38	0.48	1.18	0.73	0.30	0.18	4.30
♀, N = 2	Mean	0.93	0.45	1.15	0.57	0.48	0.33	0.46	1.10	0.65	0.28	0.17	4.05
	Min	0.88	0.45	1.10	0.56	0.46	0.33	0.45	1.03	0.60	0.26	0.16	3.70
	Max	0.98	0.45	1.20	0.58	0.50	0.33	0.48	1.18	0.70	0.30	0.18	4.40
<i>Kunungua gemina</i> sp. nov.													
♀, N = 3	Mean	0.81	0.48	1.04	0.51	0.43	0.25	0.48	0.90	0.59	0.18	0.13	4.22
	Min	0.80	0.48	1.03	0.50	0.43	0.24	0.48	0.85	0.55	0.18	0.13	4.20
	Max	0.83	0.49	1.05	0.53	0.44	0.25	0.48	0.94	0.63	0.18	0.14	4.25
<i>Kunungua ornata</i> sp. nov.													
♂, N = 2	Mean	0.99	0.58	1.14	0.61	0.49	0.30	0.55	1.04	0.70	0.19	0.15	4.03
	Min	0.98	0.56	1.14	0.60	0.49	0.28	0.53	1.03	0.70	0.18	0.15	3.90
	Max	1.00	0.59	1.15	0.63	0.49	0.33	0.58	1.05	0.70	0.20	0.15	4.15
<i>Kunungua ukerewensis</i> Odhiambo, 1962													
♂, N = 3	Mean	0.80	0.45	0.97	0.55	0.44	0.24	0.43	0.90	0.56	0.19	0.15	3.58
	Min	0.78	0.45	0.95	0.53	0.43	0.23	0.41	0.89	0.55	0.18	0.15	3.55
	Max	0.81	0.46	0.98	0.58	0.45	0.25	0.44	0.93	0.58	0.20	0.15	3.60
♀, N = 3	Mean	0.82	0.45	1.03	0.61	0.46	0.25	0.43	0.91	0.58	0.18	0.15	3.77
	Min	0.80	0.45	1.00	0.60	0.44	0.25	0.40	0.88	0.55	0.18	0.14	3.70
	Max	0.84	0.46	1.05	0.63	0.48	0.25	0.48	0.95	0.63	0.19	0.15	3.80
<i>Kunungua ukerewensis</i> Odhiambo, 1962 (light)													
♂, N = 3	Mean	0.83	0.46	1.00	0.56	0.46	0.24	0.45	0.91	0.58	0.19	0.14	3.72
	Min	0.80	0.46	0.98	0.55	0.45	0.23	0.45	0.86	0.55	0.16	0.13	3.60
	Max	0.84	0.46	1.05	0.58	0.48	0.25	0.45	1.00	0.64	0.21	0.15	3.90
♀, N = 3	Mean	0.82	0.47	1.03	0.58	0.47	0.23	0.45	0.93	0.59	0.19	0.15	3.75
	Min	0.81	0.45	0.99	0.58	0.46	0.20	0.44	0.90	0.58	0.18	0.15	3.70
	Max	0.83	0.48	1.05	0.59	0.48	0.28	0.48	0.95	0.61	0.20	0.15	3.80

Specimens	Width					Length							
	Head	Vertex	Pronot.	Calli	Collar	Head	AI	Pronot.	Pr. disc	Calli	Collar	Body	
<i>Prodromus abuyog</i> Stonedahl, 1988													
♂, N = 3	Mean	0.90	0.40	1.16	0.74	0.52	0.40	0.65	0.87	0.48	0.26	0.13	5.23
	Min	0.90	0.39	1.13	0.70	0.50	0.40	0.63	0.83	0.45	0.25	0.13	5.20
	Max	0.90	0.40	1.18	0.76	0.53	0.40	0.68	0.90	0.50	0.28	0.13	5.30
♀, N = 1		0.95	0.43	1.25	0.76	0.53	0.43	0.65	0.90	0.48	0.30	0.13	5.30
<i>Prodromus aethiopicus</i> (Poppius, 1910)													
♂? N = 1		0.76	0.36	0.99	0.73	0.55	0.48	0.53	0.78	0.38	0.25	0.15	4.20
♀, N = 1		0.75	0.38	1.01	0.75	0.58	0.48	0.61	0.85	0.43	0.30	0.13	5.10
<i>Prodromus angulatus</i> (Odhiambo, 1962)													
♂, N = 3	Mean	0.77	0.38	1.01	0.72	0.57	0.48	0.57	0.75	0.35	0.26	0.13	4.52
	Min	0.75	0.36	0.98	0.70	0.55	0.45	0.55	0.73	0.33	0.25	0.13	4.30
	Max	0.78	0.40	1.03	0.74	0.58	0.49	0.58	0.78	0.38	0.28	0.15	4.65
♀, N = 3	Mean	0.75	0.37	0.97	0.70	0.56	0.45	0.52	0.69	0.29	0.28	0.13	4.33
	Min	0.68	0.33	0.85	0.63	0.50	0.43	0.46	0.59	0.26	0.23	0.10	3.90
	Max	0.79	0.40	1.03	0.75	0.60	0.48	0.58	0.76	0.31	0.30	0.15	4.60
<i>Prodromus apoensis</i> Stonedahl, 1988													
♂, N = 1		0.75	0.35	1.06	0.68	0.50	0.40	0.55	0.78	0.43	0.23	0.13	4.70
♀, N = 1		0.73	0.35	0.98	0.60	0.48	0.38	0.55	0.73	0.39	0.24	0.10	4.50
<i>Prodromus clypeatus</i> Distant, 1904													
♂, N = 1		0.83	0.40	1.25	0.73	0.53	0.40	0.53	0.76	0.44	0.20	0.13	4.85
♀, N = 1		0.80	0.40	1.18	0.68	0.50	0.34	0.50	0.73	0.38	0.23	0.13	4.55
<i>Prodromus ibbaicus</i> Linnavuori, 1975													
♂, N = 3	Mean	0.68	0.33	1.01	0.64	0.51	0.35	0.41	0.68	0.34	0.23	0.12	4.47
	Min	0.66	0.33	0.98	0.63	0.50	0.35	0.40	0.65	0.30	0.21	0.10	4.30
	Max	0.69	0.33	1.04	0.65	0.53	0.35	0.43	0.70	0.36	0.25	0.13	4.60
♀, N = 3	Mean	0.66	0.32	1.00	0.65	0.51	0.35	0.39	0.68	0.33	0.23	0.12	4.37
	Min	0.65	0.31	0.95	0.63	0.49	0.34	0.38	0.65	0.33	0.23	0.10	4.10
	Max	0.68	0.33	1.05	0.68	0.53	0.35	0.40	0.73	0.35	0.25	0.13	4.60
<i>Prodromus incisus</i> (Odhiambo, 1962)													
♂, N = 3	Mean	0.85	0.44	1.13	0.78	0.58	0.45	0.47	0.67	0.31	0.24	0.12	4.82
	Min	0.83	0.43	1.13	0.75	0.58	0.43	0.45	0.65	0.30	0.23	0.10	4.75
	Max	0.88	0.45	1.15	0.80	0.59	0.48	0.49	0.68	0.33	0.25	0.13	4.90
♀, N = 1		0.84	0.43	1.04	0.74	0.58	0.45	0.49	0.65	0.28	0.28	0.10	4.70
<i>Prodromus kawandanus</i> Odhiambo, 1962													
♂, N = 3	Mean	0.68	0.33	0.96	0.58	0.47	0.35	0.43	0.66	0.32	0.22	0.12	4.02
	Min	0.68	0.33	0.94	0.58	0.46	0.34	0.43	0.65	0.30	0.21	0.10	4.00
	Max	0.69	0.34	0.99	0.60	0.48	0.35	0.44	0.68	0.34	0.23	0.14	4.05
♀, N = 3	Mean	0.67	0.34	0.94	0.59	0.45	0.35	0.43	0.65	0.33	0.20	0.12	4.05
	Min	0.66	0.34	0.93	0.58	0.45	0.33	0.43	0.65	0.31	0.20	0.11	4.00
	Max	0.68	0.35	0.98	0.60	0.46	0.38	0.44	0.66	0.34	0.21	0.13	4.10
<i>Prodromus melanotus</i> Carvalho, 1951													
♂, N = 3	Mean	0.69	0.33	0.96	0.58	0.45	0.35	0.58	0.73	0.46	0.16	0.10	3.83
	Min	0.69	0.33	0.95	0.55	0.45	0.34	0.58	0.73	0.43	0.14	0.10	3.80
	Max	0.70	0.35	0.99	0.60	0.45	0.36	0.60	0.73	0.49	0.20	0.10	3.90
♀, N = 1		0.73	0.38	1.00	0.60	0.45	0.34	0.60	0.79	0.48	0.21	0.10	3.90
<i>Prodromus oculatus</i> (Poppius, 1912)													
♂, N = 3	Mean	0.82	0.39	1.14	0.64	0.52	0.38	0.73	0.88	0.51	0.24	0.13	5.13
	Min	0.81	0.38	1.09	0.63	0.51	0.35	0.73	0.78	0.40	0.23	0.10	4.80
	Max	0.83	0.40	1.18	0.65	0.53	0.40	0.75	0.95	0.58	0.25	0.15	5.45
♀, N = 1		0.79	0.36	1.15	0.64	0.53	0.38	0.70	0.85	0.50	0.20	0.15	5.25
<i>Prodromus pilosus</i> (Odhiambo, 1962)													
♀, N = 3	Mean	0.76	0.40	1.17	0.77	0.58	0.48	0.63	0.87	0.43	0.29	0.15	5.37
	Min	0.74	0.39	1.15	0.75	0.55	0.48	0.63	0.83	0.40	0.28	0.13	5.20
	Max	0.78	0.40	1.20	0.78	0.60	0.48	0.65	0.90	0.45	0.30	0.18	5.50
<i>Prodromus thaliae</i> China, 1944													
♂, N = 3	Mean	0.70	0.35	0.93	0.56	0.44	0.32	0.43	0.70	0.43	0.19	0.09	3.93
	Min	0.68	0.35	0.93	0.55	0.43	0.31	0.43	0.69	0.41	0.18	0.08	3.80
	Max	0.73	0.35	0.95	0.58	0.45	0.33	0.45	0.73	0.44	0.20	0.10	4.10
♀, N = 3	Mean	0.67	0.35	0.93	0.57	0.43	0.32	0.44	0.71	0.41	0.19	0.11	4.05
	Min	0.66	0.35	0.90	0.55	0.43	0.30	0.43	0.68	0.38	0.18	0.10	4.00
	Max	0.68	0.35	0.98	0.58	0.45	0.33	0.45	0.75	0.45	0.20	0.13	4.10

## Materials and methods

### Specimens

About 350 specimens of *Kunungua*, *Prodromus*, and *Duducoris* were examined. Unique Specimen Identifiers (USIs) were attached to each specimen and are available in the material examined section. Additional label information can be accessed through the Planetary Biodiversity Inventory (PBI) Plant Bug locality database: <http://research.amnh.org/pbi/heteropterasespeciespage>. Most specimens used in this study, including holotypes of new species, are kept at the Royal Museum for Central Africa, Tervuren, Belgium (MRAC), with some specimens borrowed from the following collections:

- AMNH** American Museum of Natural History, New York (R.T. Schuh and R. Salas);  
**NHM** Natural History Museum, London (M. Webb);  
**NMWC** National Museum of Wales, Cardiff (M. R. Wilson);  
**ZISP** Zoological Institute, Russian Academy of Sciences, St. Petersburg;  
**USNM** Smithsonian National Museum of Natural History (T. J. Henry).

### Measurements

Measurements were taken using an eyepiece micrometer from one to six specimens, depending on the quantity of intact specimens available. On average, three males and three females were measured for each species (Table 1). The measurements include body length, head length and width, width of vertex, length of antennal segment I, length and width for the pronotal collar, calli, and disk. All measurements are in millimetres.

### Microscopy and illustrations

Observations and measurements were made with a Nikon SMZ 1500 stereomicroscope. Digital colour images of all specimens were taken using Canon EOS 5D Mark IV equipped with a Canon MP-E 65 mm f/2.8 1–5× Macro lens and Twin-Lite MT-26EX-RT flash. Partially focused images of each specimen or structure were stacked using the Helicon Focus 7.5.4 software. Dissections of genitalia were made following the methodology in Kerzhner and Konstantinov (1999). Images of the genitalic structures were made with a Leica DM 2500 microscope equipped with a drawing tube.

### Terminology

The terminology used in this paper follows Schuh and Weirauch (2020) except for male (Konstantinov 2003, 2019) and female (Schwartz 2011) genitalia.

## Results

### Taxonomy

#### *Prodromus* Distant, 1904

Figs 3–5

*Prodromus* Distant, 1904: 436. Type species by original designation: *Prodromus subflavus* Distant, 1904.

*Prodromopsis* Poppius, 1911: 4. Type species by original designation: *Prodromus cuneatus* Distant, 1909. Synonymised with *Sinervus* Stål, 1860 by Carvalho (1948: 191), with *Prodromus* by Odhiambo (1962: 248) and Stonedahl (1988: 70).

*Duducoris* Odhiambo, 1962: 264. Type species by original designation: *Duducoris incisus* Odhiambo, 1962. New synonym.

*Prodromus*: Odhiambo (1962: 248) (redescription, comparative discussion, key to spp.), Carvalho (1981: 80) (description, discussion, key to spp.), Stonedahl (1988: 53) (synonymy, redescription, discussion, phylogeny, key to spp.).

*Prodromopsis*: Carvalho (1948: 191) (synonymy), Odhiambo (1962: 248) (synonymy), Carvalho (1981: 80) (as valid genus), Stonedahl (1988: 70) (synonymy).

**Revised diagnosis.** Body elongate; head about twice as wide as long (Fig. 3); antennal segment I 1.1–2.0 times as long as head, with basal one-half to one-fourth distinctly narrowed (Fig. 5); eyes kidney-shaped, occasionally elongate; vertex with medial sulcus; calli usually distinctive, posterior lobe of pronotum from flattened to convex (Fig. 4); pronotum densely punctate; posterior margin of pronotal disk from straight to deeply emarginate (Fig. 3); scutellum equilateral.

**Hosts.** Host plant associations are poorly known. *Prodromus clypeatus* Distant, 1904 and *P. oculatus* (Poppius, 1912) have been reported to feed on banana (Musaceae) and young *Musa* leaves (Odhiambo 1962). *Prodromus melanonotus* Carvalho, 1951 and *P. thaliae* China, 1944 have been documented as inhabitants of *Marantochloa* and *Thalia* (Marantaceae) (Stonedahl 1988).

**Distribution.** Paleotropical.

**Discussion.** *Prodromus* was established by Distant (1904), with *P. subflavus* designated as the type species. Three species, *P. subflavus*, *P. clypeatus*, and *P. subviridis* Distant, 1904 were originally described within *Prodromus* (Distant, 1904) with 23 additional species subsequently added to the genus. The original diagnosis of *Prodromus* was based on the following combination of characters: a broad head with pedunculate eyes and a longitudinal sulcus on the vertex, antennal segment I longer than the head, segment II approximately 1.5 times longer than segment I, pronotum having a narrow collar, constriction behind calli, and swollen, coarsely punctate disk with a concave posterior margin, and cuneus longer than broad.

Poppius (1911) erected a monotypic genus *Prodromopsis* to accommodate *Prodromus cunealis* Distant, 1907 based on the more vertical head with projecting clypeus, longer antennal segments III and IV, long and narrow cuneus, and short vestiture. Carvalho (1957) synonymised *Prodromopsis*, within which nine species were

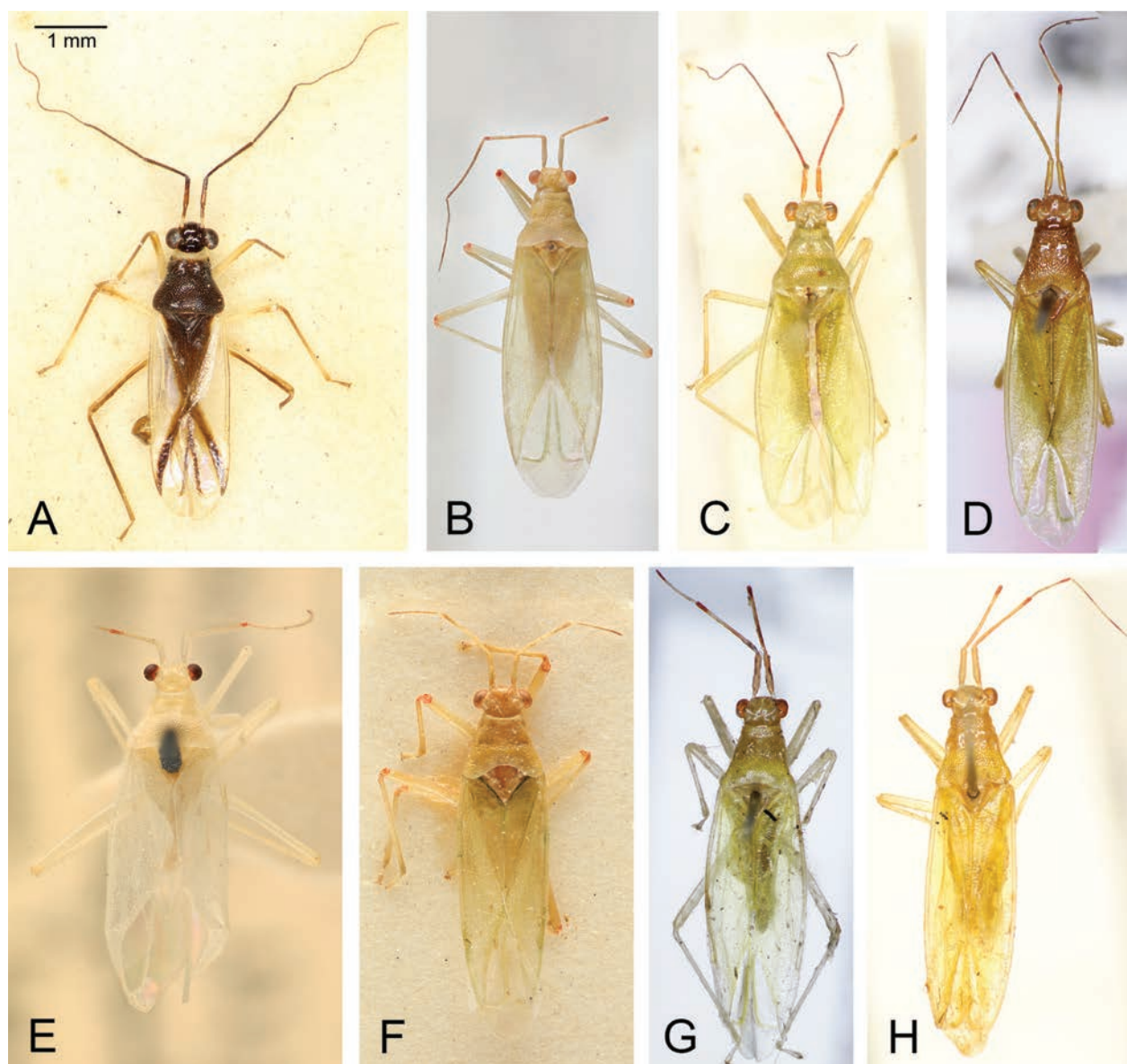


**Figure 3.** *Prodrumus* species, dorsal view. **A.** *P. melanonotus*, AMNH\_PBI 00340373; **B.** *P. ibbaicus*, ZISP\_ENT 00008385; **C.** *P. kawandanus*, AMNH\_PBI 00340355; **D.** *P. angulatus*, AMNH\_PBI 00340389; **E.** *P. clypeatus*, ZISP\_ENT 00008400; **F.** *P. incisus*, ZISP\_ENT 00008403; **G.** *P. pilosus*, AMNH\_PBI 00340363; **H.** *P. wardi*, AMNH\_PBI 00340365.

recognised at the time, with *Sinervus*. However, subsequently he reinstated the genus as valid, differentiating it from *Sinervus* based on the less pedunculate eyes, the somewhat convex anterior margin of the collar, the hind margin of disc being slightly convex, and the less narrowed cuneus (Carvalho 1981).

Carvalho (1981) considered the much longer cuneus and the more pedunculate eyes as characters suitable for unambiguously distinguishing *Prodrumpsis* from *Prodrumus*. Stonedahl (1988), however, treated *Prodrumpsis* as a junior synonym of *Prodrumus*. Thus, he characterised *Prodrumus* as having substylate to strongly pedunculate eyes and an elongate, curved cuneus, three times or more as long as broad.

Odhiambo (1962) described *Duducoris* to accommodate three newly described species from Uganda. He

considered this genus to be closely allied to *Prodrumus*, suggesting that *Duducoris* can be differentiated by a more flattened body, a non-sulcate vertex, eyes only weakly projecting above the vertex, a relatively short narrowed basal part of the antennal segment I, weakly raised calli, a pronotum deeply emarginated posteriorly, and shorter legs.

Akingbohunge (1975) described a new Nigerian species of *Duducoris*, *D. wardi* Akingbohunge, 1975, characterised by a pubescent pronotal disk, a broadly emarginate posterior margin of pronotum, and a labium reaching apex of mesosternum. A key allowing for distinguishing the four *Duducoris* species was also provided.

Stonedahl (1988), in his comprehensive revision of six eccritotarsine genera including *Prodrumus*, performed cladistic analysis of *Prodrumus* species based on a matrix of 16 bistate characters. *Duducoris* sp. was cho-

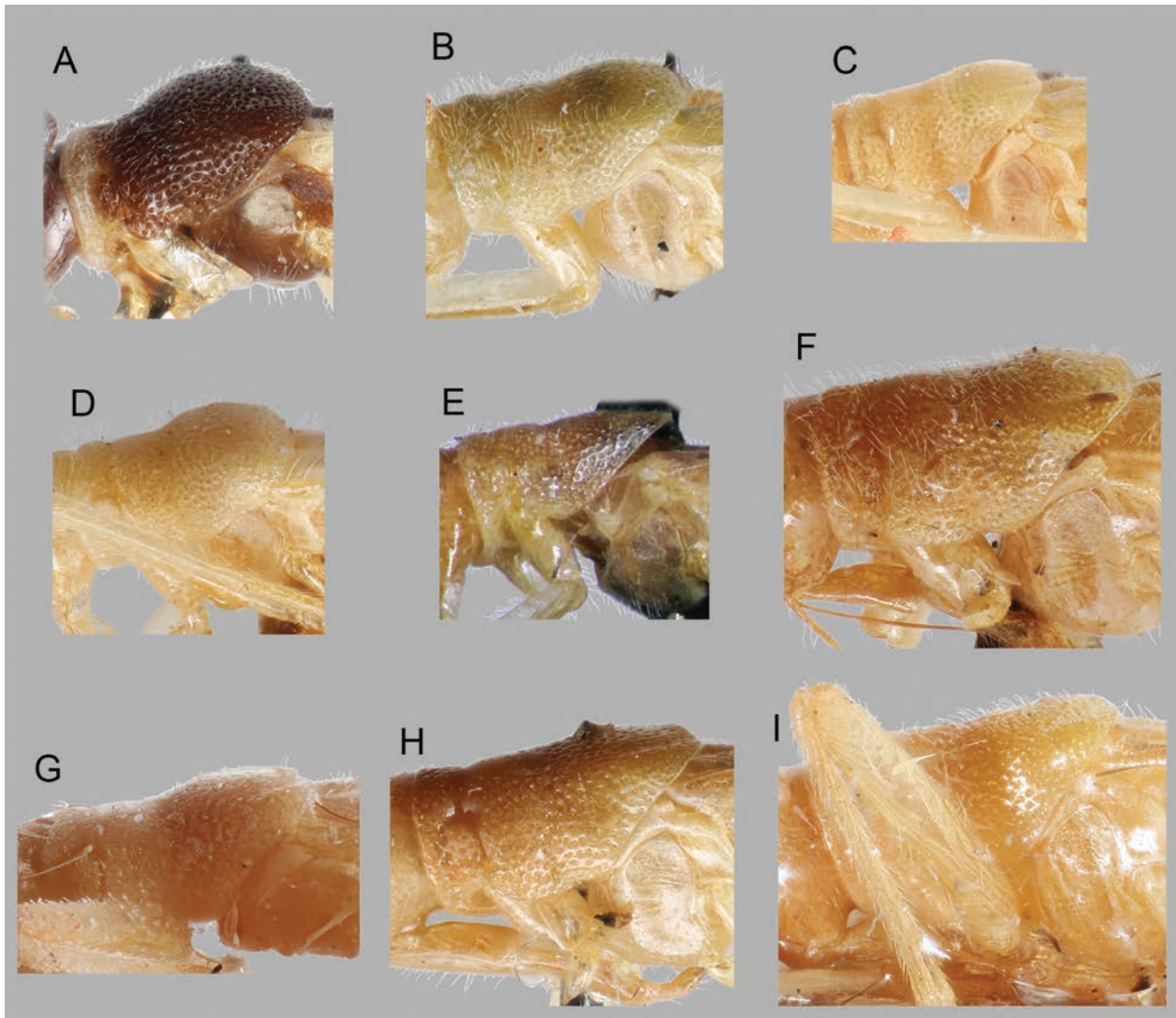


**Figure 4.** Pronotum of *Prodrumus* spp. in lateral view. **A.** *P. melanonotus*, ZISP\_ENT 00008406; **B.** *P. kawandanus*, ZISP\_ENT 00008364; **C.** *P. ibbaicus*, ZISP\_ENT 00008372; **D.** *P. thaliae*, ZISP\_ENT 00008390; **E.** *P. subflavus*, AMNH\_PBI 00340343; **F.** *P. pilosus*, ZISP\_ENT 00008409; **G.** *P. incisus*, ZISP\_ENT 00008402; **H.** *P. angulatus*, ZISP\_ENT 00008378; **I.** *P. aethiopicus*, ZISP\_ENT 00008418.

sen as the outgroup taxon, with all the characters coded as 0. Importantly, the character matrix used for analysis did not include a specific *Duducoris* species, and no apomorphies of *Prodrumus* were presented during this study. Stonedahl concluded that *Prodrumus* can be distinguished from *Duducoris* based on the combination of the following characters: a longer, less hypognathous head, a frons weakly convex or nearly straight, the basal 1/4–1/2 of the antennal segment I distinctly narrowed, the length of antennal segment III greater than or equal to the length of segment II, a pronotal disk moderately convex, femora relatively longer and narrower, usually slightly swollen distally, and the apex of the left paramere usually unmodified.

However, after we conducted a thorough examination of the specimens of various species within *Prodrumus* and *Duducoris*, a set of characters allowing for unambiguous discrimination of these genera was not revealed.

The body of *Prodrumus* spp., in particular the pronotal disk, can be weakly convex, like in *P. kawandanus* Odhiambo, 1962 (Fig. 4B), *P. ibbaicus* Linnavuori, 1975 (Fig. 4C) and *P. tafoensis* Stonedahl, 1988, while the pronotum of *Duducoris* can be raised posteriorly as in some *Prodrumus* species. The latter condition may be observed in *D. incisus* (Fig. 4G). The clypeus is not always flattened in *Prodrumus*. For instance, in *P. ibbaicus* (Fig. 5C) and *P. kawandanus* (Fig. 5D) the clypeus is as swollen as in *Duducoris* species. The thin basal part of antennal segment I may occupy from one-quarter to one-half of the segment, so that the slender basal part of the segment in *Prodrumus* and *Duducoris* may be subequal as compared to the length of antennal segment I. Eyes may be both rounded and kidney-shaped, which is typical for the majority of species, and rarely elongated, as in *P. kawandanus*, resembling the condition observed in *Duducoris*.

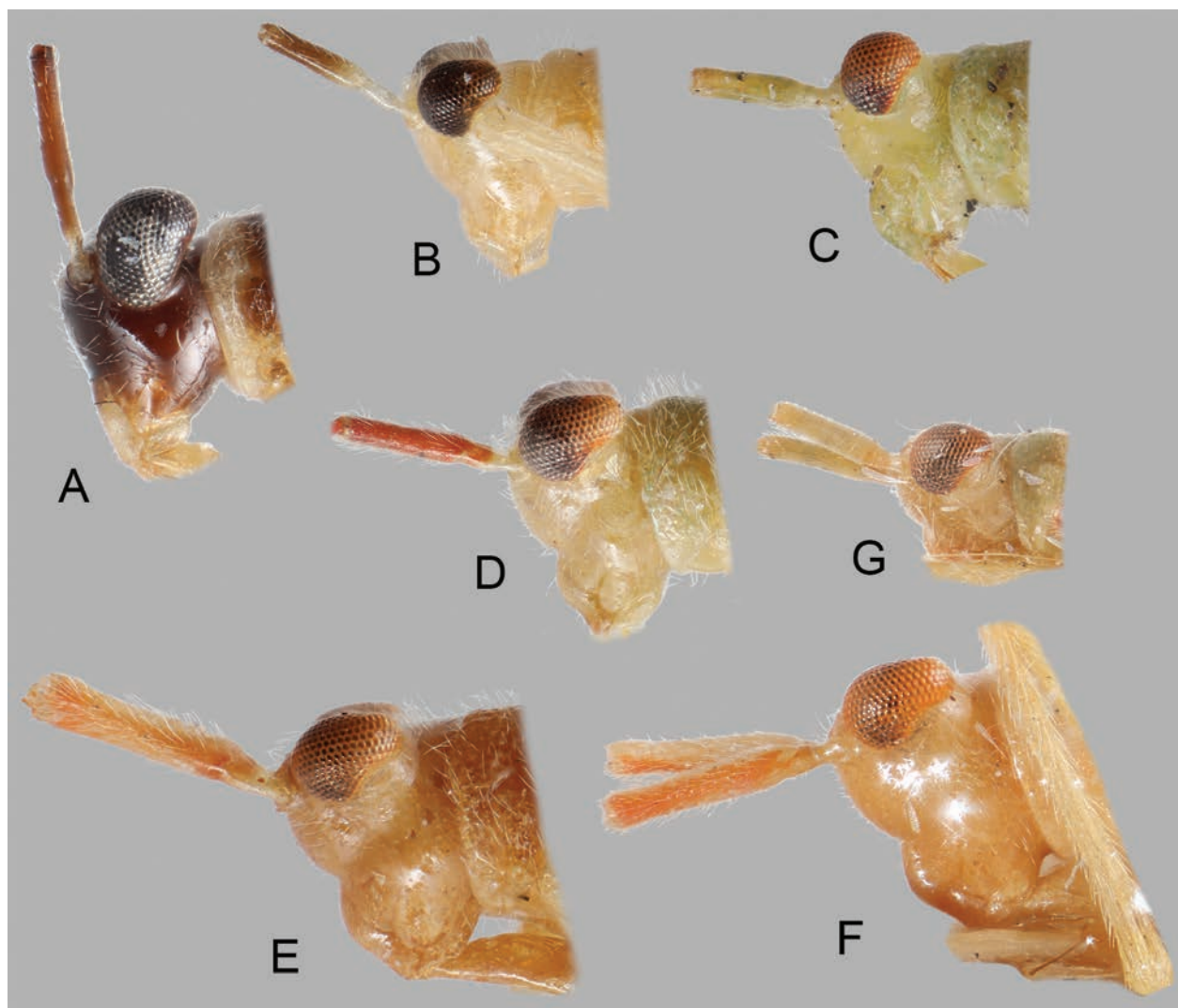


**Figure 5.** Head of *Prodrumus* spp. in lateral view. **A.** *P. melanonotus*, ZISP\_ENT 00008406; **B.** *P. thaliae*, ZISP\_ENT 00008390; **C.** *P. ibbaicus*, ZISP\_ENT 00008383; **D.** *P. kawandanus*, ZISP\_ENT 00008364; **E.** *P. pilosus*, ZISP\_ENT 00008409; **F.** *P. aethiopicus*, ZISP\_ENT 00008418; **G.** *P. incisus*, ZISP\_ENT 00009324.

According to Odhiambo (1962), the posterior margin of the pronotum in *Duducoris* is deeply emarginate. Based on our observations, this medial depression is always present, but may be poorly expressed. For instance, in *D. pilosus* Odhiambo, 1962 (Fig. 3G) the posterior margin of the pronotum resembles that of such *Prodrumus* species as *P. ibbaicus* (Fig. 3B), *P. kawandanus* (Fig. 3C), and *P. tafoensis*. The pronotum in *Prodrumus* spp. may be straight posteriorly, as in *P. melanonotus* (Fig. 3A), or slightly depressed, as in *P. subviridis*, *P. abuyog* Stonedahl, 1988, *P. apoensis* Stonedahl, 1988, and others.

According to Stonedahl (1988), *P. ibbaicus* was the sister taxon to all remaining *Prodrumus* spp. with *P. kawandanus* branching off next. These species exhibit characters traditionally considered typical for *Duducoris*: eyes weakly elevated above the vertex, frons moderately convex, anteclypeus distinctly swollen and pronotal disk flattened. In *P. kawandanus*, eyes are also elongate in dorsal and lateral views, resembling those of *Duducoris* species. However, we believe *P. ibbaicus* and *P. kawandanus* should not be

placed in *Duducoris*, as such a taxonomic act will further blur the line between *Prodrumus* and *Duducoris*.

Our investigation revealed no significant differences, which allowed us to distinguish between *Prodrumus* and *Duducoris*. Therefore, we suggest that *Duducoris* represents a specific form of the highly polymorphic genus *Prodrumus*, and thus synonymise *Duducoris* Odhiambo, 1962 with *Prodrumus* Distant, 1904. Consequently, *Prodrumus* is here redefined, containing the following 31 species:

*Prodrumus abuyog* Stonedahl, 1988 – Philippine Islands and North Borneo.

*Prodrumus aethiopicus* (Poppius, 1910), comb. nov. – Kilimanjaro, Kenya, South Sudan, Natal in South Africa.

*Prodrumus alboviridescens* (Motschulsky, 1863) nomen dubium.

*Prodrumus angulatus* (Odhiambo, 1962), comb. nov. – Uganda.

*Prodrumus apoensis* Stonedahl, 1988 – Mindanao, Philippine Islands.

- Prodromus bakeri* Stonedahl, 1988 – Luzon, Philippine Islands.
- Prodromus borneoensis* Stonedahl, 1988 – Sabah and Sarawak, Malaysia.
- Prodromus cambodiensis* Stonedahl, 1988 – Cambodia; Sarawak, Malaysia.
- Prodromus chiangmaiensis* Stonedahl, 1988 – North-western Thailand.
- Prodromus clypeatus* Distant, 1904 – Sri Lanka, Vietnam, India (Kerala), Thailand, southern China, Taiwan, Malaysia, Java, Ambon.
- Prodromus gressitti* Stonedahl, 1988 – Northwestern Thailand.
- Prodromus ibbaicus* Linnavuori, 1975 – Equatoria Province, South Sudan.
- Prodromus incisus* (Odhambo, 1962), comb. nov. – Uganda, Democratic Republic of the Congo.
- Prodromus joveri* Delattre, 1950 – Ivory Coast.
- Prodromus kawandanus* Odhambo, 1962 – Uganda and South Sudan.
- Prodromus melanonotus* Carvalho, 1951 – Ghana, Cameroon, Democratic Republic of the Congo (Haut Uele, Mauda).
- Prodromus mindanao* Stonedahl, 1988 – Mindanao and Samar, Philippine Islands.
- Prodromus nigrus* (Carvalho, 1981) – New Guinea.
- Prodromus nimbus* Delattre, 1950 – Guinea.
- Prodromus novoguineensis* Stonedahl, 1988 – Western New Guinea.
- Prodromus oculatus* (Poppius, 1912) – New Guinea, Bismark Archipelago, Solomon Islands.
- Prodromus pelagus* Stonedahl, 1988 – Sarawak, Malaysia.
- Prodromus philippinensis* (Poppius, 1915) – Luzon, Philippine Islands.
- Prodromus pilosus* (Odhambo, 1962) comb. nov. – Uganda.
- Prodromus ranau* Stonedahl, 1988 – North Borneo.
- Prodromus sabah* Stonedahl, 1988 – North Borneo.
- Prodromus subflavus* Distant, 1904 – Sri Lanka and Vietnam.
- Prodromus subviridis* Distant, 1904 – Tanintharyi Region of Myanmar.
- Prodromus tafoensis* Stonedahl, 1988 – Ghana.
- Prodromus thaliae* China, 1944 – Ghana.
- Prodromus wardi* (Akingbohunge, 1975), comb. nov. – Nigeria.

### ***Kunungua* Carvalho, 1951**

Figs 6–10

- Kunungua* Carvalho, 1951: 107. Type species by original designation: *Kunungua boxi* Carvalho, 1951.
- Kunungua*: Carvalho (1957: 107) (catalogue), Odhambo (1962: 269) (discussion).

**Revised diagnosis.** Head hammer-shaped, 0.2–0.4 times as long as wide; vertex longitudinally sulcate at middle;

eyes distinctly pedunculate; collar and pronotal disk deeply punctate, punctures dense, spacing between punctures smaller than punctures diameter, rarely fusing; posterior angles of pronotal disk rounded; calli prominently raised, divided by deep longitudinal depression; scutellum very small, only about 0.3 times as wide and 0.3–0.4 times as long as pronotum, strongly pointed at apex; membrane with thick vein, apical angle acute, membranal cell nearly reaching apex of cuneus.

**Redescription. Male. Colouration.** Antenna usually with entirely or partly darkened segments I and II; head and pronotum from ochraceous to dark brown; clavus brown to dark brown, corium cinnamon or whitish with brown bands or spots apically or medioapically, cuneus from pale brownish yellow to dark brown (as in Fig. 6A–D, F–H).

**Surface and vestiture.** Body shining, covered with dense pale erect to semierect setae; pronotum deeply punctate, punctures dense, rarely fusing, the distance between punctures less than puncture's size; punctures on calli smaller, sparse, but more dense at sides; scutellum wrinkly.

**Structure.** Body elongate, 3.4–4.1 times as long as width of pronotum; total length 3.5–4.3 mm.

Head. Strongly transverse, short in dorsal view, 0.3–0.4 times as long as wide, triangular in frontal view; eyes pedunculate, distinctly projecting above vertex in frontal view, kidney-shaped in lateral view; vertex about 1.0–1.3 times as wide as length of antennal segment I; antennal segment I 0.4–0.6 times as long as pronotum and 0.4–0.5 times as long as its width; clypeus swollen; mandibular plate subquadrate, maxillary plate trapeziform; labium relatively short, reaching from middle of fore coxa almost to hind coxa.

Thorax. Pronotum campanulate, 1.0–1.2 times as wide as long, 1.1–1.3 times as wide as head; collar 0.5–0.9 times as long as calli; calli prominently raised, divided by a deep longitudinal depression, 0.3–0.6 times as wide as pronotum; collar and calli combined length 0.3–0.4 times as long as pronotum, with deep depression behind calli extending at sides of pronotum; pronotal disk, calli and collar 0.6–0.7 times, 0.2–0.3 times, 0.1–0.2 times as long as entire pronotum, respectively; posterior angles of pronotum rounded, posterior margin straight to moderately concave; mesoscutum entirely covered with pronotum; scutellum small, 0.3–0.4 times as long as pronotum, triangular, equilateral, apically tapering.

Legs. Femora cylindrical, usually gradually thickening distally, less than two times as wide as tibiae; tarsus three-segmented, segment II almost twice as long as segment I, segment III slightly longer than segment I.

Hemelytron. Long, apex of cuneus far surpassing apex of abdomen, from semitransparent to opaque; membrane with one cell, membranal vein strongly curved apically, nearly reaching apex of cuneus; cuneus about 2.0–2.5 times as long as wide at base.

**Genitalia.** Genital capsule wider than long; aperture large, dorsoposteriorly oriented; apex of ventral wall

with lobe-shaped sclerotised processes forming paramere sockets; supragenital bridge absent (Fig. 9A–E).

Aedeagus tubular, C-shaped, with strongly sclerotised basal part and entirely membranous, non-eversible, single-lobed apical portion, without clear demarcation between phallosome and endosoma, sometimes with a dorsal outgrowth at base (Fig. 8); ductus seminis entirely membranous, apically terminating with barely recognisable secondary gonopore devoid of distinctive sculpture.

Parameres subequal in size, left paramere more or less falciform, right one somewhat S-shaped, sometimes with a flattened sensory lobe (Fig. 10).

**Female.** Similar to male in colouration, surface, vestiture, structure, and measurements. Sexual dimorphism not apparent.

**Genitalia.** Bursa copulatrix membranous, vulvar region and posterior wall devoid of any distinctive sclerotisations; sclerotised rings of dorsal labiate plate very thin and weakly sclerotised, with medially oriented outgrowth (Fig. 9F).

**Discussion.** *Kunungua* appears to be most closely related to *Prodromus* due to the hammer-shaped head with distinctly pedunculate eyes, deeply punctate pronotum, and elongate body. However, *Kunungua* can be unambiguously distinguished from *Prodromus* on the basis of the following combination of characters: head only 0.24–0.39 times as long as wide, eyes strongly pedunculate, calli prominently raised, scutellum small, only about 0.3 times as wide and 0.3–0.4 times as long as pronotum, and parameres subequal in size.

*Kunungua* resembles New World genera of the *Prodromus* complex e.g., *Sinervus*, *Sinervaspartus*, and *Spartacus*, possessing the distinctively stalked eyes, sulcate vertex, strongly elevated calli, distinctly convex pronotal disk, and more or less falciform left paramere. The colouration of *K. ukerewensis* (Fig. 6G), *K. atramentomaculata* sp. nov. (Fig. 6C), *K. gemina* sp. nov. (Fig.

6F), and *K. ornata* sp. nov. (Fig. 6D) with specific bands is similar to that of some *Sinervus* species, in particular *S. baerensprungi* Stål, 1860 and *S. minezi* Carvalho, 1990. However, these genera differ from *Kunungua* spp. in having a long and slender, sickle-shaped cuneus, a narrower collar, and confluent calli that are distinctly separated posteriorly from the pronotal disk with a deep constriction dorsally and at sides.

The external characters of *Kunungua*, specifically colouration, suggest that two groups can be recognised within *Kunungua*, the first one comprising *K. boxi* and *K. cinnamomea*, and the second one including the remaining species. *Kunungua boxi* (Fig. 6B) and *K. cinnamomea* (Fig. 6A) share the brown hemelytra, a fuscous membrane, distinctly swollen clypeus and frons, an extremely short labium, reaching procoxa only (Fig. 7F, G), antennal segment I reddish, short, 1.3–1.6 times as long as head, a comparatively short eye peduncle, oblique, longer in the basal part, a cinnamon-coloured pronotum, and a strongly curved distally membranous vein, forming an acute angle.

*Kunungua ukerewensis*, *K. atramentomaculata* sp. nov., *K. gemina* sp. nov., and *K. ornata* sp. nov. are characterised by yellowish white hemelytra with specific brownish bands (Fig. 6C, D, F–H), gradually darkening from pale yellow to brown antennal segment I, a transparent membrane, strongly pedunculate eyes, slightly swollen frons, labium reaching approximately the middle of the mesothorax, and a distinctly curved distally membranous vein, forming a right angle. Interestingly, *K. cinnamomea* appears to be the only species to possess denticles on the apex of the right paramere (Fig. 10C, E). Unfortunately, we have not dissected male genitalia of *K. boxi*, and the only existing picture of *K. boxi* parameres and aedeagus (Odhiambo 1962) appears to be of a relatively poor quality. Therefore, no conclusions can be drawn about the presence of denticles on the apex of the right paramere in *K. boxi*.

## Key to species

- 1 Posterior margin of pronotum straight; eye peduncle short, oblique, with longer posterior margin (Fig. 6A, B)..... 2
- Posterior margin of pronotum slightly concave; eye peduncle distinctive, about as long as the width of the eye from above (Fig. 6C, D, F–H) ..... 3
- 2 Femora and tibiae covered with extremely dense, robust brown setae, antennal segment II pale yellow, apically and basally darkened; antennal segment III pale yellow (Fig. 6A) ..... *K. cinnamomea*
- Femora and tibiae covered with dense, relatively thin brownish yellow setae, antennal segment II reddish brown; antennal segment III brownish (Fig. 6B)..... *K. boxi*
- 3 Pronotal collar dirty yellow to pale yellow (Fig. 6D, G, H)..... 4
- Pronotal collar dark brown (Fig. 6C, F)..... 5
- 4 Apical two thirds of antennal segment I, segment II, calli, pronotal disk, and band along inner margin of cuneus dark brown ..... 6
- Antennal segment I except for the apex, basal two thirds of segment II, pronotal disk, and band along inner margin of cuneus yellowish; calli yellowish brown (Fig. 6H) ..... *K. ukerewensis* (light form)
- 5 Corium with distinct brown transverse band starting near the apex of clavus and almost reaching costal margin (Fig. 6C)..... *K. atramentomaculata* sp. nov.
- Corium with brown longitudinal semicircular spot near apex of clavus, not extending to mesocorium (Fig. 6F) ..... *K. gemina* sp. nov.

- 6 Corium whitish, with longitudinal medioapical spot far not reaching exocorium, brown spot along medioapical margin; cuneus dark brown, membrane smoky brown, except for transparent apical part (Fig. 6G) .... *K. ukerewensis* (dark form)
- Corium whitish, with wide, oblique subapical brown band running from medioapical to costal margin; cuneus whitish yellow, with brown stripe along inner margin and narrow brown edging along costal margin; membrane transparent, whitish hyaline, with brown veins. (Fig. 6D) ..... *K. ornata* sp. nov.

***Kunungua atramentomaculata* sp. nov.**

<https://zoobank.org/6FB02238-D303-47CA-8330-D102B4E33410>

Figs 6C, 7C

**Material examined. Holotype.** ♀, DEMOCRATIC REPUBLIC OF THE CONGO: Haut Uelé: Mabaya [Mabao], 3.32°N, 28.74°E, L. Burgeon1 (ZISP\_ENT 00008427) (MRAC).

**Paratype.** DEMOCRATIC REPUBLIC OF THE CONGO: 1 ♀, Haut Uelé: Moto, 3.056°N, 29.47°E, 1920, L. Burgeon (ZISP\_ENT 00014326) (MRAC).

**Diagnosis.** Recognised by the following combination of characters: collar dark brown; corium pale yellow, with brown transverse band starting slightly above claval apex and not quite reaching costal margin, blurring distally; cuneus brown, with brown spot blurring towards base.

This species can be unambiguously distinguished from all other congeners by the presence of a brown band crossing the corium transversely, starting slightly above the claval apex, but not reaching the outer margin of the corium.

**Description. Female. Colouration** (Figs 6C, 7C). Head, except for pale yellow antennal fossa, dark brown; antennal segment I pale yellow basally, gradually darkening to brown apically, segment II dark brown, segments III and IV yellowish brown; eyes commonly dark brown; pronotum, scutellum, and clavus dark brown; corium pale yellow, with transverse brown band crossing corium, starting slightly above claval apex and nearly reaching costal margin, blurring distally; corium narrowly dark brown along costal margin in apical half; cuneus brown, basally with blurring brown spot and dark brown outer margin; membrane transparent, basal two-thirds of membrane fuscous, apical one-third whitish; coxae brown anteriorly, pale yellow posteriorly; femora pale yellow basally, dark brown at middle, brownish yellow distally; fore tibia pale yellow, darkened basally; middle tibia pale yellow, except for brown basal one-third; basal one-half of hind tibia brown, apical half pale yellow; tarsal segments I and II pale yellow, the latter slightly darkened apically; segment III greyish brown; abdomen dark brown basally and apically, middle part, comprising about one-half of abdomen, whitish yellow.

**Vestiture.** Clothed with long whitish simple setae, adpressed on hemelytron, semierect elsewhere, subequal to width of antennal segment I at middle, somewhat shorter on pronotum.

**Structure.** Total length 4.2 mm; body 3.7 times as long as width of pronotum and 4.4 times as long as pronotal length.

Head 0.3 times as long as wide, 2 times as wide as collar; antennal fossa large, removed from inner eye margin by distance subequal to its own width, located at the level of inferior eye margin; frons only slightly convex; vertex

about 1.3 times as wide as length of antennal segment I; segment I 1.7 times as long as head, 0.5 times as long as pronotum, 0.4 times as long as pronotal width; labium long, almost reaching hind coxa (Fig. 7C).

Thorax. Posterior margin of pronotum slightly concave medially (Fig. 6C); pronotum 1.2 times as wide as long, 1.2 times as wide as head; calli 0.5 times as wide as basal width of pronotum; pronotal disk, calli and collar 0.7 times, 0.2 times, and 0.2 times as long as pronotum, respectively; calli and collar together about 0.3 times as long as pronotum.

Hemelytron. Semitransparent, long, corium reaching apex of abdomen; cuneus about 1.5 times as long as wide at base (Figs 6C, 7C).

Legs. Slender, femora gradually thickening apically (Fig. 6C, 7C).

**Genitalia.** Bursa copulatrix as in *K. ukerewensis*, weakly sclerotised, with indistinct sclerotised rings of dorsal labiate plate, posterior wall entirely membranous.

**Male.** Unknown.

**Distribution.** Known from two localities in Congo, Haut Uelé.

**Host.** Unknown.

**Etymology.** The specific epithet is a Latin adjective composed of the noun *atramentum*, meaning “ink” and the adjective *maculatus*, *-a*, *-um*, meaning “spotted”, referring to the shape of the band on the corium, blurring distally and thus resembling an ink spot.

**Discussion.** While this species is known solely from two females, its distinct colouration prompted us to describe it despite the lack of known males. Given the observed variation in colour patterns within *Kunungua*, we are confident that with further collecting efforts, males could be readily associated with females.

***Kunungua boxi* Carvalho, 1951**

Figs 6B, 7F

*Kunungua boxi* Carvalho, 1951: 108.

*Kunungua boxi*: Carvalho (1957: 107) (catalogue).

**Material examined. Holotype.** ♂, GHANA: Gold coast, Amentia, 6.22°N, 1.17°W, 15 Sep 1943, H. E. Box, *Aframomum* sp. (Zingiberaceae) (AMNH\_PBI 00340367) (NHM).

**Paratypes.** GHANA: Gold coast, Amentia, 6.22°N, 1.17°W, 15 Sep 1943, H. E. Box, *Aframomum* sp. (Zingiberaceae), 2 ♂ (AMNH\_PBI 00340368, AMNH\_PBI 00340369) (NHM). Gold coast, Asuansi, 5.3°N, 1.23°E, 15 Dec 1942, H. E. Box, *Aframomum* sp. (Zingiberaceae), 1 ♀ (AMNH\_PBI 00340370) (NHM).

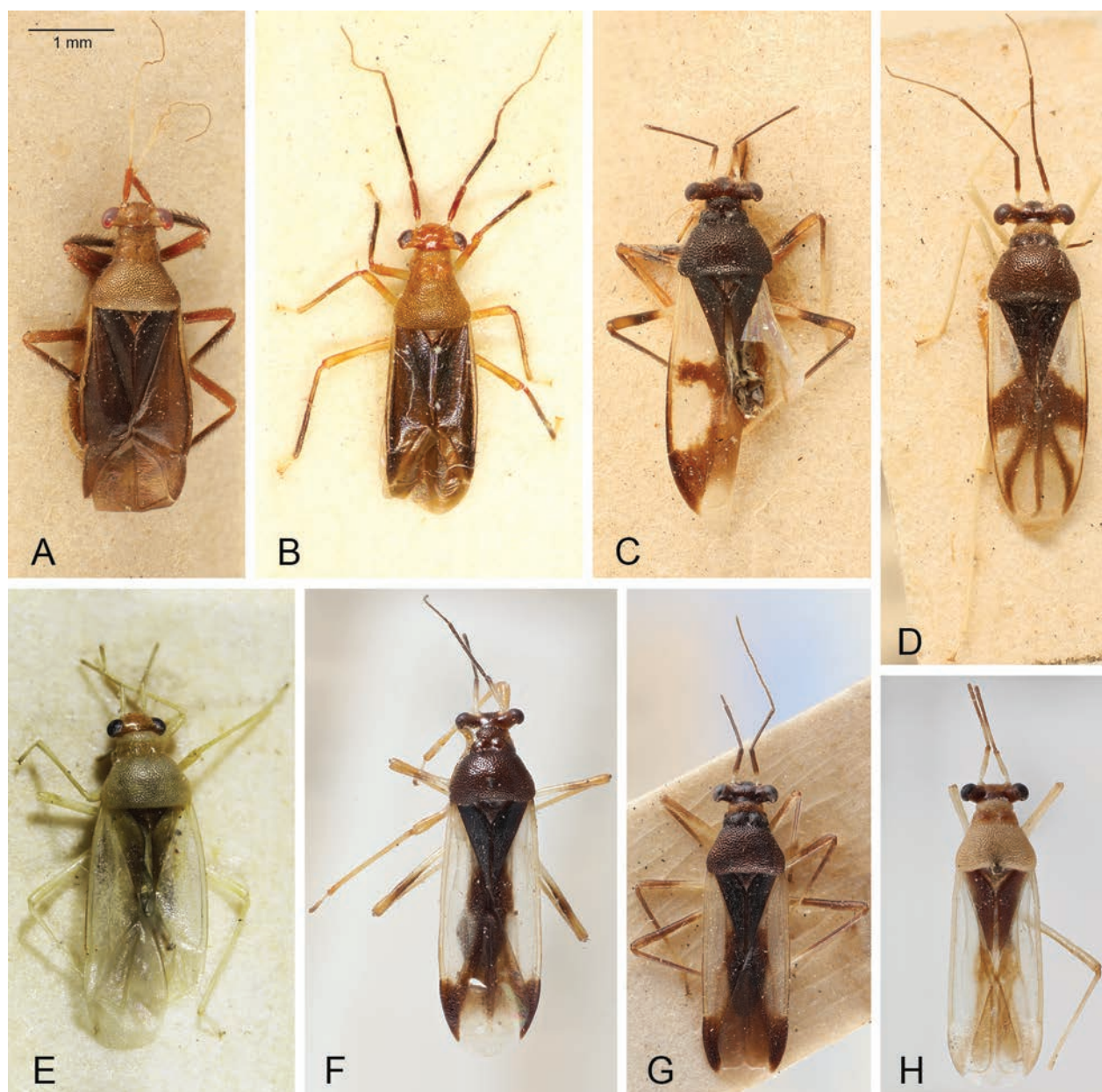


**Figure 6.** *Kunungua* species, dorsal view. **A.** *K. cinnamomea*, ZISP\_ENT 00008425; **B.** *K. boxi*, AMNH\_PBI 00340368; **C.** *K. atramentomaculata*, ZISP\_ENT 00008427; **D.** *K. ornata*, ZISP\_ENT 00008428; **E.** *K. pallida*; **F.** *K. gemina*, ZISP\_ENT 00008589; **G.** *K. ukerewensis* (dark form), ZISP\_ENT 00008413; **H.** *K. ukerewensis* (light form), ZISP\_ENT 00008433.

**Revised diagnosis.** Recognised by the following combination of characters: antennal segment I terracotta, segment II dark brown, basally terracotta, segment III brownish yellow, segment IV sandy; head reddish yellow; pronotum ochraceous; hemelytron dark brown, with dirty yellow costal margin; femora reddish yellow. Parameres similar to those of *K. ornata*.

*Kunungua boxi* is most similar to *K. cinnamomea* (Fig. 6A) in the structure, body proportions, and colouration, differing from the latter species in the comparatively sparsely distributed, pale brown setae on tibiae, especially fore tibia, as well as in the colouration of antenna, head, and femora. Refer to the discussion section of the genus for additional details.

**Redescription. Male. Colouration** (Figs 6B, 7F). Head reddish; antennal segment I terracotta, segment II dark brown, basally terracotta, segment III brownish yellow, segment IV sandy; eyes brownish scarlet; labium pale yellow, apex dark brown; collar, calli, and pronotal disk ochraceous, calli with reddish tinge; clavus and cuneus dark brown, corium dark brown with dirty yellow, gradually darkening apically costal margin; membrane fuscous, cinnamon, semitransparent; coxae pale yellow; femora reddish yellow, apically with reddish tinge; fore tibia brown, reddish basally; middle tibia brownish yellow; hind tibia brownish yellow basally, gradually darkening towards apex; tarsi pale yellow; abdomen uniformly brown.

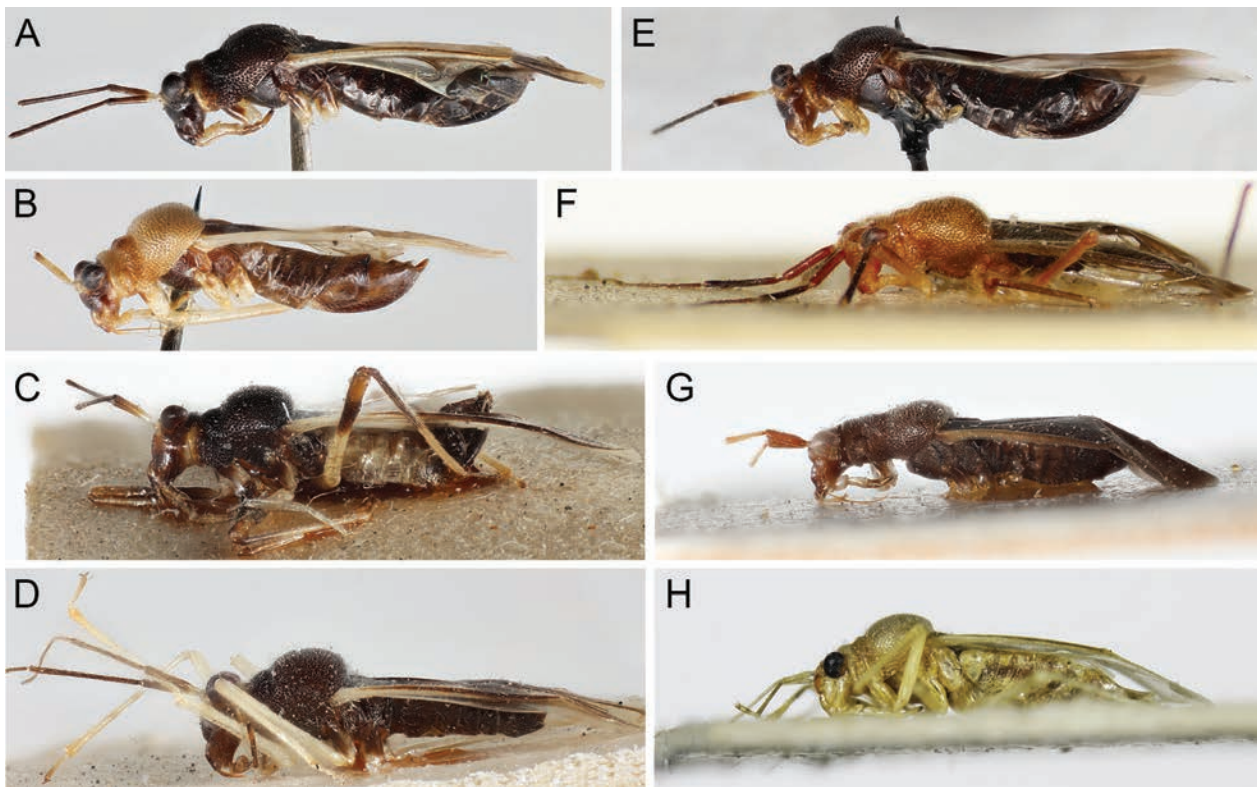


**Figure 7.** *Kunungua* species, lateral view. **A.** *K. ukerewensis* (dark form), ZISP\_ENT 00008437; **B.** *K. ukerewensis* (light form), ZISP\_ENT 00008430; **C.** *K. atramentomaculata*, ZISP\_ENT 00008427; **D.** *K. ornata*, ZISP\_ENT 00008428; **E.** *K. gemina*, ZISP\_ENT 00008415; **F.** *K. boxi*, AMNH\_PBI 00340368; **G.** *K. cinnamomea*, ZISP\_ENT 00008426; **H.** *K. pallida*.

**Vestiture.** Body covered with comparatively long simple setae, subequal to width of antennal segment I at middle, adpressed on hemelytron, semierect elsewhere, goldish on dorsum, pale brown on legs and antennal segment I.

**Structure.** Total length 3.2–3.5 mm; body 3.7–3.8 times as long as basal width of pronotum.

**Head.** Eye peduncle short, oblique, with longer posterior margin; antennal fossa large, removed from inner eye margin by about half of fossa width, located at the level of inferior eye margin; frons short, swollen; vertex about 1.0–1.2 times as wide as length of antennal segment I; segment I 0.5 times as long as pronotum; labium short, slightly surpassing fore coxa.

**Thorax.** Pronotum comparatively narrow, 1.0–1.1 times as wide as long, 1.0–1.2 times as wide as head; pronotal disk, calli, and collar 0.6 times, 0.3 times, and 0.1 times as long as entire pronotum, respectively; calli and collar together about 0.4 times as long as pronotum; posterior margin straight, not concave (Fig. 6B).

**Hemelytron.** Opaque, long, cuneus distinctly surpassing the apex of abdomen; cuneus narrowly triangular, with slightly concave inner margin, about 1.5 times as long as wide at base (Figs 6B, 7F).

**Legs.** Relatively short, robust, femora cylindrical, of about the same diameter along entire length (Fig. 6B).

**Genitalia.** Parameres. Left paramere falciform (Odhiambo 1962: figs 62–63), tapering toward the apex, apex

hook-like from the inner side; right paramere (Odhiambo 1962: figs 64–65) somewhat S-shaped, with relatively wide sensory lobe and with needle-shaped, upturned apex in lateral view. Aedeagus C-shaped, apically with single large membranous lobe (Odhiambo 1962: fig. 66).

**Female.** Colouration, structure, body proportions, and vestiture as in male.

**Distribution.** The species was originally described and is still known from two localities in Ghana, which are ca. 130 kilometers apart from each other.

**Host.** *Aframomum* sp. (Zingiberaceae).

### *Kunungua cinnamomea* Carvalho, 1951

Figs 6A, 7G, 8A, 9A, 10A–E

*Kunungua cinnamomea* Carvalho, 1951: 109.

*Kunungua cinnamomea*: Carvalho (1957: 107) (catalogue).

**Material examined.** DEMOCRATIC REPUBLIC OF THE CONGO: Nord-Kivu: Rutshuru, 1.18°S, 29.45°E, May 1937, J. Ghesquiere, 1♀ (ZISP\_ENT 00008425) (MRAC). Tshuapa: Bokuma, 0.67°S, 21.02°E, Mar 1954, R.P. Lootens, 1♂ (ZISP\_ENT 00008426) (MRAC). GABON: Estuaire: Mbel, 0.25°N, 10.18°E, Oct 1969, A. Villiers, 3♂ (ZISP\_ENT 00009332, ZISP\_ENT 00009333, ZISP\_ENT 00009335), 2♀ (ZISP\_ENT 00009334, ZISP\_ENT 00014341) (MNHN).

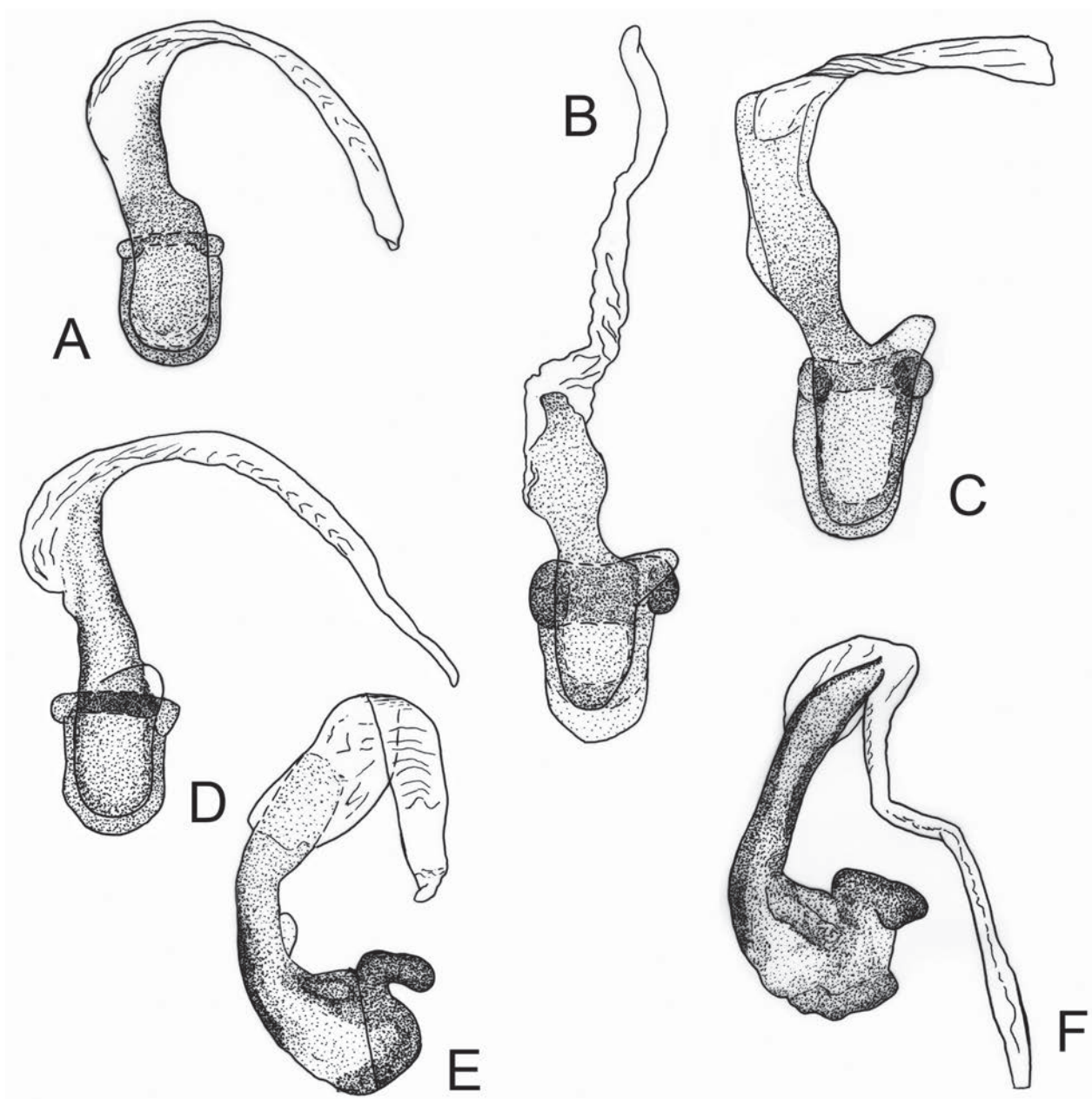


**Figure 8.** *Kunungua* species, aedeagus. **A.** *K. cinnamomea*, ZISP\_ENT 00008426; **B.** *K. ukerewensis* (dark form), ZISP\_ENT 00014329; **C.** *K. ukerewensis* (light form), ZISP\_ENT 00008433; **D, E.** *K. gemina*, ZISP\_ENT 00014338; **F.** *K. ornata*, ZISP\_ENT 00008429.

**Revised diagnosis.** Recognised by the following combination of characters: antennal segment I reddish, segments II–IV pale yellow; head cinnamon; femora reddish; right paramere apically serrate.

Most similar to *K. boxi* in the structure and colouration (see the discussion section of the genus for more details), differing from the latter species in the colour of antenna, specifically pale yellow antennal segment II, sandy head, reddish femora, and the more dense, dark brown setae on fore tibia.

**Redescription. Male. Colouration** (as in Figs 6A, 7G). Head sandy; antennal segment I reddish, segments II–IV pale yellow, sometimes segment II with reddish tinge basally; eyes scarlet; clypeus brownish; labial segments I

and II pale yellow, segments III and IV brownish yellow; pronotum sandy; corium and cuneus brown to cinnamon; clavus brown; membrane fuscous, cinnamon, semitransparent; fore coxa yellowish, middle and hind coxa brownish; femora reddish; fore tibia brown, middle and hind tibiae reddish brown; tarsus pale yellow; abdomen brown.

**Vestiture.** Body covered with simple semierect setae, brown on legs and antennal segment I, goldish brown on hemelytron, goldish elsewhere. Setae on tibiae, especially fore tibia, extremely dense, longer than tibia diameter, dark brown to brown.

**Structure.** Total length 3.5–4.3 mm; body 3.4–3.7 times as long as basal width of pronotum and 3.6–3.7 times as long as pronotal length.

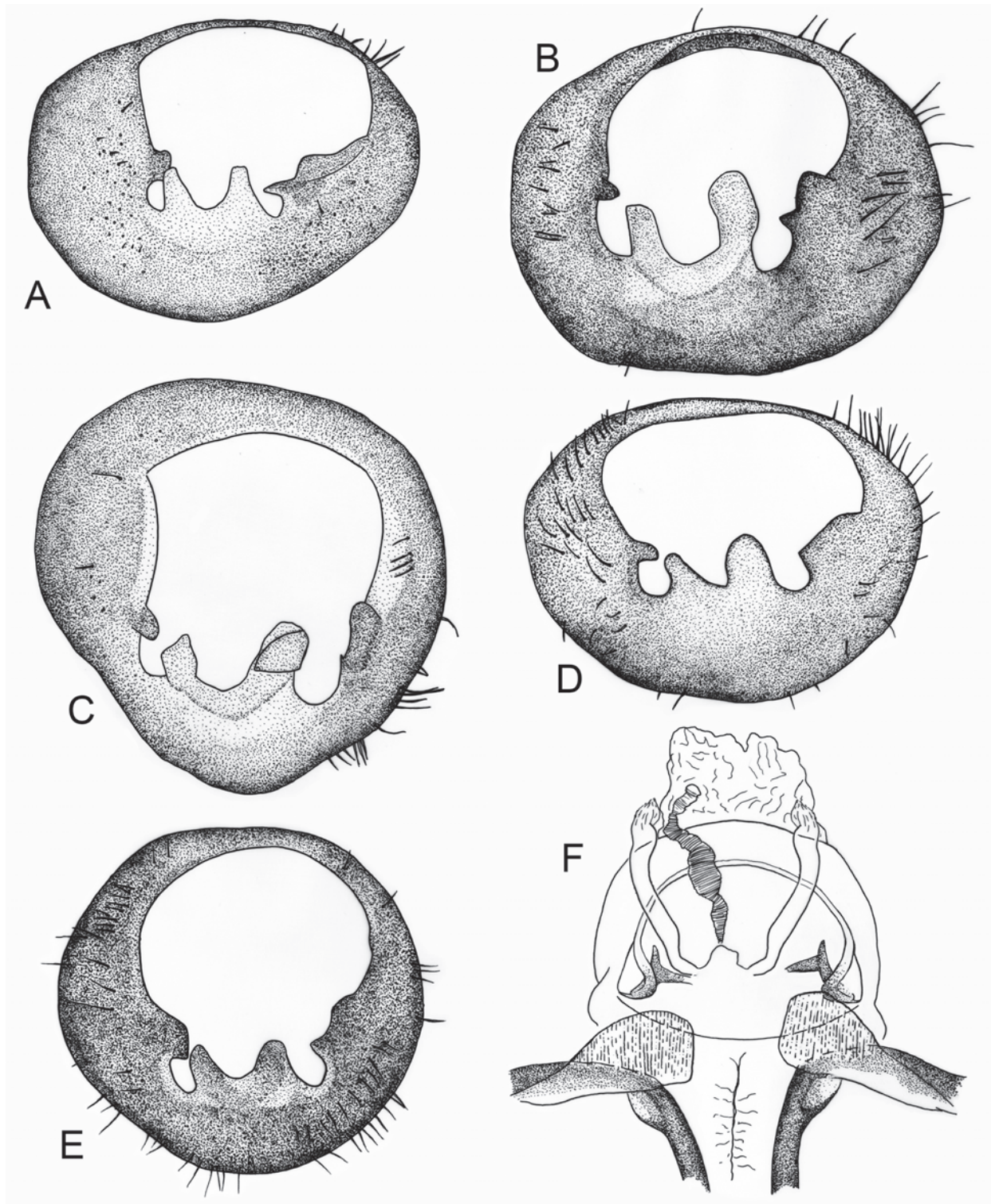


**Figure 9.** *Kunungua* species, male genital capsule and female bursa copulatrix. **A.** *K. cinnamomea*, ZISP\_ENT 00008426; **B, F.** *K. ukere-wensis* (dark form), ZISP\_ENT 00014329 (male), ZISP\_ENT 00014327 (female); **C.** *K. ukere-wensis* (light form), ZISP\_ENT 00008433; **D.** *K. gemina*, ZISP\_ENT 00014338; **E.** *K. ornata*, ZISP\_ENT 00008429. **A–E.** genital capsule; **F.** dorsal labiate plate of bursa.

Head 0.4 times as long as wide, 1.8–2 times as wide as collar; eye peduncle short, oblique, longer in basal part; antennal fossa large, removed from inner eye margin by distance comprising about half of its own width, located at the level of inferior eye margin; frons short, swollen; vertex about as wide as length of antennal segment I;

segment I 1.3 times as long as head, 0.4 times as long as pronotum, 0.4 times as long as pronotal width; labium short, reaching middle of fore coxa.

Thorax. Pronotum nearly as wide as long, 1.2 times as wide as head; calli 0.5 times as wide as basal width of pronotum; posterior margin slightly concave medially

(Fig. 6A); pronotal disk, calli, and collar 0.6 times, 0.2–0.3 times, and 0.1–0.2 times as long as pronotum, respectively; calli and collar together about 0.4 times as long as pronotum.

Hemelytron. Opaque, long, cuneus reaching distinctly beyond the apex of abdomen; cuneus about 1.5 times as long as wide at base (as in Fig. 6A, 7G).

Legs. Relatively short, robust, femora cylindrical, of about the same diameter along entire length (as in Fig. 6A).

**Genitalia.** Genital capsule. Lateral portions of cuplike sclerite lobe-shaped, apically tapering, subequal in size. Outgrowth forming outer side of right paramere socket spike-like, left outer outgrowth blunt, apically widened (Fig. 9A).

Parameres. Left paramere falciform, tapering towards apex (Fig. 10A, B); right paramere with wide, flattened sensory lobe, serrated apically, with needle-shaped, upturned apex in lateral view (Fig. 10C–E).

Aedeagus. As in Fig. 8A, C-shaped, basal part without any outgrowths.

**Female.** Colouration, surface, and vestiture as in male. Total body length 3.7–4.4 mm; antennal segment I 1.4–1.5 times as long as head; head 0.3–0.4 times as long as wide.

**Distribution.** The species was originally described from Kunungu and is currently known from two localities in Congo and one in Gabon.

**Host.** Unknown.

#### *Kunungua gemina* sp. nov.

<https://zoobank.org/6B7D4A25-3851-4E6B-AE05-F6DC0C4466F5>

Figs 6F, 7E, 8D, E, 9D, 10N–Q

**Material examined. Holotype.** ♀, DEMOCRATIC REPUBLIC OF THE CONGO: P.N.U. (Upemba National Park), Kamitungula af. Lusinga, 8.93°S, 27.21°E, 1700 m, 04 Mar 1947–07 Mar 1947, Miss G. F. de Witte, 6a (ZISP\_ENT 00008589) (MRAC).

**Paratypes.** DEMOCRATIC REPUBLIC OF THE CONGO: P.N.U. (Upemba National Park), Lusinga, 8.93°S, 27.21°E, 1760 m, 19 Mar 1947, Miss G. F. de Witte, 75a, 5♀ (ZISP\_ENT 00008415, ZISP\_ENT 00008416, ZISP\_ENT 00008417, ZISP\_ENT 00014336, ZISP\_ENT 00014337), 1♂ (ZISP\_ENT 00014338); 22 Mar 1947, Miss G. F. de Witte, 95a, 4♀ (ZISP\_ENT 00014331, ZISP\_ENT 00014332, ZISP\_ENT 00014333, ZISP\_ENT 00014334) (MRAC). P.N.U. (Upemba National Park), Kamitungula af. Lusinga, 8.93°S, 27.21°E, 1700 m, 04 Mar 1947–07 Mar 1947, Miss G. F. de Witte, 6a, 1♀ (ZISP\_ENT 00014335) (MRAC). Katanga: P.N.U. (Upemba National Park), Kabwoe sur Muye, 8.8°S, 26.85°E, 1.320 m, 13 May 1948–14 May 1948, Miss G. F. de Witte, 1603a, 1♀ (ZISP\_ENT 00014318) (MRAC).

**Other specimens examined.** DEMOCRATIC REPUBLIC OF THE CONGO: P.N.U. (Upemba National Park), Lusinga, 8.93°S, 27.21°E, 17 Mar 1947, Miss G. F. de Witte, 1♀ (ZISP\_ENT 00014317) (MRAC); 19 Mar 1947, Miss G. F. de Witte, 1♀ (ZISP\_ENT 00008416) (MRAC).

**Diagnosis.** Recognised by the following combination of characters: antennal segment I pale yellow, with dark

brown apex; collar dark brown; corium pale yellow, with elongate brown spot in medioapical area; cuneus dark brown; right paramere with needle-shaped apex.

Resembles the dark form of *K. ukerewensis* in the general appearance, body proportions, and colouration, particularly in the presence of an oval brown spot in the medioapical area of corium and the entirely darkened cuneus. *Kunungua ukerewensis* can be distinguished from the new species in having brownish yellow to yellow collar (figs 6G, H), and the shape of both parameres (Fig. 10D–G).

**Description. Female. Colouration** (Figs 6F, 7E). Head dark brown except for pale yellow antennal fossa; antennal segment I pale yellow, with dark brown apex, segments II–IV dark brown; eyes usually dark brown; pronotum, scutellum, and clavus dark brown; corium pale yellow, with longitudinal, more or less semicircular band along its inner margin starting slightly above claval apex; cuneus uniformly brown; membrane semitransparent, fuscous basally, whitish apically; coxae pale yellow; fore tibia and fore femur brownish yellow; middle and hind femora pale yellow basally, brown in middle part, brownish yellow apically; middle and hind tibiae brownish yellow, darker basally and gradually lightening apically; tarsal segment I pale yellow, segment II gradually darkening apically; segment III greyish brown; abdomen dark brown.

**Vestiture.** Clothed with whitish long simple setae, adpressed on hemelytron, semierect elsewhere, subequal to width of antennal segment I at middle, somewhat shorter on pronotum.

**Structure.** Total length 4.2–4.3 mm; body 4.0–4.1 times as long as width of pronotum and 4.5–4.9 times as long as pronotal length.

Head 0.3 times as long as wide, 1.9 times as wide as collar; antennal fossa large, removed from the inner eye margin by distance subequal to its own width, located at the level of inferior eye margin; frons flattened, only slightly convex distally; vertex about as wide as length of antennal segment I; antennal segment I 1.9–2.0 times as long as head, 0.5–0.6 times as long as pronotum, 0.4–0.5 times as long as pronotal width; labium relatively short, segment IV reaching middle of mesothorax (Fig. 7E).

Thorax. Posterior margin of pronotum slightly concave medially (Fig. 6F); pronotum 1.1–1.2 times as wide as long, 1.3 times as wide as head; calli 0.5 times as wide as basal width of pronotum; pronotal disk, calli, and collar 0.6–0.7 times, 0.2 times, and 0.1–0.2 times as long as pronotum, respectively; calli and collar together 0.3–0.4 times as long as pronotum.

Hemelytron. Semitransparent, long, corium reaching the apex of abdomen; cuneus about twice and a half as long as wide at the base (Figs 6F, 7E).

Legs. Slender, femora gradually thickening apically (Fig. 6F).

**Genitalia.** Bursa copulatrix weakly sclerotised, sclerotised rings not distinctive, posterior wall fully membranous.

**Male.** Colouration, structure, surface, and vestiture as in female.

**Genitalia.** Genital capsule. Lateral portions of cup-like sclerite lobe-shaped, right being about twice as large

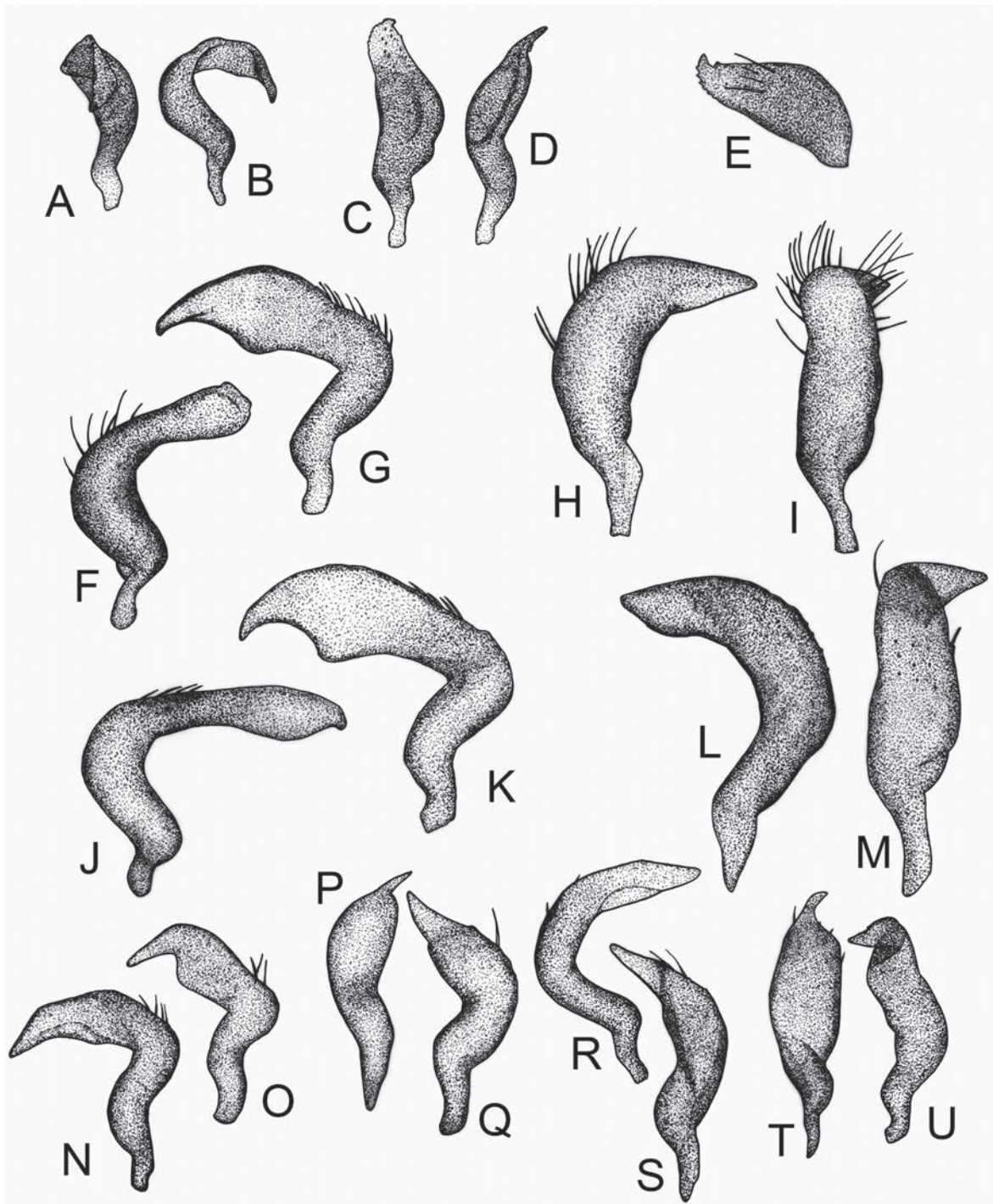


**Figure 10.** *Kunungua* species, parameres. **A–C.** *K. cinnamomea*, ZISP\_ENT 00008426; **D, E.** *K. ukerewensis* (dark form), ZISP\_ENT 00014329; **F, G.** *K. ukerewensis* (light form), ZISP\_ENT 00008433; **H, I.** *K. gemina*, ZISP\_ENT 00014338; **J, K.** *K. ornata*, ZISP\_ENT 00008429. **A–E.** *K. cinnamomea*, ZISP\_ENT 00008426; **F–I.** *K. ukerewensis* (dark form), ZISP\_ENT 00014329; **J–M.** *K. ukerewensis* (light form), ZISP\_ENT 00008433; **N–Q.** *K. gemina*, ZISP\_ENT 00014338; **R–U.** *K. ornata*, ZISP\_ENT 00008429. **A.** left paramere, lateral view; **B, R.** left paramere, ventral view; **C, I, M, T.** right paramere, lateral view; **D, H.** right paramere, dorsal view; **E.** right paramere, apex in lateral view; **F.** left paramere, anterioventral view; **G, K, N.** left paramere, dorsal view; **J.** left paramere, posterioventral view; **L, Q, U.** right paramere, ventral view; **O.** left paramere, antiodorsal view; **P.** right paramere, dorsolateral view; **S.** left paramere, dorsolateral view.

as the left one. Outgrowth forming outer side of right paramere socket wide, trapeziform, left outer outgrowth small, claw-like (Fig. 9D).

Parameres. Subequal in size; right paramere somewhat S-shaped, apically needle-shaped (Fig. 10P, Q), left

paramere falciform, apically tapering, somewhat expanded subapically (Fig. 10N, O).

Aedeagus as in Fig. 8D, E; C-shaped; with lobe-shaped, rounded, and devoid of pigmentation dorsal outgrowth of sclerotised part located close to phallobase.

**Distribution.** Known from Congo.

**Host.** Unknown.

**Etymology.** The specific epithet is the Latin adjective *geminus*, *-a*, *-um*, meaning “twin”, in allusion to the similarity of the new species and the dark form of *K. ukere-wensis* in general appearance.

***Kunungua ornata* sp. nov.**

<https://zoobank.org/E1E2B771-82ED-42E4-B14E-E1F6D40BB818>

Figs 6D, 7D, 8F, 9E, 10R–U

**Material examined. Holotype.** ♂, DEMOCRATIC REPUBLIC OF THE CONGO: Bas-Uele: Djamba, 9.82°S, 22.12°E, 25 Dec 1924, Dr H. Schouteden (ZISP\_ENT 00008428) (MRAC).

**Paratype.** DEMOCRATIC REPUBLIC OF THE CONGO: Orientale: Yangambi, 0.78°N, 24.47°E, Jun 1948, P. L. G. Benoit, 1♂ (ZISP\_ENT 00008429) (MRAC).

**Diagnosis.** Recognised by the following combination of characters: antennal segment I brown, pale yellow basally; collar brownish yellow; corium pale yellow, with wide, oblique brown band along cuneal fracture, starting near apex of clavus, reaching costal margin, and gradually narrowing laterally; cuneus pale yellow, with inner and outer margins narrowly brown; femora and tibiae pale yellow (Figs 6D, 7D).

The new species clearly differs from all congeners by the wide, oblique, gradually narrowing laterally, brown band, starting near the apex of the clavus and reaching the costal margin. While it somewhat resembles *K. gemina* in the shape of both parameres, it differs from that species in the shape of the apex of the right paramere (Fig. 10I, K), not to mention the striking differences in the colour-pattern (Fig. 6 D, F).

**Description. Male. Colouration** (Figs 6D, 7D). Head, except for pale yellow posterior and anterior margins of eye peduncle and antennal fossa, antennal segment I, except for basal pale yellow quarter, and antennal segment II dark brown, antennal segments III and IV brownish; eyes reddish brown; collar brownish yellow; calli, pronotal disk, and scutellum dark brown; corium pale yellow, with wide oblique transverse brown band along cuneal fracture, starting near apex of clavus and narrowing towards costal margin; clavus dark brown; membrane semitransparent, pale yellow, with brown membranal vein; coxae brownish, posteriorly pale yellow; femora and tibiae pale yellow; cuneus pale yellow, with brown inner and outer margins; tarsal segments I and II pale yellow, the latter brownish apically, segment III brownish; abdomen dark brown.

**Vestiture.** Clothed with whitish long simple setae, adpressed on hemelytron, semierect elsewhere, subequal to width of antennal segment I at middle, somewhat shorter on pronotum.

**Structure.** Total length 3.9–4.2 mm; body 3.4–3.6 times as long as width of pronotum and 3.7–4.0 times as long as pronotal length.

Head 0.3 times as long as wide, 2 times as wide as collar; antennal fossa large, removed from inner eye margin

by distance subequal to its own width, located at the level of inferior eye margin; frons flattened, only slightly convex distally; vertex 1.0–1.1 times as wide as length of antennal segment I, segment I 1.6–2.1 times as long as head, 0.5–0.6 times as long as pronotum, 0.5 times as long as pronotal width; labium reaching middle coxa (Fig. 7D).

Thorax. Posterior margin of pronotum slightly concave medially (Fig. 6D); pronotum 1.1 times as wide as long, 1.1–1.2 times as wide as head; calli 0.5–0.6 times as wide as basal width of pronotum; pronotal disk, calli, and collar 0.7 times, 0.2 times, and 0.1–0.2 times as long as pronotum, respectively; calli and collar together 0.3 times as long as pronotum.

Hemelytron. Semitransparent, long, corium reaching slightly beyond apex of abdomen; cuneus nearly twice and a half as long as wide at base (Figs 6D, 7D).

Legs. Slender, femora gradually thickening apically (Fig. 6D).

**Genitalia.** Genital capsule. Lateral portions of cuplike sclerite forming inner parts of paramere sockets lobe-shaped, right lobe about twice as large as left one; outgrowths forming outer sides of right and left paramere sockets trapeziform, wide and short, right one medially depressed, about twice as large as left (Fig. 9E).

Parameres. Subequal in size, left paramere slightly larger, falciform, tapering at apex (Fig. 10R, S); right paramere with a flattened sensory lobe and upturned hook-like apex (Fig. 10T, U).

Aedeagus. As in Fig. 8F; C-shaped, sclerotised basal part without any outgrowths.

**Female.** Unknown.

**Distribution.** Known from two localities in Congo.

**Host.** Unknown.

**Etymology.** The specific epithet is the Latin adjective *ornatus*, *-a*, *-um*, meaning “ornate, adorned with decorative details”, referring to the presence of a wide brown band on the corium.

***Kunungua ukerewensis* Odhiambo, 1962**

Figs 6G, H, 7A, B, 8B, C, 9B, C, F, 10F–M

*Kunungua ukerewensis* Odhiambo, 1962: 269.

**Material examined. Holotype.** ♀, TANZANIA: Mara, Tanganyika Terr. Ukerewe Island, 2.02°S, 32.98°E, R.P. Conrads (AMNH\_PBI 00340366) (NHM).

**Other specimens examined. Dark form:** DEMOCRATIC REPUBLIC OF THE CONGO: Nord-Kivu: Massif Ruwenzori, riv. Kakalari, affl. Bombi, 0.32°N, 29.78°E, 1.680 m, 28 Sep 1956, P. Vanschuytbroeck, VS738, 1♀ (ZISP\_ENT 00008437) (MRAC). Katanga: P.N.U. (Upemba National Park), Kabwoe sur Muye, 8.8°S, 26.85°E, 1.320 m, 13 May 1948–14 May 1948, Miss G. F. de Witte, 1603a, 1♂ (ZISP\_ENT 00014329) (MRAC). Katanga: Upemba National Park (P.N.U.), Gorges de la Pelenge, 7.15°S, 27.02°E, 1.150 m, 19 Jun 1947, Miss G. F. de Witte, 520a, 2♀ (ZISP\_ENT 00014327, ZISP\_ENT 00008436);

21 Jun 1947, Miss G. F. de Witte, 521a, 1♀ (ZISP\_ENT 00008412) (MRAC). Nord-Kivu: Terr. Rutshuru, 1.18°S, 29.45°E, Sep 1937, Miss. Prophylactique, 1♀ (ZISP\_ENT 00014328) (MRAC). TANZANIA: Mara, Victoria Nyanza: Ukerewe, 2.02°S, 32.98°E, Feb 1938, R. P. Conrad, 469, 2♂ (ZISP\_ENT 00008413), 1♀1♂ (ZISP\_ENT 00008414) (MRAC). **Light form:** DEMOCRATIC REPUBLIC OF THE CONGO: Nord-Kivu: Massif Ruwenzori, riv. Lume, 0.41°N, 29.78°E, 1.860 m, 12 Dec 1956, P. Vanschuytbroeck, VS 840d, 1♂ (ZISP\_ENT 00008435), 2♀ (ZISP\_ENT 00008432, ZISP\_ENT 00014330) (MRAC). Kinshasa: P.N.A. Mont Hoyo, 1.25°N, 29.82°E, 1.280 m, 07 Jul 1955–15 Jul 1955, P. Vanschuytbroeck, 13274-309, 2♂ (ZISP\_ENT 00008433, ZISP\_ENT 00008434), 2♀ (ZISP\_ENT 00008430, ZISP\_ENT 00008431) (MRAC).

**Revised diagnosis.** Recognised by the following combination of characters: antennal segment I dark brown, with pale yellow basis; collar brownish yellow; right paramere falciform, with swollen body, apically tapering (Fig. 10E, G); left paramere falciform, subapically widened, hook-like in lateral view (Fig. 10D, F).

The dark form resembles *K. gemina* sp. nov. in general appearance and colouration, particularly in the shape of the band on corium. However, this species differs from *K. ukerewensis* in having a needle-shaped apex of the right paramere (Fig. 10I), a pale yellow, apically darkened antennal segment I and a dark-brown collar (Figs 6F, 7E). The light form may be distinguished from all congeners by the same characters and additionally differs in having an almost entirely pale yellow corium and cuneus.

**Redescription. Male. Colouration. Dark form** (as in Figs 6G, 7A). Head dark brown except for brownish yellow antennal fossa, antennal segment I, except for pale yellow narrowed basal part, segments II–IV brown, clypeus from basis to apex gradually lightening from dark brown to yellowish brown; collar dirty yellow to brownish yellow; calli, pronotal disk, scutellum, clavus and cuneus dark brown; corium pale yellow, with brown, more or less rounded band along its inner margin starting slightly above claval apex; membrane transparent, fuscous basally, gradually lightening apically; coxae pale yellow, with brownish anterolateral margin; basal half of femora usually pale yellow, apical half brownish, sometimes femora uniformly pale yellow; basal half of tibiae usually brownish, apical half pale yellow, sometimes tibiae uniformly pale yellow; tarsal segment I pale yellow, segment II pale yellow basally, gradually darkening apically; segment III brownish; abdomen dark brown.

**Light form** (as in Figs 6H, 7B). Head brown except for brownish yellow antennal fossa and pale yellow clypeus, slightly darkened along margins, antennal segment I pale yellow with brown apex, basal one-third of segment II sandy, apical two-thirds brownish; eyes usually dark brown; calli and scutellum brownish yellow; collar and pronotal disk sandy; clavus brown; corium pale yellow, with sandy, indistinctly bordered band along its inner margin, starting slightly above claval apex; cuneus pale yellow, apically sandy; membrane transparent, pale fuscous basally; coxae

pale yellow, with brownish anterolateral margin; femora and tibiae pale yellow; tarsal segment I pale yellow, segment II pale yellow basally, gradually darkening apically; segment III brownish yellow; abdomen brown.

**Vestiture.** Covered with whitish setae, adpressed on hemelytron, semierect elsewhere, subequal to or slightly longer than width of antennal segment I at middle.

**Structure.** Total length 3.6–3.9 mm; body 3.6–3.8 times as long as width of pronotum and 3.9–4.2 times as long as pronotal length.

Head 0.3 times as long as wide, 1.7–1.9 times as wide as collar; antennal fossa large, removed from the inner eye margin by distance subequal to its own width, located at the level of inferior eye margin; frons flattened, only slightly convex distally; vertex 1.0–1.1 times as wide as length of antennal segment I; segment I 1.7–2.0 times as long as head, 0.5 times as long as pronotum, 0.4–0.5 times as long as pronotal width; labium relatively short, reaching middle of mesothorax (as in Fig. 7A, B).

Thorax. Posterior margin of pronotum slightly concave medially (Fig. 6G, H); pronotum about 1.1 times as wide as long, 1.2 times as wide as head; calli 0.5–0.6 times as wide as basal width of pronotum; pronotal disk, calli, and collar 0.6 times, 0.2 times, and 0.2 times as long as pronotum, respectively; calli and collar together 0.4 times as long as pronotum.

Hemelytron. Semitransparent, long, corium reaching apex of abdomen; cuneus about two-and-a-half times as long as wide at base (as in Figs 6G, H, 7A, B).

Legs. Slender, femora gradually thickening apically (Fig. 6G, H).

**Genitalia.** Genital capsule. Lateral portions of cuplike sclerite forming inner margins of paramere sockets lobe-shaped, right lobe about twice as large as left one; outgrowth forming outer side of right paramere socket trapeziform, medially depressed, left outer outgrowth small, spike-like (Fig. 9B, C).

Parameres. Subequal in size; right paramere C-shaped, with swollen, not flattened body, apically tapering (Fig. 10H, I, L, M); left paramere falciform, subapically widened, tapering at apex, hook-like in lateral view (Fig. 10F, G, J, K).

Aedeagus. As in Fig. 8B, C; C-shaped, sclerotised part with dorsal, non-pigmented, trapeziform outgrowth located close to phallobase.

**Female.** Structure, surface, and vestiture as in male. Colouration as in male, but cuneus pale yellow, with brown outer and inner margins. Total length 3.7–3.8 mm. Head 1.7–1.8 times as wide as collar; antennal segment I 1.6–2.2 times as long as head.

**Genitalia.** Bursa copulatrix weakly sclerotised, vulvar region and posterior wall devoid of any distinctive sclerotisations; sclerotised rings of dorsal labiate plate very thin and weakly sclerotised, with medially oriented sclerotised outgrowth (Fig. 9F).

**Distribution.** Originally described from Tanganyika region (Tanzania). Currently known from Congo and Tanzania.

**Host.** Unknown.

## Species excluded from *Kunungua*

### *Kunungua pallida* Linnavuori, 1975

Figs 6E, 7H

incertae sedis

*Kunungua pallida* Linnavuori, 1975: 4.

**Redescription.** (based on Linnavuori (1975) and images of the holotype). **Female. Colouration.** Pale, greenish yellow; head ochraceous; antennae, labium, calli, cuneus, and legs pale yellow, tarsal segment III darkened, greyish yellow; collar yellowish; pronotal disk and corium greyish yellow, probably greenish yellow in life; clavus uniformly greyish green.

**Surface and vestiture.** Dorsum with short, pale and erect simple setae, longest on clavus; pronotum deeply punctate; legs with short simple setae.

**Structure.** Total length 4 mm, body 2.75 times as long as broad.

Head 0.4 times as broad as pronotum; frons broadly rounded; clypeus slightly swollen; vertex with a medial furrow, 2.12 times as wide as eye; basal one-fourth of antennal segment I distinctly thinner than remainder of segment; antennal segment I related to segment II as 9:16; eye reaching collar dorsoposteriorly, neck not distinctive; labium reaching mesocoxa.

Thorax. Pronotum 1.17 times as broad as long; pronotal disk strongly convex, posterior margin straight; scutellum triangular, small, about 0.43 times as wide and 0.3 times as long as pronotum.

Legs. Slender.

Hemelytron. Semitransparent; cuneus relatively short, the distance between apex of cuneus and apex of membrane about three-quarters of cuneal length; membranal vein strongly curved distally, forming an acute angle.

**Genitalia.** Unknown.

## Discussion

*Kunungua pallida* was described from a single female collected in Southern Sudan (Linnavuori 1975). The original description was brief, lacked illustrations, and did not provide a discussion on the generic placement. No new information on this species has been published since then. According to Linnavuori (1975), *K. pallida* differs from congeners in having uniformly pale colouration, robust body, short vestiture, long labium, and the antennal fossa located close to the inner eye margin. Examination of the dorsal and lateral images of the holotype preserved in NMC and kindly provided by Dr. Wilson (Figs 6E, 7H) lead us to the conclusion that *K. pallida* does not align with the diagnosis of *Kunungua*. In contrast to other species of the genus, *K. pallida* has sessile and moderately produced posteriorly eyes, transverse pronotum with weakly raised, punctured calli and strongly convex posterior part behind calli, long labium, reaching mesocoxa, and strongly angulate membranal vein.

A combination of available characters prevents the transfer of this species to any other ecritotarsine genus. Within the Ethiopian region, six genera of this tribe are currently known, including *Bunsua* Carvalho, 1951, *Monalocoropsis* Poppius, 1912, *Prodromus*, *Rhodocoris* Schmitz, 1979, and *Stenopterocoris* China, 1944. Of these, *Bunsua* (see Yeshwanth and Konstantinov 2021; Konstantinov 2021), *Monalocoropsis* (see China 1944), and *Rhodocoris* (see Štys 1985; Stonedahl 1988) clearly differ from *K. pallida* in virtually all respects, placing them in different groups of genera.

*Stenopterocoris* (Fig. 1B) exhibits superficial similarities to *K. pallida*, such as gracile, parallel-sided body, long and thin appendages, and a heavily punctured pronotum. However, *Stenopterocoris* clearly differs in many other respects, including eyes distinctly extended posteriorly, a non-demarcated pronotal collar, three distinct depressions at the middle of the pronotum near the anterior margin, an elongated pronotum that is weakly convex posteriorly, a falciform cuneus, and an almost straight membranal vein.

*Prodromus* spp. may share some features with *K. pallida*, such as an elongate body form, a short head, a vertex with longitudinal sulcus, a bottle-shaped antennal segment I with strongly narrowed basal part, semitransparent hemelytra, and an angulate membranal vein observed in some species (Fig 3B, Stonedahl 1988: fig. 76h). However, *K. pallida* differs from all *Prodromus* spp. in many crucial character states, including sessile, clearly not pedunculate eyes adjoining the anterior margin of the pronotum, a convex vertex that does not form a necklike area, and a transverse, non-campanulate pronotum with straight posterior margin.

On a global scale, *K. pallida* appears to be most similar to *Myiocapsus* Poppius, 1914 (Stonedahl 1988: fig. 42), a genus containing nine species known from Malaysia, Western Indonesia, and Southern Philippines. However, this genus can be most easily differentiated by the shape of the right paramere and the presence of a spinelike process on the left margin of the genital capsule (Stonedahl 1988). Given that male genitalic structures are crucial for the correct generic assignment of *K. pallida*, at present we refrain from transferring it to another genus and treat this species as of uncertain generic placement.

## Acknowledgements

The second author is grateful to Eliane De Coninck (MRAC), Mick Webb (NHM), Tom Henry (USNM), Mike Wilson (NMWC), and Toby Schuh (AMNH) for providing access to collections and a supportive environment during his stay in the respective museums. Funding for the laboratory work of F. Konstantinov in this study was partly provided by the Bulgarian National Science Fund (project KP-06-PN71/13, BG-175467353-2023-130067 “Exploring the evolution of the plant bug subfamily Phylinae (Insecta, Hemiptera, Miridae): insights from phylogenetic reconstructions, host associations, and distributional patterns”). Tom Henry, Michael Schwartz, and Dávid Rédei provided helpful comments that have substantially improved the manuscript.

## References

- Akingbohunge AE (1975) Miridae (Heteroptera) of Nigeria: II. A new species of *Duducoris* Odhiambo with a new record for and comments on *Petasma deira* Odhiambo. Bulletin de l'Institut Français d'Afrique Noire. Série A, Sciences Naturelles 37: 795–800.
- Alvarez-Zapata A, Ferreira PS, Serna F (2022) A taxonomic synopsis of the Eccritotarsini (Hemiptera: Heteroptera: Miridae: Bryocorinae) of Colombia. Zootaxa 5178(2): 101–151. <https://doi.org/10.11646/zootaxa.5178.2.1>
- Carvalho JCM (1946) Mirídeos neotropicais, 23: Um gênero e tres espécies novas colecionada em Araceae e Bromeliacea (Hemiptera). Boletim do Museu Nacional (n. s.) (Zool.), Rio de Janeiro 61: 6 pp. [5 pls.]
- Carvalho JCM (1948) Mirídeos neotropicais, 34: Descrições de uma espécie nova de Falconia Distant e algumas correções sinonimicas (Hemiptera). Revista Brasileira de Biologia 7: 189–192.
- Carvalho JCM (1951) Five new genera and eleven new species of African Miridae (Hemiptera). Revue de Zoologie et de Botanique Africaines 45: 100–115.
- Carvalho JCM (1957) A catalogue of the Miridae of the world. Part I. Arquivos do Museu Nacional, Rio de Janeiro 44: 158 pp.
- Carvalho JCM (1973) On some interesting new genera and species of Miridae from Oceania (Hemiptera). Revista Brasileira de Biologia (suppl. 33): 1–9.
- Carvalho JCM (1981) The Bryocorinae of Papua New Guinea (Hemiptera, Miridae). Arquivos do Museu Nacional, Rio de Janeiro 56: 35–89.
- Cassis G, Cheng M, Tatarnic N (2016) Flattened plant bugs of the *Pandanus*-inhabiting genus *Frontimiris* (Heteroptera: Miridae) and *Pandanus spiralis*-heteropteran associations in the East Kimberley. Austral Entomology 55(4): 371–382. <https://doi.org/10.1111/aen.12199>
- China WE (1944) New and little known West African Miridae (Capsidae) (Hemiptera-Heteroptera). Bulletin of Entomological Research 35(2): 171–191. <https://doi.org/10.1017/S0007485300017399>
- Distant WL (1884) Insecta. Rhynchota. Hemiptera-Heteroptera. Biologia Centrali Americana 1: 265–304.
- Distant WL (1904) The fauna of British India, including Ceylon and Burma. Rhynchota. Taylor & Francis, London. Vol. 2, part 2, 243–503.
- Henry TJ, Howard SZ (2016) Revision of the Neotropical plant bug genus *Sinervus* Stål (Heteroptera: Miridae: Bryocorinae: Eccritotarsini), with the description of four new species and a closely related new genus. Proceedings of the Entomological Society of Washington 118(4): 533–554. <https://doi.org/10.4289/0013-8797.118.4.533>
- Kerzhner IM, Konstantinov FV (1999) Structure of the aedeagus in Miridae (Heteroptera) and its bearing to suprageneric classification. Acta Societatis Zoologicae Bohemicae 63(1–2): 117–137.
- Kirkaldy GW (1902) Memoirs on Oriental Rhynchota. Journal of the Bombay Natural History Society 14: 47–58, 294–309. [pls. A–C]
- Konstantinov FV (2003) Male genitalia in Miridae (Heteroptera) and their significance for suprageneric classification of the family. Part I: General review, Isometopinae and Psallopinae. Belgian Journal of Entomology 5: 3–36.
- Konstantinov FV (2019) Revision of *Agraptocoris* Reuter (Heteroptera: Miridae: Phylinae), with description of five new species and a review of aedeagal terminology. Arthropod Systematics & Phylogeny 77(1): 89–126.
- Konstantinov FV (2021) A new species of *Campyloneura* (Hemiptera: Heteroptera: Miridae) from Cameroon with a review of the genus. Zootaxa 4958(1): 301–312. <https://doi.org/10.11646/zootaxa.4958.1.16>
- Konstantinov FV, Knyshev AA (2015) The tribe Bryocorini (Insecta: Heteroptera: Miridae: Bryocorinae): phylogeny, description of a new genus, and adaptive radiation on ferns. Zoological Journal of the Linnean Society 175(3): 441–472. <https://doi.org/10.1111/zoj.12283>
- Konstantinov FV, Zinovjeva AN (2016) A new species of *Ambunticoris* from Sulawesi (Hemiptera: Heteroptera: Miridae). Acta Entomologica Musei Nationalis Pragae 5(1): 51–59.
- Konstantinov FV, Namyatova AA, Cassis G (2018) A synopsis of the bryocorine tribes (Heteroptera: Miridae: Bryocorinae): key, diagnoses, hosts and distributional patterns. Invertebrate Systematics 32(4): 866–891. <https://doi.org/10.1071/IS17087>
- Linnavuori RE (1975) Hemiptera of the Sudan, with remarks on some species of the adjacent countries. 4. Miridae and Isometopidae. Annales Zoologici Fennici 12: 1–118.
- Namyatova AA, Konstantinov FV, Cassis G (2016) Phylogeny and systematics of the subfamily Bryocorinae based on morphology with emphasis on the tribe Dicyphini sensu Schuh. Systematic Entomology 41(1): 3–40. <https://doi.org/10.1111/syen.12140>
- Odhiambo TR (1962) Review of some genera of the subfamily Bryocorinae (Hemiptera: Miridae). Bulletin of the British Museum (Natural History). Entomology 2(6): 245–331.
- Poppus B (1911) Beiträge zur Kenntnis der Miriden-Fauna von Ceylon. Öfversigt af Finska Vetenskaps societetens Förhandlingar 53A(2): 1–36.
- Poppus B (1914) Zur Kenntnis der Miriden, Anthocoriden und Nabiden Javas und Sumatras. Tijdschrift voor Entomologie 56(suppl.): 100–187.
- Schuh RT, Weirauch C (2020) True bugs of the world (Hemiptera: Heteroptera). Manchester, UK: Siri Scientific Press.
- Schwartz MD (2011) Revision and phylogenetic analysis of the North American genus *Slaterocoris* Wagner with new synonymy, the description of five new species and a new genus from Mexico, and a review of the genus *Scalponotatus* Kelton (Heteroptera: Miridae: Orthotylinae). Bulletin of the American Museum of Natural History 2011(354): 1–290. <https://doi.org/10.1206/354.1>
- Stål C (1860) Bidrag till Rio Janeiro-traktens Hemipter-fauna. Kungliga Svenska Vetenskapsakademiens Handlingar 2(7): 84 pp.
- Stonedahl GM (1986) *Stylopomiris*, a new genus and three species of Eccritotarsini (Heteroptera: Miridae: Bryocorinae) from Vietnam and Malaya. Journal of the New York Entomological Society 94: 226–234.
- Stonedahl GM (1988) Revisions of *Dioclerus*, *Harpedona*, *Mertila*, *Myiocapsus*, *Prodromus* and *Thaumastomiris* (Heteroptera: Miridae, Bryocorinae: Eccritotarsini). Bulletin of the American Museum of Natural History 187: 1–99.
- Štys P (1985) A new genus of Palaearctic Bryocorinae related to Afro-tropical *Rhodocoris* (Heteroptera, Miridae). Acta Entomologica Bohemoslovaca 82(6): 407–425.
- Yasunaga T, Ishikawa T (2016) Twelve new species of the Asian plant bug genus *Ernestinus* Distant (Heteroptera: Miridae: Bryocorinae: Eccritotarsini), with emphasis on unique biology and descriptions of three additional new eccritotarsine species. Insect Systematics & Evolution 47(5): 411–469. <https://doi.org/10.1163/1876312X-47052149>
- Yeshwanth HM, Konstantinov FV (2021) Review of the plant bug tribe Eccritotarsini (Hemiptera: Heteroptera: Miridae) of India and Sri Lanka with description of two new genera and six new species. European Journal of Taxonomy 745: 1–69. <https://doi.org/10.5852/ejt.2021.745.1311>

